MicroRNAs and Extracellular Vesicles in Pre-Clinical and Clinical Stroke Studies

Josie Charlotte van Kralingen
MRes, BSc (Hons)

Submitted in the fulfilment of the requirements of the degree of Doctor of Philosophy in the College of Medical Veterinary and Life Sciences, University of Glasgow.

Institute of Cardiovascular and Medical Sciences
College of Medical, Veterinary and Life Sciences
University of Glasgow

September 2016

Author's Declaration

I declare that this thesis has been entirely written by myself and is a record of work performed by myself with the exception of:

- SHRSP stroke surgery and subsequent brain tissue collection was performed by Dr. Emily Ord – the tissue was subsequently used in several experiments presented in this thesis (Figure 3.2 - Figure 3.5 and Figure 4.32).

- Data generated by Dr. Emily Ord has been presented in three separate figures (Figure 3.13, Figure 5.14 and Figure 5.17) to aid the discussion of data presented in this thesis.

- Exosomes were prepared for transmission electron microscopy and images taken with the aid of Mrs Margaret Mullin (Figure 4.2, Figure 4.34 and Figure 5.5).

- SHRSP permanent MCAO surgery and subsequent serum collection was performed by Dr. Emma Reid – the serum was subsequently used in one experiment presented in this thesis (Figure 4.33).

- Exosomes were isolated by precipitation from neuronal and glial cell media by Ms. Emma Sigfridsson – the exosomes were subsequently used in one experiment presented in this thesis (Figure 4.36).

This thesis has not been previously submitted for a higher degree. This research was carried out at the Institute of Cardiovascular and Medical Sciences, University of Glasgow, under the supervision of Dr. Lorraine M. Work, Professor I. Mhairi Macrae and Dr. Christopher McCabe.

Josie van Kralingen

September 2016

Acknowledgements

I would initially like to thank the lovely (Dr.) Lorraine (Work), for not only being such a great supervisor but also a friend, for her help and advice throughout the last 4 years and for always being on hand (in the ups and the downs). I couldn't have asked for better. I would also like to thank my other supervisors, Professor I. Mhairi Macrae and Dr. Chris McCabe, for taking the time throughout the course of my PhD to read reports and this thesis, to listen to presentations, to take an interest and to give welcome advice. Thanks to Dr. Jesse Dawson for giving us access to precious clinical samples without which much of the work presented here could not have been carried out.

Additionally I would like to thank the other members of our wee group: Hannah Martin and especially Dr. Emily Ord for her help in the lab. I am also grateful to Professor Eleanor Davies and Dr. Scott Mackenzie, my new colleagues, for being so accommodating and giving me time to concentrate on thesis writing. Thanks to those who keep the lab running (Nic, Gregor, Wendy, Elaine and Andy) and to all the other friendly faces that make the BHF GCRC such a great place to work.

A special thanks to Liz and Hannah, the best office friends ever! I'm so sad that you've left – we had such a great time together, so many good chats, lots of laughing (and crying), cups of tea and cake… and the rest. More recently thanks to Estrella, Chris, Valters and Izah, it's been good to have friends to share the stress of thesis writing with! Thanks to Estrella for keeping me company on the late nights we've stayed at work together – it would have been lonely without you!

A huge thank you to my friends and family (Gillies, van Daubs and vK) for your support and encouragement throughout my PhD. Special thanks go to: Dad for your never failing optimism and for offering to proof read my thesis although you had no idea what it would entail; the most loyal Mum in the world for always being *so* supportive and interested even (sometimes) when you didn't even know what I was blabbing on about; Amy, my baby sister and best friend.

My biggest thanks go to my other best friend. I don't think I could have got through these past few years without you Kenny. You are amazing and never complained despite having to make me dinner, drop me off at and pick me up from work at weekends and silly times of night as well as putting up with all my moans and boring thesis chat. It can't have been easy for you either and I love you all the more for it.

"Giving thanks always for all things unto God…" (Ephesians 5:20)

Table of Contents

List of Figures

List of Tables

List of Publications

Ord E.N., Shirley R., **van Kralingen J.C.**, Graves A., McClure J.D., Wilkinson M., McCabe C., Macrae I.M., Work L.M. (2012) Positive impact of pre-stroke surgery on survival following transient focal ischemia in hypertensive rats. J Neurosci Methods, **211**(2):305-308.

Tiong S.Y., Polgár E., **van Kralingen J.C.**, Watanabe M., Todd A.J. (2011) Galanin-immunoreactivity identifies a distinct population of inhibitory interneurons in laminae I-III of the rat spinal cord. Mol Pain, **7**:36.

List of Abstracts (2015-2016)

van Kralingen J.C. et al. (2016) Exosomal miRNA Profiling Following Ischaemic Stroke: clinical and pre-clinical data. International Stroke Conference, Los Angeles, USA [Oral Communication].

van Kralingen J.C. et al. (2015) Determination of microRNA profiles in extracellular vesicles isolated from serum of human stroke patients. BRAIN, Vancouver, Canada [Poster Communication].

van Kralingen J.C. et al. (2015) Determination of serum microRNA profiles in human stroke patients. UK Preclinical Stroke Symposium, Glasgow, UK [Oral Communication].

van Kralingen J.C. et al. (2015) Determination of serum microRNA profiles in human stroke patients. International Society for Extracellular Vesicles, Washington D.C., USA [Oral Communication].

van Kralingen J.C. et al. (2015) Determination of serum microRNA profiles in human stroke patients. Scottish Cardiovascular Forum, Edinburgh, UK [Oral Communication].

van Kralingen J.C. et al. (2015) MicroRNAs and Stroke: a clinical study. Glasgow Neuroscience Day, Glasgow, UK [Oral Communication].

List of Acronyms & Abbreviations

AGO	argonaute protein
AKI	acute kidney injury
Akt	protein kinase B
ath	*Arabidopsis thaliana*
ATP	adenosine triphosphate
AUC	area under the curve
BBB	blood brain barrier
Bcl-2	B-cell lymphoma 2
bFGF	basic fibroblast growth factor
BSA	bovine serum albumin
cel	*Caenorhabditis elegans*
CCA	common carotid artery
cDNA	complementary DNA
CE	cardioembolic
CT	computed tomography
Ct	cycle threshold
DNA	Deoxyribonucleic acid
DPBS	Dulbecco's Phosphate Buffered Saline
EAA	excitatory amino acids
ECA	external carotid artery
ECL	enhanced chemiluminescence
EDTA	ethylenediamine tetra-acetic acid
EGTA	ethylene glycol tetraacetic acid
eNOS	endothelial nitric oxide synthase
ESCRT	endosomal sorting complex required for transport
EV	extracellular vesicle
EXP5	exportin 5
FGFR2	fibroblast growth factor receptor 2
GAPDH	glyceraldehyde 3-phosphate dehydrogenase
GSO	gene silencing oligonucleotide
HSC70	heat shock cognate 70
HSP90	heat shock protein 90
HUVEC	human umbilical vein endothelial cells
ICA	internal carotid artery
ICH	intracerebral haemorrhage
ICV	intracerebroventricular

ILV	intraluminal vesicle
IP	intraperitoneal
IQR	inter-quartile range
IS	ischaemic stroke
IV	intravenous
IVT	intravenous thrombolysis
LA	large artery
LACI	lacunar infarct
LNA	locked nucleic acid
L-NAME	L-N^G-Nitroarginine methyl ester
lncRNA	long non-coding RNA
MCA	middle cerebral artery
miRNA	microRNA
miRNA*	microRNA passenger strand
MMP	matrix metalloproteinase
MRI	magnetic resonance imaging
mRNA	messenger RNA
mRS	modified Rankin Score
MTS	(3-(4,5-dimethylthiazol-2-yl)-5-(3-carboxymethoxyphenyl)-2-(4-sulfophenyl)-2H-tetrazolium)
MVB	multivesicular body
NADPH	Nicotinamide adenine dinucleotide phosphate
NHS	National Health Service
NIHSS	National Institute of Health Stroke Scale
NMDA	N-methyl-D-aspartate
NO	nitric oxide
NOX	NADPH oxidase
NTC	non template control
O_2^-	superoxide
PACI	partial anterior circulation infarct
PCR	polymerase chain reaction
PDCD4	Programmed cell death protein 4
PEG	synthetic polymer poly-(ethylene glycol)
PFA	paraformaldehyde
pMCAO	permanent middle cerebral artery occlusion
POCI	posterior circulation infarct
PPA	pterygopalatine artery
PPARα	peroxisome proliferator-activated receptor-α

pri-miRNA	primary miRNA
PSS	physiological salt solution
PTEN	phosphatase and tensin homolog
qRT-PCR	quantitative real time-PCR
RISC	RNA induced silencing complex
RNA	ribonucleic acid
ROC	receiver operator characteristic
ROS	reactive oxygen species
RQ	Relative Quantification
rt-PA	Recombinant tissue plasminogen activator
RT-PCR	reverse transcription polymerase chain reaction
SD	Sprague Dawley rats
SDS	sodium dodecyl sulfate
SDS-PAGE	SDS – polyacrylamide gel electrophoresis
SEM	standard error of mean
SHR	spontaneously hypertensive rats
SHRSP	spontaneously hypertensive stroke prone rat
siRNA	small interfering RNA
snoRNA	small nucleolar RNA
SVD	small vessel disease
TACI	total anterior circulation infarct
TBS	Tris-buffered saline
TBS-T	TBS with Tween-20
TE	Tris-EDTA
TIMP	tissue inhibitor of metalloproteinases
tMCAO	transient middle cerebral artery occlusion
TOAST	Trial of Org 10172 in Acute Stroke Treatment
U	unclassified
U46619	9,11-Dideoxy-11α-epoxymethanoprostaglandin F2α
UBC	ubiquitin C
UTR	untranslated region
v/v	volume/volume
w/v	weight/volume

Summary

Stroke is a leading cause of death and disability worldwide and remains a largely unmet clinical need. Despite decades of pre-clinical stroke research there are only two licensed interventions: intravenous delivery of thrombolytic recombinant tissue plasminogen activator (rt-PA) within 4.5 hours of stroke or mechanical thrombectomy. However, the number of patients eligible to receive either treatment is limited. An alternative intervention is needed, one which directly address specific aspects of stroke pathophysiology. Through their ability to alter the expression of multiple genes involved in stroke pathophysiology microRNAs (miRNA or miR) offer a novel therapeutic intervention. miRNA expression is altered both in experimental stroke and in patients with stroke. It was initially hypothesised that modulation of specific dysregulated miRNAs would be therapeutically beneficial in pre-clinical experimental ischaemic stroke. Recently, active transport of miRNAs in extracellular vesicles (EV), such as exosomes, has been demonstrated pre-clinically between cells in atherosclerosis and cardiac hypertrophy disease settings. It was therefore hypothesised that miRNAs packaged in exosomes would differ between patients with stroke and patients without stroke, raising the potential for novel exosomal miRNAs to be used as biomarkers or therapeutic agents for modulation.

In Chapter 3, investigations were carried out to test the hypotheses that modulation of either miR-494 or miR-21 would be therapeutically beneficial in pre-clinical *in vitro* models of stroke. While miR-494 expression was unchanged in brain tissue of spontaneously hypertensive stroke prone rats (SHRSP) harvested at either 24 or 72 hours following transient middle cerebral artery occlusion (tMCAO) its expression was successfully up-regulated in B50 neuronal and GPNT cerebral endothelial cell lines following delivery of miR-494 mimic in combination with siPORT, a lipid based transfection reagent. mRNA expression of putative miR-494 target genes (PTEN, MMP2 and MMP9) was investigated post-miR-494 modulation but there was no obvious change in their expression. Modulation of miR-494 expression did not appear to be therapeutically beneficial (or detrimental) when assessed by a cell survival assay (MTS). As the balance of evidence did not indicate that miR-494 would be a suitable target for modulation in experimental stroke subsequent similar experiments investigated the therapeutic potential of miR-21. Its expression was significantly increased in

SHRSP brain tissue at 72 hours following ischaemic stroke. miR-21 expression was successfully increased in cerebral endothelial cells following delivery of miR-21 mimics (with siPORT). mRNA expression of putative target genes (PDCD4 and PTEN) was unchanged following miR-21 modulation and cell survival (assessed by MTS assay) was unaffected. Subsequent experiments looked at vessel reactivity of aortae taken from miR-21$^{+/-}$ and miR-21$^{-/-}$ mice in comparison to wild type (WT) mice. Treatment of vessels with L-NAME to block endogenous nitric oxide (NO) bioavailability resulted in unopposed contraction to U46619 in WT mice while there was no change in contraction in miR-21$^{-/-}$ mice aortae, consistent with reduced basal NO bioavailability, and a detrimental phenotype associated with the loss of miR-21 expression. As the data generated in this study were primarily neutral and gave no indication that either miR-494 or miR-21 would be therapeutically beneficial in the setting of ischaemic stroke, subsequent studies focussed on investigating exosomal miRNA in ischaemic stroke.

In Chapter 4, exosomal miRNA expression was profiled in blood samples from stroke patients and subsequently in pre-clinical rodent stroke models. Patients with suspected stroke were recruited and a blood sample taken at 48 hours post-stroke. All participants gave full informed consent and the study was approved by the Scotland A Research Ethics Committee. Exosomes were isolated from 200 µL serum before RNA was extracted. A miRNA microarray was performed (OpenArray™ platform) on samples from 39 patients. Validation of results was performed by real-time quantitative polymerase chain reaction using samples from 173 patients to determine the expression levels of specific miRNAs. Microarray experiments identified 26 exosomal miRNAs that were significantly dysregulated between stroke and non-stroke patients or between specific TOAST subtypes and non-stroke controls. Of these, changes in 13 miRNAs were validated in the larger cohort and levels of 9 miRNAs (-27b, -93, -20b, -17, -199a, -30a, let-7e, -218 and -223) were found to be significantly increased in definitively diagnosed stroke patients as compared to non-stroke patients. Differences in exosomal miRNA expression were observed between TOAST subtypes with small vessel disease patients consistently having the highest levels of these miRNAs. miRNA expression did not correlate with baseline or day 7 NIHSS score, although there was a trend towards patients with better functional outcome post-stroke (as assessed by modified Rankin Score at 1 month) having a

higher level of some exosomal miRNAs. Subsequently total and exosomal miR-17 family (miRNAs -17, -93 and -20b) expression was investigated in pre-clinical models of hypertension and stroke. Total circulating miR-17 expression was unchanged between the serum of normotensive WKY and hypertensive SHRSP rats, whilst exosomal miR-17 expression was significantly increased in SHRSP vs. WKY. miR-17 family expression was unchanged in peri-infarct brain tissue of SHRSP at both 24 and 72 hours post-tMCAO. Experiments profiling total and exosomal circulating miR-17 family expression in serum of SHRSP post tMCAO or permanent MCAO revealed that expression was variable and changes observed were not significant. Cellular expression of miR-17 family miRNAs was unchanged following hypoxic challenge in neuronal, glial and cerebral endothelial cell lines and exosomal miRNA expression was highly variable, with no changes detected as significant. This study both identified and validated (for the first time) changes in exosome packaged miRNA expression in patients with stroke across differing stroke subtypes. The pre-clinical experimental findings corroborate the human data and support a functional role for these findings.

In Chapter 5 exosomal packaged miR-17 family miRNAs were delivered in pre-clinical models of ischaemic stroke (both *in vivo* and *in vitro*) to test the hypothesis that they would be therapeutically beneficial following *in vitro* hypoxic challenge or *in vivo* experimental stroke. Bioinformatics analysis highlighted a number of important target genes implicated in stroke pathophysiology for each miRNA including genes involved in the regulation of the cellular response to stress, apoptosis and angiogenesis. miRNAs were artificially loaded (by electroporation) into EVs harvested from SHRSP brain. While miRNA loaded EVs did not successfully modulate miRNA expression either *in vivo* or *in vitro* it is believed that this is a result of technical issues with the loading of the miRNAs into the EVs. This study should be repeated when miRNAs have been successfully loaded into EVs, as these experiments remain of interest.

In summary, the findings presented in this thesis confirm that packaging of miRNAs into exosomes is significantly dysregulated in stroke patients and that as a result the circulating exosomal miRNA profile is altered. This will direct future studies looking into paracrine signalling in the setting of stroke and the modulation of specific miRNAs as a novel therapy in the setting of experimental stroke.

Chapter 1 Introduction

1.1 Stroke

1.1.1 Classification

A stroke has been defined by the WHO as “rapidly developed clinical signs of focal (or global) disturbance of cerebral function, lasting more than 24 hours or leading to death, with no apparent cause other than of vascular origin" (Aho et al., 1980). This is in contrast to a transient ischaemic attack in which symptoms recover completely within 24 hours of onset.

1.1.1.1 Haemorrhagic Stroke

An intracerebral haemorrhage (ICH) is the result of the rupture of a diseased cerebral blood vessel within the cerebrum. This can cause a significant increase in pressure within the brain. While hypertension is the primary cause of ICH, other causes include trauma and blood vessel abnormalities (e.g. arteriovenous malformations). ICH accounts for 10% of all strokes (Intercollegiate Stroke Working Party, 2012, Luengo-Fernandez et al., 2013, Mozaffarian et al., 2015).

A subarachnoid haemorrhage (SAH) is the result of the rupture of a cerebral blood vessel into the subarachnoid space. Clinically, SAH is characterised by a sudden onset of severe headache and vomiting, with or without the loss of consciousness. SAH accounts for 3-5% of all strokes (Mozaffarian et al., 2015, Intercollegiate Stroke Working Party, 2012, Luengo-Fernandez et al., 2013). Of these approximately 85% are haemorrhages as a result of an intracranial aneurysm, 10% are non-aneurysmal peri-mesencephalic haemorrhages and 5% are a result of other vascular abnormalities (van Gijn and Rinkel, 2001). 10-15% of patients with SAH die before reaching hospital and a further 25% die within 24 hours of the haemorrhage (Intercollegiate Stroke Working Party, 2012).

Haemorrhagic strokes are typically associated with increased stroke severity and are further associated with a reduced 5-year life expectancy and higher mortality risk (vs. ischaemic stroke) within 3 months of stroke onset (Andersen et al., 2009, Luengo-Fernandez et al., 2013), even after stroke severity, age, sex and cardiovascular risk factors have been adjusted for.

1.1.1.2 Ischaemic Stroke

An ischaemic stroke is the result of an occlusion in a cerebral blood vessel, preventing blood (and therefore oxygen and nutrient) supply to the area of the brain which the artery or arterioles perfuse, causing rapid and often irreversible damage and cell death. Ischaemic stroke accounts for 85-87% of all stroke incidence (Mozaffarian et al., 2015, Intercollegiate Stroke Working Party, 2012, Luengo-Fernandez et al., 2013).

When patients with suspected stroke are admitted to hospital national guidelines recommend that patients are directly admitted to a hyperacute stroke unit where they can be assessed by stroke specialist clinicians (Intercollegiate Stroke Working Party, 2016, National Institute for Health and Care Excellence, 2008). Hypoglycaemia should be excluded as a cause of neurological symptoms and diagnosis of stroke should be provisionally confirmed using a validated tool such as ROSIER (Recognition of Stroke in the Emergency Room) (Nor et al., 2005). They also recommend that all patients undergo brain imaging urgently, ideally within 1 hour of arrival at hospital. Imaging techniques could include computed tomography (CT), magnetic resonance imaging (MRI) or CT angiography (Intercollegiate Stroke Working Party, 2016, National Institute for Health and Care Excellence, 2008). Where imaging results indicate a patient is eligible for treatment with Alteplase this should be administered as quickly as possible. If patients are eligible for endovascular therapy CT angiography of the aortic arch to the skull vertex should be performed as quickly as possible but treatment with Alteplase should not be delayed if this is the case. Finally, where there is diagnostic uncertainty diffusion-weighted MRI imaging should be performed. Further tests such as carotid ultrasound and echocardiography may also be performed to further identify cause of stroke.

Ischaemic strokes are classified according to their underlying stroke aetiology in a system devised by neurologists for the Trial of Org 10172 in Acute Stroke Treatment (TOAST) (Adams et al., 1993), using the clinical manifestation in each case and data collected by computed tomography (CT), magnetic resonance imaging (MRI), cardiac imaging, angiography or carotid Doppler ultrasound. There are 5 different ischaemic stroke categories: large artery atherosclerosis, cardioembolism, small-artery occlusion (or lacunae), acute stroke of other

determined aetiology or strokes of undetermined aetiology (Adams et al., 1993). Further information on each stroke subtype is given in Table 1.1. While there is not a direct relationship, the Oxford Vascular Study reports that cardioembolic stroke is associated with highest mortality and strokes as a result of small-vessel occlusion or of unknown aetiology are associated with better life expectancy (Luengo-Fernandez et al., 2013).

Table 1.1 – TOAST classification: features of stroke subtypes.
This classification system was devised by neurologists for the TOAST clinical trial (Adams et al., 1993). Features of each ischaemic stroke subtype are described in the table.

Stroke Subtype	Features
Large-artery atherosclerosis	*Clinical*: cortical or cerebellar dysfunction *Imaging*: cortical, cerebellar, brain stem, or subcortical infarct > 1.5 cm diameter *Tests*: Stenosis of extracranial internal carotid artery
Cardioembolism	*Clinical*: cortical or cerebellar dysfunction *Imaging*: cortical, cerebellar, brain stem, or subcortical infarct > 1.5 cm diameter *Tests*: cardiac source of emboli
Small-artery occlusion	*Clinical*: lacunar syndrome *Imaging*: subcortical or brain stem infarct < 1.5 cm diameter (not always detected)
Other cause	*Clinical*: cortical or cerebellar dysfunction **or** lacunar syndrome *Imaging*: cortical, cerebellar, brain stem, or subcortical infarct > 1.5 cm diameter or subcortical **or** brain stem infarct < 1.5 cm diameter *Tests*: other abnormality on tests

Another commonly used ischaemic stroke classification system is that reported by Bamford and colleagues, and classifies stroke patients according to their clinical manifestations only, and divides patients according to the vascular area affected by the infarct (Bamford et al., 1991).

1.1.2 Epidemiology

The UK age-standardised death rate for stroke has fallen by 78% since 1968 (data from 2013) and by 48% over the last decade (since 2003, data from 2013). This major improvement in stroke mortality (seen in both sexes, all races and age groups) is a result of both reduced stroke incidence and fatality and is concurrent with interventions resulting in improved control of cardiovascular risk (Mozaffarian et al., 2015, Townsend et al., 2015). Despite this reduction in stroke mortality, stroke was the 2nd leading cause of death worldwide in 2012,

killing 6.7 million people (World Health Organisation, 2014). In the UK (2014), 233,261 patients were admitted to National Health Service (NHS) hospitals with stroke as their primary diagnosis and 31,787 people (6% of all deaths) died as a result of stroke (Townsend et al., 2015). Stroke incidence in the UK is between 115-150 per 100,000 people (Feigin et al., 2014, Wang et al., 2013).

Age is the most significant risk factor for stroke: stroke risk doubles every decade after the age of 55 (Brown et al., 1996, Wolf et al., 1991). Men have a 25% higher risk of having a stroke than women and are more likely to have a stroke at a younger age (Townsend et al., 2015). Although age-specific incidence rates are lower in women than in men, these differences narrow with age, so that for the oldest patients, stroke incidence rates are approximately equal between women and men (Lewsey et al., 2009, Reeves et al., 2008, Rothwell et al., 2005).

Looking at mortality rates for stroke across the UK, the highest stroke death rates are to be found in Scotland: 60% of local authorities with the highest death rates are found there (see Figure 1.1 A). For premature (under the age of 75) stroke deaths, Glasgow City has the highest stroke death rate in the country (27 / 100,000 deaths) and 50% of local authorities with the highest premature death rates are located in Scotland (see Figure 1.1 B). The lowest death and premature death rates from stroke are primarily to be found in London and the South East of England, showing a clear geographical disparity in both incidence and mortality from stroke. This is primarily linked to social deprivation: statistics from Public Health England demonstrate that people in the most economically deprived areas of England are twice as likely to have a stroke as those from the least deprived areas (Public Health England, 2013).

Data from the Quality and Outcomes Framework used by GPs to register medical conditions of their patients (and compiled by the Stroke Association) suggests there are over 1.2 million stroke survivors living in the UK (Stroke Association, 2016). Over 50% of stroke patients are left with a disability (Intercollegiate Stroke Working Party, 2015). Furthermore, stroke is *the* leading cause of severe adult disability (even after adjustment for comorbidity and age) and the third leading cause of acquired adult disability overall (Adamson et al., 2004).

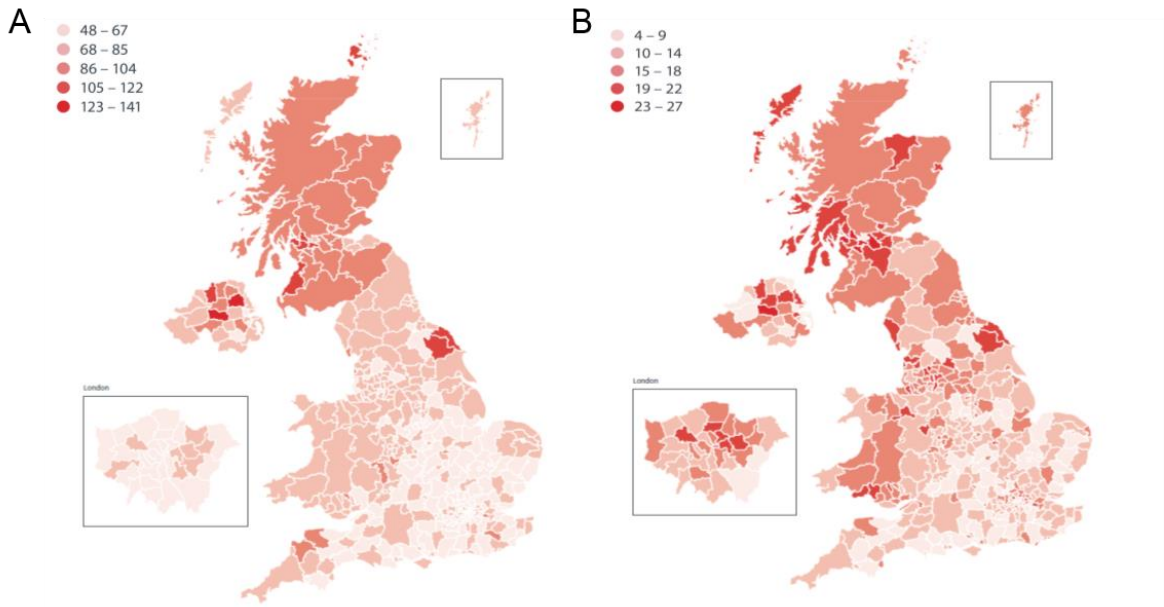

Figure 1.1 – Age Standardised Death Rates from Stroke
Map of the UK showing age-standardised death rates from stroke for men and women of all ages, per 100,000, by local authority in the UK 2011-2013 (A). Map of the UK showing age-standardised death rates from stroke in men and women under 75, per 100,000, by local authority in the UK 2011-2013 (B). Reproduced with permission from (Townsend et al., 2015).

Aside from the human cost, the NHS in England alone spent £690 million treating patients with stroke (2013-14) and NHS in Scotland spent £127 million (Townsend et al., 2015). Caring for patients with stroke accounts for 5% of total UK NHS costs (Saka et al., 2009). These sums vastly underestimate the total cost and burden of stroke in the UK, as death and long-term disability in working age people also contribute significantly.

Despite the devastating impact of stroke worldwide, research into stroke remains significantly under-funded as compared to other diseases with similar impact. Although the government and charities in the UK have recently increased the amount spent on stroke research (from £23 million in 2008 to £56 million in 2012), over double this amount was spent on research into dementia and coronary heart disease and almost 10 times as much was spent on cancer research (£544 million in 2012). The total level of funding is equivalent to £48 per person with stroke, half of the comparable spend on dementia patients, and a fifth of the spend on cancer patients (Luengo-Fernandez et al., 2014, Stroke Association, 2016). While research into diseases such as cancer and dementia is vital, it is important to remember the scale and impact of stroke. These facts

highlight the need for both a greater quantity and quality of research into stroke and new therapeutics to tackle the growing disease burden.

1.1.3 Pathophysiology

An ischaemic stroke is the result of either transient or permanent occlusion of cerebral blood flow following the occlusion of a cerebral artery – this leads to irreversible damage (infarct) along with a concomitant neurological deficit (permanent or reversible). While the brain makes up a very small percentage of total body weight (~2%) it requires 15% of total cardiac output, accounts for 20% of total body oxygen consumption and 25% of total body glucose consumption. Despite its high energy consumption the brain has a very limited capacity to store energy and is dependent on a continuous supply of oxygen and glucose, delivered via the cerebral vasculature. It is therefore very sensitive to ischaemia. It has been estimated that every minute an acute large artery stroke is left untreated, approximately 1.9 million neurons, 14 billion synapses and 12 km of myelinated fibres are lost (Saver, 2006).

Under ischaemic conditions, the brains innate inter- and intra-cellular signalling mechanisms, typically responsible for information processing, initiate an ischaemic cascade of signalling processes, facilitate cellular death and the formation of infarcted tissue (summarised in Figure 1.2 and Figure 1.3). While differences between stroke subtypes have been described in section 1.1.1, there is consistency in the cellular and molecular mechanisms that mediate ischaemic stroke. The ischaemic cascade consists of numerous processes including excitotoxicity, oxidative stress, inflammation and cell death and these will be summarised in this section.

1.1.3.1 Energy Failure

Brain tissue (especially neuronal) depends almost entirely on oxidative phosphorylation for energy production. Restriction or cessation of cerebral blood flow, as occurs in ischaemic stroke, impedes the delivery of substrates for oxidative phosphorylation, resulting in a failure of adenosine triphosphate (ATP) production. ATP is required for the maintenance of ionic gradient (active transport at ion pumps) and so with ATP depletion, membrane potential is lost

resulting in depolarisation of neurons and glia (Katsura et al., 1994, Martin et al., 1994). Membrane depolarisation results in activation of voltage-dependent Ca^{2+} channels (both pre-synaptic and somatodendritic) and excitatory amino acids (EAA), predominantly glutamate, are released into the extracellular space. Pre-synaptic and astrocytic re-uptake of EAA is an ATP-dependent process and so is disrupted (Nicholls and Attwell, 1990), leading to an even greater accumulation of EAAs within the extracellular space.

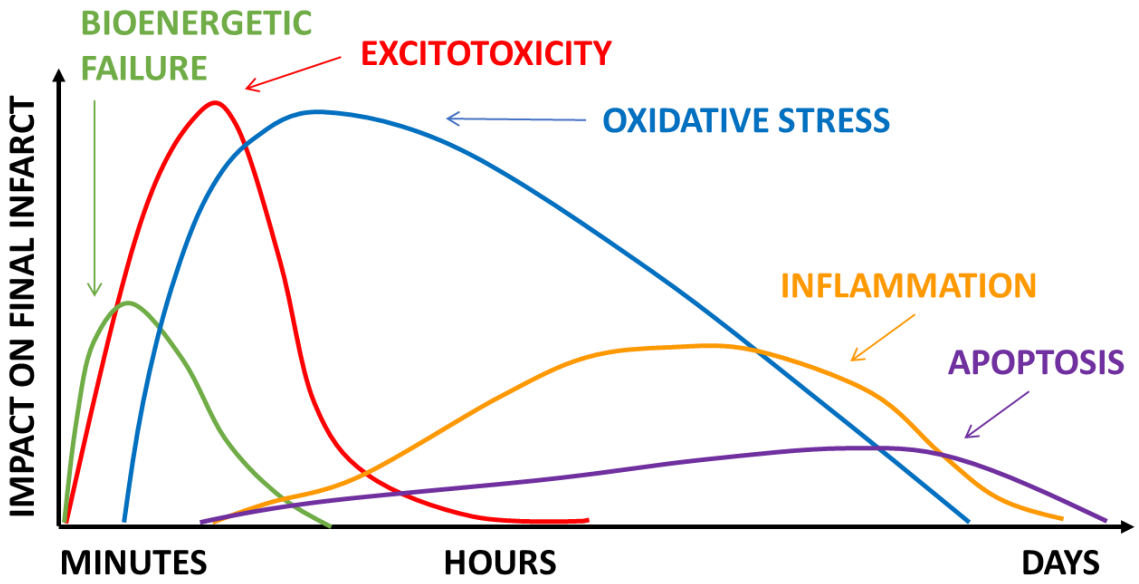

Figure 1.2 – The Ischaemic Timeline
A graph representing the temporal profile of the main pathophysiological mechanisms underlying acute ischaemic stroke and the impact of each element on final ischaemic infarct and outcome. This graph has been modified from a similar figure in (Dirnagl et al., 1999).

1.1.3.2 Excitotoxicity Mechanisms

As glutamate builds up in the extracellular space it activates *N*-methyl-D-aspartate (NMDA), α-amino-3-hydroxy-5-methyl-4-isoxazole propionic acid (AMPA) and kainate receptors, resulting in an excessive influx of Na^+, Cl^- and Ca^{2+} and efflux of K^+ ions. This causes repeated membrane depolarisation, resulting in further calcium influx and resulting EAA release, intensifying the original ischaemic insult. Excitotoxicity is the secondary damage that results from excessive glutamate release and the resulting uptake of calcium by neurons, causing acute cell death (necrosis), initiating delayed cell death (apoptosis) (Ankarcrona et al., 1995) and inflammatory pathways.

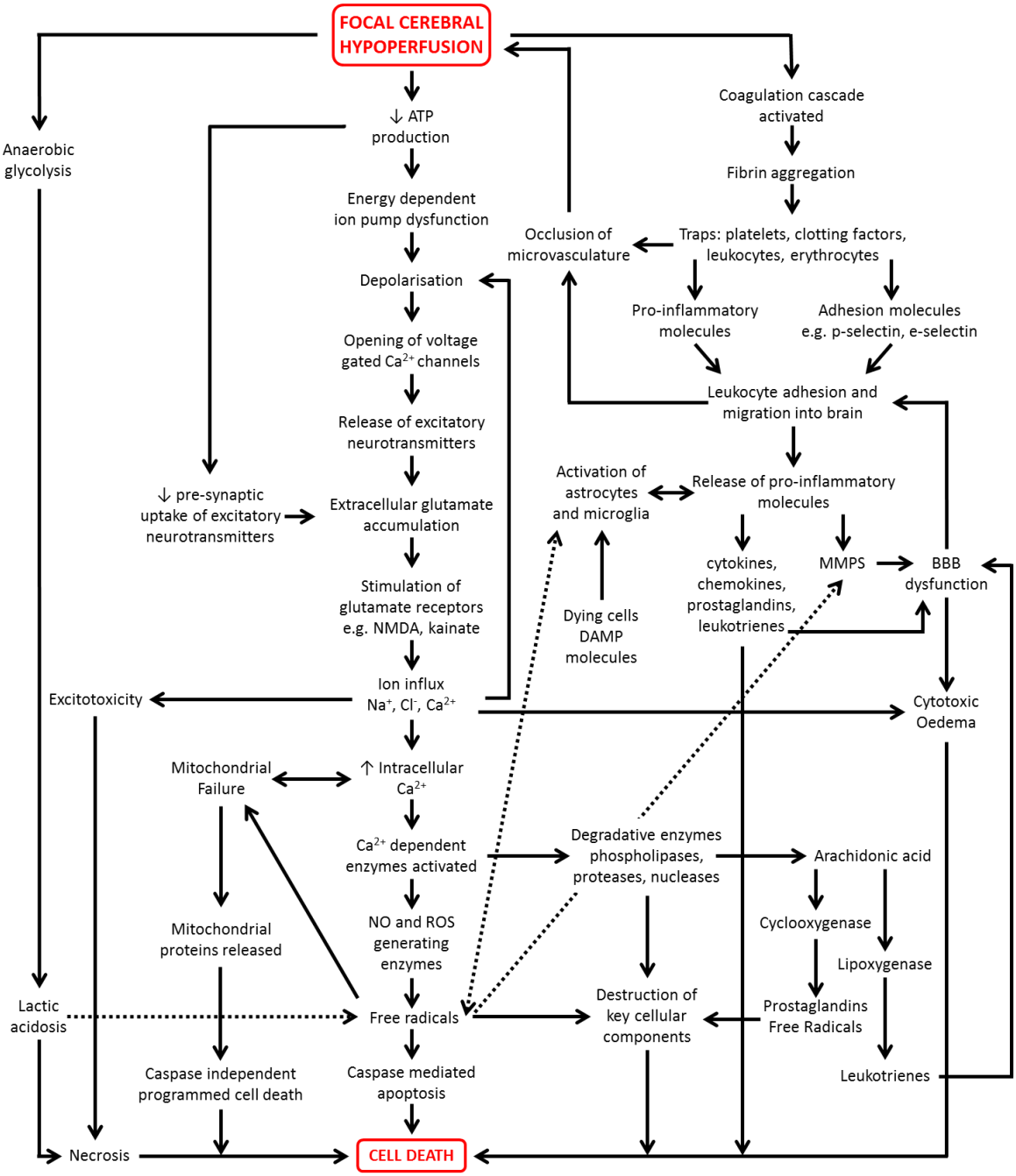

Figure 1.3 – The Ischaemic Cascade.
A diagrammatic representation of the numerous processes leading to cell death after focal cerebral hypoperfusion. Pathophysiological mechanisms underlying acute ischaemic stroke include bioenergetic failure, excitotoxicity, oxidative stress and inflammation. Dotted arrows are present only to make this diagram easier to follow and do not represent different types of pathway. Abbreviations include: BBB, blood brain barrier; DAMP, danger associated molecular pattern; MMP, matrix metalloproteinase; NO, nitric oxide; ROS, reactive oxygen species. I have used the information summarised in section 1.1.3 to create this diagram.

As the influx of Na^+ and Cl^- is excessive (greater than K^+ efflux) water follows passively, resulting in cell swelling (and death) and cerebral oedema. Oedema is cytotoxic as it affects perfusion of the area surrounding the initially infarcted brain region and can have indirect effects on otherwise unaffected brain tissue as a result of intracranial pressure, vascular compression and herniation.

Increasing concentrations of intracellular Ca^{2+} (acting as a second messenger) triggers the generation of free radicals and numerous downstream phospholipases, proteases and nucleases that degrade membranes and proteins essential for cellular integrity. Activated Ca^{2+} dependent enzymes cause considerable cellular damage and include proteases that destroy extracellular matrix proteins (e.g. laminin (Chen and Strickland, 1997)) and cytoskeletal proteins (e.g. actin and spectrin, (Furukawa et al., 1997)), calpain, endonucleases, adenosine triphosphatase as well as phospholipase A2, cyclooxygenase and nitric oxide synthase type I which generate excessive amounts of free-radical species, causing lipid peroxidation and membrane damage.

1.1.3.3 Ionic Imbalance

Although excessive Ca^{2+} is the primary cause of ionic imbalance post-ischaemic stroke, excessive zinc and potassium (Gribkoff et al., 2001) release has also been implicated as a mechanism of cell-death. Several studies (Frederickson et al., 2006, Kitamura et al., 2006b, Kitamura et al., 2006a, Sorensen et al., 1998) have demonstrated changes in zinc concentration following cerebral ischaemia and it is believed that vesicles containing zinc, stored in excitatory neurons, are released following depolarisation. The decrease in zinc concentration within presynaptic terminals is correlated with zinc accumulation within neurons and their subsequent cell death (Galasso and Dyck, 2007).

1.1.3.4 Oxidative and Nitrosative Stress

Oxidative and nitrosative stress are key mediators of tissue damage following ischaemic damage. Endogenous antioxidant defence mechanisms enable cells to deal with oxidative stress and include the regulation of reactive oxygen species (ROS) production, the elimination of ROS via neutralising enzymes and scavenger molecules and the repairing of proteins, lipids and deoxyribonucleic acid (DNA) damaged by oxidative stress. However, these have limited capability in the face of the high oxidative load and the amount of damage inflicted as a result of ischemic injury. As a result, the cell succumbs and will undergo necrosis or apoptosis (Shirley et al., 2014).

In healthy cells, mitochondria use oxygen and generate ATP (via oxidative phosphorylation at the mitochondrial respiratory chain) (Hertz, 2008). Small amounts of the ROS superoxide (O_2^-) are produced by this reaction in the mitochondrial matrix (Boveris and Chance, 1973). O_2^- is subsequently converted to hydrogen peroxide (H_2O_2) by superoxide dismutase (SOD) and leaves the mitochondria, typically acting as an intracellular messenger (Arnaiz et al., 1999, Rice, 2011). However, following ischaemic insult, oxygen is depleted (in the penumbra) favouring anaerobic production of ATP via glycolysis (Hertz, 2008) resulting in the production of lactic acid, the accumulation of which results in decreasing cellular pH and a resulting increase in ROS in parallel with an inactivation of antioxidant defence mechanisms, an increase in intracellular iron levels (Ying et al., 1999) and increased glutamate-mediated excitotoxicity (Lewerenz et al., 2010).

A second wave of ROS (O_2^-) is generated by xanthine oxidase and leakage from the mitochondrial electron transport chain, following mitochondrial depolarisation (Abramov et al., 2007). Increasing intracellular concentrations of Ca^{2+} and a variety of cytokines result in the activation of nitric oxide synthases I and II, which in turn convert L-arginine into nitric oxide (NO), a free radical with a half-life of only seconds that is both water- and lipid-soluble (Forstermann et al., 1994). Neuronal NOS is also activated directly by NMDA receptors via the adaptor postsynaptic density-95 (PSD-95). NO produced by NOS I and II reacts with $O2^-$ to produce highly toxic peroxynitrite ($ONOO^-$), an oxidant of proteins and lipids. $ONOO^-$ will spontaneously decompose to produce hydroxyl (OH^-), the most reactive of the oxygen radicals, causing the most tissue damage.

A third phase of ROS generation occurs after reperfusion and, therefore, reoxygenation. Nicotinamide adenine dinucleotide phosphate (NADPH)-oxidase (NOX), a cytoplasmic enzyme, is an important source of ROS and contributes to the amplification of oxidative stress following reoxygenation. NOX is thought to produce a significant proportion of $O2^-$ following NMDA receptor activation and ischaemia (Brennan et al., 2009, Girouard et al., 2009). Further ROS are produced by mitochondrial uncoupling.

Free radicals have important cellular effects including the inactivation of enzymes, the release of Ca^{2+} from intracellular stores, protein denaturation,

lipid peroxidation, cytoskeletal and DNA damage, chemotaxis, inhibition of mitochondrial enzymes, the formation of mitochondrial transition pores, DNA damage, PARP activation and TRPM7 channel activation (Ca^{2+} permeable) (Pacher et al., 2007). Cytochrome C, a trigger for apoptosis, is also released from mitochondria. Furthermore, nitric oxide post-transcriptionally modifies proteins, including caspases and metalloproteinases altering protein function (Gu et al., 2002). Oxidative stress therefore makes a significant contribution to cell death either through necrosis (severe oxidative stress) or apoptosis (moderate oxidative stress).

1.1.3.5 Inflammatory Pathways

The inflammatory response to ischaemic stroke begins within several hours of ischaemic insult and makes a significant contribution to the secondary insult, inducing more cell damage, microvascular stasis and disruption of the blood brain barrier (BBB) (reviewed (Iadecola and Anrather, 2011)).

Immediately following occlusion in a cerebral blood vessel there is hypoxia, changes in shear stress and ROS production – these factors combine to activate the coagulation cascade, complement, platelet and endothelial cells (Peerschke et al., 2010). Activation of the coagulation cascade results in the aggregation of fibrin molecules within the cerebral blood vessel which in turn trap platelets, clotting factors, leukocytes and erythrocytes, occluding the microvasculature (del Zoppo et al., 1991). The aggregation of activated platelets express P-selectin (an adhesion molecule) (Okada et al., 1994b, Yilmaz and Granger, 2010) and release pro-inflammatory signals, including inflammatory cytokines (e.g. IL-1α) and chemokines (CCL5, CXCL4 and CXCL7) as well as prostanoids, leukotrienes and free radicals (Iadecola and Anrather, 2011). As a result of oxidative stress there is reduced bioavailable NO which exacerbates the microvascular occlusion and so further reduces blood flow to the ischaemic area (Carden and Granger, 2000).

Cell death as a result of excitotoxicity and oxidative stress leads to further inflammatory reaction within the brain, causing increased cell damage as well as BBB disruption. Both astrocytes and microglia are activated by ROS and release numerous pro-inflammatory cytokines. However the role each cell has to play is

not clear cut: astrocytes and microglia can release both cytotoxic and/or cytoprotective substances (Iadecola and Anrather, 2011).

Recruitment of leukocytes into the brain parenchyma is mediated by adhesion molecules such as selectins, integrins and immunoglobulins. Increased expression of E- and P-selectin (Haring et al., 1996, Huang et al., 2000, Zhang et al., 1998) results in leukocyte rolling and recruitment in cerebral vessels within 4-6 hours of the ischemic insult. Subsequent to their migration they release or activate pro-inflammatory molecules that result in secondary injury (Iadecola and Anrather, 2011). Infiltration of neutrophils begins within hours of cerebral ischaemia (Buck et al., 2008) whereas infiltration of monocytes begins after several days (Che et al., 2001, Grau et al., 2001).

Cytokines are mediators of the inflammatory response and are produced by many types of cell within the brain as well as immune cells (Allan and Rothwell, 2001, Iadecola and Anrather, 2011). Important pro-inflammatory cytokines include interleukin-1 and interleukin-6 (Fassbender et al., 1994, Tarkowski et al., 1995, Vila et al., 2000), while interleukin-10 is anti-inflammatory (Vila et al., 2003) and TNFα can stimulate both inflammatory signalling leading to apoptosis and cell death as well as signalling pathways that lead to cell survival and tolerance to ischaemia (Hallenbeck, 2002). Chemokines are important mediators of cellular migration and like cytokines are produced by many cells in the brain and immune cells. Their (e.g. MCP-1, MIP-1α) increased expression following ischemic stroke is associated with further leukocyte recruitment and increased blood-brain barrier permeability (Dimitrijevic et al., 2006, Stamatovic et al., 2003) and so is believed to be detrimental.

Increasing intracellular Ca^{2+} stimulates phospholipase A_2 and therefore the arachidonic acid cascade, eventually resulting in the production of prostaglandins or leukotrienes (chemo-attractants) which are associated with BBB dysfunction, oedema and neuronal cell death (Iadecola and Anrather, 2011). There is also an up-regulation of NOS type 2 in microglia, endothelial cells and leukocytes, which has detrimental effects (as discussed in section 1.1.3.4) and an increased production of MMP2 and MMP9 by endothelial cells and leukocytes which primarily exacerbates BBB dysfunction and causes further brain damage.

The inflammatory response is eventually resolved and tissue homeostasis re-established – this is now believed to be an active process (Spite and Serhan, 2010). Resolution of the inflammatory response involves the clearing of dead cells by microglia and infiltrating macrophages. Anti-inflammatory cytokines, including TGF-β, IL-10, IL-17 and IL-23 are released by T-cells, microglia, macrophages and astrocytes (Iadecola and Anrather, 2011). Their release occurs concomitantly with the clearing away of dead cells and is believed to protect surviving cells within the ischaemic area. Finally, the production (to different extents) of growth factors such as BDNF, EPO, FGF, G-CSF, GDNF, HB-EGF, IGF-1, NGF and VEGF by microglia, astrocytes, perivascular macrophages, macrophages, endothelial cells and neurons (Iadecola and Anrather, 2011) promotes post-ischaemic neuronal sprouting, angiogenesis, neurogenesis, gliogenesis and matrix reorganisation (Greenberg and Jin, 2006).

1.1.3.6 Blood Brain Barrier Dysfunction

The BBB regulates permeability and cellular transport at the endothelial cell layer between blood and brain cells. It is made up of pericytes and tight junction proteins (e.g. occludin, claudins and junctional adhesion molecules), covered by a basal lamina that is primarily composed of collagen (type IV), fibronectin, heparan sulfate and laminin. Laminin interacts with integrins to regulate permeability and cellular transport across the BBB.

Disruption of the BBB (Yang and Rosenberg, 2011) is cytotoxic as it results in extravasation of various serum components and subsequent vasogenic oedema, which can cause further damage. Furthermore, extravasation of erythrocytes can result in haemorrhagic transformation and secondary ischemic injury. A disrupted BBB also facilitates leukocyte infiltration as discussed previously.

Disruption of the BBB is bi-phasic (Belayev et al., 1996, Huang et al., 1999, Kuroiwa et al., 1985). In the early phase (2 – 24 hours post ischemic insult) BBB disruption is primarily mediated by activation of MMP2. This is inhibited by the formation of a complex comprised of MMP2, tissue inhibitor of metalloproteinases-2 (TIMP-2) and membrane-type 1 MMP which acts to significantly limit the activity of MMP resulting in less severe injury to the BBB. However, BBB dysfunction may also be mediated by bradykinin (Aschner et al.,

1997, Kamiya et al., 1993), thrombin (Okada et al., 1994a) and other proteases. Furthermore, oxidative stress can up-regulate production of MMP9 by neurons, glia and endothelial cells leading to digestion of the endothelial basal lamina (Gidday et al., 2005).

In the later phase (24 – 72 hours post ischemic insult) BBB disruption is significantly more severe, irreversible, and is primarily mediated by the release of MMP9 from infiltrating neutrophils (Gidday et al., 2005, Rosell et al., 2008). MMP9, along with MMP3, expression is induced by cytokines and MMP9 is also activated by free radicals. Treatment with tPA (if it crosses the already disrupted BBB) can further up-regulate MMP9 expression (Tsuji et al., 2005). Unlike MMP2, the action of these metalloproteinases is unrestrained and they act on multiple substrates to disrupt the BBB.

1.1.3.7 Cell Death

Necrosis and apoptosis are the two primary mechanisms of cell death post ischaemic stroke. Necrosis is usually rapid and is characterised by plasma membrane failure, cellular (and internal organelle) oedema and finally rupture, releasing glutamate and toxins. Apoptosis, on the other hand, is highly regulated and cells die with comparatively reduced inflammation and release of genetic material. Apoptosis and necrosis can both be triggered by increased intracellular Ca^{2+} concentrations, oxidative stress and mitochondrial dysfunction.

Necrosis is the principal mechanism of ischemic cell death and is generally believed to be unregulated. However, it has been demonstrated that phosphorylation of receptor-interacting proteins (RIP) 1 and 3 can trigger pro-necrotic kinase activity and may act as a molecular switch between TNF induced apoptosis and necrosis (Cho et al., 2009, Holler et al., 2000, Zhang et al., 2009).

Apoptosis is generally associated with less severe ischaemic injury (Bonfoco et al., 1995) although severe ischaemic injury has also been linked to caspase-like enzyme activation and caspase cleavage early in the ischaemic cascade (Namura et al., 1998). Mitochondria mediate cell death in both necrosis and apoptosis (Schinzel et al., 2005) as their rupture releases both cytochrome C and a number of pro-apoptotic proteins. Cytochrome C initiates caspase-mediated apoptosis

through apoptosome complex activation, which subsequently activates caspase 3 (Green and Reed, 1998). Caspases 1 and 3 especially mediate ischemia associated apoptosis (Leist et al., 1997, Namura et al., 1998, Thornberry and Lazebnik, 1998). Caspase-independent neuronal cell death (Cho and Toledo-Pereyra, 2008) is mediated by mitochondrial proteins including apoptosis-inducing factor (AIF) and B-cell lymphoma-2 (Bcl-2)/adenovirus E1B-interacting protein (Yu et al., 2006). Apoptosis can also be triggered non-specifically by glutamate receptor activation and resulting cellular injury, mitochondrial production of ROS (Dugan et al., 1995), decreased intracellular K^+ concentrations (Yu et al., 1997) and Zn^{2+} influx.

1.1.3.8 Repair Pathways

The post-ischaemic brain undergoes both neuronal and vascular repair (neurogenesis and angiogenesis) and there is a close relationship between the pathways. Both neurogenic and angiogenic repair are mediated by numerous common mediators and signalling pathways – furthermore, neurogenesis stimulates vascular regrowth and vice versa (Arai et al., 2009, Ohab et al., 2006, Snapyan et al., 2009, Taguchi et al., 2004). Several studies have demonstrated post-ischaemic up-regulation of neurogenesis and the migration of neuroblasts towards severely infarcted striatal tissue (Arvidsson et al., 2002, Parent et al., 2002) where they express markers of developing and mature spiny neurons. Although this is believed to be an endogenous repair pathway, studies demonstrating functional activity and long-term survival of these neurons are lacking (Kernie and Parent, 2010). Angiogenesis and vasculogenesis have been detected in the penumbral regions of both human stroke patients and rodent models of ischaemic stroke (Ding et al., 2008, Krupinski et al., 1996).

1.1.3.9 Penumbra

The changes that have been described in sections 1.1.3.1 to 1.1.3.8 do not affect the whole of the ischaemic area equally. Brain tissue within the ischaemic core, where blood flow is most severely impaired, is permanently and irreversibly injured. Energy failure and the ensuing ischaemic cascade, as previously described, rapidly causes widespread cellular necrosis.

However, between the ischaemic core and healthy brain tissue lies functionally damaged tissue that is still structurally intact: the ischaemic penumbra, first described as "zones of complete electrical failure and K^+ release… with functional inactivation but not yet cell death" (Astrup et al., 1977) (see Figure 1.4). Subsequent studies have revealed the penumbra to be an area where cerebral blood flow is reduced moderately (not to the extent of the ischaemic core) and as a result energy metabolism is somewhat preserved (Baron, 1999, Markus et al., 2004, Nagesh et al., 1998, Read et al., 1998). Advances in positron emission tomography (PET) and MRI scanning now allow for the detection of the penumbra (Fisher and Bastan, 2012).

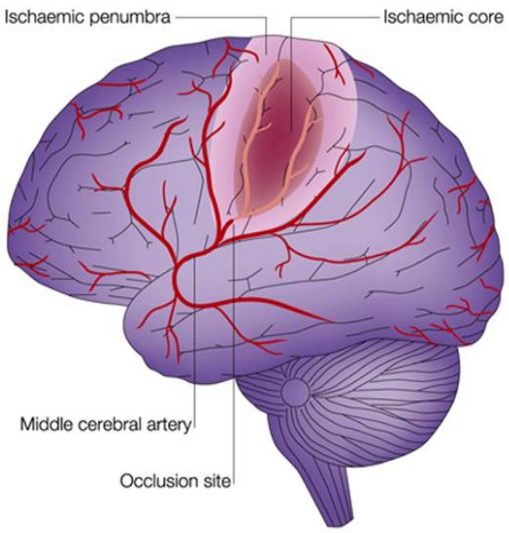

Figure 1.4 – The Ischaemic Penumbra.
An ischaemic stroke is the result of an occlusion to a cerebral blood vessel and results in rapid neuronal death in the infarct core, the region immediately surrounding the occluded artery. Surrounding the infarct core is the penumbral region, an area in which neurons may die many hours after the critical insult or may survive if reperfusion occurs in a timely manner. Image taken with permission from (Allan and Rothwell, 2001).

Penumbral tissue is often lost, absorbed into the ischaemic core, as the ischaemic cascade progresses. However, as the penumbra is a transition zone between injury and repair, it can be rescued with reperfusion and therapeutic intervention. As has been touched upon in this summary of the pathophysiology of stroke, many molecular signals in the ischaemic cascade can play biphasic roles (cytotoxic vs cytoprotective) – mechanisms that decide between cellular injury and cellular repair have yet to be discovered. While damage to the ischaemic core is irreversible, salvage of penumbral tissue is associated with

neurological improvement and recovery and so should be the target for new acute stroke therapies.

1.1.4 Therapeutics for Ischaemic Stroke

1.1.4.1 Therapeutic Challenges

The extremely complex ischaemic cascade begins within minutes of stroke onset and rapidly progresses and develops over a period of several hours. The success of any stroke treatment is therefore dependent on early treatment to prevent or limit ensuing damage. Penumbral tissue is a primary target for stroke intervention therapies and early reperfusion maximises the chance of tissue salvage. There is a clear need for novel treatments that not only result in reperfusion but also directly address specific aspects of stroke pathophysiology including cell death, cerebral oedema, oxidative stress and inflammation. While such treatments have shown promise pre-clinically, none have made the transition from bench to bedside treatment so far. Finally, therapeutic agents used must be able to cross the BBB to prove effective.

1.1.4.2 Prevention is better than cure

As currently licensed therapies for stroke are limited, preventative interventions are encouraged clinically. A 2010 study which investigated risk for stroke in 2337 ischaemic stroke patients and 3000 age and gender matched controls found the most significant risk factors for stroke, arranged in order of severity, are history of hypertension, cardiac causes, ratio of apolipoproteins, current smoking, waist-to-hip ratio, alcohol intake, diabetes mellitus, diet, depression and psychosocial stress (O'Donnell et al., 2010). Stroke is therefore to some extent a systemic disease, and risk factors that predict ischaemic stroke are also predictors for many other cardiovascular events including myocardial infarction. As a result of improved control of cardiovascular risk both stroke incidence and fatality have fallen by 78% since 1968 (data from 2013) and by 48% over the last decade (since 2003, data from 2013) (Mozaffarian et al., 2015, Townsend et al., 2015). This section will expand on modifiable risk factors for stroke and interventions that can reduce cardiovascular risk.

More than 77% of people are hypertensive on the occasion of their first stroke (Mozaffarian et al., 2015) and anti-hypertensive therapy has been associated with reductions in stroke incidence in clinical trials (Lackland et al., 2014). Even a reduction of only 10 mmHg in systolic blood pressure results in a 41% average reduction in stroke risk (Lackland et al., 2014). NICE guidelines recommend that patients with hypertension are initially treated with anti-hypertensive drugs such as angiotensin-converting enzyme (ACE) inhibitors, angiotensin-II receptor blockers (ARB) or calcium channel blockers using a monotherapy approach (National Institute for Health and Care Excellence, 2011). If hypertension is not successfully reduced using a monotherapy approach, combinations of anti-hypertensive drugs should be used (National Institute for Health and Care Excellence, 2011). Resistant hypertension may be treated using additional drugs such as thiazide diuretics. Beta blockers may also be used in patients with contraindications to ACE inhibitors or ARBs or in women of child bearing potential (National Institute for Health and Care Excellence, 2011).

Diabetes results in an over two-fold excess risk for ischaemic stroke, independent of other risk factors (Emerging Risk Factors Collaboration, 2010). A meta-analysis of clinical trials that targeted interventions at people with pre-diabetes showed this resulted in a 24% relative risk reduction in fatal and non-fatal strokes (Hopper et al., 2011).

Atrial fibrillation increases risk of stroke, independent of other risk factors, by approximately 5-fold (Wolf et al., 1991). In patients aged 50-59, 1.5% of strokes are attributable to atrial fibrillation and this increases to 23.5% in patients aged 80-89 (Wolf et al., 1991). In England it is estimated that if atrial fibrillation was adequately detected and subsequently treated, 7,000 strokes could be prevented and 2,100 lives saved (Stroke Association, 2016). NICE recommends that patients with atrial fibrillation are treated with anticoagulants to reduce the likelihood of blood clot formation (National Institute for Health and Care Excellence, 2015). Patients with valvular atrial fibrillation should be given vitamin K antagonists (e.g. warfarin) while patients with non-valvular atrial fibrillation have the choice of vitamin K antagonists or non-vitamin K antagonist oral anticoagulants (e.g. apixaban, dabigatran etc.) (National Institute for Health and Care Excellence, 2015).

The ratio of non-HDL to HDL cholesterol is associated with increased risk of ischaemic stroke, and an even stronger predictor of ischaemic stroke is the ratio of circulating ApoB to ApoA1 (O'Donnell et al., 2010). The use of statins in patients with a high risk of cardiovascular disease reduces the risk of stroke by about 25% (Heart Protection Study Collaborative Group, 2002) and reducing cholesterol levels even by 1 mmol/L reduces the risk of stroke by 21% (Amarenco and Labreuche, 2009). NICE recommends that patients with increased cardiovascular risk or established cardiovascular disease should be encouraged to make lifestyle modifications and offered atorvastatin (National Institute for Health and Care Excellence, 2014).

Current smokers have a 2- to 4-fold increased risk of stroke as compared to those who don't smoke or who have not smoked for more than 10 years (Mozaffarian et al., 2015, O'Donnell et al., 2010). Finally, increasing levels of physical activity and healthier diet are also associated with reduced risk of stroke as these can reduce occurrence of other traditional risk factors such as hypertension, diabetes mellitus and obesity.

1.1.4.3 Thrombolysis

Recombinant tissue plasminogen activator (rt-PA or Alteplase) is the only currently licenced pharmacological intervention for the treatment of acute ischaemic stroke. rt-PA works by lysing blood clots (more specifically by converting plasminogen to plasmin, which promotes the breakdown of fibrin), resulting in reperfusion of the previously ischaemic area.

The first clinical trial to test rt-PA was the Tissue Plasminogen Activator for Acute Ischemic Stroke (National Institute of Neurological Disorders and Stroke rt-PA Stroke Study Group, 1995). Patients were given rt-PA within 3 hours of stroke onset and patients receiving rt-PA were 30% more likely than controls to have no or minimal disability at 3 months. However, they were significantly more likely to have symptomatic intracerebral haemorrhage within 36 hours of stroke onset. This trial resulted in FDA approval for the use of Alteplase to treat ischaemic stroke. More recently, the subsequent European Cooperative Acute Stroke Study III (ECASS III) demonstrated safety and efficacy of Alteplase when used up to 4.5 hours following stroke (Hacke et al., 2008).

Given the small therapeutic time window in which rt-PA can be administered, only a small percentage of acute ischaemic stroke patients receive thrombolysis treatment, with statistics from the USA revealing that <10% of patients receive rt-PA (Adeoye et al., 2011, Menon et al., 2015, Saver et al., 2013). More recent statistics suggest that one in nine patients with acute stroke in the UK are treated with rt-PA (Intercollegiate Stroke Working Party, 2016). Therefore every effort should be made to improve 'door to treatment' times. Of those who do receive rt-PA within the appropriate time it has been estimated that only very few (~21%) recanalise acutely (Bhatia et al., 2010). Although successful recanalisation is one of the strongest predictors of good outcome (Bhatia et al., 2010) reducing the time in which the patient is treated post-stroke also improves outcome. Patients who are treated with thrombolytic agents within 60 minutes of stroke onset have reduced mortality and reduced incidence of intracranial haemorrhage as compared to patients who receive rt-PA after 60 minutes of stroke onset (Fonarow et al., 2011).

1.1.4.4 Clot Retrieval

Recently mechanical clot retrieval has been demonstrated to be successful in the treatment of ischaemic stroke patients. This involves the endovascular insertion of a clot retrieval device, attached to the end of a catheter. This is inserted to the site of occlusion and, following inflation of a balloon attached to the catheter, a wire net is extended to surround the clot and the catheter is subsequently removed, taking the clot with it.

Although it was previously thought that endovascular treatment (EVT) was not superior to intravenous thrombolysis (IVT), recently published multicentre clinical trials testing EVT against IVT have generated positive results (Berkhemer et al., 2015, Campbell et al., 2015, Goyal et al., 2015, Jovin et al., 2015, Saver et al., 2015). These trials show that early thrombectomy (vs. rt-PA alone) improves reperfusion, early neurological recovery and functional outcome. EVT therefore can result in good clinical outcome and has similar symptomatic haemorrhage and mortality to IVT. However as the clot must be relatively large and proximally situated within the cerebral circulation for successful thrombectomy, this may limit the patient cohort in which EVT may be used.

In the MR CLEAN trial 500 patients were recruited and of these 89% were given intravenous rt-PA (Berkhemer et al., 2015). Subsequent to IVT patients were randomised to either receive intra-arterial treatment (47% patients) or usual care alone (53% patients). Of those that received intra-arterial treatment, 82% of patients were treated using retrievable stents. Patients that received intra-arterial treatment had a 13.5% improvement in functional independence (assessed by modified Rankin score) versus control patients. Patients in this trial received intra-arterial treatment within 6 hours of stroke onset. It will be interesting to see whether future trials can extend the therapeutic time window further.

1.1.5 Pre-Clinical Models of Stroke

There are numerous *in vitro* and *in vivo* pre-clinical models of stroke. *In vitro* models typically use either primary or cultured cell lines (sometimes co-cultures) or brain slices which are subsequently subjected to oxygen glucose deprivation or high concentrations of excitotoxic agents. Novel therapeutic agents can therefore be tested in these systems, and their ability to limit cell death and other stroke pathophysiologies can be evaluated. *In vitro* models can be used effectively in proof of concept and mechanistic studies.

In vivo models typically involve the administration of focal ischaemic insults – the result of permanent or transient occlusions of cerebral blood flow that results in ischaemic stroke-like pathophysiology. Rodent models are most commonly used due to their low cost and reduced 'ethical cost'. Rodent neuroanatomy is well understood as are the molecular mechanisms of stroke pathophysiology. Furthermore, comorbid rodent models have been developed, enhancing the translatability of these models.

Both the advantages and disadvantages of pre-clinical models of ischaemic stroke have been reviewed thoroughly (Dirnagl et al., 2013, Macrae, 2011). Stroke models can predict or parallel a number of clinical phenotypes (Dirnagl et al., 2013). Important concepts common to both rodent models and clinical phenotype include the penumbra (Astrup et al., 1977), spreading ischaemic lesion as stroke pathophysiology progresses (Dreier, 2011), the effectiveness of thrombolysis (National Institute of Neurological Disorders and Stroke rt-PA Stroke

Study Group, 1995, Zivin et al., 1985), the increased risk of haemorrhage and BBB disruption following thrombolysis (Ehrenreich et al., 2009, Zechariah et al., 2010) and the ability of hypothermia to protect the brain (Hypothermia After Cardiac Arrest Study Group, 2002, Bernard et al., 2002, Rosomoff, 1957).

Despite the clinical relevance of pre-clinical models of stroke, very few treatments that show effectiveness in pre-clinical models of stroke are ultimately effective in patients (O'Collins et al., 2006). There has been a significant failure in the field to translate positive pre-clinical work into positive clinical trials. The numerous reasons for this include both the complexity of stroke and quality of pre-clinical research carried out (Dirnagl, 2016).

Stroke has an extremely complex pathophysiology, often under-estimated in pre-clinical models. There are also obvious and significant differences between species. However, many other problems or limitations of pre-clinical research could be limited or avoided with careful planning and robust study design. These problems include animal studies that are underpowered or where the effect size has been over-estimated. Furthermore, many stroke studies use stroke models that do not represent the heterogeneous, aged stroke patient population seen in the clinic. Homogenous animal populations used are usually young, predominantly male and healthy with low genetic variation. Often the timing of the therapy administered is not clinically relevant – there are a disproportionate number of studies showing efficacy with treatment delivery pre-ischaemic stroke. Off-target effects of therapeutic agents used are also rarely investigated or considered. Finally, due to negative publication bias, often only positive results are reported leading to unnecessary duplication and distortion of scientific understanding.

The STAIR and ARRIVE guidelines amongst others (Fisher et al., 2009, Kilkenny et al., 2010, Macleod et al., 2009, STAIR, 1999) provide excellent guidelines and a number of recommendations on how to improve the quality and reporting of pre-clinical stroke research and these should be rigorously adhered to, to encourage the translatability of pre-clinical research.

1.2 MicroRNAs

The central dogma of molecular biology (Crick, 1970, Crick, 1958) proposes that there is a "transfer of sequential information" from DNA to RNA to protein. It is now understood that genes within DNA are transcribed into molecules of messenger RNA (mRNA; transcripts) which are subsequently translated into amino acid chains, which can then fold into functional proteins.

At the completion of the Human Genome Project in 2001 (Lander et al., 2001) it was estimated that there were approximately 31,000 genes (less than had been previously hypothesised) and that only ~1.5% of the human genome consisted of protein coding sequence. Subsequently it has been demonstrated that approximately two thirds of genomic DNA is transcribed (Djebali et al., 2012), significantly more than the 1.5% that is translated into protein. Some of this 'non-coding' DNA is transcribed into functional non-coding RNA molecules that play a primarily regulatory role including, microRNAs (miRNA or miR), small nucleolar RNAs (snoRNA), small interfering RNAs (siRNA), long non-coding RNAs (lncRNA) as well as ribosomal RNAs (rRNA) and transfer RNAs (tRNA).

In 1993 a study was published (Lee et al., 1993) in which it was demonstrated that lin-4, a gene which partly controlled *Caenorhabditis elegans (C. elegans)* larval development, produced a pair of small RNAs (not proteins, as predicted), one of which was only 22 nucleotides in length, the first documented miRNA. The second small RNA was 61 nucleotides in length and was proposed to be a precursor of the first. These RNAs had antisense complementarity to multiple sites in the 3' UTR of the lin-14 gene and were subsequently shown to mediate translational repression of lin-14 (Lee et al., 1993, Wightman et al., 1993).

miRNAs are a class of small, single stranded regulatory RNAs, approximately 22 nucleotides in length, which post-transcriptionally regulate expression of target mRNAs. A single miRNA has the potential to regulate the expression of hundreds of different mRNAs and genes (Selbach et al., 2008). Furthermore, as over 60% of human protein-coding genes contain a minimum of 1 conserved miRNA-binding site it is hypothesised that the majority of protein-coding genes are regulated in some way by miRNAs (Friedman et al., 2009). While miRNA mediated regulation

is typically mild in nature, it can have significant biological effect when so many genes and proteins are implicated.

1.2.1 Biogenesis

miRNAs in humans are mostly encoded by introns of non-coding or coding transcripts although some miRNAs can be transcribed from exons. Occasionally multiple miRNA loci are located in close proximity (Lee et al., 2002), forming a miRNA cluster, from which miRNAs are usually co-transcribed. RNA polymerase II (RNA Pol II) transcribes miRNA (Cai et al., 2004, Lee et al., 2004) into primary miRNA (pri-miRNA) (see Figure 1.5 for a diagram of miRNA biogenesis).

Once transcribed the pri-miRNA is processed within the nucleus (Lee et al., 2002). A pri-miRNA can be over 1kb in length and is made up of a stem (33-35bp), a terminal loop and single stranded RNA segments on either side. Mature miRNA sequences are embedded within the stem-loop structure. The maturation process is initiated by the RNase III-type endonuclease Drosha within the nucleus which crops the stem-loop structure resulting in the release of a ~65 nucleotide long hairpin-shaped RNA, called pre-miRNA (Lee et al., 2003). Cleavage is mediated by Drosha in association with an essential cofactor DiGeorge syndrome chromosomal region 8 (DGCR8) – together they form a microprocessor (Denli et al., 2004, Gregory et al., 2004, Landthaler et al., 2004). The pri-miRNA is typically cleaved in such a way that there is an overhang of nucleotides created, important for export of the miRNA from the nucleus.

Following cleavage by Drosha, the pre-miRNA is exported into the cytoplasm. For nuclear export to occur the pre-miRNA forms a transport complex with exportin 5 (EXP5) and RAN·GTP, the GTP-binding nuclear protein (Bohnsack et al., 2004, Lund et al., 2004, Yi et al., 2003). As the pre-miRNA translocates through the nuclear pore complex, GTP is hydrolysed causing the transport complex to disassociate and the pre-miRNA is released into the cytoplasm.

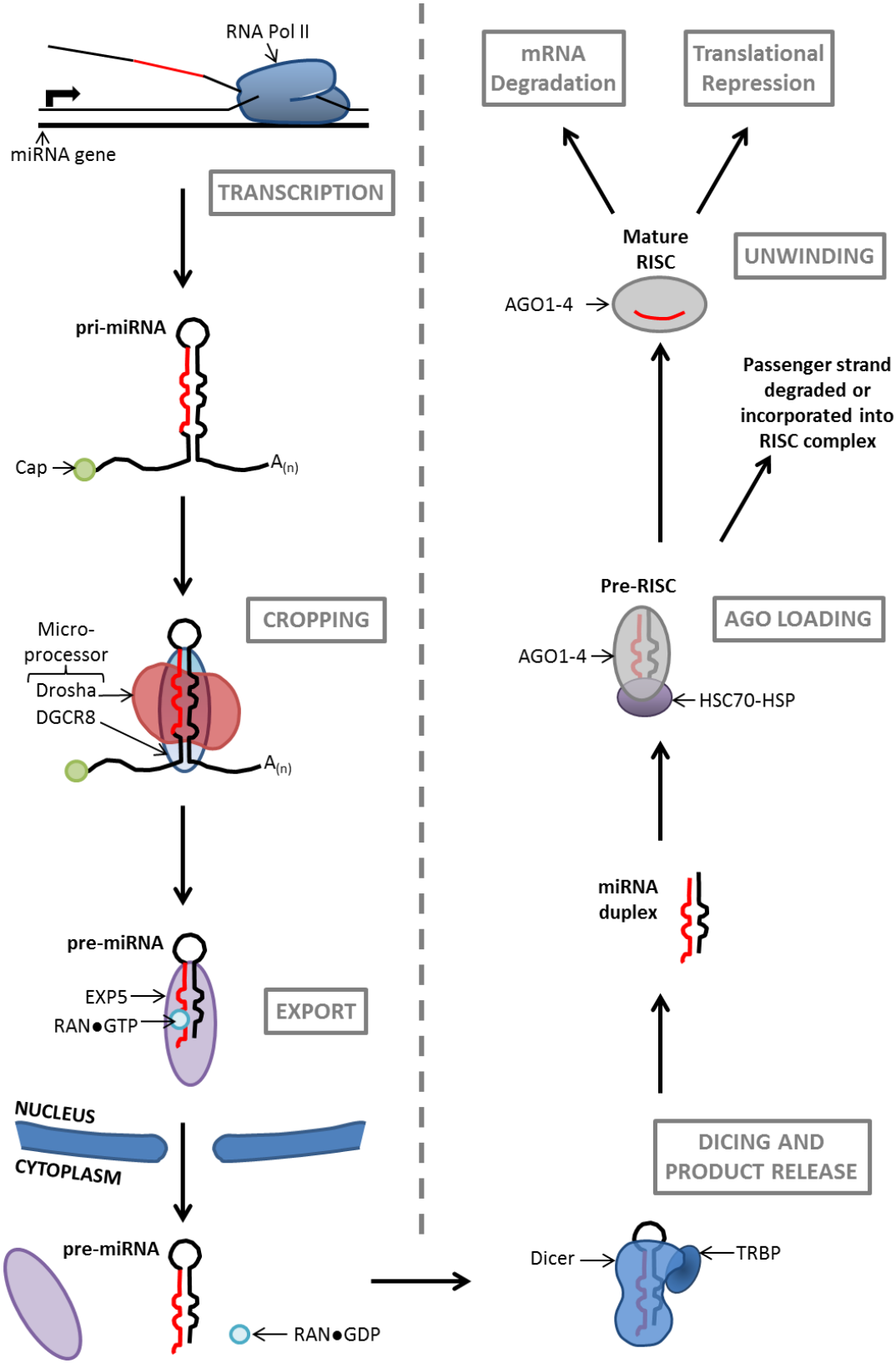

Figure 1.5 – miRNA Biogenesis
miRNAs are initially transcribed in the nucleus, forming pri-miRNAs which are subsequently cropped by a microprocessor comprised of Drosha and DCGR8 to form pre-miRNAs. Pre-miRNAs are exported from the nucleus to the cytoplasm by EXP5 where they are subsequently processed by Dicer in association with TRBP to form a double-stranded miRNA duplex. A single stand of the miRNA duplex is incorporated into the mature RISC, which then acts to inhibit mRNA expression, either by targeting the mRNA for degradation of by inhibiting its translation. The passenger strand is usually degraded. This figure was inspired by figures found in (Ha and Kim, 2014).

The terminal loop of the pre-miRNA is subsequently cleaved by Dicer, resulting in the production of dsRNA: a mature miRNA and a passenger strand. Dicer is a RNase III-type endonuclease with a catalytic centre and two RNA cleavage sites (Zhang et al., 2004) which preferentially binds to pre-miRNA with a 2 nucleotide 3' overhang (Zhang et al., 2004). The product of Dicer cleavage is an imperfect double-stranded duplex approximately 22 nucleotides in length which is subsequently loaded onto an AGO protein, forming a pre-RNA-induced silencing complex (pre-RISC) (Hammond et al., 2000, Hammond et al., 2001, Mourelatos et al., 2002, Tabara et al., 1999). In humans, all four argonaute proteins (AGO1-4) are capable of loading miRNA duplexes and there does not appear to be any miRNA sorting mechanism in place as all four proteins are associated with a wide range of miRNAs (Azuma-Mukai et al., 2008, Dueck et al., 2012, Liu et al., 2004b, Meister et al., 2004, Su et al., 2009). Loading of miRNA duplexes is an ATP-dependent process mediated by a heat shock cognate 70 (HSC70)/heat shock protein 90 (HSP90) chaperone complex.

Once the miRNA-miRNA* duplex has been loaded onto the AGO protein, the pre-RISC removes the passenger strand (miRNA*) and generates a mature RISC. While it has been shown that AGO2 has the ability to slice the passenger strand from the guide strand under certain conditions (Diederichs and Haber, 2007, Matranga et al., 2005) the majority of miRNA duplexes are unwound in an ATP-independent mechanism (Kawamata et al., 2009, Kawamata and Tomari, 2010, Yoda et al., 2010). Original models of miRNA biogenesis suggested that the passenger strand was targeted for degradation (Khvorova et al., 2003) but more recently published studies have demonstrated functional roles for miRNA* strands (e.g. (Shan et al., 2013, Yang et al., 2013)).

While the majority of miRNAs are generated by the canonical pathway, as described in detail in this section, 1% of miRNAs (Ha and Kim, 2014) follow a biogenesis pathway that can be independent of both Drosha and/or Dicer. One example of a miRNA produced in this way is miR-451 – it is not processed by Dicer but instead is loaded directly onto AGO2 and is subsequently cleaved (Cheloufi et al., 2010, Cifuentes et al., 2010, Yang et al., 2010). This produces a 30 nucleotide intermediate which is then further processed to produce the mature miR-451. Non-canonical biogenesis pathways are still poorly understood.

1.2.2 miRNA Function

1.2.2.1 Target Recognition

miRNAs recognise their target mRNAs by Watson-Crick base pairing. The mature miRNA within the RISC complex acts as a guide to argonaute, directing it to specific target mRNAs. miRNAs can recognise partially complementary binding sites which are often within the 3' untranslated region (3'UTR) of the target gene (Lee et al., 1993, Wightman et al., 1993). Nucleotides 2-7 at the 5' end of a miRNA are called the seed sequence and base pairing between the seed sequence and the mRNA is the most important factor in determining whether or not a target will be recognised and whether gene silencing will occur (Lewis et al., 2003). Occasionally, when base pairing at the seed sequence is weak (i.e. mismatch at some nucleotides) miRNA-mRNA interaction may also be mediated by base pairing at the 3'end of the miRNA (Bartel, 2009).

1.2.2.2 Translational Repression

Translation is a complex process that mediates the conversion of mRNA to protein (Jackson et al., 2010) and it is believed that miRNAs can interfere with various stages of this process. Investigations into the mechanism of miRNA-mediated gene silencing in *C. elegans* suggested that lin-4 miRNA was able to repress translation of lin-14 and lin-28 mRNA without significant effect on mRNA abundance (Olsen and Ambros, 1999, Seggerson et al., 2002). It was hypothesised that repression occurred post-translation initiation, and that the mature RISC complex caused early ribosomal dissociation from the mRNA during the elongation stage of translation (Nottrott et al., 2006, Petersen et al., 2006). However, conflicting studies suggest that translational repression occurs at the translation initiation stage, concluding that miRNAs can inhibit cap-dependent translation initiation (Humphreys et al., 2005, Pillai et al., 2005). However, a large *in vitro* ribosomal profiling study suggests that while translational repression plays a role in gene silencing it is not the primary method of gene silencing (Guo et al., 2010).

1.2.2.3 mRNA Degradation and Destabilisation

An alternative method of miRNA mediated gene silencing is that of miRNA directed cleavage of target mRNAs (Llave et al., 2002, Yekta et al., 2004). It is hypothesised that perfect base pairing between miRNAs and their target sequences on mRNAs results in endonucleolytic cleavage by Argonaute and rapid mRNA degradation. Large-scale transcriptome studies demonstrate that increasing miRNA abundance is correlated with decreasing target mRNA abundance and so indirectly support this hypothesis (Baek et al., 2008, Guo et al., 2010, Hendrickson et al., 2009, Selbach et al., 2008). However, as the majority of mRNA targets are only partially complementary to the miRNA, mRNA destabilisation appears to be the primary mechanism of mRNA degradation. This is primarily mediated by glycine-tryptophan repeat-containing (GW182) proteins which interact with the mature RISC to recruit deadenylation factors which in turn promote mRNA degradation in the 3'-5' direction (Behm-Ansmant et al., 2006, Giraldez et al., 2006, Wu et al., 2006). mRNAs are decapped at the 5' termini of the mRNA by decapping enzyme 2 (DCP2) promoting degradation in the 5'-3' direction and are subsequently degraded by cytoplasmic exonucleases (Rehwinkel et al., 2005). mRNA degradation and destabilisation by miRNAs is a major method of gene repression and probably accounts for >75% of miRNA mediated gene silencing (Baek et al., 2008, Guo et al., 2010, Hendrickson et al., 2009, Selbach et al., 2008).

1.2.3 miRNA Profiling in Stroke Patients

Circulating miRNA expression is dysregulated in patients with ischaemic stroke. A number of studies have used a non-targeted approach to profile miRNA expression in human ischaemic stroke patients. Using microarray analysis with subsequent validation of select miRNAs by quantitative real-time PCR (qRT-PCR), they have shown that the miRNAome is significantly altered post ischaemic stroke (Table 1.2). Other studies have taken a more targeted approach and only looked at expression of specific miRNAs that are associated with stroke or risk factors associated with ischaemic stroke (Table 1.3).

Initial studies profiled miRNA expression in whole blood samples collected from young stroke patients (age 18-49) within 2-24 months post-stroke (Tan et al.,

2013, Tan et al., 2009). While group sizes were small, they importantly were able to demonstrate miRNA dysregulation by microarray, even at lengthy time points post-stroke. While 138 dysregulated miRNAs detected by microarray were up-regulated only 19 were down-regulated (Tan et al., 2009). Furthermore, validation of results for six miRNAs by qRT-PCR demonstrated expression was changed in the same direction but to a greater extent than detected by microarray (Tan et al., 2009), highlighting the usefulness of microarray technology at detecting and predicting dysregulated miRNA expression. Subsequent studies have profiled miRNA expression in ischaemic stroke patients at sub-acute and acute time points and have shown that miRNA expression is dysregulated (both increased and decreased) at much earlier time points (e.g. within 3 hours) following ischaemic stroke onset (Wang et al., 2014b).

Interestingly, some of the dysregulated miRNAs detected by microarray were validated in multiple studies. One example is that of miR-106-5p which was up-regulated in plasma and serum samples collected acutely from ischaemic stroke patients (Li et al., 2015a, Wang et al., 2014b). A targeted study (Kim et al., 2015) comparing expression of miRNAs between ischaemic stroke patients and vascular risk factor control patients (in plasma within 7 days of stroke onset) also detected up-regulated miR-106a expression.

miR-126 expression was decreased in whole blood samples at acute, sub-acute and long-term time points following ischaemic stroke (vs. healthy controls) (Sepramaniam et al., 2014, Tan et al., 2009). These results were subsequently corroborated when miR-126 was shown to be down-regulated from 24h post-stroke onset until 24 weeks post-stroke in all stroke subtypes (vs. healthy controls) (Long et al., 2013). However, when patients with vascular risk factors were used as controls (Kim et al., 2015) miR-126 was shown to be unchanged in plasma samples collected within 7 days of symptom onset which may suggest that down-regulated miR-126 expression is primarily a result of chronic vascular disease rather than acute ischaemic stroke.

Table 1.2 – miRNA Profiling Studies in Ischaemic Stroke Patients
Summary of published studies that use microarray technology to profile circulating miRNA expression in human ischaemic stroke patients. Studies are listed chronologically. The final column shows the number of miRNAs validated (by qRT-PCR) to be up- or down-regulated; miRNAs with unchanged miRNA expression are not included. Abbreviations include: cardioembolic stroke patients (CE); ischaemic stroke patients (IS); intracerebral haemorrhage stroke patients (ICH); large artery stroke patients (LA); small vessel disease stroke patients (SVD); unclassified stroke patients (U).

Reference	Tissue Sample	Stroke Patients	Control Patients	Number of qRT-PCR Validated miRNAs
(Tan et al., 2009) *PloS One*	Whole blood samples from patients 6-18 months post-stroke	IS, **n=19**. LA, n=8; CE, n=5; SVD, n=3; U, n=3. Age 18-49 Array: pooled samples of different stroke subtypes and mRS scores	Healthy, **n=5**	5 miRNAs ↑ 1 miRNA ↓
(Guo et al., 2013) *Stroke*	Plasma samples from patients 1-14 days after symptom onset	Array: IS, **n=16**; ICH, n=15	Array: healthy, **n=8**	Not Attempted (for IS patients)
(Tan et al., 2013) *Int J Mol Sci*	Whole blood samples from patients 2-24 months post-stroke	IS, **n= 8**. Age 18-49	Healthy, **n=4**	Not Attempted
(Jickling et al., 2014) *PloS One*	Whole blood samples from patients within 72h of stroke onset	IS, **n=24.** LA=8, CE=8, SVD=8	Vascular risk factor patients, **n=24**	2 miRNAs ↑ 6 miRNAs ↓
(Sepramaniam et al., 2014) *Int J Mol Sci*	Whole blood samples collected within 24h, 48h and 7 days of stroke onset	IS, **n=169** Array, n=68 (pooled & individual) Validation, n=101	Healthy, **n=24.** Metabolic risk factor patients, **n=94/98**	5 miRNAs ↑ 5 miRNAs ↓
(Sørensen et al., 2014) *Transl Stroke Res*	Plasma and CSF samples collected 3 days post-stroke	IS, **n=10.** LA=3, CE=3, SVD=1, U=3	Other Neurological Disease, **n=10**	Not Attempted
(Wang et al., 2014b) *J Stroke Cerebrovasc Dis*	Plasma samples collected 0-24 hours post-stroke	IS, **n=136.** LA=60, CE=23, SVD=51, U=2 Of these: MRI(+)=76, MRI(-)=60	Healthy, **n=116**	2 miRNAs ↑ 2 miRNAs ↓
(Li et al., 2015a) *Cell Mol Neurobiol*	Serum samples collected within 24 hours of stroke onset	IS, **n=117** Array: n=4 (4 x pooled from 10) Validation: n=24 and n=53	Healthy, **n=82** Array: n=1 (pooled from 10) Validation: n=22 and n=50	3 miRNAs ↑ 1 miRNAs ↓
(Zhang et al., 2016b) *J Affect Disord*	Plasma samples collected on day of admission	Array: IS, **n=3** Validation: IS, **n=20**	Array: IS with post-stroke depression, **n=3** Validation: **n=20**	2 miRNAs ↑ 1 miRNA ↓

Table 1.3 – Targeted miRNA Profiling Studies in Ischaemic Stroke Patients
Summary of published studies that have used a targeted approach – profiling expression of selected miRNAs by qRT-PCR in human ischaemic stroke patients. Studies have been listed chronologically. Abbreviations include: cardioembolic stroke patients (CE); internal carotid artery (ICA); ischaemic stroke patients (IS); intracerebral haemorrhage stroke patients (ICH); large artery stroke patients (LA); small vessel disease stroke patients (SVD); unclassified stroke patients (U).

Reference	miRNAs	Tissue Sample	Stroke Patients	Control Patients
(Cipollone et al., 2011) *Stroke*	miRNAs -100, -127, -145, -133a, -133b (among others)	Atherosclerotic plaques from carotid endarterectomy patients with extracranial high-grade (>70%) ICA stenosis	IS, **n=22** (Patients with extracranial high grade ICA stenosis and recent atherothrombotic stroke)	Patients with extracranial high grade ICA stenosis but no stroke, **n=31**
(Zeng et al., 2011) *Front Biosci (Elite Ed)*	miRNA-210	Blood samples collected at < 3 days, 7 days and 14 days post IS	IS, **n=112**. <3 days: LA (n=22), CE (n=2), SVD (n=31). 7 days: LA (n=13), CE (n=2), SVD (n=16). 14 days: LA (n=15), CE (n=2), SVD (n=9)	Healthy, **n=60**
(Gan et al., 2012) *Genet Mol Res*	miRNA-145	Whole blood samples - no information on when sample collected	IS, **n=32.** No information on stroke subtype	Healthy, **n=14**
(Tsai et al., 2012) *J Vasc Res*	miRNAs -21, -221, -145	Serum samples collected within 7 days post-stroke	IS, **n=167**	Healthy, **n=157**. Atherosclerosis, n=66.
(Zeng et al., 2012) *Eur Neurol*	miRNA-210	Plasma samples collected within 72 hours post-stroke	IS, **n=105.** No information on stroke subtype. Good outcome, mRS≤2, n=40. Poor outcome, mRS>2, n=65.	No control subjects in this study
(Long et al., 2013) *BMC Neurol*	miRNAs -30a, -126, -let-7b	Plasma samples collected at 24h (n=38), 1 week (n=42), 4 weeks (n=40), 24 weeks (n=38), 48 weeks (n=39). Different patients at each time point	IS, **n=197.** LA (n=51), SVD (n=48), CE (n=50), U(n=48)	Age matched controls with vascular risk, **n=50** Not significantly different from IS group for characteristics recorded
(Duan et al., 2014) *J Diabetes Complications*	miRNAs -223, -146a, -495, -107	Plasma samples - no information on when sample collected	IS, **n=7.** All are LA.	Healthy, **n=8**. Diabetes mellitus, n=7. Diabetes mellitus and ischaemic stroke, n=6.

Reference	miRNAs	Tissue Sample	Stroke Patients	Control Patients
(Leung et al., 2014) *Clin Chim Acta*	miRNAs -124-3p, -16	Plasma samples collected within 24h symptom onset	Stroke, n=93. IS, **n=73** – LA (n=7), CE (n=19), SVD (n=28), U (n=20). ICH, n=19.	Healthy, **n=23.** Age and sex matched.
(Liao et al., 2014) *J Am Coll Cardiol*	miRNA-let-7g	Serum samples collected - no information on when blood samples taken	Lacunar infarction, **n=60**	No control subjects in this study
(Yang et al., 2014) *Clin Sci*	miRNA-107	Plasma samples collected within 24 hours of hospital admission	IS, **n=110.** TACI=35, PACI=31, LACI=23, POCI=21	Healthy, **n=55**
(Zhou and Zhang, 2014) *Mol Med Rep*	miRNAs – 21, -24	Plasma samples collected within 24 hours of hospital admission	Acute cerebral infarction, **n=68**	Healthy, **n=21**
(Wang et al., 2014c) *BMC Neurol*	miRNA-223	Leucocyte (from plasma) samples collected within 72 hours of onset of stroke symptoms	IS, **n=79**. LA (n=37), CE (n=5), SVD (n=9), U (n=28)	Healthy, **n=72**
(Jia et al., 2015) *Cell Biochem Funct*	miRNAs -21, -23a, -29b, -124, -145, -210, -221, -223, -483-5p	Serum samples collected within 24 hours, 7 days, 1 month, 6 months and 2 years from stroke-onset	Pilot: IS, **n=30** Validation: IS at 24 hours **n=146**, other time points, **n=49**	Pilot: Healthy, **n=30** Validation: Healthy, **n=96**
(Kim et al., 2015) *Transl Stroke Res*	miRNAs -17, -21, -106a, -126, -200b	Plasma samples collected within 7 days of symptom onset	IS, **n=83.** LA (n=35), CE (n=31), SVD (n=17)	Vascular risk factors and other neurological problems, **n=37**
(Liu et al., 2015c) *J Clin Neurosci*	miRNAs -124, -9, -219	Serum samples collected within 24 hours (all patients) and within 48 hours (n=8)	IS, **n=31.** No information on stroke subtype	Healthy, **n=11**
(Peng et al., 2015) *Transl Stroke Res*	miRNAs – let-7e, -338	Serum and CSF samples collected acutely (d1-d7), subacutely (d8-d14) and during recovery (>d15)	IS. Serum: acute (n=72), subacute (n=68), recovery (n=63). CSF: acute (n=11), subacute (n=9), recovery (n=8)	Healthy. Serum : **n=51,** CSF: **n=12**
(Huang et al., 2016) *Neurosci Lett*	miRNA -132	Serum samples collected within 3 days of hospitalisation but patients may have had stroke up to 1 year previous	IS with cognitive impairment, **n=39** IS with cognitive normality, **n=37**	Healthy, **n=38**

A further example is that of miR-145 which was shown to be sequentially increased in whole blood samples of ischaemic stroke patients (vs. healthy control patients) from 24 hours post-stroke until 6 months post-stroke (Sepramaniam et al., 2014). Up-regulated miR-145 expression was also detected in whole blood and serum samples of ischaemic stroke patients (vs. healthy controls) (Gan et al., 2012, Jia et al., 2015) but subsequently decreased in expression over time (Jia et al., 2015). Interestingly, increased miR-145 expression was also detected in the atherosclerotic plaques of patients with internal carotid artery (ICA) stenosis and recent stroke as compared to patients with ICA stenosis but no stroke (Cipollone et al., 2011). Conversely, in a conflicting study miR-145 was undetectable in a large number of ischaemic stroke patients and its expression unchanged in the remaining patients in comparison to healthy control patients (Tsai et al., 2012).

It is difficult to compare results from these studies as their methodologies vary in many different ways. Of the miRNA profiling studies listed in Table 1.2, whole blood, plasma and serum samples were all collected from ischaemic stroke patients at acute, sub-acute and long-term time points post-stroke onset. In some studies patient samples collected at different time points are grouped together to make one group of ischaemic stroke patients (e.g. (Sepramaniam et al., 2014)). Population sample sizes differ hugely, with the smallest studies looking at expression in only 4 patients per group and the largest validating changes in over 100 ischaemic stroke patients. Furthermore the majority of studies compared miRNA expression of ischaemic stroke patients to that of healthy control patients. Therefore, while miRNAs are shown to be dysregulated in these studies they may represent changes as a result of hypertension and vascular disease (risk factors for stroke) rather than the ischaemic insult itself.

Increased infarct size and resulting neurological deficit is associated with both increased and decreased expression of various miRNAs, reflecting the diverse nature of miRNAs, their targets and the role they play in ischaemic stroke. Increased expression of miRs-145, -124-3p and -16 has been associated with increased infarct size and more severe stroke (National Institute of Health Stroke Scale (NIHSS) >5) (Jia et al., 2015, Leung et al., 2014). However decreased expression of other miRNAs such as miR-124, -9, -21, -24 and -223 was also associated with increased infarct volume and NIHSS score (Liu et al., 2015c,

Wang et al., 2014c, Zhou and Zhang, 2014). Conversely, the expression of several miRNAs (let-72, miRs-338 and -219) did not correlate with NIHSS score or infarct volume (Liu et al., 2015c, Peng et al., 2015). However, several of the results quoted here are from studies which have not stated on which day the NIHSS score or infarct volume was measured (Leung et al., 2014, Wang et al., 2014c, Zhou and Zhang, 2014) and another study measured the NIHSS score on the same day as blood samples were taken – between 1 and 7 days post stroke onset meaning a very diverse range of patients (n=72) will be included, perhaps why this study didn't observe any correlations between miRNA expression and NIHSS score, highlighting the importance of careful selection of patient population groups (Peng et al., 2015).

Many of the studies discussed here have used bioinformatics to predict targets and pathways that dysregulated miRNAs may regulate. However, as these targets are generally predictions and not validated in human patients, they have not been discussed here.

A final point to notice is that many of the changes in circulating miRNA expression observed in human patients following ischaemic stroke are very modest. Several studies have also only looked at the expression of a very small number of miRNAs. Future studies should profile global miRNA expression in large, well-controlled, homogeneous patient populations to demonstrate whether multiple miRNAs are dysregulated simultaneously and which are truly dysregulated as a direct result of ischaemic stroke. Furthermore, without comprehensive mechanistic studies to investigate the function of these miRNAs it is difficult to understand whether dysregulated miRNA expression is a cause or result of ischaemic stroke pathophysiology.

1.2.4 miRNAs as Biomarkers

While the need for a biomarker to diagnose ischaemic stroke seems obsolete in Western countries, many papers cite the expense and unavailability of MRI scanning in less economically developed countries. Very little research into circulating biomarkers (other than miRs) to improve diagnosis of stroke has been performed, with most studies focussing on biomarkers that indicate increased risk of stroke (e.g. (Shoamanesh et al., 2016)), or neuroinflammatory markers

that might give indication of stroke prognosis (reviewed (Simats et al., 2016)). For a biomarker to be useful it should aid clinical decision making (e.g. whether or not to give a specific treatment). As acute treatment for stroke with reperfusion therapies is dependent on differentiating ischaemic stroke from haemorrhagic stroke and other stroke mimic conditions, treatment can be delayed due to limited access to imaging technology. Therefore "early screening to allow rapid ischemic stroke identification would speed stroke patient management and treatment" (Simats et al., 2016). As any biomarker panel would need to be extremely accurate (due to severe complications that could be a result of incorrect treatment based on inaccurate diagnosis) it seems unlikely that such a biomarker will be discovered before advances in imaging technology and better management of acute ischaemic stroke within the hospital make the need for it obsolete. Other research groups have attempted to identify biomarkers that could be used to predict stroke outcome and response to treatment, which might inform decisions about patient management. Non-modifiable factors (e.g. age and initial stroke severity) are the primary predictors of patient outcome but may have increased predictive power when combined with inflammatory biomarkers such as CRP, IL-6, TNF-α, ICAM-1 and MMP-13 (Rosell et al., 2005, Sotgiu et al., 2006, Whiteley et al., 2009).

Several studies have investigated the possibility of using miRNA expression as a biomarker for either diagnosis or prognosis in ischaemic stroke patients. Receiver operator characteristic (ROC) analysis has been used to estimate the sensitivity and specificity of certain miRNAs at distinguishing between ischaemic stroke and control patient populations. The area under a ROC curve (AUC) is an indication of how sensitive and specific a particular miRNA is: a score of 1 represents 100% specificity and 100% sensitivity. A number of studies have tested the ability of single miRNAs to distinguish between ischaemic stroke patients and non-stroke control patients. Circulating miRNAs that can distinguish between stroke and healthy control patients include miR-24 (<24 hours post-stroke, AUC 0.76) (Liu et al., 2015c) and let-7e (<7 days post-stroke, AUC 0.86) (Peng et al., 2015). 6 miRNAs detected within 7 days of stroke had high sensitivity and specificity for diagnosing between ischaemic stroke and healthy controls: miRNAs -125-2* (AUC 0.95), -27a* (AUC 0.89), -422a (AUC 0.92), -488 (AUC 0.87), -627 (AUC 0.84), and -920 (AUC 0.81) (Sepramaniam et al., 2014). However,

when these results were validated in a larger patient population the majority of AUC values decreased (Sepramaniam et al., 2014). The ability of these miRNAs to distinguish between healthy controls and patients with vascular risk but no stroke was relatively low (AUC of 0.30 to 0.67) (Sepramaniam et al., 2014). The authors conclude that changes in miRNA expression observed were therefore directly as a result of ischaemic stroke rather than other risk factors for stroke. A further study has demonstrated that circulating miRNAs (<24 hours post-stroke onset) can better distinguish between healthy controls and patients with a larger stroke than those with a smaller stroke, as detected by MRI (Wang et al., 2014b). These miRNAs included miR-4306 (AUC 0.88 vs AUC 0.95), miR-320e (AUC 0.95 vs AUC 0.98), miR-320d (AUC 0.98 vs AUC 0.99) and miR-106b-5p (AUC 0.99 vs AUC 0.96) (Wang et al., 2014b).

Alternative investigations have used a 'cocktail' of miRNAs and other markers to diagnose between ischaemic stroke patients and younger, healthy controls. For example, the serum expression of c-reactive protein (CRP) and miR-145, within 24 hours of stroke onset, gave high sensitivity and specificity (AUC 0.90) (Jia et al., 2015). Another study found that serum expression of miR-21 and miR-221 (within 7 days of stroke) in combination with traditional risk factors had the greatest ability to distinguish between ischaemic patients and healthy controls (AUC 0.93) (Tsai et al., 2012). These results highlight the need for further studies to investigate the sensitivity and specificity of biomarker panels consisting of multiple miRNAs.

Two studies have investigated the biomarker potential of miRNAs and used age matched control patients with vascular risk. Plasma samples were collected at 4 different time points and the ability of 3 miRNAs to differentiate between ischaemic stroke patients and controls was calculated (Long et al., 2013). miR-30a, miR-126 and let-7b were all increased in expression in ischaemic stroke patients and at 24 hours post stroke were able to distinguish between patient populations with AUC values of 0.91, 0.92 and 0.93 respectively (Long et al., 2013). The same miRNAs could be used to distinguish between patient populations in samples collected at 24 weeks post-stroke, showing that the time of sample collection did not significantly affect the ability of these miRNAs to differentiate between populations. Increased miR-17 expression has also been

associated with ischaemic stroke patients (AUC 0.64) in comparison to vascular risk factor control patients (Kim et al., 2015).

Unfortunately, very few studies have investigated the possibility of using miRNAs as biomarkers for prognosis following stroke. miR-210 expression has been profiled in patients with both good (mRS<2) and poor (mRS>2) functional outcome, as assessed at 3 months post-stroke. Its expression in blood samples collected up to 14 days following ischaemic stroke could partly distinguish between patients with good and poor functional outcomes (AUC 0.64) (Zeng et al., 2011). This study included samples collected at a variety of time points (< 72 hours, 7 days and 14 days post-stroke) and it is not clear which samples they used in their analysis (Zeng et al., 2011). A follow up study demonstrated that plasma levels of miR-210, in samples collected within 72 hours of stroke onset, could partially distinguish between patients with good and poor functional outcome (AUC 0.67). However, when a cocktail of biomarkers was used: expression of miR-210, pro-inflammatory cytokine IL-6 and fibrin degradation products (FDP) the sensitivity and specificity increased (AUC 0.80). This biomarker cocktail was subsequently shown to be more sensitive but less specific than NIHSS scores as a predictor of outcome (AUC 0.97) (Zeng et al., 2012).

Dysregulated miRNA expression has also been associated with stroke recurrence, post-stroke cognitive impairment and depression. Higher levels of miR-17 and miR-106a in plasma samples collected within 7 days of stroke onset are associated with recurrent stroke during a 24 month follow up period. Furthermore, increased miR-17 expression was associated with shorter event-free survival (Kim et al., 2015). Increased expression of miR-132 in serum samples collected from patients with historic stroke (<1 year) within 3 days of hospitalisation has been negatively correlated with Montreal Cognitive Assessment scores, a measure of cognitive impairment (AUC 0.96, vs. patients with no impairment) (Huang et al., 2016). Furthermore, increased plasma miR-92a-3p, and decreased miR-133a and miR-187-5p expression in samples collected on the day of hospital admission for ischaemic stroke are associated with post-stroke depression as measured by the Hamilton Depression-17 scale at 2 weeks post-stroke (Zhang et al., 2016b). These results highlight the need for future studies to investigate the prognostic power of miRNAs. If early miRNA expression

could predict how well a patient might do functionally, physiotherapy and treatment could be directed accordingly, perhaps leading to improved outcome.

A failure of all of the studies mentioned in this section is that no studies look at biomarker potential of miRNAs in relation to stroke subtype. When conventional imaging techniques fail to obtain clear images it can be difficult for clinicians to make diagnosis of stroke subtype in ischaemic stroke patients and so direct their treatment accordingly – it would therefore be beneficial to the field if all published studies listed the stroke subtype of their patients and whether separation of patients according to subtype had a beneficial or detrimental effect on the sensitivity and specificity of miRNAs to assess diagnosis and prognosis in ischaemic stroke patients.

1.2.5 Modulation of miRNAs

1.2.5.1 Increasing miRNA Expression

To increase miRNA expression synthetic miRNA duplexes (often called miRNA mimics) can be used – ideally, these will be taken up by RISC complexes and processed resulting in mRNA degradation or translational repression. The duplex contains a guide strand (a duplicate of the miRNA of interest) and a passenger strand. While the guide strand may be modified to prevent exonuclease degradation (Chiu and Rana, 2003), many modifications can interfere with RISC recognition of the miRNA. Typically it is the passenger strand that is chemically modified (e.g. by linking to a cholesterol molecule) to improve cellular uptake, promote the stability of the miRNA or to prevent loading into a RISC (reviewed (van Rooij and Kauppinen, 2014)). Furthermore, the passenger strand may be modified to contain nucleotide mismatches to stop it from acting as an anti-miR. Some modifications may inhibit degradation of the passenger strand and these are typically avoided.

Lenti-, adeno- and adeno-associated viral vectors can transfect most cell types and can all be used to increase miRNA expression. As miRNAs are susceptible to degradation by RNases they have a relatively short half-life. Viral vectors are therefore an attractive mechanism of miRNA modulation as their transduction efficiency is relatively high, and transgene expression can be sustained. Vectors

can be designed to express single miRNA mimics from RNA polymerase II promoters. More cleverly still, expression of a miRNA polycistron can mediate increased expression of multiple miRNAs from a single RNA polymerase II transcript. Clinical virus mediated delivery of miRNAs has been hampered by safety issues including immunogenicity. Virus mediated miRNA modulation has been reviewed by Liu and Berkhout and will not be further discussed here (Liu and Berkhout, 2011).

1.2.5.2 Inhibiting miRNA Expression

Inhibition of miRNA function is typically mediated, experimentally, by antisense oligonucleotides (anti-miRs). They too are usually chemically modified to increase their stability and binding affinity. An example of a typical modification includes phosphorothioate (PS) backbone linkage substitutions in the place phosphodiester (PO) linkages to improve nuclease resistance (Lennox and Behlke, 2010). These modifications reduce their glomerular filtration and therefore clearance by mediating enhanced binding to plasma proteins (Levin, 1999). Other sugar modifications include 2'-O-methyl, 2'-O-Methoxyethyl, 2'-fluoro at the 2' sugar group position and locked nucleic acid (LNA), which all act to increase the duplex melting temperature and to increase binding affinity and nuclease resistance (Lennox and Behlke, 2010, van Rooij and Kauppinen, 2014).

Initial studies using chemically modified anti-miRs used fully complementary oligonucleotides successfully (Krutzfeldt et al., 2005). Subsequently shorter LNA-modified anti-miRs have proved to be effective. These include anti-miRs fully complementary to only the first 16 nucleotides of the 5' end of a mature miRNA (Elmen et al., 2008) and LNA-modified anti-miRs complementary to only the 7-8 nucleotides of the seed sequence that are capable of inhibiting multiple miRNAs in one miRNA family that share a seed sequence (Obad et al., 2011).

miRNA sponges can also be used to inhibit multiple miRNAs from one family – the sponge mRNA contains multiple target sites that are complementary to miRNAs of interest and represses whole families of miRNAs via affinity to the seed sequence of the miRNA. Their function and use has been reviewed more fully by Ebert and Sharp (Ebert and Sharp, 2010).

1.2.5.3 Therapeutic Potential of miRNAs

Working with miRNAs is challenging as miRNA mimics and anti-miRs, even when delivered appropriately, need to avoid being degraded by serum endonucleases, detected by the immune system and cleared from the blood by the renal system. Furthermore, they must extravasate from the blood stream to reach their target tissue and miRNA mimics must also be loaded into RISC complexes to have functional effect.

Despite these caveats miRNAs remain attractive candidates for therapeutic modulation. Due to their small size and conserved sequence, miRNA mimics and anti-miRs are now readily available for most miRNAs and miRNA technology is continually being developed. Many pre-clinical studies, both in the setting of ischaemic stroke and a wider disease context, have demonstrated therapeutic effect following miRNA modulation. As one miRNA may target many hundreds of genes and as many of the genes targeted by one miRNA will often function in the same or related cellular processes or signalling cascades, even the modest modulation of a single miRNA has the potential to have a significant effect functionally – the result of accumulated modifications to multiple genes.

However, the addition of miRNA mimics to restore levels of down-regulated miRNAs may result in supra-physiological levels of miRNA, and similarly the addition of anti-miRs which are stable and potentially have very long-lasting effects may result in ablation of miRNA expression altogether (van Rooij and Kauppinen, 2014). Furthermore, given the potential of a miRNA to target many hundreds of genes, “off-target effects” are a significant possibility and make miRNAs less attractive targets for drug development by pharmaceutical companies. This is especially the case when miRNAs are delivered systemically, rather than directly to the tissue of interest, resulting in uptake by non-target tissues that may not even express the miRNA endogenously (van Rooij and Kauppinen, 2014). Therefore, targeted delivery to specific cells or tissues of interest should be considered. The use of targeted microvesicles (such as exosomes) to deliver miRNA may circumvent this problem (Johnsen et al., 2014). Furthermore as miRNA expression levels vary extensively between different cells, tissues and as a result of disease, defining appropriate levels of either up-

or down-regulation to ensure inhibition or stimulation of mRNA targets will be critical (van Rooij and Kauppinen, 2014).

Despite the challenges described here miRNA-34 in a liposome formulation is currently being tested in a Phase I, multicentre, clinical trial to investigate safety, pharmacokinetics and pharmacodynamics in patients with unresectable primary liver cancer (ID: NCT01829971 (Mirna Therapeutics, 2016)). Furthermore two compounds targeting miR-122 are being developed to treat hepatitis-C virus (HCV) infection. Miravirsen was the first miRNA-targeted drug to go to clinical trial and results from the phase II study were published in 2013 (Janssen et al., 2013) showing that treatment with Miravirsen resulted in long-lasting and dose-dependent antiviral activity, was well tolerated and had no toxic side effects or discontinuations as a result of adverse side effects. This study proves that modulation of miRNA activity is feasible therapeutically in human patients and is an inspiration for many studies seeking to provide therapeutic benefit via miRNA modulation.

1.2.6 miRNA Therapeutics for Stroke

miRNA profiling in ischaemic stroke patients has been described in section 1.2.3. Similar studies profiling miRNA expression in pre-clinical models of stroke will not be discussed here, but rather the therapeutic use of miRNAs in pre-clinical models of ischaemic stroke. Studies that have modulated miRNA expression in pre-clinical *in vivo* models of ischaemic stroke are summarised in Table 1.4.

Interestingly there are an equal number of studies demonstrating inhibition of miRNA expression is therapeutic for ischaemic stroke as there are those demonstrating the reverse. This highlights the diverse role of miRNAs post-stroke. Some are perhaps endogenous pro-survival miRNAs, repressing deleterious mRNAs - increasing expression of these miRNAs therefore increases therapeutic benefit. Others miRNAs may act to inhibit therapeutic mRNAs, and so inhibition results in de-repression of these mRNAs and therefore therapeutic effect. In either case it is evident that ischaemic stroke results in an extremely complex pathophysiology and the effects of modulating each miRNA need to be fully understood before any miRNA modulating agent could be used clinically.

In the studies listed in Table 1.4 there a number of differences between the animal and stroke models used. Of the 33 studies listed, only 2 use an animal model with co-morbidities relevant to stroke. Two studies modulate miRNA expression in spontaneously hypertensive rats (SHR) and of the remaining studies 32% modulate miRNA expression in healthy rat strains (primarily Sprague Dawley rats) and 56% in healthy mice strains (primarily C57BL/6J), with a further 2 studies using miRNA knock-out mouse models. While therapeutic benefit has been demonstrated in all of these studies, young and healthy animal models do not represent human stroke patients who are typically aged and present with a number of co-morbidities. Rigorous testing of miRNA modulation in appropriate pre-clinical models is needed to truly investigate therapeutic effect.

Furthermore, while over half of the studies used a clinically relevant model of ischaemic stroke involving ischaemia and reperfusion, i.e. transient middle cerebral artery occlusion (tMCAO), a number used permanent models of stroke, with no reperfusion. So while therapeutic benefit was observed further studies would need to test the effect of reperfusion on miRNA modulation. This is essential as the only two currently licensed treatments for ischaemic stroke are thrombolysis or thrombectomy, both of which are used to ensure reperfusion.

Table 1.4 - Therapeutic miRNA Modulation in Experimental Ischemic Stroke (*in vivo*)
A table summarising published studies that modulate miRNAs therapeutically in *in vivo* models of ischaemic stroke. Details of the miRNA modulated, animal and stroke model used, the delivery method and the time at which animals were sacrificed (post-stroke) are given. Unless otherwise stated all animals used were adult males. Abbreviations include: 4VO (4 vessel occlusion), BCCAO (bilateral common carotid artery occlusion), CCA (common carotid artery), eMCAO (embolic middle cerebral artery occlusion), H/I (hypoxia/ischaemia injury), MSC (mesenchymal stromal cell), pMCAO (permanent middle cerebral artery occlusion), SD (Sprague Dawley rat), SHR (spontaneously hypertensive rat), tMCAO (transient middle cerebral artery occlusion).

Reference	MiRNA Modulation	Animal Model	Stroke Model	Delivery Method	Animals Sacrificed (time post-stroke)
(Dharap et al., 2009) *JCBFM*	miR-145 ↓ beneficial	SHR (280-300g)	1h tMCAO	Anti-miR via osmotic mini-pump into lateral ventricle 2 days pre-tMCAO.	1 day
(Sepramaniam et al., 2010) JBC	miR-320a ↓ beneficial	SD rats	1h tMCAO	Mimics & anti-miR via ICV at reperfusion.	1 day
(Yin et al., 2010) *Neurobiol Dis*	miR-497 ↓ beneficial	C57/B6 mice	1h tMCAO	Anti-miR via ICV infusion to lateral ventricle started 2 days pre-tMCAO.	1 day
(Harraz et al., 2012) *PNAS*	miR-223 ↑ beneficial	C57BL/6 and miR-223$^{-/-}$ mice (8-12 weeks)	20min BCCAO	Adenoviral vector ↑ via stereotactic injection.	6 days
(Ouyang et al., 2012) *Neurobiol Dis*	miR-181 ↓ beneficial	C57/B6 mice (25-30g)	1h tMCAO	Plasmid (2 days pre-tMCAO) or anti-miR + DOTAP (1 day pre-tMCAO) via ICV stereotactic injection.	1 day
(Selvamani et al., 2012) *PLoS One*	let-7f ↓ beneficial	Adult female rats and age-matched males, no info on strain	eMCAO	Anti-miR via ICV injection at 4h post-MCAO.	5 days
(Deng et al., 2013) *Brain Res Bull*	miR-21 ↓ beneficial miR-224 ↓ no effect	SD rats (220-250g)	10min 4VO	Anti-miR via stereotactic injection to bilateral cerebral ventricles 24h pre-4VO.	6h, 12h and 1 day

Reference	MiRNA Modulation	Animal Model	Stroke Model	Delivery Method	Animals Sacrificed (time post-stroke)
(Doeppner et al., 2013) *Acta Neuropathol*	miR-124 ↑ beneficial	C57BL6/N mice (11-13 weeks)	45min tMCAO	Virus ↑ via stereotactic injection at 21 days pre-MCAO. No info on type of virus.	1, 2, 4, 28 and 56 days
(Khanna et al., 2013) *JCBFM*	miR-29b ↑ beneficial	C57BL6/N mice (8 weeks)	1.5h tMCAO	Lentivirus ↑ via stereotactic injection to cortex at 72h pre-tMCAO.	2 days
(Liu et al., 2013a) *Stroke*	miR-124 ↓ beneficial	C57 mice (21-23g)	pMCAO	Mimic or anti-miR + lipofectamine via ICV stereotactic injection post-tMCAO.	1 day
(Liu et al., 2013b) *JBC*	miR-17-92 cluster ↑ beneficial	C57BL/6 mice	pMCAO	Lentivirus ↑ cluster via stereotactic injection to SVZ region, 1 day pre-pMCAO.	7 days
(Moon et al., 2013) *JCBFM*	miR-181a ↓ beneficial	SD rats (280-320g)	Hypotension + 10 min CCA clamping	Anti-miR + DOTAP via stereotactic injection to hippocampus, 24 h before ischemia.	1, 3 and 7 days
(Pandi et al., 2013) *PLoS One*	miR-29c ↑ beneficial	SHR (280-300g)	1h tMCAO	Mimics via osmotic mini-pump to lateral ventricle. siRNA by stereotactic injection.	1 and 3 days
(Qiu et al., 2013) *BioMed Res Int*	miR-210 ↑ beneficial	Neonatal (d7) SD rats	CCA ligation + 2h hypoxia	Mimics or anti-miRs via stereotactic infusion into lateral ventricle.	3 days
(Sun et al., 2013) *CNS Neurosci Ther*	miR-124 ↑ beneficial	C57BL/6 mice (18-22g)	pMCAO	Mimics or anti-miRs via tail-vein injection daily for 3 days prior to MCAO.	1 day
(Xin et al., 2013b) *Stem Cells*	miR-133b ↑ beneficial	Wistar rats (270-300g)	2h tMCAO	MSCs modified to be miR-133b+ or miR-133b- via IV tail vein injection, 24h post-tMCAO.	14 days

Reference	MiRNA Modulation	Animal Model	Stroke Model	Delivery Method	Animals Sacrificed (time post-stroke)
(Zhao et al., 2013) *Stroke*	miR-424 ↑ beneficial	C57BL/6J mice (20-25g)	pMCAO	Lentivirus ↑ + polybrene via ICV injection 7 days pre-MCAO or mimic + siRNA-MATE via ICV injection 10 min post-MCAO.	Lentiviral vector = 8h, miRNA mimics = 1 day
(Chi et al., 2014) *Neuroscience*	miR-134 ↓ beneficial	C57BL/6J mice (18-22g, 6-8 weeks)	1h tMCAO	Lentivirus ↓ via stereotactic injection at 3 sites 72h pre-tMCAO.	1 day
(Qu et al., 2014) *Neurobiol Dis*	miR-139-5p ↑ beneficial	Neonatal (d10) SD rats	CCA ligation + 2.5h hypoxia	Mimic + lipofectamine via stereotactic injection to lateral ventricle at 12h post H/I.	2 and 7 days
(Vinciguerra et al., 2014) *Mol Ther*	miR-103-1 ↓ beneficial	SD rats (250-300g)	100min tMCAO	Anti-miR via ICV infusion to lateral ventricle for 48h, starting 24h pre-tMCAO or 20 min post-tMCAO.	1 and 2 days
(Wang et al., 2014a) *Neurochem Res*	miR-30a ↓ beneficial	C57BL/6J mice (22-25g)	pMCAO or 1h tMCAO	Lentivirus ↓ via stereotactic injection to cortex 5 days pre-MCAO.	pMCAO = 6h, tMCAO = 24h
(Zhao et al., 2014) *Brain Res*	miR-23a-3p ↑ beneficial	C57BL/6J mice (22g)	1h tMCAO	Mimic + lipofectamine via stereotactic injection (ICV) at 10 min post MACO.	1h, 4h, 1 day
(Zhu et al., 2014) *J Mol Neurosci*	miR-124 ↓ beneficial	SD rats (280-300g)	2h tMCAO	Anti-miR via ICV infusion to lateral ventricle at 1 day pre-tMCAO.	1 day
(Huang et al., 2015) *CNS Neurosci Ther*	miR-29c ↓ beneficial	SD rats (280-300g)	2h tMCAO	Anti-miR or mimic via ICV infusion at 1 day pre-tMCAO.	1 day
(Liu et al., 2015b) *Stroke*	miR-424 ↑ beneficial	C57BL/6 mice (22-25g)	1h tMCAO	Mimic + lipofectamine via ICV injection immediately prior to tMCAO.	1h, 4h, 1 day
(Liu et al., 2015a) *JCBFM*	miR-122 ↑ beneficial	SD rats (7-8 weeks)	1.5h tMCAO	Mimic + liposomes via IV (tail vein) or ICV injection, 5min post-tMCAO.	1 day

Reference	MiRNA Modulation	Animal Model	Stroke Model	Delivery Method	Animals Sacrificed (time post-stroke)
(Ni et al., 2015) *Brain, Behav & Immunity*	let-7c-5p ↑ beneficial	CD1 mice (25-30g)	1h tMCAO	Mimic + Entranster TM via stereotactic ICV injection, 6 days pre-MCAO.	1 and 4 days
(Stary et al., 2015) *Stroke*	miR-200c ↓ beneficial	CB57/B6 mice (8-10 weeks)	1h tMCAO	Anti-miR or mimics + DOTAP via ICV infusion, 24 hours pre-tMCAO.	1h, 3h, 1 day
(Wang et al., 2015) *JCBFM*	miR-29b ↑ beneficial	CD-1 mice (25-30g)	pMCAO	Lentivirus ↑ via stereotactic injection, 14 days pre-MCAO.	1 and 3 days
(Wei et al., 2015) *Mol Neurobiol*	miR-9 ↑ beneficial	C57/BL6 mice (8 weeks)	1.5h tMCAO	Mimics via IV for 3 days pre-tMCAO.	1h, 3h, 6h, 12h, 24h, 30 days
(Wen et al., 2015) *Mol Med*	miR-155 ↑ detrimental	C57/BL6 or miR-155$^{-/-}$ mice (25-30g)	pMCAO	Adenovirus via stereotactic injection to lateral ventricle, 24h pre-MCAO.	1 day
(Xu et al., 2015) *Exp Neurol*	miR-181 ↓ beneficial	C57/B6 mice (25-30g)	1h tMCAO	Anti-miR + DOTAP via ICV to lateral ventrical at 2h post-tMCAO or IV to internal jugular vein at 1h post-tMCAO.	1 and 2 days, 4 weeks
(Yu et al., 2015) *J Cell Biochem*	miR-22 ↑ beneficial	SD rats (260-320g)	1.5h tMCAO	Adenovirus ↑ via stereotactic injection into 2 brain sites, 3 days pre-tMCAO.	1 day

miRNAs have been successfully modulated when delivered *in vivo* either by the use of mimics and anti-miRs (with or without additional transfection reagents) (approximately 68%) and viral vectors (29%). The only study to modulate miRNA expression differently used modified mesenchymal stromal cells that were either miR-133b+ or miR-133b- (this study is discussed further in section 1.3.5).

The vast majority of studies (90%) which modulated miRNA expression *in vivo* have done so by direct delivery to the brain via stereotactic injection or osmotic-mini pump infusion into a lateral ventricle. A number of studies have demonstrated successful miRNA modulation by IV delivery, typically to the tail vein (Liu et al., 2015a, Wei et al., 2015, Xin et al., 2013b) with one study delivering to the internal jugular vein (Xu et al., 2015). IV delivery has been compared to intracerebroventricular (ICV) infusion in two separate studies. The first compared ICV infusion of a miR-181a anti-miR with IV delivery (Xu et al., 2015). miR-181a anti-miR was mixed with the cationic lipid DOTAP and infused into the lateral cerebral ventricle at 2 hours post-tMCAO in C57/B6 mice or delivered IV 1 hour post-tMCAO into the internal jugular vein. ICV infusion of the anti-miR reduced miR-181a levels in the brain significantly, infarct size by 35% (vs. control anti-miR) at 48h post-tMCAO and significantly improved neurological deficits over a 28 day period. IV delivery of the anti-miR also reduced miR-181a levels in the brain significantly (although to a lesser degree) and this was also associated with significantly reduced infarct size and improved neurological score. The second compared ICV and IV delivery of miR-122 mimic (Liu et al., 2015a). Interestingly, the miR-122 mimic was 'wrapped' using PEG-liposomes (liposomes containing synthetic polymer poly-(ethylene glycol)). PEG-liposomes have been shown to have extended blood-circulation time and reduced mononuclear phagocyte system uptake, important when delivering IV, and for this reason are sometimes called stealth liposomes (Immordino et al., 2006). Sprague Dawley rats were given miR-122 mimic IV or ICV within 5 mins of tMCAO (Liu et al., 2015a). Within 24h of tMCAO IV delivery of mimic resulted in up-regulated circulating expression of miR-122 in a dose-dependent fashion, no data are given on expression following ICV delivery. ICV delivery of mimic did not reduce infarct size or improve neurological impairment, unlike IV delivery which significantly improved both. These studies show that modulating miRNA expression by IV delivery of either miRNA mimic or anti-miR, a clinically relevant

model of delivery, holds therapeutic potential and can result in significant improvements to infarct size and neurological score following ischaemic stroke.

The majority of studies described in Table 1.4 modulate miRNA expression pre-ischaemic stroke and go on to demonstrate therapeutic benefit post-ischaemic stroke. While these proof of concept studies are necessary, drug delivery pre-stroke is clearly not appropriate for clinical treatment of stroke. Ten studies have shown therapeutic effect with delivery post-stroke, but of these six studies deliver within 20 mins post-stroke (usually at the point of reperfusion, although not all studies make this clear). While these studies are important, they do not extend the therapeutic time window past what is currently available with treatment by rtPA within 4.5 hours or thrombectomy within 6 hours. Of the remaining studies, miR-181 anti-miR was delivered at 1 and 2 hours post-stroke (Xu et al., 2015) and let-7f anti-miR was delivered by ICV to rats at 4 hours-post embolic stroke (Selvamani et al., 2012). Furthermore, miR-139-5p mimic was delivered by stereotactic injection to neonatal Sprague Dawley rats at 12 hours post-hypoxia/ischemia injury (Qu et al., 2014) and modified mesenchymal stromal cells (MSCs) were administered IV to Wistar rats at 24 hours post-tMCAO (Xin et al., 2013b). Modulating miRNA expression post-stroke can result in therapeutic benefit and future studies should focus on delivery post-stroke.

Over 50% of studies sacrificed animals within 24 hours of stroke, giving a good indication of therapeutic benefit as assessed by reduced infarct volume. However, in these studies there was limited measurement of functional outcome or the impact of the decreased lesion size. It is worth considering that in models using tMCAO the lesion would not necessarily be complete at 24 hours post-stroke. Of 14 studies that sacrificed animals after 24 hours, 11 sacrificed study animals within 7 days of stroke and the remaining 3 looked at therapeutic effect from 2 weeks to 56 days post-stroke. Delivery of miR-133b modified MSCs post-tMCAO resulted in functional improvement (assessed by adhesive removal test and foot-fault test) up until 14 days post-stroke in Wistar rats (Xin et al., 2013b). Mice treated with miR-9 mimic delivered pre-tMCAO had improved functional outcome up to 28 days post-stroke as assessed by neurological score, rotarod and staircase test (Wei et al., 2015). Finally, viral mediated increases in miR-124 expression pre-stroke, were associated with improved functional outcome in C57BL6/N mice, up to 56 days post-stroke, as assessed by rotarod and tightrope

tests and a modified water maze test (Doeppner et al., 2013). Studies that have investigated positive therapeutic effect within 24 hours should now look at longer-term time points to see if the trend towards therapeutic effect continues long-term.

As has been discussed in section 1.1.3, ischaemic stroke results in an extremely complex pathophysiology. Interestingly, the miRNAs modulated in these *in vivo* studies play a part in modulating many of these processes, including cell death and apoptosis, cerebral oedema, oxidative stress, BBB dysfunction, inflammation and neurogenesis and angiogenesis. While the majority of these studies only look at a single or small number of miRNA targets it would be interesting to see if multiple miRNAs could be used to target multiple ischaemic stroke processes simultaneously and so result in even greater therapeutic benefit.

A number of studies from separate groups have modified the same miRNA with differing results. This is the case for both miR-124 and miR-29. Viral mediated increased miR-124 expression in C57BL6/N mice resulted in reduced infarct volume, oedema and improved functional outcome (Doeppner et al., 2013). Similarly, systemic delivery of miR-124 mimic via tail vein injection 3 days prior to permanent MCAO (pMCAO) in C57BL6 mice resulted in reduced infarct volume (Sun et al., 2013). However in a conflicting study, delivery of both mimic and anti-miR to C57 mice via ICV injection post-stroke revealed that inhibition of miR-124 expression resulted in reduced infarct volume and de-repression of iASPP (an evolutionarily conserved inhibitor of p53) (Liu et al., 2013a). Furthermore, using a miR-124 anti-miR, delivered by ICV infusion 1 day pre-tMCAO in Sprague Dawley rats resulted in decreased infarct volume and de-repression of Ku70, a suppressor of Bax-mediated apoptosis (Zhu et al., 2014).

Several studies have investigated miR-29b and miR-29c modulation in 4 different animal models and present results that are similarly complicated. Three studies demonstrate that increased miR-29 expression is beneficial with 1 study showing the opposite. Inhibition of miR-29c via ICV infusion of anti-miR 1 day pre-tMCAO in Sprague Dawley rats resulted in decreased infarct size (assessed by TTC staining), improved neurological score, increased Birc2 and Bak1 (anti-apoptotic) mRNA and protein expression and decreased apoptosis (Huang et al., 2015). Conversely, osmotic infusion of pre-miR-29c into the lateral ventricle of SHR rats

resulted in significantly reduced infarct volume (assessed by cresyl violet staining) (Pandi et al., 2013). Similarly, lentiviral mediated increased miR-29b expression in C57BL6/N mice resulted in reduced lesion volume (assessed by MRI), improved functional recovery and attenuated stroke-induced neurodegeneration, mediated in part by activity of the 12-lipoxygenase pathway (Khanna et al., 2013). Finally, lentiviral mediated increased miR-29b expression in CD-1 mice resulted in reduced infarct volume (assessed by cresyl violet staining), inhibited aquaporin 4 up-regulation, alleviated brain oedema and attenuated BBB breakdown (Wang et al., 2015).

These conflicting studies investigating the effect of miR-124 and miR-29 modulation on outcome from stroke are difficult to compare and to interpret as different stroke and animal models, delivery method and sacrifice time points have been used (see Table 1.4 for further details). It is interesting, however, that one miRNA or miRNA cluster can target so many different pathways in ischemic stroke and this demonstrates the huge therapeutic potential of miRNA modulation in the setting of experimental ischaemic stroke, if thoroughly investigated and carefully targeted.

1.3 Exosomes

The term extracellular vesicle, defined as a “membrane vesicle containing cytosol from the secreting cells enclosed in a lipid bilayer” (Colombo et al., 2014), describes a number of different vesicles with a diverse range of origins, composition, function and size.

The term exosome was first used for vesicles (40-100 nm) released from a number of different cultured cell types (Trams et al., 1981) but was subsequently used to describe vesicles of endosomal origin, secreted during reticulocyte differentiation (assessed in *in vitro* cultures of sheep reticulocytes) as a result of the fusion of multivesicular bodies (MVBs) and the plasma membrane (Johnstone et al., 1987).

Exosomes are defined primarily by their size and origin. They are lipid bilayer particles, released from cells and are generally agreed to be between 30-120 nm in diameter. Some studies have expanded the size range to include particles as

small as 20 nm and as wide as 150 nm in diameter (Ibrahim and Marbán, 2016). The terms ectosome, microparticle and microvesicle generally refer to much larger vesicles released by budding from the plasma membrane, between 150-1000 nm in diameter. As exosomes (originally intraluminal endosomal vesicles) are secreted by the fusion of the endosome with the plasma membrane (resulting in release of exosomes into extracellular space) they contain markers of their biogenesis. Recently, the International Society for Extracellular Vesicles has provided criteria for the definition of exosomes (Lötvall et al., 2014). This includes the presence in exosome isolates of a number of "exosome enriched" proteins, including transmembrane or lipid-bound extracellular proteins (e.g. tetraspanins such as CD9, CD63) and cytosolic proteins with membrane or receptor binding capacity (e.g. endosome or membrane-binding proteins such as TSG101 and a number of annexins) (Figure 1.6).

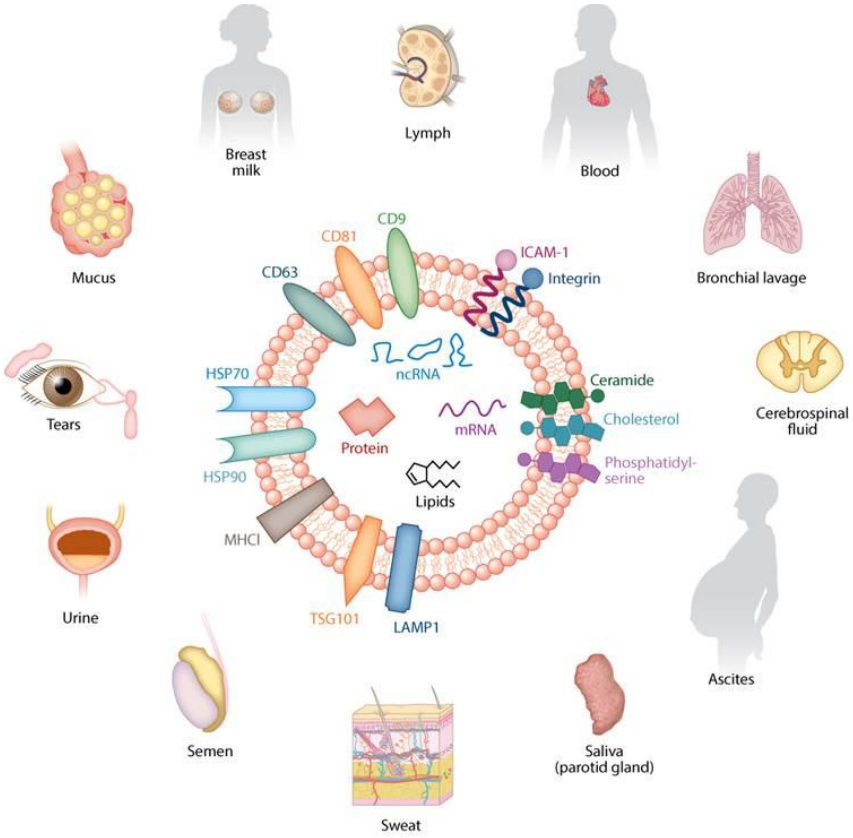

Figure 1.6 – Exosome Characteristics.
Exosomes are small vesicles with a diameter range of 30-120 nm and are secreted by all cell types. The lipid bilayer is enriched in cholesterol, ceramide and phosphatidylserine and has a differing lipid content to that of the parent cell. Markers present in most exosomes include tetraspanins (CD9, CD63, CD81), heat shock proteins, adhesion molecules and markers of the endosomal sorting complexes required for transport (LAMP1, TSG101). This figure was reproduced with permission from (Ibrahim and Marbán, 2016).

Exosomes have now been shown to be released from cells of many different organisms and have been isolated from a varied range of bodily fluids, including blood, urine, saliva, breast milk, amniotic fluid, ascites, cerebrospinal fluid, bile and semen (Figure 1.6).

1.3.1 Biogenesis

Unlike microvesicles which are formed by the outward budding of the plasma membrane and apoptotic bodies which are shed from dying cells, exosomes are released as a result of the fusion of loaded multivesicular bodies (MVBs) with the plasma membrane. MVBs typically form via the endocytic pathway. Endosomes mature into late (vs. early) endosomes (Stoorvogel et al., 1991) and during this process intraluminal vesicles (ILVs) gather within the lumen, formed by inward budding of the endosomal membrane. ILVs may contain proteins, lipids and RNAs (Ibrahim and Marbán, 2016). MVBs will often be targeted for degradation and so fuse with lysosomes containing lysosomal hydrolases that degrade the content of the MVB. However, other MVBs are targeted for secretion and these fuse with the plasma membrane and release the ILVs, now called exosomes, into the extracellular space (Raposo et al., 1996). Microvesicles and apoptotic bodies have similar membrane lipid content to the plasma membrane of the cell they originate from while exosomes shed from MVBs are likely to have differential membrane lipid content to their cell of origin.

It is now believed that there are multiple MVBs within each cell carrying differential markers that result in some being targeted for degradation and others being targeted for exocytosis – this targeting of MVBs remains poorly understood (Colombo et al., 2014). MVBs targeted for exocytosis are often cholesterol positive (Mobius et al., 2003), CD63 positive with an EGF-receptor (White et al., 2006) and CD9 positive (Buschow et al., 2009). MVBs targeted for degradation contain lysobisphosphatidic acid (White et al., 2006).

The endosomal sorting complex required for transport (ESCRT) is partly responsible for processing within the endocytic pathway. ESCRT is made up of ~30 proteins that assemble into four different complexes (ESCRT-0, -I, -II and –III) with a number of associated proteins (e.g. VPS4, VTA1, ALIX and PDCD6IP) and is involved in endosome biogenesis and exosome release (Hanson and

Cashikar, 2012, Hurley and Hanson, 2010). It is likely that MVB and ILV formation (mediated ESCRT-dependently or independently) is related to the cargo sorted within each cell (Carayon et al., 2011). Exosome release also appears to be differentially regulated, both molecularly and mechanistically, depending on the cell type of origin.

1.3.2 Targeting of Exosomes

Exosomes are intercellular messengers and secreted exosomes from one cell can interact with recipient cells, resulting in functional changes. The specificity of these exosome-recipient cell interactions is conferred by surface ligands on both the exosome and the plasma membrane of the recipient cell. Examples in the literature include: ICAM-1 dendritic cell extracellular vesicles interact with LFA-1 on dendritic cells (Segura et al., 2005); α2,3-sialic acid positive splenocyte extracellular vesicles interact with CD169+ (lectin receptor) macrophages in the spleen and lymph node (Saunderson et al., 2014); heparan sulfate proteoglycans on tumour cell extracellular vesicles increase cellular uptake into tumour cells (Christianson et al., 2013). However, many of these pairings are probably limited to specific exosomes from a certain cell type and a specific recipient cell type.

Exosomes can mediate intercellular communication either with or without internalisation into their recipient cells. For example, exosomes bearing MHC peptide complexes can be ‘captured’ by dendritic cells, and the MHC peptide complexes presented to antigen-specific T-cells without the need for internalisation of the exosome or reprocessing (Denzer et al., 2000, Segura et al., 2007). However, many studies demonstrate internalisation of exosomes occurring by a variety of mechanisms, including (but not limited to): proteolytic cleavage of exosomes releasing soluble ligands, lipid membrane fusion, internalisation by receptor-mediated endocytosis or uptake by phagocytosis, pinocytosis or micropinocytosis (Ibrahim and Marbán, 2016). Larger extracellular vesicles (or aggregations of exosomes) are likely to induce phagocytosis whereas small exosomes can be internalised by non-phagocytic processes as have been described above (Colombo et al., 2014). Similarly to exosome-target interactions, the mechanism of uptake is likely to be specific to exosomes from a certain cell type and their recipient cells.

Membrane fusion of exosomes with either the plasma membrane or the endocytic compartment limiting membrane is essential for the release of the content of an exosome into the cytosol of a recipient cell. This has been demonstrated in three important studies. The addition of exosomes labelled with a fluorescent R18 lipid probe to recipient tumour and dendritic cells resulted in increased fluorescence in these cells – fusion of the exosome membrane with the membrane of the recipient cells was subsequently demonstrated (Montecalvo et al., 2012, Parolini et al., 2009). Furthermore, when dendritic cells (expressing luciferase) were incubated with luciferin-loaded exosomes, the release of internal exosome components into the cytosol of the recipient dendritic cells was demonstrated (Montecalvo et al., 2012). Interestingly, the content of the exosomes involved in dendritic cell intercellular communication included functionally active miRNAs. Finally, a recent study investigating anthrax toxin infection demonstrated that the lethal factor component of anthrax is contained in exosomes which are protected from proteolytic degradation for some time both *in vitro* and *in vivo,* before releasing the lethal factor into the cytosol by back fusion with the MVB limiting membrane (Abrami et al., 2013).

Exosomes have been detected in a wide variety of biological fluids (see Figure 1.6) but it is difficult to investigate their fate *in vivo,* following their secretion by a cell within an organ or artificial delivery of exosomes either systemically or to a specific organ. Exosomes detected in the blood can bear markers of endothelial and immune cells (both found in blood vessels) but also, for example, of distant tumours (in cancer patients) - exosomes can therefore travel through the endothelium into blood circulation. Initially it was believed that exosomes could remain stable in the blood for a significant amount of time but more recent studies have demonstrated a very short half-life of exosomes in blood following IV injection. Exosomes generated from B16-BL6 murine melanoma cells (luciferase labelled) were delivered intravenously to BALB/c mice. These exosomes had a half-life of approximately 2 minutes and disappeared quickly from blood circulation, distributing first to the liver and then to the lungs (preferred sites of metastasis) (Takahashi et al., 2013). A similar study isolated exosomes from C57BL/6 splenocytes and labelled them with biotin (Saunderson et al., 2014). Labelled exosomes were delivered IV and

were rapidly cleared from the blood of C57BL/6 mice, with a half-life of approximately 2 minutes (Saunderson et al., 2014). However, exosomes could still be detected in the spleen after 2 hours, suggesting that exosome reservoirs may still exist after the majority have been cleared from the circulation. These studies also highlight how exosomes of differing cellular origins target different organs *in vivo*, an important consideration when using exosomes therapeutically. Other studies have successfully demonstrated modification of exosomes to alter organ targeting, for example, exosomes generated from engineered dendritic cells expressing Lamp2b (an exosomal membrane protein) fused to the neuron-specific RVG peptide, specifically delivered siRNA to neurons, microglia and oligodendrocytes in the brain when delivered IV to C57BL/6 mice (Alvarez-Erviti et al., 2011). A recent study has demonstrated that exosome dose, delivery method, cellular origin of exosomes and targeting of exosomes all affect bio-distribution of exosomes *in vivo* (Wiklander et al., 2015).

1.3.3 Exosomes and miRNA

A breakthrough in exosome research came in 2007 when it was demonstrated, for the first time, that exosomes could carry nucleic acids (Valadi et al., 2007). In a seminal paper exosomes were demonstrated to contain both mRNA and miRNA which could be delivered to cells and act functionally. Following the delivery of mouse exosomes to human cells, mouse proteins were detected in the human cells, which had previously existed as mRNA in the mouse exosomes – data consistent with the hypothesis that mRNA shuttled in the mouse exosomes had been translated (Valadi et al., 2007). Subsequently miRNAs were also detected in vesicles isolated from plasma and glioblastoma tumour cells (Hunter et al., 2008, Skog et al., 2008).

As a result of the fact that different miRNA sequences are preferentially secreted or retained within cells it is clear that exosomal miRNAs are not randomly secreted. Comparison of intracellular and extracellular miRNA shows specific miRNA sequences are selected for extracellular export (Montecalvo et al., 2012). Furthermore, miRNAs whose expression was increased in exosomes released from breast cancer cells were packaged differently to miRNAs whose expression was unaltered by malignancy (neutral miRNAs) (Palma et al., 2012).

Neutral miRNAs were packaged in much larger exosomes, enriched in CD44. The more complex mechanisms of RNA cargo selection are yet to be elucidated.

There has been controversy over whether the majority of circulating miRNAs are found within exosomes or not. It was initially believed that the majority of miRNAs in human serum and plasma co-fractionated with Argonaute2 ribonucleoprotein complexes (Arroyo et al., 2011) and that only a minority of specific miRNAs appeared to be associated with exosomes. It was subsequently shown that circulating miRNAs could form complexes with high-density lipoproteins (Vickers et al., 2011). However, there is now compelling evidence that miRNAs circulating in the serum exist primarily within exosomes (Gallo et al., 2012). Isolating exosomes from human serum was shown to increase the sensitivity of miRNA detection (Gallo et al., 2012).

Within the brain it has been proposed that exosomal mediated miRNA release is a method of adjusting gene silencing levels, for example in synaptic plasticity (Goldie et al., 2014). Exosome mediated inter-cellular communication has also been demonstrated between primary cortical neurons and astrocytes *in vitro* resulting in alterations in target protein expression (Morel et al., 2013). Furthermore, administration of exosomes from young rats, enriched in miR-219, promoted myelination in older rats (Pusic and Kraig, 2014).

Exosomal miRNAs have been shown to be involved in cancer (e.g. (Melo et al., 2014)) and cardiovascular disease. Active transport of miRNAs in exosomes was demonstrated pre-clinically in atherosclerosis (Hergenreider et al., 2012). Cells transduced with KLF2 (Kruppel-like factor 2, a shear-response transcription factor) generated exosomes that were enriched in specific miRNAs, including the miR-143/145 cluster. These exosomes were shown to mediate a reduction in atherosclerotic lesion formation in $ApoE^{-/-}$ mice. Studies in cardiac hypertrophy demonstrated that fibroblasts secreted miR-21* enriched exosomes (Bang et al., 2014a), unusual in that miRNA passenger (*) strands are conventionally believed to undergo intracellular degradation. miR-21* enriched exosomes were shown to mediate cardiomyocyte hypertrophy: their uptake through an endocytic pathway resulted in the down-regulation of several targets, which effectively triggered hypertrophy. Other studies have demonstrated the involvement of exosomal miRNAs in arrhythmia and cardiomyopathy (Ibrahim and Marbán, 2016).

1.3.4 Therapeutic Potential of Exosomes

Exosomes have huge potential as vehicles for delivering therapeutic agents to the brain (Johnsen et al., 2014). Their small size means that they can cross the BBB (e.g. (Alvarez-Erviti et al., 2011). The use of self-derived exosomes means that undesired immunogenicity is limited (if not absent), meaning exosomes are a very safe way to deliver therapeutic agents (Lakhal and Wood, 2011). Exosomes can also be modified to target certain organs or tissues, and so drug delivery can be very specific, even if administered intravenously. For example, exosomes engineered to express a peptide that specifically binds to the acetylcholine receptor, containing BACE1 siRNA significantly reduced BACE1 expression in the brain of C57BL/6 mice following systemic administration (Alvarez-Erviti et al., 2011). Additionally, miRNAs can be rapidly degraded by RNases in the blood and so exosomes are an excellent tool to protect miRNAs and provide stability and to enable the delivery of intact miRNAs to target cells.

However, the involvement of exosomes in health and disease is poorly understood. Important aspects of exosome biology, including the biogenesis, secretion, uptake and targeting of exosomes, are not yet fully established. Furthermore, exosomes can mediate the replication and propagation of transmissible pathogens. Exosomes are clearly a valuable tool for the delivery of therapeutic agents but must be used in a careful and controlled manner.

1.3.5 Exosomes and Stroke

To date very little has been published concerning exosomes in the setting of ischaemic stroke. Circulating miRNA expression was profiled in a small number of ischaemic stroke and ICH patients (Guo et al., 2013) in a study which went on to isolate CD63+ microvesicles by ultracentrifugation and to compare expression of 5 miRNAs between total plasma isolates and microvesicle isolates in healthy control and ICH patients. miRNAs-365, -27a, -150*, -34c-3p and -24 were not present in the plasma of healthy controls (n=3-4) but were detected in the plasma of ICH patients (n=3-5). Furthermore, microvesicle expression of these miRNAs was increased in ICH patients as compared to healthy controls, although no indication of the statistical significance of this increase is given. Unfortunately the patient populations used in this study were extremely small

and microvesicle miRNA expression was not investigated in the ischaemic stroke patient cohort. Despite these caveats this study is the first to demonstrate compartmentalisation of miRNAs in the setting of stroke.

Total and exosomal circulating expression of miR-126 has been compared in transient and permanent *in vivo* models of ischemic stroke (Chen et al., 2015). Exosomes were isolated by precipitation. miR-126 was detected in both total and exosomal isolates harvested from the serum of Wistar rats following either tMCAO or pMCAO (n=27/group) or sham procedure (n=5) at 3 hours and 24 hours post-stroke. miR-126 exosomal expression was decreased at 3 hours following both tMCAO and pMCAO but normalised close to pre-ischemic baseline levels at 24 hours. Total serum expression of miR-126 was decreased at 3 hours in the permanent model but not the transient and it is clear that serum miR-126 expression was much more variable, consistent with more highly regulated exosomal miRNA expression. However, expression of miR-126 in sham operated animals is not shown making results harder to interpret. Serum but not exosomal miR-126 expression (at 3 hours) correlated significantly with infarct volume.

Previous work within our own group (Breen, 2015) profiled expression of specific miRNAs (miR-19b, miR-93, miR-106a and miR-532) in the serum of SHRSP at 24 and 72 hours post-tMCAO. The expression of several miRNAs was significantly up-regulated at 24 hours (miR-19b, miR-532) and 72 hours (miR-532) post-tMCAO. However, the exosomal expression of a number of miRNAs was up-regulated at 24 hours (miR-19b, miR-106a) and at 72 hours (miR-19b, miR-93, miR-106a) to a much greater extent than had been observed in the total serum analysis. Comparison of miRNA expression at specific time points would suggest that miRs -19b, -93 and -106a are compartmentalised within the exosomes.

These studies suggest that circulating exosomes containing miRNAs are present in both human stroke patients and in *in vivo* pre-clinical models of ischaemic stroke. Further studies should be performed to elucidate the full extent of exosomal miRNA expression in ischaemic stroke patients and whether these exosomally packaged miRNAs have a functional role to play in ischaemic stroke.

Two studies published by Michael Chopp's research group have demonstrated the therapeutic use of exosomes in the setting of pre-clinical ischaemic stroke. The

first involved IV delivery of MSC exosomes to Wistar rats at 24 hours post-tMCAO (Xin et al., 2013a). MSCs were cultured from bone marrow harvested from healthy Wistar rats. Treatment with exosomes isolated from MSCs did not reduce lesion volume at 28 days post-stroke but did significantly improve functional outcome as assessed by foot fault test and neurological score. Furthermore, treatment with exosomes isolated from MSCs increased axonal density, synaptophysin staining (an indicator of synaptic plasticity) and appeared to promote neurogenesis and angiogenesis post-stroke (as assessed by increased Brd-U staining, a marker of cell proliferation, co-localised with markers for migrating neuroblasts or sprouting capillaries) within the ischaemic boundary zone (or penumbra) (Xin et al., 2013a).

Subsequently MSCs were modified to have up-regulated or down-regulated miR-133b expression (Xin et al., 2013b). These MSCs were shown to produce exosomes that were miR-133b+ or miR-133-. Similarly to their previous study Wistar rats were given miR-133b+, miR-133b- MSCs, naïve MSCs or PBS at 24 hours post-tMCAO. All types of MSC improved functional recovery (assessed by adhesive-removal and foot fault test) at day 14 post-tMCAO. However, compared to naïve MSC treatment, miR-133b+ MSCs significantly improved and miR-133b- MSCs significantly decreased functional recovery. MSCs were (again) shown to improve angiogenesis and neurogenesis and the effect was enhanced with miR-133b+ MSCs. In this study MSCs were also transfected with a plasmid containing a CD63-GFP fusion protein gene and rats were subsequently treated with these cells post-tMCAO. Exosomes released by MSCs (CD63-GFP+) were detected in adjacent astrocytes and neurons of the ischemic boundary zone demonstrating communication between MSCs and neural cells. These studies demonstrate the potential of using exosomes to modulate miRNA expression therapeutically in the setting of ischaemic stroke.

1.4 General Aims

Ischaemic stroke is a devastating condition and remains a largely unmet clinical need, with only a limited percentage of stroke patients eligible to receive rt-PA or thrombectomy. Stroke is therefore a significant cause of death and disability worldwide. This thesis will investigate whether miRNAs (especially those packaged within exosomes) are dysregulated following ischaemic stroke and whether they can be modulated therapeutically to improve outcome.

My hypothesis is that as miRNAs are modulated following ischaemic stroke and play a functional role in stroke pathophysiology, modulation of miR-494 and miR-21 (dysregulated miRNAs) will be a novel therapy in pre-clinical experimental ischaemic stroke, resulting in inhibition of stroke pathophysiology and/or promotion of recovery.

Furthermore, I hypothesise that the packaging of miRNAs into exosomes will be significantly dysregulated in human stroke patients and that as a result the circulating miRNA/exosome profile will be significantly altered.

Specifically, the aims of this project include:

1. To modulate specific miRNAs in *in vitro* models of ischaemia, namely hypoxia-reoxygenation injury, to assess resulting functional outcome and to determine regulation of gene targets by specific miRNAs.

2. To characterise exosomal miRNA expression in the serum of a human ischaemic stroke patient population and identify miRNAs that are differentially regulated as a result of ischaemic stroke.

3. To assess the use of exosomes as a method for the delivery of miRNA modulating agents and to modulate miRNA expression of specific miRNAs dysregulated in human ischaemic stroke patients, using exosomes, in *in vitro* and *in vivo* models of pre-clinical ischaemic stroke.

Chapter 2 Materials and Methods

2.1 General laboratory practice

Laboratory reagents and equipment were of the highest commercially available standard. Hazardous chemicals were handled and disposed of in compliance with Control of Substances Hazardous to Health (COSHH) guidelines. Laboratory coats, nitrile powder-free gloves and fume hoods were used where appropriate.

2.2 Cell Culture

All tissue culture was performed under sterile conditions in standard biological safety class II vertical laminar flow cabinets. Cabinets were cleaned with 1% Virkon and 70% ethanol before and after use. Cells were grown in humidified incubators at 37˚C in a 5% CO_2 atmosphere.

2.2.1 Maintenance of Established Cell Lines

Cells were maintained with appropriate cell culture media (see Table 2.1) and grown in a monolayer, replenishing media between passages when necessary. Cells were passaged upon reaching 80% confluence using 0.05% (1X) trypsin-ethylenediamine tetra-acetic acid (trypsin-EDTA; Gibco, Paisley, UK) with regular passaging preventing overgrowth and loss of surface contact. Trypsin is a proteolytic enzyme that acts to disrupt proteins mediating cell-cell interactions and EDTA chelates divalent cations that act to strengthen these interactions. Cells were washed twice with Dulbecco's Phosphate Buffered Saline, without calcium (Ca^{2+}) or magnesium (Mg^{2+}) (DPBS; Gibco, Paisley, UK) before 3-5 mL of trypsin-EDTA was added. Cells were incubated with trypsin-EDTA at 37ºC for several minutes until the majority of adherent cells had detached from the surface of the flask and before cell death occurred. An equal volume of complete media (containing serum) was immediately added to prevent further trypsinisation. The cell suspension was centrifuged at 1500 rpm for 5 minutes to remove remaining trypsin-EDTA and the cell pellet resuspended in complete media. When necessary a haemocytometer was used to count cells to allow for the accurate seeding of cells to a specific seeding density.

Table 2.1 - Details of the cell lines used and their culture medium.
All media and supplements obtained from Gibco®, Paisley, UK or Sigma-Aldrich®, Irvine, UK..

Cell Type	Description	Cell Culture Medium
B50	Immortalised rat neuronal cells from a neuroblastoma	Dulbecco's Modified Eagle Medium (DMEM): low glucose (1g/L), sodium pyruvate [without L-glutamine, Phenol Red, HEPES] supplemented with 10% (v/v) Heat Inactivated Fetal Bovine Serum (FBS), 1% (v/v) penicillin (100 units/mL), 100 µg/mL streptomycin and 2 mM L-Glutamine.
B92	Immortalised rat glial cells from a neuroblastoma	Dulbecco's Modified Eagle Medium (DMEM): low glucose (1g/L), L-glutamine, sodium pyruvate and phenol red [without HEPES] supplemented with 10% (v/v) Heat Inactivated Fetal Bovine Serum (FBS), 1% (v/v) penicillin (100 units/mL), 100 µg/mL streptomycin and 2 mM L-Glutamine.
GPNT	Immortalised rat cerebral endothelial (vascular) cells	Ham's F-10 Nutrient Mix: L-Glutamine and Phenol Red [without HEPES] supplemented with 10% (v/v) Heat Inactivated Fetal Bovine Serum (FBS), 1% (v/v) penicillin (100 units/mL), 100 µg/mL streptomycin, 2 mM L-Glutamine, 2 ng/mL basic fibroblast growth factor (bFGF) and 80 µg/mL heparin. N.B. All plasticware used for the culture of GPNT cells was pre-coated for 5 hours (minimum) with 10 µg/cm^2 collagen (Type I solution from rat tail). Plasticware was rinsed twice with DPBS before use.

Cells were checked visually for bacterial or fungal infection on a daily basis. Cells used throughout the laboratory were tested for mycoplasma infection on a regular basis by laboratory technicians using qRT-PCR (LookOut® mycoplasma qPCR detection kit, Sigma-Aldrich).

2.2.2 Modulation of microRNAs *in vitro*

2.2.2.1 Modulation of microRNAs via Transfection Agent

GPNT cells were transfected with miR-21 and miR-494 miRNA mimics and anti-miRs using siPORT™ NeoFX™ Transfection Agent (Invitrogen). To investigate the effect of modulating miRNA expression cells were seeded in 12 well plates at 5 x 10^4 cells/well (if harvesting RNA) and in 6 well plates at 1 x 10^5 cells/well (if harvesting protein) and in 96 well plates at 2 x 10^3 cells/well (if using cells for MTS assay).

When modulating miR-21 expression, cells were transfected on Day 1 following seeding on Day 0 (see Figure 2.1, A and B). When transfecting cells in a 12 well plate, miRNA mimics and anti-miRs (and their scrambled controls) were diluted appropriately with OPTI-MEM® Reduced Serum Medium (Invitrogen) to make a total volume of 50 µL. Similarly siPORT™ *NeoFX*™ Transfection Agent (Invitrogen) was diluted with OPTI-MEM® to a total volume of 50 µL (3µL siPORT™ NeoFX™ + 47 µL OPTI-MEM® = 50 µL). The diluted miRNAs and siPORT™ NeoFX™ were mixed and allowed to incubate for 10 minutes at room temperature before the complete solution (100 µL) was added to 900 µL of fresh media to give a final concentration of 30 nM for mature miRNA mimics (and controls) and 100 nM for anti-miRs (and controls). When transfecting a 96 well plate 0.5 µL of siPORT was added to 9.5 µL OPTI-MEM®, added to 10 µL diluted miR and delivered into 80 µL of fresh media. When transfecting a 6 well plate 5 µL of siPORT was added to 95 µL OPTI-MEM®, added to 100 µL diluted miR and delivered into 1.8 mL of fresh media.

A

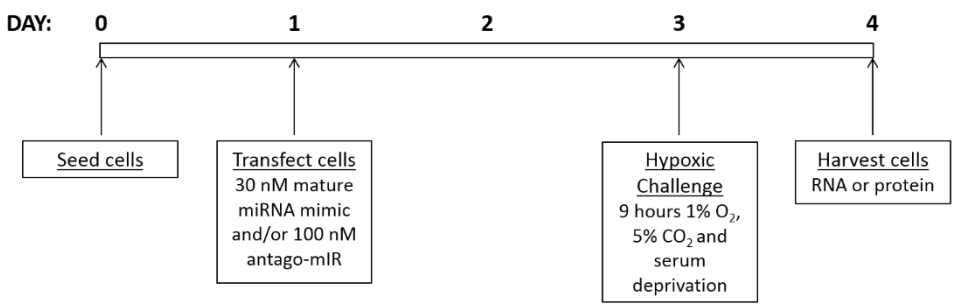

B

Condition	Day 1 cells transfected with:
#1	
#2	transfection reagent only
#3	30 nM scrambled miRNA mimic (control)
#4	30 nM miRNA mimic
#5	100 nM scrambled antago-miR (control)
#6	100 nM antago-miR

C

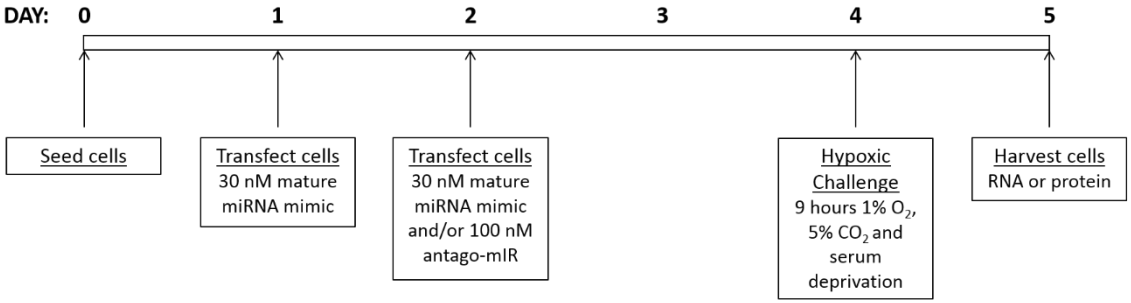

D

Condition	Day 1 cells transfected with:	Day 2 cells transfected with:
#1		
#2	transfection reagent only	transfection reagent only
#3	30 nM scrambled miRNA mimic (control)	30 nM scrambled miRNA mimic (control) + 100 nM scrambled antago-miR (control)
#4	30 nM scrambled miRNA mimic (control)	30 nM scrambled miRNA mimic (control) + 100 nM antago-miR
#5	30 nM miRNA mimic	30 nM miRNA mimic + 100 nM scrambled antago-miR (control)
#6	30 nM miRNA mimic	30 nM miRNA mimic + 100 nM antago-miR
#7	30 nM miRNA mimic	30 nM miRNA mimic

Figure 2.1 – Protocol for transfecting cells with miRNA mimics and anti-miRs.
This diagram illustrates the protocol for delivering mature miRNA mimics and anti-miRs (A) to GPNT cells and a more complicated protocol (B) to be used when limited effect of transfection with the anti-miR alone is observed, and the conditions/controls used in each experiment (B and D).

When optimising a protocol to modulate miR-494 expression, limited down-regulation of miRNA expression was observed following transfection with miR-494 anti-miR. To overcome this hurdle, cells were transfected with mature miRNA mimics, anti-miRs or their respective controls over 2 days following seeding, as illustrated in Figure 2.1 (C and D). On the first day following seeding cells were transfected with mature miRNA mimics and their controls and on the second day with a repeated delivery of the mature miRNA mimic, followed by delivery of the anti-miR. miRNA mimics and anti-miRs were delivered using siPORT™ NeoFX™ Transfection Agent as described above. Cells were allowed to rest for 48 hours following transfection before being subjected to hypoxic challenge.

Pre-miR™ miRNA Precursor rno-miR-21-3p, Pre-miR™ miRNA Precursor rno-miR-494-3p and their control Cy™3 dye-labelled Pre-miR™ Negative Control #1 and *miR*Vana® miRNA Inhibitor rno-miR-21-3p, *miR*Vana® miRNA Inhibitor rno-miR-494-3p and its control miRVana™ miRNA Inhibitor Negative Control #1 were purchased from Invitrogen and made up to a stock concentration of 30 μM.

2.2.2.2 Modulation of microRNAs via miRNA Loaded Exosomes

To investigate the effect on miRNA expression of delivering exosomes loaded with miRNAs of interest, B50 cells were grown in 12 well plates and miRNA loaded exosomes were delivered both pre- and post-hypoxia.

When investigating pre-hypoxic challenge delivery, B50 cells were seeded at 5 x 10^4 cells/well on Day 0 and 875 ng of either naïve exosomes, miR-20b loaded exosomes or miR-93 loaded exosomes were delivered directly to the cell culture medium on Day 1. The cells were subject to hypoxic challenge on Day 2 and harvested for RNA on Day 3 (Figure 2.2, A and B).

When investigating post-hypoxic challenge delivery, B50 cells were seeded on Day 0 at 2.5 x 10^4 cells/well. Cells were subject to a 9 hour hypoxic challenge on Day 2 and immediately following reoxygenation, 875ng of either naïve exosomes, miR-20b loaded exosomes or miR-93 loaded exosomes were delivered directly to the cell culture media. The cells were harvested for RNA on Day 4. The protocol is illustrated in Figure 2.2 (C and D).

A

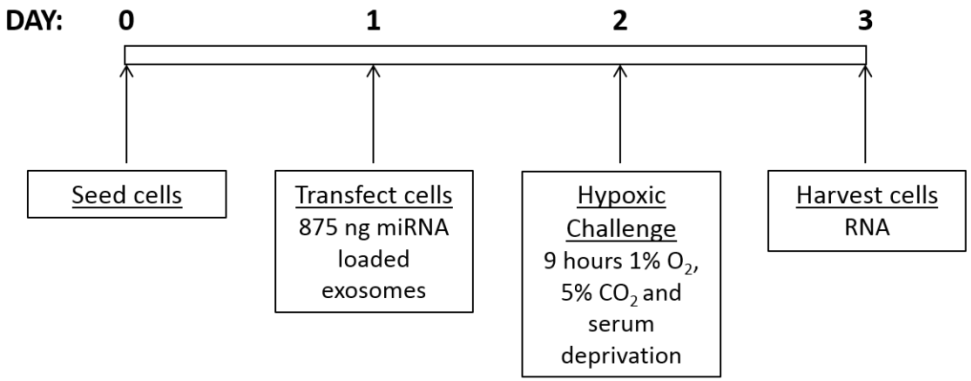

B

Condition	Day 1 cells transfected with:
#1	
#2	875 ng naïve exosomes
#3	875 ng miR-20b loaded exosomes
#4	875 ng miR-93 loaded exosomes

C

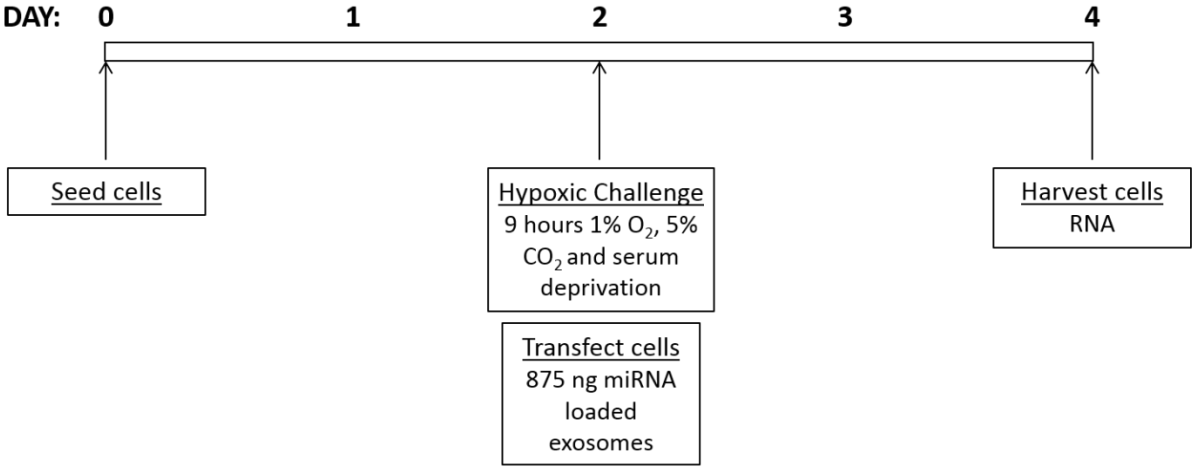

D

Condition	Day 2 cells transfected with:
#1	
#2	875 ng naïve exosomes
#3	875 ng miR-20b loaded exosomes
#4	875 ng miR-93 loaded exosomes

Figure 2.2 – Protocol for delivering miRNA loaded exosomes to B50 neuronal cells.
This diagram illustrates the protocol for delivering miRNA loaded exosomes pre-hypoxia (A) and post-hypoxia (C) and the number and nature of the conditions and controls used in each experiment (B and D).

2.2.3 Hypoxic Challenge

Cells (in cell culture plates) were washed once with DPBS before an appropriate volume of serum free media was added. The cell culture plate was placed inside the hypoxic chamber (Modular Incubator Chamber Mic-101, Bilrups-Rothenberg) which was subsequently semi-sealed. The hypoxic chamber was perfused with gas (1% O_2, 5% CO_2 and balance N_2) at a rate of 20 L/minute for 4 minutes, ensuring all atmospheric air had been flushed out of the chamber. The hypoxic chamber was then completely sealed before being placed in a 37ºC incubator for 9 hours. Typically, cells were removed from the chamber and serum free media replaced with complete media, before being left for 24 hours of reoxygenation, after which the cells were harvested or processed for subsequent analysis.

2.2.4 Harvesting of Cells

When harvesting RNA, the cells were washed twice with DPBS before 700 µL (per well) of QIAzol Lysis Reagent (Qiagen, Manchester, UK) was added. Adherent cells were gently rubbed away from the surface of the cell culture plate using the rubber end of a sterile 1 mL syringe plunger. The lysed cell suspension was transferred to a 1.5 mL eppendorf and placed on dry ice until transferred to a -80ºC freezer for long term storage.

When harvesting protein, cells were washed twice with DPBS before 500 µL (per well) of Radio-Immunoprecipitation Assay buffer (RIPA; 20 mM Tris pH 7.5, 150 mM NaCl, 2.5 mM sodium pyrophosphate, 1 mM EDTA, 1 mM ethylene glycol tetraacetic acid (EGTA), 1 mM ß-glycerophosphate, 1 mM sodium orthovanadate, 1mM phenylmethylsulfonyl fluorid (PMSF), 1 µg/mL leupeptin, 1% (v/v) Triton-X-100) was added. A smaller volume of RIPA buffer was added when a more concentrated protein sample was required. RIPA buffer efficiently lyses cells and solubilises proteins but does not degrade proteins or interfere with their biological activity.

2.2.5 Cryo-Preservation and Recovery of Cultured Cell Lines

To harvest cells for cryo-preservation, cells were trypsinised and centrifuged as described in section 2.2.1. The cell pellet was then resuspended in 2 mL complete media supplemented with 10% (v/v) dimethyl sulphoxide (DMSO;

Thermo Scientific™). The cell suspension was aliquoted (1 mL per aliquot) into a cryo-preservation vial and cooled at a constant -1ºC / minute to -80ºC using a Mr Frosty™ Freezing Container (Thermo Scientific™) containing isopropanol. Frozen cells were stored indefinitely in liquid nitrogen.

To recover cryo-preserved cells, frozen vials were removed from liquid nitrogen and rapidly thawed, before 10 mL of pre-warmed (to 37ºC) complete media was added slowly, allowing for a gradual change in the osmotic gradient. Cells were centrifuged at 1500 rpm for 5 minutes to remove any remaining DMSO, the cell pellet was resuspended in complete media and the total volume added to a T-75 cm^3 cell culture flask.

2.3 Functional *In Vitro* Assays

2.3.1 Western Blotting

Early in the presented study (Chapter 3) western blots were carried out on cell lysates to detect changes in the expression of cellular proteins such as phosphatase and tensin homolog (PTEN). The antibodies used are summarised in Table 2.2.

2.3.1.1 Quantification of Protein Concentration

The protein concentration of each individual cell lysate was determined using a Pierce BCA Protein Assay Reagent (Thermo Scientific) with reference to a standard curve generated using bovine serum albumin (BSA). Clear 96 well plates containing protein samples mixed with BCA Protein Assay Reagent were left to incubate for 30 minutes at 37ºC before they were read using a spectrophotometer at an absorbance of 562 nm.

2.3.1.2 Western Blots with ECL detection

Protein lysates were denatured using a sample denaturation buffer (62.5 mM Tris [pH 6.8], 2% (w/v) sodium dodecyl sulfate (SDS), 10% (v/v) glycerol, 1.25% (v/v) ß-mercaptoethanol and 0.01% (w/v) bromophenol blue), which induced a negative charge on the protein via the association of SDS which promoted the

migration of the protein towards the anode. The solution was heated in either a heat block or a thermal cycler to 95˚C for 5 minutes.

GPNT cell protein lysates (3.9 – 12.1 μg, maximum protein concentration possible) were loaded onto precast gels (4-20% Mini-Protean® TGX™ Precast Gels, 10 well, 30μL/well; Bio-Rad) and separated and resolved by SDS – polyacrylamide gel electrophoresis (SDS-PAGE) at 200 V. A ladder of molecular weight markers (Amersham ECL Rainbow Molecular Weight Markers, GE Healthcare Life Sciences) was used as a reference for the proteins detected.

Proteins were transferred overnight (at 4˚C) to a 0.45 μM (pore size) polyvinylidene difluoride (PVDF) membrane (Amersham Hybond™-P, GE Healthcare Life Sciences) using a wet transfer system. Transfer buffer was made up to a final concentration of 0.25 M Tris, 1.92 M Glycine, 1% (w/v) SDS and 20% (v/v) methanol. When protein transfer was completed, membranes were blocked by incubation in either 10% (w/v) non-fat milk (Marvel) or 10% (w/v) BSA, if investigating the activity of phosphorylated proteins, for 6-8 hours at room temperature, with agitation.

After removal of the blocking agent the primary antibody (made up in 5% BSA in 1 X TBS) was added and left to incubate overnight at 4˚C. The membrane was then washed 6 times with Tris buffered saline containing 0.1% tween-20 (1 X TBS-T) for 10 minutes. When investigating phosphorylated protein expression, the initial 4 washes were with 5% (w/v) BSA made up in 1 X TBS-T.

Appropriate horse radish peroxidase (HRP) coupled secondary antibodies (made up in 5% (w/v) BSA in 1 X TBS) were then added and left to incubate for 1 – 1.5 hours at room temperature with agitation. Polyclonal swine anti-rabbit immunoglobulins HRP coupled secondary antibody (DAKO) was diluted at 1:2000 in 5% (w/v) BSA (in 1 X TBS-T) and incubated with the membrane for 1 - 1.5 hours. Washes (as above) were repeated and the membrane was then developed using Amersham™ ECL™ Western Analysis System (GE Healthcare Life Sciences) according to the manufacturer's instructions.

Western blots were then scanned using a ChemiDoc™ XRS+ System (Bio-Rad) and quantified using Quantity One® 4.6.8. software using the "Volume" function.

Table 2.2 – Antibodies used for Western Blot.
This table summarises the antibodies used, their antibody type, their product number, the company they were purchased from and the dilution they were used at in this study.

Antibody	Antibody Type	Company	Product No.	Dilution Used
PTEN	Rabbit Monoclonal	Cell Signalling	#9559	1:1000
Phospho-PTEN (Ser380/Thr382/383)	Rabbit Polyclonal	Cell Signalling	#9554	1:1000
Akt	Rabbit Polyclonal	Cell Signalling	#9272	1:1000
Phospho-Akt (Ser473)	Rabbit Polyclonal	Cell Signalling	#9271	1:1000
GAPDH	Rabbit Monoclonal	Cell Signalling	#2118	1:1000

2.3.2 Gelatin Zymography

GPNT cell protein lysates were re-suspended in 1 X Zymogram Sample Buffer without reducing agent (62.5 mM Tris-HCl [pH 6.8], 25% (v/v) glycerol, 4% (w/v) SDS, 0.01% (w/v) Bromophenol Blue; Bio-Rad). 1.7 – 3.5 μg of protein lysate (maximum concentration possible) was loaded onto precast gels (Ready Gel® 10% Zymogram Gel, Bio-Rad) and separated and resolved by electrophoresis at 100 V. A ladder of molecular weight markers (Amersham ECL Rainbow Molecular Weight Markers, GE Healthcare Life Sciences) was used as a reference for the proteins detected.

Following electrophoresis the gel was re-natured by incubation with 2.5% Triton X-100 (1 X Renaturation Buffer; Bio-Rad) for 30 minutes at room temperature, with gentle agitation. Subsequently the gel was incubated in a development buffer containing 50 mM Tris-HCl [pH 7.5], 200 mM NaCl and 5 mM $CaCl_2$ (1 X Development Buffer; Bio-Rad) for 36-48 hours at 37˚C. Gels were then stained by incubation (with agitation) for 1 hour at room temperature with 0.5% (w/v) Coomassie Blue made up in 10% (v/v) acetic acid and 40% (v/v) methanol. Gels were later repeatedly washed with de-staining solution (10% (v/v) acetic acid and 40% (v/v) methanol) until clear bands appeared on the blue background. Typically 1 hour of washes were required.

Zymogram gels were then scanned using a ChemiDoc™ XRS+ System (Bio-Rad) and quantified using Quantity One® 4.6.8. software using the "Volume" function – this expresses results in arbitrary units as a sum of the intensities of the pixels within the volume boundary area multiplied by the pixel area.

2.3.3 MTS Assay

To assess cell viability post-transfection with miRNAs, a CellTiter 96® AQ_{ueous} One Solution Cell Proliferation Assay (Promega) was used. GPNT cells were cultured in 96 well plates, transfected with miRNA mimics or anti-miRS and subjected to hypoxic challenge as described in sections 2.2.2.1 and 2.2.3.

24 hours after reoxygenation (following hypoxic challenge or control normoxic conditions) the cells were washed twice with DPBS and 100 μL of fresh media was then added to each well. 20 μL of CellTiter 96® AQueous One Solution Reagent was then added directly to each well. This was carried out in a darkened tissue culture hood, due to the light sensitive nature of the solution. Adding 20μL of reagent gave a final concentration of 333μg/mL MTS (3-(4,5-dimethylthiazol-2-yl)–5-(3-carboxymethoxyphenyl)–2-(4-sulfophenyl)-2H-tetrazolium) and 25 μM phenazine methosulfate (PMS).

The cells were subsequently incubated for 1-3 hours at 37˚C in a humidified, 5% CO_2 atmosphere. Viable cells were able to bio-reduce MTS into a formazan product, soluble in tissue culture medium, which caused a colourimetric change in the cell culture media. The absorbance was recorded every 30 minutes at 490 nm using a SpectraMax M2 plate reader (Molecular Devices) until the assay reached maximum sensitivity. The quantity of formazan product produced as measured by absorbance at 490 nm was taken to be directly proportional to the number of viable, living cells in cell culture. Absorbance was also measured in a well containing media and MTS reagent, but no cells, to measure background absorbance.

2.4 General Molecular Biology Techniques

2.4.1 RNA Extraction

Throughout this study RNA was extracted from cells, tissue, serum and exosomes using the Qiagen miRNeasy Micro Kit (Qiagen, Crawley, UK). RNA extractions were performed in a standard biological safety class II vertical laminar flow cabinet to prevent exposure to toxic phenol fumes.

Cells were vortexed with 700 μL QIAzol lysis reagent to homogenise the sample. Tissue samples, stored at -80˚C, were cut on dry ice (to approximately 50 mg) to prevent degradation of RNA at room temperature, before being placed into 700 μL QIAzol reagent and being homogenised using a Qiagen TissueLyser (at 25 Hz, for 30 seconds, repeated 2 times). When isolating RNA from serum samples, 1000 μL of QIAzol was added to 200 μL total serum and homogenised by a brief vortex. When isolating RNA from exosomes, the exosome pellet was resuspended in 100 μL DPBS before 700 μL of QIAzol was added and the sample vortexed. To release all of the RNA contained in a sample it was important that plasma membranes of cells and organelles were completely disrupted and so thorough homogenisation of samples was vital.

Following the addition of QIAzol and homogenisation the sample was incubated at room temperature for 5 minutes to promote the dissociation of nucleoprotein complexes. 140 μL of chloroform (200 μL for serum samples) was then added to the sample and vortexed for 15 seconds to ensure thorough mixing, important for phase separation. The sample was subsequently centrifuged at 12,000 x g for 15 minutes at 4˚C. Following centrifugation a clear separation of sample was visible: a pink organic phase, a white interphase and an upper colourless aqueous phase which contained the RNA. The upper aqueous phase was transferred to a new collection tube using a Gilson pipette before approximately 1.5 X volume of 100% ethanol was added, typically around 600 μL (900 μL for serum samples). This was mixed thoroughly by pipetting up and down.

700 μL of the ethanol/sample mix was then added to a RNeasy Mini spin column in a collection tube and centrifuged at 10,000 x g for 30 seconds at room temperature to allow the RNA to bind to the silica membrane of the spin

column. The flow through was discarded and the step was repeated with any remaining sample. The column was washed to remove any impurities, using two buffers supplied with the kit. Initially 700 μL RWT Buffer was added to the column and centrifuged briefly and the flow through discarded. RPE Buffer (500 μL) was added and the column centrifuged (repeated once) before the column was spun at 16,000 x g for 1 minute to dry the spin column membrane, ensuring no ethanol was carried over during RNA elution as this can interfere with downstream analysis of RNA expression.

Finally the RNeasy Mini spin column was transferred to a new 1.5 mL RNase-free eppendorf. An appropriate volume of RNase-free water (typically 30-50 μL) was then pipetted directly on to the spin column membrane and left for 1 minute before being centrifuged for 1 minute at 10,000 x g to elute the RNA. The eluate was then pipetted back onto the spin column membrane and centrifuged again to give a higher yield of RNA. The spin column was discarded and RNA stored at -80˚C until used.

The concentration and quality of each RNA sample was determined by taking an average of 2 readings using a NanoDrop™ (ND-1000 spectrophotometer; Thermo Scientific).

2.4.1.1 DNase Treatment of RNA

When extracting RNA from cells or tissue, samples were treated with DNase to remove contaminating genomic DNA – this is important when using the RNA in applications sensitive to very small amounts of genomic DNA including reverse transcription polymerase chain reaction (RT-PCR). This step was not performed when extracting RNA from serum or exosomes.

To DNase treat the RNA, after the addition of 350μL RWT buffer (usually 700μL) and centrifugation at 10,000 x g for 30 seconds, 80 μL of DNase (made up in RDD Buffer according to manufacturer's instructions) was pipetted directly onto the spin column membrane and left at room temperature for 15 minutes. Subsequently a further 350 μL of RWT Buffer was added and the spin column centrifuged again at 10,000 x g for 30 seconds. The remaining part of the RNA extraction protocol was carried out as described in section 2.4.1.

2.4.2 Reverse Transcription Polymerase Chain Reaction (RT-PCR)

2.4.2.1 RT-PCR for Investigating microRNA Expression

Reverse transcription reactions were performed for each specific miRNA of interest and for a control miRNA, to allow for normalisation of the data generated. When investigating miRNA expression in rat tissue (*in vivo* or *in vitro*) U87 was used as a control and when investigating miRNA expression in serum or exosomes, samples were spiked with a known amount of *C. elegans* miRNA-39.

To create cDNA for miRNA analysis the Taqman® microRNA Reverse Transcription Kit (Life Technologies) was used. A single reaction contained 1 mM of each dNTP, 3.33 U/µL Multiscribe™ Reverse Transcriptase, 1 X Reverse Transcription Buffer, 0.25 U/µL RNase Inhibitor (provided with the kit), 1 X TaqMan® microRNA Reverse Transcription primer (Life Technologies) and a total of 5 ng RNA. Nuclease-free water was added to make a reaction volume of 7.5 µL. Non-template controls (NTC) were used for each specific miRNA primer - nuclease-free water was added in the place of RNA. Reverse transcription was carried out using a thermal cycler (PTC-225, MJ Research): 16ºC for 30 minutes (this allows for the binding of the miRNA primer), 42ºC for 30 minutes (this is when reverse transcription takes place) and 85ºC for 5 minutes (to inactivate the reverse transcription enzyme). cDNA samples were stored at -20ºC until used.

2.4.2.2 RT-PCR for Investigating Gene Expression

To create cDNA for gene analysis the TaqMan Reverse Transcription Reagents kit (Life Technologies) was used. A single reaction contained 1 X Reverse Transcription Buffer, 5.5 mM $MgCl_2$, 0.5 mM of each dNTP, 2.5 µM random hexamers, 0.4 U/µL RNase Inhibitor and 1.25 U/µL Multiscribe™ Reverse Transcriptase and between 200-1000 ng of total RNA (this was kept consistent within experiments). Nuclease-free water was added to make a reaction volume of 20 µL. Non-template controls (NTC) were used in which nuclease-free water was added in the place of RNA. Reverse transcription was carried out using a thermal cycler (PTC-225, MJ Research): 25ºC for 10 minutes (this allows for the annealing of primers), 48ºC for 30 minutes (when reverse transcription takes place) and 95ºC for 5 minutes (to inactivate the reverse transcriptase enzyme). When the reaction had completed each sample was diluted by the addition of 30

µL nuclease-free water, this did not significantly affect gene expression levels but ensured plenty of cDNA was available for future experiments. Samples were then stored at -20ºC until used.

2.4.3 qRT-PCR

TaqMan® qRT-PCR was used to quantify the expression of specific mRNAs and miRNAs within cells, tissue, serum and exosomes. To measure the expression of a specific mRNAs/miRNAs, fluorescent signal, produced proportionally during the amplification of cDNA was measured.

Each TaqMan® qRT-PCR assay is labelled with a fluorescent reporter dye (5' end, e.g. VIC or FAM) and a quencher molecule (3' end). During amplification, if the target mRNA/miRNA sequence is present the TaqMan probe binds and anneals and *Taq* DNA polymerase (within the reaction mix) degrades the TaqMan® probe, resulting in the cleavage the quencher molecule from the probe. This allows the fluorescent reporter dye to be detected. If a TaqMan® probe binds to a target sequence, the amount of fluorescence produced in each amplification cycle is proportional to the amount each specific mRNA/miRNA is amplified each cycle. Conversely, if the target mRNA/miRNA sequence is not present, the TaqMan probe does not bind and so remains intact, meaning any fluorescence released from the reporter dye is transferred to the quencher molecule, and no fluorescence is detected - this is known as fluorescence resonance energy transfer (FRET).

The fluorescence of miRNA/genes of interest was normalised to that of control ('housekeeper') miRNA/genes, which were chosen for their relatively stable expression throughout a particular set of samples, allowing for the comparison of expression levels between all samples.

To investigate miRNA expression TaqMan® miRNA RT-PCR probes were used (see Table 2.3). Each reaction was made up of 1 X TaqMan® Universal PCR Master Mix II (no UNG), 1 X TaqMan® miRNA qRT-PCR probe and nuclease-free water was added to make a total volume of 9.3 µL, to which was added 0.7 µL of cDNA produced at the miRNA RT-PCR step (see section 2.4.2.1).

To investigate mRNA expression TaqMan® Gene Expression assays were used (see Table 2.4). Each reaction was made up of 1 X TaqMan® Universal PCR Master Mix II (no UNG), 1 X TaqMan® Gene Expression probe and nuclease-free water was added to make a total volume of 8.5 µL, to which was added 1.5 µL of diluted cDNA produced at the mRNA RT-PCR step (see section 2.4.2.2).

Experiments were performed in 384-well plates using an ABI Prism 7900HT Sequence Detection System (Applied Biosystems). The reaction was initiated by heating the sample mixture to 95ºC for 10 minutes (denaturation) which was followed by 40 cycles of 95ºC for 15 seconds (further denaturation) and 60ºC for 60 seconds (primer and probe annealing and primer extension).

Data were collected when PCR amplification was in the exponential phase and analysed using the ΔΔCt method (Livak and Schmittgen, 2001). The cycle threshold (Ct) of a particular sample is the number of amplification cycles required for the fluorescence dye emissions to reach a specific level. The data are normalised by calculating the ΔCt, the difference between the Ct of the miRNA or gene of interest and the Ct of the control (housekeeper) miRNA or gene. The mean ΔCt of a number of biological replicates for the same mRNA/miRNA was then calculated. ΔΔCt was subsequently calculated using the following equation:

$$\Delta\Delta Ct = \Delta Ct\ (treated\ samples) - \Delta Ct\ (untreated\ or\ control\ samples)$$

Relative quantification (RQ), which is essentially the fold increase or decrease in miRNA/mRNA expression between a group of treated samples and the control samples, is calculated using the following equation:

$$RQ = 2^{-\Delta\Delta Ct}$$

RQ of a specific miRNA/mRNA is always given relative to the expression in the control group, whose expression is always given as 1. qRT-PCR analysis was performed using Microsoft Excel and GraphPad Prism.

Table 2.3 – List of miRNA TaqMan® assays used in this study.
The table also gives details of their miRBase Identifier (accession number) and their respective assay IDs (as used by Life Technologies).

Assay Name	miRNA	miRBase Identifier	Assay ID
cel-miR-39	cel-miR-39-3p	MIMAT0000010	000200
hsa-let-7e	hsa-let-7e-5p	MIMAT0000066	002406
hsa-miR-17	hsa-miR-17-5p	MIMAT0000070	002308
hsa-miR-20b	hsa-miR-20b-5p	MIMAT0001413	001014
hsa-miR-27b	hsa-miR-27b-3p	MIMAT0000419	000409
hsa-miR-29b	hsa-miR-29b-3p	MIMAT0000100	000413
hsa-miR-30a-5p	hsa-miR-30a-5p	MIMAT0000087	000417
hsa-miR-31	hsa-miR-31-5p	MIMAT0000089	002279
hsa-miR-32	hsa-miR-32-5p	MIMAT0000090	002109
hsa-miR-34b	hsa-miR-34b-5p	MIMAT0000685	000427
hsa-miR-93	hsa-miR-93-5p	MIMAT0000093	001090
hsa-miR-199a-3p	hsa-miR-199a-3p	MIMAT0000232	002304
hsa-miR-206	hsa-miR-206	MIMAT0000462	000510
hsa-miR-218	hsa-miR-218-5p	MIMAT0000275	000521
hsa-miR-223*	hsa-miR-223-5p	MIMAT0004570	002098
hsa-miR-323-3p	hsa-miR-323a-3p	MIMAT0000755	002227
hsa-miR-376a	hsa-miR-376a-3p	MIMAT0000729	000565
hsa-miR-451	hsa-miR-451a	MI0001729	001141
hsa-miR-454	hsa-miR-454-3p	MIMAT0003885	002323
hsa-miR-520b	hsa-miR-520b	MIMAT0002843	001116
hsa-miR-549	hsa-miR-549a	MIMAT0003333	001511
hsa-miR-660	hsa-miR-660-5p	MIMAT0003338	001515
hsa-miR-1291	hsa-miR-1291	MIMAT0005881	002838
rno-miR-21	rno-miR-21-5p	MIMAT0000076	000397
rno-miR-494	rno-miR-494-3p	MIMAT0003193	462468_mat
U87	U87	NCBI Accession: AF272707	001712

Table 2.4 – List of mRNA TaqMan® assays used in this study.
The table also gives details of their respective Assay IDs (as used by Life Technologies).

Gene Name	Assay ID
UBC	Rn01789812_g1
GAPDH	Rn01482168_m1
ß-ACT	Rn01447976_m1
18S	Rn03928990_g1
B2M	Rn00560865_m1
MMP2	Rn01538170_m1
MMP9	Rn00579162_m1
PTEN	Rn01538170_m1

2.4.4 DNA Extraction/Purification

DNA was extracted using a PureLink® Genomic DNA Mini Kit (Invitrogen). Ear clips from miR-21$^{+/-}$ and miR-21$^{-/-}$ mice pups were placed in an eppendorf and immersed in a mixture of 180 µL PureLink Genomic Digestion Buffer and 20 µL Proteinase K. The eppendorf containing the ear clip and digestion buffer was incubated at 55˚C in a water bath for a minimum of 4 hours, typically overnight. The eppendorf was vortexed to ensure complete lysis and then centrifuged at 16,000 x g for 3 minutes at room temperature to remove any particulate materials. The supernatant was then transferred to a fresh, sterile eppendorf. 20 µL RNase A was added to the lysate, to remove transcript copies from the sample, which was subsequently vortexed and incubated at room temperature for 2 minutes. 200 µL PureLink Genomic Lysis/Binding Buffer was added and the solution vortexed. This was followed by the addition of 200 µL 100% ethanol and further vortexing to precipitate the DNA.

The complete lysate, approximately 640 µL, was added to a PureLink Spin Column sitting in a collection tube, and the column was centrifuged for 1 minute at 10,000 x g, to allow the sample to bind to the membrane. The collection tube with the flow through was discarded and the spin column placed in a fresh collection tube. Next the sample was washed with buffers supplied with the extraction kit to remove impurities: 500 µL Wash Buffer 1 was added to the column and the column centrifuged at 10,000 x g for 1 minute. The collection tube with the flow through was again discarded and the spin column placed in a fresh collection tube, to which was added 500 µL Wash Buffer 2. The column was centrifuged at 16,000 x g for 3 minutes, before being placed in a 1.5 mL eppendorf, and the previous collection tube discarded. Finally, 30 µL PureLink Genomic Elution buffer was added to the column which was then incubated for 1 minute at room temperature before being centrifuged at 16,000 x g for 1 minute. The resulting eluate contained genomic DNA and was re-added to the spin column and centrifuged again at 16,000 x g for 1.5 minutes to give a higher yield of genomic DNA. The spin column was then discarded and the DNA stored at -20˚C until needed for further experiments.

2.4.5 Genotyping of Transgenic Animals

2.4.5.1 Genotyping of miR-21$^{-/-}$ Mice

PCR was carried out using primers specific for the miR-21 region of the genome (Forward: 5'-GGG CGT CGA CCC GGC TTT AAC AGG TG-3' and Reverse: 5'-GGG CGT CGA CGA TAC TGC TGC TGT TAC CAA G-3'; Eurofins MWG Operon).

A master mix was prepared for each PCR reaction, comprised of 5 µL 5 X Green GoTaq® Flexi Buffer, 3 µL 25 mM $MgCl_2$ solution, 0.5 µL 10 mM PCR nucleotide mix, 1 µL 10 µM forward primer, 1 µL 10 µM reverse primer, 0.125 µL GoTaq® DNA Polymerase (5U/µL) and 12.88 µL nuclease free water. To this was added 1.5 µL of 20 ng/µL DNA making a solution that contained 1 X Green GoTaq® Flexi Buffer, 3 mM $MgCl_2$ solution, 0.2 mM of each dNTP, 0.4 µM forward primer, 0.4 µM reverse primer and 0.625 U GoTaq® DNA polymerase. Aside from the primers, all components for the master mix were purchased from Promega.

To amplify the transcript of interest, the sample was heated to at 95˚C for 2 minutes, followed by 35 cycles of 95˚C for 15 seconds, 62.3˚C for 35 seconds, 72˚C for 30 seconds. A final cycle of 72˚C for 5 minutes completed the PCR. If not being used immediately PCR products were stored at -20˚C.

PCR product was subsequently loaded into a 2% agarose gel containing ethidium bromide and run at 100 V for approximately 30 minutes. They were then visualised using a ChemiDoc™ XRS+ System (Bio-Rad). Genotype was determined by the size of specific bands on the gel: the knock-out allele band was at 330 bp and the wild type allele band at 469 bp, see Figure 2.3.

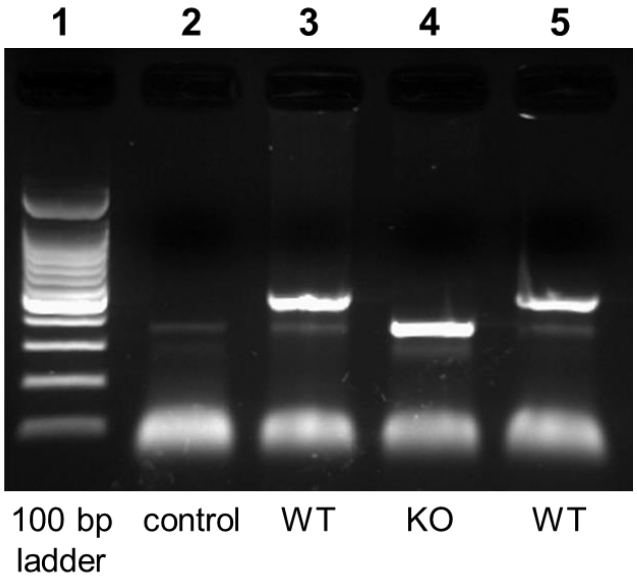

Figure 2.3 – Genotyping of miR-21$^{-/-}$ Mice.
Lane 1: 100 bp ladder. Lane 2: control sample (PCR master mix, no DNA). Lane 3: 469 bp band is visible indicating a WT mouse. Lane 4: 330 bp band is visible indicating a miR-21$^{-/-}$ (knockout) mouse. Lane 5: 469 bp band is visible indicating a WT mouse.

2.4.5.2 Genotyping of miR-21$^{+/-}$ Mice

PCR was carried out using primers specific for a GFP tag (Forward: 5'-TCT TCT TCA AGG ACG ACG GCA ACT-3' and Reverse: 5'-TGT GGC GGA TCT TGA AGT TCA CCT-3'; Eurofins MWG Operon).

A master mix was prepared for each PCR reaction, comprised of 5 µL 5 X Green GoTaq® Flexi Buffer, 2 µL 25 mM $MgCl_2$ solution, 1 µL 10 mM dNTPs, 1 µL 10 µM forward and reverse primer mix, 0.25 µL GoTaq® DNA Polymerase (5U/µL) and 14.75 µL nuclease free water. To this was added 1 µL of 20ng/µL DNA making a solution that contained 1 X Green GoTaq® Flexi Buffer, 2 mM $MgCl_2$ solution, 0.4 mM of each dNTP, 0.4 µM forward primer, 0.4 µM reverse primer and 1.25 U GoTaq® DNA polymerase. Aside from the primers, all components for the master mix were purchased from Promega.

To amplify the transcript of interest, the sample was heated to at 95˚C for 2 minutes, followed by 32 cycles of 95˚C for 30 seconds, 60˚C for 30 seconds, 72˚C for 60 seconds. A final cycle of 72˚C for 5 minutes completed the PCR. If not being used immediately the PCR products were stored at -20˚C.

PCR product was loaded into a 2% agarose gel containing ethidium bromide and run at 100 V for approximately 30 minutes. They were then visualised using a ChemiDoc™ XRS+ System (Bio-Rad). Genotype was determined by the presence of a specific band on the gel, the 216bp GFP band (see Figure 2.4).

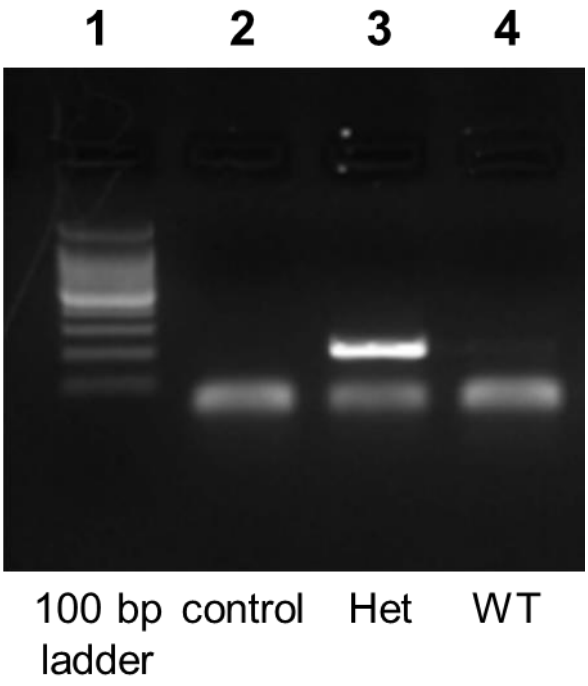

Figure 2.4 – Genotyping of miR-21$^{+/-}$ Mice.
Lane 1: 100 bp ladder. Lane 2: control sample (PCR master mix, no DNA). Lane 3: 216 bp GFP band is visible indicating a heterozygous miR-21$^{+/-}$ mouse. Lane 4: 216 bp GFP band is not visible indicating WT mouse.

2.5 Working with Exosomes

2.5.1 Exosome Isolation

2.5.1.1 Exosome Isolation from Serum

Exosomes were isolated from both human and rat serum using Total Exosome Isolation Reagent (from serum) (Invitrogen). Serum samples were thawed at room temperature and placed on wet ice until needed. The samples were then centrifuged for 30 minutes at 2,000 x g at 4˚C to remove any remaining cellular debris. 200 μL of supernatant was removed without disturbing the pellet and transferred to a fresh eppendorf. To this 40 μL of Total Exosome Isolation Reagent was added and the mixture vortexed until homogenous before being incubated at 4˚C for 30 minutes to precipitate exosomes. The mixture was

subsequently centrifuged for 10 minutes at 10,000 x g at room temperature. The supernatant was removed by pipette and the remaining exosome pellet was gently resuspended in 100 μL of DPBS and vortexed before being stored at 4˚C (short-term) or -80˚C (long-term).

2.5.1.2 Exosome Isolation from Cell Culture Media

Exosomes in this study were isolated from cell culture media by ultra-centrifugation. Cells were grown in 6 well plates. After initial seeding (Day 0) cells were incubated as normal (see section 2.2) until hypoxic challenge (Day 2). After cells were subjected to 9 hours of hypoxic or normoxic conditions media was collected and replaced with fresh cell culture media. Subsequently, cell culture media was collected (Day 3) prior to the cells being harvested, 24 hours post-reoxygenation. In total, for each biological 'n', approximately 24 mL of 'normoxic' media was collected and 18 mL of 'hypoxic' media.

To isolate exosomes from cell culture media, the media was filtered through a 0.22 μM syringe filter (Minisart® NML 16534K, cellulose acetate membrane; Sartorius) into Ultra-Clear™ Tubes (Thinwall, 17 mL, 16 x 102 mm; Beckman Coulter) before being ultra-centrifuged at 25.4 k rpm (~82,000 x g) for 2 hours at 4˚C (SW 32.1 Ti rotor, Optima™ L-80 XP Ultracentrifuge; Beckman Coulter). The supernatant was poured off and the tubes inverted on to tissue paper to drain. The exosome pellets (usually not visible) in each tube were resuspended in 1 mL DPBS (or more if required) and all samples were then pooled into 1 Ultra-Clear™ Tube before being ultra-centrifuged again at 25.4 k rpm for 1.5 hours at 4˚C. The supernatant was again poured off and the tube inverted on top off tissue paper before the final exosome pellet was resuspended in a small volume of DPBS (typically 300 – 500 μL) and stored at -80˚C until used.

2.5.1.3 Exosome Isolation from Brain Tissue

The protocol for isolating exosomes from brain tissue was optimised for use in our laboratory by Dr. Emily Ord and was developed using the protocol published by Perez-Gonzalez and colleagues (Perez-Gonzalez et al., 2012). Typically, exosomes were isolated from 6 brain hemispheres at one time. Initially, each brain hemisphere was incubated in 20 U/mL Papain (Sigma-Aldrich) made up in 3

mL of Hibernate®-E Medium (Gibco) for 15 minutes at 37˚C. Papain is a cysteine protease with wide specificity and is used here as it is more efficient and less destructive than other proteases and so suitable for the isolation of exosomes. Hibernate®-E Medium is a basal nutrient media (serum free) used for the short-term maintenance of brain tissue.

The brain hemispheres were subsequently removed from the Papain solution and placed into fresh 15 mL falcon tubes containing 6 mL ice-cold Hibernate®-E solution before the brain tissue was gently homogenised using a 5 mL syringe and serially smaller needle gauges (18G, 19G, 21G, 23G and 25G). Once fully homogenised a further 1 volume of ice-cold Hibernate®-E was added to the brain homogenate, which was homogenised again if required. The brain homogenate was filtered using a Falcon® 40 μM Cell Strainer (Corning) into a petri dish. The filtrate was then transferred into numerous 2 mL eppendorfs. The petri dish was washed with Hibernate®-E to make sure no sample was wasted and added to further 2 mL eppendorfs. The aliquoted filtrate was then centrifuged at 2,000 x g for 30 minutes at 4˚C to remove cellular debris. The supernatant was removed and placed in fresh 2 mL eppendorfs before being centrifuged at 12,000 x g for 45 minutes at 4˚C. Subsequently, the supernatant was filtered through a 0.22 μM syringe filter (Minisart® NML 16534K, cellulose acetate membrane; Sartorius) into an Ultra-Clear™ Tube (Thinwall, 17 mL, 16 x 102 mm; Beckman Coulter) before being ultra-centrifuged at 25.4 k rpm for 2 hours at 4˚C (SW 32.1 Ti rotor, Optima™ L-80 XP Ultracentrifuge; Beckman Coulter). The supernatant was poured off and the tubes inverted on to tissue paper to drain. The exosome pellets (usually visible) in each tube were resuspended in 1 mL DPBS (or more if required) and all samples were then pooled into 1 Ultra-Clear™ Tube before being ultra-centrifuged again at 25.4 k rpm for 1.5 hours at 4˚C. The supernatant was again poured off and the tube inverted on top off tissue paper before the final exosome pellet was resuspended in a small volume of DPBS (typically 300 – 500 μL) and stored at -80˚C until used.

2.5.2 NanoSight

Exosomes were visualised and their concentration quantified using Nanoparticle Tracking Analysis (NTA) on a NanoSight LM10 (Malvern). Approximately 500 μL of

diluted exosome sample (1:100 or 1:1000 in DPBS) was injected into the LM10 Viewing Unit using a syringe. The viewing unit was then placed onto the microscope stage, the laser was turned on and the stage adjusted until a clear view of the particles present in the solution was obtained, using a 20 X magnification microscope (with camera attached). The laser beam passing through the sample chamber illuminated particles in the path of the beam. Once a clear image could be seen through the microscope oculars, the image was diverted to the camera. The position and focus were adjusted as needed and a 60 second movie recorded, recording the particles moving under Brownian motion. NTA software tracked the movement of individual particles and calculated their hydrodynamic diameter using the Stokes-Einstein equation. A minimum of 3 recordings were taken for each sample and a representative recording picked. The operator was blinded to the sample name and subtype to prevent systematic bias in the selection of representative recordings.

2.5.3 Loading of microRNA into exosomes

The protocol for synthetically loading miRNA into exosomes was optimised by Dr. Emily Ord and based on a previously published protocol (El-Andaloussi et al., 2012). To load miRNAs into exosomes, miRNA mimic was mixed in an equal ratio with exosomes and electroporated using Geneflow Electroporation Cuvettes (Sterile, 1mm electrode, Red Cap; Geneflow) and a Bio-Rad MicroPulser™ Electroporator.

Initially the concentration of an exosome sample was calculated by BCA assay and exosomes diluted to a concentration of 0.56 µg/µL in 50 mM Trehalose (Sigma-Aldrich). Subsequently an equal volume (to the diluted exosome sample) of 0.56 µg/µL miRNA mimic was made up in 50 mM Trehalose. These were mixed together and left on wet ice for 45 minutes. Trehalose was used to prevent the exosomes aggregating, ensuring efficient transfer of miRNA to exosome.

Subsequently 125 µL of exosome/miRNA mimic mixture was added to an electroporation cuvette and given a 400 V pulse using a Bio-Rad MicroPulser™ Electroporator. Immediately following the electroporation pulse 875 µL of ice cold 1% (w/v) BSA (Sigma-Aldrich) was added to the cuvette and mixed by pipetting. The complete sample was then transferred to a falcon tube sitting in

wet ice. Once the complete amount of exosome/miRNA mixture had been electroporated it was left on ice for approximately 30 minutes.

The electroporated exosome mixture was then transferred into an Ultra-Clear™ Tube (Thinwall, 17 mL, 16 x 102 mm; Beckman Coulter) before being ultra-centrifuged at 25.4 k rpm for 1.5 hours at 4˚C (SW 32.1 Ti rotor, Optima™ L-80 XP Ultracentrifuge; Beckman Coulter). The supernatant was poured off and the tubes inverted on to tissue paper to drain. The electroporated exosome pellet (usually visible) was resuspended in 1 mL DPBS (or more if required) and ultra-centrifuged again at 25.4 k rpm for 1.5 hours at 4˚C. The supernatant was again poured off and the tube inverted on top off tissue paper before the final exosome pellet was resuspended in a small volume (100 – 300 μL) of sterile DPBS (if being used *in vitro*) or sterile 0.9% (w/v) sodium chloride (Baxter, Newbury, UK) (if being used *in vivo*) and stored at -80˚C until used.

2.6 Human Patient Exosomal miRNA Study

2.6.1 Patient Recruitment

This study was approved by the Scotland A Research Ethics Committee (reference number: 11/SS/0077) and all patients involved gave informed, written consent. Between the 31st January 2012 and 19th August 2014 217 patients were recruited at the Acute Stroke Unit, Western Infirmary, Glasgow. Patients presenting at the Western Infirmary with stroke-like symptoms were referred to the Acute Stroke Unit where they were assessed by stroke-specialist clinicians and subsequently re-assessed at 48 hours, 7 days, 1 month and 3 months post-presentation.

Initially a detailed cardiovascular patient history was taken, prescription medication recorded and a medical examination performed. Diagnosis was aided by one or several of the following investigations: CT scan, MRI scan, Carotid Doppler ultrasound, angiography, echocardiogram, electrocardiogram and cardiac monitor. Patients were then officially diagnosed as having a definite ischaemic stroke, a possible ischaemic stroke or as a non-stroke patient. Non-stroke patients usually presented with symptoms of stroke but were subsequently given a differential diagnosis: for example, severe migraine.

Definite stroke patients were classified according to TOAST criteria (Adams et al., 1993) which categorises patients according to their stroke pathophysiology, as having a stroke as a result of large artery atherosclerosis, a cardioembolism, a small vessel occlusion or a stroke with an unknown aetiology.

At each visit stroke severity was assessed using the 42-point NIHSS, and at 1 and 3 months post-stroke outcome from stroke was assessed using mRS (a measure of disability), the Barthel Index (assesses performance in activities of daily living) and the Stroke Impact Scale (a measure of how stroke has affected quality of life for the patient).

After initial recruitment at the Western Infirmary a number of patients withdrew their consent. For a further number of patients there was an insufficient volume of serum harvested or remaining and so in the present study serum samples from 173 patients were used. In the OpenArray exosomal miRNA expression was profiled in 39 patients: of which there were non-stroke (n=10), large artery (n=9), cardioembolic (n=10) and small vessel (n=10) patients. Expression of carefully selected miRNAs was validated by qRT-PCR in a larger population of 173 patients: of which there were non-stroke (n=34) and stroke (n=139) patients. In the stroke patient population there were large artery (n=22), cardioembolic (n=40), small vessel (n=37) and unclassified (n=40) patients.

2.6.2 Sample Collection

Peripheral blood samples were collected when patients presented at the Western Infirmary, and subsequently at 48 hours, 7 days, 1 month and 3 months post-stroke or presentation at the Acute Stroke Unit, in the case of non-stroke patients. In this study blood samples collected at 48 hours post-incident onset were used. To isolate serum, blood samples were allowed to clot for 20 minutes and then were centrifuged at 3,000 x g for 15 minutes. The isolated serum was aliquoted and stored at -80˚C until used.

2.6.3 miRNA OpenArray

In this study miRNA expression was profiled in exosomes isolated from the serum of human patients. Exosomes were isolated as described in section 2.5.1 and resuspended in 100 µL PBS. Total RNA was extracted from the exosome

suspension using a miRNeasy Micro Kit (as described in section 2.4.1). The OpenArray experiment consisted of reverse transcription of RNA, pre-amplification of cDNA, and qRT-PCR on the OpenArray panel. A diagram summarising the OpenArray workflow is shown in Figure 2.5.

2.6.3.1 Reverse Transcription

cDNA was synthesised from total exosomal RNA harvested from serum of human patients using the TaqMan® MicroRNA Reverse Transcription Kit (Applied Biosystems). As a result of low RNA yield from the exosomes isolated from serum an optimised low sample input protocol was used (Life Technologies, 2011).

For each sample, cDNA was synthesised for two pre-defined pools of different miRNAs (Pool A or Pool B; 750 miRNA in total with 375 covered by each primer pool) – this allowed for the simultaneous reverse transcription of hundreds of miRNAs and endogenous controls. A total of 9.9 ng RNA was loaded into each reaction (3.3 μL of RNA at 3 ng/μL). Each reaction was also spiked with 2.5 ng of an exogenous spike-in control (*Arabidopsis thaliana*: ath-miR-159a). In summary, each reaction was made up of 1 X Megaplex™ RT Primers (Pool A or Pool B), 1 X dNTPs with a dTTP Inhibitor (29 U/μL), Multiscribe™ Reverse Transcriptase (10 U/μL), 1 X Reverse Transcription Buffer, 3 mM $MgCl_2$, RNase Inhibitor (0.25 U/μL) to which was added 2.5 ng of ath-miR-159a and a total of 9.9 ng exosomal RNA, all made up to a total volume of 7.5 μL with nuclease-free water.

Reverse transcription was performed in a 96 well plate and underwent sequential incubation in a thermal cycler: 16˚C for 2 minutes, 40˚C for 1 minute and 50˚C for 1 second (repeated for another 39 cycles) followed by an incubation at 85˚C for 5 minutes to complete the thermal cycling. cDNA was stored at -20˚C until pre-amplification was performed.

2.6.3.2 Pre-Amplification of cDNA

cDNA synthesised by RT-PCR was pre-amplified using TaqMan® PreAmp Master Mix and Megaplex™ PreAmp Primer Mix (Pool A or Pool B). Each reaction contained 1 X TaqMan® PreAmp Master Mix, 1 X Megaplex™ PreAmp Primer Mix,

the complete volume of cDNA synthesised previously (7.5 μL) and nuclease-free water to make a total volume of 40 μL.

Pre-amplification was performed in a 96 well plate which underwent sequential incubation: at 95˚C for 10 minutes, 55˚C for 2 minutes, 72˚C for 2 minutes, [95˚C for 15 seconds and 60˚C for 4 minutes, repeated for another 15 cycles] followed by an incubation at 99.9˚C for 10 minutes.

Each reaction was then diluted 1:20 using 0.1 X Tris-EDTA (TE) buffer, to make a total volume of 60 μL. The diluted pre-amplified cDNA was then stored at -20˚C until the OpenArray® experiment was performed. The diluted pre-amplified cDNA is only stable for 10-14 days following pre-amplification and so the OpenArray® experiments were completed in a timely fashion.

2.6.3.3 OpenArray®

The OpenArray® experiment was run using TaqMan® OpenArray® Human MicroRNA Panels. To load samples onto the OpenArray® panels, 12.5 μL of diluted (Pool A or Pool B) pre-amplified sample was first added to 36.75 μL of TaqMan® OpenArray® Real-Time PCR Master Mix, making a total volume of 49.25 μL. 5 μL of this was transferred (by pipetting) into one well in an OpenArray® 384-Well Sample Plate. This was repeated a further 7 times, making a total of 8 wells each containing 5 μL of a particular sample (either Pool A or Pool B).

Samples were subsequently loaded (from each 384-Well Sample Plate) onto a TaqMan® OpenArray® Human MicroRNA Panel using a QuantStudio™ 12K Flex AccuFill™ System. To prevent systematic bias as a result of card data generation, samples from each stroke subtype were randomised across 13 TaqMan® OpenArray® Human MicroRNA Panels. Loaded MicroRNA panels were then loaded into an OpenArray® Real-Time PCR instrument and panels underwent thermal cycling at 50˚C for 2 minutes, 95˚C for 10 minutes and (95˚C for 15 seconds and 60˚C for 1 minute, repeated for another 39 cycles).

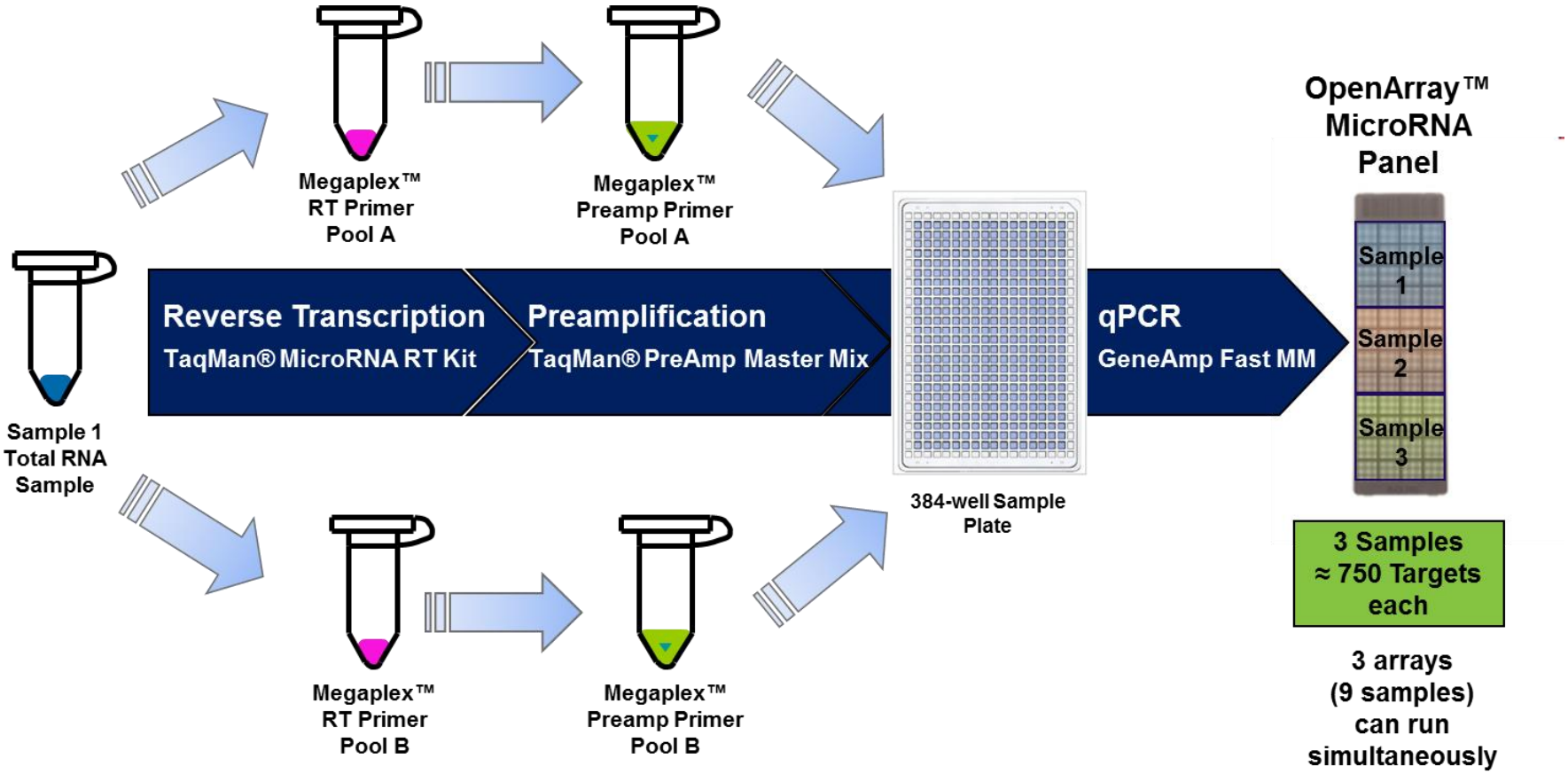

Figure 2.5 – OpenArray Workflow
This diagram summarises steps in the OpenArray workflow including reverse transcription of total RNA, the pre-amplification of cDNA and qRT-PCR performed on OpenArray™ MicroRNA Panels. In the reverse transcription step, cDNA was synthesised for two pre-defined pools of different miRNAs (Pool A or Pool B, 375 miRNAs in each primer pool) allowing for simultaneous reverse transcription of hundreds of miRNAs. This figure was adapted from information provided by Life Technologies.

2.6.3.4 OpenArray® Data Analysis

Data generated was analysed using DataAssist™ software. Data was normalised to the exogenous spike-in control (ath-miR-159a) and ΔCt values calculated and compared to non-stroke patient (control) values. Results for each individual miRNA were analysed using a two-tailed, Student's unpaired t-test.

2.6.4 OpenArray Validation by qRT-PCR

The expression of 13 miRNAs, detected as being differentially expressed by the OpenArray, was validated by qRT-PCR in a larger patient population. If possible all miRNAs whose expression was identified as being significantly changed by OpenArray would have been validated by qRT-PCR in the larger patient population. However, budget constraints meant that only 13 miRNAs could be validated in this way. miRNAs whose expression was determined to be significantly dysregulated by t-test (either in stroke vs. non-stroke or stroke subtype vs. non-stroke) were prioritised as were those miRNAs whose expression appeared to be 'turned on' in ischaemic stroke patients. Finally, those miRNAs whose expression appeared to be 'turned off' in all stroke subtypes or in small vessel disease stroke patients were taken forward for validation in the larger patient population. miRNAs altered in small vessel disease patients were prioritised over those 'turned off' in large artery and cardioembolic disease patients as small vessel disease stroke was hypothesised to be biologically and phenotypically quite different to large vessel and cardioembolic stroke.

2.6.4.1 Reverse Transcription

RNA was extracted from exosomes isolated from serum, as described earlier. RNA concentration and purity was determined and RNA diluted to a concentration of 2 ng/μL.

cDNA was synthesised by RT-PCR from the total RNA of isolated exosomes using the TaqMan® MicroRNA Reverse Transcription Kit. Each reaction contained 1 mM dNTPs, 3.33 U/μL Multiscribe™ Reverse Transcriptase, 1 X Reverse Transcription Buffer, 0.25 U/μL RNase Inhibitor, 1 X Reverse Transcription Buffer, 5 ng *C.Elegans* miR-39 (exogenous spike-in control) and 5 ng of sample RNA. RT-PCR was performed in 96 well plates and samples under sequential incubation: 16˚C

for 30 minutes, 42˚C for 30 minutes and 85˚C for 5 minutes. cDNA was stored at -20˚C until pre-amplification was performed. To control for the presence of contaminating RNA, a PCR-only experiment was carried out using otherwise identical conditions without input template RNA.

2.6.4.2 Pre-Amplification of cDNA

cDNA synthesised by RT-PCR was pre-amplified using TaqMan® PreAmp Master Mix. A pooled assay mix was created by mixing TaqMan® probes for 14 miRNAs of interest: *C.Elegans* miR-39, hsa-miR-27b, mmu-miR-93, hsa-miR-520b, hsa-miR-660, hsa-miR-20b, hsa-miR-30a-5p, hsa-miR-218, hsa-miR-17, hsa-miR-199a-3p, hsa-miR-223#, hsa-miR-376a, hsa-miR-549, hsa-let-7e. TaqMan® probes were mixed, giving a final concentration of 0.2 X for each probe.

Each pre-amplification reaction contained 1 X TaqMan® PreAmp Master Mix, 0.05 X pooled assay mix and 8.25 ng cDNA, made up to a total volume of 50 µL using nuclease free water. Reactions underwent sequential incubation in a 96 well plate at 95˚C for 10 minutes, followed by 95˚for 15 seconds and 60˚C for 4 minutes, repeated for another 13 cycles. The pre-amplified cDNA product was then diluted 1:5 with 1 X TE buffer. Diluted pre-amplified cDNA was stored at -20˚C until qRT-PCR was performed.

2.6.4.3 qRT-PCR

To profile miRNA expression qRT-PCR was performed using TaqMan® miRNA RT-PCR probes. Each reaction contained 1 x TaqMan® Universal PCR Master Mix II (no UNG), 1 X TaqMan® miRNA RT-PCR probe and nuclease-water added to make a total volume of 8 µL to which was added 2 µL of diluted pre-amplified cDNA. Duplicate reactions were run for each sample on a 384-well plate which was incubated as previously described in section 2.4.3.

2.6.4.4 Statistical Analysis

Data generated in the OpenArray Validation study were analysed as previously described in section 2.4.3. Data were normalised to the expression of the exogenous spike-in control: *C.Elegans* miR-39. RQ values were compared to the values for non-stroke patients. Results were analysed using a one-way-ANOVA

with post-hoc Dunnett's test. Statistical significance was taken at $p<0.05$. Statistics were calculated using GraphPad Prism.

2.7 *In Vivo* Methods

All animals were housed in controlled environmental conditions: ambient temperatures (20 - 26˚C) and humidity (40 - 70%) were maintained along with alternating 12 hour light and dark cycles. All animals were kept in standard polycarbonate cages in small groups of two to three and were fed ad libitum standard rat chow (rat and mouse No. 1 maintenance diet, Special Diet Services, UK) and untreated water. Work with experimental animals was in accordance with the Animal Scientific Procedures Act 1986 under the project licence held by Dr Delyth Graham, PPL 60/4286. All studies were approved by the University of Glasgow's Ethics Review Committee.

2.7.1 Animal Models

An inbred colony of stroke-prone spontaneously hypertensive rats (SHRSP) was maintained "in-house" by brother – sister mating. Lab microsatellite screening was carried out routinely to confirm the homozygosity of all loci within a random group from the colony. SHRSP demonstrate several physiological markers of cardiovascular disease, including hypertension, altered glucose handling and increased basal inflammatory status and are therefore comorbid and so are ideal candidates for modelling clinical stroke.

Transgenic mice were used in studies investigating the effect of miR-21 expression *in vivo*. Adult male miR-21$^{-/-}$ mice, with a mixed genetic background of S129/C57, and their WT littermates, were used to investigate the effect of knock-out of miR-21 expression. The mice were obtained by the University of Glasgow in collaboration with Professor Rhonda Bassel-Duby and Ms Cheryl Nolen (Olson Laboratory, UT Southwestern Medical Center, TX, USA). A local colony was set up at the University of Glasgow and animals were bred in house and males placed on procedure when they weighed 25-30 g. PCR of the miR-21 flanking region confirmed the genotype (see section 2.4.5.1).

Adult male miR-21$^{+/-}$ mice, with a B6/C3/F1 background, and their WT littermates, were used to investigate the effect of over-expression of miR-21. The mice were originally obtained by the University of Glasgow in collaboration with Dr Mark Hatley (St Jude Children's Research Hospital, Memphis, TN, USA). A colony was set up at the University of Glasgow and mice for these studies were bred in house and males used for experimental procedure when they weighed 25-30 g. PCR of GFP determined whether the mouse was heterozygous for the transgene (see section 2.4.5.2).

2.7.2 Preparation of animals for surgery

To prepare for any aseptic animal surgery, the operating table and surrounding area was initially disinfected using chlorhexidine solution before being covered with sterile drapes. All surgical instruments were autoclaved and instruments were also sterilised between surgeries to ensure every animal was operated on using sterile surgical instruments. Sterilised instruments were only placed within the sterile area of the table. Consumables used such as swabs, needles and suture materials, were sterile and only used within their stated expiry dates. The surgeon wore a sterile gown and sterile gloves.

Anaesthesia in SHRSP rats was induced in a Perspex chamber using 1.5 L/min 100% oxygen and 5% isoflurane. When the rat was sufficiently anaesthetised (typically after several minutes) an intubation tube (16-guage cannula) was inserted into the trachea, using a metal guide wire. To ensure sufficient visibility the mouth was held open using a plastic speculum and a surgical lamp was used to illuminate the throat and therefore the oesophageal-tracheal junction. SHRSP animals were artificially ventilated throughout experimental procedures: 0.3 L/min 100% oxygen, 2.5 mL stroke volume at 65 beats/minute (Harvard Model 683, Small Animal Ventilator; Harvard Apparatus, Cambridge, UK). Isoflurane levels were monitored throughout the duration of experimental procedures to maintain an appropriate depth of anaesthesia (typically ~3%).

During surgical procedures a rectal probe (VetTech Solutions Ltd, UK) was used to monitor body temperature and a heat lamp was used to keep temperature within appropriate physiological limits (37.5˚C ± 1˚C).

2.7.3 Cranial Burrhole

To improve survival in SHRSP rats following 45 minute tMCAO surgery, pre-stroke cranial burrhole surgery was carried out 4 or 5 days prior to stroke surgery. A previous study carried out within our group (Ord et al., 2012) has demonstrated that pre-stroke general anaesthesia combined with cranial burrhole surgery improved survival and reduced the weight loss associated with tMCAO surgery, whilst not affecting systolic blood pressure, infarct volumes or neurological deficit. This is therefore an important methodological refinement for the tMCAO procedure, especially when it is carried out in SHRSP, an animal model that has many co-morbidities associated with clinical stroke.

SHRSP rats were anesthetised, intubated and ventilated as previously described (section 2.7.2). Animals were then placed in the prone position in a stereotaxic frame (Ultra Precise Lab Standard Stereotaxic Frame for Rat; Stoelting, Dublin, Ireland) and positioned carefully, as illustrated in Figure 2.6. The head was secured in place using stereotaxic ear bars. The skin covering the skull was first shaved before being disinfected using chlorhexidine solution.

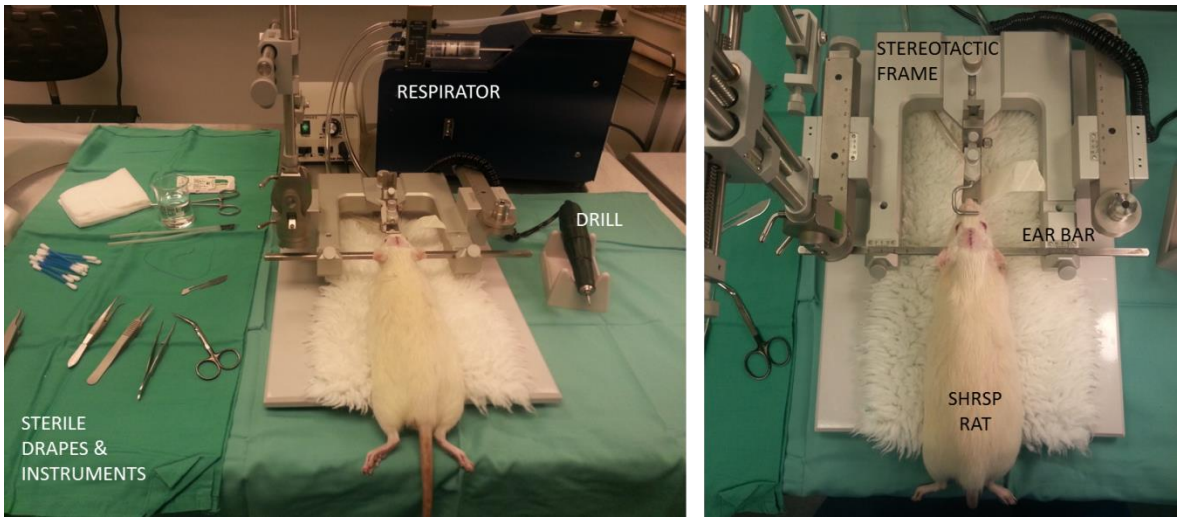

Figure 2.6 – Cranial burrhole surgery.
Photographs illustrating surgical set-up for pre-stroke cranial burrhole surgery. SHRSP rat is intubated, artificially ventilated and positioned in stereotaxic frame. Sutured incision above the skull is visible.

When the head was secure and the skin disinfected, a small incision was made in skin above the skull and the superficial fascia gently rubbed away using sterile cotton buds. Small retractors were used when necessary to keep the surgical area clear. A 1mm diameter burrhole was drilled (Tech 2000 Handpiece,

Microtorque Control Box; Ram Products, Dayton, NJ, USA). The dura was then pierced using a 24G Hamilton syringe needle. The burrhole was later sealed using dental cement (Prontolute; Wright Cotterell, UK). The procedure typically lasted about 30 minutes, not exceeding 40 minutes at any time.

To recover the animal, the isoflurane supply was turned off but mechanical ventilation with 100% oxygen at 0.3 L/min was maintained until independent breathing was observable. After the animal reached full consciousness it was moved to a recovery room where it was checked regularly.

2.7.4 Transient Middle Cerebral Artery Occlusion (tMCAO)

SHRSP rats were anesthetised as previously described (section 2.7.2). Intraluminal filaments (Doccol Corporation, CA, USA) were used to occlude the origin of the middle cerebral artery (MCA) inducing experimental stroke, a modified version of the protocol first described in 1989 (Longa et al., 1989) (illustrated in Figure 2.7). Throughout the surgery an operating microscope (M651, Leica Microsytems, UK) was used.

Initially, an area on the neck was shaved, and the area disinfected with chlorhexidine solution before a midline neck incision was made, and subcutaneous fatty tissue dissected. The left common carotid artery (CCA) was exposed and two retractors placed between the digastric, sternomastoid and sternohyoid muscles to keep the CCA visible. The CCA was exposed at the point of its bifurcation into the internal and external carotid arteries. The CCA was occluded – a ligature made of 5/0 silk suture (Sofsilk; Covidien, UK) was used to tie a square knot. The occipital artery was electrocoagulated using bayonet pointed tip bipolar forceps (Eschmann, Lancing, UK). The external carotid artery (ECA) was then temporarily ligated and a loose suture loop was tied around the internal carotid artery (ICA) and tension was applied. The pterygopalatine artery (PPA) was also temporarily ligated to ensure the intraluminal filament was advanced correctly up the ICA.

Tension was applied to the CCA, ECA and ICA and a small incision was made immediately below the bifurcation of the CCA using microscissors. A silicone-coated nylon filament, 0.37 mm in diameter (Doccal Corporation, CA, USA), was

inserted through the incision and advanced approximately 22 mm up the ICA, until resistance was felt. The origin of the middle cerebral artery (MCA) was occluded as a result. The filament was kept in place for 45 minutes using a ligature (Figure 2.7 A-C). If a sham procedure was being performed the filament was advanced as has been described but then immediately withdrawn and the surgery was continued as is subsequently described.

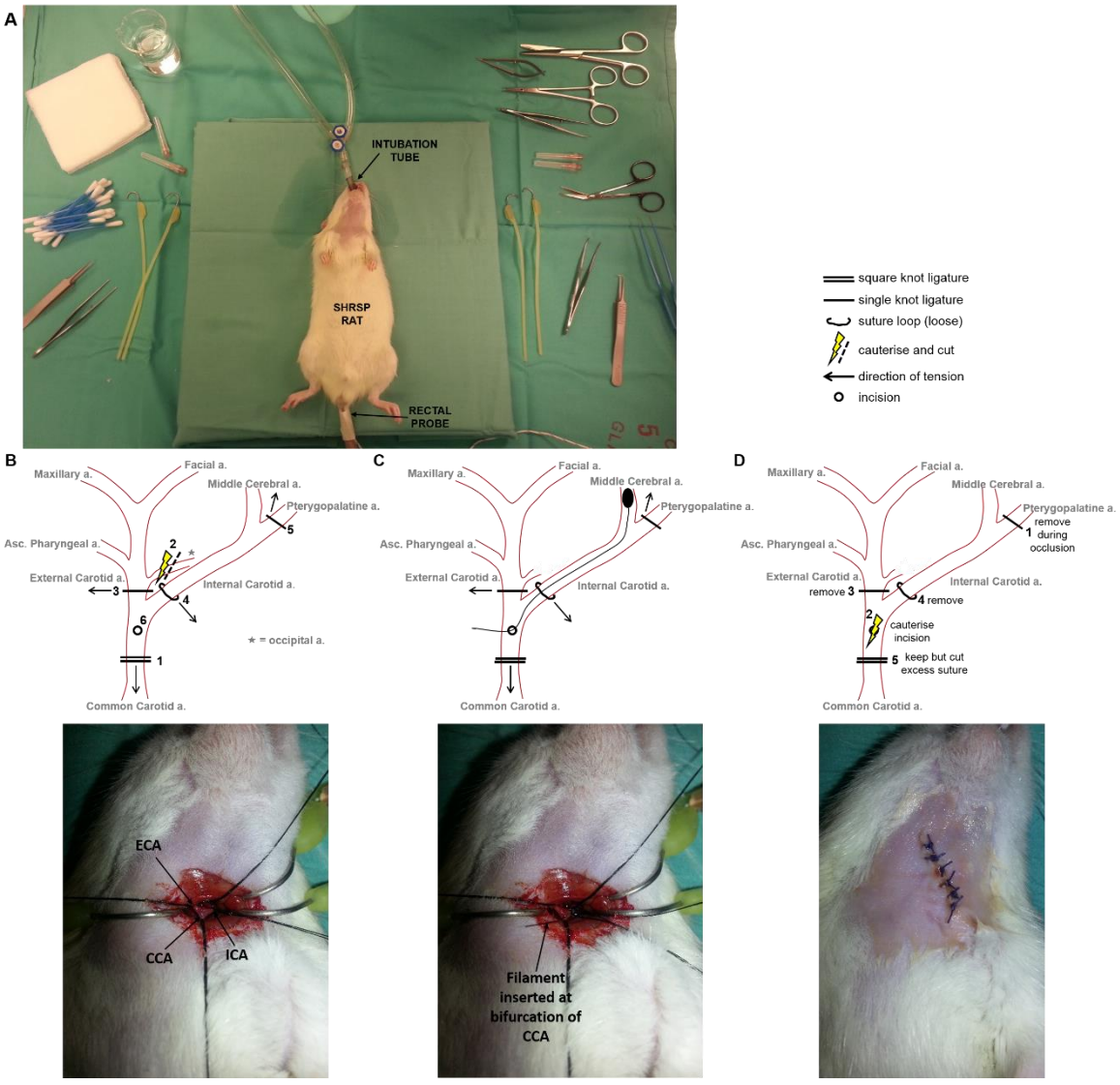

Figure 2.7 – tMCAO Surgery
Photograph illustrating surgical set up for tMCAO procedure (A). SHRSP is intubated and artificially ventilated, in supine position and in an aseptic surgical area. CCA, ECA, ICA and PPA ligated with silk sutures (B). Bifurcation of CCA to ICA/ECA visible. Intraluminal filament inserted at bifurcation of CCA, filament left in place for 45 minutes, occluding origin to MCA (C) After 45 minutes intraluminal filament is removed, incision electrocoagulated, ligatures removed and wound sutured using absorbance sutures (D).

After 45 minutes the intraluminal filament was removed and the incision of the CCA sealed by electrocoagulation. Ligatures were removed from the PPA and ECA and the suture loop from the ICA. The ligature on the CCA was left in place

and surplus suture cut away. Retractors were removed and the muscles of the neck gently massaged into place. Finally the neck wound was sutured using 4/0 vicryl absorbance suture (FS-2 needle, Ethicon, Livingston, UK) (Figure 2.7D).

To recover the animal, the isoflurane supply was turned off but mechanical ventilation with 100% oxygen at 0.3 L/min was maintained until independent breathing was observable. While the animal was recovering 2 mL of 0.9% (w/v) sodium chloride (Baxter, Newbury, UK) was given subcutaneously to prevent dehydration. After the animal reached full consciousness it was moved to a recovery room where it was checked regularly.

2.7.5 Tail-Cuff Plethysmography

To measure conscious systolic blood pressure in SHRSP rats a non-invasive computerised tail-cuff was used. SHRSP rats were warmed using heat lamps for 20 minutes. To restrain the free movement, each rat was gently wrapped in a surgical drape. A pneumatic pressure cuff and pneumatic pressure sensor were placed on the tail, the sensor distal to the cuff – both were controlled by a Programmed Electro Sphygmomanometer. Average systolic blood pressure measurements were calculated using a minimum of six consistent separate indirect pressure measurements. SHRSP rats were trained to become habituated to the pressure cuff and sensor before actual measurements were recorded.

2.7.6 Intra-nasal Delivery of Exosomes

Anaesthesia was induced in SHRSP rats as described in section 2.7.2, but rats were only allowed to become lightly anaesthetised. They were then placed in the supine position, with their nose inside a nose cone where they continued to receive light isoflurane anaesthesia (1.5 L/min 100% oxygen with 2-3% isoflurane) for the duration of the intra-nasal administration, typically several minutes. Immediately prior to each intra-nasal dose the rat was pulled away from the nose cone and the tip of a Gilson pipette (range: 2 - 20 µL) was placed at the tip of the rat's nare. 7.5 µL of solution (either 0.9% sterile saline or 2.5 µg/µL exosomes) was then delivered to the nare in one bolus. The head was placed inside the nose cone again and the rat was allowed to inhale the solution for approximately 30 seconds. A matching dose was then delivered in the same way

to the opposite nare. This was repeated twice so that each rat received a total volume of 30 µL, 15 µL in each nare. The rat was then placed in its cage in the supine position and allowed to recover from the anaesthesia.

2.7.7 Animal Sacrifice

Naïve rats and mice were killed using Schedule 1 methods of termination, whilst SHRSP rats put on procedure were killed by transcardiac perfusion fixation or removal of the heart under terminal anaesthesia.

2.7.7.1 Schedule 1

Naïve rats were typically killed by exposure to carbon dioxide in rising concentrations. Each rat was placed into a chamber into which carbon dioxide (CO_2) gas was subsequently flushed (8 L/min of 100% CO_2). When the animal was observed to be unconscious a maximal flow of CO_2 (10 L/min of 100% CO_2) was flushed into the chamber for 2 minutes. The carbon dioxide was then turned off and the rat left inside the sealed chamber for a further 2 minutes. The rat was then checked for any signs of life. If signs of life were present the rat was replaced inside the chamber and if absent death was ensured by neck dislocation.

Mice were typically killed by concussion of the brain by striking the cranium against the side of a bench. This caused immediate loss of consciousness and/or death. Death was ensured by neck dislocation. This Schedule 1 method was only carried out by fully trained animal technicians.

2.7.7.2 Cardiac Puncture Blood Sampling

In this study cardiac puncture blood samples were only taken terminally. Anaesthesia was induced (as described in section 2.7.2), and the rat was left within the induction box until very deeply anaesthetised. The rat was then placed in the supine position, with the head inside a nose cone where it continued to receive deep isoflurane anaesthesia (1.5 L/min 100% oxygen with 5% isoflurane). A transverse incision was then made below the sternum to expose the thoracic cavity and rib cage. The rib cage was cut at either side to expose the beating heart. A 19-gauge needle attached to a 5 mL syringe was then

inserted into the left ventricle and blood was removed slowly to prevent the heart collapsing. Animals were then euthanised as described in sections 2.7.7.3 or 2.7.7.4.

Typically 5 mL of blood was easily removed. This was injected into 2 mL eppendorfs and allowed to clot for approximately 30 minutes at room temperature. The clotted blood samples were then centrifuged for 2000 x g for 10 minutes at 4ºC. The clear supernatant (serum) was immediately removed using a Gilson pipette and transferred to a fresh eppendorf. Serum aliquots were frozen at -80ºC until used for further analysis.

2.7.7.3 Perfusion Fixation

Chemical fixation was used as a method of euthanasia to preserve tissue. Typically chemical fixation was achieved using 4% paraformaldehyde (PFA) which maintains cellular definition of tissue, stabilising cell morphology and disabling proteolytic enzymes. It also strengthens the tissue to withstand downstream processing and/or staining.

To perfusion fix SHRSP rats, the rat was deeply anaesthetised and the heart exposed as described in section 2.7.7.2. A 16-gauge needle (blunted) was inserted into the apex of the heart and advanced until visible in the aorta. A hemostat was used to clamp the needle into place. An incision was then made on the right atrium and the process of exsanguination begun. Simultaneously pressure was applied (120 mmHg) resulting in the perfusion of heparinised (10 U/mL) saline. The rat was perfused with heparinised saline until the liver appeared ‘clear’ of blood and the outflow from the right atrium was free from blood. The animal was then perfused with 4% PFA until firm and stiff to touch. The head was removed and submerged in 4% PFA for a further 24 hours. The brain was then carefully removed and stored in 4% PFA for another 24 hours before being placed in PBS, to be kept until tissue processing was carried out.

2.7.7.4 Euthanasia to allow harvesting of fresh tissue

If fresh (rather than fixed) tissue was required, the animal was terminally anaesthetised and the thoracic cavity and heart exposed as described in section 2.7.7.2. The heart was then removed to ensure permanent cessation of

circulation. Any organs being used for further analysis were removed from the body as quickly as possible, placed in eppendorfs and stored in liquid nitrogen until they could be placed in a -80ºC freezer for long-term storage.

2.8 *Ex Vivo* Methods

2.8.1 Isolation of Aorta

Adult male miR-21$^{-/-}$ mice, miR-21$^{+/-}$ mice and their wild type litter mates were killed as described in section 2.7.7.1. The aorta was carefully removed and ring segments of aorta arterial tissue (2-3 mm in length) were dissected, taking care not to denude the endothelium.

2.8.2 Wire Myography

The endothelium-intact aorta ring was then mounted on a small vessel wire myograph (DMT). The vessels were bathed at 37˚C in gassed Krebs physiological saline solution (118 mM NaCl, 4.8 mM KCl, 2.5 mM $CaCl_2$, 1.2 mM $MgSO_4$, 1.2 mM KH_2PO_4, 24 mM $NaHCO_3$ and 11 mM glucose; PSS). Aortic rings were mounted under 1.0 g resting tension and changes in isometric tension were recorded using signal transducers and displayed using a Powerlab data acquisition unit and LabChart software (ADInstruments).

The tissue was allowed to equilibrate for approximately 60 minutes (tension was gradually increased) before each experiment and aorta rings were initially contracted with a high concentration (125 mM) potassium solution (KPSS; made by equimolar substitution of KCl for NaCl in PSS).

9,11-Dideoxy-11α-epoxymethanoprostaglandin $F_{2\alpha}$ (U46619, Sigma-Aldrich), a stable analogue of endoperoxide prostaglandin H_2 and a thromboxane (TP) receptor agonist (Abramovitz et al., 2000) was added to the organ bath ($1x10^{-9}$ M – $3x10^{-6}$ M) so that cumulative concentration-response curves could be constructed. Contractile responses to U46619 were calculated as a percentage of the maximum contraction and are expressed as the mean ± S.E.M. The influence of endogenous nitric oxide on the response to U46619 in endothelium-intact tissue was investigated using the nitric oxide synthase inhibitor, L-nitro-arginine methyl ester (L-NAME; $1x10^{-4}$ M).

Acetylcholine chloride (Sigma-Aldrich), a muscarinic receptor agonist and vasodilator and carbachol (or carbamylcholine, Sigma-Aldrich) a more stable analogue of acetylcholine, were added to the organ bath ($1x10^{-8}$ M – $3x10^{-5}$ M) so that a cumulative concentration-response curve could be constructed. The relaxation responses were calculated as a percentage of the maximum contraction, following a dose of U46619, calculated to contract the vessel to 80% of its original maximum contraction.

2.9 Bias and Blinding of Experiments

In the *in vitro* experiments the experimenter was not blinded to the treatment being given to each well. However, efforts were made to ensure that treatments were allocated to cell culture plates in such a way that no one group would be especially exposed to evaporation (for example). When cells were harvested from each well and collected into eppendorfs for downstream analysis, each eppendorf was labelled only with a number to ensure the experimenter was not aware of the treatment the cells had received when performing RNA analysis or other downstream analysis.

When analysing miRNA expression in human serum samples (Chapter 4) the experimenter was blinded to the stroke subtype and was not given access to phenotypic data concerning the patient. During RNA extractions, RT-PCR and qRT-PCR experiments samples were arranged according to sample number, and therefore the order in which patients were recruited into the study. The experimenter remained blinded until data analysis was complete.

In the *in vivo* experiments described in Chapter 5 the experimenter was not blinded to the nature of treatment being given to each animal. As these were pilot experiments blinding to treatment was not deemed necessary. Animals were not formally randomised to a particular treatment group. However, only a small number of animals were available to use each week (due to low animal stock in the animal unit and only a small percentage of these animals meeting weight and age requirements) and so all the animals available were typically used. In each week the experiments were performed all treatments were given (i.e. if there were 3 animals being used in 1 week, each would receive a different treatment: sterile saline, miR-93 loaded exosomes or miR-20b loaded

exosomes). Had the full animal study been carried out, efforts would have been made to ensure the experimenters were completely blinded and animals randomised to treatment groups to prevent bias.

2.10 Statistical Analysis of Results

Results described in the text are typically expressed as mean ± standard error of the mean (SEM). Statistical analysis was carried out using GraphPad Prism software. If 'n' numbers were sufficient (minimum n=8 in each group) data was tested for normality using the D'Agostino & Pearson omnibus normality test function on GraphPad Prism. On normally distributed data the most commonly used statistical tests were unpaired two-tailed Student's t-test and one-way analysis of variance (ANOVA) with either Bonferroni, Dunnet or Tukey post-hoc correction for multiple comparisons. If data was not normally distributed, a Mann Whitney test was used instead of a t-test and a Kruskal-Wallis test instead of a one-way ANOVA. When performing correlation analysis, if data was normally distributed a Pearson product-moment correlation coefficient calculation was used – where these have been calculated results are displayed as R^2 values. If data was not normally distributed a Spearman's Rank-Order Correlation calculation was used – where these have been calculated results are displayed as ρ values.

Chapter 3 Early Investigations into Candidate miRNAs

3.1 Introduction

Numerous studies have shown that modulation of miRNA expression may be therapeutically beneficial in the setting of pre-clinical ischaemic stroke. These studies have been discussed in greater detail in section 1.2.6. miR-494 and miR-21 are potential candidates for modulation in the setting of experimental stroke. Here studies that present evidence implicating the importance of these miRNAs in the setting of ischaemic stroke will be introduced.

3.1.1 miR-494

miR-494 is located on chromosome 14 and is part of the 14q32 miRNA cluster (Figure 3.1). This is one of the largest polycistronic clusters and in humans is comprised of 54 different miRNAs. A miRNA cluster denotes miRNAs processed together in one primary transcript. miR-494 is expressed ubiquitously with highest expression in reproductive tissue such as the cervix, placenta, ovary, testes and prostrate (miRNA Map 2.0) (Hsu et al., 2008). Studies to date investigating miR-494 expression and modulation have been primarily cancer focussed and these are summarised by Tay and colleagues (Tay et al., 2016).

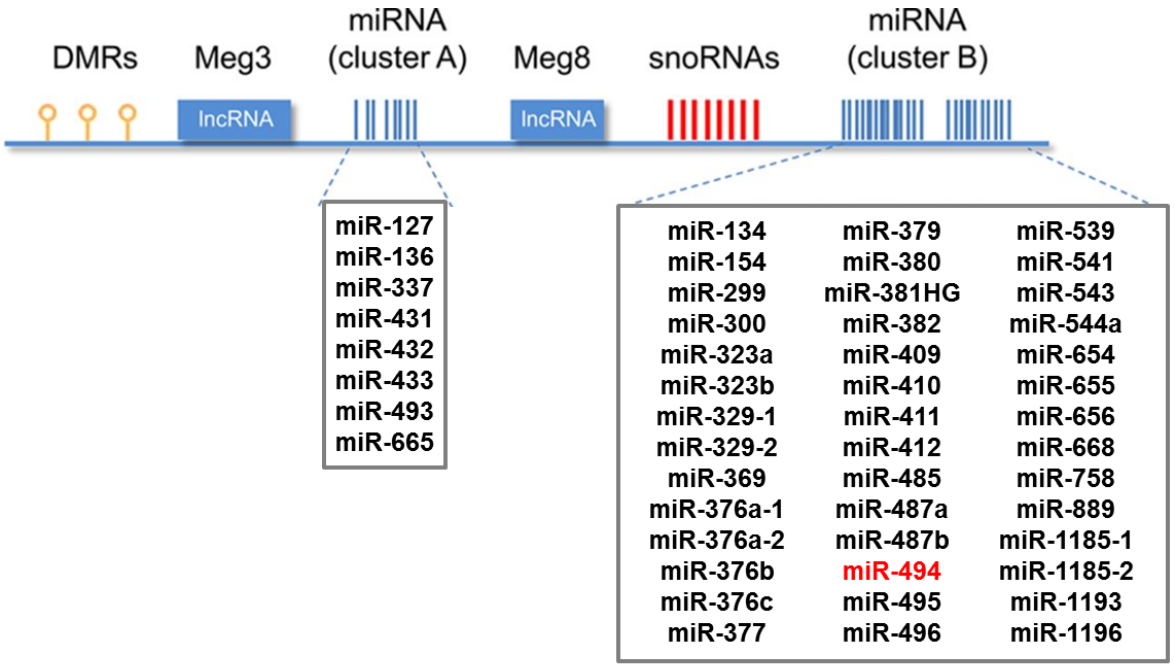

Figure 3.1 – Schematic Illustration of the 14q32 miRNA Cluster
MicroRNAs are listed by number and not in order of their chromosomal location. Abbreviations include: DMR, DNA methylated region; lncRNA, long noncoding RNA; snoRNA, small nucleolar RNAs. Figure adapted from (Dimmeler and Yla-Herttuala, 2014).

3.1.1.1 miR-494 and Cardiovascular Disease

miR-494 expression is increased (~2-fold; non validated microarray data) in *ex vivo* murine ischaemic hearts subjected to 45 minutes of global no-flow ischaemia followed by 2 hours of reperfusion (Ren et al., 2009). miR-494 was subsequently shown to be significantly increased *in vivo* in murine hearts following 30-minute left anterior descending artery occlusion in comparison to sham operated animals (Wang et al., 2010). It was further increased with 1 hour of reperfusion but was significantly decreased after 24 hours of reperfusion (Wang et al., 2010). Conversely, miR-494 was decreased (~1.5-fold; non validated microarray data) in the left ventricle of human hearts in end-stage heart failure in comparison to normal hearts (Thum et al., 2007). miR-494 was also down-regulated in plasma samples taken from patients in heart failure and in patients with heart failure with reduced left ventricular ejection fraction (HFREF) but not in patients with heart failure with preserved left ventricular ejection fraction (HFPEF) in comparison to healthy control patients (Wong et al., 2015). However, miR-494 was not found to be a particularly good biomarker for either heart failure or HFREF as assessed by ROC analysis (Wong et al., 2015).

Transgenic mice with cardiac-specific over-expression of miR-494 had improved functional recovery (assessed by contractile performance) following global no-flow ischaemia/reperfusion injury (Langendorff system, *ex vivo*), and also reduced lactate dehydrogenase release and apoptosis (Wang et al., 2010). Furthermore, *in vivo*, miR-494 transgenic mice had a reduced infarct size following myocardial infarct in comparison to WT control mice (Wang et al., 2010). In this setting miR-494 was found to negatively regulate a number of pro-apoptotic (ROCK1, PTEN, CAMKIIδ) and anti-apoptotic (FGFR2 and LIF) proteins both *in vivo* in miR-494 transgenic mice hearts and *in vitro* in adult cardiomyocytes (Wang et al., 2010).

Other studies investigating miR-494 in cardiovascular disease have shown, conversely, that miR-494 knockdown is beneficial and miR-494 over-expression detrimental. Over-expression of miR-494 contributed to acute kidney injury (AKI) in C57BL/6 mice following experimentally induced ischaemia/reperfusion injury (following bilateral renal artery occlusion) (Lan et al., 2012). Lentiviral vectors designed to over-express miR-494 were injected into the renal artery of mice

and decreased kidney function, increased renal apoptosis, reduced expression of activating transcription factor 3 (AFT3) and induced inflammatory markers such as IL-6, MCP-1, P-selectin and NFκB (Lan et al., 2012). Urinary (but not serum) expression of miR-494 was subsequently shown to be up-regulated in human AKI patents in intensive care in comparison to both healthy control patients and intensive care patients with no AKI (Lan et al., 2012).

miR-494 knockdown via administration of gene silencing oligonucleotides (GSOs) prior to experimentally induced hind limb ischemia (induced by single femoral artery ligation) improved blood flow recovery (Welten et al., 2014). mRNA expression of target genes of miR-494: toll-like receptor 4 (TLR4), ADP-ribosylation factor 6 (ARF6) and fibroblast growth factor receptor 2 (FGFR2) were found to be increased *in vivo* in the left adductor muscle following treatment with GSO-miR-494 (Welten et al., 2014). *In vitro* experiments showed an increase in proliferation of primary human umbilical arterial myofibroblasts following treatment with GSO-miR-494 but no change in the proliferation of human umbilical arterial endothelial cells or human umbilical arterial smooth muscle cells (Welten et al., 2014). Increased outgrowth of neo-vessels was observed in 5-day collagen-embedded murine thoracic aortic ring explants following GSO-miR-494 treatment (Welten et al., 2014). However, the mechanisms by which miR-494 knockdown improved blood flow recovery are unclear as GSO-miR-494 treatment did not affect capillary density or arteriogenesis *in vivo* (Welten et al., 2014). A follow up paper demonstrated reduced carotid artery atherosclerotic lesion development and increased plaque stability in hypercholesterolemic $ApoE^{-/-}$ mice following IV delivery of GSO-miR-494 4 days following placement of semi-constrictive collars around both carotid arteries to induce carotid artery plaque formation (Wezel et al., 2015). Knock-down of miR-494 expression in carotid arteries resulted in up-regulated mRNA expression of miR-494 targets: IL33, TIMP3 and TGFβ2 (Wezel et al., 2015).

These studies, taken in combination with the fact that miR-494 can regulate expression of both pro- and anti-apoptotic proteins suggest that miR-494 plays a complex role in the regulation of tissue homeostasis.

3.1.1.2 miR-494 and Stroke

miR-494 expression was up-regulated in whole blood samples of young (aged 18-49 years) ischaemic stroke patients collected between 2-24 months post-stroke (Tan et al., 2013) and in whole blood samples collected from patients within 24 hours of stroke onset (Sepramaniam et al., 2014) in comparison to healthy control patients (non-validated microarray data). Expression of miR-494 was also increased approximately 15-fold in plasma samples collected from haemorrhagic stroke patients between 1-14 days post-symptom onset in comparison to healthy control patients (Guo et al., 2013). Although these changes are interesting, none have been validated by qRT-PCR.

A study profiling miRNA expression in male SD rats post-tMCAO found that miR-494 expression was increased in both brain tissue and blood at 24 and 48 hours post-stroke (Jeyaseelan et al., 2008). The increase in expression peaked at 24 hours in brain tissue but still remained elevated at 48 hours in comparison to sham tissue. Within blood samples its expression was essentially unchanged at 24 hours but substantially increased at 48 hours post-stroke (Jeyaseelan et al., 2008). Subsequently a putative target of miR-494, Visinin-like 1 (VSNL1), was shown to be down-regulated in the brains of SD at 24 hours post-reperfusion, negatively correlating with the increase in miR-494 expression (Jeyaseelan et al., 2008). These results were confirmed in a separate study where miR-494 was shown to be increased in ipsilateral brain tissue of male SD rats at 24 hours post-tMCAO in comparison to sham operated rats and Bcl-2, a target of miR-494, was decreased in the same tissue (Zhai et al., 2012). Adult male Fischer rats subjected to pMCAO had increased miR-494 expression at 30 minutes and 6 hours post-stroke (as assessed by microarray) – expression returned to basal levels at 7 days post-stroke and was decreased at 14 days but in comparison to healthy animals rather than sham operated animals (Gubern et al., 2013). In this study (Gubern et al., 2013) increases in miR-494 expression were shown to occur at the critical time point post-pMCAO when the penumbra is evolving and being absorbed into the infarct (Hossmann, 2012) - this suggests that miR-494 may be relevant to the acute evolution of ischaemic damage.

The only study (published to date) to modulate miR-494 expression within the brain did so in C57BL/6 mice 2 weeks prior to a Parkinson's Disease (PD)

phenotype being induced (by IP injection of MPTP neurotoxin) via stereotactic injection of lentiviral vectors designed to increase miR-494 expression (Xiong et al., 2014). miR-494 was shown to inhibit DJ-1 expression, an oxidative sensor protein thought to help protect cells from oxidative insult. DJ-1 expression is also reduced in the substantia nigra of PD patients. miR-494 over-expression enhanced neurodegeneration as assessed by a swim test and a loss of dopaminergic neurons in the substantia nigra (Xiong et al., 2014).

Endogenous increases in circulating and brain miR-494 expression in response to ischaemic insult suggest that this is either an endogenous repair response that is insufficient to protect tissue or that it is part of the ischaemic injury cascade, contributing to cell death. The majority of studies discussed here have demonstrated that increased miR-494 expression is detrimental to functional outcome following ischaemic insult. However, these studies were predominantly investigating miR-494 modulation within the peripheral vasculature. The role of miR-494 within the brain and following ischaemic stroke is yet to be elucidated. By modulating miR-494 expression we may be able to influence final infarct volume, vascular function, apoptosis and neurological deficit.

3.1.2 miR-21

miR-21 is a highly conserved miRNA, located on chromosome 17. It is expressed ubiquitously with highest expression in the lung, followed by the kidney and bladder (miRNA Map 2.0) (Hsu et al., 2008). miR-21 has an important role to play in a wide range of biological processes including development, cancer, cardiovascular disease and inflammation. It is classified as an oncomiR as it has been found to be differentially regulated in many forms of cancer but more recently has also been found to play a role in numerous cardiovascular and pulmonary diseases, for example, cardiac and pulmonary fibrosis and myocardial infarction (Jazbutyte and Thum, 2010, Krichevsky and Gabriely, 2009).

3.1.2.1 miR-21 and Cardiovascular Disease

Elevated miR-21 expression has been associated with myocardial infarction (MI). miR-21 has been shown to be increased in plasma of patients with acute MI in comparison to healthy age-matched controls, patients with acute heart failure,

angina or chest pain syndrome (Olivieri et al., 2014, Yao et al., 2011). However, in a separate study, circulating miR-21 expression was significantly decreased at 2 days post-MI in comparison to control patients but increased at 5 days post-MI before returning to normal by 90 days post-MI (Zile et al., 2011). Increased miR-21 expression has also been associated with angina and cardiac hypertrophy (Cheng et al., 2007, Ren et al., 2013, Sayed et al., 2007, van Rooij et al., 2006).

miR-21 is involved in vascular remodelling, affecting both smooth muscle cells and endothelial cells. As miR-21 has been shown to be significantly up-regulated within the cerebral vasculature of SHRSP following tMCAO (assessed by *in situ* hybridisation) (Breen, 2015) the expression and regulation of miR-21 within the vasculature is of special interest in the context of stroke.

Expression of miR-21 is increased following vascular injury (Ji et al., 2007) and hypoxia (Sarkar et al., 2010), is post-transcriptionally induced by TGF-ß and BMP signalling (Davis et al., 2008, Kang et al., 2012) and is increased in human arteries with arteriosclerosis obliterans (Wang et al., 2011). Furthermore its circulating (serum) expression is sequentially decreased in patients with calcified and non-calcified coronary artery plaques in comparison to control patients (with chest pain but no coronary plaques), but increased sequentially in macrophages of patients with calcified and non-calcified plaques in comparison to control patients (Fan et al., 2014). Furthermore circulating miR-21 expression negatively correlated with serum MMP9 expression (Fan et al., 2014). miR-21 expression was also increased in atherosclerotic plaques obtained from aortic, carotid and femoral arteries in comparison to non-atherosclerotic left internal thoracic arteries (Raitoharju et al., 2011).

miR-21 signalling negatively regulates the expression of PDCD4 (Davis et al., 2008, Sarkar et al., 2010, Wang et al., 2012), PTEN (Ji et al., 2007), Sprouty 2 (SPRY2) (Sarkar et al., 2010), peroxisome proliferator-activated receptor-α (PPARα) (Sarkar et al., 2010), tropomyosin1 (TPM1) (Wang et al., 2011), transcription factor specificity protein-1 (SP1) (and subsequently cystathionine gamma-lyase, a major H_2S generating enzyme) (Yang et al., 2012) and increases expression of phosphorylated Akt, Bcl-2 (Ji et al., 2007), smooth muscle α-actin (SMA) and calponin (Davis et al., 2008).

These proteins have targets which in turn regulate cell proliferation (Ji et al., 2007, Sarkar et al., 2010, Wang et al., 2011, Yang et al., 2012), migration (Sarkar et al., 2010, Wang et al., 2012), differentiation (Yang et al., 2012) and apoptosis (Ji et al., 2007) as well as the induction of a contractile phenotype (Davis et al., 2008) in vascular smooth muscle cells. miR-21 signalling also plays a role in the proliferation and apoptosis of vascular adventitial fibroblasts and myofibroblasts (Wang et al., 2012) as well as neo-intimal lesion formation (Ji et al., 2007).

Within endothelial cells miR-21 is highly expressed (Kuehbacher et al., 2007) and has been found to play an important regulatory role. Expression of miR-21 was induced by shear stress in human umbilical vein endothelial cells (HUVECs) (Weber et al., 2010, Zhou et al., 2011), but reduced in late passage senescent human aorta endothelial cells (in comparison to early passage) (Rippe et al., 2012) and following treatment with bFGF in HUVECs (Sabatel et al., 2011).

miR-21 signalling in endothelial cells modulated expression of downstream targets including PTEN (Weber et al., 2010), PPARα, vascular cell adhesion molecule-1, monocyte chemotactic protein-1 (Zhou et al., 2011), RhoB (Sabatel et al., 2011), collagen I and III, elastin, Smad2, Smad5, Smad7, CTGF, MMP2, MMP10 and TIMP-4 (Zhang et al., 2013).

Overexpression of miR-21 reduced apoptosis, increased eNOS phosphorylation and levels of nitric oxide in endothelial cells (Weber et al., 2010), promoted monocyte adhesion, part of a pro-inflammatory response to shear stress (Zhou et al., 2011) and also impaired cell proliferation, migration and angiogenesis in HUVECs (Sabatel et al., 2011). Reduction in miR-21 expression was associated with decreased cell proliferation and eNOS but increased apoptosis and inflammation in human aortic endothelial cells (Rippe et al., 2012). Reduced miR-21 expression was also associated with reduced proliferation, migration and tube forming capacity in retinal microvascular endothelial cells (Guduric-Fuchs et al., 2012). Interestingly, endothelial specific miR-21 knock-out mice demonstrated both structural and functional aorta remodelling (Zhang et al., 2013). miR-21 knock-out in this setting resulted in decreased diastolic blood pressure, maximal tension depression, impaired endothelium-dependent relaxation and a decrease in compliance (Zhang et al., 2013).

This evidence suggests that miR-21 has an important role to play in modulating both vascular smooth muscle and endothelial cell biology. Furthermore inhibition of apoptosis and promotion of proliferation are, in theory, interesting treatment strategies for regenerative medicine in the cardiovascular system.

3.1.2.2 miR-21 and Stroke

Circulating miR-21 expression has been profiled in a number of human ischaemic stroke patient populations and these are summarised in Table 3.1.

Table 3.1 – miR-21 Expression in Ischaemic Stroke Patients.
A table summarising published studies that have profiled circulating miR-21 expression in human ischaemic patients by qRT-PCR. Abbreviations: IS, ischaemic stroke; * indicates change in expression was statistically significant.

Reference	miR-21 Expression	Sample Used	Control Patients
(Tan et al., 2009)	*↑ IS vs. control	Whole blood collected 6-18 months post IS	Healthy, no details of age
(Tsai et al., 2012)	*↑ IS vs. control	Serum collected <7 days post IS onset	Healthy, younger but p-values adjusted for age
(Wang et al., 2014b)	*↑ IS vs. control	Plasma collected <24 hours post IS onset	Healthy, age-matched
(Jia et al., 2015)	**Not changed** IS vs. control	Serum collected < 24 hours post IS onset	Healthy, age-matched
(Kim et al., 2015)	**Not changed** IS vs. control	Plasma collected < 7 days post IS onset	Some vascular risk factors, age-matched
(Zhou and Zhang, 2014)	*↓ IS vs. control	Plasma collected < 24 hours post IS onset	Healthy, younger (not significant)

In contradictory studies circulating miR-21 expression was shown to increase (Tan et al., 2009, Tsai et al., 2012, Wang et al., 2014b), remain unchanged (Jia et al., 2015, Kim et al., 2015) and to decrease (Zhou and Zhang, 2014) following ischaemic stroke. miRNA expression was profiled in differently processed blood samples that had been collected at differing time points post-stroke so the results are not directly comparable. However, the most important discrepancies appear to be between the patient (and control) populations used. Only three of the studies provide information on the stroke subtype breakdown of their patient populations (Kim et al., 2015, Tsai et al., 2012, Wang et al., 2014b) and so it is impossible to know whether differences in miR-21 expression observed

are a result of differing stroke subtypes within the patient populations used. Of note, the only studies that observed differences in miR-21 expression used healthy control patients. Had miR-21 expression been compared to age-matched, vascular risk factor controls, it is possible that no differences would have been observed, as is the case in the study published by Kim and colleagues. Similarly, miR-21 expression was significantly increased in serum samples collected from ischaemic stroke patients within 7 days of stroke in comparison to healthy control patients but was not significantly increased in comparison to samples collected from asymptomatic patients with carotid atherosclerosis (Tsai et al., 2012).

In pre-clinical models of stroke *in situ* hybridisation has been used to show up-regulated miR-21 expression in coronal brain sections of Wistar rats following embolic MCAO in comparison to its expression in the contralateral hemisphere (Buller et al., 2010). miR-21 expression was especially increased in neuronal cells of the ischaemic boundary zone (peri-infarct) at 2 and 7 days post-stroke (Buller et al., 2010). Furthermore, increased miR-21 expression was associated with areas of reduced TUNEL staining, suggesting reduced apoptosis in these areas (Buller et al., 2010). In a separate study qRT-PCR analysis demonstrated increased miR-21 expression in the hippocampus of SD rats at 24 hours post ischaemia/reperfusion injury (induced by transient 4 vessel occlusion) in comparison to sham operated animals (Deng et al., 2013). Furthermore, increases in miR-21 expression correlated with increases in MMP9 expression (Deng et al., 2013). *In vitro* cell culture experiments have also demonstrated increased miR-21 expression in secondary neuronal (N2A) cells following hypoxic insult with 24 hours of reoxygenation (Zhou and Zhang, 2014). Conversely, miR-21 expression was decreased in primary rat microglial cells at 3, 6 and 12 hours post hypoxic insult (with reoxygenation) (Zhang et al., 2012). These studies suggest that miR-21 is differentially expressed between cell subtypes following ischaemic or hypoxic insult.

Up-regulation of miR-21 expression (via delivery of miRNA mimics) protected primary cortical neurons *in vitro* from oxygen and glucose deprivation (Buller et al., 2010). Protection was hypothesised to be mediated by miR-21 induced down-regulation of Fas ligand (part of the TNFα family), a cell death inducing ligand (Buller et al., 2010). Consistent with this, increased miR-21 expression (via

delivery of miRNA mimic) was shown to induce repression of Fas ligand – this protected against activated microglia induced neuronal apoptosis following hypoxic insult *in vitro* (Zhang et al., 2012). Finally, stereotactic injection of anti-miR-21 to bilateral cerebral ventricles 24 hours prior to 4 vessel occlusion in Sprague Dawley rats resulted in a down-regulation of MMP9 expression (Deng et al., 2013). However, data on the effect of anti-miR-21 on infarct volume and other functional measures of outcome was not presented or commented on in this study (Deng et al., 2013).

A number of studies have demonstrated that over-expression of miR-21 is therapeutically beneficial following traumatic brain injury, reducing lesion volume, brain oedema and BBB damage (Ge et al., 2015, Ge et al., 2016, Ge et al., 2014). miR-21 targeted PTEN, Angiopoietin-1, Tie-2, NF-κB and a number of inflammatory cytokines – resulting in an inhibition of apoptosis and a promotion of angiogenesis (Ge et al., 2015, Ge et al., 2016, Ge et al., 2014).

The evidence presented here suggests that miR-21 has an important role to play within the brain and vasculature following ischaemic stroke and therefore may have an influence on final infarct volume, apoptosis, vascular function, angiogenesis and neurological deficit – supporting the hypothesis that miR-21 modulation may prove to be an effective novel therapeutic in the setting of experimental stroke.

3.1.3 Hypotheses

The hypotheses of the present study were as follows:

- Modulation of miR-494 (and concomitant modulation of its gene targets) will be therapeutically beneficial in pre-clinical models of experimentally induced stroke.

- Modulation of miR-21 (and concomitant modulation of its gene targets) will be therapeutically beneficial in pre-clinical *in vitro* models of stroke.

3.1.4 Aims

The aims of the present study were as follows:

- To assess the extent of miR-494 modulation following delivery of miR-494 mimics and anti-miRs to secondary neuronal and cerebral endothelial cells.

- To assess the effect of miR-494 modulation *in vitro* by quantifying changes in expression and activity of miR-494 gene targets and by assessing measures of functional outcome, such as cell survival, following hypoxic challenge.

- To assess the extent of miR-21 modulation following delivery of miR-21 mimics and anti-miRs to a secondary cerebral endothelial cell line.

- To assess the effect of miR-21 modulation *in vitro* by quantifying changes in expression of its target genes and by assessing measures of functional outcome, such as cell survival, following hypoxic challenge.

- To assess the effect of miR-21 modulation *ex vivo* by quantifying changes in vessel contraction and relaxation using wire myography in the aortae of transgenic miR-21$^{-/-}$ and miR-21$^{+/-}$ mice.

3.2 Results

3.2.1 miR-494

Pilot data, collected prior to the start of the presented study (by a research student in our group), demonstrated that miR-494 expression was increased in the brain of SHRSP post-tMCAO (data not shown here). miR-494 expression was significantly increased in ischaemic infarct tissue of SHRSP rats at 3, 6 and 24 hours post-tMCAO, as compared to its expression in matched tissue from sham operated rats. The increase in expression was most marked at 24 hours. miR-494 expression was moderately decreased in ischaemic periphery (or peri-infarct) tissue of SHRSP rats at 3 hours, unchanged as compared to sham operated rats at 6 hours and significantly increased at 24 hours but not to the extent observed in the ischaemic core. This data suggested that miR-494 was dysregulated in the brain of SHRSP rats following stroke. This data, in combination with the studies discussed in the introduction of this chapter, suggested that miR-494 was a good candidate miRNA for modulation in pre-clinical models of stroke.

The expression of miR-494 and several of its putative target genes was subsequently profiled in ipsilateral infarct, peri-infarct and remainder (i.e. non-infarcted ipsilateral) brain tissue of SHRSP rats, collected at both 24 and 72 hours post-tMCAO. The brain tissue used in this study was previously collected in a study carried out by Dr. Emily Ord. A T_2-weighted MRI scan was performed prior to animal sacrifice to allow for the accurate dissection of the infarct and peri-infarct brain regions. In the pilot study, discussed above, infarct and peri-infarct tissue was assessed visually only.

miR-494 expression was not significantly increased in ipsilateral infarct, peri-infarct or remainder tissue at either 24 or 72 hours post-stroke as compared to sham operated animals: 24 hours infarct (RQ 0.85 ± 0.12 vs. 1.00 ± 0.05); 24 hours peri-infarct (RQ 1.13 ± 0.16 vs. 1.00 ± 0.17); 24 hours remainder (RQ 1.35 ± 0.17 vs. 1.00 ± 0.24); 72 hours infarct (RQ 0.74 ± 0.10 vs. 1.00 ± 0.13); 72 hours peri-infarct (RQ 0.93 ± 0.05 vs. 1.00 ± 0.13); 72 hours remainder (RQ 1.09 ± 0.12 vs. 1.00 ± 0.09) (Figure 3.2).

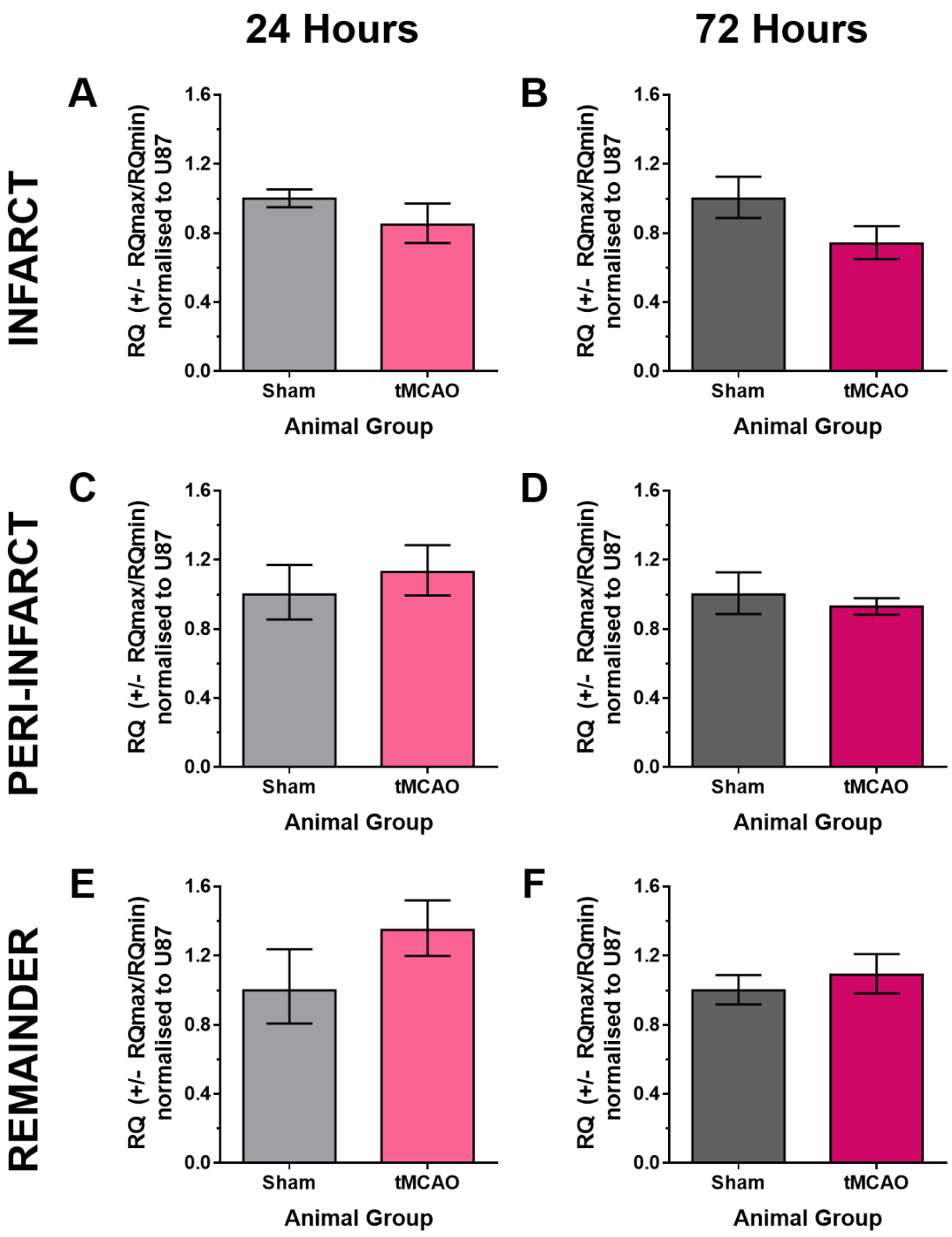

Figure 3.2 – miR-494 Expression in SHRSP tMCAO Brain
The expression of miR-494 was assessed in infarct (A, B), peri-infarct (C, D) and remainder (E, F) brain tissue of SHRSP rats at 24 hours (A, C, E) and 72 hours (B, D, F) following 45 min tMCAO (coloured bars) or sham operation (grey bars) (n=6/group). Statistical probability of differences in expression observed were calculated using unpaired Student's t-test with Bonferroni corrections, vs. sham operated rats. Change in miRNA expression was assessed by qRT-PCR and relative quantification (RQ) calculated from ΔΔCt following normalisation to a housekeeper miRNA, U87, and compared to miRNA expression in the sham operated rats. Data shown is RQ ± RQmax/RQmin. Brain tissue collected by and used with permission of Dr. Emily Ord.

When analysing the data presented in Figure 3.2 - Figure 3.5 a Bonferroni correction was applied to each t-test performed to correct for the fact that miRNA or gene expression was being examined in three different brain tissue sections (infarct, peri-infract and remainder) from the same animals (e.g. sham and tMCAO SHRSP rats at 24 hours). To make the Bonferroni correction we divided the critical P value (α) by the number of comparisons being made. Therefore, with a α value of 0.05, and three comparisons (infarct, peri-infarct and remainder), the new p-value required for significance was: $\frac{0.05}{3} = 0.0167$.

The mRNA expression of PTEN, a validated target of both miR-494 and miR-21, was significantly decreased in infarct, peri-infarct and remainder tissue at both 24 and 72 hours post-stroke as compared to sham operated animals: 24 hours infarct (RQ 0.48 ± 0.05 vs. 1.00 ± 0.08); 24 hours peri-infarct (RQ 0.69 ± 0.11 vs. 1.00 ± 0.14); 24 hours remainder (RQ 0.63 ± 0.09 vs. 1.00 ± 0.12); 72 hours infarct (RQ 0.25 ± 0.08 vs. 1.00 ± 0.05); 72 hours peri-infarct (RQ 0.50 ± 0.12 vs. 1.00 ± 0.04); 72 hours remainder (RQ 0.62 ± 0.09 vs. 1.00 ± 0.12) (Figure 3.3).

The mRNA expression of MMP2, a putative target of miR-494 and validated target of miR-21, was significantly increased in infarct tissue at 24 hours post-tMCAO as compared to sham operated animals (RQ 1.50 ± 0.13 vs. 1.00 ± 0.09) but unchanged in peri-infarct (RQ 1.08 ± 0.15 vs. 1.00 ± 0.18) and in remainder tissue (RQ 1.21 ± 0.10 vs. 1.00 ± .16) (Figure 3.4). MMP2 expression was significantly increased in infarct, peri-infarct and remainder tissue at 72 hours post-tMCAO as compared to sham operated animals: infarct (RQ 2.55 ± 0.28 vs. 1.00 ± 0.14); peri-infarct (RQ 2.61 ± 0.35 vs. 1.00 ± 0.11); remainder (RQ 2.14 ± 0.30 vs. 1.00 ± 0.03) (Figure 3.4).

The mRNA expression of MMP9 (a predicted target of miR-494 and validated target of miR-21) was also profiled. MMP9 was significantly increased in infarct, peri-infarct and remainder tissue at 24 hours post-tMCAO as compared to sham animals: infarct (RQ 3.46 ±1.64 vs. 1.00 ± 0.54); peri-infarct (RQ 2.95 ± 1.01 vs. 1.00 ± 0.28); remainder (RQ 5.08 ± 1.14 vs. 1.00 ± 0.38) (Figure 3.5). However, MM9 expression was unchanged in brain tissue of SHRSP rats at 72 hours as compared to sham operated rats: infarct (RQ 1.21 ± 0.30 vs. 1.00 ± 0.20); peri-

infarct (RQ 1.94 ± 0.81 vs. 1.00 ± 0.17); remainder (RQ 1.22 ± 0.73 vs. 1.00 ± 0.32) (Figure 3.5).

Despite the fact that miR-494 expression was not altered in the brain tissue of SHRSP rats at 24 and 72 hours following tMCAO in the present study it was hypothesised that modulation of miR-494 expression could still be therapeutic in the setting of ischaemic stroke as a number of its putative gene targets are implicated in ischaemic stroke. Furthermore, their expression (PTEN, MMP2 and MMP9) is significantly dysregulated in stroke and modulation of miR-494 may lead to therapeutic benefit via modulation of the expression of these target genes.

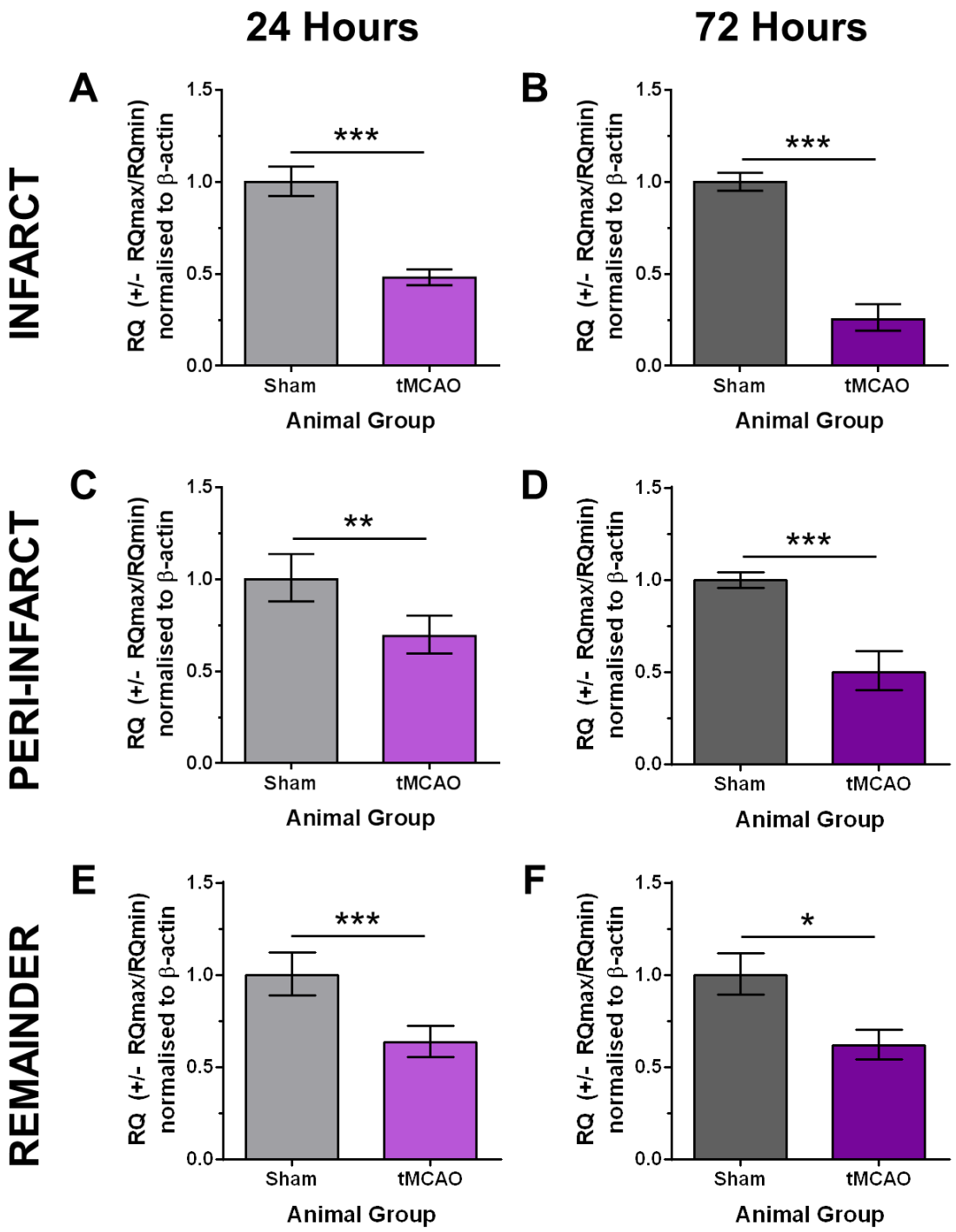

Figure 3.3 – PTEN Expression in SHRSP tMCAO Brain
The expression of PTEN was assessed in infarct (A, B), peri-infarct (C, D) and remainder (E, F) brain tissue of SHRSP rats at 24 hours (A, C, E) and 72 hours (B, D, F) following 45 min tMCAO (coloured bars) or sham operation (grey bars) (n=6/group). Statistical probability of differences in expression observed were calculated using unpaired Student's t-test with Bonferroni corrections, vs. sham operated rats: *p<0.05; **p<0.01; ***p<0.001. Change in mRNA expression was assessed by qRT-PCR and relative quantification (RQ) calculated from ΔΔCt following normalisation to a housekeeper mRNA, β-actin, and compared to mRNA expression in the sham operated rats. Data shown is RQ ± RQmax/RQmin. Brain tissue collected by and used with permission of Dr. Emily Ord.

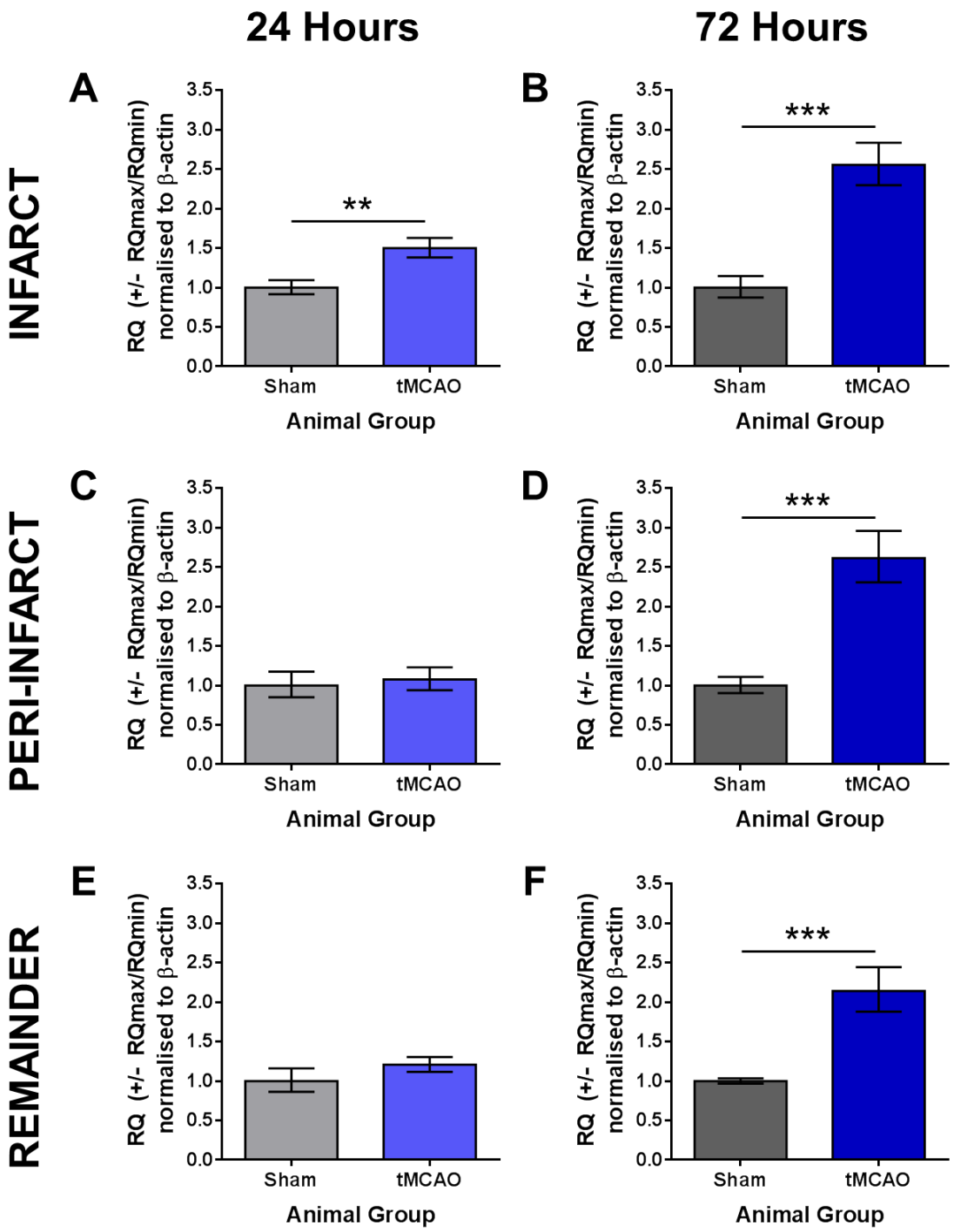

Figure 3.4 – MMP2 Expression in SHRSP tMCAO Brain
The expression of MMP2 was assessed in infarct (A, B), peri-infarct (C, D) and remainder (E, F) brain tissue of SHRSP rats at 24 hours (A, C, E) and 72 hours (B, D, F) following 45 min tMCAO (coloured bars) or sham operation (grey bars) (n=6/group). Statistical probability of differences in expression observed were calculated using unpaired Student's t-test with Bonferroni corrections, vs. sham operated rats: **p<0.01; ***p<0.001. Change in mRNA expression was assessed by qRT-PCR and relative quantification (RQ) calculated from ΔΔCt following normalisation to a housekeeper mRNA, β-actin, and compared to mRNA expression in the sham operated rats. Data shown is RQ ± RQmax/RQmin. Brain tissue collected by and used with permission of Dr. Emily Ord.

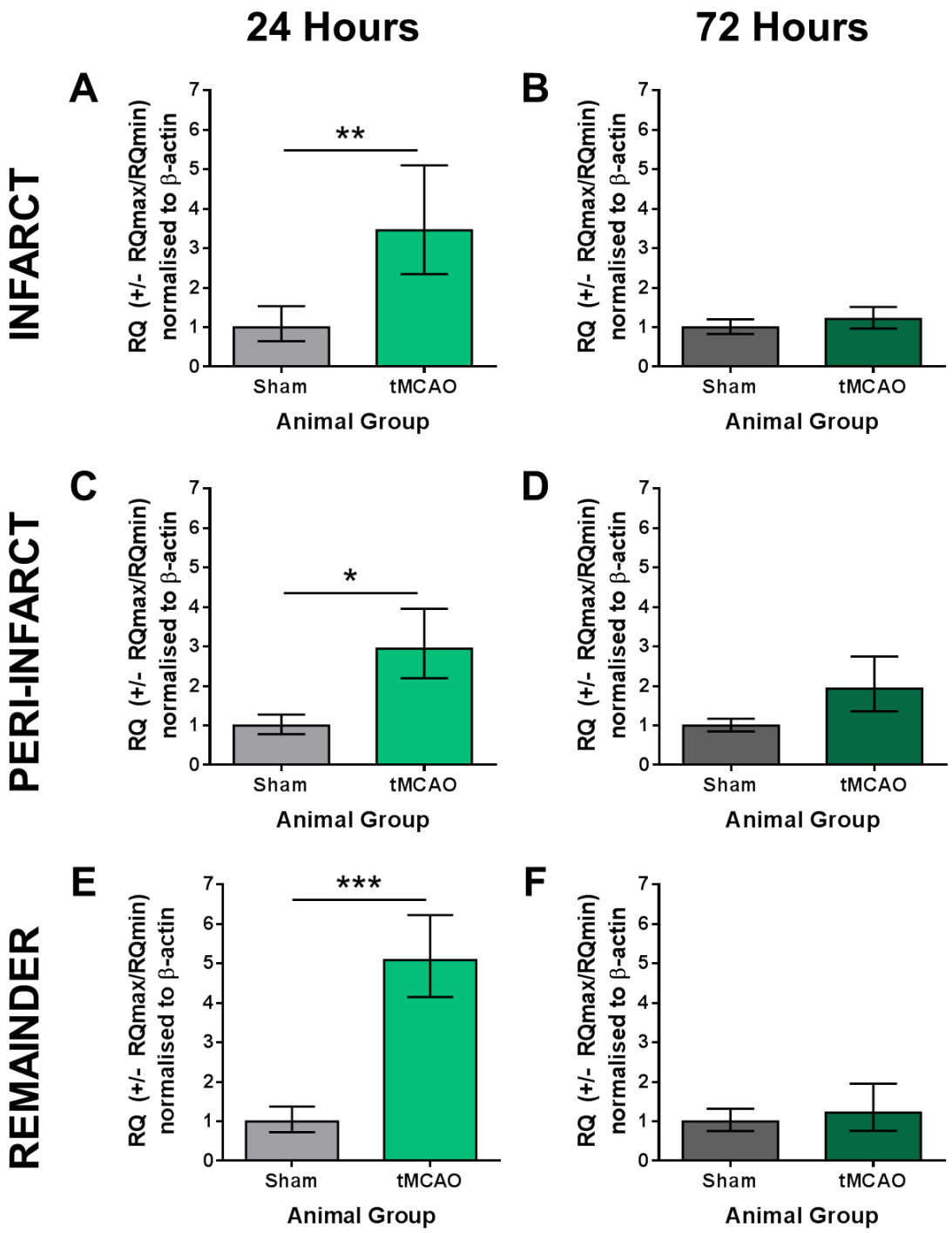

Figure 3.5 – MMP9 Expression in SHRSP tMCAO Brain
The expression of MMP9 was assessed in infarct (A, B), peri-infarct (C, D) and remainder (E, F) brain tissue of SHRSP rats at 24 hours (A, C, E) and 72 hours (B, D, F) following 45 min tMCAO (coloured bars) or sham operation (grey bars) (n=6/group). Statistical probability of differences in expression observed were calculated using unpaired Student's t-test with Bonferroni corrections, vs. sham operated rats: *p<0.05; **p<0.01; ***p<0.001. Change in mRNA expression was assessed by qRT-PCR and relative quantification (RQ) calculated from ΔΔCt following normalisation to a housekeeper mRNA, β-actin, and compared to mRNA expression in the sham operated rats. Data shown is RQ ± RQmax/RQmin. Brain tissue collected by and used with permission of Dr. Emily Ord.

miR-494 expression was initially modulated *in vitro,* in B50 neuronal and GPNT cerebral endothelial cells, via the delivery of mature miRNA mimics and miRNA anti-miRs, delivered using siPORT, a lipid based transfection agent (Figure 3.6). miR-494 expression was unchanged in NTC B50 cells following hypoxic challenge as compared to normoxic cells (1/ΔCt 0.156 ± 0.0052 vs. 0.170 ± 0.0016) (Figure 3.6A). miR-494 expression was also unchanged in both normoxic and hypoxic B50 cells following delivery of siPORT, the mature mimic control (+C) or the anti-miR control (-C) as compared to their NTC treated counterparts. miR-494 expression was significantly increased following delivery of miR-494 mimic in normoxic (RQ 175.51 vs. 1.00 ± 0.04) and hypoxic (RQ 195.96 ± 7.67 vs. 1.00 ± 0.17) cells in comparison to matched NTC control cells (Figure 3.6A). However, miR-494 expression was not significantly modulated following delivery of miR-494 anti-miR to B50 cells: normoxic (RQ 1.18 ± 0.09 vs. 1.00 ± 0.04); hypoxic (RQ 0.72 ± 0.05 vs. 1.00 ± 0.17) (Figure 3.6A).

miR-494 expression was subsequently modulated in GPNT cerebral endothelial cells (Figure 3.6B). miR-494 expression was unchanged in NTC GPNT cells following hypoxic challenge as compared to normoxic cells (1/ΔCt 0.098 ± 0.002 vs. 0.092 ± 0.0005). miR-494 expression was also unchanged in both normoxic and hypoxic GPNT cells following delivery of siPORT, the mature mimic control (+C) or the anti-miR control (-C) as compared to their NTC treated counterparts. miR-494 expression was increased to an even greater extent in GPNT cells than was observed in the B50 cells following delivery of miR-494 mimic as compared to expression in NTC control cells: normoxic (RQ 6999.12 ± 967.43 vs. 1.00 ± 0.04); hypoxic (RQ 1911.75 ± 257.96 vs. 1.00 ± 0.16) (Figure 3.6B). Surprisingly, miR-494 expression was also significantly increased following delivery of miR-494 anti-miR to GPNT cells in comparison to its expression in NTC control cells: normoxic (RQ 6.62 ± 2.57 vs. 1.00 ± 0.04); hypoxic (RQ 3.43 ± 3.73 vs. 1.00 ± 0.16) (Figure 3.6B).

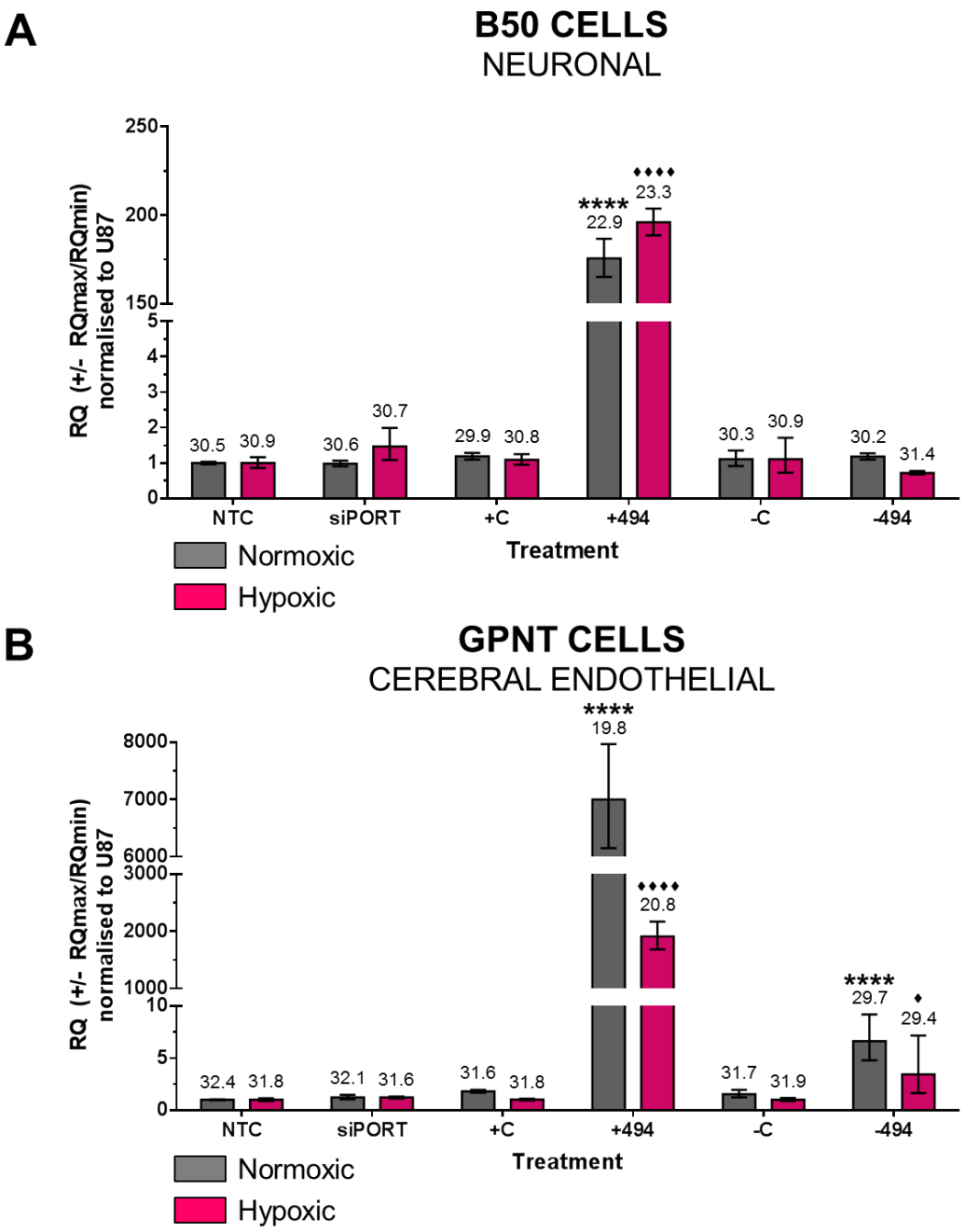

Figure 3.6 – miR-494 Modulation in B50 and GPNT Cells
B50 (A) and GPNT (B) cells were transfected with the transfection agent alone (siPORT C), mature mimic control (+C), mature miR-494 mimic (+494), anti-miR control (-C) or anti-miR-494 (-494) or did not receive any treatment (NTC). miR-494 expression was assessed in cell lysates harvested 24 hours following hypoxic challenge (pink) or control normoxic conditions (grey) (n=2). Change in miRNA expression was assessed by qRT-PCR and relative quantification (RQ) calculated from ΔΔCt following normalisation to a housekeeper miRNA, U87, and compared to miRNA expression in the NTC control cells. Data shown is RQ ± RQmax/RQmin. Raw Ct values are given above each column. Statistical probability of differences in expression observed were calculated using unpaired Student's t-test with Tukey's Multiple Comparisons Test. Selected statistical significances are shown on the graph: ****p<0.0001 vs. normoxic NTC cells; ♦p<0.05, ♦♦♦♦p<0.0001 vs hypoxic NTC cells.

As we were interested in the effects of both miR-494 over-expression and knock-down a refined transfection protocol was designed in which cells were transfected with miR-494 modulating agents over 2 days (Figure 3.7 A and B). On the first day GPNT cells were transfected with mature miR-494 mimic or mimic control and on the second with a repeated dose of miR-494 mimic and either anti-miR-494 or an anti-miR control. This protocol was designed to show knock-down of miR-494 following artificial up-regulation so that the effect of both over-expression and subsequent knock-down of miR-494 expression could be examined.

As before, miR-494 expression was unchanged in NTC hypoxic GPNT cells as compared to normoxic NTC cells (1/ΔCt 0.036 ± 0.0001 vs. 0.037 ± 0.0002) (Figure 3.7 C). miR-494 expression was also unchanged in both normoxic and hypoxic GPNT cells following delivery of siPORT, the mature mimic control/anti-miR control (+C + -C) or mature mimic control/anti-miR-494 (+C + -494) as compared to their NTC treated counterparts. miR-494 expression was significantly increased following delivery of miR-494 mimic/anti-miR control (+494 + -C) in both normoxic (RQ 5986.66 ± 279.71 vs. 1.00 ± 0.12) and hypoxic (RQ 10031.14 ± 148.15 vs. 1.00 ± 0.04) cells as compared to matched NTC control cells (Figure 3.7 C). Although miR-494 expression was significantly increased in normoxic cells treated with miR-494 mimic/anti-miR-494 as compared to NTC treated cells (RQ 8.02 ± 1.92 vs. 1.00 ± 0.12), its expression was significantly down-regulated in comparison to +494 + -C treated cells. Similarly, miR-494 expression was significantly increased in hypoxic cells treated with mature miR-494/anti-miR-494 in comparison to NTC treated cells (RQ 465.98 ± 245.88 vs. 1.00 ± 0.04) but was significantly down-regulated in comparison to +494 + -C treated cells. Furthermore, there was a significant difference in miR-494 expression between normoxic and hypoxic +494 + -494 treated cells (1/ΔCt normoxic 0.042 ± 0.0006 vs. 0.053 ± 0.0016) (Figure 3.7 C).

A

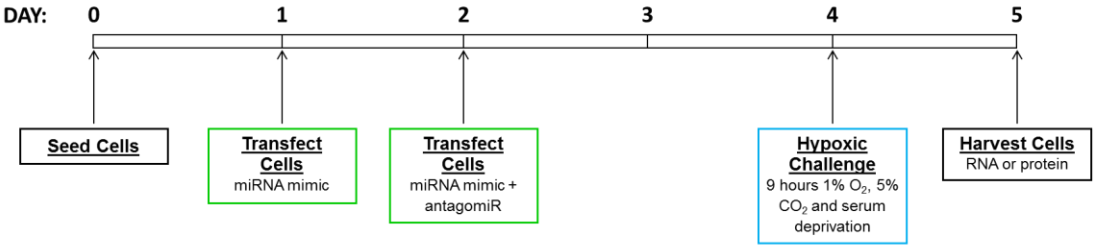

B

	Day 1	Day 2	
		1	2
NTC	NTC	NTC	
siPORT C	siPORT	siPORT	
+C + -C	+C	+C	-C
+C + -494	+C	+C	-494
+494 + -C	+494	+494	-C
+494 + -494	+494	+494	-494

C

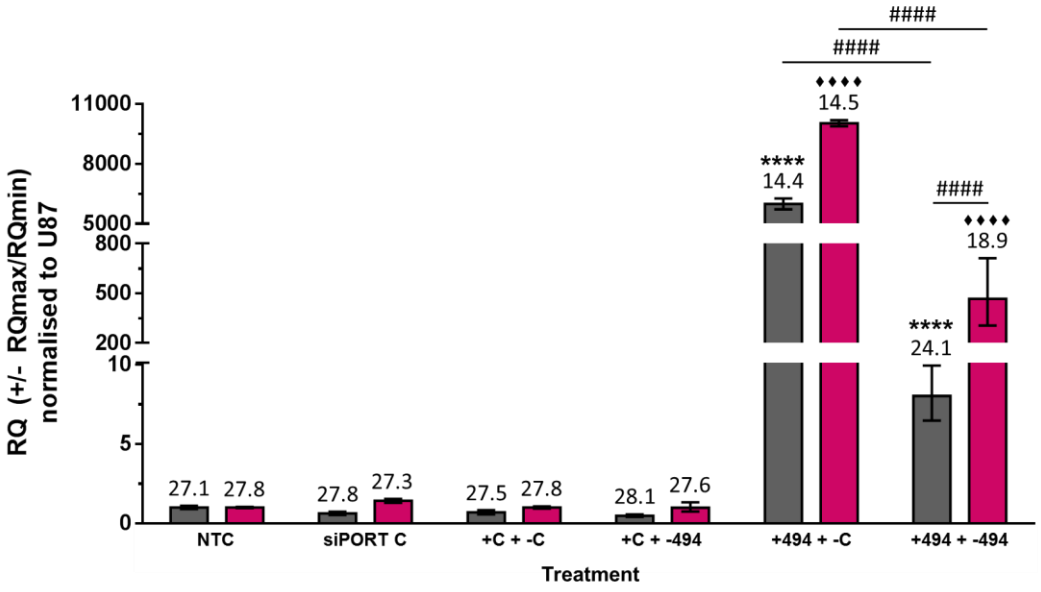

Figure 3.7 – miR-494 Modulation in GPNT Cells
GPNT cells were transfected over 2 days according to the protocol shown (A and B). GPNT cells were transfected with either transfection agent alone (siPORT C), mature mimic control followed by anti-miR control (+C + -C), mature mimic control followed by anti-miR-494 (+C + -494), mature miR-494 mimic followed by anti-miR control (+494 + -C), mature miR-494 mimic followed by anti-miR-494 (+494 + -494) or did not receive any treatment (NTC). miR-494 expression was assessed in cell lysates harvested 24 hours following hypoxic challenge (pink) or control normoxic conditions (grey) (n=3). Change in miRNA expression was assessed by qRT-PCR and relative quantification (RQ) calculated from ΔΔCt following normalisation to a housekeeper miRNA, U87, and compared to miRNA expression in the NTC control cells. Data shown is RQ ± RQmax/RQmin. Raw Ct values are given above each column. Statistical probability of differences in expression observed were calculated using one-way ANOVA with Tukey's Multiple Comparisons Test. Selected statistical significances are shown on the graph: ****p<0.0001 vs. normoxic NTC cells; ♦♦♦♦p<0.0001 vs hypoxic NTC cells; ####p<0.0001 for selected pair.

Gene expression of putative miR-494 target genes (PTEN, MMP2 and MMP9) was subsequently analysed in the GPNT cells in which miR-494 expression had been modulated. However, as the expression of housekeeper genes traditionally used in our research (GAPDH and ß-actin) were unstable in GPNT cells following hypoxic challenge it was important that another endogenous control gene was found that remained stable in GPNT cells following hypoxic challenge. To this end a TaqMan Array Rat Endogenous Control 96-well Plate (Applied Biosystems®) was run. The plate contained 16 gene expression assays for genes previously shown to be good candidates for housekeeper genes. The genes tested were as follows: 18S, ARBP, ACTB, B2M, GAPDH, GUSB, HMBS, HPRT, PGK1, PPIA, PPIB, RPLP2, TBP, TFRC, UBC and YWHAZ. In this experiment expression of the 16 housekeeper genes were evaluated in 3 normoxic and 3 hypoxic GPNT cell lysates. The average Ct of each gene in the 6 cell lysates tested is given in Table 3.2 along with the standard deviation. The gene with the highest standard deviation in the 6 samples tested was TBP (average Ct 29.92, SD 2.04). The gene with the lowest standard deviation in the samples tested was UBC (average Ct 20.45, SD 1.10). While a standard deviation of under 0.5 is desirable for any housekeeper gene, the expression of UBC was more stable than that of GAPDH and ß-actin in these cell lysates.

The results were subsequently validated by comparing expression of ß-actin and UBC in GPNT cells in which miR-494 expression had been modulated (Figure 3.8). The average expression of ß-actin in these cells was 21.62 (Ct), with a standard deviation of 0.98. The average expression of UBC in these cells was 24.34 (Ct) with a standard deviation of 0.90. While the expression of UBC was more stable than that of ß-actin it was still considered too variable in this particular experiment to be used as a housekeeper when calculating relative quantification of miR-494 target genes.

Table 3.2 – Housekeeper Optimisation Results
Gene expression was assessed in GPNT cell lysates harvested 24 hours following hypoxic challenge or control normoxic conditions (n=3/condition). Gene expression was assessed by qRT-PCR using a TaqMan Array Rat Endogenous Control 96-Well Plate. Data shown is average Ct and standard deviation.

Housekeeper	Average Ct	Standard Deviation
TBP	29.92	2.04
PPIB	22.02	1.50
ARBP	22.60	1.42
HMBS	28.34	1.39
YWHAZ	25.63	1.39
PPIA	20.91	1.38
GUSB	29.09	1.37
HPRT	23.97	1.37
TFRC	32.50	1.36
ACTB	20.86	1.30
RPLP2	20.63	1.29
18S	21.45	1.27
PGK1	24.18	1.27
GAPDH	23.67	1.26
B2M	20.08	1.16
UBC	20.45	1.10

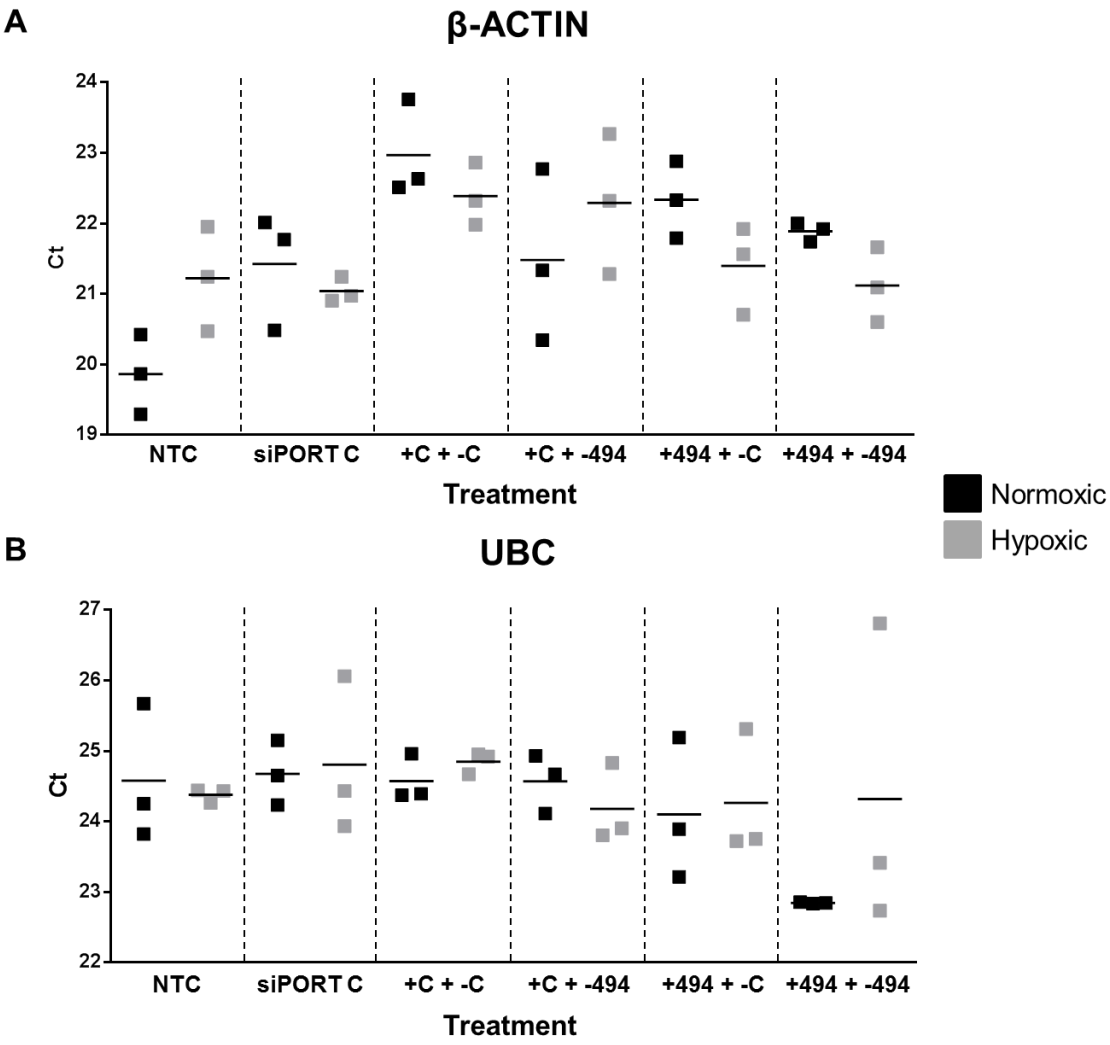

Figure 3.8 – Housekeeper Expression post miR-494 Modulation
GPNT cells were transfected over 2 days with either transfection agent alone (siPORT C), mature mimic control followed by anti-miR control (+C + -C), mature mimic control followed by anti-miR-494 (+C + -494), mature miR-494 mimic followed by anti-miR control (+494 + -C), mature miR-494 mimic followed by anti-miR-494 (+494 + -494) or did not receive any treatment (NTC). β-actin (A) and UBC (B) expression was assessed in cell lysates harvested 24 hours following hypoxic challenge (grey) or control normoxic conditions (black) (n=3, representative graph shown here of 1 experiment). Change in gene expression was assessed by qRT-PCR. Data shown is raw Ct values.

PTEN, MMP2 and MMP9 expression was assessed in GPNT cells following modulation of miR-494. Although miR-494 expression was robustly modulated *in vitro* there were no obvious changes in expression of target genes in relation to miRNA modulation (Figure 3.9). However, it was difficult to analyse the data properly as expression of target genes varied hugely, even within treatment groups and this was more pronounced when looking at expression of MMP2 and MMP9, where endogenous levels of mRNA expression were low (Ct values of over 32).

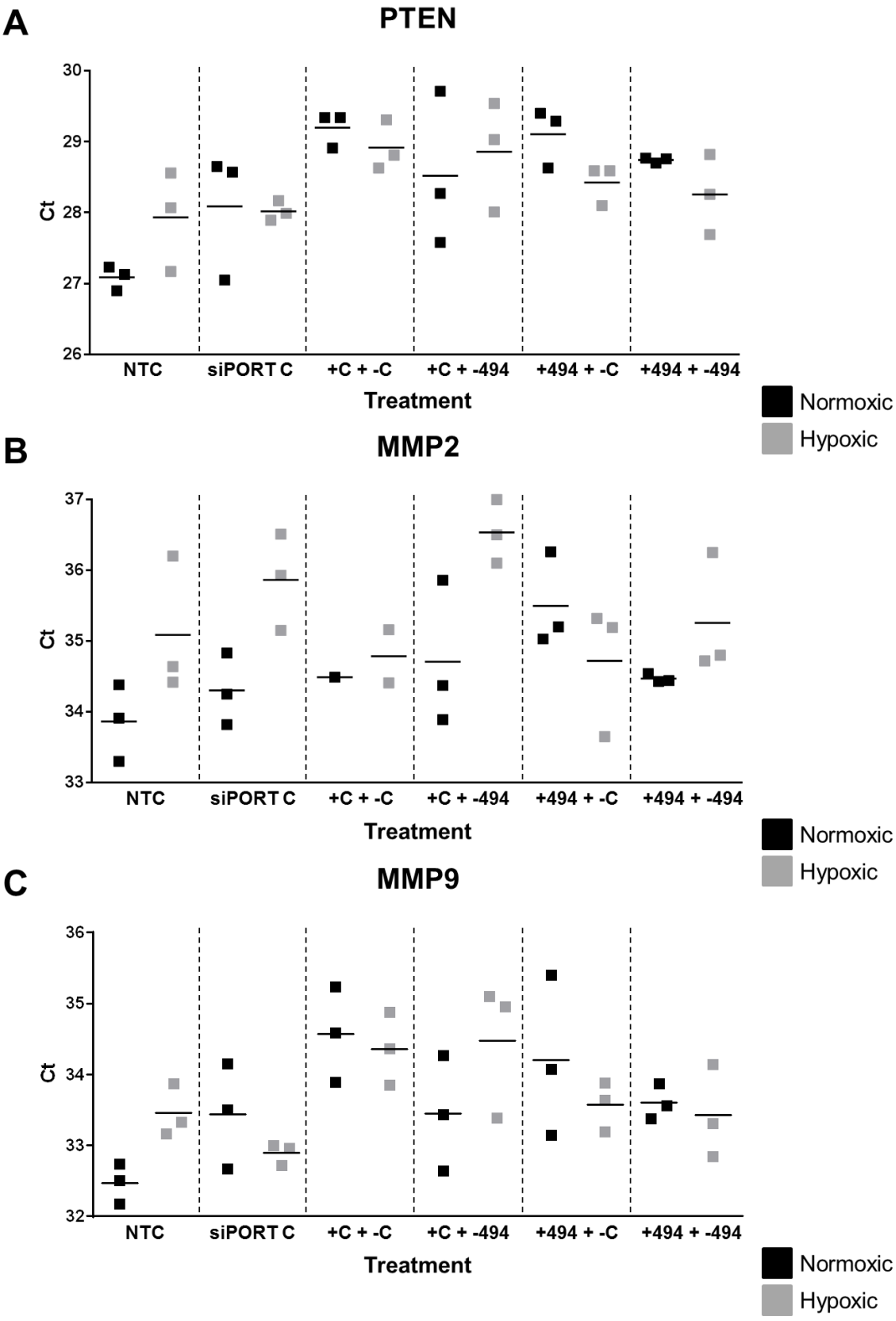

Figure 3.9 - Gene Expression post-miR-494 Modulation
GPNT cells were transfected over 2 days with either transfection agent alone (siPORT C), mature mimic control followed by anti-miR control (+C + -C), mature mimic control followed by anti-miR-494 (+C + -494), mature miR-494 mimic followed by anti-miR control (+494 + -C), mature miR-494 mimic followed by anti-miR-494 (+494 + -494) or did not receive any treatment (NTC). PTEN (A), MMP2 (B) and MMP9 (C) mRNA expression was assessed in cell lysates harvested 24 hours following hypoxic challenge (grey) or control normoxic conditions (black) (n=3, representative graph shown here of n=1 experiment). Change in gene expression was assessed by qRT-PCR. Data shown is raw Ct values.

miRNAs can regulate target gene expression by degrading (initially by destabilising) the target mRNA. However, miRNAs can also act to repress the translation of target mRNA or inhibit translation initiation without significantly affecting transcriptome expression. Although rapid mRNA degradation probably accounts for >75% of miRNA mediated gene silencing (Baek et al., 2008, Guo et al., 2010, Hendrickson et al., 2009, Selbach et al., 2008) it is plausible that modulation of miR-494 expression could affect the protein expression of target genes without affecting their transcriptome expression.

As no significant changes in the transcriptome expression of PTEN, MMP2 and MMP9 were observed following miR-494 modulation *in vitro,* the activity of target genes were assessed by western blot and gelatin zymography. PTEN acts to inhibit phosphorylation of Akt, a protein kinase that acts downstream of PTEN. To investigate the expression of PTEN and Akt, cell lysates were separated by gel electrophoresis and Western blot analysis was performed. Antibodies for PTEN, total and phosphorylated Akt proteins and a housekeeper protein, GAPDH, were bought and experiments were carried out to optimise the conditions necessary for this experiment (Figure 3.10). However the phosphorylated Akt bands were difficult to quantify meaningfully due to high background staining.

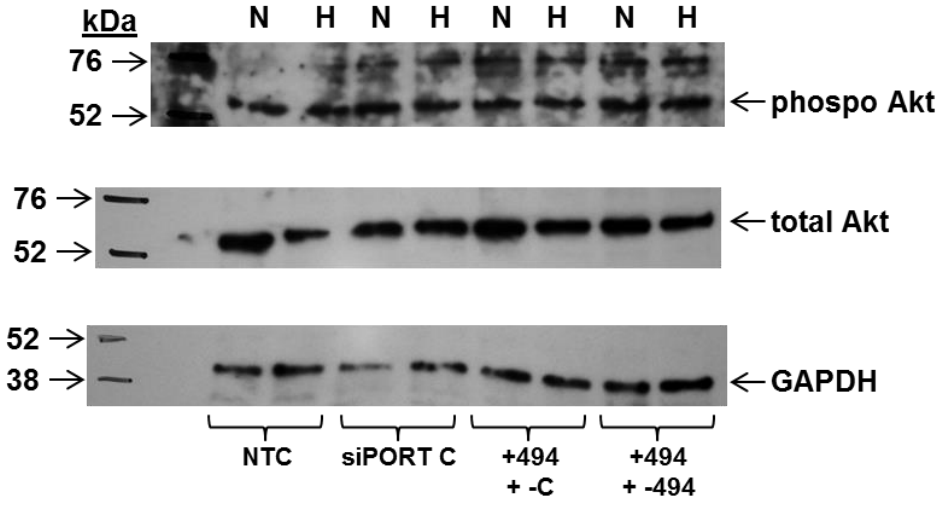

Figure 3.10 – Western Blot Optimisation
Phosphorylated and total Akt and GAPDH protein expression was assessed in GPNT cell lysates. GPNT cells were transfected over 2 days with either transfection agent alone (siPORT C), mature miR-494 mimic followed by anti-miR control (+494 + -C), mature miR-494 mimic followed by anti-miR-494 (+494 + -494) or did not receive any treatment (NTC). Protein expression was assessed in cell lysates harvested 24 hours following hypoxic challenge (H) or control normoxic conditions (N). Change in protein expression was assessed by gel electrophoresis and Western blot. Western blots were scanned using Quantity One® 4.6.8 software. Representative graph is shown of 1 optimisation experiment.

To investigate MMP2 and MMP9 activity *in vitro* following miR-494 modulation gelatin zymography was performed. miR-494 expression was modulated as described previously in GPNT cells – GPNT cell lysates were subsequently separated by gel electrophoresis in gelatin containing polyacrylamide gels. Protein lysates were not denatured prior to gel electrophoresis and subsequent Coomassie staining of the gels (blue) allowed bands of proteolytic activity (white) to be visualised. Although the experiments were carefully optimised it was difficult to obtain clear images of the white bands showing protein activity due to the fact that they were very small (see results from an optimisation experiment, Figure 3.11 A). Quantification of the zymogram gel revealed no obvious changes in either MMP2 or MMP9 activity following miR-494 modulation in GPNT cells (Figure 3.11 B and C). The experimental protocol needed to be further refined before additional experiments were carried out.

As the difficulties in assessing protein expression of miR-494 target genes became apparent, the importance of carrying out assays to investigate the functional effect of miR-494 modulation *in vitro* became clear. To assess the functional significance of miR-494 modulation a MTS cell viability assay was performed on GPNT cells in which miR-494 had been previously modulated. A MTS assay is a colorimetric method of determining the number of viable cells in a cell culture experiment. MTS is bio-reduced by cells into a formazan product that is soluble in tissue culture medium. The absorbance can subsequently be measured directly from the cell culture plate and is directly proportional to the number of living cells in culture.

Following hypoxic challenge in GPNT cells there was a significant reduction in cell viability of NTC treated cells (arbitrary units 0.80 ± 0.03 vs.1.28 ± 0.06) as was expected (Figure 3.12). However following treatment with either siPORT C, mimic control/anti-miR control (+C + -C), mimic control/anti-miR-494 (+C + -494), miR-494 mimic/anti-miR control (+494 + -C) and miR-494 mimic/anti-miR-494 (+494 + -494) there were equivalent reductions in cell viability following hypoxic challenge (Figure 3.12). Normoxic +C + -C treated cells also had significantly reduced cell viability as compared to normoxic NTC cells (1.08 ± 0.03 vs. 1.28 ± 0.06). These results indicated that modulation of miR-494 expression (either over-expression or subsequent knock-down) did not have any

therapeutic effect on the survival of GPNT cerebral endothelial cells following hypoxic challenge.

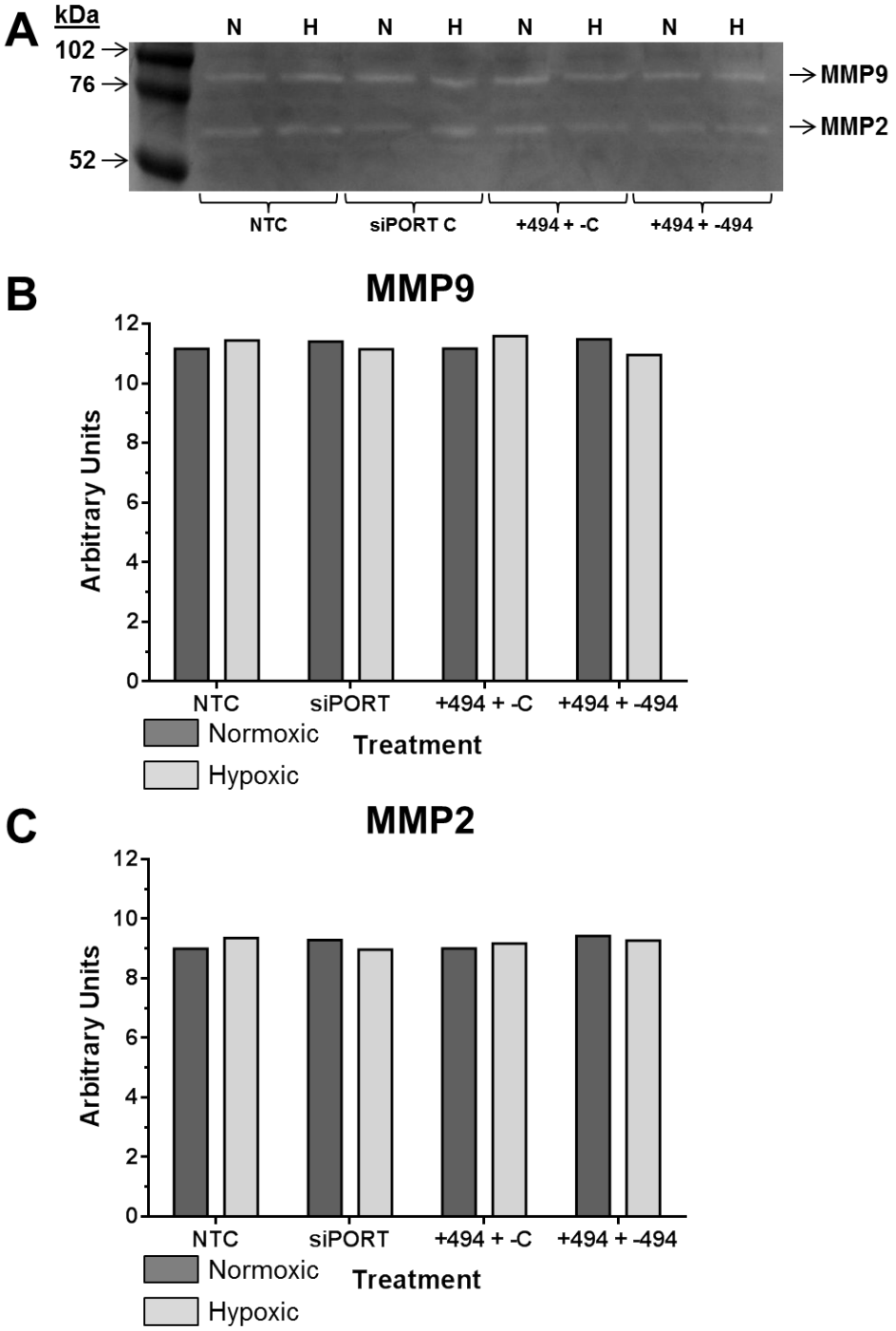

Figure 3.11 - Gelatin Zymography Optimisation
MMP2 (A, C) and MMP9 (A, B) activity was assessed in GPNT cell lysates. GPNT cells were transfected over 2 days with either transfection agent alone (siPORT C), mature miR-494 mimic followed by anti-miR control (+494 + -C), mature miR-494 mimic followed by anti-miR-494 (+494 + -494) or did not receive any treatment (NTC). MMP2 and MMP9 activity was assessed in cell lysates harvested 24 hours following hypoxic challenge (H, light grey) or control normoxic conditions (N, dark grey). Changes in MMP2 and MMP9 were assessed by gelatin zymography. Zymogram gels were scanned and analysed using Quantity One® 4.6.8 software. Arbitrary units represent the intensity of the pixels multiplied by the volume of the band. Representative graphs are shown of 1 optimisation experiment.

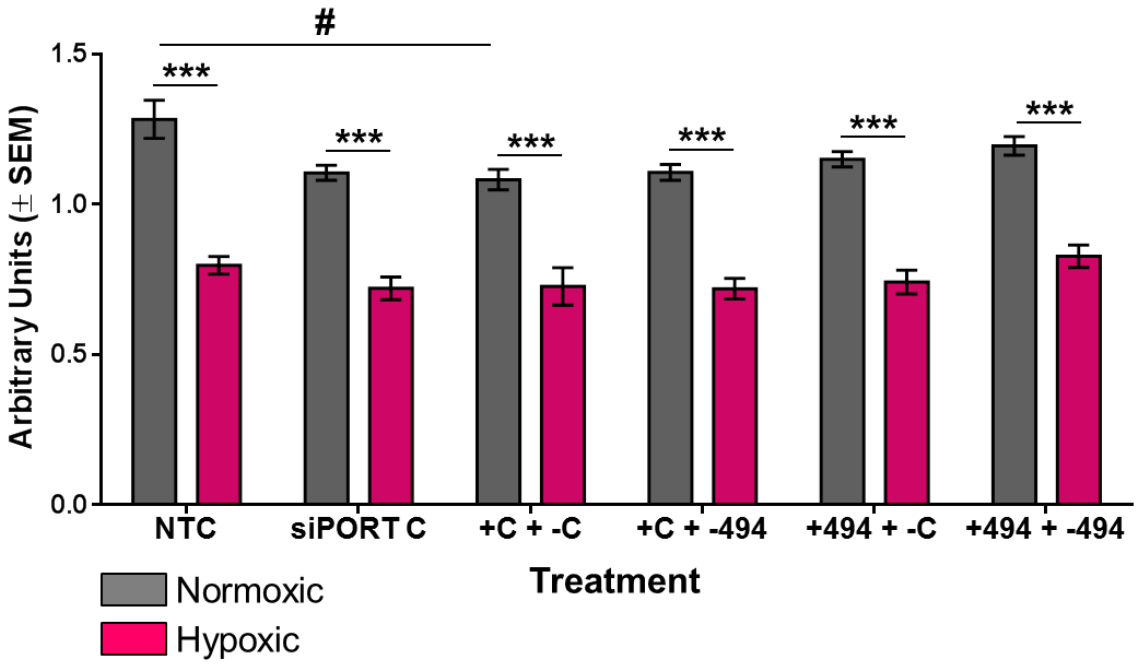

Figure 3.12 – Cell Survival post miR-494 Modulation
GPNT cells were transfected over 2 days with either transfection agent alone (siPORT C), mature mimic control followed by anti-miR control (+C + -C), mature mimic control followed by anti-miR-494 (+C + -494), mature miR-494 mimic followed by anti-miR control (+494 + -C), mature miR-494 mimic followed by anti-miR-494 (+494 + -494) or did not receive any treatment (NTC). Cell viability was assessed by a MTS cell viability assay following hypoxic challenge (pink) or control normoxic conditions (grey) (n=3). The quantity of formazan product as measured by absorbance at 490nm is directly proportional to the number of living cells in culture. Data shown is the absorbance in arbitrary units. Statistical probability of differences in cell viability observed were calculated using one-way ANOVA with Tukey's Multiple Comparisons Test: ***p<0.001 vs. normoxic counterpart cells; #p<0.05 for pair shown.

It is plausible that miR-494 modulation affected (or could affect) the expression of target genes such as PTEN, MMP9 and MMP2, although there is no obvious indication of this in our pilot, optimisation data. However, this is not important therapeutically if overall miR-494 modulation has no functional effect. We have demonstrated that robust up-regulation of miR-494 expression had no effect (either for better or worse) on cell survival following hypoxic challenge. It was therefore determined that the balance of evidence indicated that miR-494 was not a suitable therapeutic target for modulation in experimental stroke.

3.2.2 miR-21

3.2.2.1 *In Vitro* miR-21 Modulation

Modulation of miR-21 as a potential novel therapy in the setting of ischaemic stroke was subsequently investigated in pre-clinical models of ischaemic stroke. This work was carried out in conjunction with an *in vivo* study performed by Dr. Christopher Breen as part of his PhD project in which he tested whether transgenic mouse models with miR-21 over-expression or knock-down had altered outcome and/or functional recovery from experimentally induced ischaemic stroke.

Data collected by Dr. Emily Ord showed that miR-21 expression was increased in peri-infarct ipsilateral tissue of SHRSP rats at both 24 hours and 72 hours post-tMCAO (Figure 3.13). miR-21 expression was increased, non-significantly, almost four-fold in ipsilateral peri-infarct tissue at 24 hours in comparison to expression in matched tissue from sham operated animals (RQ 3.91 ± 0.49 vs. 1.00 ± 1.09) and two-fold in contralateral peri-infarct tissue (RQ 1.98 ± 0.45 vs. 1.00 ± 0.18) at the same time point (Figure 3.13 A and C). At 72 hours miR-21 expression was increased over seven-fold in ipsilateral peri-infarct tissue in comparison to expression in matched tissue from sham operated animals (RQ 7.53 ± 1.86 vs. 1.00 ± 0.93) and increased to a much smaller, but still significant, extent in matched contralateral tissue (RQ 3.72 ± 0.64 vs. 1.00 ± 0.28) (Figure 3.13 B and D).

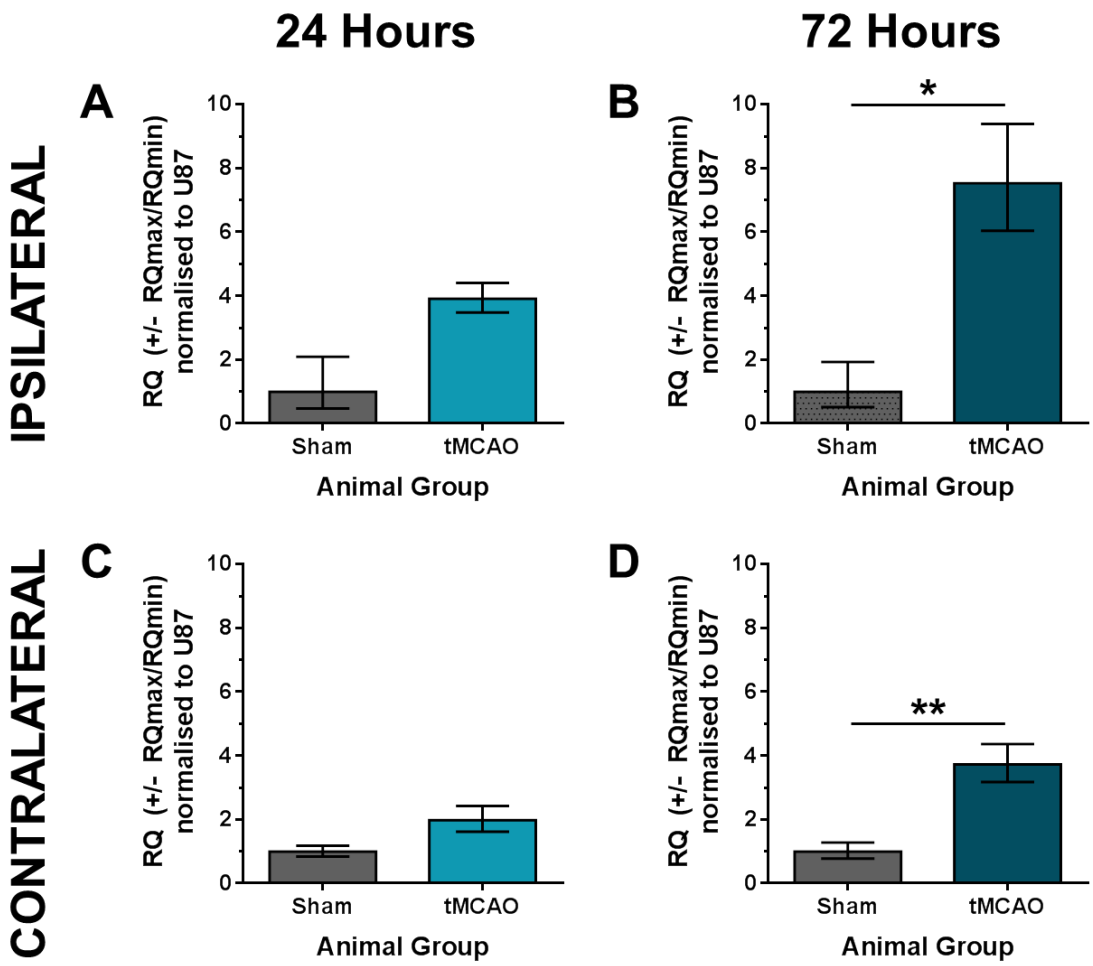

Figure 3.13 – miR-21 Expression in SHRSP Rat Brain post-tMCAO
The expression of miR-21 was assessed in ipsilateral (A, B) and contralateral (C, D) peri-infarct brain tissue of SHRSP rats at 24 hours (A, C) and 72 hours (B, D) following 45 min tMCAO (coloured bars) or sham operation (grey bars) (n=6/group). Statistical probability of differences in expression observed were calculated using unpaired Student's t-test with Bonferroni corrections, vs. sham operated rats. Change in miRNA expression was assessed by qRT-PCR and relative quantification (RQ) calculated from ΔΔCt following normalisation to a housekeeper miRNA, U87, and compared to miRNA expression in sham operated rats. Data shown is RQ ± RQmax/RQmin. Data courtesy of Dr. Emily Ord.

miR-21 expression was modulated in GPNT cerebral endothelial cells *in vitro* via the delivery of mature miRNA mimics and miRNA anti-miRs, delivered using siPORT transfection agent (Figure 3.14). miR-21 expression was unchanged in NTC GPNT cells following hypoxic challenge as compared to normoxic cells (1ΔCt 1.34 ± 0.19 vs. 1.66 ± 0.47) (Figure 3.14). miR-21 expression was also unchanged in both normoxic and hypoxic GPNT cells following delivery of siPORT and the mature mimic control (+C). Following treatment with the anti-miR control (-C) miR-21 expression was decreased in normoxic cells as compared to normoxic NTC treated cells (RQ 0.70 ± 0.11 vs. 1.00 ± 0.12). However expression of miR-21 in hypoxic –C treated cells was not significantly decreased in comparison to hypoxic

NTC treated cells (RQ 0.88 ± 0.08 vs. 1.00 ± 0.09). miR-21 expression was successfully increased following delivery of miR-21 mimic in normoxic (RQ 3.26 ± 0.41 vs. 1.00 0.12) and hypoxic (RQ 1.69 ± 0.18 vs. 1.00 ± 0.09) cells in comparison to matched NTC control cells (Figure 3.14). However similarly to what we observed following miR-494 modulation, miR-21 expression was not significantly decreased following delivery of miR-21 anti-miR to GPNT cells: normoxic (RQ 0.73 ± 0.08 vs. 1.00 ± 0.12); hypoxic (RQ 0.78 ± 0.12 vs. 1.00 ± 0.09) (Figure 3.14).

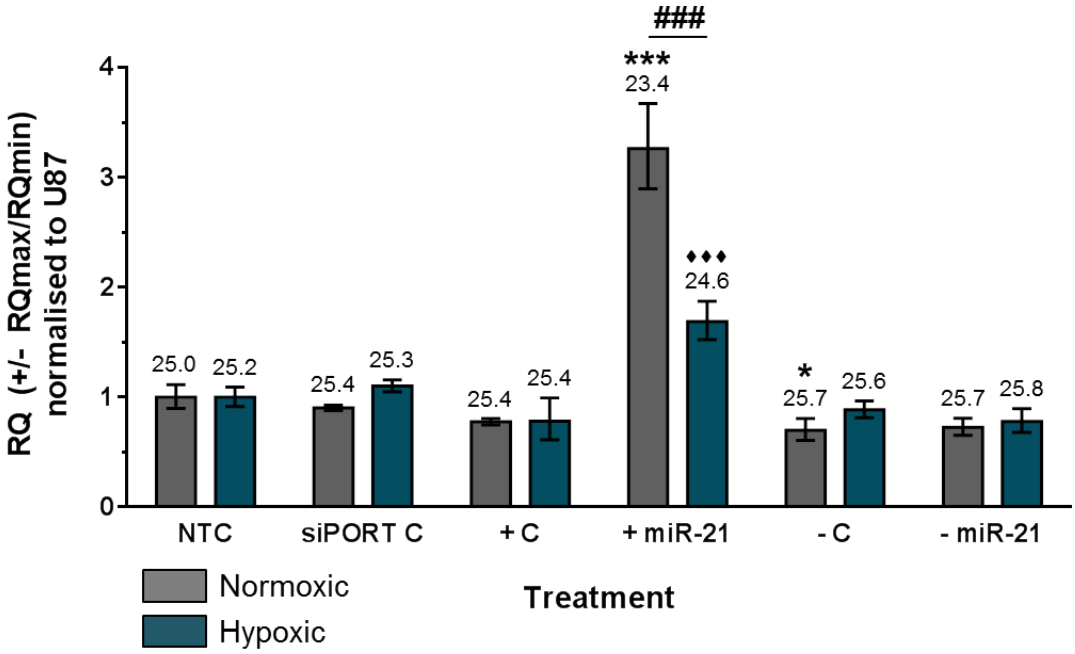

Figure 3.14 – miR-21 Modulation in GPNT Cells
GPNT cells were transfected with the transfection agent alone (siPORT C), mature mimic control (+ C), mature miR-21 mimic (+ miR-21), anti-miR control (- C) or anti-miR-21 (- miR-21) or did not receive any treatment (NTC). miR-21 expression was assessed in cell lysates harvested 24 hours following hypoxic challenge (blue) or control normoxic conditions (grey) (n=3). Change in miRNA expression was assessed by qRT-PCR and relative quantification (RQ) calculated from ΔΔCt following normalisation to a housekeeper miRNA, U87, and compared to miRNA expression in NTC control cells. Data shown is RQ ± RQmax/RQmin. Raw Ct values are shown above each column. Statistical probability of differences in expression observed were calculated using unpaired Student's t-test with Tukey's Multiple Comparisons Test. Selected statistical significances are shown on the graph: *p<0.05, ***p<0.001 vs. normoxic NTC cells; ♦♦♦p<0.001 vs hypoxic NTC cells, ###p<0.001 vs. for selected pair.

Gene expression of experimentally validated miR-21 target genes (PTEN, PDCD4, SPRY1, MMP9 and MMP2) was subsequently analysed in the GPNT cells in which miR-21 expression had been modulated. PTEN expression was unchanged in hypoxic NTC treated cells as compared to normoxic NTC treated cells (1/ΔCt 0.15 ± 0.004 vs. 0.155 ± 0.003) (Figure 3.15A). Expression of PTEN was also unchanged following treatment with controls (siPORT C, mimic control or anti-miR control). Furthermore, despite robust up-regulation of miR-21 *in vitro* there was no observable change in PTEN expression in comparison to NTC treated cells: normoxic (RQ 0.91 ± 0.03 vs. 1.00 ± 0.08); hypoxic (RQ 0.88 ± 0.01 vs. 1.00 ± 0.13) (Figure 3.15A). Similarly PDCD4 expression was unchanged in hypoxic NTC treated cells as compared to normoxic NTC treated cells (1ΔCt 0.12 ± 0.008 vs. 0.14 ± 0.006) (Figure 3.15B). Expression of PDCD4 was also unchanged following treatment with controls and also miR-21 mimic despite significant up-regulation of miR-21 expression: normoxic (RQ 0.78 ± 0.18 vs. 1.00 ± 0.25) and hypoxic (RQ 1.19 ± 0.20 vs. 1.00 ± 0.51) (Figure 3.15B).

Expression of target genes was variable following miR-21 modulation, even within treatment groups, as was also observed following miR-494 modulation. This was especially pronounced in the case of SPRY1, MMP2 and MMP9 where endogenous levels of mRNA expression were low (data not shown). The data was so variable that it was difficult to interpret and so the results are not presented here.

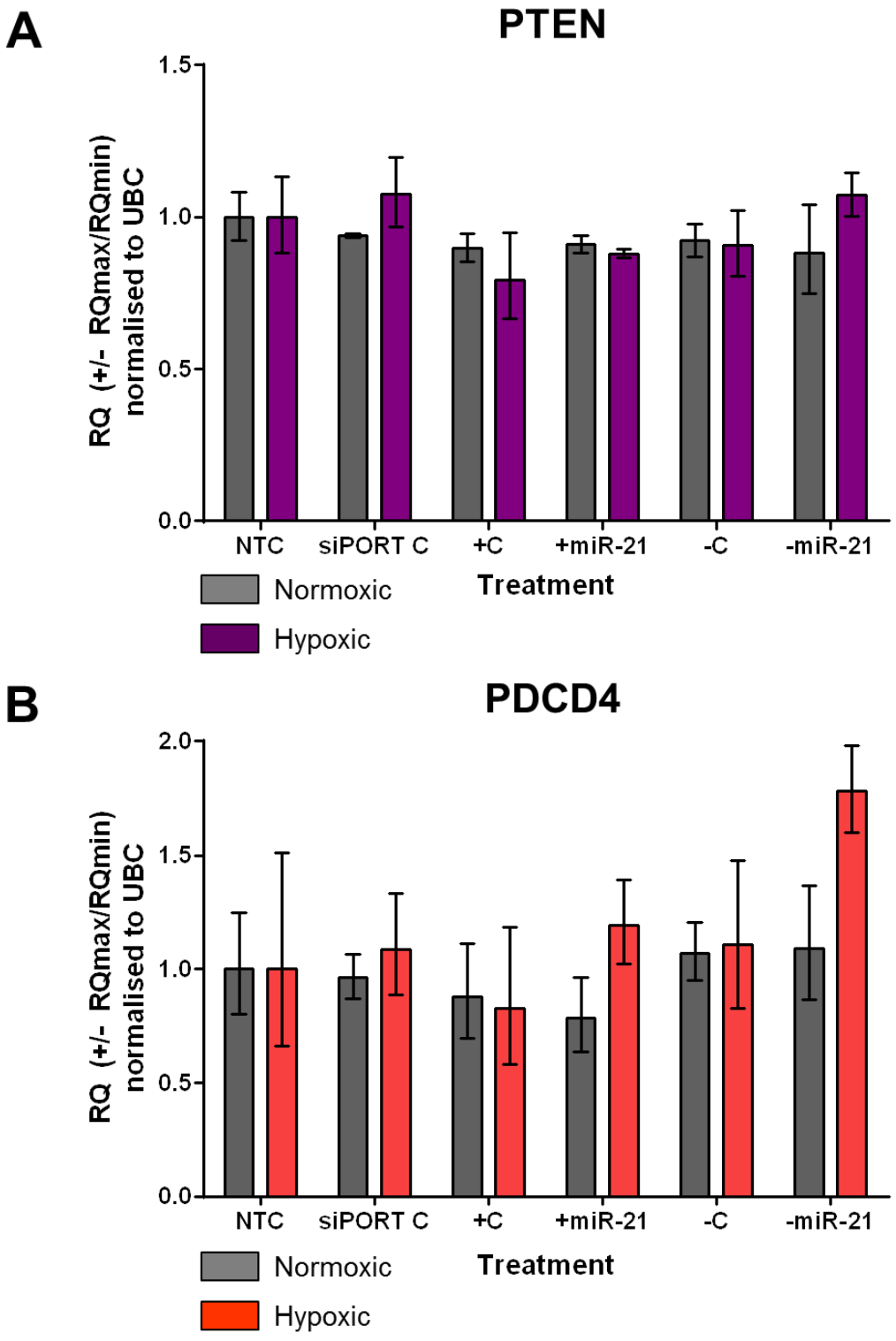

Figure 3.15 – Gene Expression post-miR-21 Modulation
GPNT cells were transfected with the transfection agent alone (siPORT C), mature mimic control (+ C), mature miR-21 mimic (+ miR-21), anti-miR control (- C) or anti-miR-21 (- miR-21) or did not receive any treatment (NTC). PTEN (A) and PDCD4 (B) expression was assessed in cell lysates harvested 24 hours following hypoxic challenge (coloured bars) or control normoxic conditions (grey) (n=3). Change in mRNA expression was assessed by qRT-PCR and relative quantification (RQ) calculated from ΔΔCt following normalisation to a housekeeper mRNA, UBC, and compared to mRNA expression in the NTC control cells. Data shown is RQ ± RQmax/RQmin. Statistical probability of differences in expression observed was calculated using unpaired Student's t-test with Tukey's Multiple Comparisons Test.

To assess the functional significance of miR-21 up-regulation a MTS cell viability assay was performed on GPNT cells in which miR-21 had been modulated. Following hypoxic challenge in GPNT cells there was a significant reduction in cell viability of NTC treated cells (arbitrary units 0.75 ± 0.07 vs.1.38 ± 0.03) (Figure 3.16), similar to what was observed previously (Figure 3.12). Treatment with control agents (siPORT C, mimic control and anti-miR control) did not result in any changes in cell viability following hypoxic challenge in comparison to their normoxic matched cells (Figure 3.16). Despite significant up-regulation of miR-21 in the GPNT cells there was no change in cell survival following treatment with miR-21 mimic in hypoxic cells in comparison to hypoxic NTC treated cells: (0.79 ± 0.05 vs. 0.75 ± 0.07). Treatment with anti-miR-21 did result in a significant reduction in cell viability in normoxic cells in comparison to normoxic NTC treated cells (1.11 ± 0.06 vs. 1.38 ± 0.03). miR-21 up-regulation did not appear to have any therapeutic benefit on the cell survival of GPNT cerebral endothelial cells following hypoxic challenge.

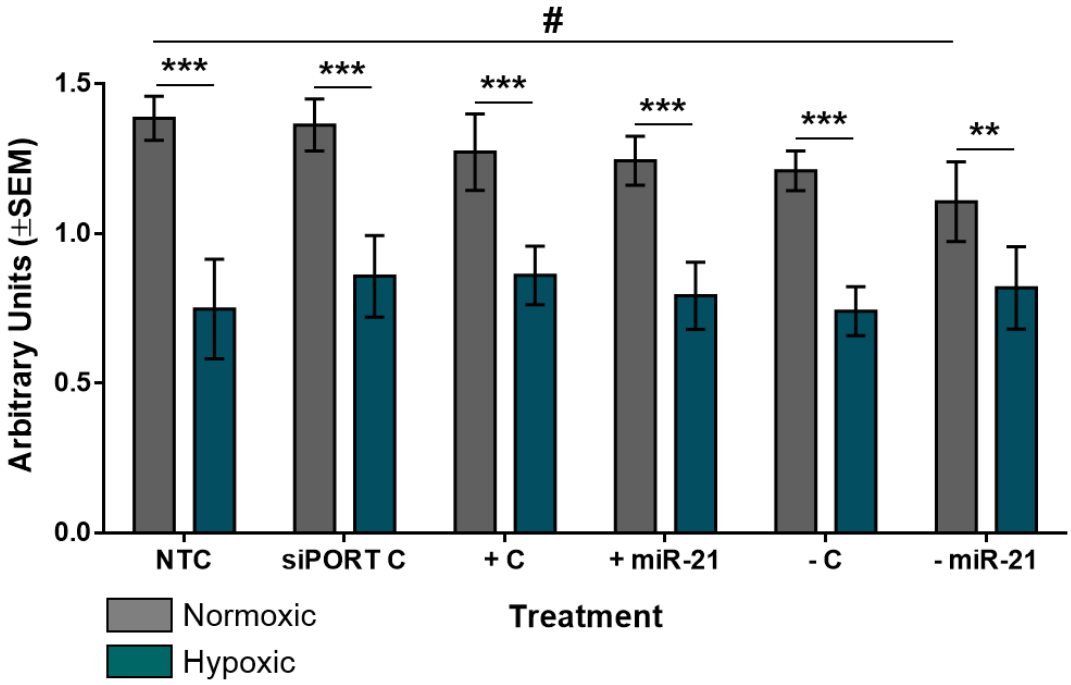

Figure 3.16 – Cell Survival post miR-21 Modulation
GPNT cells were transfected with the transfection agent alone (siPORT C), mature mimic control (+ C), mature miR-21 mimic (+ miR-21), anti-miR control (- C) or anti-miR-21 (- miR-21) or did not receive any treatment (NTC). Cell viability was assessed by a MTS cell viability assay following hypoxic challenge (blue) or control normoxic conditions (grey) (n=3). The quantity of formazan product as measured by absorbance at 490nm is directly proportional to the number of living cells in culture. Data shown is the absorbance in arbitrary units. Statistical probability of differences in cell viability observed were calculated using one-way ANOVA with Tukey's Multiple Comparisons Test: **p<0.01, ***p<0.001 vs. normoxic counterpart cells; #p<0.05 for pair shown.

3.2.2.2 Myography

Studies carried out within our group had previously shown that miR-21 is increased in the cerebrovasculature of SHRSP following tMCAO (Breen, 2015). To further investigate the possible effects of an increase in miR-21 expression on the vasculature wire myography experiments were carried out using aorta from miR-21 transgenic mice models. Two mouse models were used: a miR-$21^{-/-}$ with global knock-out of miR-21 (and its background WT strain as a control) and a miR-$21^{+/-}$ strain with heterozygous global over-expression of miR-21 (and its background WT strain as a control).

U46619 ($1x10^{-9}$ – $3x10^{-6}$ M) was used to induce concentration dependent contraction of endothelium intact rings of male mouse aortae (Figure 3.17 and Figure 3.18). U46619 is a stable synthetic analogue of endoperoxide prostaglandin (PGH_2) and acts as a thromboxane A_2 receptor agonist, causing smooth muscle contraction. L-NAME is a nitric oxide synthase inhibitor that allows vasoconstriction to happen unopposed by inhibiting basal NO release. Pre-treatment of aortae with L-NAME ($1x10^{-4}$) therefore resulted in increased maximal contraction of the aortae following treatment with U46619 in both WT strains: miR-21 knock-out WT strain ($p<0.0001$) (Figure 3.17A) and miR-21 over-expression WT strain ($p=0.0001$) (Figure 3.18A). The increased maximal contraction obtained following treatment with L-NAME was consistent with inhibition of basal nitric oxide activity. In miR-$21^{-/-}$ mice this enhancement of contraction, following treatment with L-NAME, was completely ablated ($p=0.847$) (Figure 3.17B) suggesting there was no (or very limited) endothelial basal NO activity consistent with a detrimental phenotype associated with the specific loss of miR-21 expression. In aortae from miR-$21^{+/-}$ heterozygous mice there was enhanced sensitivity to U46619 in comparison to the WT aortae and an increase in maximal contraction in the presence of L-NAME (Figure 3.18B). The aortae from the miR-$21^{+/-}$ mice demonstrated the most significant change in contraction following L-NAME treatment as not only was contraction enhanced overall ($p<0.0001$), there was as a significant increase in sensitivity, demonstrated by a significant difference between the EC_{50} values following treatment with L-NAME (U46619 EC_{50}: 5.28×10^{-8} vs. U46619 + L-NAME EC_{50} 3.53×10^{-8}; $p=0.0011$).

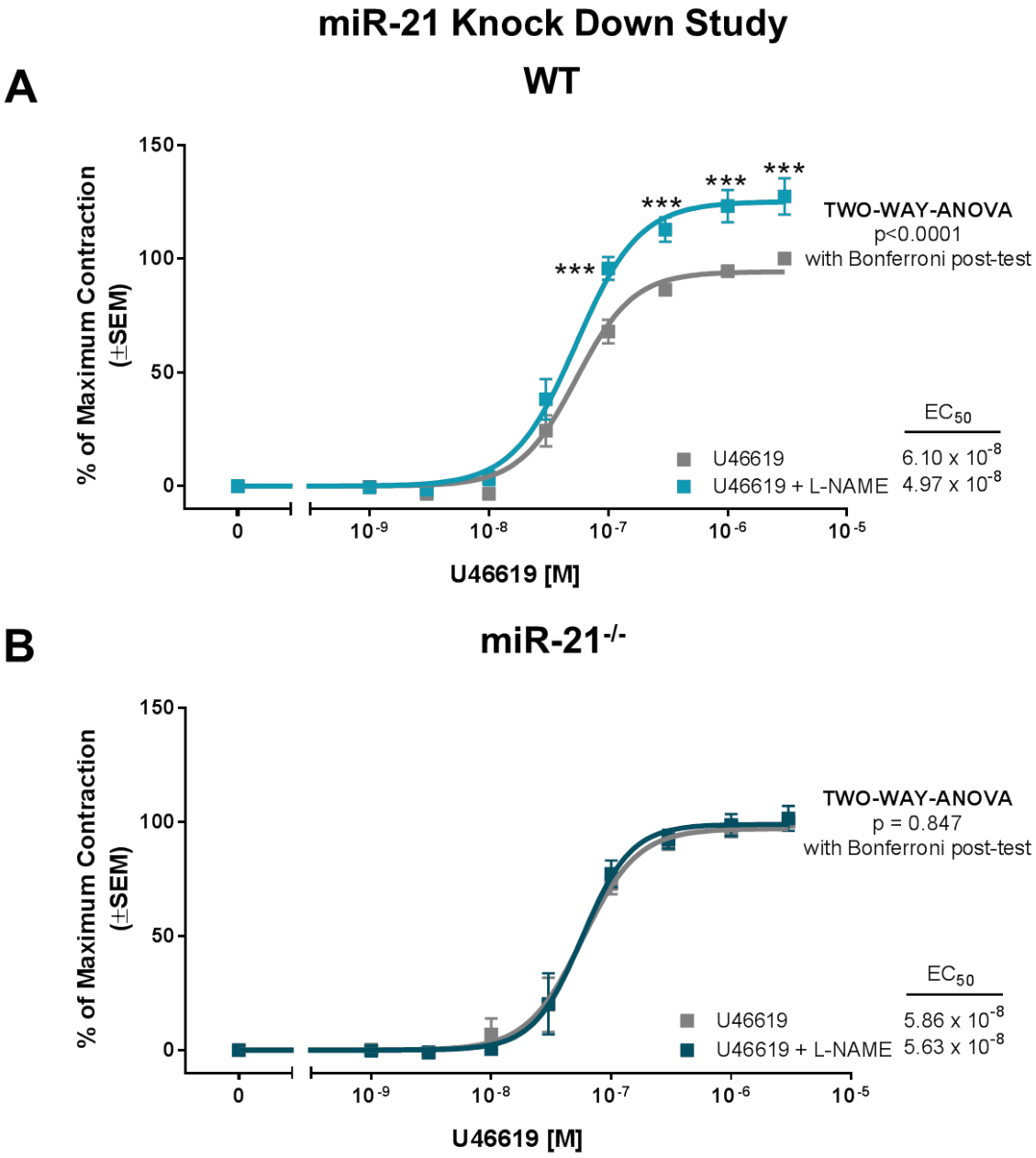

Figure 3.17 – Vessel Contractility in Aorta of miR-21$^{-/-}$ Mice
The concentration-dependent contractile effect of U46619 (1x10^{-9} – 3x10^{-6} M) was examined following pre-treatment with L-NAME (1x10^{-4} M) in WT (A) and miR-21$^{-/-}$ mice (B). Each point is the mean ± SEM of several observations: (A) n=9 (B) n=7. Statistical significance was assessed by two-way-ANOVA with Bonferroni's Multiple Comparisons Test: probability values for overall difference in contraction following pre-treatment with L-NAME are given on the graph; ***p<0.001 significant difference in contraction of aortae treated with L-NAME vs. aortae treated with U46619 alone for a specific concentration. Statistical significance of differences between EC_{50} values was assessed by extra sum of squares F test.

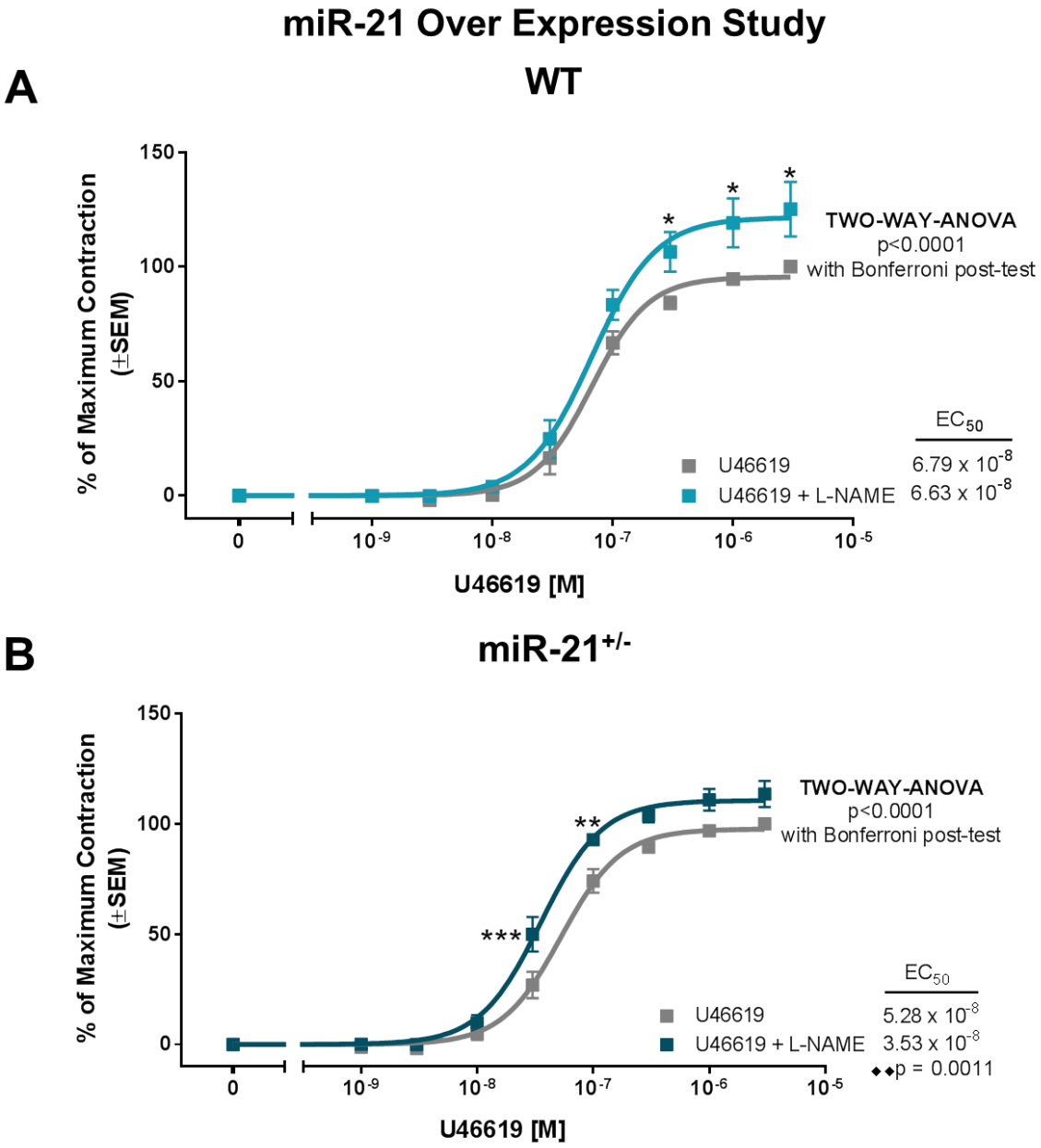

Figure 3.18 – Vessel Contractility in Aorta of miR-21$^{+/-}$ Mice
The concentration-dependent contractile effect of U46619 (1x10^{-9} – 3x10^{-6} M) was examined following pre-treatment with L-NAME (1x10^{-4} M) in WT (A) and miR-21$^{+/-}$ mice (B). Each point is the mean ± SEM of several observations: (A) n=9 (B) n=9. Statistical significance was assessed by two-way-ANOVA with Bonferroni's Multiple Comparisons Test: probability values for overall difference in contraction following pre-treatment with L-NAME are given on the graph; *p<0.05, **p<0.01; ***p<0.001 significant difference in contraction of aortae treated with L-NAME vs. aortae treated with U46619 alone for a specific concentration. Statistical significance of differences between EC$_{50}$ values was assessed by extra sum of squares F test: ♦♦p<0.01.

Acetylcholine ($1x10^{-8}$ – $3x10^{-5}$ M) was used to induce concentration dependent relaxation of endothelium-intact rings of male mouse aortae. While acetylcholine did induce relaxation of miR miR-$21^{-/-}$ and WT aortae (as assessed by two-way ANOVA, p=0.0001) this was primarily in the WT aortae (Figure 3.19A). A sigmoidal curve could not be fitted this data. There was no difference in the relaxation curves between the two mouse strains (p=0.866) (Figure 3.19A). These results were possibly a result of experimental error and/or the unstable nature of acetylcholine as a drug. Before adding acetylcholine to the organ bath the aortae were pre-contracted to approximately 80% of their original maximal contraction using an appropriate dose of U46619. However, it took some time to work out an appropriate level of pre-contraction and so these experiments will need to be repeated to get a true result. Furthermore, acetylcholine can be rapidly degraded – for this reason carbachol was used to investigate vessel relaxation in miR-$21^{+/-}$ and WT mice. Carbachol ($1x10^{-8}$ – $3x10^{-5}$ M) induced concentration dependent relaxation of miR-$21^{+/-}$ and WT mice aortae ($p<0.0001$) but there was no difference in the relaxation induced between the miR-$21^{+/-}$ and WT mice aortae (p=0.138) (Figure 3.19B).

The results from the myography experiments looked interesting and were consistent with our hypothesis that miR-21 modulation could have a therapeutic effect in the setting of ischaemic stroke although further work is needed to complete these experiments and to expand on them. However, in the light of the negative results obtained following miR-21 modulation in the *in vitro* study (presented here) and the *in vivo* study (Breen, 2015) it was decided to stop the experiments early and focus on a new study, presented as part of this thesis in Chapter 4 and Chapter 5.

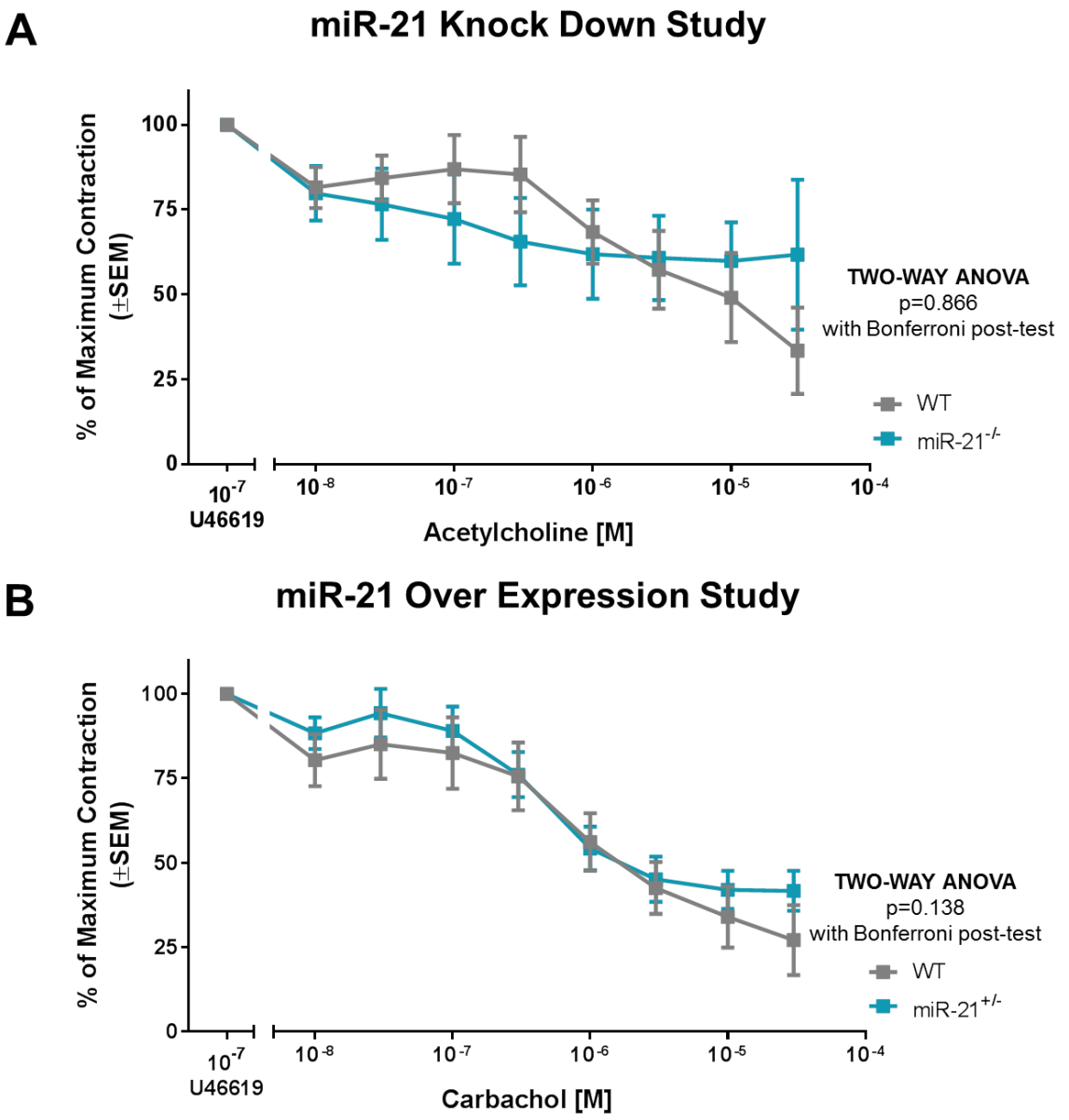

Figure 3.19 – Vessel Relaxation in Aorta of miR-21$^{-/-}$ and miR-21$^{+/-}$ Mice
The concentration-dependent relaxation effect was examined following treatment with acetylcholine (1x10^{-8} – 3x10^{-5} M) (A) or carbachol (1x10^{-8} – 3x10^{-5} M) (B) in the aorta of male WT and miR-21$^{-/-}$ mice (A) and WT and miR-21$^{+/-}$ mice (B). Each point is the mean ± SEM of several observations: (A) n=7-9/group (B) n=9/group. Statistical significance was assessed by two-way-ANOVA with Bonferroni's Multiple Comparisons Test: probability values for overall difference in relaxation between WT and either miR-21$^{-/-}$ or miR-21$^{+/-}$ aortae are given on the graph

3.3 Discussion

It was hypothesised that modulation of two candidate miRNAs, miR-494 and miR-21, would prove therapeutically beneficial in pre-clinical ischaemic stroke studies. The presented studies focussed on assessing the extent of miRNA modulation *in vitro* following delivery of miRNA mimics and anti-miRs. Subsequently the effect of miR modulation was assessed by profiling the expression of putative miRNA target genes and carrying out functional assays to measure cell survival following ischaemic insult. To investigate the effect of miR-21 on the vasculature wire myography experiments were performed on vessels taken from miR-21 transgenic mice.

Initial results demonstrated that, unlike pilot data and previously reported studies, miR-494 was not up-regulated at either 24 or 72 hours post-stroke in ipsilateral brain tissue of SHRSP rats following 45 minute tMCAO. SHRSP have a number of comorbidities that are often present in human patients including hypertension, hypertriglyceridemia, hypercholesterolemia, nephropathy, insulin resistance and hyperinsulinemia (Nagaoka et al., 1976). miR-494 had previously been shown to be up-regulated post-stroke in the brain tissue of healthy, normotensive rats such as SDs (Jeyaseelan et al., 2008, Zhai et al., 2012) and Fischer (Gubern et al., 2013). Circulating miR-494 expression was also increased in human ischaemic stroke patients but this microarray data was not validated and was compared to expression in healthy control patients (Sepramaniam et al., 2014, Tan et al., 2013). Therefore, if basal miR-494 expression is increased as a result of comorbidities such as hypertension, increased miR-494 expression may appear enhanced in these studies and might not have been observed if unhealthy, co-morbid controls had been used. Pilot data collected by a student in our group suggested that miR-494 was significantly increased in SHRSP at 24 hours post-tMCAO, especially in the ischaemic infarct and to a lesser extent in the ischaemic peri-infarct (penumbra), even when compared to hypertensive SHRSP sham operated animals. However, group sizes in the pilot study were approximately half (n=2-4/group) of those in the presented study (n=6/group). Furthermore, in the present study the infarct and peri-infarct areas were identified by T2-weighted MRI scan and tissue was isolated very carefully. In the pilot study peri-infarct tissue was only visually assessed before dissection

meaning that data shown here is more likely to be a true representation of what is occurring biologically.

miR-21 expression was increased in ipsilateral and contralateral peri-infarct SHRSP brain tissue following tMCAO. This is consistent with a number of pre-clinical and clinical studies where miR-21 expression was shown to be increased in brain tissue post embolic MCAO or 4 vessel occlusion in Wistar and SD rats (Buller et al., 2010, Deng et al., 2013) and in blood samples collected from ischaemic stroke patients at a number of time points post-stroke in comparison to healthy control patients (Tan et al., 2009, Tsai et al., 2012, Wang et al., 2014b). Interestingly, circulating miR-21 expression was unchanged in stroke patients when compared to patients with vascular risk or other neurological problems (Kim et al., 2015).

Transcriptome expression of PTEN, MMP2 and MMP9 was significantly altered in brain tissue of SHRSP rats following tMCAO. These three genes are validated targets of miR-21 and while only PTEN is a validated target of miR-494, MMP9 and MMP2 are predicted targets. miRNAs usually act to negatively regulate gene expression and in the present study up-regulated miR-21 expression is associated with down-regulated PTEN expression in peri-infarct tissue at both 24 and 72 hours post-stroke. Increased miR-21 expression is also associated with decreased PTEN and increased pAkt expression in VSMCs and HUVECs (Ji et al., 2007, Weber et al., 2010). Furthermore, following ICV infusion with miR-21 mimic the protein (but not transcriptome) expression of PTEN was decreased and that of pAkt increased (Ge et al., 2014) in the brains of SD following traumatic brain injury.

In the present study MMP2 mRNA expression was increased significantly in infarct tissue at 24 hours post-tMCAO and in infarct, peri-infarct and remainder tissue at 72 hours post-tMCAO. Furthermore, MMP9 mRNA expression was shown to be significantly up-regulated in all brain tissue at 24 hours post-tMCAO but unchanged at 72 hours post-tMCAO. Activation of MMP2 following reperfusion is associated with early phase BBB disruption (Yang and Rosenberg, 2011). MMP9 is increased as a result of oxidative stress and is also released from infiltrating neutrophils and is primarily linked with later phase (24 to 72 hours post ischaemic insult) BBB disruption (Yang and Rosenberg, 2011). A study investigating MMP9 expression in a rodent model of stroke demonstrated

significant increases in MMP9 expression at 3, 6, 12 and 24 hours post-stroke, but did not investigate expression at later time points (Park et al., 2009). It is possible that the time points assessed in the present study do not adequately reflect the rapidly evolving changes in MMP2 and MMP9 expression post-ischaemic insult, which would explain why we do not observe significant increases in MM9 mRNA expression at 72 hours post-stroke in the present study.

Previously, mice with endothelial specific miR-21 knock out had increased MMP2 expression when compared to WT mice (Zhang et al., 2013). This would suggest that up-regulated MMP2 expression in the present study is not connected to increased miR-21 expression.

Human macrophages treated with miR-21 mimic had increased expression and secretion of MMP9 (Fan et al., 2014) although decreased miR-21 expression in the serum of patients with non-calcified coronary plaques was also associated with increased MMP9 expression (Fan et al., 2014). Increased miR-21 expression in SD rats following transient 4 vessel occlusion positively correlated with increased MMP9 expression and treatment with anti-miR-21 resulted in decreased MMP9 expression *in vivo* (Deng et al., 2013). The increased MMP9 expression observed in the present study is therefore consistent with MMP9 being a target of miR-21.

miR-494 and miR-21 expression was successfully up-regulated *in vitro* using mature miRNA mimics. However, there was no decrease in miRNA expression following delivery with either miR-494 or miR-21 anti-miRs, although miR-494 expression was down-regulated when anti-miRs were delivered after first up-regulating miR-494 expression with miR-494 mimics. Despite robust increases in both miR-21 and miR-494 expression following treatment with miRNA mimics there was no obvious effect of increased miRNA expression on transcriptome expression of target genes. If it had been possible to carry out a screening experiment to assess the whole transcriptome this may have detected changes in novel targets of miR-494 and miR-21 not considered in the present study.

Numerous studies have demonstrated differential transcriptome and protein expression following miRNA modulation so it is possible that while transcriptome expression of target genes was unchanged protein expression was modulated.

For this reason we had planned to assess PTEN and Akt expression by Western Blot and MMP2 and MMP9 activity by gelatin zymography. Unfortunately in the time we had to carry out these experiments we were not able to optimise the methodology sufficiently to get usable results. However, if the protein expression of target genes such as PTEN (which regulates Akt activity as part of an endogenous pro-survival pathway) was changed we would have expected to see changes in cell survival, as assessed by MTS assay. In the present study there was no change in cell survival following treatment with miRNA mimics post-hypoxic insult.

One hypothesis for why there was no observable change in target transcriptome expression or cell survival following increased miR-494 or miR-21 expression is that miRNA expression was increased to supraphysiological levels, inducing counter regulatory mechanisms to counteract the increase (van Rooij and Kauppinen, 2014). This could especially be the case with miR-494 modulation where its expression was increased over 5000-fold following treatment with miR-494 mimic. The dose of miRNA mimic used had been optimised previously (Breen, 2015) and it was hypothesised that if a lower dose was given it might not have sufficiently perturbed the cellular homeostasis to induce the modulation of target genes. The same dose of both miR-494 and miR-21 mimic was used but resulted in much greater over-expression of miR-494 than miR-21, reflecting the lower endogenous expression of miR-494.

An alternative hypothesis for why we did not observe any changes in cell survival following increased miR-494 or miR-21 expression is that the mimics delivered *in vitro* were not being processed by the cells to which they were delivered. Recently, total levels of miRNA expression (assessed by qRT-PCR) were compared to the expression of miRNAs bound to Argonaute (assessed by Argonaute immunoprecipitation) following transfection with miRNA mimics (Thomson et al., 2013). MDA-MB-231 cells were transfected with miRNA mimic using Lipofectamine or HiPerfect transfection reagents. Significant increases in miRNA expression (assessed by qRT-PCR) were observed following transfection with miRNA mimic but also when the mimic was added following cell lysis. miRNAs must be incorporated into RISC to be functional - these results therefore demonstrate that qRT-PCR data does not necessarily reflect true functionality of the miRNA. Argonaute immunoprecipitation revealed that the amount of RISC

associated miRNA expression was much lower than what had been demonstrated by qRT-PCR, suggesting that most of the transfected mimic was not bound to Argonaute and was therefore non-functional (Thomson et al., 2013). They subsequently demonstrated that the majority of transfected miRNA co-localised with lysosomes suggesting that miRNA mimics are retained (non-functionally) within vesicles and then amplified by qRT-PCR following cell lysis (Thomson et al., 2013).

The lack of functional effect following transfection with miRNA mimics *in vitro* in the presented study is consistent with the hypothesis that miRNA mimics were not functionally processed by the cells to which they were delivered. However, there is not enough data to support this conclusion. In the present study mimics and anti-miRs for both miR-21 and miR-494 were purchased from Invitrogen. miR-21 mimics (Sabatel et al., 2011, Wang et al., 2012, Weber et al., 2010, Yang et al., 2012, Zhou et al., 2011) and anti-miRs (Sarkar et al., 2010, Wang et al., 2012, Weber et al., 2010, Zhou et al., 2011) also purchased from Invitrogen, have been successfully used (by several studies already cited in this chapter) to modulate miR-21 expression with functional effect. The miR-21 modulating agents were used at similar concentrations in the present study to those used by previous studies in a number of primary and secondary cell types. Therefore, to fully understand the results presented here it would have been beneficial to carry out similar argonaute immunoprecipitation experiments to assess the level of miRNA that was being functionally incorporated into the cells. To further assess the effect of miRNA modulation in the present study it would have been useful if experiments to assess the protein expression and activity of target genes had been fully optimised and if other functional assays, to measure cell death, apoptosis and angiogenesis (for example), had been performed.

Wire myography experiments in the present study revealed differences in the contractility of aortae of transgenic mice with either global knock-down or over-expression of miR-21. In WT mice strains the maximal contraction of the aorta following pre-treatment with L-NAME was increased, consistent with inhibition of basal nitric oxide activity. In miR-$21^{-/-}$ this increase in contraction was completely ablated suggesting abnormal endothelial basal nitric oxide activity consistent with a detrimental phenotype associated with a loss of miR-21 expression. In miR-$21^{+/-}$ heterozygous mice the increase in maximal contraction

in the presence of L-NAME was significantly enhanced as compared to WT mice consistent with a beneficial effect of the increase in miR-21 expression. These results are consistent with those of Zhang and colleagues who demonstrated abnormal endothelial activity in mice with endothelium specific miR-21 knockout (Zhang et al., 2013). In their study the aorta of miR-21 knock-out mice were shown to have reduced maximal contraction in response to norepinephrine and endothelial dysfunction was further demonstrated by decreased sensitivity to acetylcholine when assessing endothelium dependent relaxation (Zhang et al., 2013). In the present study acetylcholine was not successful at inducing vessel relaxation in either WT or miR-21$^{-/-}$ mice. Although these experiments were further optimised and carbachol was successfully used to induce endothelium dependent relaxation in miR-21$^{+/-}$ mice, the vessel relaxation experiments in miR-21$^{-/-}$ mice were not repeated due to lack of time. However, in general the results are consistent with those of Zhang and colleagues and suggest that vessel contractile response and the ability of the endothelium to produce nitric oxide are impaired in miR-21$^{-/-}$ mice. This is also consistent with experiments demonstrating increased eNOS phosphorylation (at serine 1177) and NO production in HUVECs transfected with miR-21 mimic (Weber et al., 2010). HUVEC transfection with anti-miR-21 also reduced eNOS phosphorylation (Weber et al., 2010).

miR-21$^{+/-}$ mice were not protected from ischaemic stroke *in vivo* but there was a significant increase in mortality of miR-21$^{-/-}$ mice post-tMCAO as compared to WT mice suggesting a detrimental phenotype associated with loss of miR-21 expression (Breen, 2015). These results are consistent with those obtained in the present study. To investigate this further it would have been interesting to expand on the myography experiments performed on the aorta, part of the peripheral vasculature, and characterise the vessel reactivity of the cerebrovasculature of miR-21 transgenic mice, including the middle cerebral artery. If it had been possible to do this it would have provided information as to the importance of miR-21 modulation in the brain and context of ischaemic stroke. There are numerous differences between the peripheral and cerebral vasculature, including higher NADPH oxidase activity in intracranial vessels in association with increased Nox4 expression (Miller et al., 2005). Further experiments could also be expanded to compare endothelium-dependent and

endothelium-independent relaxation, so that the results could be compared more directly to those of previous studies (Zhang et al., 2013).

While the data generated in the present study was primarily neutral microRNAs-494 and -21 remain interesting candidates for modulation as novel therapeutic agents for the treatment of ischaemic stroke. If more time had been allotted to this project, allowing for further optimisation of experiments, interesting data may have been generated.

Chapter 4 Exosomal Packaged microRNAs in Clinical and Pre-Clinical Stroke

4.1 Introduction

The discovery of miRNAs and other non-coding RNAs has demonstrated that there are additional levels of cell-type specific gene regulation, important in both health and disease. Various miRNAs have been implicated as being dysregulated in both human stroke patients (Table 1.2 - Table 1.3) and in pre-clinical models of stroke. Importantly, a number of publications have shown modulation of miRNA expression to be effective therapeutically in pre-clinical models of stroke (Table 1.4).

miRBase (v21), the online registry of miRNAs, lists 1881 human miRNA stem loop sequences. For every stem loop sequence there are two individual miRNAs (guide and passenger strands; -5p and -3p strands). Every year many new miRNAs are discovered and the latest version of miRBase contains 5441 new mature miRNAs, including the first miRNAs in 17 species (Kozomara and Griffiths-Jones, 2014). While qRT-PCR is the gold standard methodology for sensitive, quantitative profiling of both mRNA and miRNA expression, it is limited in the number of samples and miRNAs that can be assessed at one time. Microarray screening technology is therefore the methodology of choice for global analysis of miRNA expression and produces unbiased (non-targeted), genome wide miRNA profiles.

While a number of microarray technologies exist TaqMan® OpenArray® MicroRNA Panels (used in this study) run 1000s of 33 nL reactions simultaneously on 3072-well microfluidic OpenArray® Plates that contain dried TaqMan® primers and probes for up to 758 miRNAs and controls. The fluorescence from each individual reaction is read and quantified by specialised microarray scanners. As each panel can hold up to 3 samples and 3 panels can be run simultaneously in a matter of hours, this allows for very high throughput miRNA screening in a large number of samples. Furthermore, this technology can profile miRNA expression using as little as 10-100 ng of input RNA.

Many high profile studies have successfully used large-scale microarray assays to profile miRNA expression in a range of tissue types (Liu et al., 2004a) or to profile changes in miRNA expression during the onset and development of disease, including cardiovascular disease and cancer (Chen et al., 2008, Fichtlscherer et al., 2010, Lu et al., 2005). Furthermore, miRNA expression has

been profiled in human stroke patients using array technology (Table 1.2) (Guo et al., 2013, Jickling et al., 2014, Li et al., 2015b, Sepramaniam et al., 2014, Sørensen et al., 2014, Tan et al., 2013, Tan et al., 2009, Wang et al., 2014b, Zhang et al., 2016b).

While circulating miRNA expression has been profiled in stroke patients, many of these studies profile expression in a very small number of stroke patients, do not look at the effect of stroke subtype on miRNA expression and compare expression in stroke patients to healthy control patients (as discussed more fully in section 1.2.3). These studies demonstrate how microarray technology can be used effectively to highlight candidate miRNAs of interest. There is, however, a clear need for a larger scale study that takes these additional factors into consideration, and attempts to more fully validate (by qRT-PCR) the changes observed by microarray.

Furthermore, very little is known about how exosomal miRNA expression differs from that of total circulating miRNA expression in the setting of ischaemic stroke. Only one published study, to date, has investigated exosomal miRNA expression in human stroke patients (Guo et al., 2013). This study performed a microarray on pooled samples from healthy control patients, ischaemic stroke patients and intracerebral haemorrhage (ICH) patients. They subsequently selected 5 miRNAs dysregulated in ICH patients but unaffected by patient gender and validated their expression by qRT-PCR in ICH patients. Of these miRs, 3 were detected by microarray to be also dysregulated in ischaemic stroke (IS) patients, the remaining 2 were unchanged in IS patients in comparison to control patients. The supernatant and multivesicular expression of these miRs was then compared in healthy controls and ICH patients. Although they did not investigate the multivesicular miRNA expression of IS patients, this study is the first to demonstrate compartmentalisation of miRNAs in the setting of stroke.

Pre-clinically, exosomal miR-126 expression has been shown to be down-regulated in serum of Wistar rats at 3 hours post-tMCAO or pMCAO but normalised close to pre-ischaemic levels at 24 hours post-stroke (Chen et al., 2015). Total serum expression of miR-126 was decreased at 3h post-pMCAO but not tMCAO, therefore the dysregulation of miR-126 was exosome specific in this case. Furthermore, serum expression of miR-126 was more variable than the

exosomal expression, hinting at more highly regulated exosomal miRNA expression.

Previous work within our own group used microarray technology to profile total serum miRNA expression in human patients (n=16 stroke, n=14 vascular risk factor controls) at 48 hours post-stroke (Breen, 2015). Validation of candidate miRNAs (miRs -19b, -20b, -21, -27a, -93, -106a, -139, -331, -374, -532, -590-5p and -885) was attempted by qRT-PCR in a larger patient population (n=55 stroke, n=20 vascular risk factor controls). Changes in expression of the 12 candidate miRNAs did not validate when assessed by qRT-PCR in the validation study patient population. However, when expression of these miRNAs was broken down in terms of stroke subtype there appeared to be differences in expression of some miRNAs between different stroke subtypes (miRs -19b, -21, -93, -331, -374, -590-5p and -885), with miRNA expression being especially up-regulated in large artery stroke patients (non-significantly). Exosomal expression of 4 miRs (-19b, -93, -106a and -139) was investigated in the serum of human patients and their expression was found to be increased as compared to non-stroke patients but not significantly. Finally the total and exosomal expression of 4 miRs (-19b, -93, -106a and -532) was compared in SHRSP serum at 24 and 72 hours post-tMCAO and the exosomal expression (but not the total expression) of miRs-19b, -93 and -106a were found to be significantly upregulated in SHRSP serum at 72 hours post-stroke. Total miR-532 expression was increased as compared to sham operated animals but not exosomal miR-532 expression.

These studies suggest that circulating exosomes containing miRNAs are present both in human stroke patients and in pre-clinical models of ischaemic stroke and hint at the importance of exosomal packaged miRNAs, as compared to miRNAs circulating freely in the serum. This work could be successfully built on by harnessing the power of microarray technology to profile exosomal packaged miRNA expression in a large number of stroke patients. Dysregulated exosomal miRNAs could then be investigated further to test the hypothesis that these miRNAs have a functional role to play in the setting of ischaemic stroke.

4.1.1 Hypotheses

The hypotheses of the present study were as follows:

- Packaging of miRNAs into exosomes will be significantly dysregulated in ischaemic stroke patients and as a result of this the circulating exosomal miRNA profile will be significantly altered.

- Exosomal miRNA profiles will be useful in phenotyping patients where clinical imaging has proved inconclusive and may serve to direct patient care or to predict functional outcome of patients.

- miRNAs dysregulated in ischaemic stroke patients will be similarly dysregulated in pre-clinical models of ischaemic stroke and comparison of total and exosomal miRNA expression in these models may provide insights into the functional role of exosomal packaged miRNAs following stroke.

4.1.2 Aims

The aims of this chapter were as follows:

- To profile miRNA expression in exosomes isolated from the serum of ischaemic stroke patients at 48 hours post-stroke by miRNA OpenArray experiment and to identify dysregulated miRNAs.

- To validate candidate miRNAs (as identified by OpenArray) by qRT-PCR in a large ischaemic stroke patient population.

- To relate changes in exosomal miRNA expression to stroke subtype and clinical outcome from stroke.

- To profile expression of selected miRNAs (dysregulated in ischaemic stroke patients) in pre-clinical models of ischaemic stroke.

4.2 Ischaemic Stroke Patient Results

4.2.1 Characterisation of Exosomes Isolated from Human Patients

Extracellular vesicles were isolated from serum taken from ischaemic stroke patients at 48 hours post-stroke onset. To verify that isolated vesicles were indeed exosomes (as hypothesised), vesicles were visualised, measured and quantified using NanoSight technology and transmission electron microscopy.

4.2.1.1 NanoSight

Extracellular vesicles were isolated by precipitation from 200µL of human serum using Exosome Isolation Reagent (Life Technologies). They were then visualised and quantified using a NanoSight LM10 (Figure 4.1). An example NanoSight trace for a representative serum sample shows that the majority of extracellular vesicles are found within the size range 30-120 nm (Figure 4.1A), with a small number of larger vesicles present (all <~450 nm). The average concentration of vesicles (within the size range 30–120 nm) in the serum of stroke patients was more than double the concentration of vesicles of the same size in non-stroke patients (5.2 ± 0.7 $x10^8$ particles/mL vs. 2.4 ± 0.4 $x10^8$ particles/mL), although this change was not statistically significant (Figure 4.1B). Furthermore, there were no significant differences in average concentration of extracellular vesicles found in the serum of different stroke patient subtypes (Figure 4.1C).

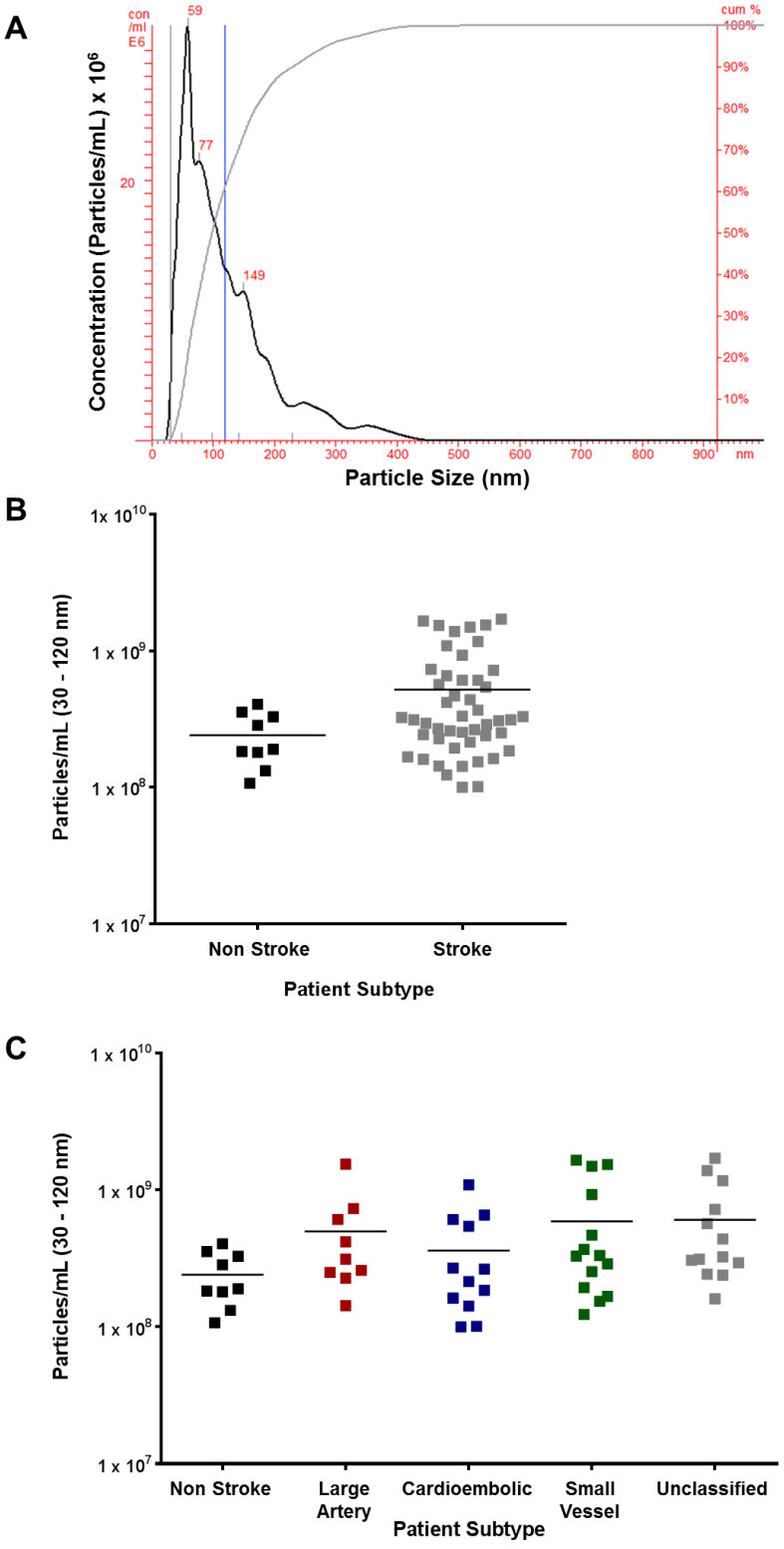

Figure 4.1 – Exosome Quantification by NanoSight
The concentration of exosomes (between 30-120 nm) isolated from 200 µL of human serum was determined for each sample using a NanoSight LM10. An example NanoSight trace for a representative sample is shown (A). The black trace indicates the concentration of exosomes with increasing particle size, while the blue trace shows the cumulative percentage of exosomes with increasing particle size. The concentration of exosomes was assessed in stroke patients (n=48) and non-stroke patients (n=9) (B). Exosome sample concentrations were also evaluated in different stroke subtypes: large artery (n=9), cardioembolic (n=12), small vessel disease (n=14) and unclassified (n=13) (C). Probability was assessed using unpaired Student's t-test, vs. non-stroke control patients (B) and one-way-ANOVA with a Dunnett's Multiple Comparison Test (C).

4.2.1.2 Transmission Electron Microscopy

Exosomes were subsequently visualised on a transmission electron microscope (TEM). To isolate exosomes for this procedure, exosomes were precipitated from serum using Exosome Isolation Reagent. The exosome pellet was subsequently resuspended in 2% paraformaldehyde before being fixed onto Formvar-carbon coated electron microscope (EM) grids according the protocol provided in Current Protocols in Cell Biology (Théry et al., 2006). Samples were contrasted using uranyl oxalate before being contrasted and embedded in a mixture of 4% uranyl acetate and 2% methyl cellulose. In this experiment it was difficult to obtain clear images where the methyl cellulose film was too thick. Furthermore, the exosome preparations were contaminated by other membranes and proteins that were also precipitated with the exosomes during the exosome isolation procedure. Exosomes were embedded and prepared for electron microscopy by Mrs Margaret Mullin.

Electron microscopy of exosomes, from extracellular vesicle isolations from two human patients, revealed both cup-shaped and more rounded membrane vesicles (Figure 4.2 A and B). Representative images were selected from the images taken and the diameter of every vesicle present in each image measured. Patient A had suffered a cardioembolic stroke; their median vesicle size was 63.0 nm, with an inter-quartile range (IQR) of 53.8 – 84.5 nm (Figure 4.2C). Patient B had suffered a small vessel disease stroke; their median vesicle size was 40.0 nm, with an IQR of 31.8 – 53.0 nm (Figure 4.2C). While the median vesicle isolated from the cardioembolic patient was ~58% bigger than that of the small vessel patient it is impossible to tell how representative these results are without visualising exosomes from further human patients by electron microscopy. These results primarily serve to show that the vast majority of vesicles isolated by precipitation fall within the exosome size range of 30 – 120 nm.

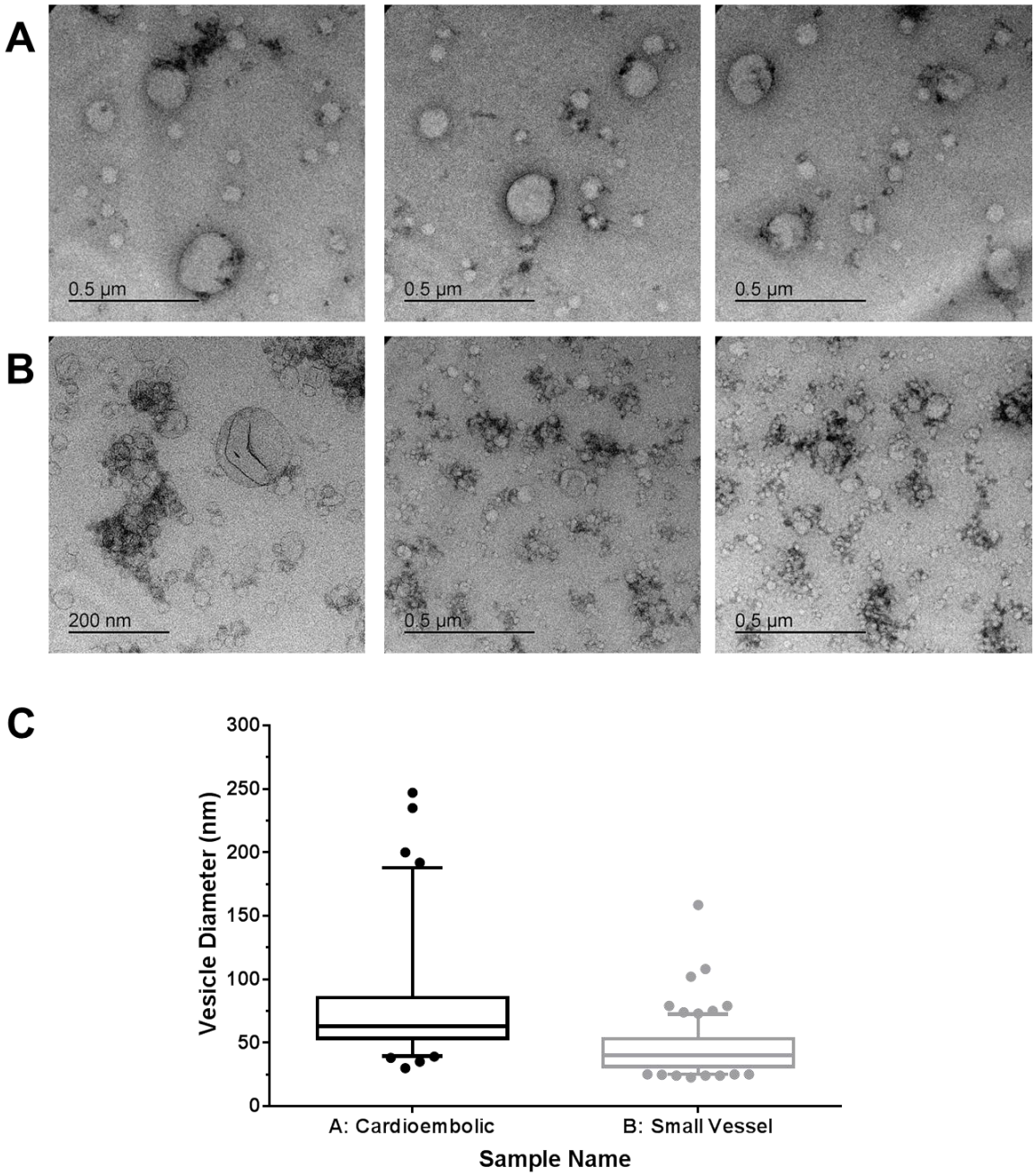

Figure 4.2 – TEM of Human Extracellular Vesicles
Electron-microscopic observation of whole-mounted exosomes purified from human serum by precipitation. Representative images of exosome isolates from two human patient samples (A - cardioembolic and B – small vessel) obtained by transmission electron microscopy showing both larger microvesicles and exosomes. A box and whisker plot to show the diameter of vesicles in representative images (n=4) (C). Plots show 5th percentile, Q1, Q2, Q3 and 95th percentile with values outside of this represented by scatter dots. Diameter was measured twice on every vesicle in each representative image and the longest diameter value was taken for each vesicle to create this graph.

4.2.2 OpenArray® Screen Design & Analysis

Microarray analysis was performed using the TaqMan® OpenArray® Human MicroRNA Panels (Life Technologies). Each panel contained 3 individual arrays and each array can profile 754 unique human miRNA sequences (plus 4 control sequences) for one sample. Sequence data for the array was sourced from miRBase (Kozomara and Griffiths-Jones, 2014). Samples were prepared and experiments completed as described in section 2.6.3. In the OpenArray experiment described here 13 TaqMan® OpenArray® Human MicroRNA Panels were used, profiling miRNA expression in 39 patient samples.

4.2.2.1 Normalisation and Data Analysis

Raw data collected from the OpenArray experiments was combined using DataAssist™ software. DataAssist™ was used to perform quality control analysis on the raw data, to perform sample normalisation for each assay and to perform quality control analysis on the normalised data. The data were subsequently exported and ΔCt values were calculated by normalising data to the exogenous spike-in control (*Arabidopsis thaliana* miR-159a; ath-miR-159a). ΔCt values for stroke patients were compared to non-stroke patient (control) values. Statistical significance for each individual miRNA was calculated using a two-tailed, Student's unpaired t-test.

4.2.2.2 Experimental Design

In order to profile exosomal miRNAs differentially regulated in ischaemic stroke patients, RNA was extracted from exosomes that had been isolated from serum harvested from ischaemic stroke patients at 48 hours post-stroke onset. The experiment was designed to document significant changes in miRNA expression between non-stroke control patients and ischaemic stroke patients but also to highlight differences between ischaemic stroke subtypes. A total of 39 patient samples were analysed by OpenArray of which 10 were non-stroke control patients and 29 were ischaemic stroke patients: large artery (n=9), cardioembolic (n=10) and small vessel (n=10).

Comparisons were made between ΔCt values of ischaemic stroke patients and non-stroke control patients to highlight exosomal miRNAs dysregulated primarily

as a result of cerebrovascular ischaemia. Furthermore, comparisons were made between individual stroke subtypes and non-stroke control patients. It was hypothesised that this would give more detailed information about whether miRNAs were dysregulated specifically in connection with differing stroke subtypes or only as a direct result of ischaemia in general. The majority of studies published to date, looking at miRNA expression in stroke patients, either make no comparison between stroke subtype and miRNA expression or do not give information as to the breakdown of their patient population with regard to stroke subtype.

4.2.3 OpenArray® Study Patient Population Demographics

The demographics of patients used in the OpenArray study are summarised in Table 4.1 and Table 4.2. In the OpenArray study serum samples from 39 patients (from the full cohort of 173 patients) were used. Serum samples were initially collected from patients who presented at the Western Infirmary with stroke-like symptoms and were referred to the Acute Stroke Unit where they were assessed by stroke-specialist clinicians. Patients were reassessed at 48 hours, 7 days, 1 month and 3 months post-symptom onset and serum samples were collected at each time point when possible.

Non stroke control patients were those patients who presented with symptoms of stroke but were subsequently given a differential diagnosis following medical imaging and clinical examination: for example, severe migraine. Importantly the non-stroke control patients were aged, hypertensive and on similar medication to the stroke patients, but this will be discussed more fully in section 4.2.5. Table 4.1 and Table 4.2 demonstrate that patient groups in the OpenArray study were matched as closely as possible for age, gender and medical history. There are no significant differences between non-stroke control and ischaemic stroke patients in any category recorded (Table 4.1). After examining demographical data for stroke patients in relation to stroke subtype it is clear that there are no significant differences in gender or age although large artery patients are slightly younger (median age 63 years vs. 70-73.5 years in other stroke subtypes). A higher number of cardioembolic stroke patients are in atrial fibrillation than any other patient subtype (50% vs. non-stroke 30%; large artery 0%; small vessel 0%) but this is expected for this stroke subtype. Differences in

miRNA expression observed in the OpenArray study can therefore be assumed to be a result of differences in patient subtype rather than of the age or general health of the patients.

Table 4.1 – OpenArray Patient Characteristics
This table summarises demographical data for the patients used in the OpenArray study. The gender, median age and number of patients positive for a number of risk factors for stroke and/or on prescribed medication are recorded. A Fisher's Exact Test was used to calculate whether differences observed between non-stroke control and ischaemic stroke patients were statistically significant. ✞ indicates a Student's t-test was used to calculate probability.

		Non-Stroke	Stroke	p (Fisher's test)
Age & Gender	n	10	29	n/a
	Male, % (n)	70.0 (7)	75.9 (22)	0.696
	Median Age	70	73	0.544✞
Risk Factors for Ischaemic Stroke	Hypertension, % (n)	70.0 (7)	51.7 (15)	0.464
	Atrial Fibrillation, % (n)	30.0 (3)	17.2 (5)	0.399
	Diabetes (Type 1 or 2), % (n)	30.0 (3)	24.1 (7)	0.696
	Hyperlipidaemia, % (n)	30.0 (3)	31.0 (9)	1.000
	PVD, % (n)	0.0 (0)	0.0 (0)	1.000
	Smoker, % (n)	30.0 (3)	31.0 (9)	1.000
	Ex-Smoker, % (n)	30.0 (3)	20.7 (6)	0.669
	Previous TIA, % (n)	0.0 (0)	3.4 (1)	1.000
	Previous Stroke, % (n)	20.0 (2)	13.8 (4)	0.636
	Family History, % (n)	10.0 (1)	13.8 (4)	1.000
Medication	rtPA, % (n)	n/a	34.5 (10)	n/a
	ACE, % (n)	40.0 (4)	17.2 (5)	0.197
	Alpha Blocker, % (n)	10.0 (1)	0.0 (0)	0.256
	Anticoagulant, % (n)	10.0 (1)	3.4 (1)	0.452
	Antiplatelet, % (n)	60.0 (6)	27.6 (8)	0.124
	ARB, % (n)	0.0 (0)	10.3 (3)	0.556
	Beta Blocker, % (n)	40.0 (4)	31.0 (9)	0.704
	Blood Pressure Treatment, % (n)	70.0 (7)	51.7 (15)	0.464
	CCB, % (n)	40.0 (4)	10.3 (3)	0.057
	Loop Diuretic, % (n)	30.0 (3)	13.8 (4)	0.344
	Oral Hypoglycaemic Drugs, % (n)	20.0 (2)	6.9 (2)	0.267
	Spironolactone, % (n)	10.0 (1)	3.4 (1)	0.452
	Statin, % (n)	60.0 (6)	44.8 (13)	0.480
	Thiazide, % (n)	20.0 (2)	6.9 (2)	0.267

Table 4.2 – Open Array Patient Characteristics (Stroke Subtype)
This table summarises demographical data for the patients used in the OpenArray study. The gender, median age and number of patients positive for a number of risk factors for stroke and/or on prescribed medication are recorded. A Chi-Square Test was used to calculate whether differences observed between patient groups were statistically significant. ✞ indicates a One-Way ANOVA with Tukey's multiple comparisons test was used to calculate probability.

		Non-Stroke	Large Artery	Cardioembolic	Small Vessel	p (Chi-square test)
Age & Gender	n	10	9	10	10	n/a
	Male, % (n)	70.0 (7)	88.9 (8)	70 (7)	70 (7)	0.730
	Median Age	70.0	63.0	73.5	73.5	0.192✞
Risk Factors for Ischaemic Stroke	Hypertension, % (n)	70.0 (7)	33.3 (3)	70.0 (7)	50.0 (5)	0.306
	Atrial Fibrillation, % (n)	30.0 (3)	0.0 (0)	50.0 (5)	0.0 (0)	0.013
	Diabetes (Type 1 or 2), % (n)	30.0 (3)	22.2 (2)	30.0 (3)	20.0 (2)	0.936
	Hyperlipidaemia, % (n)	30.0 (3)	22.2 (2)	50.0 (5)	20.0 (2)	0.459
	PVD, % (n)	0.0 (0)	0.0 (0)	0.0 (0)	0.0 (0)	-
	Smoker, % (n)	30.0 (3)	55.6 (5)	30.0 (3)	10.0 (1)	0.126
	Ex-Smoker, % (n)	30.0 (3)	33.3 (3)	20.0 (2)	10.0 (1)	0.611
	Previous TIA, % (n)	0.0 (0)	0.0 (0)	10.0 (1)	0.0 (0)	0.395
	Previous Stroke, % (n)	20.0 (2)	11.1 (1)	10.0 (1)	20.0 (2)	0.879
	Family History, % (n)	10.0 (1)	11.1 (1)	20.0 (2)	10.0 (1)	0.890
Medication	rtPA, % (n)	n/a	44.4 (4)	30.0 (3)	30.0 (3)	0.751
	ACE, % (n)	40.0 (4)	11.1 (1)	10.0 (1)	30.0 (3)	0.312
	Alpha Blocker, % (n)	10.0 (1)	0.0 (0)	0.0 (0)	0.0 (0)	0.395
	Anticoagulant, % (n)	10.0 (1)	11.1 (1)	0.0 (0)	0.0 (0)	0.526
	Antiplatelet, % (n)	60.0 (6)	22.2 (2)	40.0 (4)	20.0 (2)	0.219
	ARB, % (n)	0.0 (0)	0.0 (0)	20.0 (2)	10.0 (1)	0.285
	Beta Blocker, % (n)	40.0 (4)	22.2 (2)	40.0 (4)	30.0 (3)	0.813
	Blood Pressure Treatment, % (n)	70.0 (7)	33.3 (3)	60.0 (6)	60.0 (6)	0.423
	CCB, % (n)	40.0 (4)	11.1 (1)	0.0 (0)	20.0 (2)	0.122
	Loop Diuretic, % (n)	30.0 (3)	11.1 (1)	20.0 (2)	10.0 (1)	0.630
	Oral Hypoglycaemic Drugs, % (n)	20.0 (2)	11.1 (1)	10.0 (1)	0.0 (0)	0.536
	Spironolactone, % (n)	10.0 (1)	0.0 (0)	10.0 (1)	0.0 (0)	0.572
	Statin, % (n)	60.0 (6)	44.4 (4)	60.0 (6)	30.0 (3)	0.478
	Thiazide, % (n)	20.0 (2)	11.1 (1)	10.0 (1)	0.0 (0)	0.536

4.2.4 OpenArray® Results

553 miRNAs (out of possible 754 miRNAs) were detected by the microarray. Of these 93 were detected in ≥ 30% of patients in at least one patient subtype (i.e. non-stroke, large artery, cardioembolic or small vessel). Ideally candidate miRNAs would have expression in >90% patients. Very few miRNA met these criteria. Although this could be a result of using a low sample input (LSI) protocol (see section 2.6.3), the RNA input (ng of RNA) used was that recommended by Life Technologies for their LSI protocol. In a report published by Life Technologies the LSI protocol was demonstrated to detect 92% of the miRNAs detected using the standard protocol (Life Technologies, 2011). As a result of the small number of miRNAs detected in >90% of patients we examined differences in expression of miRNAs present in a much smaller proportion of patients than we would have otherwise. Where possible an unpaired Student's t-test was used to calculate statistical significance of differences observed between patient groups.

A number of miRNAs: hsa-miR-27b, hsa-miR-93, hsa-miR-520b and hsa-miR-660 were dysregulated in the exosomes of ischaemic stroke patients as compared to non-stroke patient controls (Figure 4.3). Of these, 3 miRNAs were increased in stroke patients and only hsa-miR-660 was significantly decreased in stroke patients. These results are summarised in Table 4.3.

Other exosomal miRNAs were either exclusively or especially dysregulated in one specific stroke subtype (Figure 4.4 - Figure 4.6). hsa-miR-93 and hsa-miR-20b were increased in large artery patients while hsa-miR-30a-5p was decreased (Figure 4.4). hsa-miR-520b was increased in cardioembolic patients while hsa-miR-660 and hsa-miR-218 were down-regulated in these patients (Figure 4.5). Finally, hsa-miR-17, hsa-miR-93 and hsa-miR-199a-3p were increased in small vessel disease stroke patients whilst hsa-miR-660 was downregulated (Figure 4.6). These results are summarised in Table 4.3.

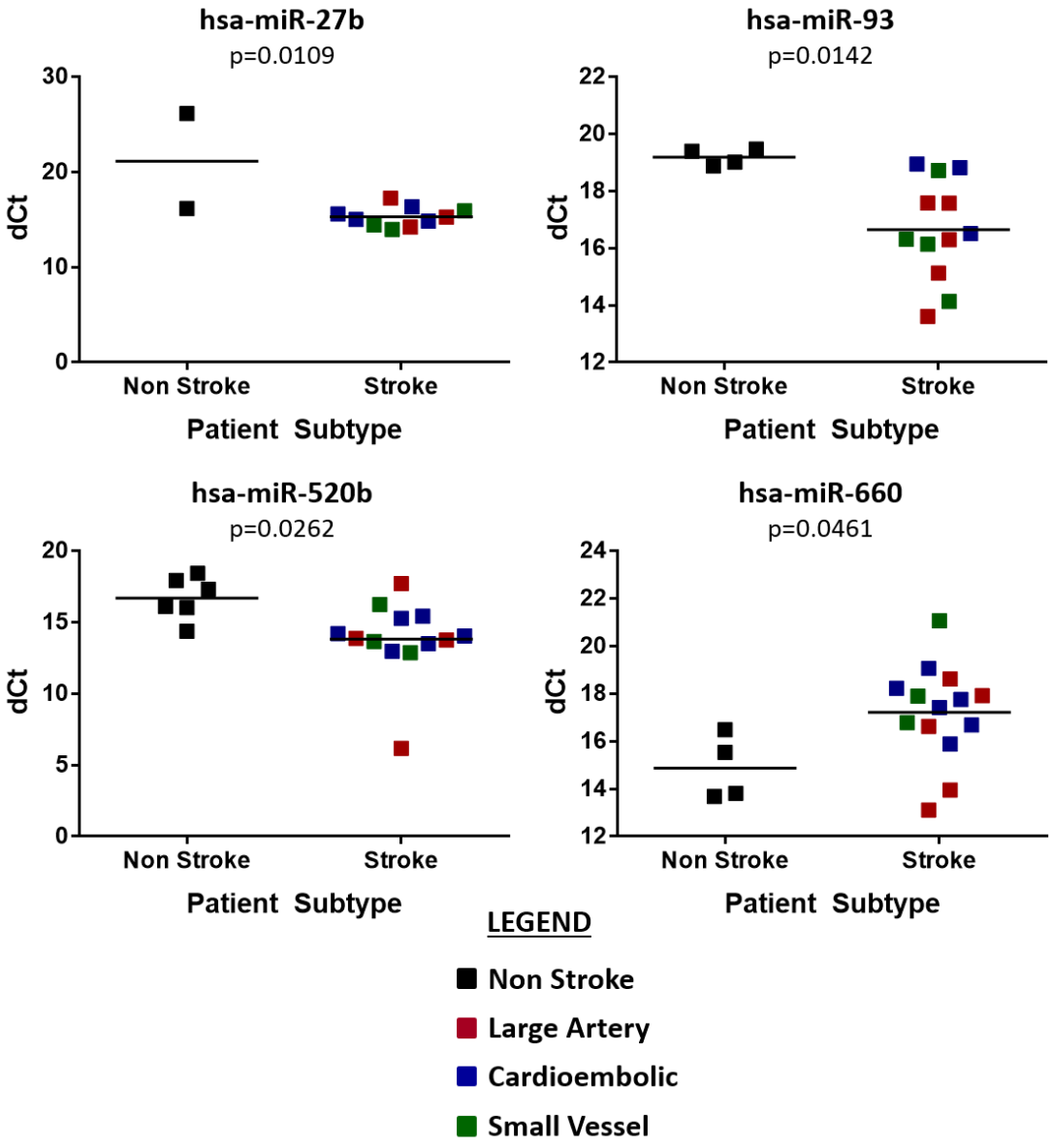

Figure 4.3 – miRNAs Dysregulated in Stroke Patients
Exosomal expression of hsa-miR-27b, hsa-miR-93, hsa-miR-520b and hsa-miR-660 was profiled in stroke patients. Exosomal miRNA expression was assessed from miRNA extracted from exosomes harvested from the serum of control non stroke patients (n=10) and large artery (n=9), cardioembolic (n=10) and small vessel disease (n=10) stroke patients. Changes in miRNA expression were assessed by OpenArray and data shown are ΔCt values. Data was normalised to a spike housekeeper miRNA, ath-miR-159a. Probability values were calculated using unpaired Student's t-test, vs. non stroke control patients.

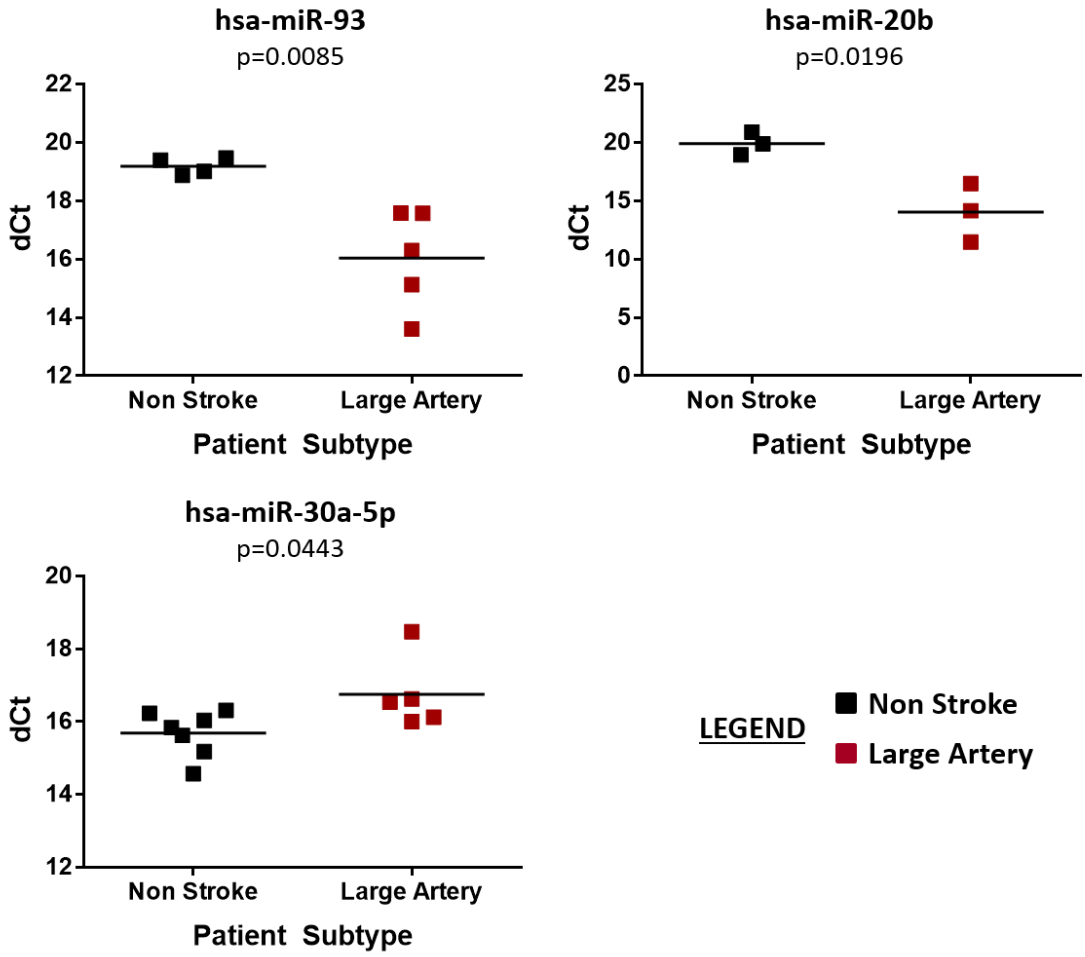

Figure 4.4 – miRNAs Dysregulated in Large Artery Stroke Patients
Exosomal expression of hsa-miR-93, hsa-miR-20b and hsa-miR-30a-5p was profiled in large artery stroke patients. Exosomal miRNA expression was assessed from miRNA extracted from exosomes harvested from the serum of control non stroke patients (n=10) and large artery (n=9) stroke patients. Changes in miRNA expression were assessed by OpenArray and data shown are ΔCt values. Data was normalised to a spike housekeeper miRNA, ath-miR-159a. Probability values were calculated using unpaired Student's t-test, vs. non stroke control patients.

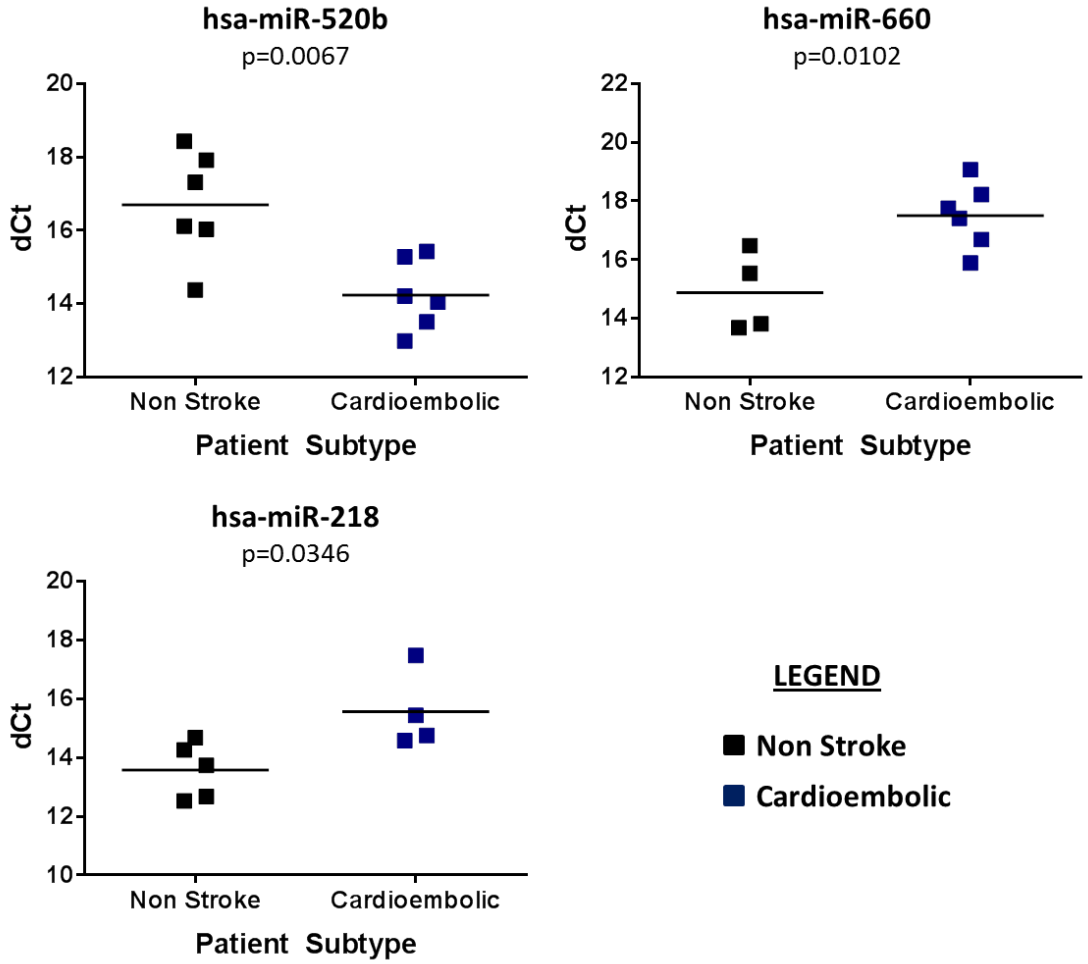

Figure 4.5 – miRNAs Dysregulated in Cardioembolic Stroke Patients
Exosomal expression of hsa-miR-520b, hsa-miR-660 and hsa-miR-218 was profiled in cardioembolic stroke patients. Exosomal miRNA expression was assessed from miRNA extracted from exosomes harvested from the serum of control non stroke patients (n=10) and cardioembolic (n=10) stroke patients. Changes in miRNA expression were assessed by OpenArray and data shown are ΔCt values. Data was normalised to a spike housekeeper miRNA, ath-miR-159a. Probability values were calculated using unpaired Student's t-test, vs. non stroke control patients.

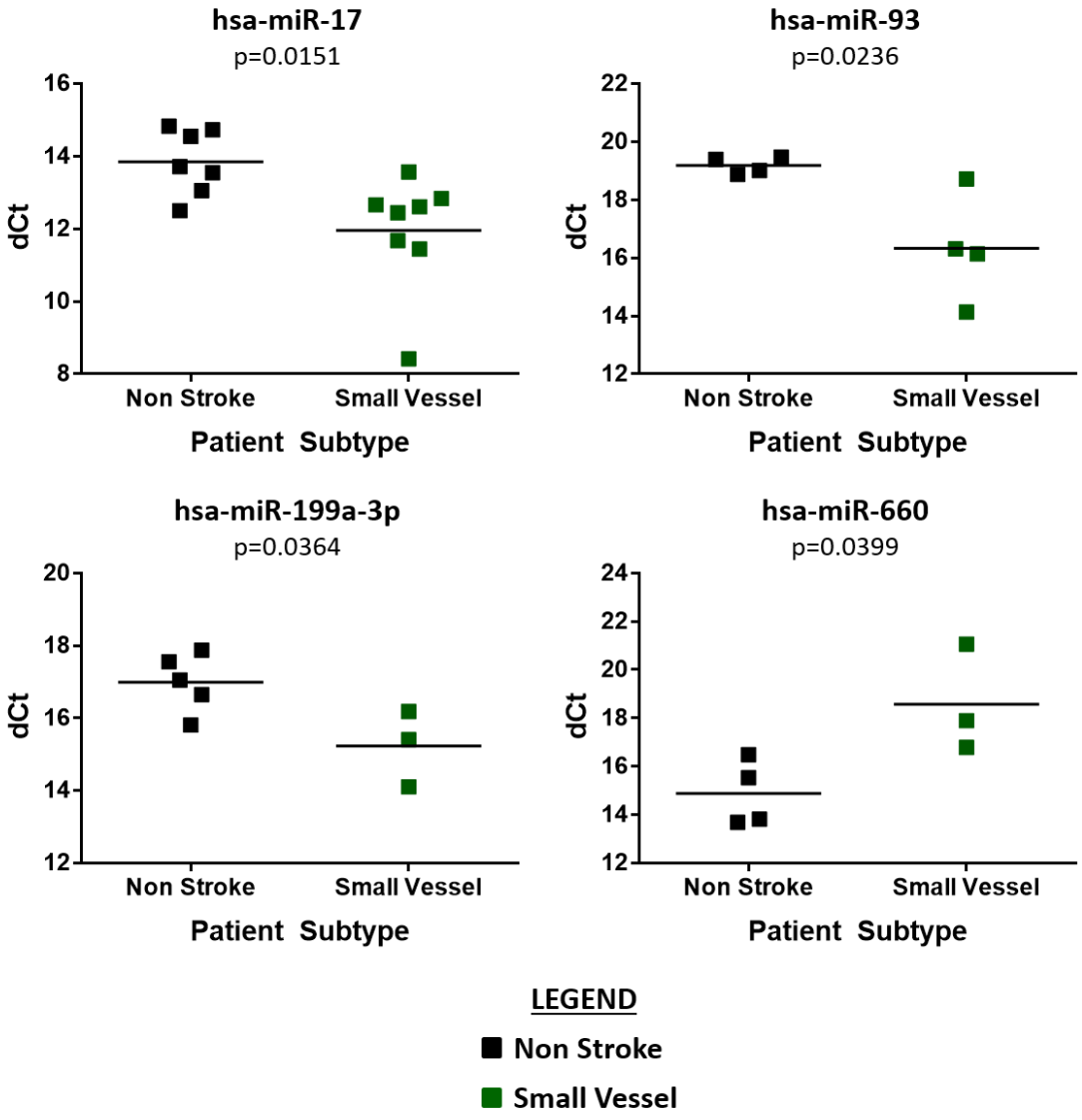

Figure 4.6 – miRNAs Dysregulated in Small Vessel Disease Stroke Patients
Exosomal expression of hsa-miR-17, hsa-miR-93, hsa-miR-199a-3p and hsa-miR-660 was profiled in small vessel disease stroke patients. Exosomal miRNA expression was assessed from miRNA extracted from EVs harvested from the serum of control non stroke patients (n=10) and small vessel disease (n=10) stroke patients. Changes in miRNA expression were assessed by OpenArray and data shown are ΔCt values. Data was normalised to a spike housekeeper miRNA, ath-miR-159a. Probability values were calculated using unpaired Student's t-test, vs. non stroke control patients.

Table 4.3 – Dysregulated miRNAs detected by OpenArray
A table summarising miRNAs that were shown to be dysregulated by OpenArray and whether they were selected for validation. The average Ct value for each miRNA in each patient group is given with the direction of change and the probability of changes being statistically significant (as assessed by two-tailed Student's unpaired t-test) in comparison to non-stroke control patients. Black text indicates changes that were statistically significant, as opposed to the grey text which indicates miRNAs where the change in miRNA expression was not statistically significant. Exosomal miRNA expression was assessed from miRNA extracted from exosomes harvested from the serum of control non stroke patients (n=10) and large artery (n=9), cardioembolic (n=10) and small vessel disease (n=10) stroke patients.

miRNA	Average Ct Value T-Test p-value (calculated from dCt)					Selected for Validation?
	Non Stroke	Stroke (All)	Large Artery	Cardioembolic	Small Vessel	
hsa-miR-27b	34.51	27.81 ↑ p=0.011	28.38 ↑ p=0.248	27.42 ↑ p=0.139	27.76 ↑ p=0.191	✓
mmu-miR-93	31.18	29.13 ↑ p=0.014	28.34 ↑ p=0.008	30.11 ↑ p=0.169	29.38 ↑ p=0.024	✓
hsa-miR-520b	29.30	26.42 ↑ p=0.026	25.28 ↑ p=0.100	26.66 ↑ p=0.007	27.45 ↑ p=0.064	✓
hsa-miR-660	26.49	29.30 ↓ p=0.046	28.36 ↓ p=0.421	29.44 ↓ p=0.010	30.58 ↓ p=0.040	✓
hsa-miR-20b	32.43	28.72 ↑ p=0.056	26.49 ↑p=0.020	30.47 ↑ p=0.171	29.79 ↑ p=0.168	✓
hsa-miR-30a-5p	27.30	28.09 ↓ p=0.177	29.17 ↓ p=0.044	26.84 ↑ p=0.255	27.99 ↓ p=0.743	✓
hsa-miR-218	25.59	25.79 ↓ p=0.915	25.01 ↑ p=0.646	27.92 ↓ p=0.035	25.28 ↑ p=0.508	✓
hsa-miR-17	26.07	25.03 ↑ p=0.118	25.07 ↑ p=0.123	25.78 ↑ p=0.793	24.26 ↑ p=0.015	✓
hsa-miR-199a-3p	29.09	26.07 ↑ p=0.265	23.33 ↑ p=0.185	28.21 ↑ p=0.278	26.68 ↑ p=0.036	✓

In other cases, where miRNAs appeared to be either ‘switched on’ or ‘switched off’ no probability could be calculated and so these miRNAs were labelled as ‘ON-OFF’ or ‘OFF-ON’ (Table 4.4 - Table 4.5). hsa-miR-223* was turned on in large artery patients, while hsa-miR-454 and hsa-miR-323-3p were turned on in cardioembolic patients and hsa-miR-376a in small vessel disease patients (Table 4.4). Other miRNAs appeared to be switched off following ischaemic stroke. hsa-miR-31 and hsa-miR-1291 appeared to be switched off in all stroke subtypes as compared to non-stroke patients (Table 4.5). hsa-miR-338-5p and hsa-miR-572 were turned off in large artery and cardioembolic patients whilst hsa-miR-508 was turned off in cardioembolic and small vessel disease stroke patients, as compared to non-stroke control patients (Table 4.5). hsa-let-7d was switched off in large artery patients (Table 4.5). A number of miRNAs were switched off in cardioembolic patients alone: hsa-miR-1274a, hsa-miR-186, hsa-miR-192, mmu-miR-374-5p and hsa-miR-766 (Table 4.5). miRNAs hsa-let-7e and hsa-miR-549 were turned off in small vessel disease patients alone (Table 4.5).

The 26 unique miRNAs identified here as candidate miRNAs of interest are summarised in Table 4.3 - Table 4.5. While microarray experiments are very useful for the discovery of dysregulated miRNAs, variability in microarray results and limited dynamic range can limit the sensitivity and specificity of microarray experiments. Furthermore, extremely small reaction volumes (33 nL) and false positives can reduce the reliability of microarray data. Changes observed therefore must be independently validated by qRT-PCR to ensure that miRNAs of interest are indeed dysregulated and to investigate to what extent.

Of the 26 candidate miRNAs identified 17 were selected for validation by qRT-PCR (a selection had to be made due to budget constraints). All miRNAs with statistically significant differences between patient groups (as assessed by t-test) were selected for validation. All miRNAs that appeared to be switched on following stroke were also selected for validation. Of the 13 miRNAs that appeared to be switched off following ischaemic stroke, the 2 miRNAs that were switched off in all patient groups were selected. Furthermore the 2 miRNAs that were switched off only in small vessel disease patients were selected as small vessel disease stroke is the most phenotypically different to the other stroke subtypes and so we were keen to investigate differences in this stroke subtype.

Table 4.4 – miRNAs turned on following stroke (OpenArray)
A table summarising miRNAs that were shown to be turned on following stroke, as detected by OpenArray, and whether or not they were selected for validation. The average Ct value for each miRNA in each patient group is given with the direction of change in comparison to non-stroke control patients. Black text indicates where miRNA expression was detected as being turned on, grey text indicates where miRNA expression was not detected. 'Not detected' indicates miRNA expression was non-detectable in ≥ 90% of patients. Exosomal miRNA expression was assessed from miRNA extracted from exosomes harvested from the serum of control non stroke patients (n=10) and large artery (n=9), cardioembolic (n=10) and small vessel disease (n=10) stroke patients.

miRNA	Average Ct Value T-Test p-value (calculated from dCt)					Selected for Validation?
	Non Stroke	Stroke (All)	Large Artery	Cardioembolic	Small Vessel	
hsa-miR-223*	Not detected	29.13 OFF - ON	29.81 OFF - ON	28.56 OFF - ON	28.60 OFF - ON	✓
hsa-miR-454	Not detected	28.25 OFF - ON	Not detected OFF - OFF	30.93 OFF - ON	Not detected OFF – OFF	✓
hsa-miR-323-3p	Not detected	29.82 OFF - ON	30.86 OFF - ON	30.05 OFF - ON	28.83 OFF - ON	✓
hsa-miR-376a	Not detected	29.34 OFF - ON	29.00 OFF – ON	29.67 OFF – ON	29.29 OFF - ON	✓

Table 4.5 – miRNAs turned off following stroke (OpenArray)
A table summarising miRNAs that were shown to be turned off following stroke, as detected by OpenArray, and whether or not they were selected for validation. The average Ct value for each miRNA in each patient group is given with the direction of change and the probability of changes being statistically significant (as assessed by two-tailed Student's unpaired t-test) in comparison to non-stroke control patients. Black text indicates where miRNA expression was detected as being turned off, grey text indicates where miRNA expression remained detectable. 'Not detected' indicates miRNA expression was non-detectable in ≥ 90% of patients. Exosomal miRNA expression was assessed from miRNA extracted from exosomes harvested from the serum of control non stroke patients (n=10) and large artery (n=9), cardioembolic (n=10) and small vessel disease (n=10) stroke patients.

miRNA	Average Ct Value T-Test p-value (calculated from dCt)					Selected for Validation?
	Non Stroke	Stroke (All)	Large Artery	Cardioembolic	Small Vessel	
hsa-miR-31	29.18	28.84 ↑ p=0.571	Not detected ON - OFF	Not detected ON - OFF	Not detected ON - OFF	✓
hsa-miR-1291	28.64	24.39 ↑ p=0.993	Not detected ON - OFF	Not detected ON - OFF	Not detected ON - OFF	✓
hsa-miR-338-5p	31.50	31.92 ↓ p=0.785	Not detected ON - OFF	Not detected ON - OFF	33.80 ↓ p=0.516	×
hsa-miR-508	28.98	25.10 ↑ p=0.170	26.03 ↑ p=0.359	Not detected ON - OFF	Not detected ON - OFF	×
hsa-miR-572	28.04	29.14 ↑ p=0.715	Not detected ON - OFF	Not detected ON - OFF	29.22 ↓ p=0.960	×
hsa-let-7d	29.84	28.42 ↑ p=0.155	Not detected ON - OFF	28.61 ↑ p=0.396	28.44 ↑ p=0.289	×
hsa-miR-1274a	31.48	27.51 ↑ p=0.055	27.16 ↑ p=0.066	Not detected ON - OFF	28.22 ↑ p=0.118	×
hsa-miR-186	29.83	30.71 ↓ p=0.539	28.04 ↑ p=0.154	Not detected ON - OFF	32.25 ↓ p=0.122	×
hsa-miR-192	28.43	29.43 ↓ p=0.735	32.35 ↓ p=0.220	Not detected ON - OFF	26.51 ↑ p=0.428	×
mmu-miR-374-5p	30.02	27.49 ↑ p=0.260	26.76 ↑ p=0.221	Not detected ON - OFF	27.82 ↑ p=0.609	×
hsa-miR-766	28.16	27.42 ↑ p=0.685	27.81 ↑ p=0.752	Not detected ON - OFF	26.71 ↑ p=0.494	×
hsa-let-7e	30.15	28.05 ↑ p=0.338	26.38 ↑ p=0.248	28.69 ↑ p=0.743	Not detected ON - OFF	✓
hsa-miR-549	30.93	31.39 ↓p=0.678	30.59 ↑ p=0.614	32.22 ↓ p=0.089	Not detected ON - OFF	✓

4.2.5 Validation Study Patient Population Demographics

Demographical information for the full cohort of patients used in the validation study is listed in Table 4.6 (non stroke vs. stroke) and Table 4.7 (non stroke vs. stroke subtype).

There is no significant difference between the gender or age of the non-stroke and ischaemic stroke patient populations. However the stroke patients are moderately older (median age of 68 years vs. 63.5 years for non-stroke) (Table 4.6). This is because cardioembolic patients are significantly older than all other stroke-subtypes (median age of 75 years vs. non stroke, 63.5 years; large artery 62.5 years; small vessel, 64 years; unclassified, 67 years) (Table 4.7). The patients of other stroke subtypes are not significantly older than the non-stroke control patients.

While the percentage of stroke patients in atrial fibrillation is not significantly higher than that of the non-stroke control patients (15.6% vs. 8.8%), when the difference is broken down in terms of stroke subtype it is clear that a significantly higher proportion of cardioembolic patients are in atrial fibrillation than any other patient subgroup (60% vs. non-stroke 8.8%, large artery 0%, small vessel 2.7% and unclassified 5%). Fisher's exact test also detected statistically significant differences between the percentage of patients who were ex-smokers (32.4% non-stroke vs. 13.3% stroke) or who had a history of TIA (23.5% non-stroke vs. 8.1% stroke) between the ischaemic stroke and non-stroke control patients. However, in both these cases the non-stroke patients had a higher percentage of these patients, indicating that differences we observe in exosomal miRNA expression will not be as a result of comparing stroke population expression to healthy non-stroke control patients. Furthermore, when the differences are broken down to represent stroke subtype (Table 4.7) it is clear there are no significant differences between any particular stroke subtype and the non-stroke patients.

There are no statistically significant differences between the prescribed medication that non-stroke and stroke patients received prior to their arrival at hospital.

As was discussed in sections 1.1.2 and 1.1.4.2 some of the most important risk factors for ischaemic stroke include age, hypertension, ratio of apolipoproteins, current smoking and diabetes. For these factors (excepting age, as discussed) there is no significant difference between our patient populations. This gives confidence that any changes in exosomal miRNA expression observed are a direct result of stroke pathophysiology and aren't confounded as a result of co-morbidity or medication.

Table 4.6 – Validation Study Population Characteristics
This table summarises demographical data for the full cohort of patients used in the validation study. The gender, median age and number of patients positive for a number of risk factors for stroke and/or on prescribed medication are recorded. A Fisher's Exact Test was used to calculate whether differences observed between non-stroke control and ischaemic stroke patients were statistically significant. ✞ indicates a Mann Whitney U Test was used to calculate probability.

		Non-Stroke	Stroke	p (Fisher's test)
Age & Gender	n	34	173	n/a
	Male, % (n)	55.9 (19)	63.0 (109)	0.446
	Median Age	63.5	68	0.055✞
Risk Factors for Ischaemic Stroke	Hypertension, % (n)	38.2 (13)	32.9 (57)	0.557
	Atrial Fibrillation, % (n)	8.8 (3)	15.6 (27)	0.427
	Diabetes (Type 1 or 2), % (n)	20.6 (7)	13.9 (24)	0.303
	Hyperlipidaemia, % (n)	17.6 (6)	20.8 (36)	0.817
	PVD, % (n)	5.9 (2)	0.6 (1)	0.071
	Smoker, % (n)	26.5 (9)	26.0 (45)	1.000
	Ex-Smoker, % (n)	32.4 (11)	13.3 (23)	0.011
	Previous TIA, % (n)	23.5 (8)	8.1 (14)	0.014
	Previous Stroke, % (n)	14.7 (5)	11.0 (19)	0.559
	Family History, % (n)	11.8 (4)	12.7 (22)	1.000
Medication	rtPA, % (n)	n/a	22.5 (39)	n/a
	ACE, % (n)	23.5 (8)	18.5 (32)	0.483
	Alpha Blocker, % (n)	0.0 (0)	0.6 (1)	1.000
	Anticoagulant, % (n)	5.9 (2)	4.6 (8)	0.670
	Antiplatelet, % (n)	41.2 (14)	29.5 (51)	0.225
	ARB, % (n)	2.9 (1)	5.2 (9)	1.000
	Beta Blocker, % (n)	29.4 (10)	20.2 (35)	0.258
	Blood Pressure Treatment, % (n)	41.2 (14)	39.3 (68)	0.850
	CCB, % (n)	14.7 (5)	14.5 (25)	1.000
	Loop Diuretic, % (n)	2.9 (1)	8.7 (15)	0.480
	Oral Hypoglycaemic Drugs, % (n)	5.9 (2)	5.8 (10)	1.000
	Spironolactone, % (n)	2.9 (1)	1.2 (2)	0.418
	Statin, % (n)	47.1 (16)	34.7 (60)	0.179
	Thiazide, % (n)	8.8 (3)	8.7 (15)	1.000

Table 4.7 – Validation Study Population Characteristics
This table summarises demographical data for the patients used in the validation study. The gender, median age and number of patients positive for a number of risk factors for stroke and/or on prescribed medication are recorded. A Chi-Square Test was used to calculate whether differences observed between patient groups were statistically significant. ✞ indicates that a Kruskal-Wallis Test was used to calculate probability.

		Non-Stroke	Large Artery	Cardioembolic	Small Vessel	Unclassified	p (Chi-square test)
Age & Gender	n	34	22	40	37	40	n/a
	Male, % (n)	55.9 (19)	77.3 (17)	70.0 (28)	70.3 (26)	47.5 (19)	0.076
	Median Age	63.5	62.5	75.0	64.0	67.0	0.0012✞
Risk Factors for Ischaemic Stroke	Hypertension, % (n)	38.2 (13)	36.4 (8)	45.0 (18)	32.4 (12)	47.5 (19)	0.667
	Atrial Fibrillation, % (n)	8.8 (3)	0.0 (0)	60.0 (24)	2.7 (1)	5.0 (2)	<0.0001
	Diabetes (Type 1 or 2), % (n)	20.6 (7)	13.6 (3)	20.0 (8)	13.5 (5)	20.0 (8)	0.884
	Hyperlipidaemia, % (n)	17.6 (6)	13.6 (3)	30.0 (12)	21.6 (8)	32.5 (13)	0.343
	PVD, % (n)	5.9 (2)	0.0 (0)	0.0 (0)	0.0 (0)	2.5 (1)	0.256
	Smoker, % (n)	26.5 (9)	54.5 (12)	25.0 (10)	37.8 (14)	22.5 (9)	0.066
	Ex Smoker, % (n)	32.4 (11)	22.7 (5)	15.0 (6)	10.8 (4)	20.0 (8)	0.200
	Previous TIA, % (n)	23.5 (8)	9.1 (2)	7.5 (3)	13.5 (5)	10.0 (4)	0.276
	Previous Stroke, % (n)	14.7 (5)	9.1 (2)	7.5 (3)	18.9 (7)	17.5 (7)	0.553
	Family History, % (n)	11.8 (4)	4.5 (1)	10.0 (4)	18.9 (7)	25.0 (10)	0.163
Medication	rtPA, % (n)	n/a	36.4 (8)	25.0 (10)	27.0 (10)	27.5 (11)	0.810
	ACE, % (n)	23.5 (8)	22.7 (5)	17.5 (7)	24.3 (9)	27.5 (11)	0.882
	Alpha Blocker, % (n)	0.0 (0)	4.5 (1)	0.0 (0)	0.0 (0)	0.0 (0)	0.141
	Anticoagulant, % (n)	5.9 (2)	4.5 (1)	15.0 (6)	2.7 (1)	0.0 (0)	0.052
	Antiplatelet, % (n)	41.2 (14)	31.8 (7)	47.5 (19)	24.3 (9)	40.0 (16)	0.282
	ARB, % (n)	2.9 (1)	9.1 (2)	7.5 (3)	2.7 (1)	7.5 (3)	0.731
	Beta Blocker, % (n)	29.4 (10)	22.7 (5)	42.5 (17)	16.2 (6)	17.5 (7)	0.053
	Blood Pressure Treatment, % (n)	41.2 (14)	45.5 (10)	55.0 (22)	37.8 (14)	55.0 (22)	0.438
	CCB, % (n)	14.7 (5)	18.2 (4)	20.0 (8)	13.5 (5)	20.0 (8)	0.918
	Loop Diuretic, % (n)	2.9 (1)	4.5 (1)	15.0 (6)	13.5 (5)	7.5 (3)	0.318
	Oral Hypoglycaemic Drugs, % (n)	5.9 (2)	4.5 (1)	7.5 (3)	2.7 (1)	12.5 (5)	0.522
	Spironolactone, % (n)	2.9 (1)	0.0 (0)	2.5 (1)	2.7 (1)	0.0 (0)	0.786
	Statin, % (n)	47.1 (16)	50.0 (11)	52.5 (21)	29.7 (11)	42.5 (17)	0.317
	Thiazide, % (n)	8.8 (3)	18.2 (4)	10.0 (4)	2.7 (1)	15.0 (6)	0.310

4.2.6 Validation Study Results

As the microarray experiment included a pre-amplification step, it was decided that a trial qRT-PCR experiment should be carried out to decide whether a pre-amplification step would also be needed in the validation study. The exosomal expression of the 17 candidate miRNAs selected for validation and the housekeeper miRNA, *Caenorhabditis elegans* miR-39 (cel-miR-39), were therefore profiled in 6 randomly chosen patient samples (Table 4.8).

Table 4.8 – Exosomal miRNA Expression (standard qRT-PCR)
miRNA expression of 18 miRNAs was assessed in 6 randomly chosen patient samples. miRNA expression was assessed by qRT-PCR in exosomes isolated from serum samples and collected at 48 hours post-stroke. In the table the average Ct, standard deviation and SEM of the expression of each miRNA has been given.

miRNA	Average Ct	Standard Deviation	SEM
cel-miR-39-3p	22.70	0.04	0.02
hsa-let-7e-5p	28.18	0.77	0.31
hsa-miR-17-5p	30.53	1.02	0.42
hsa-miR-93-5p	30.86	0.52	0.21
hsa-miR-30a-5p	31.30	0.86	0.35
hsa-miR-199a-3p	31.94	1.38	0.56
hsa-miR-660-5p	32.20	1.10	0.45
hsa-miR-27b-3p	32.34	1.11	0.45
hsa-miR-20b-5p	33.15	1.54	0.63
hsa-miR-218-5p	33.87	0.86	0.35
hsa-miR-520b	33.95	2.19	0.90
hsa-miR-454-3p	35.75	1.46	0.60
hsa-miR-223-5p	35.95	2.56	1.04
hsa-miR-376a-3p	36.85	1.74	0.71
hsa-miR-549a	37.15	0.77	0.31
hsa-miR-31-5p	37.83	2.48	1.01
hsa-miR-1291	38.56	1.58	0.64
hsa-miR-323-3p	38.65	1.53	0.62

Where miRNAs had Ct values between 30 and 35 expression was deemed adequate. Where miRNAs had Ct values of over 35 expression was considered to be low and a pre-amplification step was deemed necessary. The majority of miRNAs investigated had adequate miRNA expression in the 6 samples profiled (Table 4.8). However, it was hypothesised that if the expression of these miRNAs

was decreased in the remaining 167 samples not profiled, in comparison to these samples, then the expression of these miRNAs could fall below a Ct of 35 (i.e. ≥ 35). It was therefore decided essential that a pre-amplification step was introduced to the protocol (for all miRNAs) to ensure sufficient expression of miRNAs for accurate detection and quantification by qRT-PCR.

Subsequently a small experiment was carried out to test the effectiveness of pre-amplification and to investigate whether this would introduce variability into the data (Figure 4.7 and Table 4.9). Expression of each miRNA was assessed by standard qRT-PCR in a number of samples and then subsequently assessed by qRT-PCR in samples in which a pre-amplification step had been performed as part of the protocol. In the majority of samples miRNA expression pre-amplified evenly in comparison to standard miRNA expression (Figure 4.7A). However, in samples with very low endogenous miRNA expression, miRNAs did not always pre-amplify equally, with examples including hsa-miR-323-3p and hsa-miR-1291 (Figure 4.7B). The difference (average number of cycles) between standard miRNA expression and pre-amplified miRNA expression, for each miRNA tested, is shown in Table 4.9. As a result of this experiment 4 miRNAs were not taken forward for validation by qRT-PCR in the full patient cohort: hsa-miR-323-3p, hsa-miR-1291, hsa-miR-454 and hsa-miR-31.

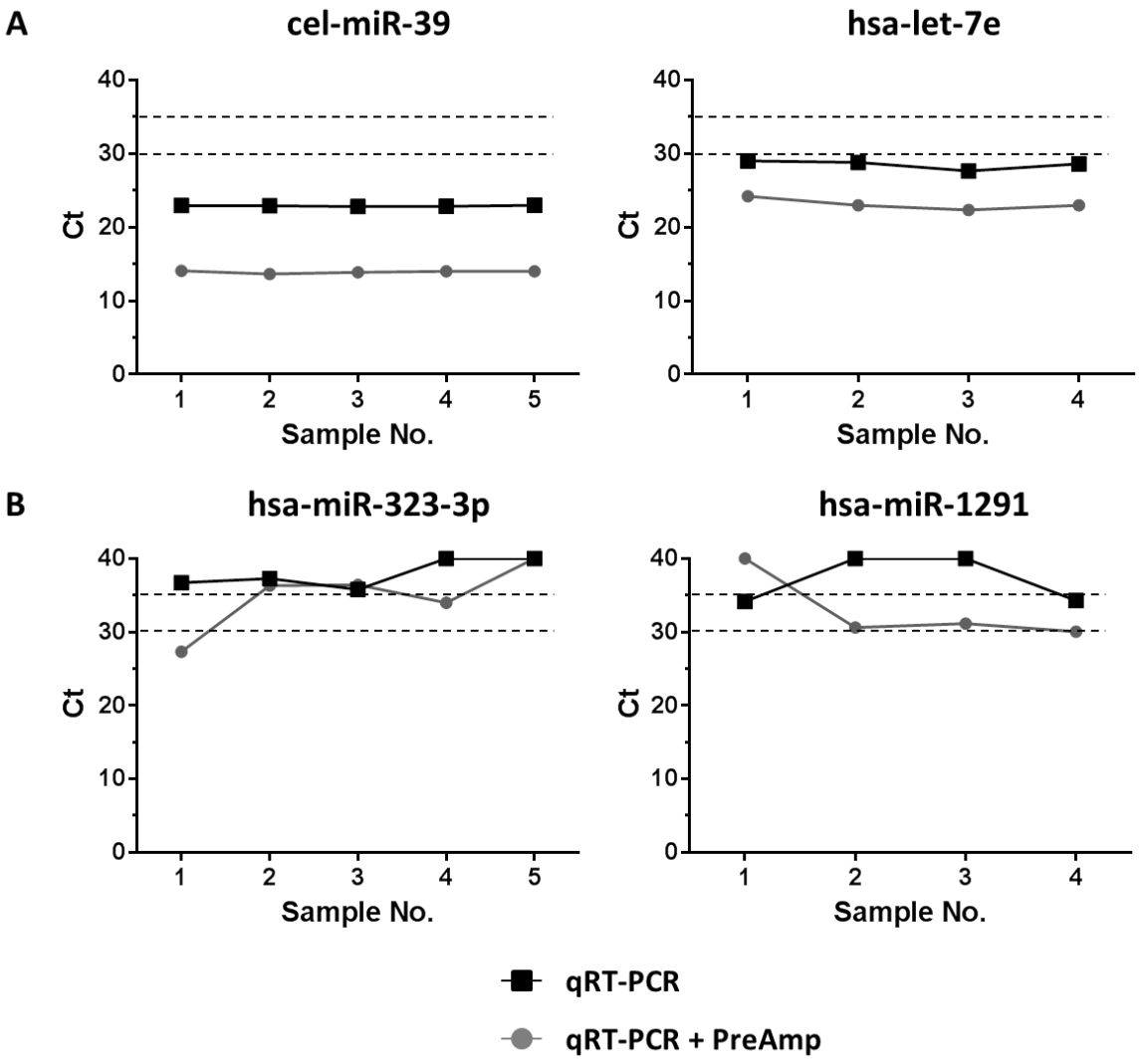

Figure 4.7 – Pre-Amplification of miRNA
miRNA expression of 18 miRNAs was assessed in randomly chosen patient samples (n=4-5). Expression of 4 representative miRNAs is shown here. cel-miR-39, hsa-let-7e (A) hsa-miR-323-3p and hsa-miR-1291 (B) miRNA expression was assessed by qRT-PCR in exosomes isolated from serum samples and collected at 48 hours post-stroke. miRNA expression was profiled with and without a pre-amplification step. Data shown is raw Ct values.

Table 4.9 – Pre-Amplification of miRNA
miRNA expression of 18 miRNAs was assessed in randomly chosen patient samples (n=4-5). miRNA expression was assessed by qRT-PCR in exosomes isolated from serum samples and collected at 48 hours post-stroke. miRNA expression was also assessed by qRT-PCR in the same samples that had been subjected to a pre-amplification step. Data shown is the average raw Ct value for each miRNA and the average differences in the number of cycles between the two methods has been calculated.

miRNA	qRT-PCR (Average Ct)	qRT-PCR + PreAmp (Average Ct)	No. Cycles Improved
cel-miR-39	22.88	13.80	9.08
hsa-let-7e	28.53	23.13	5.40
hsa-miR-17	30.77	19.93	10.84
hsa-miR-93	30.85	24.55	6.29
hsa-miR-30a-5p	31.30	25.69	5.61
hsa-miR-199a-3p	32.08	25.35	6.73
hsa-miR-660	32.54	26.26	6.27
hsa-miR-27b	32.82	27.53	5.29
hsa-miR-520b	33.43	29.19	4.24
hsa-miR-218	33.84	30.79	3.05
hsa-miR-20b	33.96	23.74	10.22
hsa-miR-31	35.05	40.00	-4.95
hsa-miR-454	35.05	25.88	9.17
hsa-miR-223#	35.79	28.34	7.45
hsa-miR-376a	35.79	29.77	6.02
hsa-miR-549	36.31	29.92	6.39
hsa-miR-1291	37.10	32.95	4.20
hsa-miR-323-3p	37.95	34.80	3.93

The exosomal expression of 13 miRNAs was assessed in the validation study cohort (n=173). Of these patients, 37 were unable to have their diagnosis of ischaemic stroke confirmed by conventional imaging and so they are termed 'possible', the diagnosis for all remaining ischaemic stroke patients is termed 'definite'. Possible stroke patients may have a milder stroke phenotype and so we have compared expression between non-stroke and all stroke patients, and non-stroke and only definite stroke patients, to see if this difference affects miRNA expression.

Exosomal **hsa-miR-27b** is significantly increased in all stroke patients as compared to non-stroke patients (RQ 1.62 ± 0.16 vs. 1.00 ± 0.18) (Figure 4.8A) and is also significantly increased in definite stroke patients as compared to non-stroke controls (RQ 1.72 ± 0.20 vs. 1.00 ± 0.18) (Figure 4.8B). Furthermore, while its expression is moderately increased in large artery stroke patients, it is significantly increased in small vessel disease patients, as compared to non-stroke control patients (RQ 2.24 ± 0.47 vs. 1.00 ± 0.18) (Figure 4.8C). Interestingly, expression of hsa-miR-27b is unchanged in unclassified patients relative to non-stroke patients. There is no correlation between hsa-miR-27b and the age (R^2 = 0.00766) or gender of the patients (Figure 4.8 D and E). Although has-miR-27b expression is increased (non-significantly) in male large artery patients as compared to female patients, this probably reflects the small number of female patients in this particular stroke subtype (n=5).

Other miRNAs were dysregulated in a similar manner.

hsa-miR-93 is not significantly increased in the exosomes of all stroke patients as compared to non-stroke patients (RQ 1.51 ± 0.15 vs. 1.00 ± 0.18) (Figure 4.9A) but is significantly increased in definite stroke patients as compared to non-stroke controls (RQ 1.61 ± 0.19 vs. 1.00 ± 0.18) (Figure 4.9B). Its expression is slightly increased in large artery and cardioembolic stroke patients but is only significantly increased in small vessel disease patients as compared to non-stroke control patients (RQ 2.23 ± 0.47 vs. 1.00 ± 0.18) (Figure 4.9C). Expression of hsa-miR-93 is unchanged in unclassified patients relative to non-stroke patients. There is no correlation between hsa-miR-93 and the age (R^2 = 0.00115) or gender of the patients (Figure 4.9 D and E).

Exosomal **hsa-miR-20b** is significantly increased in all stroke patients as compared to non-stroke patients (RQ 1.66 ± 0.17 vs. 1.00 ± 0.19) (Figure 4.10A) and is also significantly increased in definite stroke patients as compared to non-stroke controls (RQ 1.75 ± 0.20 vs. 1.00 ± 0.19) (Figure 4.10B). While its expression is moderately increased in large artery and cardioembolic stroke patients, it is only significantly increased in small vessel disease patients as compared to non-stroke control patients (RQ 2.36 ± 0.47 vs. 1.00 ± 0.19) (Figure 4.10C). Expression of hsa-miR-20b is unchanged in unclassified patients relative to non-stroke patients. There is no correlation between hsa-miR-20b and the age (R^2 = 0.000259) or gender of the patients (Figure 4.10 D and E).

hsa-miR-17 is also significantly increased in the exosomes of all stroke patients as compared to non-stroke patients (RQ 1.54 ± 0.15 vs. 1.00 ± 0.16) (Figure 4.11A) and is similarly increased in definite stroke patients as compared to non-stroke controls (RQ 1.55 ± 0.19 vs. 1.00 ± 0.16) (Figure 4.11B). hsa-miR-17 is significantly increased in small vessel disease patients as compared to non-stroke patients (RQ 2.15 ± 0.40 vs. 1.00 ± 0.16) (Figure 4.11C). There was no correlation between hsa-miR-17 and patient age (R^2 = 0.0000134) or patient gender (Figure 4.11 D and E).

Interestingly three miRNAs with up-regulated exosomal expression in stroke patients as compared to non-stroke patient controls (in the present study) belong to one miRNA family. hsa-miR-17, hsa-miR-93 and hsa-miR-20b all belong to the miR-17 family (Figure 4.12). While these miRNAs are transcribed from separate chromosomes (hsa-miR-17 from chromosome 13, hsa-miR-93 from chromosome 7 and hsa-miR-20b from chromosome X) they have similar sequences and identical seed sequences (Figure 4.12A). The seed sequence is important for miRNA-target interaction and so miRNAs with identical seed sequences are thought to have mRNA targets in common.

miRWalk 2.0 was used to generate a list of predicted targets for the three miRNAs. Predicted genes from 12 databases were looked at: miRWalk, Microt4, miRanda, mirbridge, miRDB, miRMap, miRNAMap, Pictar2, PITA, RNA22, RNAhybrid and Targetscan. Only gene targets that were predicted by 7 or more databases were counted as a positive hit, and of these miRNAs -17-5p, -93-5p and -20b-5p have 1873 predicted gene targets in common (Figure 4.12C).

miRWalk and miRTarBase were used to generate a list of experimentally validated microRNA-gene target interactions, of these miRNAs -17-5p, -93-5p and -20b-5p only have 2 gene targets in common. This is primarily because very few targets of hsa-miR-20b-5p have been experimentally validated to date.

A significant number (over 100) of the predicted gene targets for miRNAs in this family are involved in the regulation of programmed cell death and apoptosis. Furthermore, a number of these targets are specifically believed to be involved in the regulation of neuron apoptosis. A slightly smaller number of predicted targets (approximately 90) are involved in the cellular response to stress and of these some are specifically involved in the response to oxygen levels and hypoxia. A large proportion of these miRNA-gene target interactions have been validated experimentally and these will be discussed further in Chapter 5.

miRNAs -17-5p, -93-5p and 20b-5p have a very similar pattern of expression in relation to stroke subtype (Figure 4.9 - Figure 4.11). The expression of all three miRNAs increased more than 2-fold in small vessel disease stroke patients as compared to non-stroke control patients. As these three miRNAs from the same family are dysregulated in such a similar way we have increased confidence in the biological significance of these results.

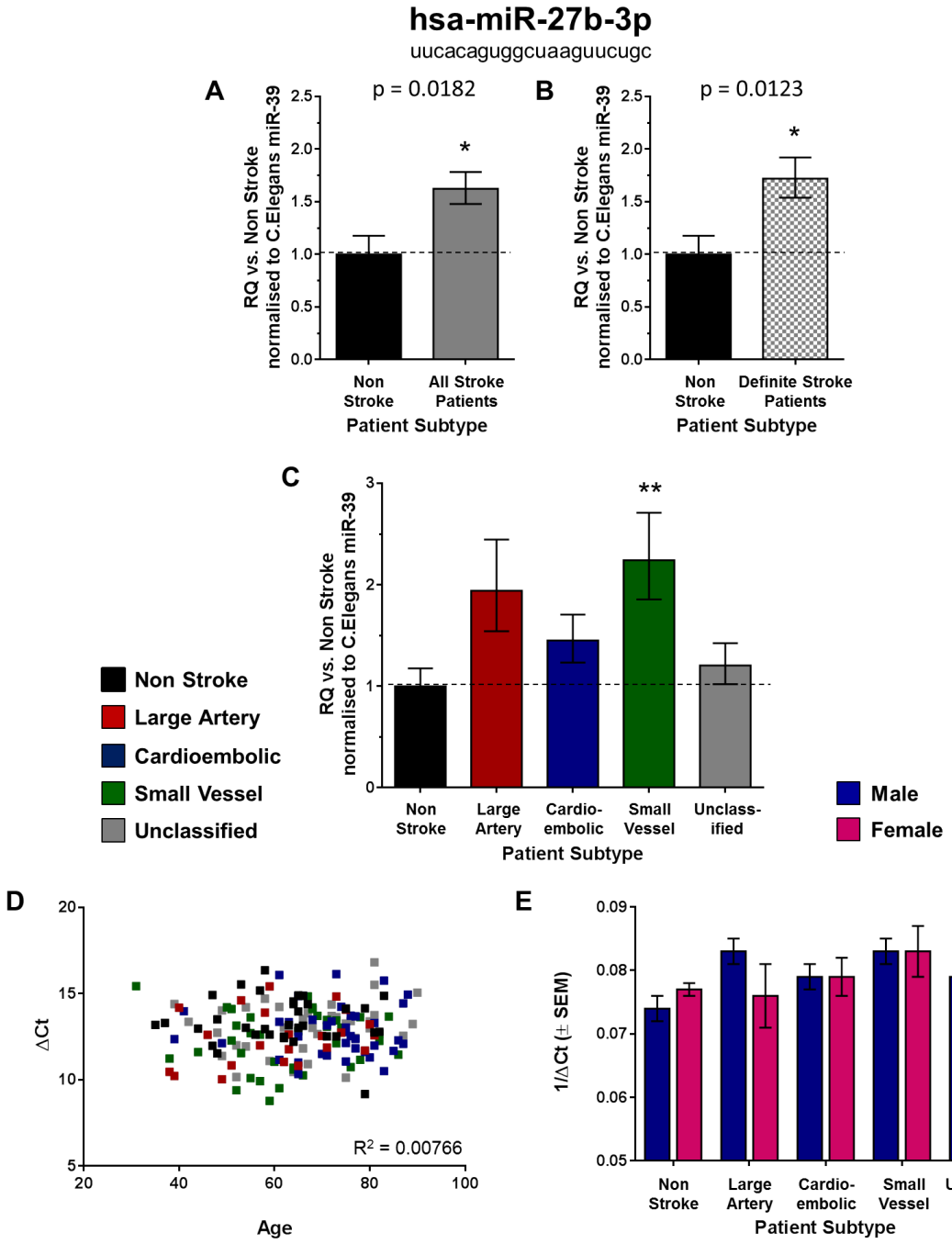

Figure 4.8 – hsa-miR-27b Validation
The exosomal expression of hsa-miR-27b was profiled in all stroke patients (this includes possible stroke patients) (n=139) (A) and in definite stroke patients (n=102) (B) as compared to non-stroke patients (n=34). Probability values were calculated using unpaired Student's t-test, vs. non-stroke control patients, *p<0.05. hsa-miR-27b expression was also assessed specifically in large artery (n=22), cardioembolic (n=40), small vessel (n=37) and unclassified (n=40) stroke patients and compared to non-stroke patients (n=34) (C). Probability values were calculated using one-way-ANOVA with post-hoc Dunnett's test, **p<0.01. Change in miRNA expression was assessed at 48 hours post-stroke by qRT-PCR and relative quantification (RQ) calculated from ΔΔCt following normalisation to a spike housekeeper miRNA, cel-miR-39 and compared to miRNA expression in the non-stroke control patients. Data shown is RQ ± RQmax/RQmin. Patient age was correlated against hsa-miR-27b exosomal expression (D). Data shown are ΔCt values. R^2 value was calculated by Pearson product-moment correlation coefficient. The effect of gender on hsa-miR-27b expression was investigated (E). Data shown is 1/ΔCt (±SEM). Probability was calculated using a one-way-ANOVA with a Bonferroni Multiple Comparison Test.

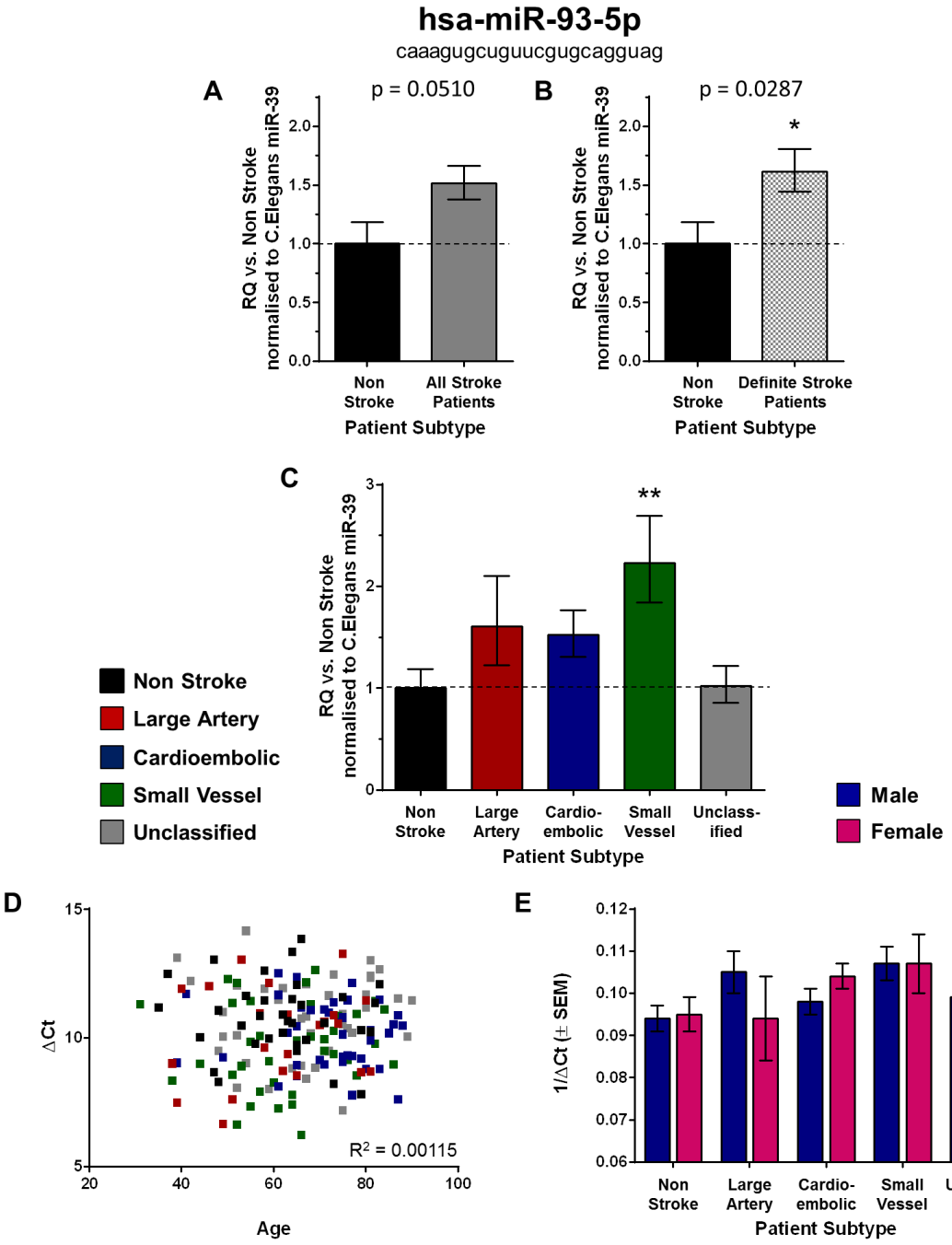

Figure 4.9 – hsa-miR-93 Validation
The exosomal expression of hsa-miR-93 was profiled in all stroke patients (this includes possible stroke patients) (n=139) (A) and in definite stroke patients (n=102) (B) as compared to non-stroke patients (n=34). Probability values were calculated using unpaired Student's t-test, vs. non-stroke control patients, *p<0.05. hsa-miR-93 expression was also assessed specifically in large artery (n=22), cardioembolic (n=40), small vessel (n=37) and unclassified (n=40) stroke patients and compared to non-stroke patients (n=34) (C). Probability values were calculated using one-way-ANOVA with post-hoc Dunnett's test, **p<0.01. Change in miRNA expression was assessed at 48 hours post-stroke by qRT-PCR and relative quantification (RQ) calculated from ΔΔCt following normalisation to a spike housekeeper miRNA, cel-miR-39 and compared to miRNA expression in the non-stroke control patients. Data shown is RQ ± RQmax/RQmin. Patient age was correlated against hsa-miR-93 exosomal expression (D). Data shown are ΔCt values. R^2 value was calculated by Pearson product-moment correlation coefficient. The effect of gender on hsa-miR-93 expression was investigated (E). Data shown is 1/ΔCt (±SEM). Probability was calculated using a one-way-ANOVA with a Bonferroni Multiple Comparison Test.

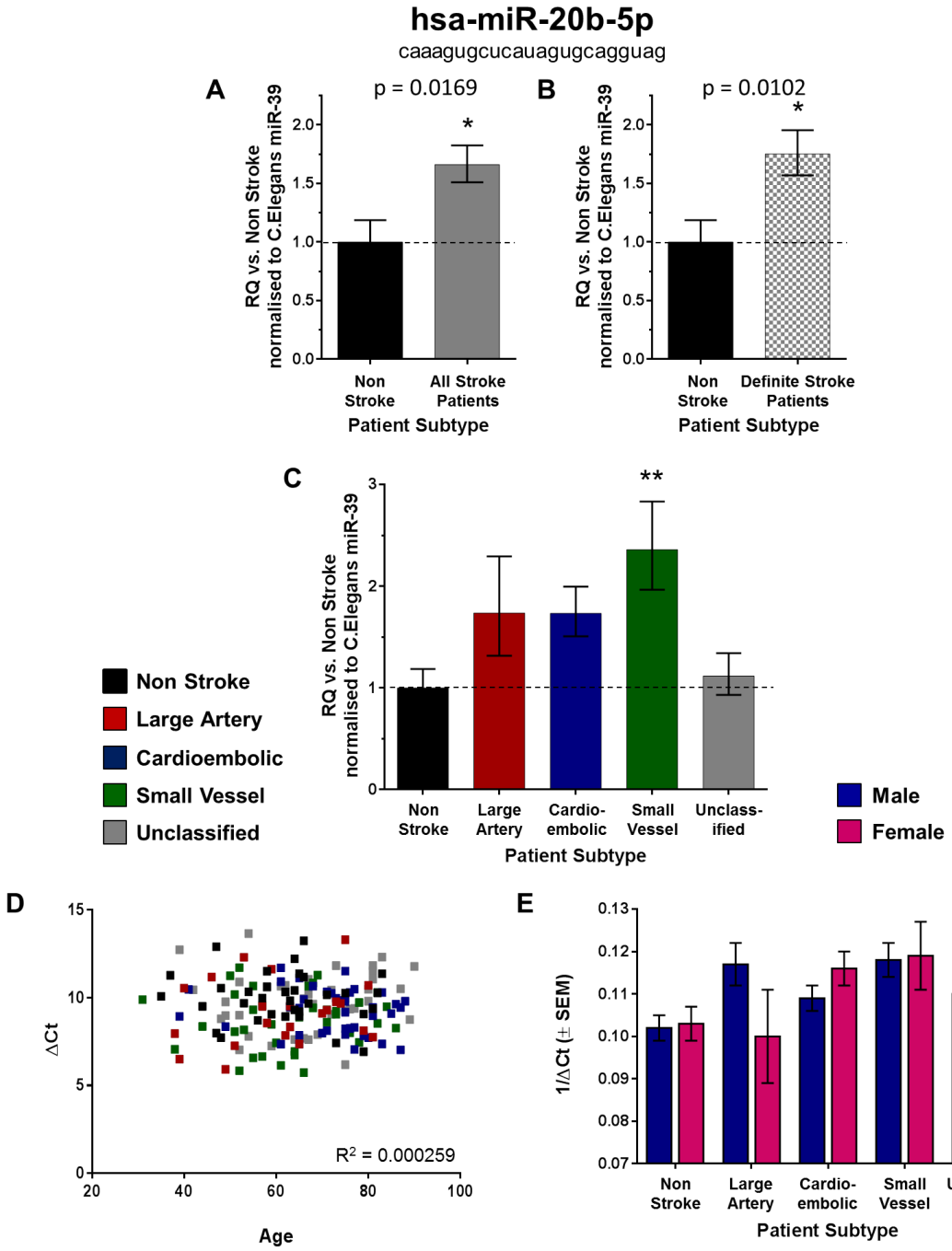

Figure 4.10 – hsa-miR-20b Validation
The exosomal expression of hsa-miR-20b was profiled in all stroke patients (this includes possible stroke patients) (n=139) (A) and in definite stroke patients (n=102) (B) as compared to non-stroke patients (n=34). Probability values were calculated using unpaired Student's t-test, vs. non-stroke control patients, *p<0.05. hsa-miR-20b expression was also assessed specifically in large artery (n=22), cardioembolic (n=40), small vessel (n=37) and unclassified (n=40) stroke patients and compared to non-stroke patients (n=34) (C). Probability values were calculated using one-way-ANOVA with post-hoc Dunnett's test, **p<0.01. Change in miRNA expression was assessed at 48 hours post-stroke by qRT-PCR and relative quantification (RQ) calculated from ΔΔCt following normalisation to a spike housekeeper miRNA, cel-miR-39 and compared to miRNA expression in the non-stroke control patients. Data shown is RQ ± RQmax/RQmin. Patient age was correlated against hsa-miR-20b exosomal expression (D). Data shown are ΔCt values. R^2 value was calculated by Pearson product-moment correlation coefficient. The effect of gender on hsa-miR-20b expression was investigated (E). Data shown is 1/ΔCt (±SEM). Probability was calculated using a one-way-ANOVA with a Bonferroni Multiple Comparison Test.

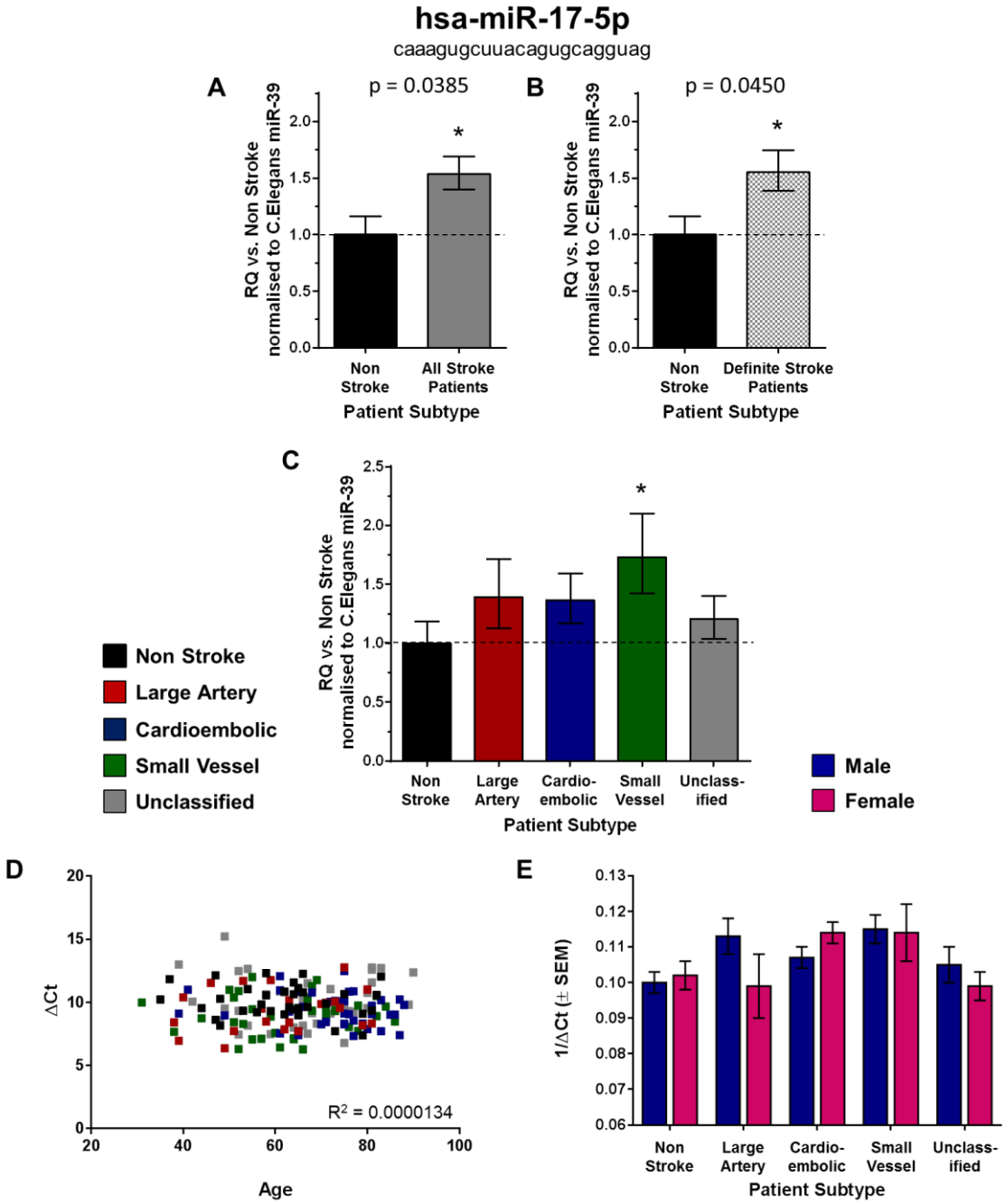

Figure 4.11 – hsa-miR-17 Validation
The exosomal expression of hsa-miR-17 was profiled in all stroke patients (this includes possible stroke patients) (n=139) (A) and in definite stroke patients (n=102) (B) as compared to non-stroke patients (n=34). Probability values were calculated using unpaired Student's t-test, vs. non-stroke control patients, *p<0.05. hsa-miR-17 expression was also assessed specifically in large artery (n=22), cardioembolic (n=40), small vessel (n=37) and unclassified (n=40) stroke patients and compared to non-stroke patients (n=34) (C). Probability values were calculated using one-way-ANOVA with post-hoc Dunnett's test, *p<0.05. Change in miRNA expression was assessed at 48 hours post-stroke by qRT-PCR and relative quantification (RQ) calculated from ΔΔCt following normalisation to a spike housekeeper miRNA, cel-miR-39 and compared to miRNA expression in the non-stroke control patients. Data shown is RQ ± RQmax/RQmin. Patient age was correlated against hsa-miR-17 exosomal expression (D). Data shown are ΔCt values. R^2 value was calculated by Pearson product-moment correlation coefficient. The effect of gender on hsa-miR-17 expression was investigated (E). Data shown is 1/ΔCt (±SEM). Probability was calculated using a one-way-ANOVA with a Bonferroni Multiple Comparison Test.

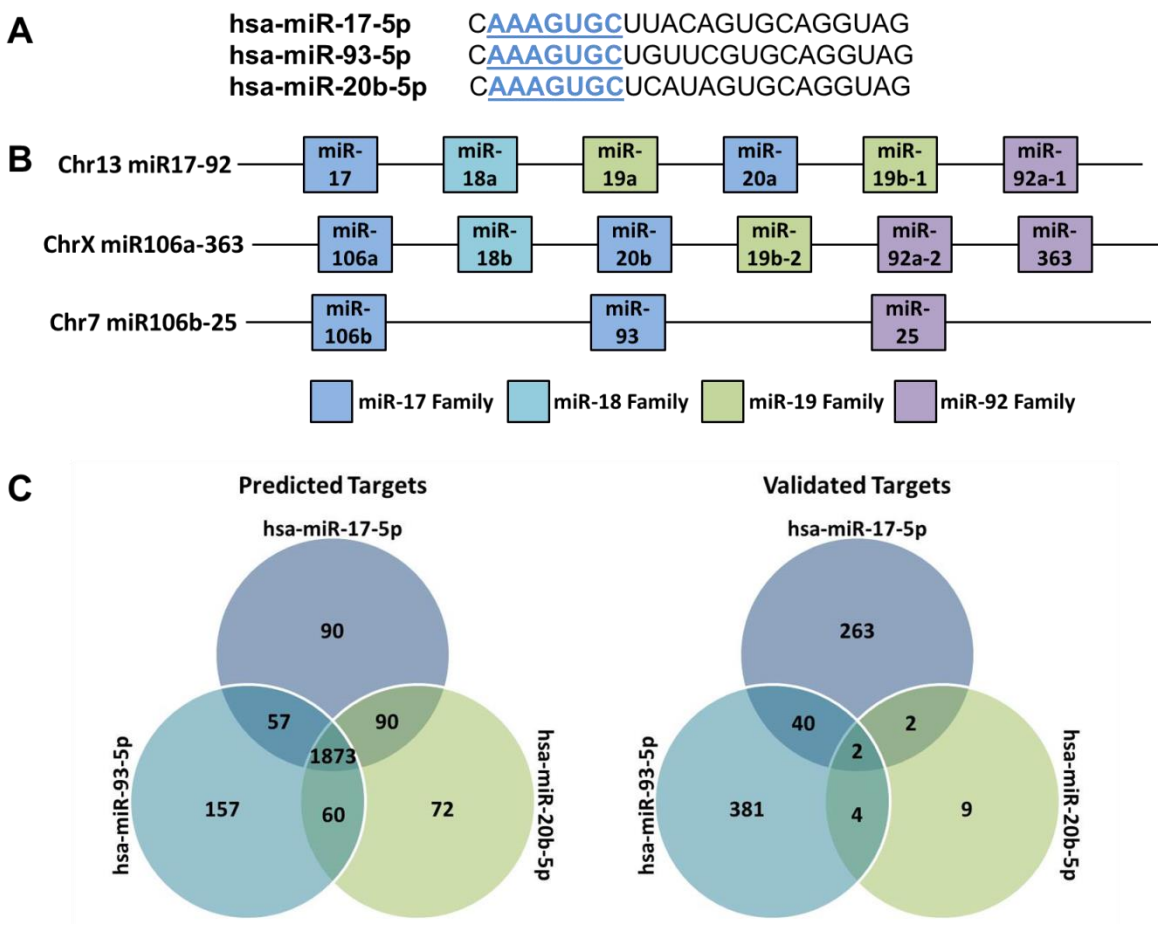

Figure 4.12 – miR-17 Family
miRNAs -17, -93 and -20b have identical seed sequences (in blue, underlined) (A) and belong to the miR-17 family (B) despite being transcribed from separate chromosomes. miRNAs -17, -93 and -20b share a number of predicted and experimentally validated gene targets (C).

hsa-miR-199a-3p is not significantly increased in the exosomes of all stroke patients as compared to non-stroke patients (RQ 1.56 ± 0.18 vs. 1.00 ± 0.20) (Figure 4.13A) but is significantly increased in definite stroke patients as compared to non-stroke patients (RQ 1.66 ± 0.30 vs. 1.00 ± 0.20) (Figure 4.13B). hsa-miR-199a-3p is significantly increased in small vessel disease patients as compared to non-stroke control patients (RQ 2.29 ± 0.48 vs. 1.00 ± 0.20) (Figure 4.13C) but not in large artery and cardioembolic patients. Its expression was unchanged in unclassified patients as compared to non-stroke patients (RQ 0.96 ± 0.24 vs. 1.00 ± 0.20). There was no correlation between hsa-miR-199a-3p expression and the patients age (R^2 = 0.00425) or gender (Figure 4.13 D and E).

Exosomal **hsa-miR-30a-5p** is also not significantly increased in all stroke patients as compared to non-stroke patients (RQ 1.47 ± 0.14 vs. 1.00 ± 0.19) (Figure 4.14A) but is significantly increased in definite stroke patients as compared to

non-stroke patients (RQ 1.53 ± 0.17 vs. 1.00 ± 0.19) (Figure 4.14B). hsa-miR-30a-5p is moderately increased in large artery and cardioembolic stroke patients but only significantly increased in small vessel disease patients as compared to non-stroke control patients (RQ 1.97 ± 0.36 vs. 1.00 ± 0.19) (Figure 4.14C). Its expression was unchanged in unclassified patients as compared to non-stroke patients (RQ 1.00 ± 0.20 vs. 1.00 ± 0.19). There was no correlation between hsa-miR-30a-5p expression and the patients age (R^2 = 0.00215) or gender (Figure 4.14 D and E).

hsa-let-7e is not significantly increased in the exosomes of all stroke patients as compared to non-stroke patients (RQ 1.38 ± 0.12 vs. 1.00 ± 0.14) (Figure 4.15A) but is significantly increased in definite stroke patients as compared to non-stroke patients (RQ 1.45 ± 0.15 vs. 1.00 ± 0.14) (Figure 4.15B). hsa-let-7e is somewhat increased in large artery and cardioembolic stroke patients but only significantly increased in small vessel disease patients as compared to non-stroke control patients (RQ 1.85 ± 0.33 vs. 1.00 ± 0.14) (Figure 4.15C). Its expression was unchanged in unclassified patients as compared to non-stroke patients (RQ 0.97 ± 0.19 vs. 1.00 ± 0.14). There was no correlation between hsa-let-7e expression and the patients age (R^2 = 0.00198) (Figure 4.15D). Male unclassified patients had a significantly higher level of hsa-let-7e expression than corresponding female patients (1/ΔCt 0.093 ± 0.003 vs. 0.085 ± 0.003) (Figure 4.15E).

Exosomal **hsa-miR-218** is not significantly increased in all stroke patients as compared to non-stroke patients (RQ 1.45 ± 0.14 vs. 1.00 ± 0.30) (Figure 4.16A) but is significantly increased in definite stroke patients as compared to non-stroke patients (RQ 1.64 ± 0.20 vs. 1.00 ± 0.30) (Figure 4.16B). hsa-miR-218 is not significantly increased in any stroke patient subtype as compared to non-stroke control patients (Figure 4.16C). Furthermore, there was no correlation between hsa-miR-218 expression and the patients age (R^2 = 0.0215) or gender (Figure 4.16 D and E).

hsa-miR-223 is not significantly increased in the exosomes of all stroke patients as compared to non-stroke patients (RQ 3.96 ± 1.17 vs. 1.00 ± 0.81) (Figure 4.17A) but is significantly increased in definite stroke patients as compared to non-stroke patients (RQ 4.71 ± 1.61 vs. 1.00 ± 0.81) (Figure 4.17B). hsa-miR-223

was not detected in a number of samples (i.e. Ct >40). For the purposes of data analysis these samples were given a Ct of 40. This resulted in the data being non-normally distributed but appropriate statistical tests were used to compensate for this. hsa-miR-223 was not significantly increased in any specific stroke subtype as compared to non-stroke controls although it was increased eight-fold in cardioembolic patients (RQ 8.06 ± 3.51 vs. 1.00 ± 0.81) (Figure 4.17C). There was no correlation between hsa-miR-223 expression and the patients age ($\rho = 0.0471$) or gender (Figure 4.17 D and E).

The exosomal expression of four miRNAs was unchanged as a result of ischaemic stroke: **miR-520b, miR-660, miR-376a and miR-549a** (Figure 4.18 - Figure 4.21). Their expression was not significantly altered in either all stroke patients or definite stroke patients (Figure 4.18 - Figure 4.21 A and B) or in any particular stroke subtype (Figure 4.18 - Figure 4.21 C). There was no correlation between their expression and patient age (Figure 4.18 - Figure 4.21 D). Furthermore, patient gender did not appear to have any effect on their expression (Figure 4.18 - Figure 4.21 E), with the exception that male large artery stroke patients had a significantly higher level of miR-376a expression than their female counterparts (Figure 4.20E). There was no effect of gender on miR-376a expression observable in other stroke patient subtypes.

The effect of treatment with rtPA on exosomal miRNA expression was also investigated. Treatment with rtPA did not have any effect on the expression of the miRNAs already discussed here (data not shown).

In the present study we have found 3 miRNAs significantly increased in the exosomes of all stroke patients vs. controls, 9 exosomal miRNAs that are significantly increased in definite stroke patients vs. controls and 7 miRNAs that are significantly increased in small vessel disease patients vs. non-stroke control patients. Interestingly, for all of these miRNAs, unclassified patients have, on average, a very similar level of miRNA expression to non-stroke patients.

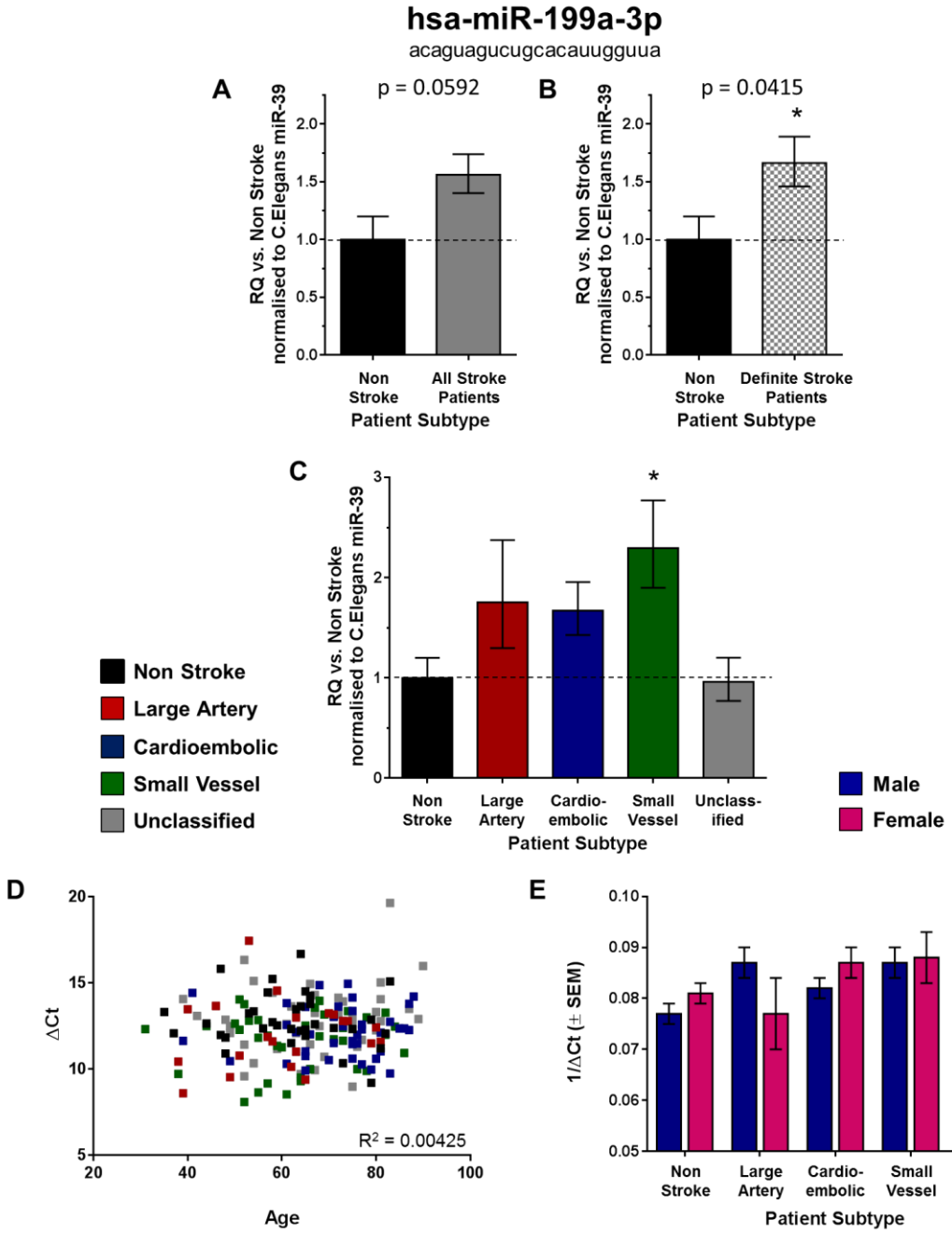

Figure 4.13 – hsa-miR-199a-3p Validation
The exosomal expression of hsa-miR-199a-3p was profiled in all stroke patients (this includes possible stroke patients) (n=139) (A) and in definite stroke patients (n=102) (B) as compared to non-stroke patients (n=34). Probability values were calculated using unpaired Student's t-test, vs. non-stroke control patients, *p<0.05. hsa-miR-199a-3p expression was also assessed specifically in large artery (n=22), cardioembolic (n=40), small vessel (n=37) and unclassified (n=40) stroke patients and compared to non-stroke patients (n=34) (C). Probability values were calculated using one-way-ANOVA with post-hoc Dunnett's test, *p<0.05. Change in miRNA expression was assessed at 48 hours post-stroke by qRT-PCR and relative quantification (RQ) calculated from ΔΔCt following normalisation to a spike housekeeper miRNA, cel-miR-39 and compared to miRNA expression in the non-stroke control patients. Data shown is RQ ± RQmax/RQmin. Patient age was correlated against hsa-miR-199a-3p exosomal expression (D). Data shown are ΔCt values. R^2 value was calculated by Pearson product-moment correlation coefficient. The effect of gender on hsa-miR-199a-3p expression was investigated (E). Data shown is 1/ΔCt (±SEM). Probability was calculated using a one-way-ANOVA with a Bonferroni Multiple Comparison Test.

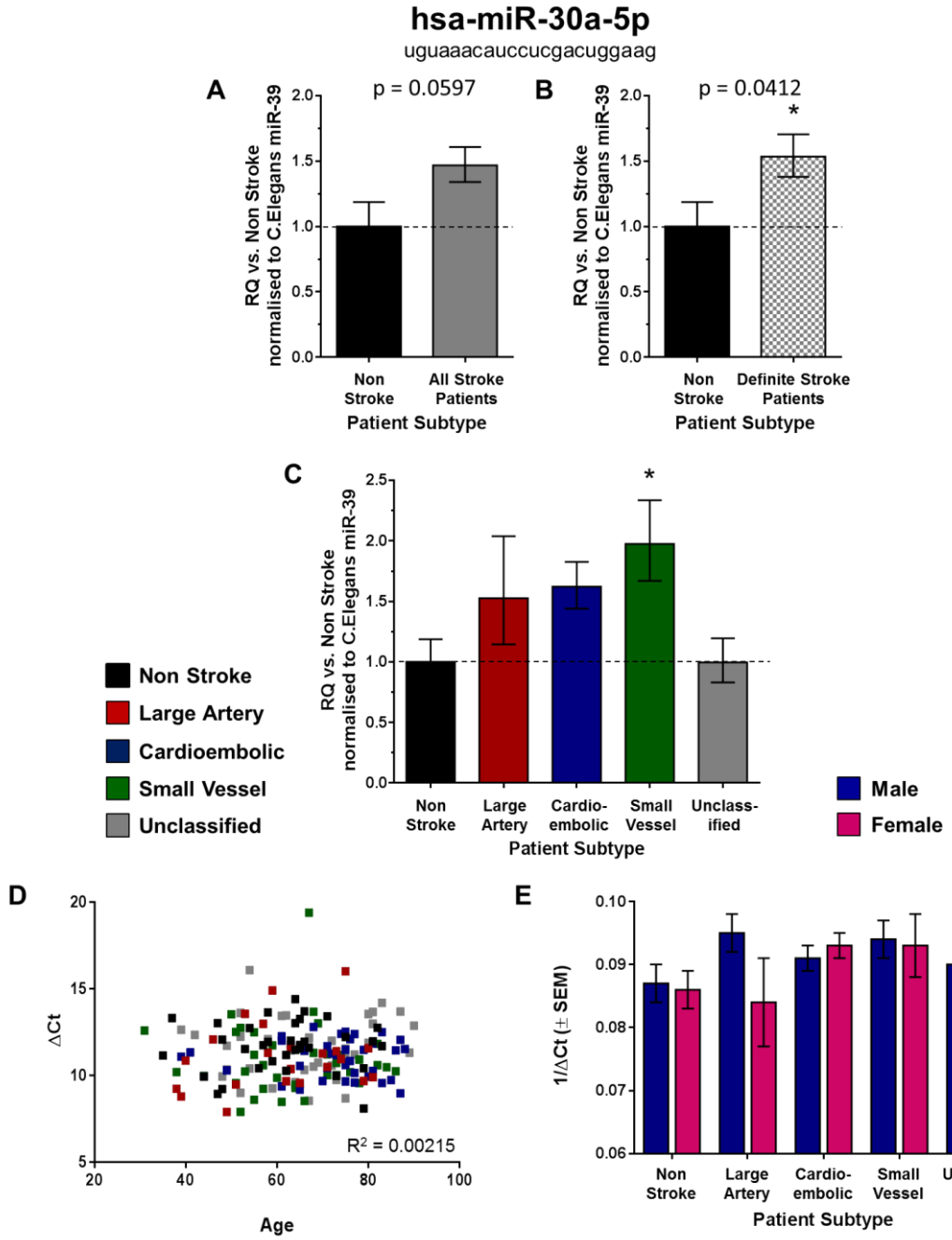

Figure 4.14 – hsa-miR-30a-5p Validation
The exosomal expression of hsa-miR-30a-5p was profiled in all stroke patients (this includes possible stroke patients) (n=139) (A) and in definite stroke patients (n=102) (B) as compared to non-stroke patients (n=34). Probability values were calculated using unpaired Student's t-test, vs. non-stroke control patients, *p<0.05. hsa-miR-30a-5p expression was also assessed specifically in large artery (n=22), cardioembolic (n=40), small vessel (n=37) and unclassified (n=40) stroke patients and compared to non-stroke patients (n=34) (C). Probability values were calculated using one-way-ANOVA with post-hoc Dunnett's test, *p<0.05. Change in miRNA expression was assessed at 48 hours post-stroke by qRT-PCR and relative quantification (RQ) calculated from ΔΔCt following normalisation to a spike housekeeper miRNA, cel-miR-39 and compared to miRNA expression in the non-stroke control patients. Data shown is RQ ± RQmax/RQmin. Patient age was correlated against hsa-miR-30a-5p exosomal expression (D). Data shown are ΔCt values. R^2 value was calculated by Pearson product-moment correlation coefficient. The effect of gender on hsa-miR-30a-5p expression was investigated (E). Data shown is 1/ΔCt (±SEM). Probability was calculated using a one-way-ANOVA with a Bonferroni Multiple Comparison Test.

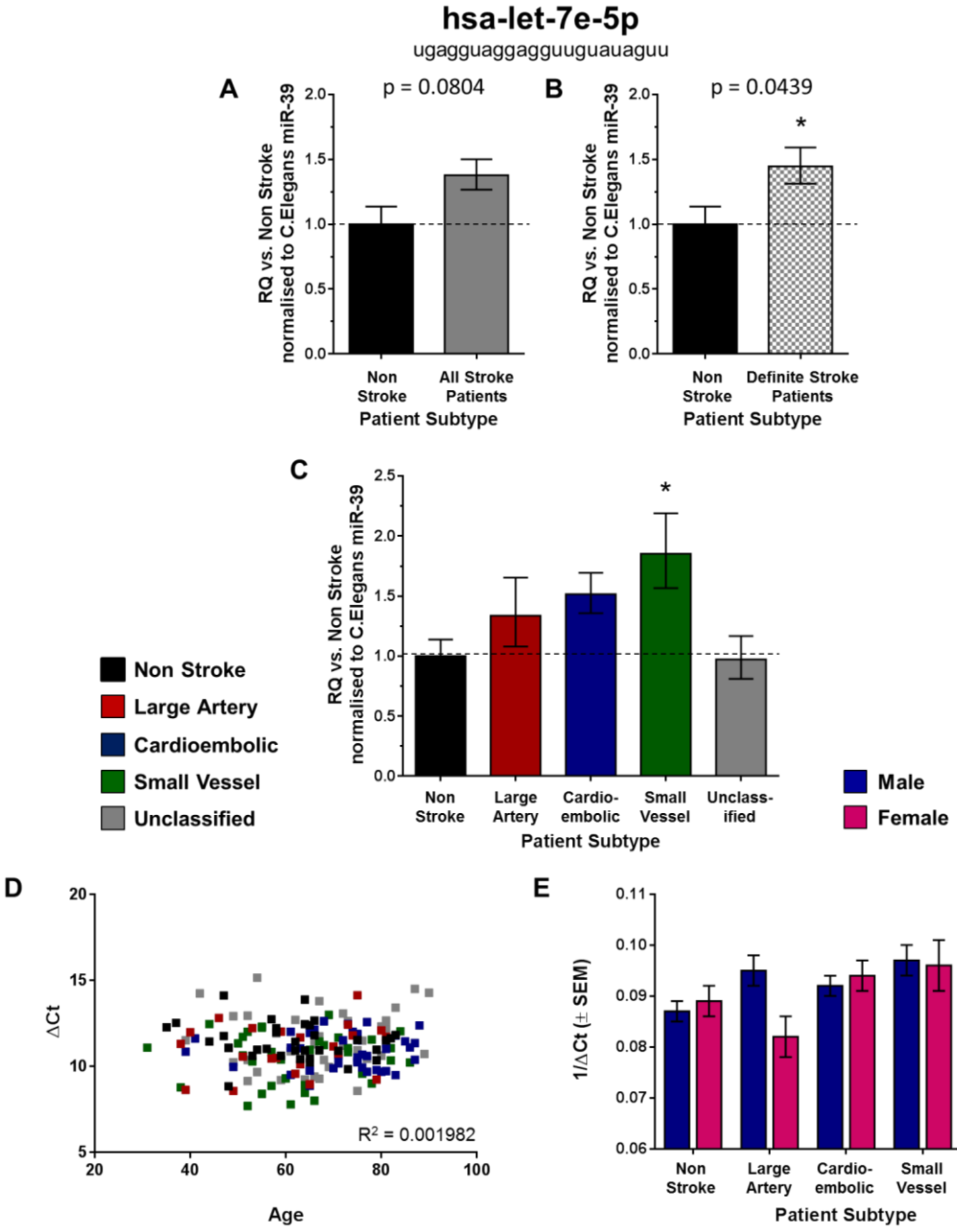

Figure 4.15 – hsa-let-7e Validation
The exosomal expression of hsa-let-7e was profiled in all stroke patients (this includes possible stroke patients) (n=139) (A) and in definite stroke patients (n=102) (B) as compared to non-stroke patients (n=34). Probability values were calculated using unpaired Student's t-test, vs. non-stroke control patients, *p<0.05. hsa-let-7e expression was also assessed specifically in large artery (n=22), cardioembolic (n=40), small vessel (n=37) and unclassified (n=40) stroke patients and compared to non-stroke patients (n=34) (C). Probability values were calculated using one-way-ANOVA with post-hoc Dunnett's test, *p<0.05. Change in miRNA expression was assessed at 48 hours post-stroke by qRT-PCR and relative quantification (RQ) calculated from ΔΔCt following normalisation to a spike housekeeper miRNA, cel-miR-39 and compared to miRNA expression in the non-stroke control patients. Data shown is RQ ± RQmax/RQmin. Patient age was correlated against hsa-let-7e exosomal expression (D). Data shown are ΔCt values. R^2 value was calculated by Pearson product-moment correlation coefficient. The effect of gender on hsa-let-7e expression was investigated (E). Data shown is 1/ΔCt (±SEM). Probability was calculated using a one-way-ANOVA with a Bonferroni Multiple Comparison Test, *p<0.05.

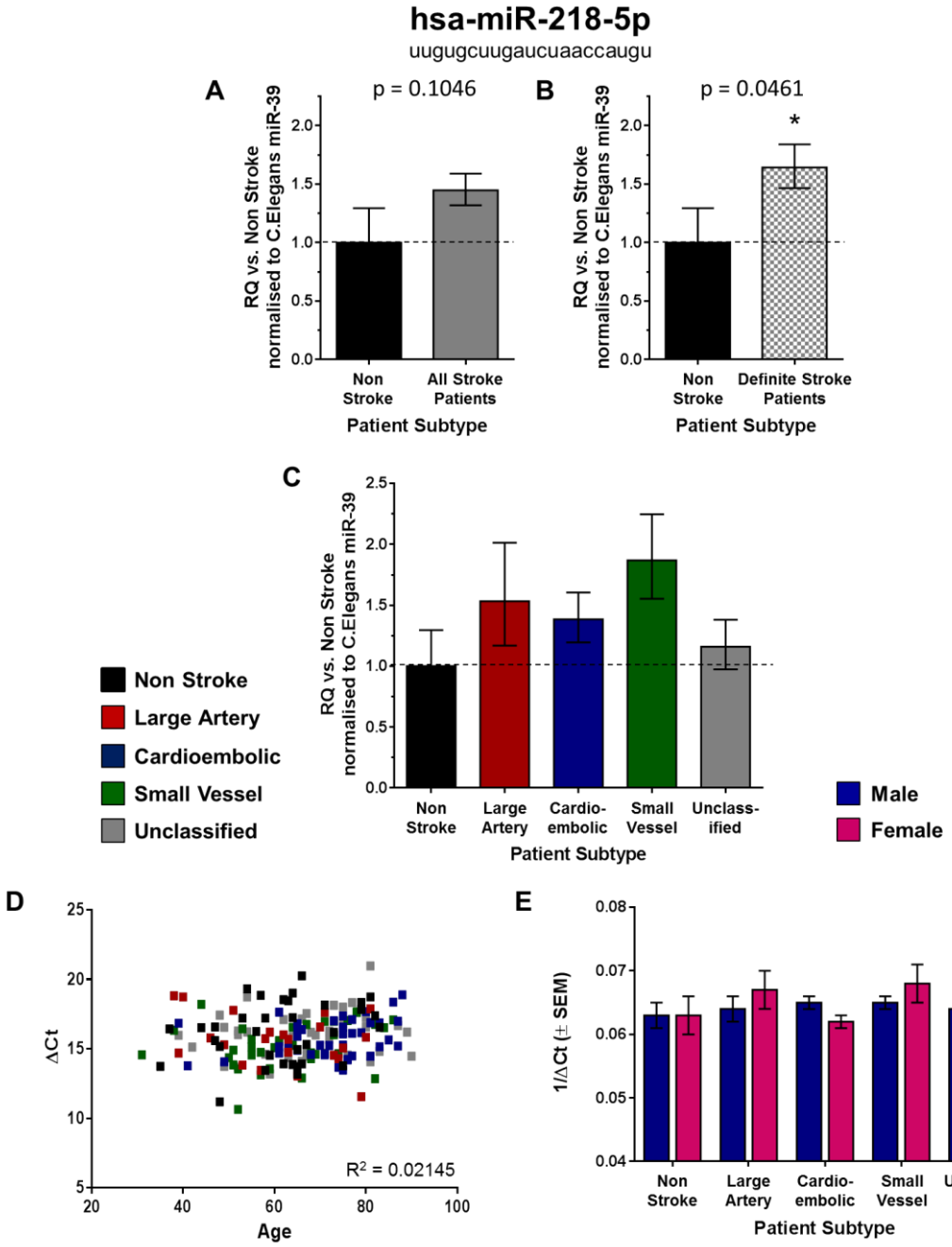

Figure 4.16 – hsa-miR-218-5p Validation
The exosomal expression of hsa-miR-218-5p was profiled in all stroke patients (this includes possible stroke patients) (n=139) (A) and in definite stroke patients (n=102) (B) as compared to non-stroke patients (n=34). Probability values were calculated using unpaired Student's t-test, vs. non-stroke control patients, *p<0.05. hsa-miR-218-5p expression was also assessed specifically in large artery (n=22), cardioembolic (n=40), small vessel (n=37) and unclassified (n=40) stroke patients and compared to non-stroke patients (n=34) (C). Probability values were calculated using one-way-ANOVA with post-hoc Dunnett's test. Change in miRNA expression was assessed at 48 hours post-stroke by qRT-PCR and relative quantification (RQ) calculated from ΔΔCt following normalisation to a spike housekeeper miRNA, cel-miR-39 and compared to miRNA expression in the non-stroke control patients. Data shown is RQ ± RQmax/RQmin. Patient age was correlated against hsa-miR-218-5p exosomal expression (D). Data shown are ΔCt values. R^2 value was calculated by Pearson product-moment correlation coefficient. The effect of gender on hsa-miR-218-5p expression was investigated (E). Data shown is 1/ΔCt (±SEM). Probability was calculated using a one-way-ANOVA with a Bonferroni Multiple Comparison Test.

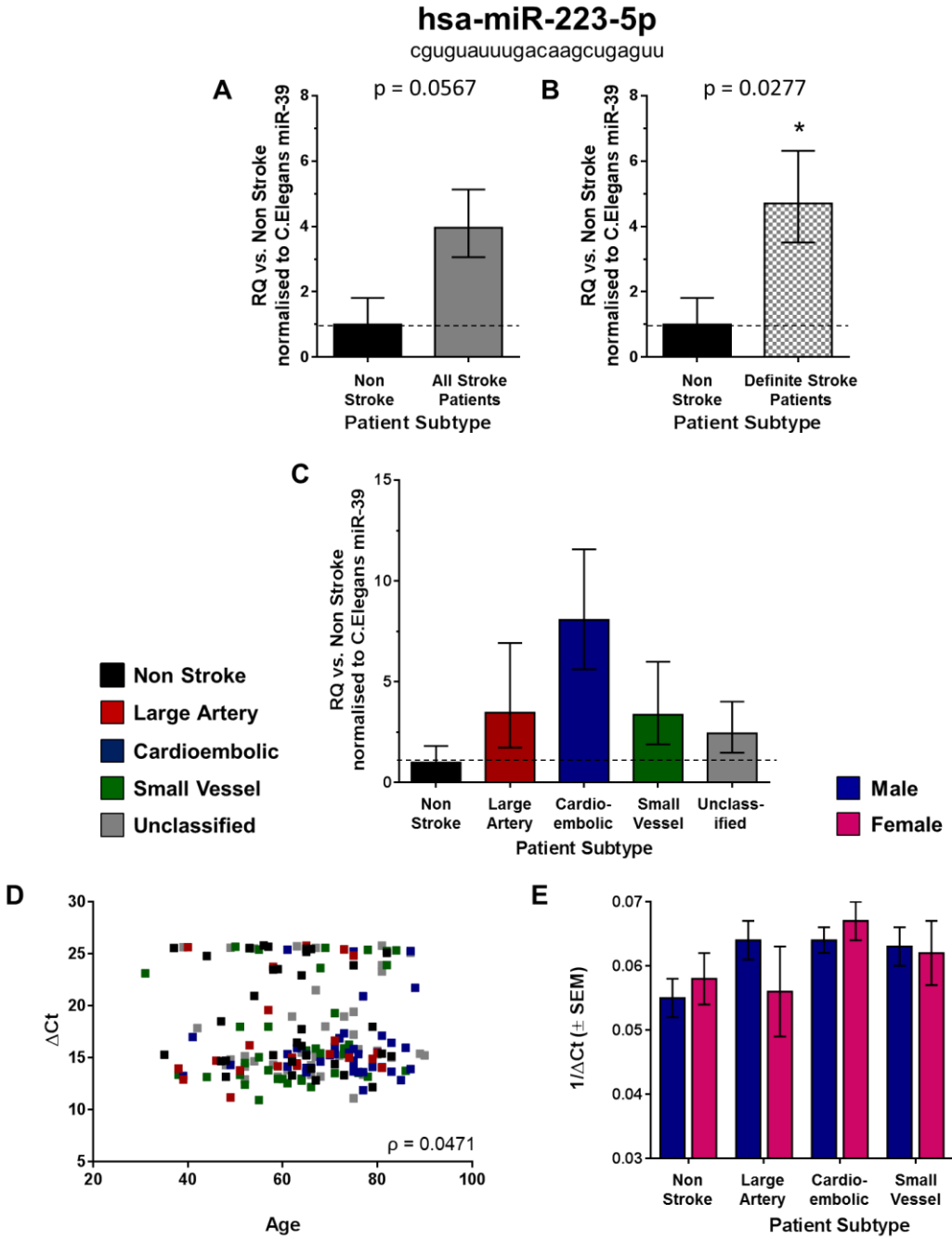

Figure 4.17 – hsa-miR-223-5p Validation
The exosomal expression of hsa-miR-223-5p was profiled in all stroke patients (this includes possible stroke patients) (n=139) (A) and in definite stroke patients (n=102) (B) as compared to non-stroke patients (n=34). Probability values were calculated using Mann-Whitney U test, vs. non-stroke control patients, *p<0.05. hsa-miR-223-5p expression was also assessed specifically in large artery (n=22), cardioembolic (n=40), small vessel (n=37) and unclassified (n=40) stroke patients and compared to non-stroke patients (n=34) (C). Probability values were calculated using a Kruskal-Wallis H test with post-hoc Dunn's multiple comparisons test. Change in miRNA expression was assessed at 48 hours post-stroke by qRT-PCR and relative quantification (RQ) calculated from ΔΔCt following normalisation to a spike housekeeper miRNA, cel-miR-39 and compared to miRNA expression in the non-stroke control patients. Data shown is RQ ± RQmax/RQmin. Patient age was correlated against hsa-miR-223-5p exosomal expression (D). Data shown are ΔCt values. ρ was calculated by Spearman's Rank-Order Correlation. The effect of gender on hsa-miR-223-5p expression was investigated (E). Data shown is 1/ΔCt (±SEM). Probability was calculated using a Kruskal-Wallis H test with post-hoc Dunn's multiple comparisons test.

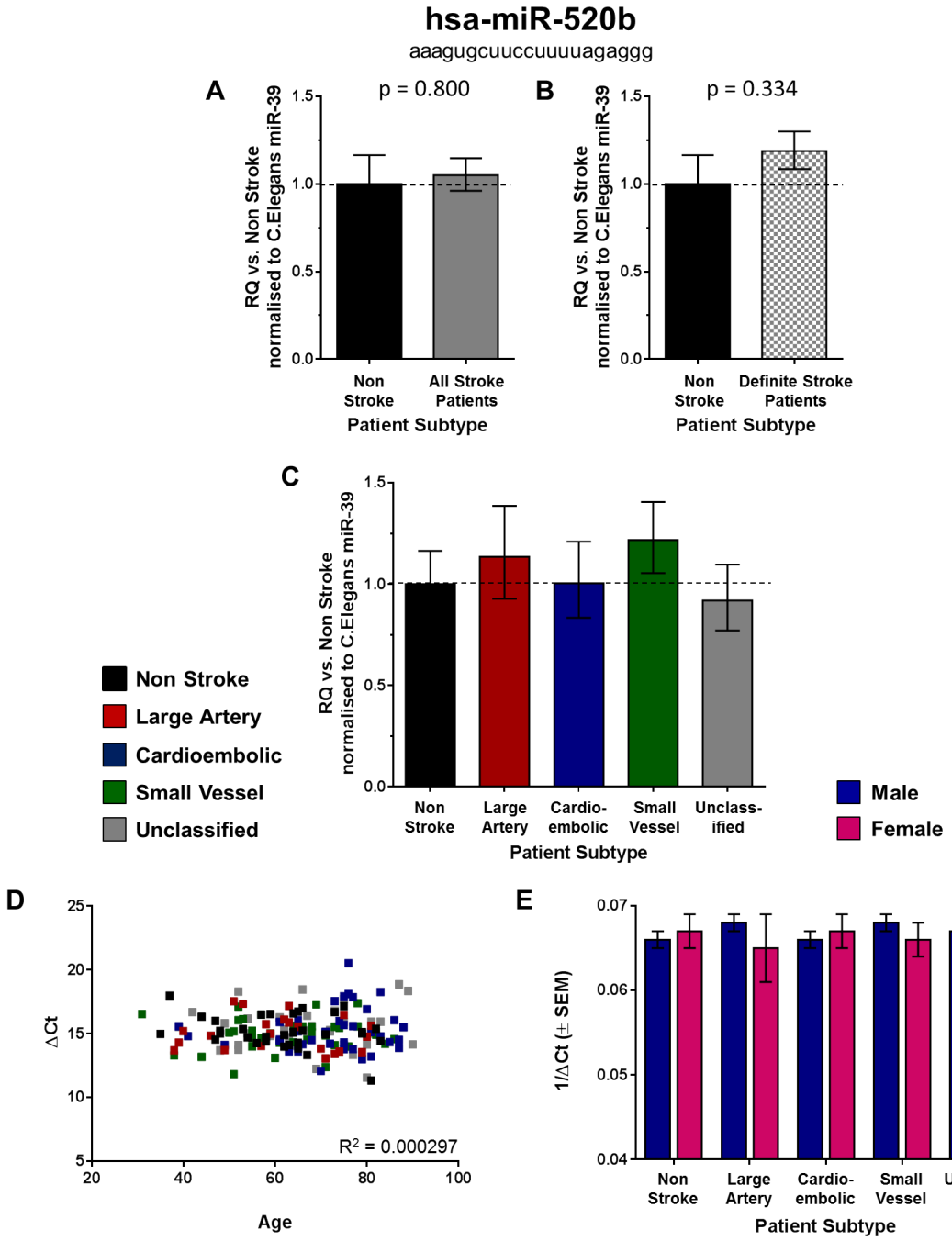

Figure 4.18 – has-miR-520b Validation
The exosomal expression of hsa-miR-520b was profiled in all stroke patients (this includes possible stroke patients) (n=139) (A) and in definite stroke patients (n=102) (B) as compared to non-stroke patients (n=34). Probability values were calculated using unpaired Student's t-test, vs. non-stroke control patients. hsa-miR-520b expression was also assessed specifically in large artery (n=22), cardioembolic (n=40), small vessel (n=37) and unclassified (n=40) stroke patients and compared to non-stroke patients (n=34) (C). Probability values were calculated using one-way-ANOVA with post-hoc Dunnett's test. Change in miRNA expression was assessed at 48 hours post-stroke by qRT-PCR and relative quantification (RQ) calculated from ΔΔCt following normalisation to a spike housekeeper miRNA, cel-miR-39 and compared to miRNA expression in the non-stroke control patients. Data shown is RQ ± RQmax/RQmin. Patient age was correlated against hsa-miR-520b exosomal expression (D). Data shown are ΔCt values. R^2 value was calculated by Pearson product-moment correlation coefficient. The effect of gender on hsa-miR-520b expression was investigated (E). Data shown is 1/dCt (±SEM). Probability was calculated using a one-way-ANOVA with a Bonferroni Multiple Comparison Test.

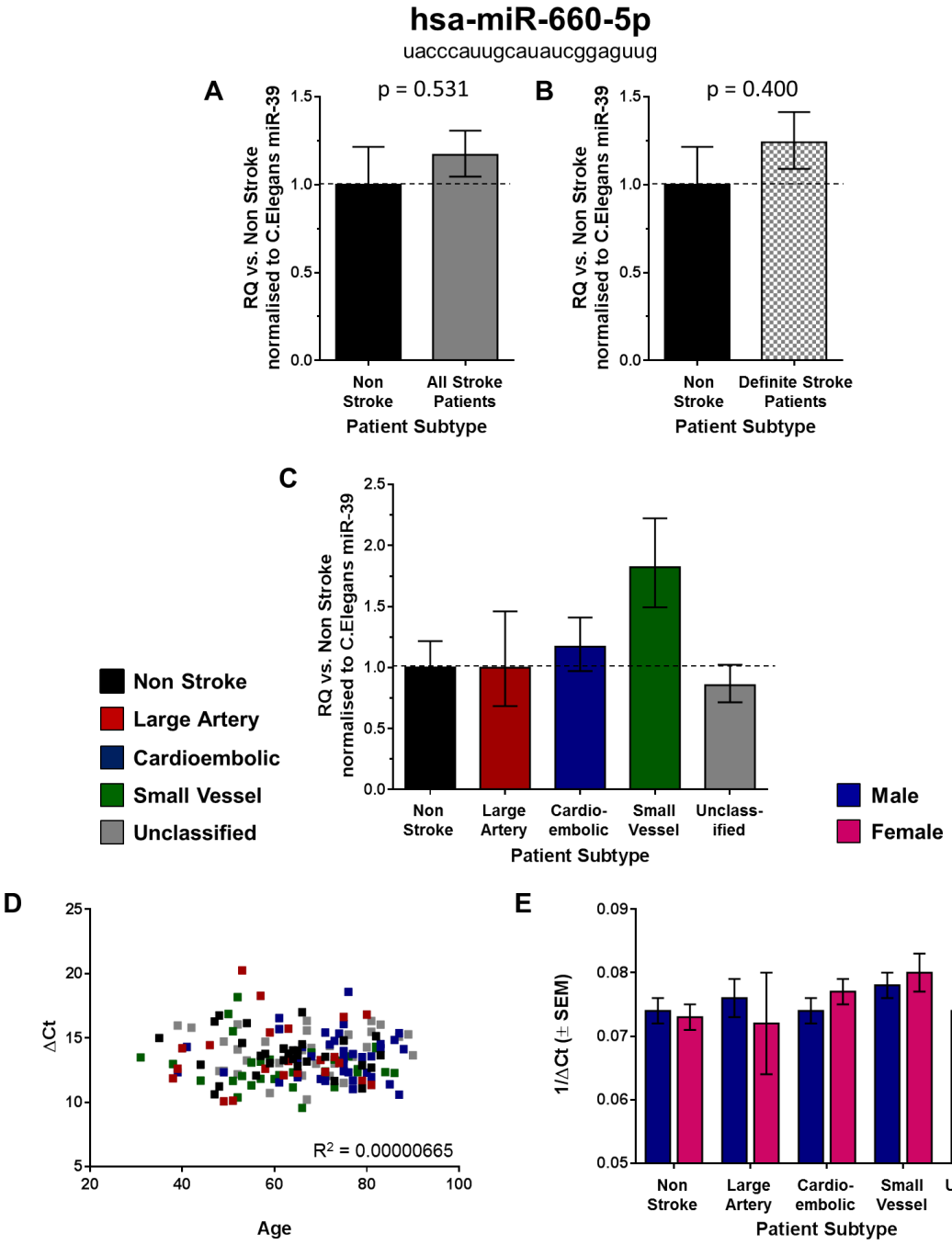

Figure 4.19 – hsa-miR-660 Validation
The exosomal expression of hsa-miR-600 was profiled in all stroke patients (this includes possible stroke patients) (n=139) (A) and in definite stroke patients (n=102) (B) as compared to non-stroke patients (n=34). Probability values were calculated using unpaired Student's t-test, vs. non-stroke control patients. hsa-miR-660 expression was also assessed specifically in large artery (n=22), cardioembolic (n=40), small vessel (n=37) and unclassified (n=40) stroke patients and compared to non-stroke patients (n=34) (C). Probability values were calculated using one-way-ANOVA with post-hoc Dunnett's test. Change in miRNA expression was assessed at 48 hours post-stroke by qRT-PCR and relative quantification (RQ) calculated from ΔΔCt following normalisation to a spike housekeeper miRNA, cel-miR-39 and compared to miRNA expression in the non-stroke control patients. Data shown is RQ ± RQmax/RQmin. Patient age was correlated against hsa-miR-660 exosomal expression (D). Data shown are ΔCt values. R^2 value was calculated by Pearson product-moment correlation coefficient. The effect of gender on hsa-miR-660 expression was investigated (E). Data shown is 1/dCt (±SEM). Probability was calculated using a one-way-ANOVA with a Bonferroni Multiple Comparison Test.

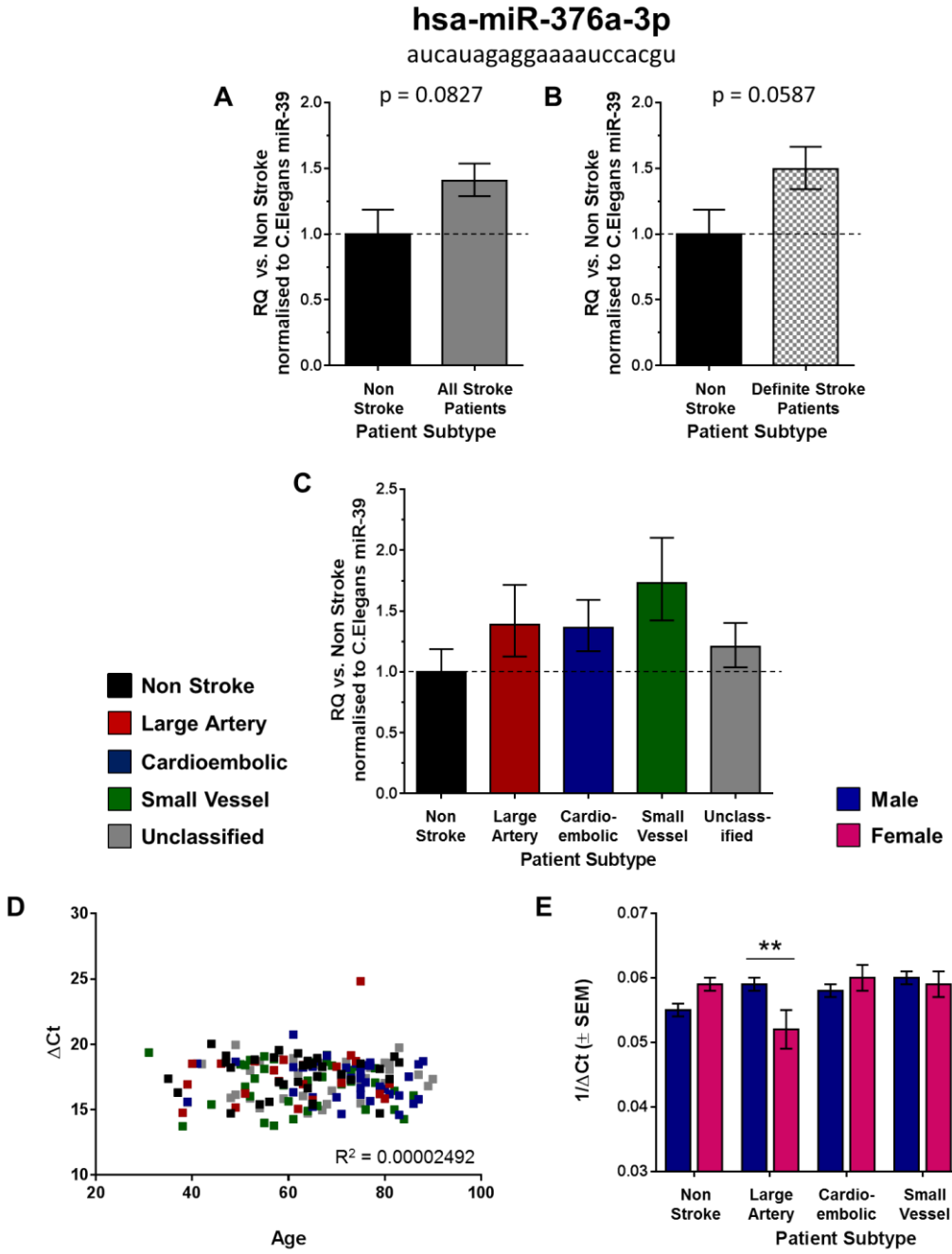

Figure 4.20 – hsa-miR-376a-3p Validation
The exosomal expression of hsa-miR-376a-3p was profiled in all stroke patients (this includes possible stroke patients) (n=139) (A) and in definite stroke patients (n=102) (B) as compared to non-stroke patients (n=34). Probability values were calculated using unpaired Student's t-test, vs. non-stroke control patients. hsa-miR-376a-3p expression was also assessed specifically in large artery (n=22), cardioembolic (n=40), small vessel (n=37) and unclassified (n=40) stroke patients and compared to non-stroke patients (n=34) (C). Probability values were calculated using one-way-ANOVA with post-hoc Dunnett's test. Change in miRNA expression was assessed at 48 hours post-stroke by qRT-PCR and relative quantification (RQ) calculated from ΔΔCt following normalisation to a spike housekeeper miRNA, cel-miR-39 and compared to miRNA expression in the non-stroke control patients. Data shown is RQ ± RQmax/RQmin. Patient age was correlated against hsa-miR-376a-3p exosomal expression (D). Data shown are ΔCt values. R^2 value was calculated by Pearson product-moment correlation coefficient. The effect of gender on hsa-miR-376a-3p expression was investigated (E). Data shown is 1/ΔCt (±SEM). Probability was calculated using a one-way-ANOVA with a Bonferroni Multiple Comparison Test.

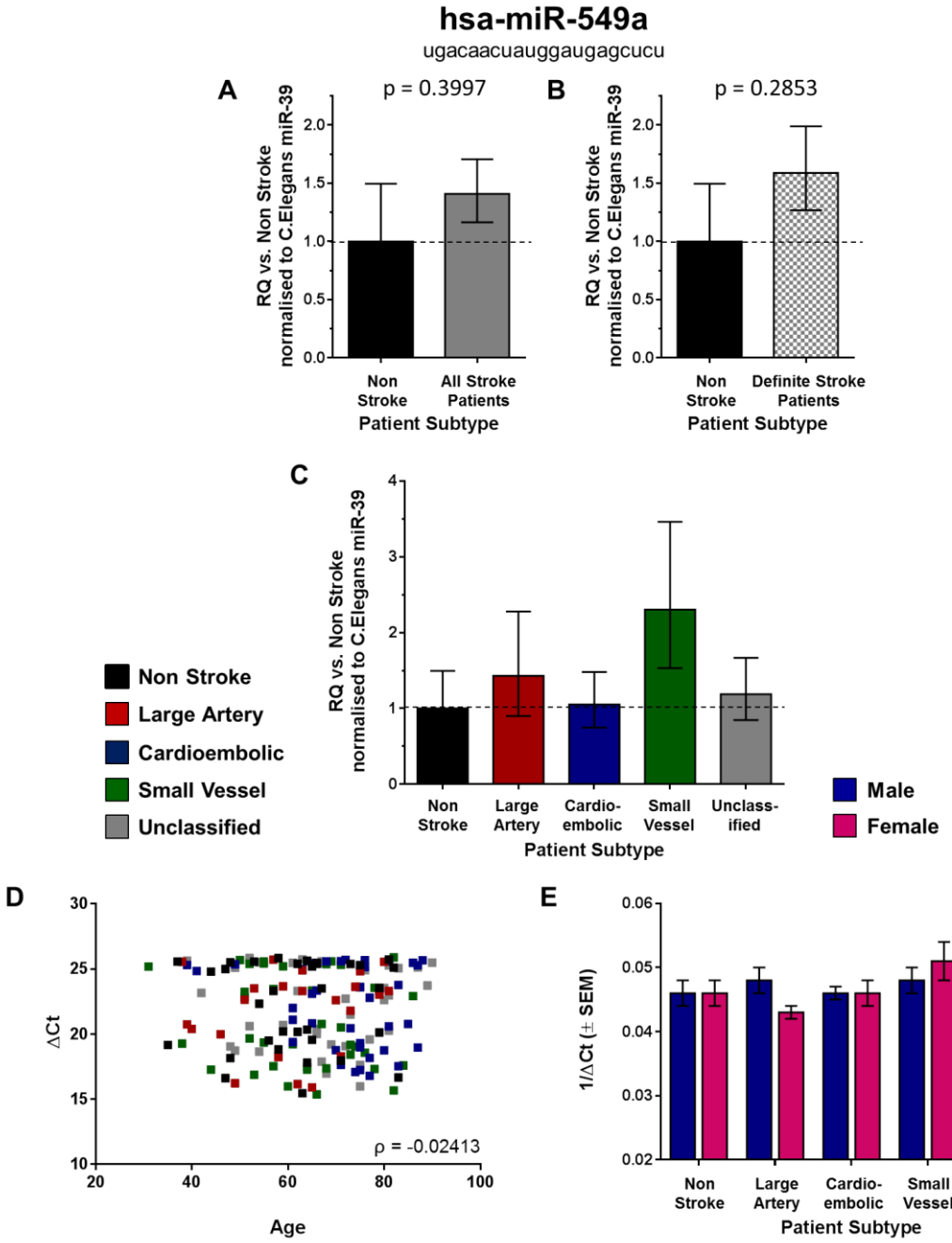

Figure 4.21 – hsa-miR-549a Validation
The exosomal expression of hsa-miR-549a was profiled in all stroke patients (this includes possible stroke patients) (n=139) (A) and in definite stroke patients (n=102) (B) as compared to non-stroke patients (n=34). Probability values were calculated using Mann-Whitney U test, vs. non-stroke control patients. hsa-miR-549a expression was also assessed specifically in large artery (n=22), cardioembolic (n=40), small vessel (n=37) and unclassified (n=40) stroke patients and compared to non-stroke patients (n=34) (C). Probability was calculated using a Kruskal-Wallis H test with post-hoc Dunn's multiple comparisons test. Change in miRNA expression was assessed at 48 hours post-stroke by qRT-PCR and relative quantification (RQ) calculated from ΔΔCt following normalisation to a spike housekeeper miRNA, cel-miR-39 and compared to miRNA expression in the non-stroke control patients. Data shown is RQ ± RQmax/RQmin. Patient age was correlated against hsa-miR-549a exosomal expression (D). Data shown are ΔCt values. ρ was calculated by Spearman's Rank-Order Correlation. The effect of gender on hsa-miR-549a expression was investigated (E). Data shown is 1/ΔCt (±SEM). Probability was calculated using a Kruskal-Wallis H test with post-hoc Dunn's multiple comparisons test.

4.2.7 miRNA Expression and Clinical Outcome from Stroke

In the present study we examined the relationship between exosomal expression of 7 miRNAs and the clinical outcome of ischaemic stroke patients. These miRNAs are miRs -27b, -93, -20b, -17, 30a, 199a and let-7e and were all increased in definite stroke patients vs. non-stroke patients and were also all increased in small vessel disease vs. non-stroke control patients. In this study we have used two measures of clinical outcome: the NIHSS and the mRS, both widely used by clinicians in the UK and worldwide. The NIHSS is an impairment scale based on 15 measurements and is intended to evaluate both neurological outcome and the degree of physical recovery in patients with stroke. It assesses levels of consciousness, extraocular movements, visual fields, facial muscle relaxation, extremity strength, sensory function, coordination (ataxia), language (aphasia), speech (dysarthria) and hemi-inattention (neglect). It is commonly used as an initial assessment tool and to plan post-acute care. Patients can score from 0 – 42, with 0 indicating no stroke, 1 to 4 a minor stroke, scores of 5 to 20 moderate strokes and scores over 21 indicating severe stroke. The second measure of clinical outcome used in this study is the modified Rankin scale. This is a scale used to measure the degree of disability in a patient post-stroke and their level of dependence for carrying out daily activities. It is often used as an outcome measure in clinical trials for stroke. Patients can score from 0 – 6. Scores of 0 and 1 indicate the patient has either no disability or that they are able to carry out all previous activities without assistance despite minor symptoms. Scores 2 - 5 indicate increasing levels of disability and a score of 6 indicates patient death.

Exosomal hsa-miR-17 expression does not correlate with NIHSS scores at either baseline (Figure 4.22A-E) or at day 7 (Figure 4.22F-J). NIHSS scores at baseline do not correlate with hsa-miR-17-5p expression (R^2 = 0.0028) (Figure 4.22A). If these results are broken down further to examine differences in correlation between the different stroke subtypes only very small changes are observed: large artery (R^2 = 0.0058) (Figure 4.22B), cardioembolic (R^2 = 0.12) (Figure 4.22C), small vessel (R^2 = 0.00013) (Figure 4.22D) and unclassified (R^2 = 0.012) (Figure 4.22E). NIHSS scores at day 7 also do not correlate with hsa-miR-17-5p expression (R^2 = 0.0094) (Figure 4.22F). When broken down further to examine the differences between the different stroke subtypes it is clear there are only

very small differences between correlations: large artery (R^2 = 0.13) (Figure 4.22G), cardioembolic (R^2 = 0.045) (Figure 4.22H), small vessel (R^2 = 0.00054) (Figure 4.22I) and unclassified (R^2 = 0.00038) (Figure 4.22J).

If exosomal expression of miR-17 is compared between patients with a mRS score (at 1 month) of ≤1 (patients with no disability) and patients with a score ≥2 (patients with slight to significant disability), we can see that there is a slight trend towards higher expression of miR-17 in patients with improved outcome following stroke (RQ 1.00 ± 0.19 vs. 0.69 ± 0.13, p=0.14) (Figure 4.22K). This change is not significant but if the change in expression is broken down to reveal differences between differing stroke subtypes it becomes clear that this is most likely because miR-17 expression is only associated with improved functional recovery in large artery and unclassified stroke patients, although these changes are also not significant (Figure 4.22L).

When examining the relationship between exosomal expression of miRNAs and the clinical outcome of ischaemic stroke patients a number of similarities were observed between different miRNAs and their relationship to clinical outcome. For this reason the results for the following 6 miRNAs have been summarised briefly here. The exosomal expression of hsa-miR-20b, hsa-miR-93, hsa-miR-27b, hsa-miR-30a, hsa-miR-199a and hsa-let-7e does not correlate with NIHSS scores for all stroke patients at baseline or day 7 (Figure 4.23 - Figure 4.28 A and F). When broken down further to examine differences between stroke subtypes, although there are small changes between stroke subtypes, there is no significant correlation between any individual stroke subtype and exosomal expression of any one miRNA (Figure 4.23 - Figure 4.28 B-E and G-J).

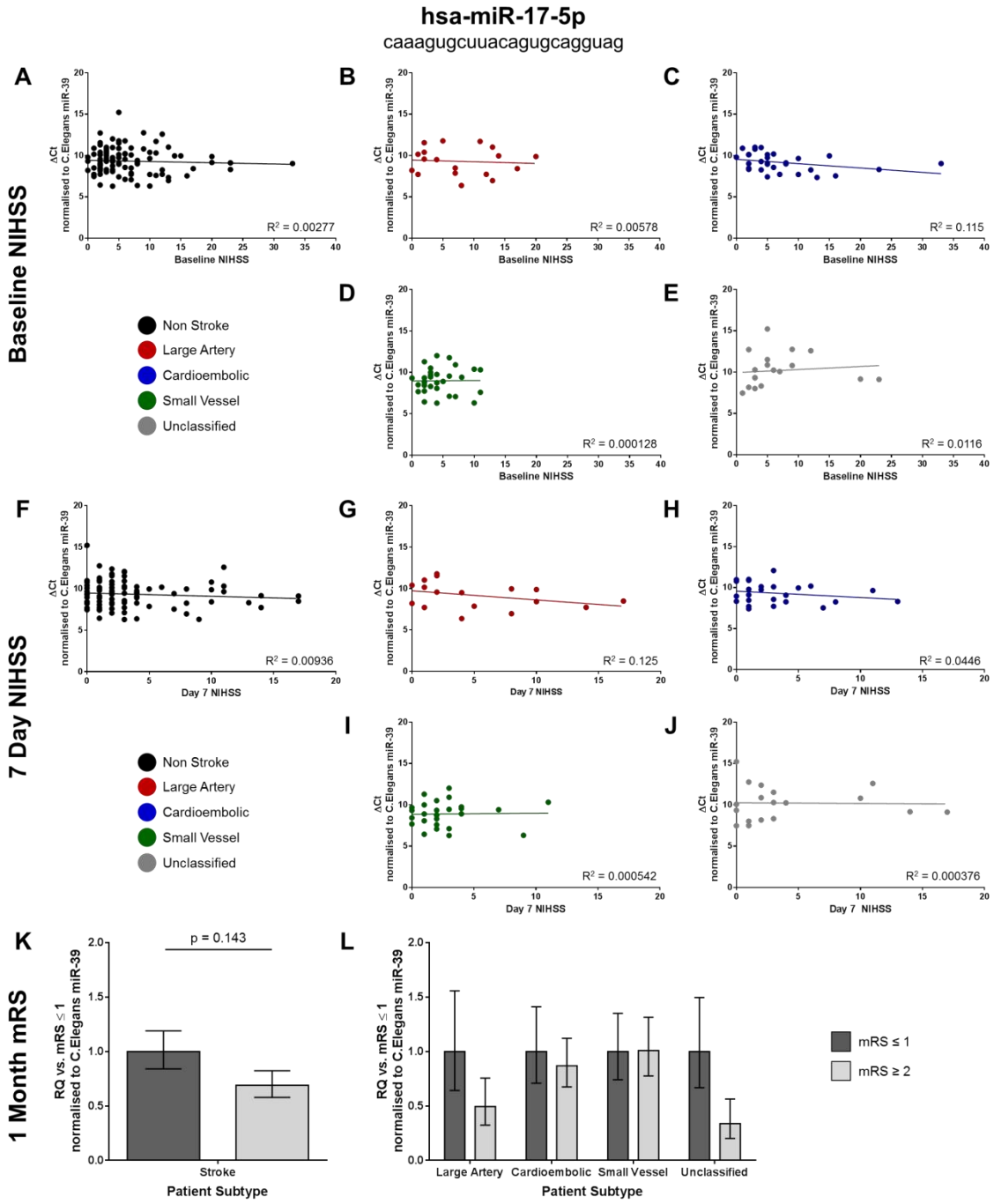

Figure 4.22 – has-miR-17 and Clinical Outcome
NIHSS scores at baseline are correlated against ΔCt values for hsa-miR-17 expression for all definite stroke patients (A), large artery (B), cardioembolic (C), small vessel (D) and unclassified stroke patients (E). NIHSS scores at day 7 post-stroke are correlated against ΔCt values for hsa-miR-17 expression for all definite stroke patients (F), large artery (G), cardioembolic (H), small vessel (I) and unclassified stroke patients (J). R^2 values are calculated by Pearson product-moment correlation coefficient. hsa-miR-17 expression is compared between stroke patients with a 1 month mRS ≤ 1 and those with a mRS ≥ 2 (K). Probability was calculated using unpaired Student's t-test. For each stroke subtype hsa-miR-17 expression was compared between stroke patients with a 1 month mRS ≤ 1 and those with a mRS ≥ 2 (L). Probability values were calculated using a one-way-ANOVA with a Sidak's Multiple Comparisons Test. Data shown is RQ ± RQmax/RQmin. Exosomal miRNA expression was assessed from miRNA extracted from exosomes harvested from the serum of large artery (n=19), cardioembolic (n=32), small vessel disease (n=31) and unclassified (n=20) stroke patients. Change in miRNA expression was assessed by qRT-PCR, data was normalised to a spike housekeeper miRNA, cel-miR-39.

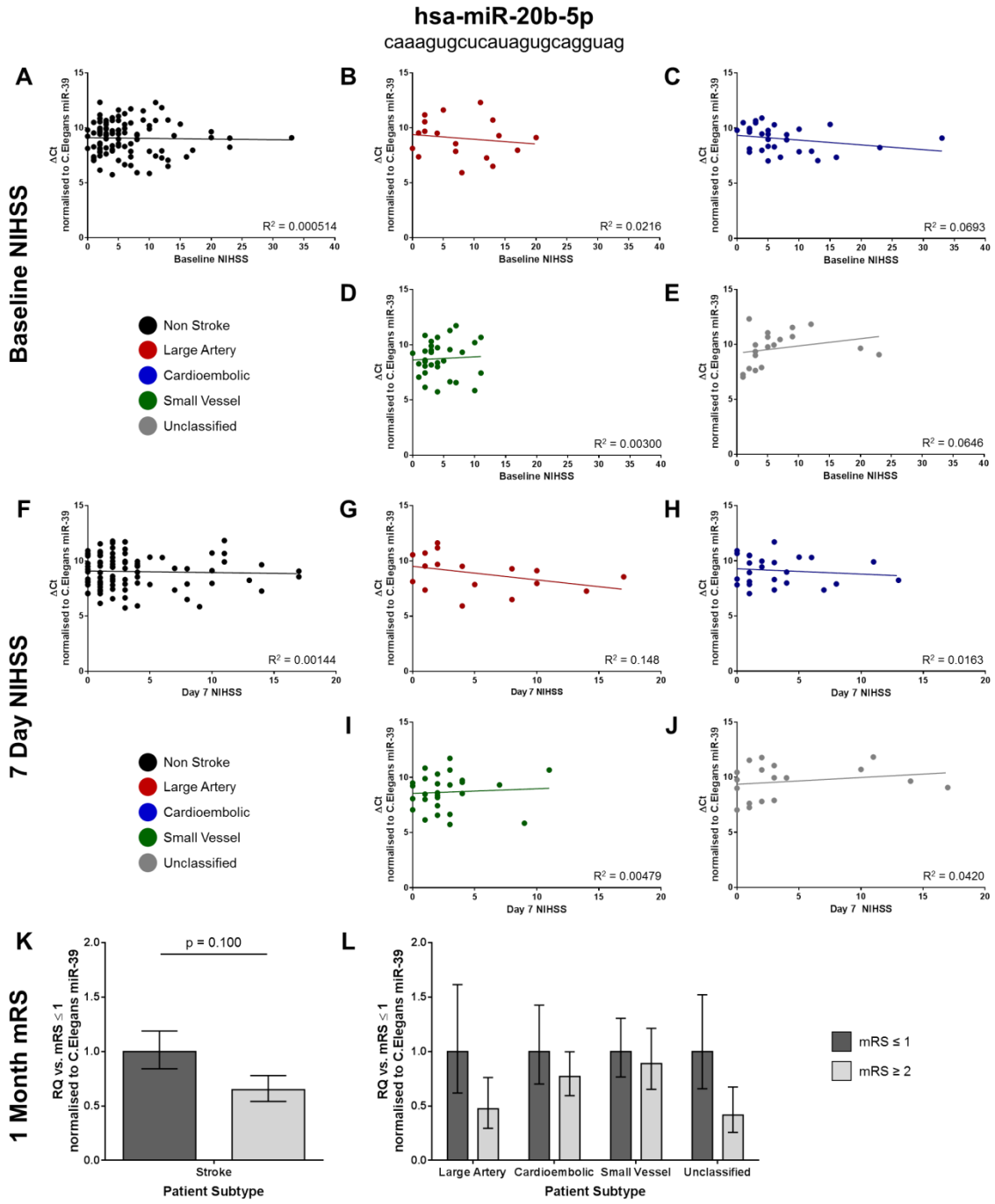

Figure 4.23 – hsa-miR-20b and Clinical Outcome
NIHSS scores at baseline are correlated against ΔCt values for hsa-miR-20b expression for all definite stroke patients (A), large artery (B), cardioembolic (C), small vessel (D) and unclassified stroke patients (E). NIHSS scores at day 7 post-stroke are correlated against ΔCt values for hsa-miR-20b expression for all definite stroke patients (F), large artery (G), cardioembolic (H), small vessel (I) and unclassified stroke patients (J). R^2 values are calculated by Pearson product-moment correlation coefficient. hsa-miR-20b expression is compared between stroke patients with a 1 month mRS ≤ 1 and those with a mRS ≥ 2 (K). Probability was calculated using unpaired Student's t-test. For each stroke subtype hsa-miR-17 expression was compared between stroke patients with a 1 month mRS ≤ 1 and those with a mRS ≥ 2 (L). Probability was calculated using a one-way-ANOVA with a Sidak's Multiple Comparisons Test. Data shown is RQ ± RQmax/RQmin. Exosomal miRNA expression was assessed from miRNA extracted from exosomes harvested from the serum of large artery (n=19), cardioembolic (n=32), small vessel disease (n=31) and unclassified (n=20) stroke patients. Change in miRNA expression was assessed by qRT-PCR, data was normalised to a spike housekeeper miRNA, cel-miR-39.

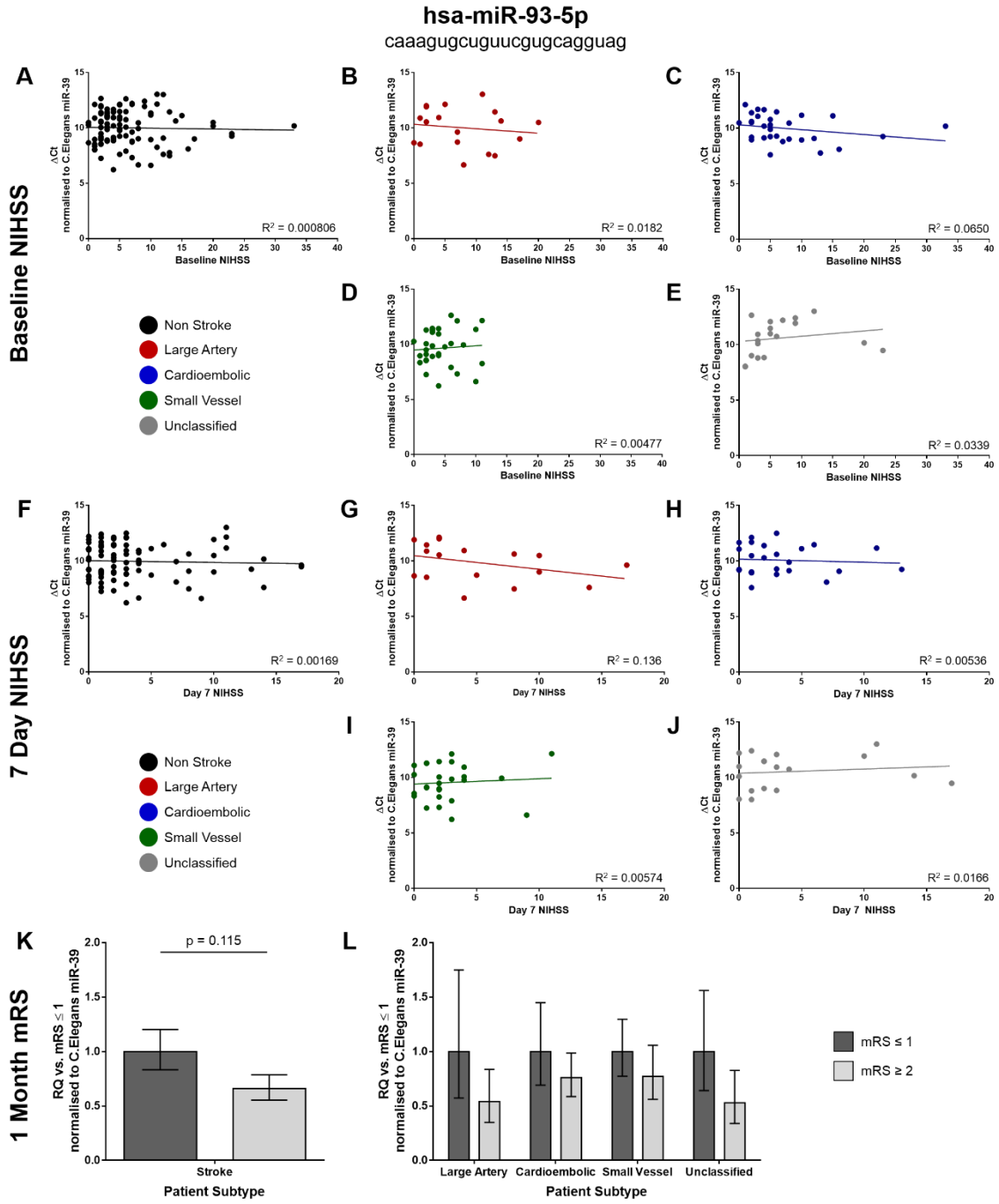

Figure 4.24 – hsa-miR-93 and Clinical Outcome
NIHSS scores at baseline are correlated against ΔCt values for hsa-miR-93 expression for all definite stroke patients (A), large artery (B), cardioembolic (C), small vessel (D) and unclassified stroke patients (E). NIHSS scores at day 7 post-stroke are correlated against ΔCt values for hsa-miR-93 expression for all definite stroke patients (F), large artery (G), cardioembolic (H), small vessel (I) and unclassified stroke patients (J). R^2 values are calculated by Pearson product-moment correlation coefficient. hsa-miR-93 expression is compared between stroke patients with a 1 month mRS ≤ 1 and those with a mRS ≥ 2 (K). Probability was calculated using unpaired Student's t-test. For each stroke subtype hsa-miR-93 expression was compared between stroke patients with a 1 month mRS ≤ 1 and those with a mRS ≥ 2 (L). Probability was calculated using a one-way-ANOVA with a Sidak's Multiple Comparisons Test. Data shown is RQ ± RQmax/RQmin. Exosomal miRNA expression was assessed from miRNA extracted from exosomes harvested from the serum of large artery (n=19), cardioembolic (n=32), small vessel disease (n=31) and unclassified (n=20) stroke patients. Change in miRNA expression was assessed by qRT-PCR, data was normalised to a spike housekeeper miRNA, cel-miR-39.

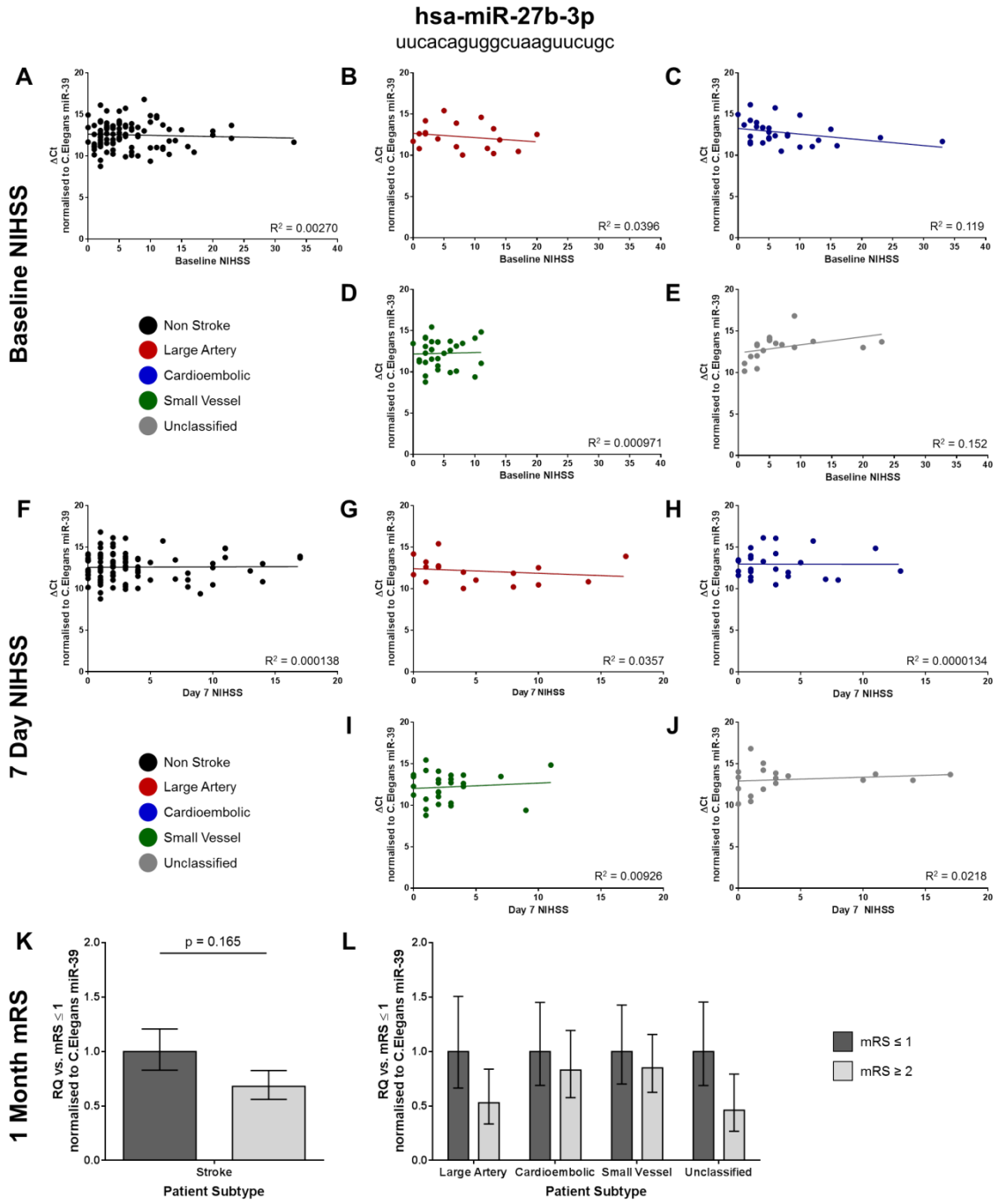

Figure 4.25 – hsa-miR-27b and Clinical Outcome
NIHSS scores at baseline are correlated against ΔCt values for hsa-miR-27b expression for all definite stroke patients (A), large artery (B), cardioembolic (C), small vessel (D) and unclassified stroke patients (E). NIHSS scores at day 7 post-stroke are correlated against ΔCt values for hsa-miR-27b expression for all definite stroke patients (F), large artery (G), cardioembolic (H), small vessel (I) and unclassified stroke patients (J). R^2 values are calculated by Pearson product-moment correlation coefficient. hsa-miR-27b expression is compared between stroke patients with a 1 month mRS ≤ 1 and those with a mRS ≥ 2 (K). Probability was calculated using unpaired Student's t-test. For each stroke subtype hsa-miR-27b expression was compared between stroke patients with a 1 month mRS ≤ 1 and those with a mRS ≥ 2 (L). Probability was calculated using a one-way-ANOVA with a Sidak's Multiple Comparisons Test. Data shown is RQ ± RQmax/RQmin. Exosomal miRNA expression was assessed from miRNA extracted from exosomes harvested from the serum of large artery (n=19), cardioembolic (n=32), small vessel disease (n=31) and unclassified (n=20) stroke patients. Change in miRNA expression was assessed by qRT-PCR, data was normalised to a spike housekeeper miRNA, cel-miR-39.

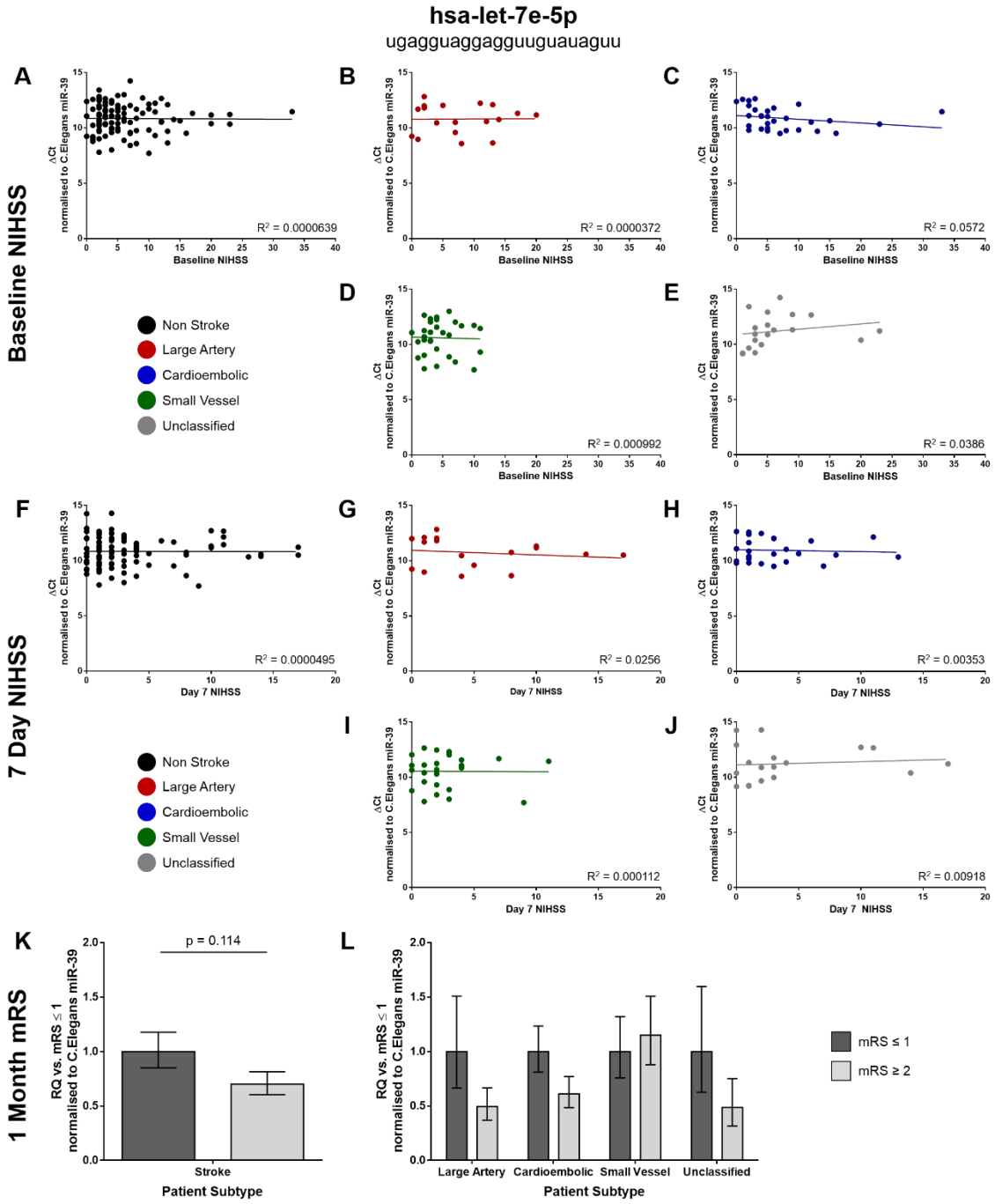

Figure 4.26 – hsa-let-7e and Clinical Outcome
NIHSS scores at baseline are correlated against ΔCt values for hsa-let-7e expression for all definite stroke patients (A), large artery (B), cardioembolic (C), small vessel (D) and unclassified stroke patients (E). NIHSS scores at day 7 post-stroke are correlated against ΔCt values for hsa-let-7e expression for all definite stroke patients (F), large artery (G), cardioembolic (H), small vessel (I) and unclassified stroke patients (J). R^2 values are calculated by Pearson product-moment correlation coefficient. hsa-let-7e expression is compared between stroke patients with a 1 month mRS ≤ 1 and those with a mRS ≥ 2 (K). Probability was calculated using unpaired Student's t-test. For each stroke subtype hsa-let-7e expression was compared between stroke patients with a 1 month mRS ≤ 1 and those with a mRS ≥ 2 (L). Probability was calculated using a one-way-ANOVA with a Sidak's Multiple Comparisons Test. Data shown is RQ ± RQmax/RQmin. Exosomal miRNA expression was assessed from miRNA extracted from exosomes harvested from the serum of large artery (n=19), cardioembolic (n=32), small vessel disease (n=31) and unclassified (n=20) stroke patients. Change in miRNA expression was assessed by qRT-PCR, data was normalised to a spike housekeeper miRNA, cel-miR-39.

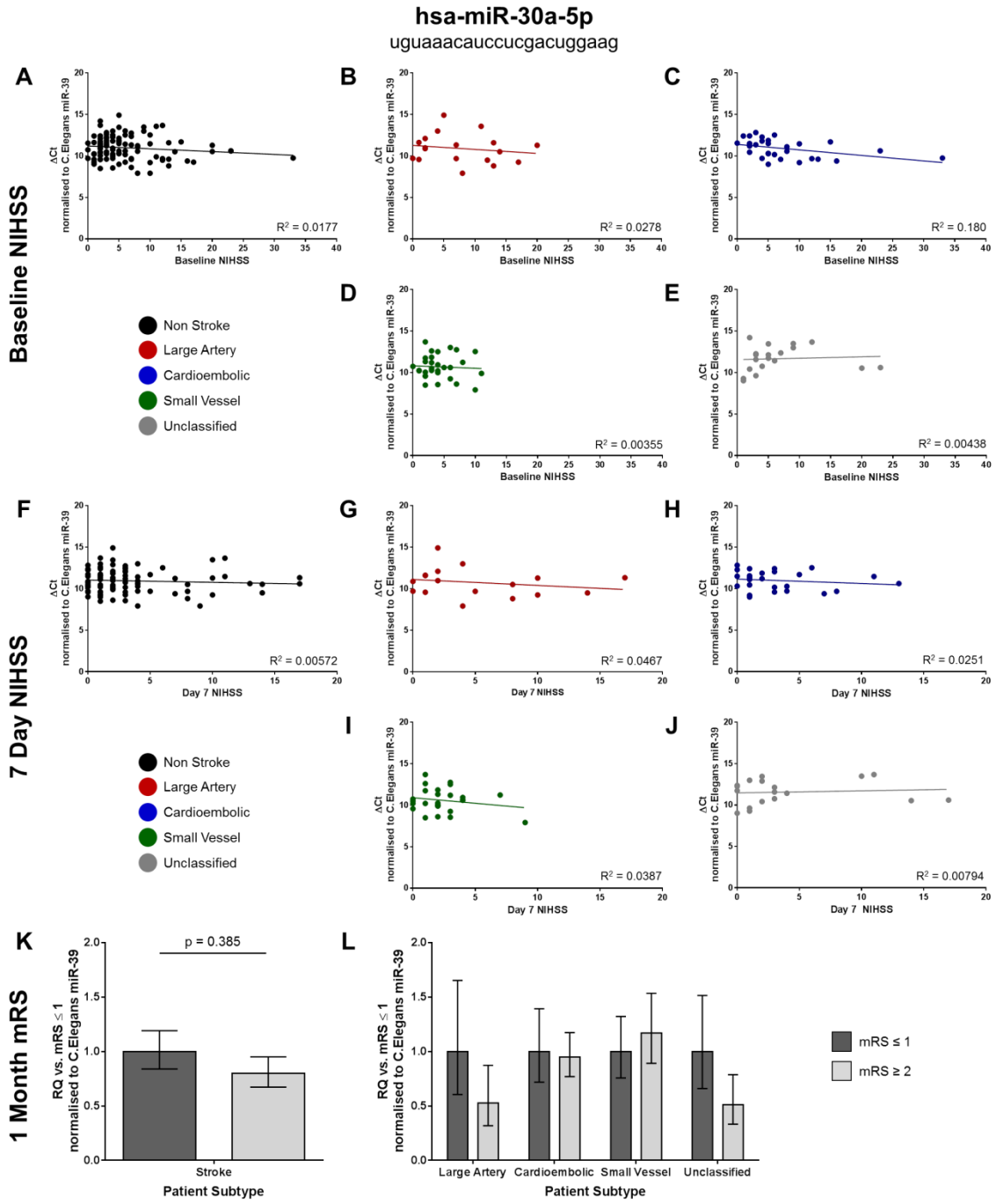

Figure 4.27 – hsa-miR-30a-5p and Clinical Outcome
NIHSS scores at baseline are correlated against ΔCt values for hsa-miR-30a-5p expression for all definite stroke patients (A), large artery (B), cardioembolic (C), small vessel (D) and unclassified stroke patients (E). NIHSS scores at day 7 post-stroke are correlated against ΔCt values for hsa-miR-30a-5p expression for all definite stroke patients (F), large artery (G), cardioembolic (H), small vessel (I) and unclassified stroke patients (J). R^2 values are calculated by Pearson product-moment correlation coefficient. hsa-miR-30a-5p expression is compared between stroke patients with a 1 month mRS ≤ 1 and those with a mRS ≥ 2 (K). Probability was calculated using unpaired Student's t-test. For each stroke subtype hsa-miR-30a-5p expression was compared between stroke patients with a 1 month mRS ≤ 1 and those with a mRS ≥ 2 (L). Probability was calculated using a one-way-ANOVA with a Sidak's Multiple Comparisons Test. Data shown is RQ ± RQmax/RQmin. Exosomal miRNA expression was assessed from miRNA extracted from exosomes harvested from the serum of large artery (n=19), cardioembolic (n=32), small vessel disease (n=31) and unclassified (n=20) stroke patients. Change in miRNA expression was assessed by qRT-PCR, data was normalised to a spike housekeeper miRNA, cel-miR-39.

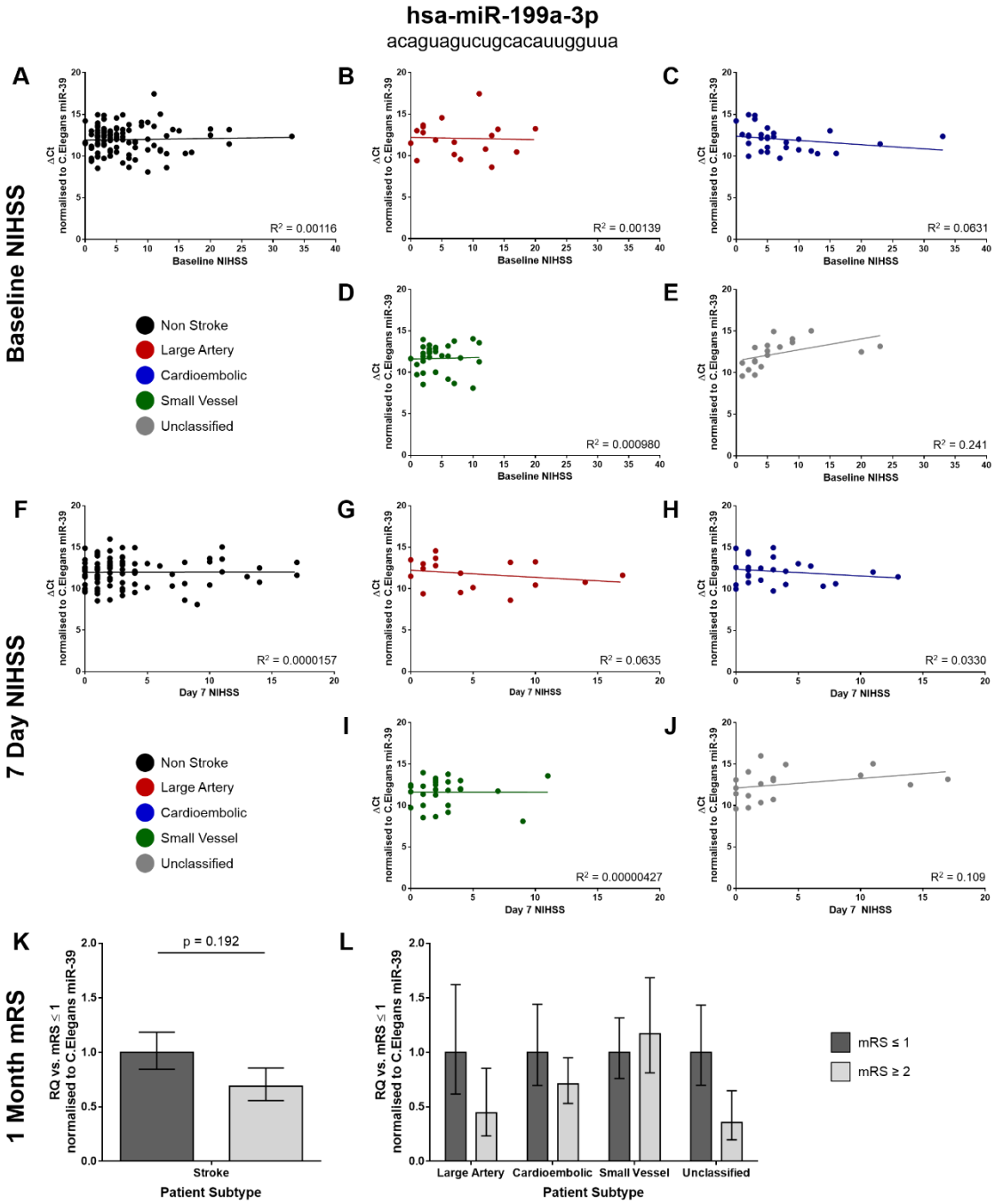

Figure 4.28 – miR-199a-3p and Clinical Outcome
NIHSS scores at baseline are correlated against ΔCt values for hsa-miR-199a-3p expression for all definite stroke patients (A), large artery (B), cardioembolic (C), small vessel (D) and unclassified stroke patients (E). NIHSS scores at day 7 post-stroke are correlated against ΔCt values for hsa-miR-199a-3p expression for all definite stroke patients (F), large artery (G), cardioembolic (H), small vessel (I) and unclassified stroke patients (J). R^2 values are calculated by Pearson product-moment correlation coefficient. hsa-miR-199a-3p expression is compared between stroke patients with a 1 month mRS ≤ 1 and those with a mRS ≥ 2 (K). Probability was calculated using unpaired Student's t-test. For each stroke subtype hsa-miR-199a-3p expression was compared between stroke patients with a 1 month mRS ≤ 1 and those with a mRS ≥ 2 (L). Probability was calculated using a one-way-ANOVA with a Sidak's Multiple Comparisons Test. Data shown is RQ ± RQmax/RQmin. Exosomal miRNA expression was assessed from miRNA extracted from exosomes harvested from the serum of large artery (n=19), cardioembolic (n=32), small vessel disease (n=31) and unclassified (n=20) stroke patients. Change in miRNA expression was assessed by qRT-PCR, data was normalised to a spike housekeeper miRNA, cel-miR-39.

There is a slight (non-significant) trend toward higher exosomal expression of hsa-miR-20b, hsa-miR-93, hsa-miR-27b and hsa-let-7e in patients without a disability in comparison to patients with a disability (mRS ≤ 1 vs. mRS ≥ 2, p ≤ 0.15) (Figure 4.23 - Figure 4.26 K). For these miRNAs the increased miRNA expression is primarily associated with improved functional recovery in large artery and unclassified patients, although this trend is not significant (Figure 4.23 - Figure 4.26 L). Changes in exosomal expression of hsa-miR-30a and hsa-miR-199a are not, on average, associated with improved functional recovery ((mRS ≤ 1 vs. mRS ≥ 2, p ≥ 0.15) in ischaemic stroke patients (Figure 4.27 - Figure 4.28 K).

We failed to observe a direct correlation between the exosomal expression of any one individual miRNA and clinical outcome from stroke. We hypothesised that small changes in multiple miRNAs could be associated with improved outcome from stroke. To examine whether a panel of multiple miRNAs could be used to predict clinical outcome from stroke ΔCt scores from different miRNAs were combined to give an aggregate score. Initially, ΔCt scores for miRNAs -17, -93 and -20b were combined. As these 3 miRNAs belong to one miRNA family we hypothesised that their combined score would be biologically significant and would detect whether their expression was associated with improved functional recovery from stroke (Figure 4.29). We subsequently tested the aggregate ΔCt score of all 7 miRNAs previously investigated (miR-17, miR-93, miR-20b, miR-27b, miR-199a-3p, miR-30a-5p and hsa-let-7e) (Figure 4.30).

NIHSS scores at baseline do not correlate with the aggregate ΔCt score for miR-17 family expression (R^2 = 0.001) (Figure 4.29A). When broken down further to examine the differences in correlation between the different stroke subtypes there is very little change: large artery (R^2 = 0.015) (Figure 4.29B), cardioembolic (R^2 = 0.083) (Figure 4.29C), small vessel (R^2 = 0.0022) (Figure 4.29D) and unclassified (R^2 = 0.034) (Figure 4.29E). NIHSS scores at day 7 also do not correlate with the aggregate ΔCt score for miR-17 family miRNAs (R^2 = 0.004) (Figure 4.29F); large artery (R^2 = 0.14) (Figure 4.29G), cardioembolic (R^2 = 0.019) (Figure 4.29H), small vessel (R^2 = 0.0033) (Figure 4.29I) and unclassified (R^2 = 0.0095) (Figure 4.29J). As shown previously, there is a trend towards higher expression of miR-17 family miRNAs in patients without disability in comparison

to those with disability (RQ 1.00 ± 0.69 vs. 0.26 ± 0.18, p=0.08) (Figure 4.29K). This change is not significant but if we break down the expression to look at the differences between differing stroke subtypes it is clear that increased miR-17 family expression is chiefly associated with improved functional recovery in large artery and unclassified stroke patients, and to a lesser extent in cardioembolic and small vessel disease stroke patients (Figure 4.29L). Using the aggregate miRNA score resulted in a greater difference in miRNA expression, on average, between patients with and without disability. However, as the data were much more variable, it is difficult to tell whether this improved the sensitivity and specificity of using miRNA expression to predict clinical outcome.

Finally, NIHSS scores at baseline do not correlate with the aggregate ΔCt score for 7 selected miRNAs (R^2 = 0.0029) (Figure 4.30A); large artery (R^2 = 0.039) (Figure 4.30B), cardioembolic (R^2 = 0.11) (Figure 4.30C), small vessel (R^2 = 0.0044) (Figure 4.30D) and unclassified (R^2 = 0.13) (Figure 4.30E). Furthermore, NIHSS scores at day 7 also do not correlate with the aggregate ΔCt score for 7 selected miRNAs (R^2 = 0.0021) (Figure 4.30F); large artery (R^2 = 0.088) (Figure 4.30G), cardioembolic (R^2 = 0.016) (Figure 4.30H), small vessel (R^2 = 0.025) (Figure 4.30I) and unclassified (R^2 = 0.038) (Figure 4.30J). There is a trend towards a higher aggregate miRNA score in patients without disability (RQ 1.00 ± 2.06 vs. 0.15 ± 0.35, p=0.26) (Figure 4.30K). Using the aggregate the score of 7 miRNAs increased the variability of the data very significantly, without showing any improved association with clinical outcome from stroke. ROC curve analysis demonstrated that an aggregate miRNA score was neither specific nor sensitive at predicting clinical outcome (by mRS score) (AUC: 0.51) (Figure 4.30L). Aggregate miRNA score (of 7 selected miRNAs), therefore, does not predict clinical outcome from stroke.

One striking observation is the difference between the ranges of clinical outcome scores for each stroke subtype. We have observed a significant increase in expression of 7 miRNAs in small vessel disease patients and yet these patients have the ‘smallest’ strokes and best clinical outcome as measured by NIHSS scores at baseline and day 7.

We have identified and validated changes in exosomal packaged miRNA expression in stroke patients and across different stroke subtypes. Multiple

miRNAs from one miRNA family were dysregulated similarly, giving increased confidence in these results. While we have failed to establish a link between exosomal miRNA expression and clinical outcome from stroke, these data will direct future studies looking into paracrine signalling in stroke and the modulation of specific miRNAs as a novel therapy in the setting of experimental stroke.

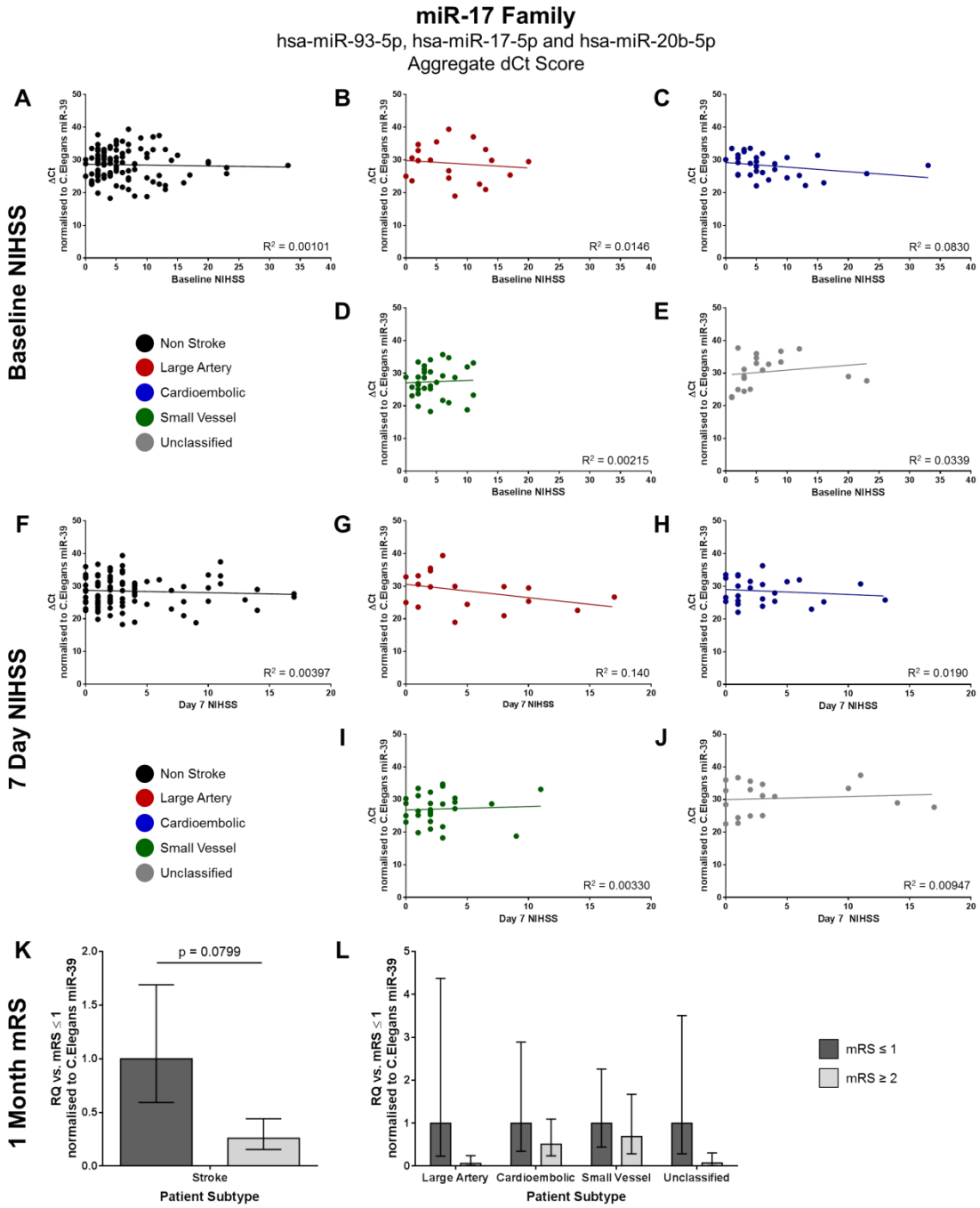

Figure 4.29 – miR-17 Family and Aggregate Score
NIHSS scores at baseline are correlated against aggregate miR-17 family ΔCt values for all definite stroke patients (A), large artery (B), cardioembolic (C), small vessel (D) and unclassified stroke patients (E). NIHSS scores at day 7 post-stroke are correlated against aggregate miR-17 family ΔCt values for all definite stroke patients (F), large artery (G), cardioembolic (H), small vessel (I) and unclassified stroke patients (J). R^2 values are calculated by Pearson product-moment correlation coefficient. miR-17 family miRNA expression is compared between stroke patients with a 1 month mRS ≤ 1 and those with a mRS ≥ 2 (K). Probability was calculated using unpaired Student's t-test. For each stroke subtype miR-17 family miRNA expression was compared between stroke patients with a 1 month mRS ≤ 1 and those with a mRS ≥ 2 (L). Probability was calculated using a one-way-ANOVA with a Sidak's Multiple Comparisons Test. Data shown is RQ ± RQmax/RQmin. Exosomal miRNA expression was assessed from miRNA extracted from exosomes harvested from the serum of large artery (n=19), cardioembolic (n=32), small vessel disease (n=31) and unclassified (n=20) stroke patients. Change in miRNA expression was assessed by qRT-PCR, data was normalised to a spike housekeeper miRNA, cel-miR-39.

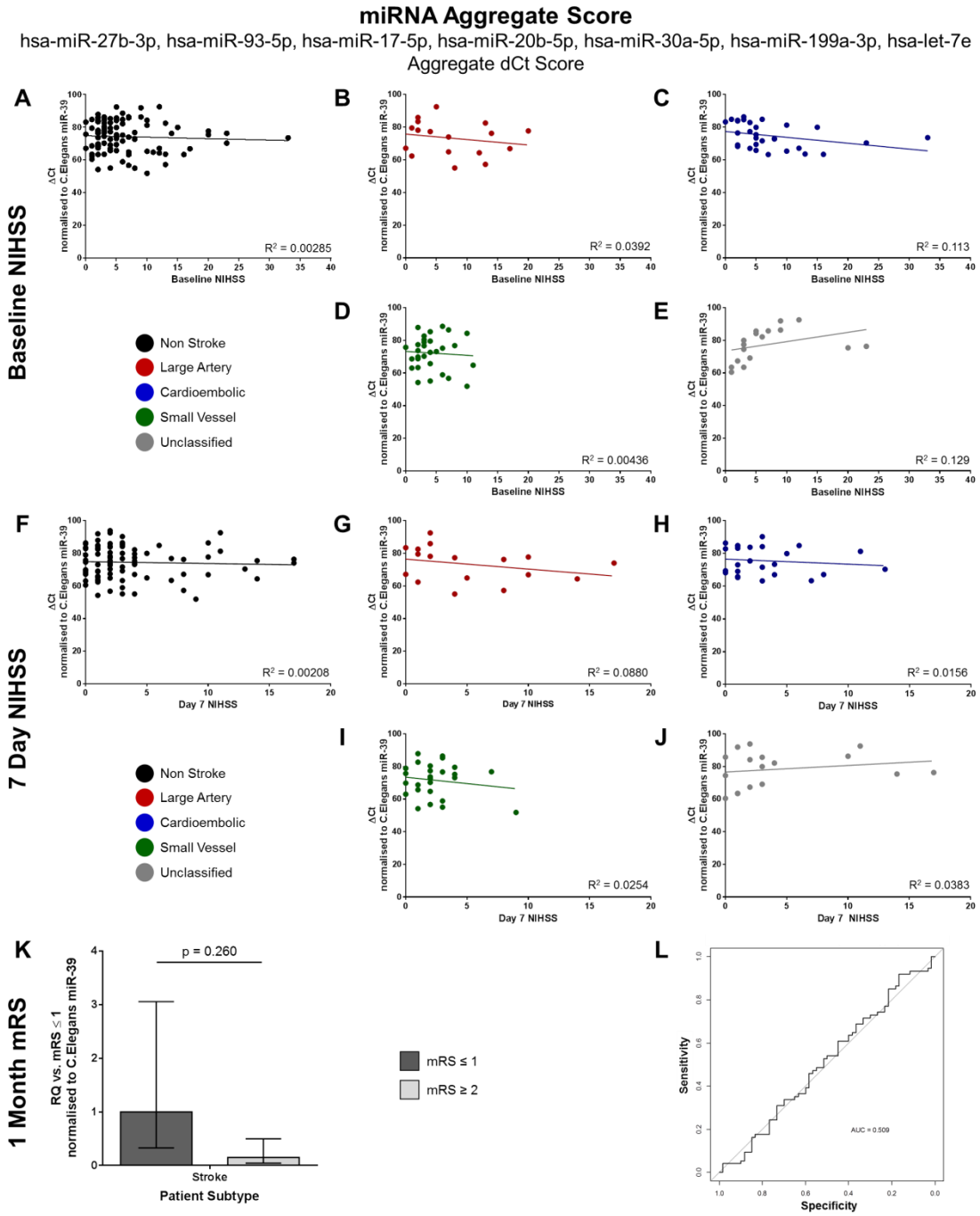

Figure 4.30 – Aggregate dCt and Clinical Outcome
NIHSS scores at baseline are correlated against aggregate ΔCt values for 7 miRNAs for all definite stroke patients (A), large artery (B), cardioembolic (C), small vessel (D) and unclassified stroke patients (E). NIHSS scores at day 7 post-stroke are correlated against aggregate ΔCt values for 7 miRNAs for all definite stroke patients (F), large artery (G), cardioembolic (H), small vessel (I) and unclassified stroke patients (J). R^2 values are calculated by Pearson product-moment correlation coefficient. Aggregate ΔCt values for 7 miRNAs were compared between stroke patients with a 1 month mRS ≤ 1 and those with a mRS ≥ 2 (K). Data shown is RQ ± RQmax/RQmin. Probability was calculated using unpaired Student's t-test. ROC analysis was used to assess whether an aggregate ΔCt score for 7 miRNAs could be used to distinguish between patients with a 1 month mRS scores ≥ 2 as compared to patients with a mRS ≤ 1 in any stroke subtype, as assessed by ROC analysis (L). Exosomal miRNA expression was assessed from miRNA extracted from exosomes harvested from the serum of large artery (n=19), cardioembolic (n=32), small vessel disease (n=31) and unclassified (n=20) stroke patients. Change in miRNA expression was assessed by qRT-PCR, data was normalised to a spike housekeeper miRNA, cel-miR-39.

4.3 Pre-Clinical Results

4.3.1 Ex Vivo Analysis of Cellular and Exosomal miRNA Expression

To further investigate whether changes in miRNA expression observed were a direct result of stroke pathology or a result of pre-existing vascular dysfunction we assessed exosomal miRNA expression in normotensive WKY and hypertensive SHRSP rats and in SHRSP rats that had been subjected to either tMCAO or pMCAO. Furthermore, to assess whether expression of miRNAs was selectively increased in exosomes, or increased more generally within the circulation, we compared exosomal miRNA expression against total serum miRNA expression. Initially it was decided that miRNAs would be taken forward for further analysis whose expression was most radically altered or those miRNAs who were biologically related (belonging to the same miRNA cluster or family). All 7 miRNAs whose expression was increased in ischaemic stroke patients were altered to a similar extent. We therefore selected miRs -17, -93 and -20b, belonging to the miR-17 family, for further analysis. These miRNAs from the same miRNA family were dysregulated in a similar manner in our human stroke patients, and this gave us increased confidence in the biological significance of these results.

Initially we compared miRNA expression between naïve normotensive WKY and hypertensive SHRSP rats (Figure 4.31). Total serum expression of miR-17, -93 and -20b expression was unchanged between WKY and SHRSP rats, however exosomal expression of these miRNAs was increased in SHRSP rats. Total serum miR-17 expression was unchanged in SHRSP rats as compared to WKY (RQ SHRSP 1.01 ± 0.38 vs. WKY 1.00 ± 0.28, p=0.99) (Figure 4.31A) whereas exosomal miR-17 expression was significantly increased in SHRSP rats (RQ 4.59 ± 1.57 vs. 1.00 ± 0.78, p=0.046) (Figure 4.31B). Total serum miR-93 expression was also unchanged in SHRSP rats as compared to WKY (RQ 1.09 ± 0.27 vs. 1.00 ± 0.33, p=0.81) (Figure 4.31C). Although there was a trend towards increased exosomal miR-93 expression in SHRSP rats, this change was not significant (RQ 2.47 ± 0.32 vs. 1.00 ± 0.53, p=0.076) (Figure 4.31D). Similarly total serum miR-20b expression was unchanged in SHRSP rats as compared to WKY (RQ 1.13 ± 0.37 vs. 1.00 ± 0.33, p=0.77) (Figure 4.31E) and there was a trend towards increased

exosomal miR-20b expression but this was non-significant (RQ 2.01 ± 0.54 vs. 1.00 ± 0.36, p=0.11) (Figure 4.31F).

We subsequently profiled miRNA expression in SHRSP rats post-MCAO. We initially assessed miR-17 family miRNA expression in historic peri-infarct brain tissue collected in a study carried by Dr. Emily Ord. SHRSP rats were subjected to a 45 min tMCAO and were subsequently sacrificed at either 24 or 72 hours post-tMCAO. At the point of sacrifice brain tissue was dissected into ipsilateral and contralateral hemispheres and each hemisphere was further divided into infarct, peri-infarct and remainder (any leftover) tissue. Infarct and peri-infarct areas were identified by T2-weighted MRI scan. miRs -17, -93 and -20b were unchanged in both ipsilateral and contralateral hemispheres at both 24 hours and 72 hours post-tMCAO.

miR-17 expression was unchanged at 24 hours in ipsilateral peri-infarct tissue in tMCAO SHRSP rats as compared to sham operated rats (RQ 1.19 ± 0.16 vs. 1.00 ± 0.08) and contralateral tissue (RQ 0.83 ± 0.09 vs. 1.00 vs. 0.14) (Figure 4.32A). Similarly, at 72 hours miR-17 expression was unchanged in ipsilateral peri-infarct tissue (RQ 0.83 ± 0.19 vs. 1.00 ± 0.24) and in the equivalent contralateral tissue (RQ 0.99 ± 0.17 vs. 1.00 ± 0.16) as compared to matched tissue in sham operated rats (Figure 4.32B).

miR-93 expression was also unchanged at 24 hours in ipsilateral peri-infarct tissue in tMCAO SHRSP rats as compared to sham operated rats (RQ 1.18 ± 0.07 vs. 1.00 ± 0.03) and in contralateral tissue (RQ 1.00 ± 0.03 vs. 1.00 vs. 0.03) (Figure 4.32C). At 72 hours miR-93 expression was unchanged in ipsilateral peri-infarct tissue (RQ 0.91 ± 0.08 vs. 1.00 ± 0.11) and in the equivalent contralateral tissue (RQ 1.07 ± 0.09 vs. 1.00 ± 0.05) as compared to matched tissue in sham operated rats (Figure 4.32D).

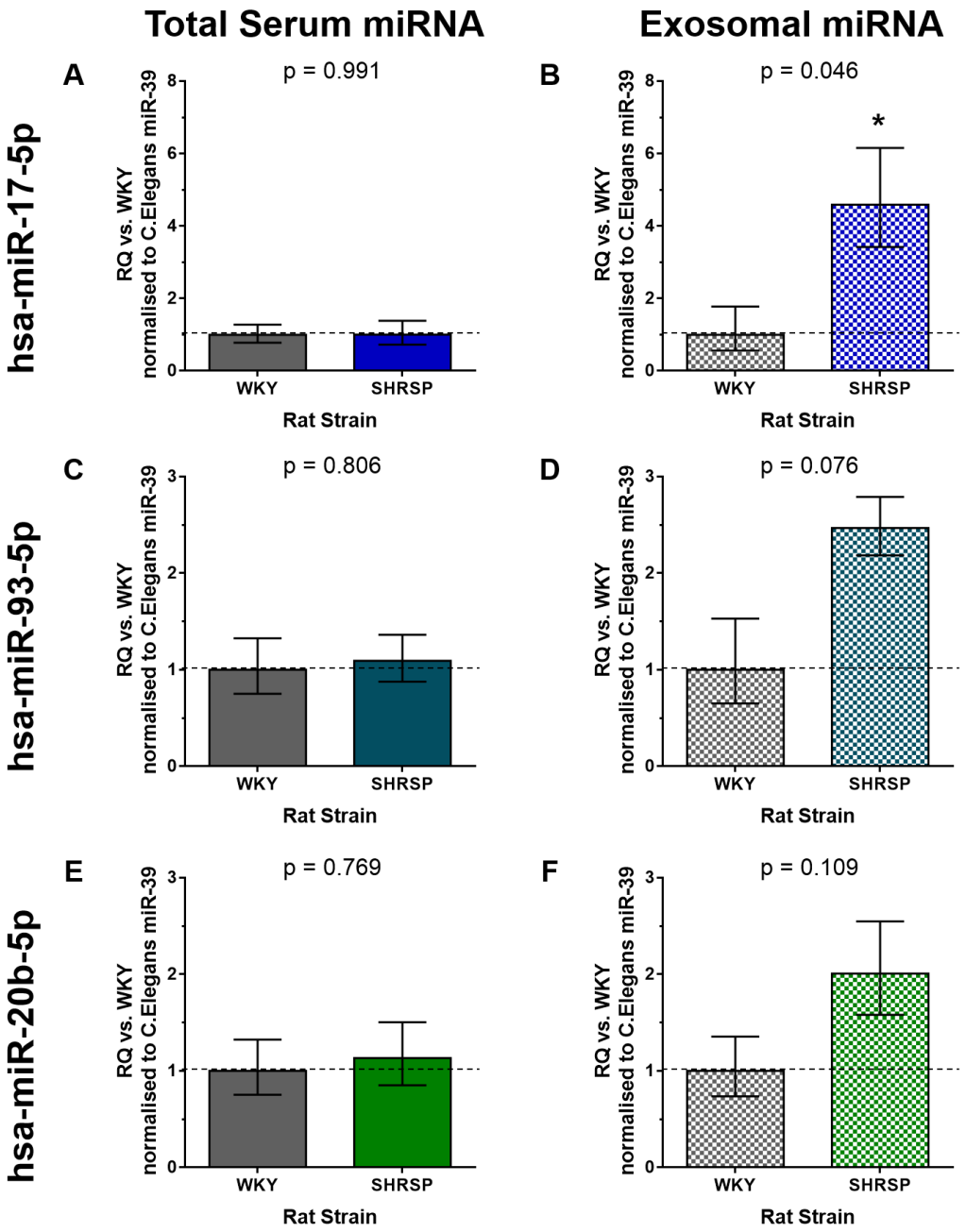

Figure 4.31 – Serum miR-17 Family Expression in Naïve WKY and SHRSP Rats
The total serum expression of hsa-miR-17-5p (A), hsa-miR-93-5p (C) and hsa-miR-20b-5p (E) was assessed in both naïve normotensive WKY and hypertensive SHRSP rats (n=5/group). Exosomal miRNA expression of hsa-miR-17-5p (B), hsa-miR-93-5p (D) and hsa-miR-20b-5p (F) was also assessed in both naïve WKY and SHRSP rats (n=5/group). Statistical probability of differences in expression observed were calculated using unpaired Student's t-test, vs. WKY rats. Change in miRNA expression was assessed by qRT-PCR and relative quantification (RQ) calculated from ΔΔCt following normalisation to a spike housekeeper miRNA, cel-miR-39 and compared to miRNA expression in the WKY rats. Data shown is RQ ± RQmax/RQmin.

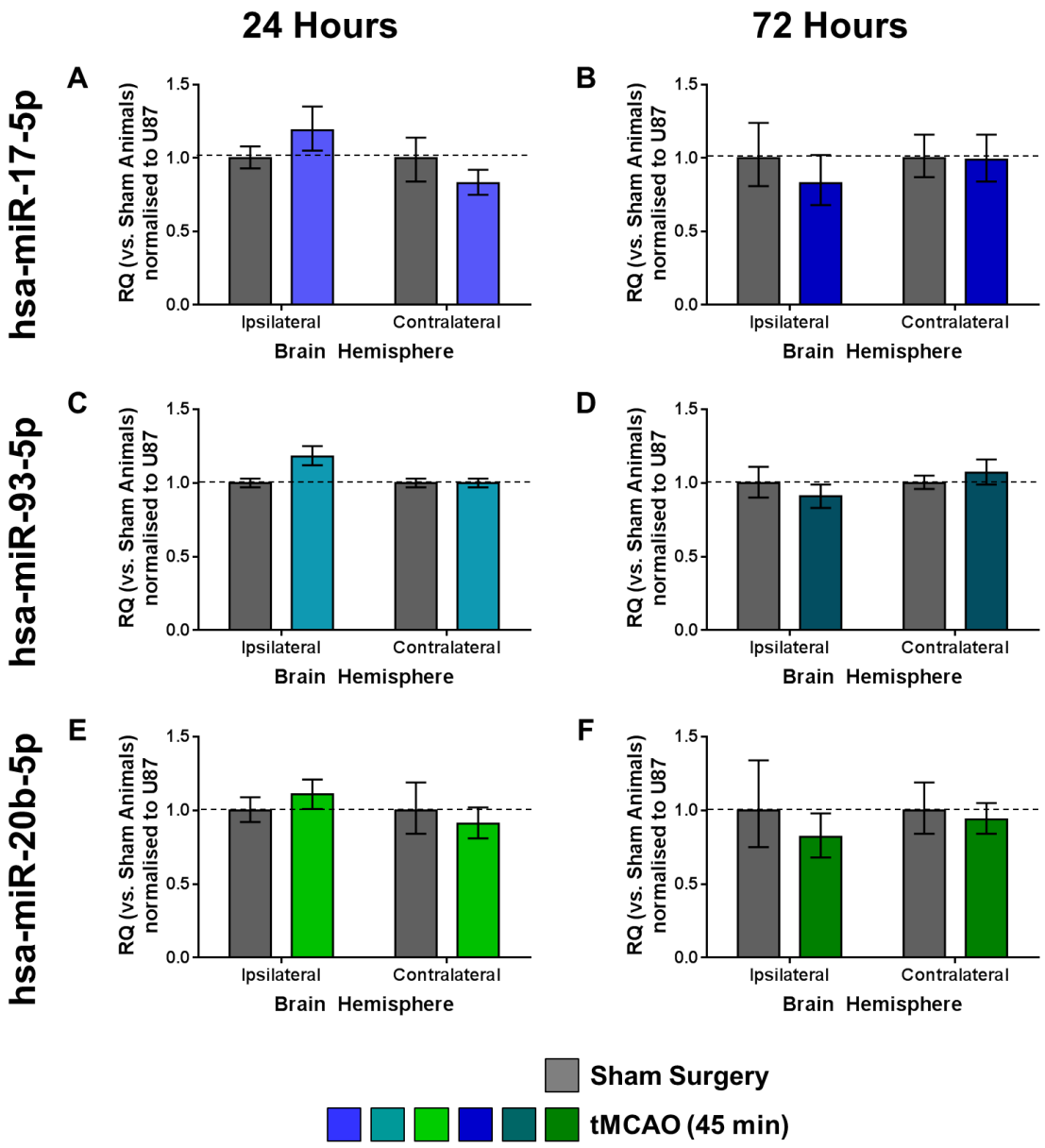

Figure 4.32 – miR-17 Family Expression in SHRSP Brain
The expression of hsa-miR-17-5p (A, B), hsa-miR-93-5p (C, D) and hsa-miR-20b-5p (E, F) was assessed in peri-infarct tissue of SHRSP rats at 24 hours (A, C, E) and 72 hours (B, D, F) following 45 min tMCAO (coloured bars) or sham operation (grey bars) (n=6/group). Statistical probability of differences in expression observed were calculated using unpaired Student's t-test with Bonferroni's Multiple Comparisons Test, vs. sham operated rats. Change in miRNA expression was assessed by qRT-PCR and relative quantification (RQ) calculated from ΔΔCt following normalisation to a housekeeper miRNA, U87, and compared to miRNA expression in the sham operated rats. Data shown is RQ ± RQmax/RQmin. Brain tissue collected by and used with permission of Dr. Emily Ord.

Finally, miR-20b expression was unchanged at 24 hours in ipsilateral peri-infarct tissue in tMCAO SHRSP rats as compared to sham operated rats (RQ 1.11 ± 0.10 vs. 1.00 ± 0.09) and unchanged in contralateral tissue (RQ 0.91 ± 0.11 vs. 1.00 vs. 0.19) (Figure 4.32E). At 72 hours miR-20b expression was also unchanged in ipsilateral peri-infarct tissue (RQ 0.82 ± 0.16 vs. 1.00 ± 0.34) and in the

equivalent contralateral tissue (RQ 0.94 ± 0.11 vs. 1.00 ± 0.19) as compared to matched tissue in sham operated rats (Figure 4.32F).

We subsequently profiled circulating total and exosomal miR-17 family miRNA expression in SHRSP rats subjected to tMCAO and pMCAO (Figure 4.33). Serum from SHRSP subjected to pMCAO was collected by Dr. Emma Reid.

Total serum expression of miR-17 was moderately increased in rats at 24 hours following tMCAO (RQ 2.21 ± 0.65 vs. 1.00 ± 0.31) and further increased in SHRSP at 24 hours following pMCAO (RQ 2.96 ± 2.33 vs. 1.00 ± 0.31) as compared to sham operated rats (Figure 4.33A), although all changes were not significant. Exosomal expression of miR-17 was moderately decreased in SHRSP following tMCAO (RQ 0.47 ± 0.05 vs. 1.00 ± 0.52) and unchanged following pMCAO (RQ 1.10 ± 0.75 vs. 1.00 ± 0.52) (Figure 4.33B). All changes in expression were not significant.

The total expression of miR-93 followed the same pattern and was moderately increased in SHRSP at 24 hours following tMCAO (RQ 1.74 ± 0.51 vs. 1.00 ± 0.29) and further increased following pMCAO (RQ 2.72 ± 1.53 vs. 1.00 ± 0.29) (Figure 4.33C). Exosomal expression of miR-93 was somewhat decreased at 24 hours following tMCAO (RQ 0.53 ± 0.1 vs. 1.00 ± 0.68) but increased following pMCAO (RQ 1.69 ± 0.77 vs. 1.00 ± 0.68) (Figure 4.33D). All changes in expression were not significant.

Similarly, there was a trend towards increased total miR-20b expression following tMCAO (RQ 2.16 ± 0.21 vs. 1.00 ± 0.46) and pMCAO (RQ 2.54 ± 1.54 vs. 1.00 ± 0.46) (Figure 4.33E). Exosomal expression of miR-20b was moderately decreased at 24 hours following tMCAO (RQ 0.58 ± 0.08 vs. 1.00 ± 0.29) but increased following pMCAO (1.38 ± 0.55 vs. 1.00 ± 0.29) (Figure 4.33F). The changes observed here were not significant.

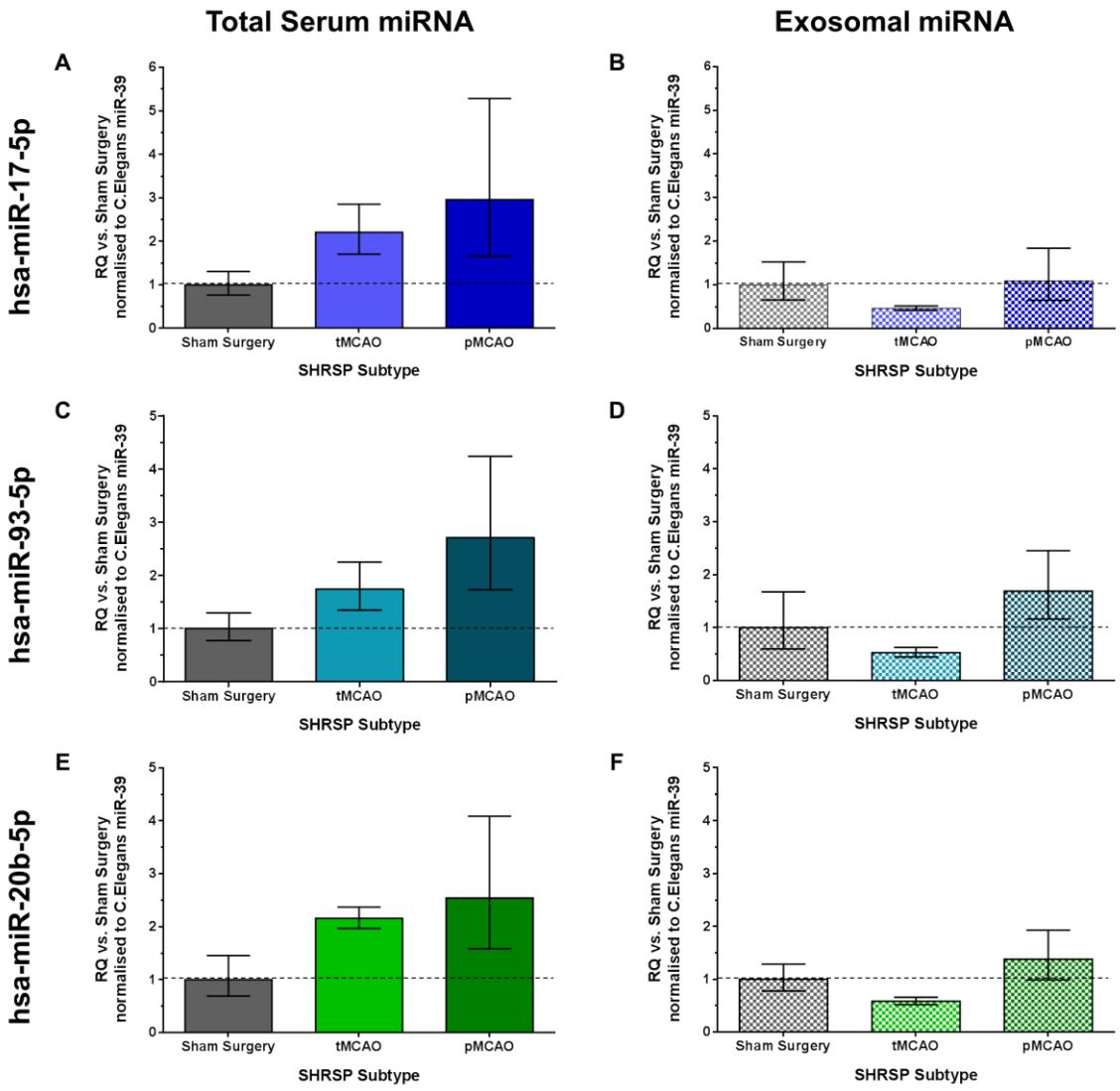

Figure 4.33 – Circulating miR-17 Family Expression post-MCAO
Total expression of hsa-miR-17-5p (A), hsa-miR-93-5p (C) and hsa-miR-20b-5p (E) was assessed in serum of SHRSP rats at 24 hours following 45 min tMCAO (n=3), permanent MCAO (pMCAO) (n=5) or sham operation (grey bars) (n=3). Exosomal expression of hsa-miR-17-5p (B), hsa-miR-93-5p (D) and hsa-miR-20b-5p (F) was assessed in the serum of the same SHRSP rats. Statistical probability of differences in expression observed were calculated using one-way ANOVA with Tukey's multiple comparisons test. Change in miRNA expression was assessed by qRT-PCR and relative quantification (RQ) calculated from ΔΔCt following normalisation to a spike housekeeper miRNA, cel-miR-39, and compared to miRNA expression in the sham operated rats. Data shown is RQ ± RQmax/RQmin. pMCAO surgery and subsequent collection of serum was carried out by Dr. Emma Reid and serum was used for these experiments with her permission.

4.3.2 Characterisation of Exosomes Isolated from SHRSP serum

Exosomes were visualised on a transmission electron microscope, as described in section 4.2.1.2. Exosomes were embedded and prepared for electron microscopy by Mrs Margaret Mullin.

Electron microscopy of exosomes isolated from the serum of two SHRSP rats demonstrated the presence of rounded membrane vesicles (Figure 4.34 A and B). Representative images were selected from the images taken of each exosome isolation, and the diameter of every vesicle present in each image measured. SHRSP 1 had a median vesicle size of 73.0 nm, with an IQR of 59.1 – 90.2 nm (Figure 4.34 C). SHRSP 2 had a median vesicle size of 80.9 nm, with an IQR of 63.9 – 99.3 nm (Figure 4.34 C). These results primarily show that the vast majority of vesicles isolated by precipitation from SHRSP serum fall within the exosome size range of 30 – 120 nm.

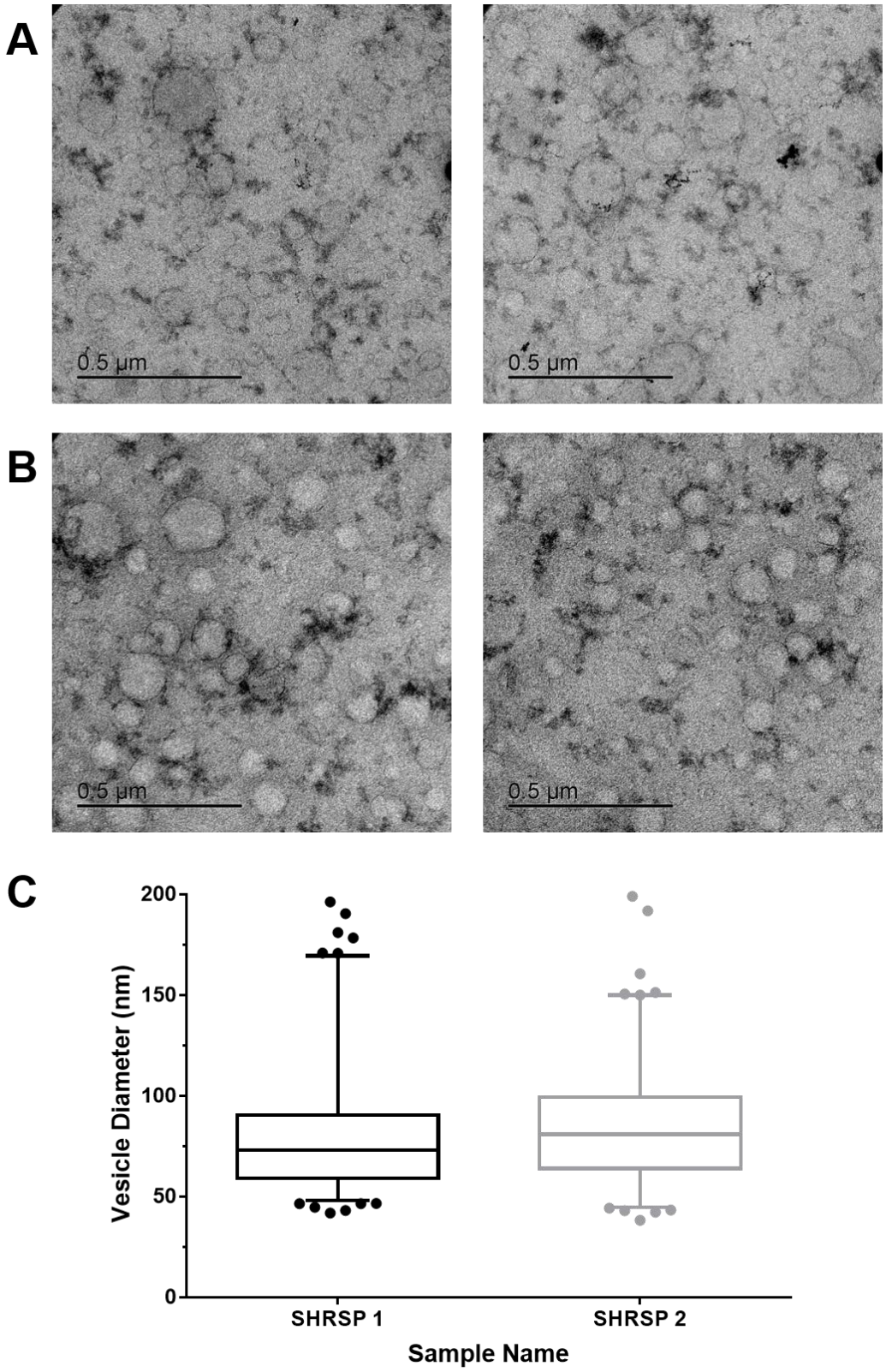

Figure 4.34 – TEM of SHRSP Serum Extracellular Vesicles
Electron-microscopic observation of whole-mounted exosomes purified from SHRSP serum by precipitation. Representative images of exosome isolates from two SHRSP serum samples (SHRSP 1, A; SHRSP 2, B) obtained by transmission electron microscopy showing both larger microvesicles and exosomes. A box and whisker plot to show the diameter of vesicles in representative images (n=4) (C). Plots show 5th percentile, Q1, Q2, Q3 and 95th percentile with values outside of this represented by scatter dots. Diameter was measured twice on every vesicle in each representative image and the longest diameter value was taken for each vesicle to create this graph.

4.3.3 In Vitro Analysis of Cellular and Exosomal miRNA Expression

To assess the *in vitro* exosomal expression of dysregulated miRNAs (as first detected in human stroke patients), three different secondary cell lines were used: neuronal (B50), cerebral endothelial (GPNT) and glial (B92). The cells were subjected to a 9 hour hypoxic challenge or left entirely in normoxic conditions before being reoxygenated for 24 hours. The cells were then harvested to investigate total miRNA expression and media was collected, from which exosomes were isolated. We were interested to see if exosomal miRNA expression was increased in all of these cell lines or only in specific brain cell types.

Total cellular expression of miR-17 was completely unchanged in neuronal (B50) cells following hypoxic challenge (RQ 1.00 ± 0.01 [hypoxic] vs. 1.00 ± 0.02 [normoxic]) (Figure 4.35A). This was also the case for miR-93 (RQ 0.99 ± 0.02 vs. 1.00 ± 0.04) (Figure 4.35B) and miR-20b (RQ 0.97 ± 0.02 vs. 1.00 ± 0.03) (Figure 4.35C) expression in B50 cells.

Cellular expression of miR-17 was not significantly increased in hypoxic cerebral endothelial cells (GPNT) as compared to its expression in normoxic cells (RQ 1.24 ± 0.06 vs. 1.00 ± 0.10) (Figure 4.35A). The expression of miR-93 and miR-20b was unchanged following hypoxic challenge in cerebral endothelial cells (RQ 1.13 ± 0.09 vs. 1.00 ± 0.11 and RQ 1.06 ± 0.03 vs. 1.00 ± 0.09) (Figure 4.35 B and C).

Similarly, cellular expression of miR-17 and miR-93 was not significantly increased in hypoxic glial (B92) cells are compared to expression in normoxic cells (RQ 1.16 ± 0.06 vs. 1.00 ± 0.02) (Figure 4.35A), (RQ 1.17 ± 0.09 vs. 1.00 ± 0.03) (Figure 4.35B). Cellular expression of miR-20b was unchanged in hypoxic glial cells as compared to normoxic cells (RQ 0.99 ± 0.003 vs. 1.00 ± 0.03) (Figure 4.35C).

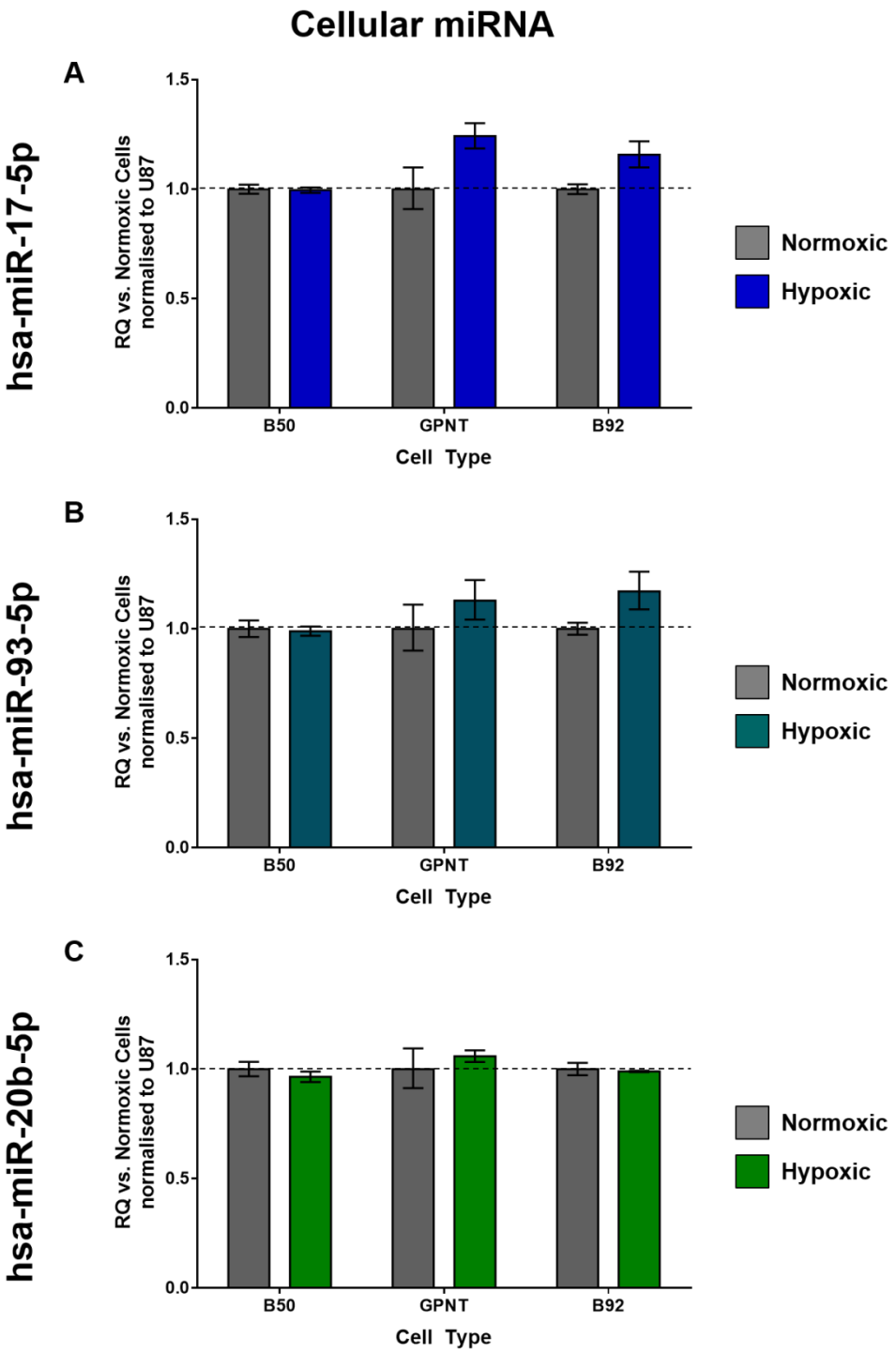

Figure 4.35 – Cellular miR-17 Family Expression (*in vitro*)
The expression of hsa-miR-17-5p (A), hsa-miR-93-5p (B) and hsa-miR-20b-5p (C) was assessed in both normoxic and hypoxic B50, GPNT and B92 cells (n=3/group). Statistical probability of differences in expression observed were calculated using unpaired Student's t-test with Bonferroni's Multiple Comparisons Test, vs. normoxic cells for each cell type. Change in miRNA expression was assessed following 24 hours of reoxygenation post-9 hour hypoxic challenge, by qRT-PCR. Relative quantification (RQ) was calculated from ΔΔCt following normalisation to a spike housekeeper miRNA, cel-miR-39 and compared to miRNA expression in the normoxic cells. Data shown is RQ ± RQmax/RQmin.

Media (from the same experiment as described above) was collected as described in section 2.5.1.2 and exosomes were subsequently isolated by

ultracentrifugation. Exosomal expression of miR-17 family miRNAs was then profiled. Expression of the same miRNAs was also profiled in exosomes isolated by precipitation (using Exosome Isolation Reagent) collected by Ms. Emma Sigfridsson in identical experiments.

In general miRs-17, -93 and -20b appeared to be down-regulated in exosomes collected by ultracentrifugation from hypoxic B50 and GPNT cells but up-regulated in B92 hypoxic exosomes, although all changes observed were non-significant. The data collected were very variable and this isolation method will need to be refined further. Data shown here are from a biological n=3. Repeating the experiment may also have reduced the variability in the data. As the data stands, it is very difficult to interpret. Specifically, miR-17 exosomal expression was, on average, decreased in exosomes isolated from hypoxic B50 cells (RQ 0.35 ± 0.81 vs. 1.00 ± 0.96), unchanged in GPNT cells (1.11 ± 0.19 vs. 1.00 ± 0.99) and increased in B92 cells (RQ 3.93 ± 10.22 vs. 1.00 ± 0.39) (Figure 4.36A). miR-93 exosomal expression was, on average, decreased in exosomes isolated from hypoxic B50 cells (RQ 0.20 ± 0.90 vs. 1.00 ± 3.64) and GPNT cells (0.14 ± 0.14 vs. 1.00 ± 3.91) and increased in B92 cells (5.38 ± 58.40 vs. 1.00 ± 2.29) (Figure 4.36C). Finally, miR-20b expression was also, on average, decreased in hypoxic B50 cells (RQ 0.22 ± 1.48 vs. 1.00 ± 6.04) and GPNT cells (0.29 ± 0.25 vs. 1.00 ± 3.12) and increased in B92 cells (4.38 ± 47.36 vs. 1.00 ± 3.11) (Figure 4.36E). All changes were non significant.

However, when expression of miR-17 family miRNAs was profiled in exosomes isolated by precipitation (n=6) there was a trend towards an increase in expression in both B50 and B92 cells (Figure 4.36), although changes observed were not statistically significant. Specifically miR-17 expression was increased in exosomes isolated from both hypoxic B50 (RQ 1.59 ± 0.26 vs. 1.00 ± 0.51) and B92 (RQ 2.22 ± 0.62 vs. 1.00 vs. 1.21) cells (Figure 4.36B). Similarly, the exosomal expression of miR-93 was increased by a small amount, on average, in hypoxic B50 cells (RQ 1.25 ± 0.18) and by a larger amount in hypoxic B92 cells (RQ 1.69 ± 0.42 vs. 1.00 ± 1.12) as compared to their normoxic counterparts (Figure 4.36D). The expression of miR-20b was unchanged in exosomes isolated from hypoxic B50 cells (1.04 ± 0.08 vs. 1.00 vs. 0.09) and hypoxic B92 cells (0.93 ± 0.08 vs. 1.00 ± 0.24) as compared to normoxic cells (Figure 4.36F).

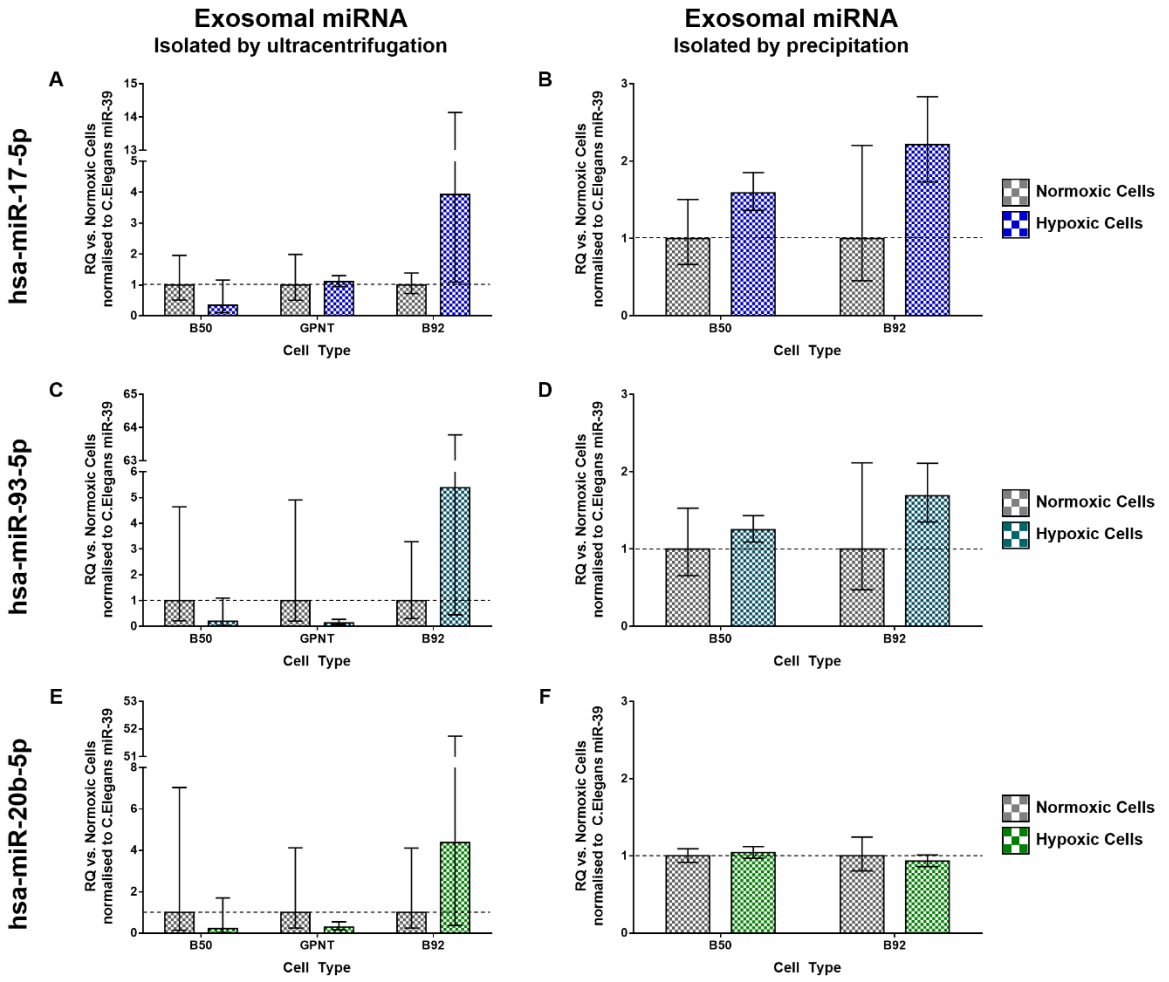

Figure 4.36 – Exosomal miR-17 Family Expression (*in vitro*)
The expression of hsa-miR-17-5p (A), hsa-miR-93-5p (C) and hsa-miR-20b-5p (E) was assessed in exosomes isolated by ultracentrifugation from the media of both normoxic and hypoxic B50, GPNT and B92 cells (n=3/group). Statistical probability of differences in expression observed were calculated using unpaired Student's t-test, vs. normoxic cells for each cell type. The expression of hsa-miR-17-5p (B), hsa-miR-93-5p (D) and hsa-miR-20b-5p (F) was also assessed in exosomes isolated by precipitation from the media of both normoxic and hypoxic B50 and B92 cells (n=6/group). Statistical probability of differences in expression observed were calculated using unpaired Student's t-test with Bonferroni's Multiple Comparisons Test, vs. normoxic cells for each cell type. Change in miRNA expression was assessed following 24 hours of reoxygenation post 9 hour hypoxic challenge, by qRT-PCR. Relative quantification (RQ) was calculated from ΔΔCt following normalisation to a spike housekeeper miRNA, cel-miR-39 and compared to miRNA expression in the normoxic exosomes. Data shown is RQ ± RQmax/RQmin.

Finally, the changes in miR-17 family miRNA expression, detailed in this chapter, have been summarised in Table 4.10 to allow for a quick comparison of data gleaned in the human study and pre-clinical *in vivo* and *in vitro* studies.

Table 4.10 – Summary of miR-17 Family Results
A table summarising results from the OpenArray and validation studies in human ischaemic stroke patients, and the *in vivo* pre-clinical and *in vitro* studies. The comparison made is indicated and unless otherwise stated in human patients comparisons were made at 48 hours post-stroke onset and in pre-clinical models at 24 hours. The tissue type and whether total or exosomal miRNA expression was examined is also indicated. Exosomal (P) indicates exosomes isolated via precipitation while exosomal (U) indicates exosomes isolated by ultracentrifugation. Arrows indicate the direction of change and where results were significant the level of significance is given: *p<0.05, **p<0.01 vs. control. The figure in which data can be found is also given. Abbreviations include: NS, non-stroke; LA, large artery; CE, cardioembolic; SVD, small vessel disease; U, unclassified.

	Comparison	Tissue Type	Total vs. Exosomal	miRNA			Figures
				miR-17	miR-93	miR-20b	
Human: OpenArray	All Stroke vs. NS	Serum	Exosomal (P)	↑	↑*	↑	Figure 4.3 - Figure 4.6 Table 4.3
	LA vs. NS			↑	↑**	↑*	
	CE vs. NS			↑	↑	↑	
	SVD vs. NS			↑*	↑*	↑	
Human: Validation	All Stroke vs. NS	Serum	Exosomal (P)	↑*	↑	↑*	Figure 4.9 - Figure 4.11
	All Stroke (definite) vs. NS			↑*	↑*	↑*	
	LA vs. NS			↑	↑	↑	
	CE vs. NS			↑	↑	↑	
	SVD vs. NS			↑*	↑**	↑**	
	U vs. NS			↔	↔	↔	
Pre-clinical: *in vivo*	SHRSP naïve vs. WKY naïve	Serum	Total	↔	↔	↔	Figure 4.31
			Exosomal (P)	↑*	↑	↑	
	SHRSP tMCAO vs. SHRSP sham	Brain: ipsilateral	Total	↑	↑	↔	Figure 4.32
		Brain: contralateral	Total	↓	↔	↔	
		Serum	Total	↑	↑	↑	Figure 4.33
			Exosomal (P)	↓	↓	↓	
	SHRSP tMCAO vs. SHRSP sham (72 hrs)	Brain: ipsilateral	Total	↔	↔	↓	Figure 4.32
		Brain: contralateral	Total	↔	↔	↔	
	SHRSP pMCAO vs. SHRSP sham	Serum	Total	↑	↑	↑	Figure 4.33
			Exosomal (P)	↑	↑	↑	
Cellular: *in vitro*	Normoxic vs. Hypoxic	B50 neuronal cell line	Total	↔	↔	↔	Figure 4.35
			Exosomal (U)	↓	↓	↓	Figure 4.36
			Exosomal (P)	↑	↑	↔	
		GPNT cerebral endothelial cell line	Total	↑	↑	↑	Figure 4.35
			Exosomal (U)	↔	↓	↓	Figure 4.36
		B92 glial cell line	Total	↑	↑	↔	Figure 4.35
			Exosomal (U)	↑	↑	↑	Figure 4.36
			Exosomal (P)	↑	↑	↔	

4.4 Discussion

The causes and consequences of ischaemic stroke are numerous and complex. It was hypothesised that miRNAs are dysregulated following ischaemic stroke either as a consequence of, or, as regulators of, stroke pathophysiology, and subsequently interact with gene networks with far reaching consequences. The presented studies focus on the identification of novel exosomal miRNAs with potential roles in stroke pathophysiology, using microarray technology. The study looked for exosomal miRNAs dysregulated in all ischaemic stroke patients but also exosomal miRNAs that were differentially regulated in particular stroke subtypes. Validation by qRT-PCR was performed in a large patient population to confirm changes in expression of candidate miRNAs identified by microarray. More in depth analysis of validated exosomal miRNA expression sought to relate changes in exosomal miRNA expression to stroke subtype and clinical outcome from stroke. Further studies profiled the expression of selected dysregulated human exosomal miRNAs in pre-clinical models of ischaemic stroke to elucidate further the origin and cause of dysregulated exosomal miRNA expression.

Of the 9 miRNAs (-27b, -93b, -20b. –17, -199a-3p, -30-5p, -let-7e, -218 and -223) that were found to be up-regulated in exosomes of definite ischaemic stroke patients a number have previously been documented in studies profiling miRNA expression in human stroke patients. As this is the first study, to our knowledge, to profile miRNA expression within exosomes in ischaemic stroke patients, we can only make comparisons between the present study and total circulating miRNA expression in other studies.

We have demonstrated increased exosomal expression of miRs-17, -93 and -20b, miRNAs that belong to the miR-17 family. Of these miRNAs only miR-17 expression has been validated by other published studies to be significantly dysregulated in human patients following stroke. Total miR-17 expression is increased in the plasma of acute ischaemic stroke patients (collected within 7 days of stroke) in comparison to expression in control patients with either vascular risk or other neurological problems (Kim et al., 2015). However, in this study the blood pressure and percentage of patients with diabetes (amongst other factors) was significantly less in the control patients than the ischaemic stroke patients (Kim et al., 2015). Average miR-17 expression was shown to be

unchanged in cardioembolic stroke patients but increased in small vessel disease patients and even further in large artery patients, although these differences were not significant, unlike in the present study. Increased miR-17 expression was also associated with plaque enhancement (as assessed by MRI) and a shorter stroke-free survival time, during a 33 month follow up period (Kim et al., 2015). Total miR-17, miR-93 and miR-20b expression was also detected by microarray technology to be increased in whole blood samples from stroke patients, and especially in small vessel patients (vs. large artery) as compared to healthy control patients, although these changes were not validated by qRT-PCR and the number of patients profiled was low (Tan et al., 2009). miR-17 expression has been investigated pre-clinically in the setting of ischaemic stroke (Liu et al., 2013b) and this will be discussed further in Chapter 5.

Studies investigating total miRNA expression will also inevitably profile exosomal expression in part (RNA is usually extracted from total and not separated serum or plasma) and so it is difficult to tell whether the changes in exosomal expression we have observed in the present study are only found within exosomes or whether expression of these miRs is increased within the serum *and* within exosomes.

The only study to date to compare total and exosomal miRNA expression in human stroke patients collected plasma samples from ICH stroke patients, and examined the difference in expression of 5 miRNAs between the plasma supernatant and microvesicle fractions as separated by ultracentrifugation (Guo et al., 2013). In healthy controls, miR-27a (part of the miR-27 family), miR-24 (clustered with miR-27b) and 3 other miRNAs were not detectable in the supernatant but were found in microvesicles. In ICH patients, these miRNAs were found both in the supernatant and in the microvesicles, and in some cases at a much higher level than in the healthy control patients, although no indication of statistical difference is given (Guo et al., 2013). It would be interesting to carry out similar analysis on our own samples, but given the limited volume of serum that was available for this study, precipitation using exosome isolation reagent was deemed the best method to make as much use as possible of the limited sample. Pre-clinically, differences between total and exosomal serum expression of miR-126 have been investigated in Wistar rats following transient or permanent ischaemic stroke (Chen et al., 2015). miR-126 was detected in both

total serum and exosomes. There was a trend towards similar directions of change in both total and exosomal miR-126 expression at a number of time points post-stroke. However serum miR-126 expression was much more variable than exosomal miR-126 expression, consistent with more highly regulated exosomal microRNA expression (Chen et al., 2015).

To investigate differences between total and exosomal miRNA expression further, we subsequently assessed both total and exosomal expression of miRs-17, -93 and -20b in pre-clinical clinical models of stroke. These miRNAs were selected as they belong to the same miRNA family and this gave us increased confidence in the biological significance of their dysregulation following stroke. Exosomal (and not total) expression of these miRs was increased in the serum of naïve SHRSP rats as compared to WKY rats, although only significantly in the case of miR-17. Expression of all three miRs was unchanged in peri-infarct tissue harvested from both the ipsilateral and the equivalent tissue from the contralateral hemispheres of SHRSP rats in comparison to sham operated rats, sacrificed at either 24 or 72 hours post-tMCAO. Finally, circulating total and exosomal expression of these miRs was examined in SHRSP following either tMCAO, pMCAO or sham surgery and there were no significant increases in miRNA expression at 24 hours following stroke.

The present study was designed to detect exosomal miRNA expression that was dysregulated as a direct result of stroke. The non-stroke control population was therefore carefully selected and we have shown that there are no significant differences between our non-stroke control and stroke patient populations for a number of important characteristics, including hypertension, other risk factors for stroke and for the prescribed medication patients were receiving. Furthermore, the pre-clinical models of stroke used were chosen carefully to represent our human patients as best as possible. SHRSP rats are an excellent model of human ischaemic stroke, not only do they develop stroke spontaneously, they present with a number comorbidities that are often present in human patients, including hypertension, nephropathy, insulin resistance, hyperinsulinemia, hypertriglyceridemia and hypercholesterolemia (Nagaoka et al., 1976). WKY, on the other hand, are normotensive, healthy rats. Our human data shows dysregulated miRNA expression post-ischaemic stroke and our pre-clinical data shows trends towards increased expression of the same miRNAs

post-pMCAO. This is consistent with the hypothesis that these miRNAs are actively packaged into exosomes as a direct result of ischaemic stroke.

The *in vitro* data presented in this study are more conflicting – when we profiled miRNA expression *in vitro*, we were directly assessing the effect of hypoxia alone on differing brain cell types and we found no increase in total miRNA expression and only a trend towards an increase in glial cell secreted exosomal expression that was not significant. The *in vitro* data presented are very variable and so experimental protocols need to be optimised and experiments repeated before we can conclude more from these data. However, a recently published study profiling the miRNA content of exosomes released by cardiac progenitor cells isolated from Sprague Dawley rats following hypoxic insult revealed that miR-17 and miR-20 were up-regulated (Gray et al., 2015). Therefore, the fact that miRNAs in this family are dysregulated in a similar way in the present study is consistent with miR-17 family miRs being packaged into exosomes as a direct result of the brain's response to ischaemic conditions. However, the pre-clinical model used in the study (cardiac progenitor cells from healthy rats) (Gray et al., 2015) cannot be directly compared to data gleaned in our own carefully phenotyped human patients and co-morbid pre-clinical models of ischaemic stroke.

Alternatively, the data presented here could also be consistent with the hypothesis that aberrant packaging of selected miRNAs into exosomes is part of an underlying vascular pathology that renders patients and SHRSP susceptible to stroke. In the present study the clinical patient populations were carefully selected to ensure that dysregulated miRNA expression observed could be concluded to be a direct result of stroke. Seven miRNAs were subsequently shown to be especially dysregulated in small vessel disease patients in the clinical study. Furthermore miR-17 family miRNAs were increased (some significantly) in naïve SHRSP (vs. WKY) but not significantly further increased following pre-clinical stroke. SHRSP are accepted by some to be a valid model of human cerebral small vessel disease (Bailey et al., 2009, Hainsworth and Markus, 2008, Wardlaw et al., 2013). This being said, they (and no other animal model) can mimic every aspect of human small vessel disease and while useful, SHRSP cannot be used to make direct deductions as to the pathogenesis of human SVD (Hainsworth et al., 2012). However, SHRSP rats demonstrate modest endothelial

and perivascular tissue defects as early as 5 weeks of age (before hypertension has set in), including impaired “impaired endothelial tight junctions, poor myelination, overactive microglia, and a tendency for glial scarring that can be detected by protein expression” (Wardlaw et al., 2013). SHRSP have non-specific inflammation and BBB permeability changes at as early as 5 weeks of age (Wardlaw et al., 2013) and are also spontaneously hypertensive with blood pressure rising progressively from normal levels at age 4 weeks to a plateau at around 20 weeks in male rats (Yamori et al., 1976). Cerebrovascular lesions can also develop spontaneously, and the incidence of these increases from being rare at less than 12 weeks of age to an incident rate of over 80% at 30 weeks of age in male rats (Tagami et al., 1987, Yamori and Horie, 1977). The naïve SHRSP rats used in this study were 20-22 weeks old and would therefore have many characteristics of cerebral small vessel disease. Therefore, the data presented in this study could also be interpreted to be consistent with the hypothesis that miRNAs detected in this study are packaged into exosomes as a result of underlying cerebral vascular disease which predisposes patients to either an ischaemic stroke or maybe more specifically a small vessel disease stroke. While cerebral ischaemia as a result of stroke may result in a further (but non-significant) increase in expression of these miRNAs, this may not be the primary cause of their increase in expression, which would explain why expression is increased in large artery and cardioembolic patients to a lesser extent.

A previous study within our own research group (Breen, 2015) profiled total miRNA expression in serum samples using the same microarray technology as used in the present study and compared expression to a similar cohort of vascular risk control patients as has been used in the present study. While the patient population investigated was smaller, miRNAs selected for validation failed to validate in a large patient population (IS: n=55, non-stroke: n=20). Some of the miRNAs profiled were examined in the present study including miR-20b and miR-93 (both unchanged in IS vs. control). Other miRNAs studied are related to miRNAs investigated in this study, including miR-27a (miR-27 family) and miR-106a (miR-17 family), both of which were unchanged in IS patients in comparison to control patients (Breen, 2015). As many of the patient samples used in this study were also used in the present study where a number of interesting dysregulated miRNAs were identified, this highlights the importance

of looking at exosomal packaged miRNA expression. Furthermore, these data from the same carefully phenotyped stroke and control patient populations (although smaller *n*) when taken in combination with our data are consistent with the hypothesis that a number of miRNAs are selectively and actively packaged into exosomes, hence their expression is unchanged when total miRNA content is investigated but increased when exosomal miRNA content is analysed.

Other exosomal miRNAs (not part of the miR-17 family) detected as being dysregulated in the present study have been shown to be dysregulated in ischaemic stroke patients in other studies. Total miRNA expression was profiled in both plasma and CSF samples collected 3 days post-stroke, using microarray technology (Sørensen et al., 2014). Expression of miR-27b was one of the 21 most frequently detected miRNAs in CSF, and was significantly increased in ischaemic stroke patients in comparison to patients with other neurological diseases such as dementia or multiple sclerosis. Interestingly, miR-199a-3p (passenger strand), which we found to be significantly up-regulated in exosomes of ischaemic stroke patients was unchanged in the CSF of ischaemic stroke patients in this study, although neither of these changes were validated by qRT-PCR (Sørensen et al., 2014). A separate study profiling total miRNA expression in plasma samples collected 24 hours following stroke found miR-199a-5p (lead strand) to be upregulated in IS patients in comparison to healthy controls and especially in patients with embolic stroke as opposed to thrombotic stroke (although results were not validated by qRT-PCR) (Li et al., 2015a).

Interestingly, the only other passenger strand miRNA we found to be dysregulated in our samples, miR-223-5p, has also been profiled in a number of other studies. miR-223 is increased in whole blood samples collected from ischaemic stroke patients within 6-18 months of their stroke as compared to its expression in healthy control patients (Tan et al., 2009). Leukocytes isolated from plasma of ischaemic stroke patients within 72 hours of stroke onset had significantly higher levels of miR-223 than their healthy control counterparts (Wang et al., 2014c). This study also profiled the expression of miR-223 in relation to stroke subtype and found that average expression was only significantly increased in large artery and small vessel disease, was unchanged in unclassified patients and was decreased in cardioembolic patients. Furthermore the expression was significantly increased in stroke patients at 24h and 72h post-

stroke, but not at 48h post stroke (Wang et al., 2014c), the time point at which we collected serum from patients in our study. miR-223 was also negatively correlated with NIHSS score and infarct volume (Wang et al., 2014c). Subsequent studies have shown unchanged miR-223 expression in the serum of stroke patients at 24 hours following stroke onset as compared to healthy controls (Jia et al., 2015) and in the plasma of large artery patients as compared to healthy controls (Duan et al., 2014). Pre-amplified expression of miR-223-5p was relatively low in the present study (average Ct: 31.9 including 30 patients where the miRNA was not detected), which is why this miRNA was not taken forward for further investigation. None of the studies mentioned here provide information on which strand of miR-223 they investigated and so we assume they were profiling expression of the lead strand, miR-223-3p, which may explain differences both in level and profile of expression in relation to stroke subtype.

A seminal study investigating exosomal paracrine signalling between cardiac fibroblasts and cardiomyocytes found that cardiac fibroblasts secrete exosomes that contained a relatively high abundance of miRNA passenger strand miRNAs, which were previously believed to undergo intracellular degradation (Bang et al., 2014b). Specifically they found exosomal miR-21-3p, a passenger strand miRNA, was secreted in exosomes and acted to induce cardiomyocyte hypertrophy, possibly by the inhibition of proteins SORBS2 and PDLIM5 (Bang et al., 2014b). This highlights the possible functional importance of exosomal packaged passenger strand miRNAs within our own study and if possible it would be interesting to investigate the functional activity of these exosome bound miRNAs further.

In the present study, OpenArray data predicted a decrease in miR-30a-5p expression but its exosomal expression was subsequently shown to be increased in ischaemic stroke patients, and especially so in small vessel disease patients. Total miR-30a expression was profiled in relation to stroke subtype in the plasma of ischaemic stroke patients and compared to that of age-matched controls with vascular risk, at a number of time points (Long et al., 2013). In this study miR-30a was found to be decreased in all stroke subtypes at 24 hours, 1 week, 4 weeks and 24 weeks post-stroke but unchanged at 48 weeks post-stroke in relation to control patients (Long et al., 2013). miR-30a was also a specific and sensitive diagnostic marker for ischaemic stroke (AUC consistently >0.91

regardless of time point chosen) (Long et al., 2013). Importantly this study was well powered and used appropriate control patients, similarly to the present study. The differences in results observed here (Long et al., 2013) in comparison to the presented data could therefore be a direct result of differences in exosomal and total miRNA expression. Another possibility would be the time point at which miRNA expression was investigated. In the present study exosomal miR-30a-5p was shown to be increased at 48 hours post-stroke whereas in that of Long and colleagues this time-point was not investigated. Secondary ischaemic damage, as a result of inflammation for example, peaks at around 48-72 hours post-stroke (see Figure 1.2) and may begin to resolve within a week post ischaemic insult. As miRNA expression changes temporally post-stroke it is feasible that miR-30a-5p is temporarily increased between 48-72 hours post-stroke. Further experiments profiling exosomal miRNA expression in samples collected at longitudinal time points from the patients recruited in the present study would help to resolve this discrepancy.

Exosomal let-7e miRNA expression was shown (in the present study) to be up-regulated in the serum of ischaemic stroke patients at 48 hours post-stroke. These data are consistent with a couple of studies profiling total miRNA expression in IS patients. Total let-7e expression was increased in whole blood samples of IS patients collected within 72h of stroke onset in relation to vascular risk factor control patients (Jickling et al., 2014). Total let-7e expression was also profiled in serum and CSF samples collected from IS patients acutely (24 hours to 1 week), subacutely (2 weeks) and during recovery (≥3 weeks) and compared to expression in healthy control patients (Peng et al., 2015). let-7e expression was most increased acutely but significantly increased at all 3 time points studied. This was also the case for total let-7e expression within the CSF. While its' serum expression did not correlate with NIHSS scores, it was found to be good diagnostic biomarker for stroke in relation to healthy controls (AUC 0.86) (Peng et al., 2015).

While studies investigating miRNA expression in the setting of ischaemic stroke have shown effects of both age and gender on miRNA expression (for example, (Selvamani et al., 2014)), we did not observe any correlation between exosomal miRNA expression and age. Furthermore, of the miRNAs we took forward for further investigation, only the exosomal expression of let-7e was altered in

relation to gender, and only in unclassified male patients (vs. matched females) and not in stroke patients as a whole. The stroke and control patient populations used in the present study were carefully selected, and although the non-stroke control patients were younger (not significantly) they had a very similar gender ratio to their stroke patient counterparts.

As we were interested in exosomal packaged miRNAs released as a cause of or directly as a result of ischaemic stroke, the serum samples we used in this study (collected at 48h post-stroke) may not be ideal. However, we were keen to profile exosomal miRNA expression in as many patients as possible to give the study the power needed to detect small changes in miRNA expression. As many as 6 in 10 stroke patients arrive at A&E later than 4.5 hours post-stroke onset, the therapeutic window for rtPA treatment, often as a result of having had a stroke during sleep or not taking symptoms seriously and so delaying arrival at hospital (Stroke Association, 2016). Some even arrive as late as 24 hours post-stroke. For this reason we decided to profile miRNA expression in samples collected at 48 hours, a time point for which we had a sample for every patient enrolled in the study and one that is still sub-acute. Furthermore, published studies that profile total miRNA expression at various time points following stroke did not show significant changes in miRNA expression over early time points post-stroke (Long et al., 2013, Peng et al., 2015).

It would be interesting to profile both total and exosomal miRNAs highlighted in the present study, in a patient population at risk of stroke (such as our control population) with a long-term follow up to determine whether dysregulated miRNA expression could be used to identify individuals especially susceptible to ischaemic stroke. This would also help to elucidate whether aberrant exosomal miRNA signalling is part of an underlying vascular pathology that causes patients to have or be susceptible to stroke, or whether these exosomal miRNAs are released directly following a stroke and cerebral ischaemia. In the present study serum samples were also collected at 7 days, 1 month and 3 months post-stroke and are available for exosomal miRNA profiling though there was not sufficient time in this study to perform these experiments.

In the present study it was hypothesised that dysregulated exosomal miRNAs could be used as biomarkers, either to phenotype patients where diagnosis was

unclear (unclassified patients, and 'possible' stroke patients) or as predictors of clinical outcome. We investigated the possibility of using the expression of 7 miRNAs either individually or their combined scores for diagnosis or prognosis and in both cases found that no single exosomal miRNA or group of miRNAs in this study could be used for this purpose. Although the average expression of these miRNAs changed between non-stroke and stroke patients and between stroke subtypes, their expression overlapped considerably between groups. ROC analysis performed to assess the ability of exosomal miRNA expression to differentiate between stroke subtypes showed that the overlap in expression for miRNA expression between stroke-subtypes was too great to allow for this diagnosis (data not shown). Although there was a trend towards the expression of each miRNA being higher in patients with better functional outcome from stroke, these changes were not significant. Even when the scores for each miRNA were combined, to give extra power to the analysis, ROC analysis showed that this score could not sensitively or specifically predict clinical outcome from stroke, when comparing 1 month mRS scores of ≤1 and those ≥2. Very few published studies present data on this: miRs -30a, -126, let-7b (Long et al., 2013) and miR-17 (Kim et al., 2015) have been tested for their diagnostic capability and miRs -210 (Zeng et al., 2012, Zeng et al., 2011) and -132 (Huang et al., 2016) for their prognostic capability. Although it is difficult to assess whether the results of the present study are typical of what is observed in studies of this kind (as very few have been published in setting of IS) the lack of predictive ability of miRNAs is likely reflective of the very heterogeneous stroke population, in comparison to other diseases where miRNAs have been more successfully used as biomarkers such as heart failure and cancer.

If circulating dysregulated exosomal miRNAs could be found whose expression overlapped less between patient groups these would be ideal candidates for diagnostic or prognostic biomarkers. Liquid biopsies are advantageous over other types of tissue biopsy as they have a reduced risk to the patient and a reduced cost to the health service provider. Tissue biopsies may also result in sample bias, depending on the location of the tissue extraction. Furthermore, while RNA is very sensitive to degradation miRNAs remain detectable and relatively stable following many freeze thaw cycles (data not shown). miRNAs within exosomes

are further protected from degradation and so are excellent candidates for stable biomarkers that will provide an unbiased comparison between patients.

The only two licenced interventions for ischaemic stroke are rt-PA and thrombectomy and both must be administered within hours of the onset of stroke in order to prove successful. Time constraints associated with exosome isolations, RNA extractions and subsequent PCR reactions mean that it is unlikely that exosomal miRNA expression could ever be used diagnostically in more economically developed countries where imaging technologies such as CT and MRI are readily available. However, in patients where diagnosis by conventional imaging fails, as a result of mild stroke, or technical problems, exosomal miRNA expression may provide an additional tool for stratifying patients. Furthermore a biomarker to stratify patients according to predicted clinical outcome would be useful both in identifying patients that will benefit most from intensive physical rehabilitation or other treatment and for informing patients of their prognosis.

In the present study TaqMan® OpenArray® MicroRNA Panels were used. While a low sample input was used (10 ng input RNA vs. 100 ng) Life Technologies provide an adapted protocol for samples with low RNA yield. Life Technologies report that using 10 ng of input RNA and following their adapted protocol will result in detection of 92% of the miRNAs detected when using 100 ng of RNA (Life Technologies, 2011). In the present study 553 miRNAs were detected in at least 1 sample (out of 39) and of these, 93 were detected in greater than 30% of patients in one particular subtype. Ideally candidate miRNAs taken forward for validation would have been detected in over 90% of patients. The fact that so few miRNAs met this criteria is possibly a result of the lower sample input RNA. To get as much out of the data set as possible we examined differences in miRNA expression between non-stroke and stroke patients in every miRNA detected in at least 30% of patients in one particular stroke subtype. 26 miRNAs were detected as being dysregulated in stroke patients. The fact that many miRNAs were not detected in a number of samples in the microarray is not the result of using exosomal miRNA (vs. total serum miRNA), as when validated by qRT-PCR the majority of miRNAs were detectable in every sample. Similar studies using microarray technology to profile circulating miRNA expression in human patients post-stroke (Table 1.2) often do not report the total number of miRNAs detected or the percentage of samples the miRNAs detected were present in, so it is

difficult to compare our results to array data collected in other studies. Of these studies (Table 1.2) dysregulated miRNAs (detected by microarray) taken forward for validation were selected randomly (Tan et al., 2009, Zhang et al., 2016a), if they had a fold change of greater than 1.2 (Jickling et al., 2014, Sepramaniam et al., 2014) or 2.0 (Li et al., 2015b, Wang et al., 2014b, Zhang et al., 2016a) or if the miRNAs had previously been reported in the literature (Li et al., 2015b). None of these studies comment on the percentage of samples each miRNA had to be present in to be taken forward for validation.

Of the 13 miRNAs selected for validation from the microarray data, 3 miRNAs were detected as being up-regulated in all stroke patients (vs. non-stroke control): miR-27b, miR-20b and miR-17. These results were positively validated by qRT-PCR and the direction of change was the same. A further 9 miRNAs were shown to up-regulated (by qRT-PCR) in definite stroke patients (vs. non-stroke control) – of these 7 were up-regulated in the OpenArray study but miR-30a and miR-218 were detected as being down-regulated (although non-significantly). Very few studies profile miRNA expression in relation to stroke subtype. Stroke subtype is rarely taken into account in experimental design and is only occasionally commented on following data generation. In the present study we were especially interested in differences in miRNA expression between stroke subtypes and designed the experiment to include (as much as possible) approximately equivalent group sizes for each stroke subtype. In the present study we have demonstrated that 7 miRNAs are up-regulated in small vessel disease patients (vs. non-stroke controls, by qRT-PCR). Of these 5 were shown to be up-regulated in small vessel disease patients in the OpenArray study (although only 3 of these changes were significantly different) but miR-30a was detected as being down-regulated in the OpenArray (non-significant) and let-7e was detected as being switched off in small vessel patients.

While microarray technology has been used in many studies, of the 9 studies (Table 1.2) that use this technology to profile miRNA expression in stroke only 6 studies (Jickling et al., 2014, Li et al., 2015b, Sepramaniam et al., 2014, Tan et al., 2009, Wang et al., 2014b, Zhang et al., 2016a) validate expression of some miRNAs by qRT-PCR. Several studies report whether their qRT-PCR data validated the changes seen in the microarray, with some miRs changing to a greater extent than observed in the array (Tan et al., 2009), others changing to

a significantly lesser extent than the array (Li et al., 2015a, Sepramaniam et al., 2014). Other studies reported miRs that either were unchanged in the array but changed by qRT-PCR (Tan et al., 2009) and additional studies either did not report any or all their array data (Jickling et al., 2014, Li et al., 2015a) or represented their array data by a heat map which made it difficult to interpret (Wang et al., 2014b, Zhang et al., 2016b). Of the 13 miRNAs validated by qRT-PCR, 7 were positively validated and a further 2 miRNAs were shown to be significantly different (but in an opposite direction to predicted). This is a success rate of over 50% and justifies the use of microarray technology for the identification of novel dysregulated miRNAs. Had it been possible to increase the quantity of input RNA used in the microarray we hypothesise that this may have increased the quality of the data generated and have further increased the success rate.

Microarray technology, developed for high throughput global analysis of changes in mRNA levels, has been widely used for analysis of changes in miRNA expression in many different diseases. These experiments produce large amounts of data and analysis is time consuming. Furthermore, not all dysregulated miRNAs identified can be validated by qRT-PCR. Of the 26 miRNAs identified by OpenArray as dysregulated in stroke patients only 13 were taken forward for validation by qRT-PCR in the larger patient population as the expense and time taken to profile even these miRNAs was considerable. This means there are other miRNAs, previously uncharacterised in the setting of stroke whose expression and role in ischaemic stroke was not investigated further.

Normalisation of microarray and qRT-PCR data when investigating circulating miRNA expression remains challenging as there is not a universal reference gene or miRNA for normalisation (Jarry et al., 2014). As RNA extraction, reverse transcription and amplification efficiencies can all vary between the samples used it is important to have a signal to normalise to. Traditionally an endogenous “housekeeper” miRNA or small nucleolar RNA would be used. However, it is difficult to find either a single circulating miRNA or panel of miRNAs that are stable in samples from patients with disease as profound as ischaemic stroke. For this reason in the present study an external control (cel-miR-39 spike in) was used. The addition of an external spike can correct for differences in RNA recovery and qPCR efficiency but it does not take into account endogenous

differences in miRNA expression. However, due to the lack of a suitable endogenous control the use of an external control was appropriate for the present study.

In conclusion, in the present study we have identified and validated changes in exosomal packaged miRNA expression in stroke patients and across different stroke subtypes. Furthermore, multiple miRNAs from one miRNA family were dysregulated similarly giving us increased confidence in the biological significance of these results. While we have failed to establish a link between exosomal miRNA expression and clinical outcome from stroke, these miRNAs remain interesting candidates for further investigation. These results will direct future studies looking into paracrine signalling in stroke and the modulation of specific miRNAs as a novel therapy in the setting of experimental stroke.

Chapter 5 Therapeutic Delivery of miRNA Loaded Extracellular Vesicles

5.1 Introduction

There is an unmet need for novel treatments for ischaemic stroke. miRNA modulation has proved to be therapeutically beneficial in models of pre-clinical stroke (see Table 1.4). Although the majority of these studies deliver miRNA modulating agents prior to the occurrence of stroke, a number of studies deliver therapeutic agents post-stroke, a more clinically relevant delivery time point.

Of these, a number of studies modulated miRNA expression by the direct delivery of mature miRNA mimics or anti-miRs (Selvamani et al., 2012, Sepramaniam et al., 2010, Vinciguerra et al., 2014). ICV infusion of an anti-miR for miR-320a at reperfusion proved therapeutically beneficial (assessed by reduced infarct volume) following 1h tMCAO in Sprague Dawley rats (Sepramaniam et al., 2010). ICV injection of a let-7f anti-miR 4 hours post embolic MCAO in adult female rats resulted in reduced cortical and striatal infarcts and preserved sensorimotor function (Selvamani et al., 2012). miR-103-1 anti-miR delivered via ICV infusion to the lateral ventricle for 48 hours, starting 20 mins post-tMCAO in Sprague Dawley rats resulted in reduced infarct volume and neurological deficit (Vinciguerra et al., 2014).

Interestingly, several studies have modulated miRNA expression using transfection agents, such as Lipofectamine™ (a cationic liposome formulation that complexes with nucleic acid molecules, allowing them to overcome the electrostatic repulsion of the cell membrane and to be taken up by the cell). miR-124a anti-miR delivered in lipofectamine via ICV stereotactic injection following pMCAO in C57 mice resulted in a reduction of infarct volume (Liu et al., 2013a). miR-424 mimic with siRNA-MATE was delivered via ICV injection 10 minutes post-pMCAO in C57BL/6J mice and resulted in reduced cerebral infarct and oedema volume (Zhao et al., 2013). Stereotactic injection of miR-139-5p mimic with lipofectamine at 12 hours post hypoxia/ischaemia injury in neonatal Sprague Dawley rats reduced infarct volume when assessed at both 48 hours and 7 days (Qu et al., 2014). miR-23a-3p mimic with lipofectamine delivered via ICV stereotactic injection at 10 minutes post tMCAO in C57BL/6J mice reduced infarct volume (Zhao et al., 2014). miR-181 anti-miR delivered with DOTAP either via ICV to the lateral ventricle at 2 hours post-tMCAO or via IV delivery to the internal jugular vein at 1 hour post-tMCAO in C57/B6 mice resulted in long

lasting (up to 4 weeks) reduced infarct volume, neurological deficit and improved behavioural outcome (Xu et al., 2015). Finally, miR-122 mimic was delivered in PEG-liposomes via IV delivery to the tail vein or ICV injection at 5 mins post-tMCAO in Sprague Dawley rats and reduced infarct volume and attenuated neurological impairment (Liu et al., 2015a).

The only study to date to modulate miRNA expression, post-stroke, by a different method, used MSCs that had been modified to be miR-133b positive or negative (Xin et al., 2013b). The miR modified MSCs were delivered by IV injection to the tail vein of Wistar rats, 24 hours post-tMCAO and resulted in improved functional recovery (Xin et al., 2013b).

The majority of these studies modulate miRNA expression via the delivery of mature miRNA mimics or anti-miRs either systemically, by stereotactic injection or by ICV infusion. While miRNA modulation is undoubtedly achievable via these methods, they are not readily transferable to clinical treatment of human stroke patients. As time is of the essence in the treatment of ischaemic stroke, invasive stereotactic injection and ICV infusion delivery of therapeutic agents may not be suitable, aside from the other practical, safety and cost considerations, which would be significant. However, if the primary aim of the therapeutic intervention is to promote repair and regeneration, then delivery can be delayed and stereotactic administration may become a viable option. An example of this is the Pilot Investigation of Stem Cells in Stroke (PISCES) clinical trial (Kalladka et al., 2016) where human neural stem-cells from an immortalised cell line were administered by stereotactic injection 6-60 months following stroke. Systemic delivery of miRNA modulating agents is not ideal as the possibility of off-target effects is considerable, furthermore it is possible that therapeutic agents delivered would not reach or cross the BBB in an efficient manner.

Intra-nasal delivery is a potential alternative strategy for delivering therapeutic agents to the CNS and has been used successfully pre-clinically as a simple method to deliver therapeutic agents to the brain. It is practical, non-invasive and bypasses the BBB. It was first developed to target neurotrophic factors (e.g. nerve growth factor and fibroblast growth factor-2) to the CNS (Frey, 1991). Therapeutic agents delivered intra-nasally travel to the central nervous system via the olfactory and trigeminal neural pathways (Figure 5.1). The nasal cavities

of both humans and rodents are innervated by the olfactory and trigeminal nerves. Initial studies attributed the connection between the nasal cavity and the CNS to the olfactory pathway alone (Frey et al., 1997, Thorne et al., 1995). However, more recently the trigeminal pathway has also been implicated in intra-nasal delivery to the CNS – it is thought to be able to deliver therapeutic agents to caudal brain regions and the spinal cord (Ross et al., 2004, Thorne et al., 2004). Intra-nasal delivery of therapeutic agents results in a very rapid transfer to the brain, and this implicates extracellular transport (as opposed to axonal) as the primary method of transfer (Lochhead and Thorne, 2012). Studies carried out in human patients show that that intra-nasal delivery of therapeutic agents to the CNS is possible, and is not a phenomena unique to rodents and their significantly smaller brains (Lochhead and Thorne, 2012).

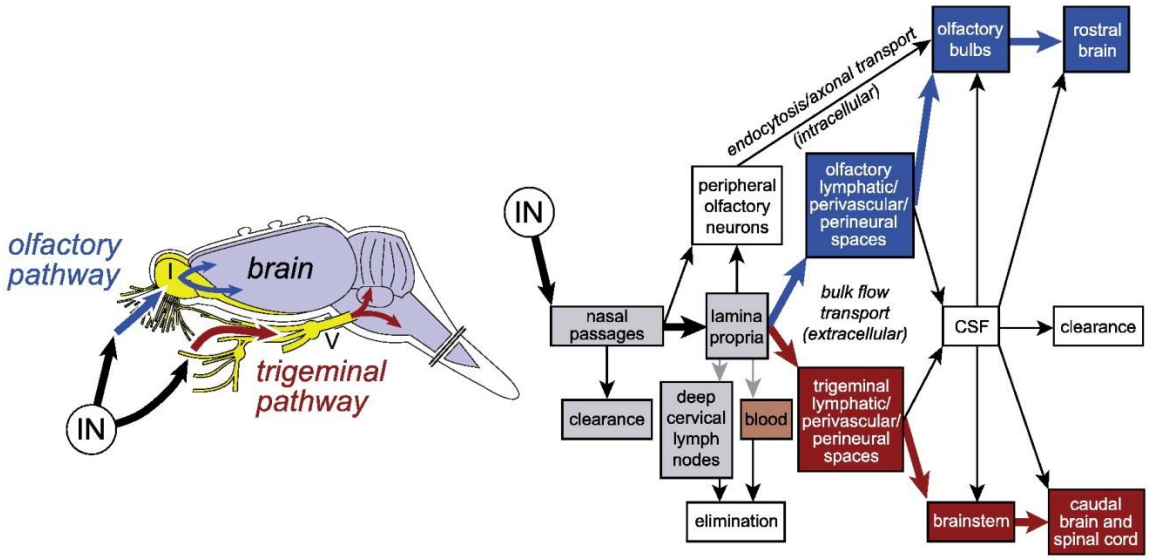

Figure 5.1 – Intra-nasal Delivery Pathways
This diagram illustrates the olfactory and trigeminal neural pathways. Exosomes delivered intra-nasally are believed to cross the olfactory epithelium, bypassing the blood brain barrier to deliver agents directly to the central nervous system. Image used with permission from (Lochhead and Thorne, 2012).

No study, to date, has modulated miRNA expression in the setting of ischaemic stroke via intra-nasal delivery of a miRNA modulating agent. However studies such as those published by Jae-Kyu Roh's research group in South Korea (Kim et al., 2014, Lee et al., 2012) provide evidence that modulating miRNA expression intra-nasally may be beneficial for the treatment of neurological disorders.

Intra-nasal delivery of anti-miR-206 (suspended in PBS) to Tg2576 transgenic mice, a pre-clinical model of Alzheimer's Disease, resulted in anti-miR delivery

to the olfactory bulb, cortex and hippocampus within 24 hours (Lee et al., 2012). Expression of BDNF, a target of miR-206, is reduced in the Alzheimer's Disease brains. Its expression was increased following delivery of the anti-miR in all 3 brain regions. Furthermore, mice that were treated with the anti-miR had improved hippocampal memory function as compared to vehicle treated animals at 1 week following treatment, as assessed by 2 different behavioural tests (Lee et al., 2012). Enhancing BDNF expression by intra-nasal delivery of anti-miR-206 is therefore a novel therapy for the treatment of Alzheimer's Disease.

Interestingly, modulation of let-7c by the intra-nasal delivery of an anti-miR proved therapeutically effective in a pre-clinical ICH model of stroke (Kim et al., 2014). Intra-nasal delivery of the anti-miR-let-7c (suspended in DEPC treated water) immediately following ICH induction, in Sprague Dawley rats, reduced brain water content (at 72 hours post ICH) and reduced staining for markers of neutrophil infiltration, activated microglia and apoptosis. Furthermore, animals treated with anti-miR had improved neurological function scores as compared to vehicle treated animals, but only at 4 and 5 weeks post-stroke (not significantly different in the first 3 weeks post-treatment) (Kim et al., 2014).

In the present study we propose modulating the expression of miRNAs via intra-nasal delivery of miRNA modulating agents, encapsulated in exosomes, as a novel therapy for ischaemic stroke. Exosomes are endogenous transport vesicles and so are excellent tools for drug delivery (Johnsen et al., 2014). They are small (30 – 120 nm) and can cross the BBB. 'Self-derived' exosomes can also overcome problems with immunogenicity. Furthermore, some exosomes have natural selective properties for target cells – if this power was harnessed or modified correctly, exosomes could be used to delivery miRNA modulating agents with high specificity, and therefore fewer side effects.

Exosomes have been used to deliver siRNA specifically to the mouse brain (following systemic administration): exosomes targeted to the neuron specific RVG peptide and containing BACE1 siRNA significantly reduced BACE1 expression in the brain of C57BL/6 mice as compared to mice treated with exosomes alone or the siRNA delivered via a cationic liposome-based transfection reagent (Alvarez-Erviti et al., 2011). Exosomes have also been used to deliver therapeutic agents intra-nasally. A series of papers have demonstrated the rapid

uptake of exosomes into the brain (and especially microglial cells) following intra-nasal delivery and subsequent therapeutic effect following delivery of therapeutic agents (Zhuang et al., 2016, Zhuang et al., 2011). C57BL/6J mice treated intra-nasally with exosomes containing curcumin were protected from LPS-induced brain inflammation (Zhuang et al., 2011). Furthermore curcumin exosomes reduced the progression of experimentally induced autoimmune encephalomyelitis and delayed brain tumour growth following injection of brain tumour stimulating cells in the GL26 mouse tumour model (Zhuang et al., 2011). Subsequently, intra-nasal delivery of exosome like nanovectors, derived from the juice of grapefruit, coated with folic acid (to target folate receptor positive tumour cells) and loaded with miR-17 resulted in up-regulation of miR-17 expression and delayed brain tumour growth (Zhuang et al., 2016). These studies confirm that exosomes are a novel and powerful way to deliver therapeutic agents to the brain.

In the present study we propose modulating the expression of miR-17 family miRNAs: miRs -17, -93 and -20b. The exosomal expression of these miRNAs was up-regulated in the serum of human stroke patients, and especially small vessel disease patients, at 48 hours post-stroke (Chapter 4).

Basic bioinformatics was carried out to find out more about the target genes of miRs -17, -93 and -20b – miRWalk 2.0 software (an atlas of predicted and validated miRNA-target interactions) and DAVID (a functional annotation tool) were used to generate information about target genes. Figure 5.2 gives more information on how this was carried out. As the 3 miRNAs belong to one miRNA family and have identical seed sequences (the part of the miRNA important for miRNA-target interactions), they share a large number of predicted and validated gene targets (Figure 4.12) and a relatively high percentage of these targets have the potential to be involved in stroke pathophysiology. If miR-93 is taken as an example (Figure 5.2) – of its 2147 predicted gene targets 427 miRNA-gene target interactions have been experimentally validated. Of these 43 (~10%) are involved in the regulation of programmed cell death and apoptosis, 27 (~6%) are involved in the cellular response to stress and 31 (~7%) are involved in repair processes such as proliferation, axonogenesis and angiogenesis.

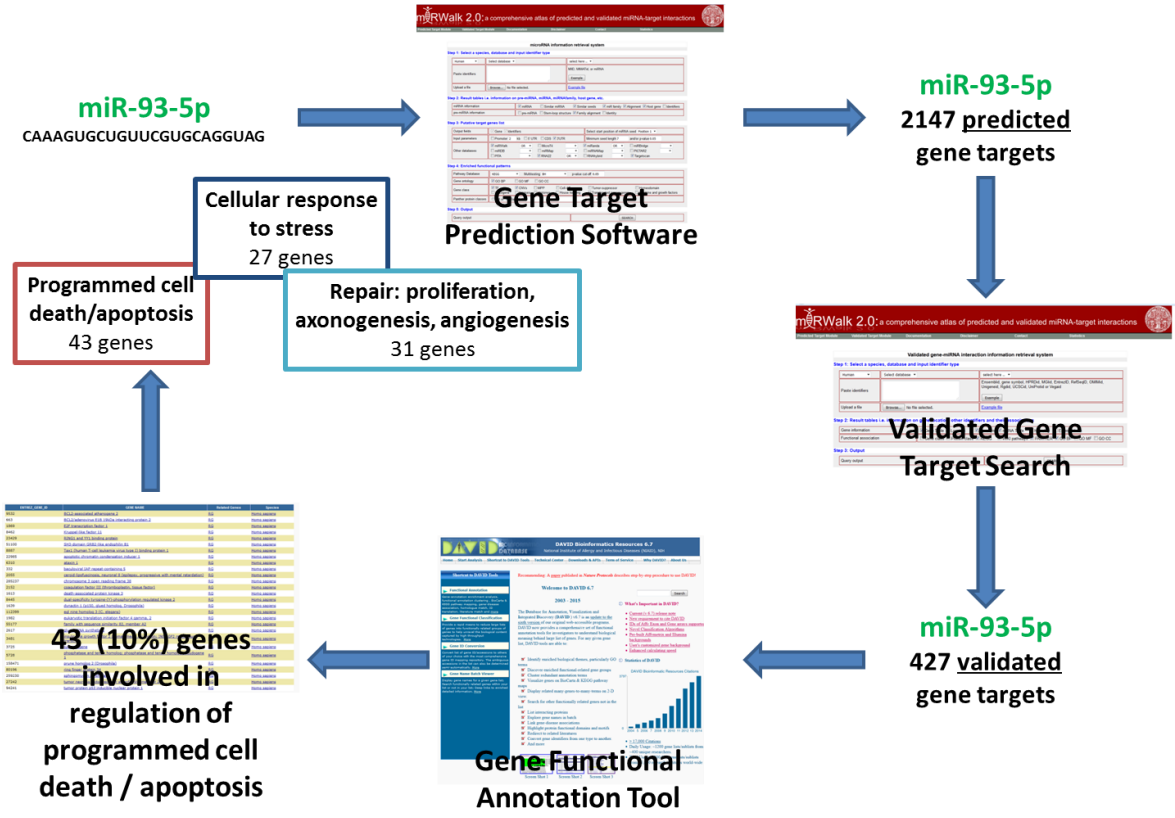

Figure 5.2 – miR-17 Family Bioinformatics Example
An example of the process used to find out information about the target genes for each miRNA in the miR-17 family. The mature miRNA sequence was entered into a gene target prediction software: miRWalk 2.0. miRWalk 2.0 combines results from 12 different miRNA-gene target prediction algorithms. Only gene targets predicted by 7 or more algorithms were accepted as predicted hits. To narrow down the list of gene targets, experimentally validated targets were investigated using the same software. The list of experimentally validated targets was then entered into the Database for Annotation, Visualization and Integrated Discovery (DAVID), where the Gene Ontology function for Biological Processes was used. This sorted experimentally validated target genes into various biological processes. Biological processes that could be involved in the pathophysiology of ischaemic stroke were selected and target genes listed.

Only one study to date has investigated miR-17 family miRNAs in the setting of ischaemic stroke (Liu et al., 2013c). The expression of miRNAs in the miR-17-92 cluster (of which miR-17 is one) were up-regulated in neural progenitor cells harvested from C57BL/6J mice 7 days post-pMCAO. However, miR-17 was not significantly up-regulated unlike other members of the miR-17-92 cluster. miRNAs in the miR-106b-25 cluster (of which miR-93 is one) (see Figure 4.12) were down-regulated in neural progenitor cells following pMCAO. miR-93 was not significantly down-regulated. Inhibition of miRs -18a and -19a (miR-17-92 cluster) in neural progenitor cells reduced proliferation and increased apoptosis. miR-18a and -19a were subsequently found to target PTEN and FasL, inducers of apoptosis (Liu et al., 2013c). The study concluded that the miR-17-92 cluster

mediates the proliferation and survival of neural progenitor cells following stroke.

miR-25 (a member of the miR-106b-25 cluster, of which miR-93 is a member) has also been demonstrated to be up-regulated following tMCAO in young Sprague Dawley rats and further increased following repetitive transcranial magnetic stimulation (Guo et al., 2014). ICV injection of anti-miR-25, immediately prior to tMCAO surgery, resulted in increased p57 protein expression (a negative regulator of cell proliferation) and reduced proliferation in cells of the ipsilateral sub-ventricular zone at 7 days post-tMCAO.

In non-stroke related models of ischaemia, miR-17 and miR-20 are up-regulated in exosomes released by cardiac progenitor cells isolated from Sprague Dawley rats following hypoxic insult (Gray et al., 2015). miR-93 has been shown to be up-regulated in mouse strains with increased perfusion recovery following experimentally induced hindlimb ischaemia (Hazarika et al., 2013). Furthermore, *in vivo* overexpression of miR-93 improved perfusion recovery and increased capillary density in C57BL/6J and BALB/cJ mice, whilst intravenous delivery of anti-miR-93 resulted in reduced perfusion recovery following induced hindlimb ischaemia (Hazarika et al., 2013). p21 and p53 were found to be targets of miR-93 in this setting (Hazarika et al., 2013). miR-20b has been shown to be down-regulated in ischaemia-reperfused Sprague Dawley rat heart and to target VEGF and HIF1α (Mukhopadhyay et al., 2012). miR-20b is also down-regulated in whole blood samples of patients with peripheral arterial disease as compared to healthy control patients (Stather et al., 2013).

There is a clear need for novel, clinically relevant therapeutics to treat ischaemic stroke and the various processes of the debilitating ischaemic cascade. We therefore propose delivering miRNA-17 family loaded exosomes intra-nasally, post-stroke, in our *in vivo* pre-clinical models of ischaemic stroke and subsequently assessing therapeutic efficacy.

5.1.1 Hypotheses

The hypotheses of the present study were as follows:

- Artificial loading of specific miRNAs into extracellular vesicles will prove an efficient tool for modulating miRNA expression *in vivo* and *in vitro*.

- Intra-nasal delivery of miRNAs packaged in extracellular vesicles will be an effective and clinically relevant method of modulating miRNA expression *in vivo*.

- Modulation of miR-17 family miRNAs via delivery of miRNA loaded extracellular vesicles will result in therapeutic benefit following pre-clinical stroke or *in vitro* hypoxic challenge.

5.1.2 Aims

The aims of the present study were as follows:

- To assess the extent of modulation of specific miRNAs following intra-nasal delivery of extracellular vesicle packaged miR-17 family miRNAs *in vivo* post tMCAO.

- To assess the therapeutic effect of modulation of miR-17 family miRNAs post-stroke by measuring functional recovery (assessed by behavioural testing) and infarct size.

- To assess the extent of modulation and therapeutic effect of modulation of miR-17 family miRNAs post-hypoxic challenge *in vitro* by quantifying miRNA expression and using functional assays to assess therapeutic effect.

5.2 Methodology

5.2.1 miRNAs Selected for Therapeutic Delivery

Following the results of the exosomal miRNA profiling study in human patients, we selected miRs -17, -93 and -20b, from the miR-17 family, as interesting candidates for modulation in our pre-clinical models of stroke.

Due to time and cost constraints it was not possible to examine the effect of all 3 miRNAs in our *in vivo* pre-clinical model of stroke. miR-17 had previously been investigated in the setting of pre-clinical stroke, and the miR-17-92 cluster shown to be therapeutic – mediating proliferation and survival of neural progenitor cells following stroke (Liu et al., 2013c). As miRs-93 and -20b were therefore more novel in the setting of ischaemic stroke they were taken forward for further investigation. miR-93 has a higher endogenous level of expression in SHRSP rat brain than miR-20b (average Ct 27 vs. 32) and in SHRSP serum (average Ct 27 vs. 31) and it was not clear whether both miRNAs would be modulated to the same extent following equivalent doses of miRNA modulating agents. miRs -93 and -20b were therefore both taken forward for pilot testing *in vivo* to investigate which miRNA showed the greatest change in expression following modulation by delivery of miRNA mimic loaded exosomes.

5.2.2 Loading of miRNAs into Exosomes

miRNA mimics were synthetically loaded into exosomes by electroporation, using a protocol optimised for our group by Dr. Emily Ord. This protocol was developed from a protocol originally published by El-Andaloussi and colleagues (El-Andaloussi et al., 2012) and involves the insertion of miRNAs (by electroporation) into EVs, previously isolated from the brains of SHRSP rats. This protocol is summarised in Figure 5.3 and is given in detail in sections 2.5.1.3 and 2.5.3. During electroporation short duration, high voltage electrical field pulses cause the reversible breakdown of the cellular membrane, via the formation of pores. The pores allow small molecules (such as oligonucleotides) to be introduced into the EV. Uptake of oligonucleotides continues until the pores close.

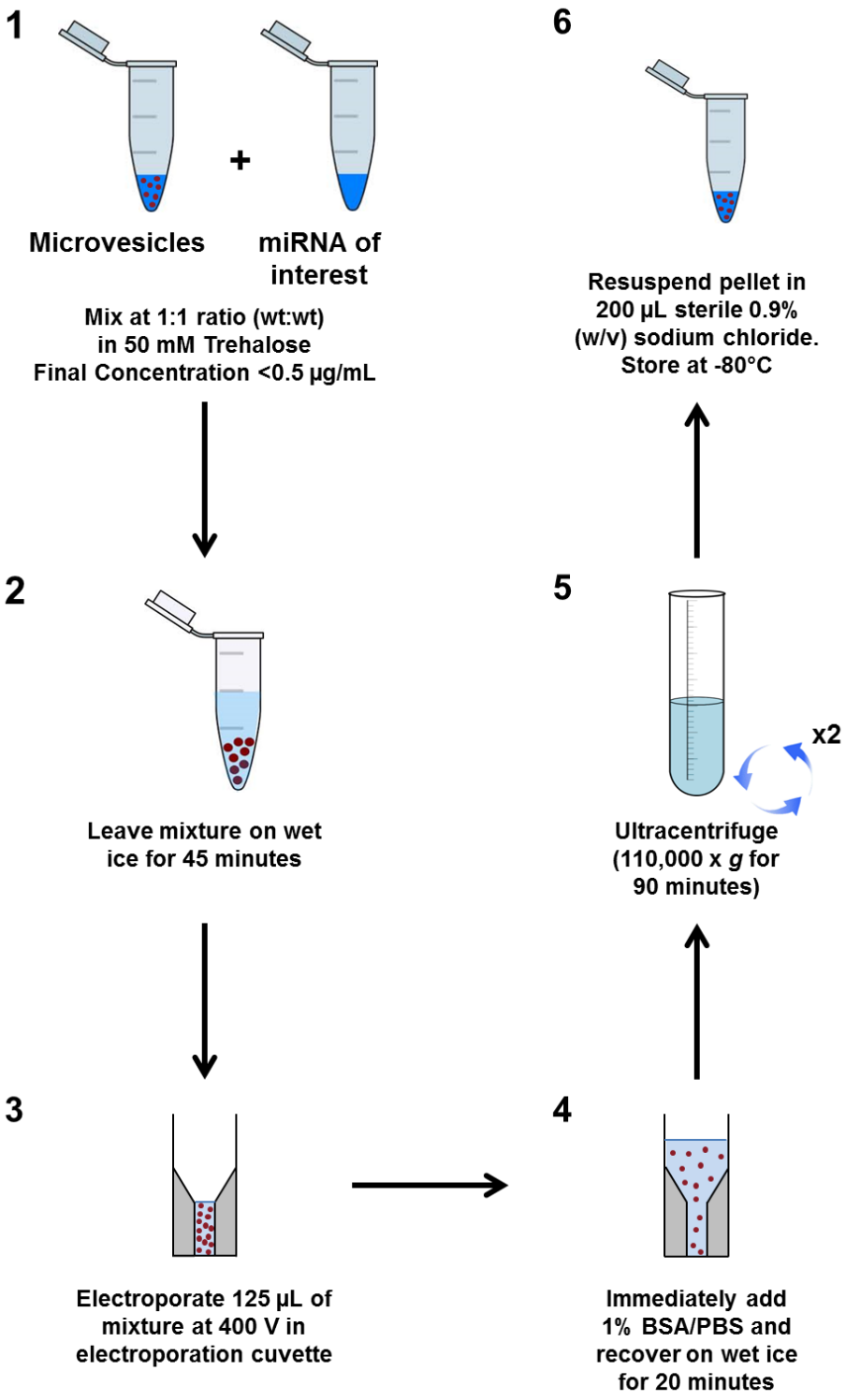

Figure 5.3 – Exosome Electroporation Protocol
miRNAs were loaded into EVs previously isolated from SHRSP rat brain. 1. The mimic for the miRNA of interest was initially mixed in a 1:1 ratio with EVs. Both were diluted in 50 mM Trehalose. 2. The mixture was left on wet ice for 45 minutes. 3. A small volume of EV/miRNA mimic mixture (125 µL) was added to an electroporation cuvette and given a 400 V pulse in a Bio-Rad MicroPulser™. 4. Immediately following electroporation ice cold 1% (w/v) BSA (875 µL) was added and mixed with the electroporated EVs before being transferred to a falcon tube on wet ice and left for 20 minutes. 5. The electroporated EV mixture was then ultra-centrifuged at 25.4 k rpm for 1.5 hours before the EV pellet was resuspended in DPBS and ultra-centrifuged again at 25.4 k rpm for 1.5 hours. 6. The EV pellet was then resuspended in 200 µL 0.9% (w/v) sodium chloride (sterile) before being stored at -80ºC until use.

5.2.3 Delivery of Exosomal miRNAs

For the *in vivo* experiments in the present study, miRNA loaded EVs were administered intra-nasally in SHRSP rats. A complete protocol is given in section 2.7.6. This method had previously been used by Dr. Emily Ord, who demonstrated successful up-regulation of miR-520b following intra-nasal delivery of miR-520b loaded exosomes to naïve SHRSP rats. Four deliveries of 100 µg of miR-520b exosomes over 2 days resulted in substantial up-regulation of miR-520b in the olfactory bulb tissue and rostral brain tissue.

For the *in vitro* experiments in the present study, miRNA loaded EVs were added directly to cell culture medium (see section 0 for a complete protocol). This method had previously been used by Dr. Emily Ord – miR-520b was up-regulated in B50 neuronal cells following delivery of 875 ng exosomes into the cell culture medium 1 day after the cells were seeded. miR-520b expression was assessed 2 days after cells were treated with exosomes.

5.3 Results

5.3.1 Characterisation of miRNA Loaded EVs

EVs were isolated by sequential centrifugation from 8 SHRSP brain hemispheres. A portion of these EVs were subsequently loaded with miRNA-93 or miR-20b via electroporation. They were then visualised and quantified using a NanoSight LM10 (Figure 5.4). These experiments were performed twice (Batch #1 and Batch #2) to create enough extracellular vesicles to use in the presented study. The NanoSight traces show that while there some extracellular vesicles in each sample that were within the exosome size range of 30-120 nm (~15-20%), the majority of EVs were moderately larger. The mean particle size of naïve EVs in Batch #1 was 176 nm and in Batch#2 was 172 nm. The mean particle size of electroporated EVs in Batch #1 was 180 nm and in Batch #2 184 nm.

EVs were subsequently visualised on a transmission electron microscope. EVs were isolated or electroporated as usual, before the pellet was resuspended in 2% paraformaldehyde before being fixed onto Formvar-carbon coated electron microscope (EM) grids according the protocol provided in Current Protocols in Cell Biology (Théry et al., 2006). Samples were contrasted using uranyl oxalate before being contrasted and embedded in a mixture of 4% uranyl acetate and 2% methyl cellulose. In this experiment it was difficult to obtain clear images where the methyl cellulose film was too thick. Extracellular vesicles were embedded and prepared for electron microscopy by Mrs Margaret Mullin.

Electron microscopy of negatively stained naïve (Figure 5.5A) and electroporated (Figure 5.5B) extracellular vesicle samples revealed predominantly cup-shaped membrane vesicles. Representative images were selected from the images taken for each extracellular vesicle isolation. While image quality and the angle at which the EVs embedded in the methyl cellulose membrane made it difficult to take accurate measurements, it is clear the majority of vesicles isolated are 200 nm or less in diameter, as the NanoSight also demonstrated.

A

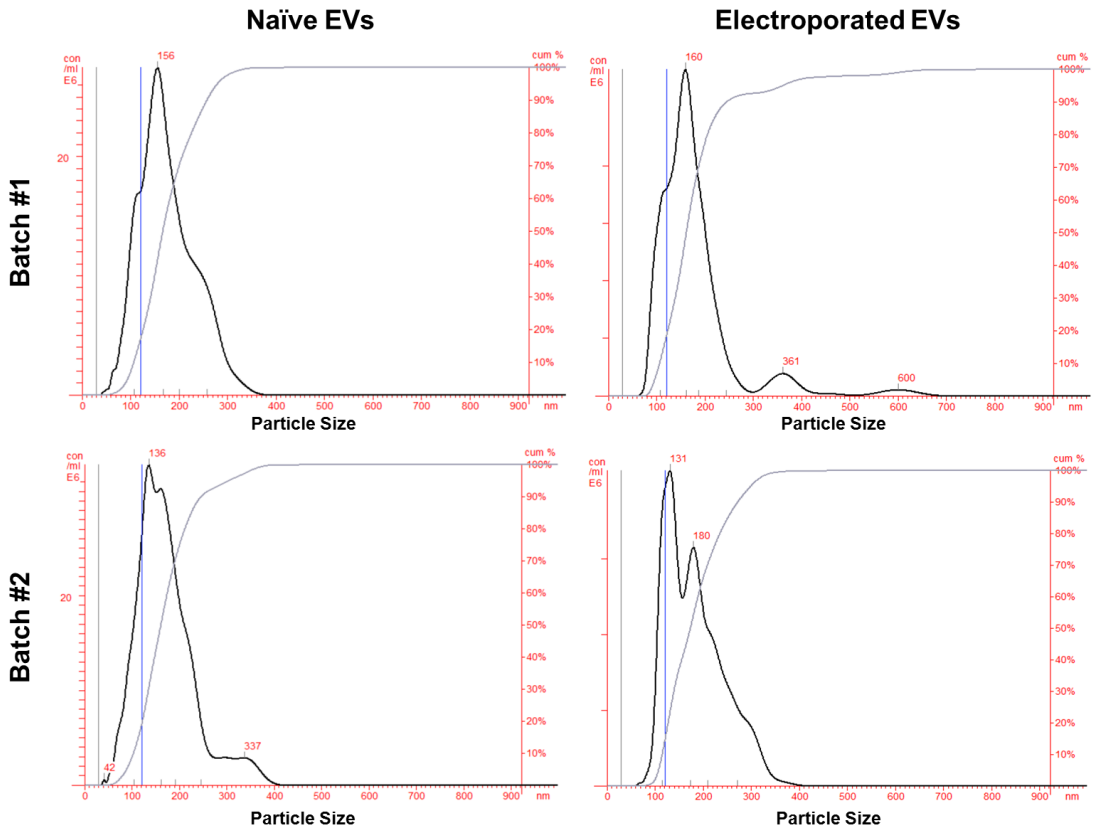

B

Batch	Concentration: all particles (particles/mL)	Concentration: particles 30-120 nm (particles/mL)	Mean Particle Size	Mode Particle Size	Standard Deviation
#1 Naive	3.28 x 10^{12}	5.5 x 10^{11}	176 nm	156 nm	55 nm
#1 Electroporated	5.96 x 10^{11}	1.08 x 10^{11}	180 nm	160 nm	85 nm
#2 Naïve	4.12 x 10^{12}	7.68 x 10^{11}	172 nm	136 nm	60 nm
#2 Electroporated	4.68 x 10^{11}	6.8 x 10^{10}	184 nm	131 nm	59 nm

Figure 5.4 - NanoSight Characterisation of Extracellular Vesicles
Naïve EVs were isolated from 8 SHRSP brain hemispheres. A portion of these EVs were subsequently electroporated with miR-93 or miR-20b. The concentration of particles within each sample was determined using a NanoSight LM10. NanoSight traces for each sample are shown (A). The black trace indicates the concentration of exosomes with increasing particle size, while the grey trace shows the cumulative percentage of exosomes with increasing particle size. The concentration of particles of all sizes, the concentration of particles sized 30-120 nm, the mean particle size, the mode particle size and the standard deviation for each sample is also listed (B).

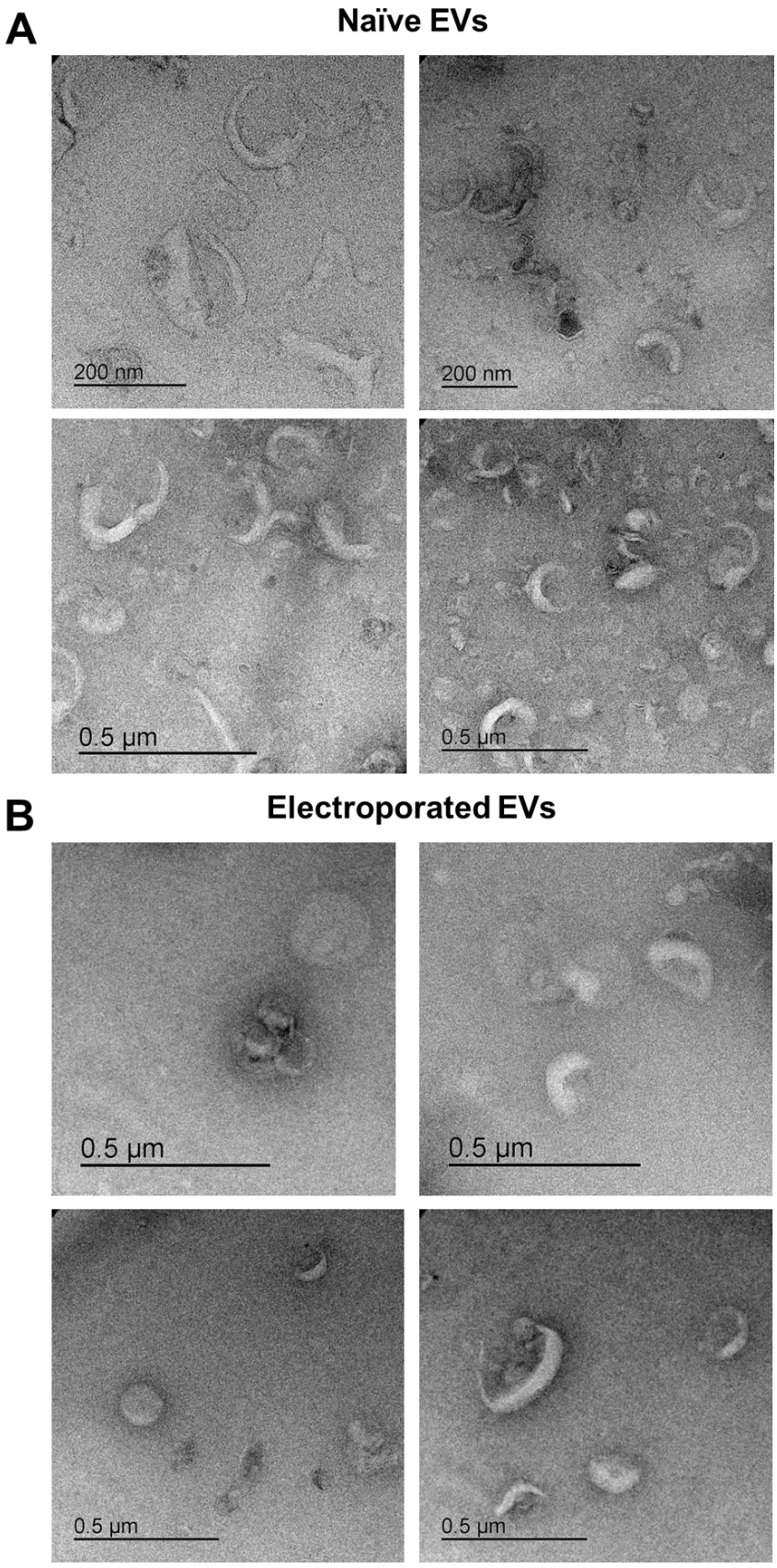

Figure 5.5 - TEM Characterisation of Extracellular Vesicles
Electron-microscopic observation of whole-mounted EVs. EVs were isolated from 8 SHRSP brain hemispheres. A portion of these extracellular vesicles were subsequently electroporated with miR-93. Representative images of naïve (A) and miR-93 loaded electroporated (B) extracellular vesicles obtained by transmission electron microscopy showing both larger microvesicles and exosome sized vesicles.

5.3.2 Delivery of miRNA Loaded EVs *in vivo*

5.3.2.1 Delivery of miRNA Loaded EVs to SHRSP post-tMCAO

A protocol was designed to assess the therapeutic effect of modulating miR-17 family miRNAs post-stroke via intra-nasal delivery of miR-17 family loaded EVs *in vivo* (Figure 5.6).

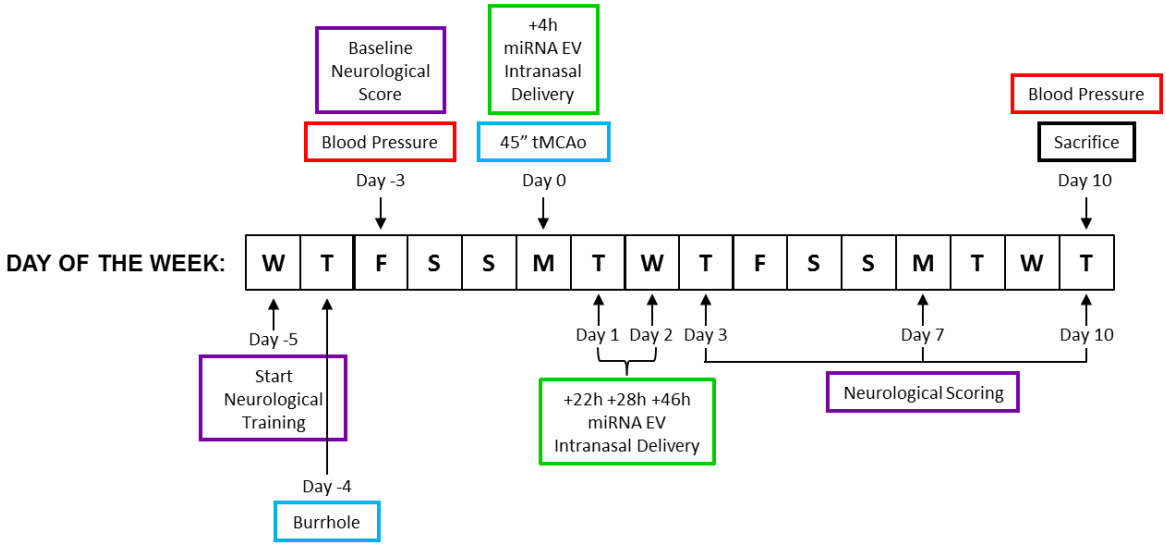

Figure 5.6 - Animal Study Protocol
This diagram illustrates the planned protocol for the animal study. Neurological and behavioural test training was to start 5 days prior to tMCAO surgery. A pre-stroke cranial burrhole was to be performed 4 days prior to tMCAO surgery. 3 days prior to stroke surgery a baseline neurological score was to be measured along with baseline blood pressure. On Day 0 a 45 minute tMCAO surgery was to be performed. 4 hours post-reperfusion the first intra-nasal delivery of miRNA loaded EVs was to be administered, followed by subsequent equivalent intra-nasal deliveries at 22, 28 and 46 hours post-reperfusion. Neurological and behavioural tests were to be performed on days 3, 7 and 10 post-tMCAO surgery. Finally, on day 10 the SHRSP was to have a final blood pressure measurement recorded before being sacrificed by transcardial perfusion fixation.

SHRSP rats were to receive miR-93 or miR-20b loaded EVs and control animals were to receive either naïve EVs or sterile saline. The protocol involved the measurement of baseline blood pressure and neurological and behavioural scores before tMCAO surgery would be performed on Day 0 of the protocol. At 4 hours post-reperfusion the first dose of intra-nasal miRNA loaded EVs were to be administered. Subsequently on days 1 and 2 of the protocol, miRNA loaded EVs were to be administered at 22, 28 and 46 hours post-reperfusion. Behavioural tests were to be repeated on days 3, 7 and 10, following which each SHRSP rat was to have blood pressure measurements recorded before being sacrificed by transcardial perfusion fixation. Subsequently, their brains were to be sectioned

and tissue stained with haemotoxylin and eosin (H&E) to identify infarcted tissue which would be quantified. The primary end points chosen to demonstrate therapeutic effect of miR-17 family loaded EVs were reduced infarct size and improved neurological score in SHRSP as compared to SHRSP that received naïve EVs (not loaded with any particular miRNA) or sterile saline.

Due to time and cost constraints the therapeutic effect of only 1 EV packaged miRNA could be examined in the full animal study. Therefore, to assess the extent of modulation of miR-93 and miR-20b *in vivo* following post-tMCAO intra-nasal delivery of these EV packaged miRNAs, a pilot study was designed (Figure 5.7) in which these EV miRNAs would be delivered post-stroke at the same time points as in the planned animal study. However, SHRSP rats would be sacrificed at Day 3, rather than Day 10, and miRNA expression measured, to allow for quick identification of which miRNA was modulated the most.

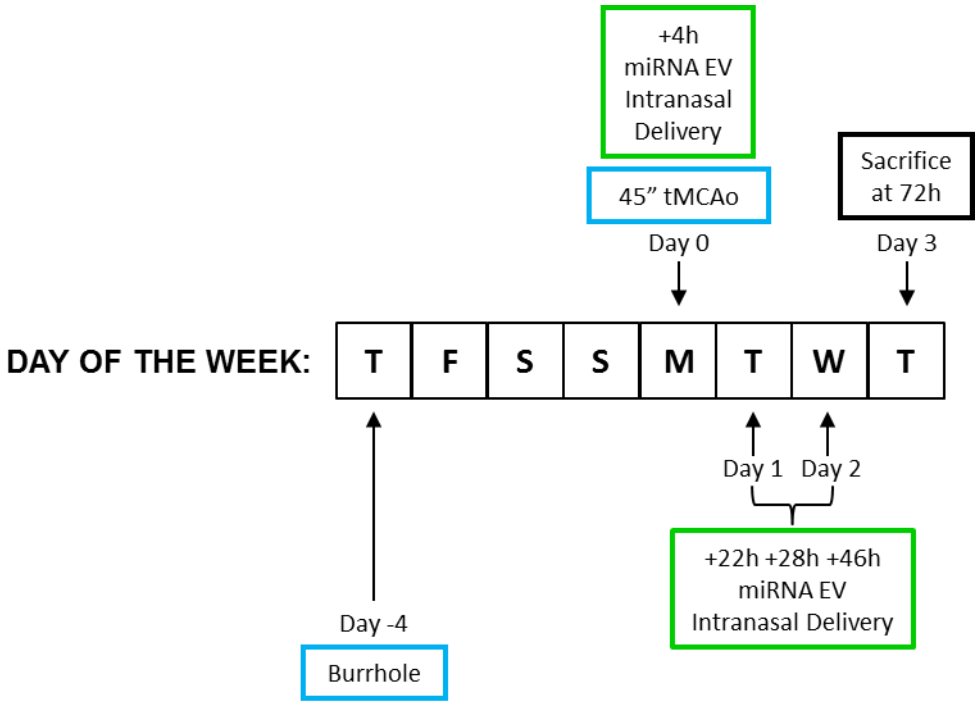

Figure 5.7 - Pilot Study Experimental Plan
This diagram illustrates the protocol for the pilot study which aimed to discover the extent of modulation of miRs -93 and -20b following delivery of EV packaged miRNAs. A pre-stroke cranial burrhole was performed 4 days prior to tMCAO surgery. On day 0 a 45 minute tMCAO surgery was performed. 4 hours post-reperfusion the first intra-nasal delivery of miRNA loaded EVs was to be administered (75 µg). Subsequent equivalent intra-nasal deliveries were given at 22, 28 and 46 hours post-reperfusion. Finally, on day 3 the SHRSP was euthanised and fresh brain tissue harvested and immediately frozen in liquid nitrogen.

In the pilot study, animals were euthanised by terminal anaesthesia and removal of the heart to allow for the harvesting of fresh tissue, in which miRNA expression could be studied (for a full description see section 2.7.7.4). Tissue needed for further analysis (in this case, brain) was removed from the body as quickly as possible. The brain tissue harvested was then quickly sectioned as is shown in Figure 5.8. The cerebellum and olfactory bulbs were initially separated from the cerebral hemispheres. The cerebral hemispheres were sectioned into 4 slices, and in each slice the cortex was separated from the striatum in each hemisphere. All brain sections were then placed in eppendorfs and stored in liquid nitrogen until they could be placed in a -80ºC freezer for long-term storage. The aim of sectioning tissue in this way was to discover areas of the brain where modulation of miRNA expression was greatest and to help discover the mechanisms by which EVs were taken up by the brain and the pathway by which their effect was mediated.

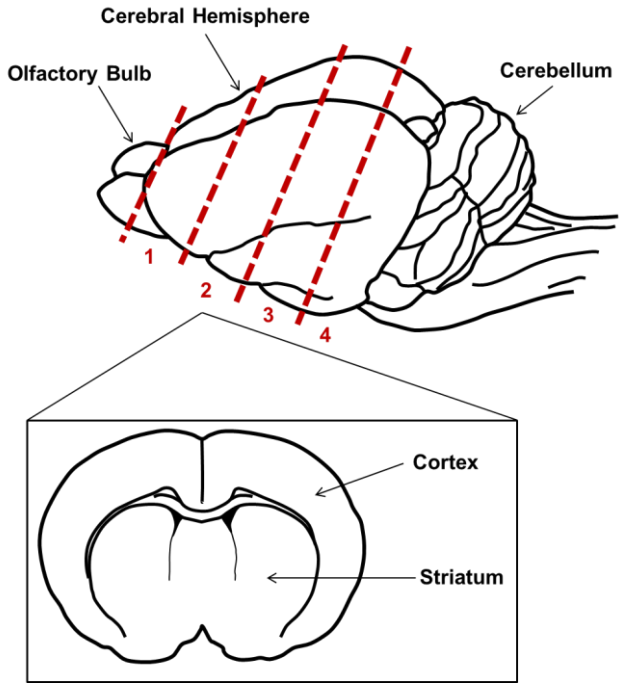

Figure 5.8 – Illustration of Brain Tissue Sectioning
The brain tissue was carefully but quickly removed from freshly euthanised SHRSP rats. The cerebellum and olfactory bulbs were initially separated from the cerebral hemispheres. The cerebral hemispheres were subsequently sectioned into 4 slices and in each slice the cortex was separated from the striatum in each hemisphere.

In the pilot study we aimed to profile miRNA expression in 9 SHRSP rats: SHRSP that received sterile saline (n=3), miR-93 EVs (n=3) or miR-20b EVs (n=3) post-tMCAO. Unfortunately there was a high mortality rate in some animal groups.

This is illustrated in the Kaplan Meier Analysis of SHRSP survival in the pilot study (Figure 5.9). 3 animals received sterile saline but only 1 survived to 72 hours, 3 animals received miR-93 EVs and all survived to 72 hours and 5 animals received miR-20b EVs, of which 2 survived to 72 hours. While the greatest percentage survival was observed in animals who received miR-93 EVs, there is no significant difference in the survival curves, as assessed by log-rank test.

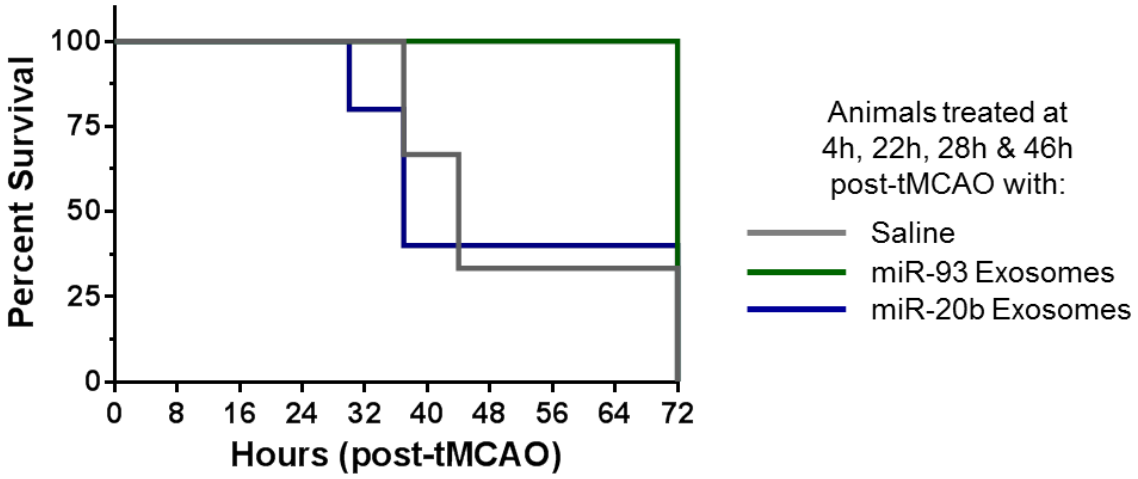

Figure 5.9 – Kaplan Meier Analysis of Animal Survival in Pilot Study
Survival probability is plotted over time, showing the greatest percentage survival in animals who received miR-93 EVs relative to control (sterile saline) or other treatment (miR-20b EVs) after tMCAO. The animals used in the pilot study are shown, with time plotted as hours post-reperfusion in tMCAO surgery. Animal groups were SHRSP rats who underwent tMCAO surgery and received sterile saline (n=3), miR-93 EVs (n=3) or miR-20b EVs (n=5). Survival curves were compared by log-rank test with all comparisons non-significant.

These surgeries were very time intense as a result of the staggered EV delivery timings. As there were significant time constraints it was decided to stop the pilot study early and examine miRNA expression in the animal tissue collected up until that point. miRNA expression was analysed in all animals that survived to 72 hours (Figure 5.10 and Figure 5.11) and also in animals that were euthanised prematurely or found immediately after death (data not shown).

In this chapter miRNA expression is sometimes expressed as $1/\Delta Ct$ rather than RQ, as in previous chapters. This is so that any endogenous differences in basal miRNA expression following treatment with exosomes or hypoxic challenge can be observed between control groups. As an increased ΔCt actually reflects a lower level of miRNA expression data is presented as $1/\Delta Ct$ so that the graphs reflect the real change of direction.

miR-93 expression was not increased in the brain tissue of animals that received miR-93 EVs post-tMCAO surgery, as compared to animals that received sterile saline (Figure 5.10). Although there is only 1 animal in the saline treated group, miR-93 expression appears to be unchanged in the majority of tissue sections examined. miR-93 expression was moderately increased in contralateral S1 tissue of animals treated with miR-93 EVs. In all other tissue sections harvested from animals treated with miR-93 EVs, miR-93 expression was unchanged or even slightly decreased as compared to animals treated with saline.

miR-20b expression was also not increased in the brain tissue of animals that received miR-20b EVs post-tMCAO surgery, as compared to animals that received sterile saline (Figure 5.11). While it is difficult to make firm conclusions from these results due to the low 'n' in both animal groups, miR-20b expression appeared to be unchanged in the majority of tissue sections examined. Its expression was moderately decreased in some brain sections of animals that received miR-20b EVs (ipsilateral C3, CB; contralateral C2, CB) as compared to SHRSP that received sterile saline. In other brain sections miR-20b expression was moderately increased in SHRSP that received miR-20b EVs post-tMCAO (ipsilateral S4; contralateral C4, S1) as compared to those who received saline.

However, as the small changes observed in miR-93 and miR-20b expression, following treatment with miR loaded EVs, do not occur in a consistent manner, or in a pattern that would be expected following intra-nasal delivery and on the whole miRNA expression is unchanged, it is difficult to tell whether the changes observed are a result of the intra-nasal exosomal delivery, the stroke itself or simply, the low 'n' number and variability between the severity of stroke in these animals. In Chapter 4 it was demonstrated that total miR-93 and miR-20b expression is not altered in either ipsilateral or contralateral peri-infarct tissue of SHRSP rats at either 24 or 72 hours post-stroke (Figure 4.32).

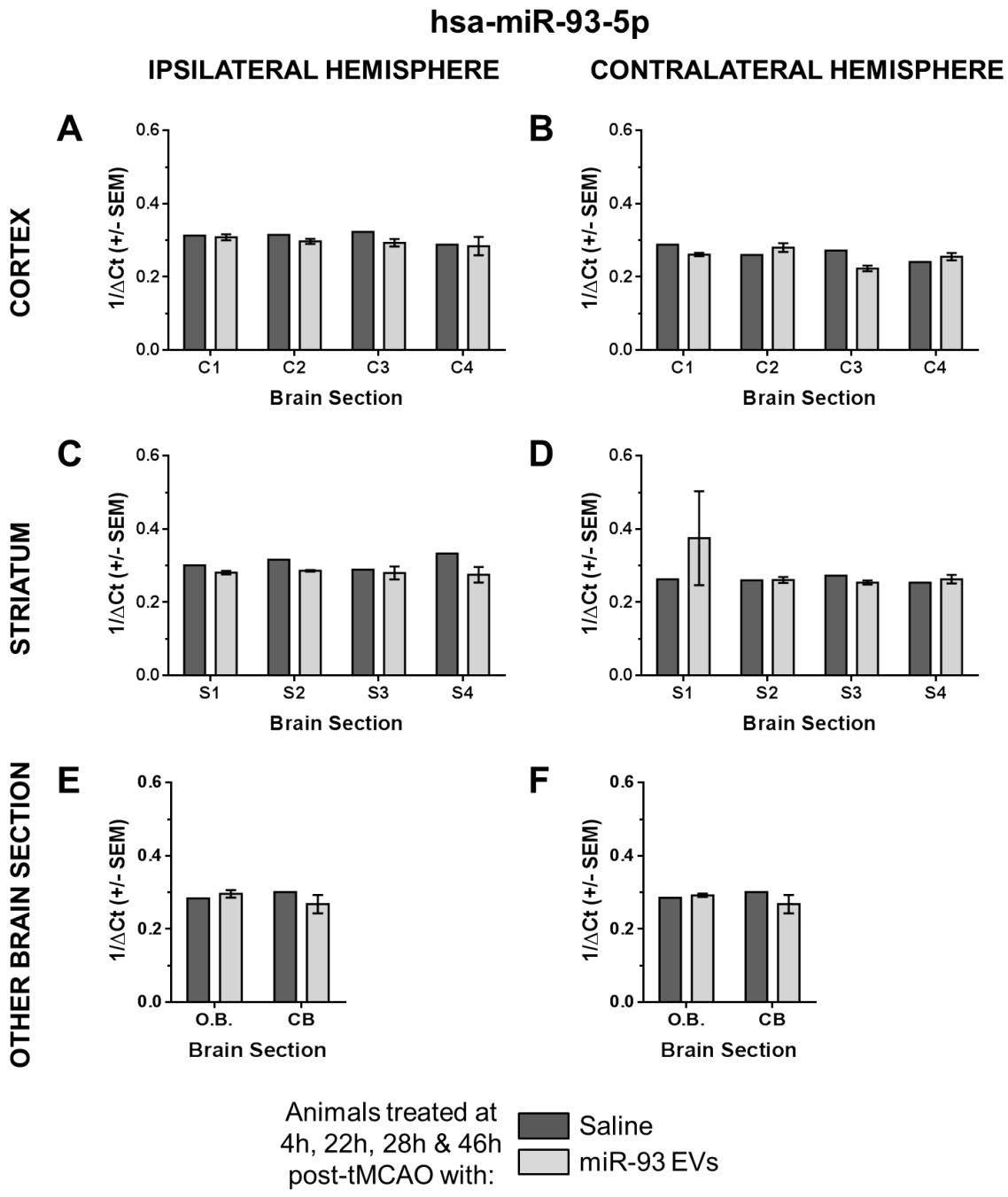

Figure 5.10 - miR-93 EV Delivery post-tMCAO
The expression of miR-93 was assessed in the brain tissue of SHRSP rats who received 300 µg of miR-93 EVs (n=3) or an equivalent volume of sterile saline (n=1) post-tMCAO. miR-93 expression was assessed in ipsilateral and contralateral cortex (A, B), striatum (C,D) and olfactory bulb and cerebellum (E,F) tissue. miRNA expression was assessed at 72 hours post-reperfusion from tMCAO surgery, by qRT-PCR. Expression was normalised to that of U87. Data shown is 1/ΔCt values (± SEM). Abbreviations include: C1, cortex section 1; S1, striatum section 2; O.B., olfactory bulb; CB, cerebellum.

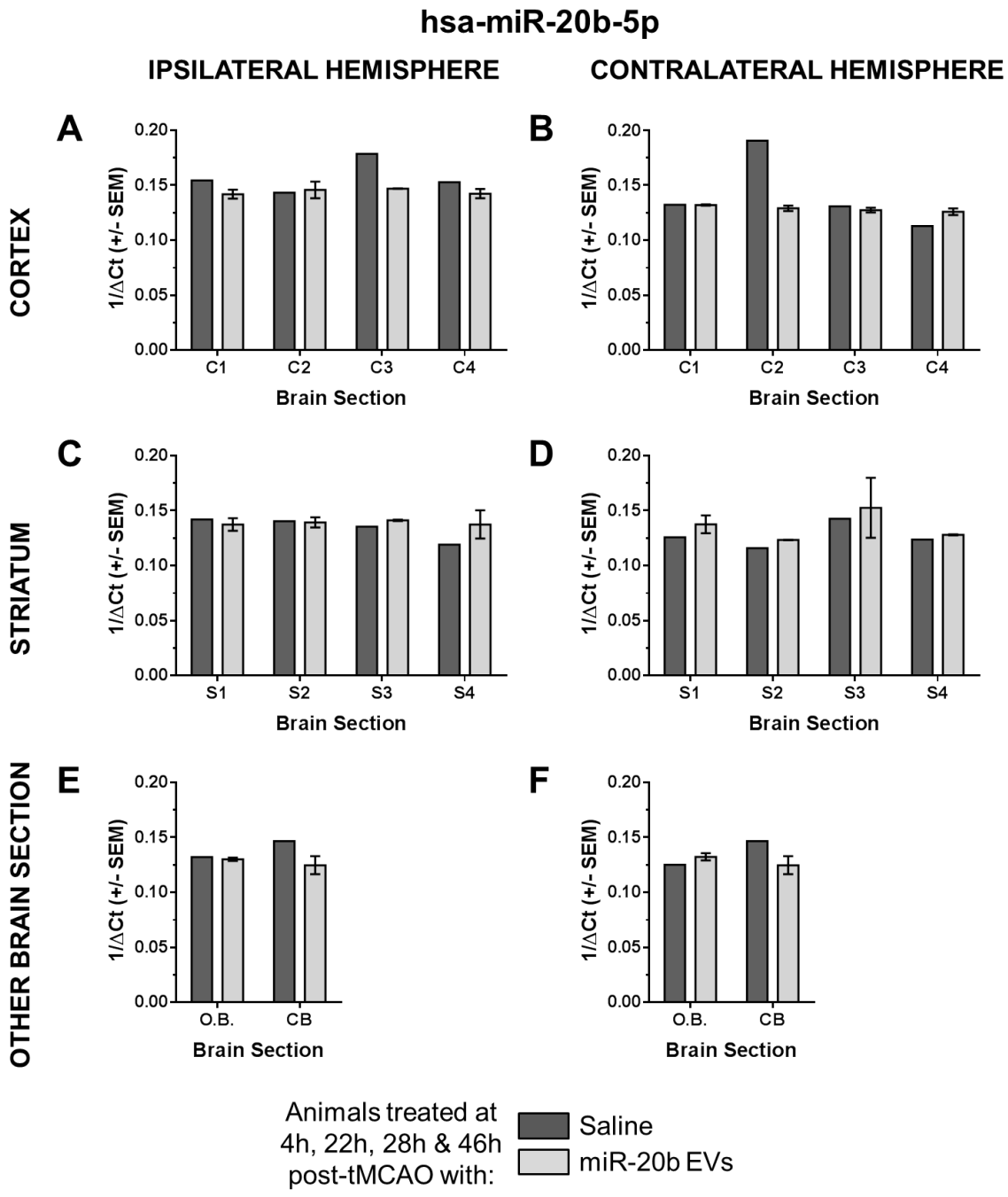

Figure 5.11 - miR-20b EV Delivery post-tMCAO
The expression of miR-20b was assessed in the brain tissue of SHRSP rats who received 300 µg of miR-20b EVs (n=2) or an equivalent volume of sterile saline (n=1) post-tMCAO. miR-20b expression was assessed in ipsilateral and contralateral cortex (A, B), striatum (C,D) and olfactory bulb and cerebellum (E,F) tissue. miRNA expression was assessed at 72 hours post-reperfusion from tMCAO surgery, by qRT-PCR. Expression was normalised to that of U87. Data shown is 1/ΔCt values (± SEM). Abbreviations include: C1, cortex section 1; S1, striatum section 2; O.B., olfactory bulb; CB, cerebellum.

As a result of the data presented here it was decided that it would not be prudent to proceed with the full animal study when there was uncertainty as to the extent of miRNA modulation following intra-nasal delivery of miR-loaded EVs. Instead, new experiments were designed to try and elucidate whether miRNA expression was altogether unchanged following exosomal miRNA delivery (i.e. a problem with the miRNA loaded EVs) or whether intra-nasal delivery was not successful as a result of concomitant health issues associated with tMCAO surgery. To this end, a small study where miR-20b loaded EVs were delivered to naïve rats was carried out.

5.3.2.2 Delivery of Exosomal miRNAs to Naïve SHRSP

To examine whether miRNA expression was increased in naïve rats following intra-nasal delivery of miRNA loaded EVs, naïve rats were given four deliveries of 75 µg miRNA loaded EVs over a period of 2 days (total 300 µg). Control animals were given an equivalent volume of sterile saline. Rather than delivering the EVs at the time points used when delivering post-tMCAO a protocol was followed (Figure 5.12) that had previously been successfully used in our group to modulate miR-520b expression in naïve rats. The naïve SHRSP rats were sacrificed on Day 5 of the protocol and fresh brain tissue harvested and immediately frozen.

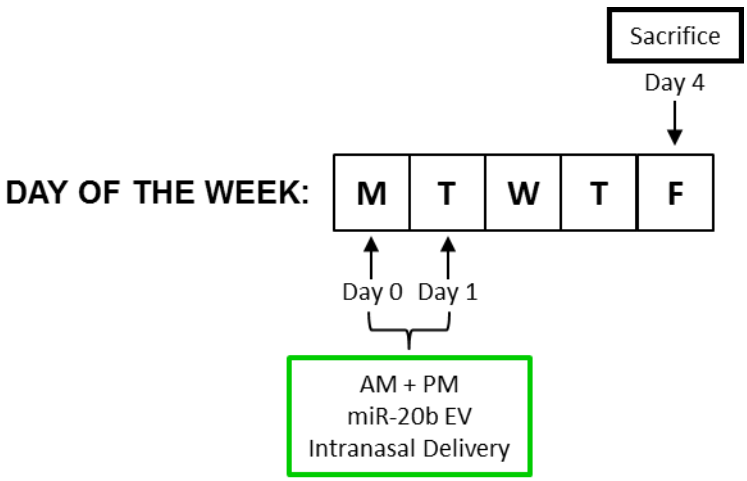

Figure 5.12 - Delivery of EVs to Naïve SHRSP, Experiment Protocol
This diagram illustrates the protocol followed for the study which aimed to discover the extent of modulation of miR-20b in naïve SHRSP rats following delivery of miR-20b EVs. On Days 0 and 1 intra-nasal deliveries of miR-20b EVs (75 µg each time) were given in the morning and evening (4 deliveries, 300 µg total) to naïve SHRSP rats. On Day 5 animals were euthanised and fresh brain, lung and kidney tissue was harvested and immediately frozen in liquid nitrogen.

Due to cost constraints only miR-20b EVs (and not miR-93 EVs) were given to naïve rats (n=3). As miR-20b has a lower endogenous level of expression in the brain than miR-93 this miRNA was chosen as it was hypothesised that a greater level of modulation would be observed following modulation of a miRNA with lower endogenous expression (as was observed in previous studies, Chapter 3).

miR-20b expression was unchanged in the brain tissue of naïve SHRSP rats which had received 300 µg of miR-20b EVs (via intra-nasal delivery) as compared to SHRSP rats which had received saline (Figure 5.13). While no differences in the expression of miR-20b between the two animal groups were statistically significant, there appeared to be a small decrease in miR-20b expression in some brain tissue sections following treatment with miR-20b EVs, similar to what was observed following delivery post-tMCAO, as compared to expression in saline treated animals. miR-20b expression was decreased in ipsilateral C1, S2, S4 and contralateral C2, S1, S2 and O.B. tissue. While miR-20b expression was not increased in brain tissue following intra-nasal delivery of miR-20b EVs, importantly, it was also not increased in either lung or kidney tissue (Figure 5.13 E and F).

As miR-20b expression was not modulated in either naïve (Figure 5.13) or tMCAO (Figure 5.11) rats following delivery of miR-20b EVs in comparison to control animals this confirmed that failed modulation of miRNA expression in tMCAO rats was not a result of health complications associated with tMCAO surgery.

Dr. Emily Ord had previously successfully delivered miR-520b loaded EVs to naïve rats (Figure 5.14). Although the tissue in this experiment was sectioned in a different way to the tissue in the present study, there was an obvious and significant increase in miR-520b expression in olfactory bulb, L1 and L2 tissue in animals that received miR-520b EVs as compared to those who received saline. In the ipsilateral hemisphere miR-520b was increased, on average, 4.0 fold in olfactory bulb, L1 and L2 tissue and 1.7 fold in L3 tissue in animals that received miR-520b EVs as compared to those who received saline: olfactory bulb (RQ 4.21 ± 0.67 vs. 1.00 ± 0.52), L1 (RQ 3.21 ± 1.14 vs. 1.00 ± 0.36), L2 (4.60 ± 1.27 vs. 1.00 ± 0.24), L3 (1.73 ± 0.36 vs. 1.00 ± 0.43) (Figure 5.14). Similarly, in the contralateral hemisphere miR-520b expression was increased 4.9 fold in olfactory bulb, L1 and L2 tissue (on average) and 1.6 fold in L3 tissue in animals

treated with miR-520 EVs as compared to those who received saline: olfactory bulb (RQ 4.21 ± 0.67 vs. 1.00 ± 0.52), L1 (RQ 4.71 ± 1.92 vs. 1.00 ± 0.49), L2 (5.73 ± 2.83 vs. 1.00 ± 0.41), L3 (1.59 ± 0.35 vs. 1.00 ± 0.61) (Figure 5.14).

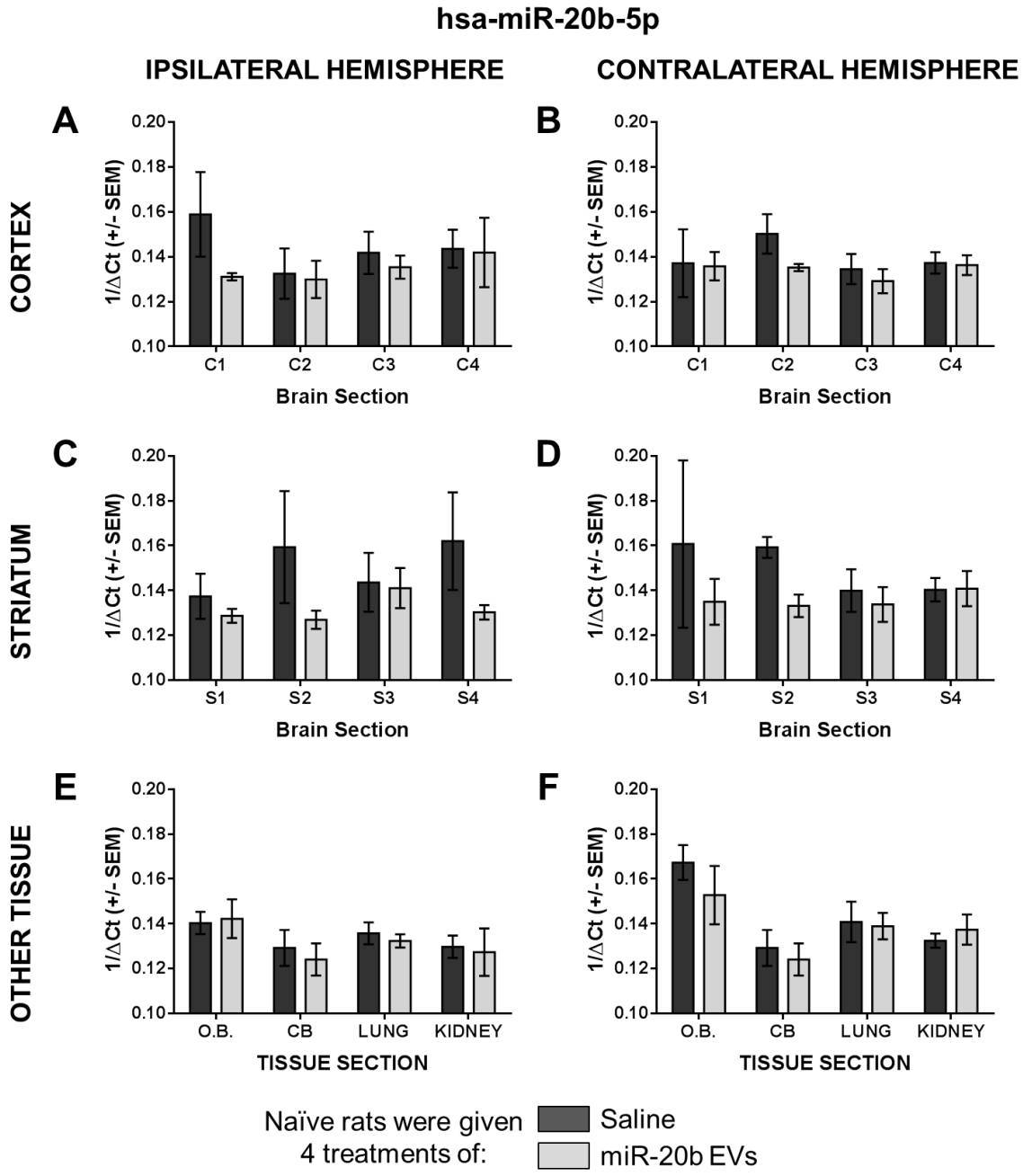

Figure 5.13 - miR-20b EV Delivery to Naïve Rats
The expression of miR-20b was assessed in the brain, lung and kidney tissue of SHRSP rats who received 300 µg of miR-20b EVs (n=3) or an equivalent volume of sterile saline (n=3). 75 µg of miR-20b EVs were delivered in the morning and evening of Day 0 and Day 1 of the protocol. miR-20b expression was assessed in ipsilateral and contralateral cortex (A, B), striatum (C,D) and olfactory bulb, cerebellum, lung and kidney (E,F) tissue. miRNA expression was assessed at Day 4, by qRT-PCR. Expression was normalised to that of U87. Data shown is 1/∆Ct values (± SEM). Probability was calculated using a one-way-ANOVA with Sidak's Multiple Comparisons Test. Abbreviations include: C1, cortex section 1; S1, striatum section 2; O.B., olfactory bulb; CB, cerebellum.

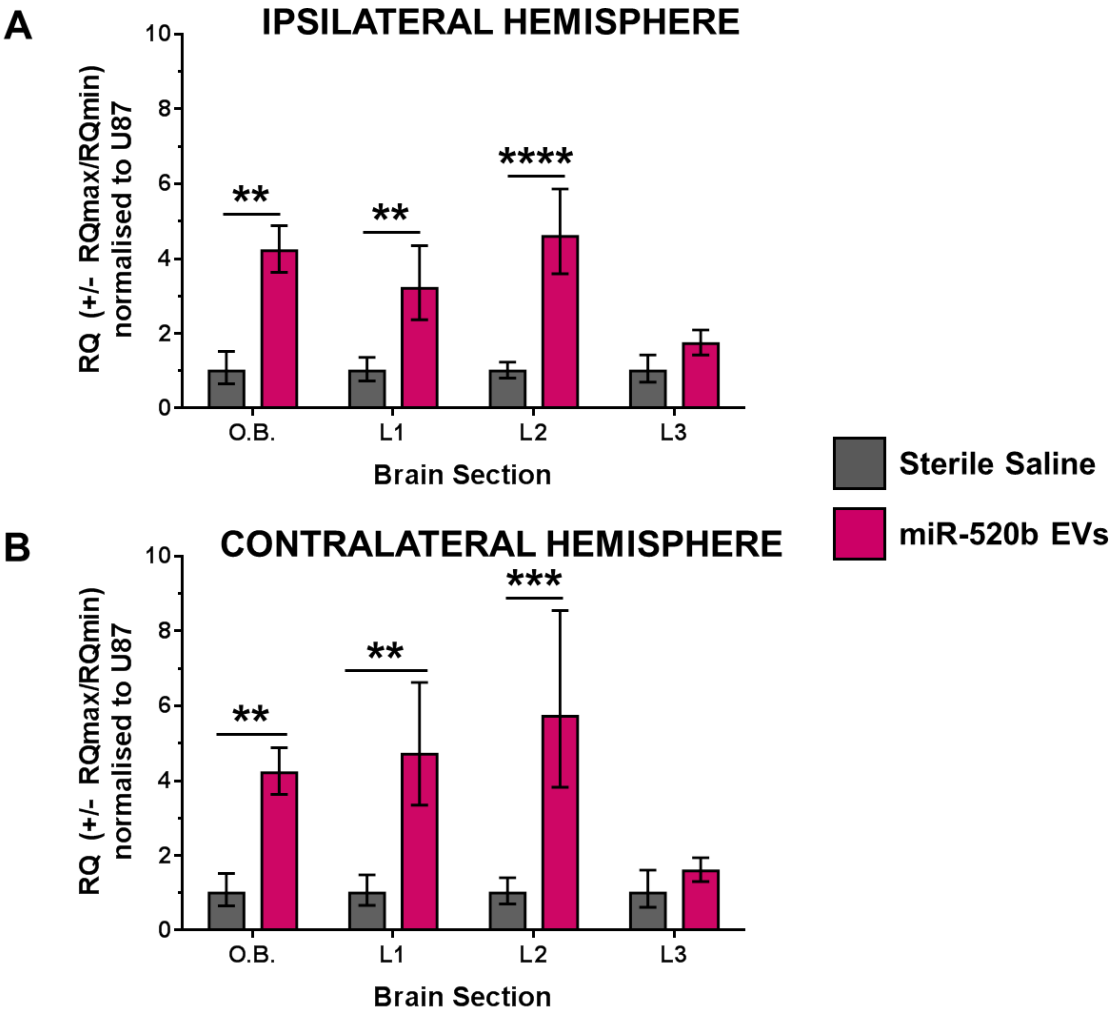

Figure 5.14 – Delivery of miR-520b EVs *in vivo*
The expression of miR-520b was assessed in the brain tissue of SHRSP rats who received 400 µg of miR-520b EVs (n=3) or an equivalent volume of sterile saline (n=4). 100 µg of miR-520b EVs were delivered in the morning and evening of Day 0 and Day 1 of the protocol. miR-520b expression was assessed in ipsilateral (A) and contralateral (B) olfactory bulb and cerebral tissue. Cerebral tissue was sectioned into 4 levels, miRNA expression was only profiled in L1-L3. Change in miRNA expression was assessed at Day 4 by qRT-PCR and relative quantification (RQ) calculated from ΔΔCt following normalisation to U87 and compared to miRNA expression in the saline treated rats. Data shown is RQ ± RQmax/RQmin. Probability was calculated using a one-way-ANOVA with Sidak's Multiple Comparisons Test: **p<0.01; ***p<0.001. Abbreviations include: O.B., olfactory bulb; L1, cerebral level/section 1. Data courtesy of Dr. Emily Ord.

Modulation of miR-93 and miR-20b expression was not achieved following post-stroke treatment with miR-93 or miR-20b EVs. miR-20b expression was also not modulated in naïve SHRSP rats following treatment with miR-20b EVs. However, modulation of miR-520b expression was clearly demonstrated in naïve SHRSP rats following treatment with miR-520b exosomes. Basal expression of miR-520b is between that of miR-93 and miR-20b (Avg Ct ~30), and so miR-520b should not have been more readily modulated as a result of its lower endogenous expression. It was therefore hypothesised that *in vivo* miRNA expression of some

miRNAs or miRNA families is more tightly regulated than that of others, making it more difficult to modulate expression of miR-93 and miR-20b than miR-520b.

As we were unable to modulate miRNA expression *in vivo* we proposed modulating miRNA expression and assessing therapeutic effect following delivery of miR loaded EVs in our *in vitro* models of ischaemic stroke.

5.3.3 Delivery of miRNA Loaded EVs *in vitro*

To examine whether delivery of miR-20b and miR-93 loaded EVs would modulate miRNA expression and result in therapeutic benefit, EVs were administered in our *in vitro* model of stroke (hypoxic injury with reperfusion). Two protocols were designed, the first where miRNA loaded EVs were delivered to cells pre-hypoxic challenge (to provide proof of concept data) and the second where miRNA loaded EVs were delivered to cells post-hypoxic challenge, a more clinically relevant route of delivery. Experiments were planned where miRNA loaded EVs would be delivered to 3 different cell types: B50 neuronal cells, B92 glial cells and GPNT cerebral endothelial cells.

To demonstrate that miRNA expression was increased following administration of miRNA loaded EVs, B50 cells were given miRNA loaded EVs pre- and post-hypoxic challenge (Figure 5.15 and Figure 5.16).

Where miR-93 EVs were administered to B50 cells pre-hypoxic challenge there was no significant increase in miR-93 expression (Figure 5.15B). miR-93 expression was slightly decreased in vehicle treated hypoxic cells as compared to normoxic cells (1/ΔCt 0.77 ± 0.05 vs. 0.94 ± 0.17). Treatment with naïve EVs reduced expression of miR-93 in normoxic cells vs. vehicle treated cells but increased expression in hypoxic cells vs. their vehicle treated counterparts. While miR-93 expression was slightly increased in normoxic cells treated with miR-93 EVs as compared to those treated with naïve EVs (1/ΔCt 0.95 ± 0.16 vs. 0.79 ± 0.13) it was not increased when compared to vehicle treated cells. miR-93 expression was slightly increased in hypoxic cells following treatment with miR-93 EVs when compared to vehicle treated cells (1/ΔCt 1.05 ± 0.1 vs. 0.77 ± 0.05) but not when compared to hypoxic cells treated with naïve EVs. All comparisons were non-significant.

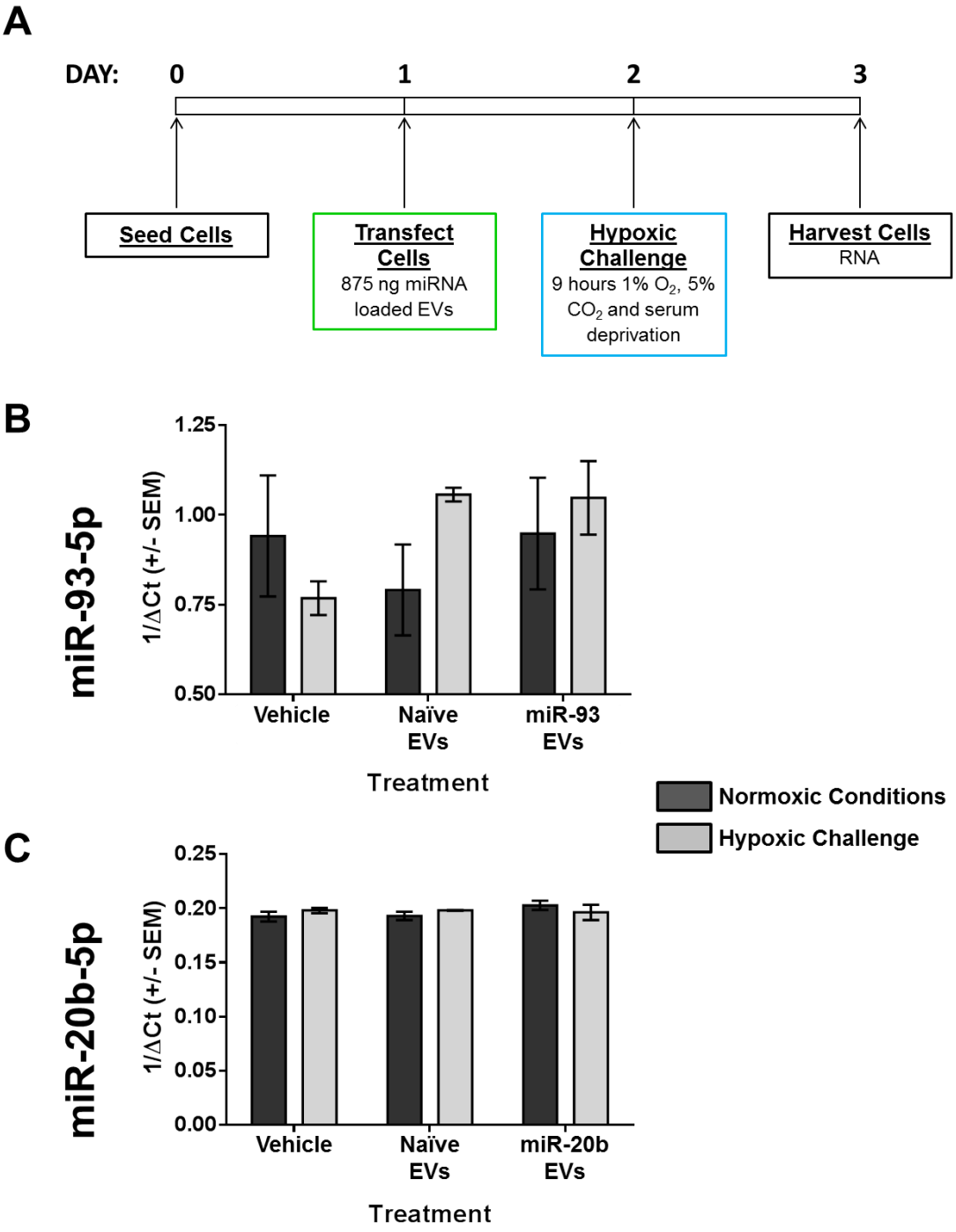

Figure 5.15 - Delivery of miRNA Loaded EVs pre-Hypoxic Challenge
The experimental protocol for pre-hypoxic challenge EV delivery is given (A). B50 neuronal cells were seeded in 12 well plates on Day 0. On Day 1 875ng of miR-93 or miR-20b loaded EVs were added to the cell culture medium. Cells were subjected to a 9 hour hypoxic challenge on Day 2 before being harvested on Day 3. The expression of miR-93 (B) and miR-20b (C) was assessed in B50 neuronal cells which had received 875 ng of naïve EVs, miRNA loaded EVs or an equivalent volume of PBS (n=3). miRNA expression was assessed at Day 3, by qRT-PCR. Expression was normalised to that of U87. Data shown is 1/ΔCt values (± SEM). Probability was calculated using a one-way-ANOVA with Tukey's Multiple Comparisons Test.

When miR-20b EVs were administered to B50 cells pre-hypoxic challenge there were no changes in miR-20b expression (Figure 5.15C). miR-20b expression was

unchanged in vehicle treated cells following hypoxic challenge as compared to normoxic cells (1/ΔCt 0.20 ± 0.003 vs. 0.19 ± 0.005). Treatment with naïve EVs did not alter miR-20b expression (1/ΔCt hypoxic 0.20 ± 0.0003 vs. normoxic 0.19 ± 0.004). Similarly, treatment with miR-20b EVs did not modulate miR-20b expression in B50 cells (1/ΔCt hypoxic 0.20 ± 0.007 vs. normoxic 0.20 ± 0.004).

Where miR-93 EVs were administered to B50 cells post-hypoxic challenge there was also no significant changes in miR-93 expression (Figure 5.16B). miR-93 expression was slightly increased in vehicle treated hypoxic cells as compared to normoxic cells (1/ΔCt 0.86 ± 0.10 vs. 0.76 ± 0.14). Treatment with naïve EVs increased expression of miR-93 in normoxic and hypoxic cells vs. their counterpart vehicle treated cells (1/ΔCt normoxic 0.94 ± 0.01 vs. 0.76 ± 0.14 and hypoxic 1.02 ± 0.08 vs. 0.86 ± 0.10). In normoxic cells treated with miR-93 EVs expression of miR-93 was unchanged as compared to vehicle treated cells and decreased as compared to cells treated with naïve EVs (1/ΔCt 0.79 ± 0.03). In hypoxic cells treated with miR-93 EVs, expression of miR-93 was slightly increased as compared to vehicle treated cells but unchanged in comparison to cells treated with naïve EVs (1/ΔCt 1.04 ± 0.12). All comparisons were non-significant.

When miR-20b EVs were administered to B50 cells post-hypoxic challenge there were no changes in miR-20b expression (Figure 5.16C). miR-20b expression was unchanged in vehicle treated cells following hypoxic challenge as compared to normoxic cells (1/ΔCt 0.18 ± 0.006 vs. 0.18 ± 0.01). Treatment with naïve EVs did not modulate expression of miR-20b in normoxic or hypoxic cells in comparison to their counterpart vehicle treated cells (1/ΔCt normoxic 0.19 ± 0.005 vs. 0.18 ± 0.01 and hypoxic 0.18 ± 0.02 vs. 0.18 ± 0.006). In normoxic cells treated with miR-20b EVs, expression of miR-20b was unchanged as compared to vehicle or naïve EV treated cells (1/ΔCt 0.21 ± 0.002). In hypoxic cells treated with miR-20b EVs, expression of miR-20b was slightly increased as compared to vehicle and naïve EV treated cells (1/ΔCt 0.23 ± 0.04). All comparisons were non-significant.

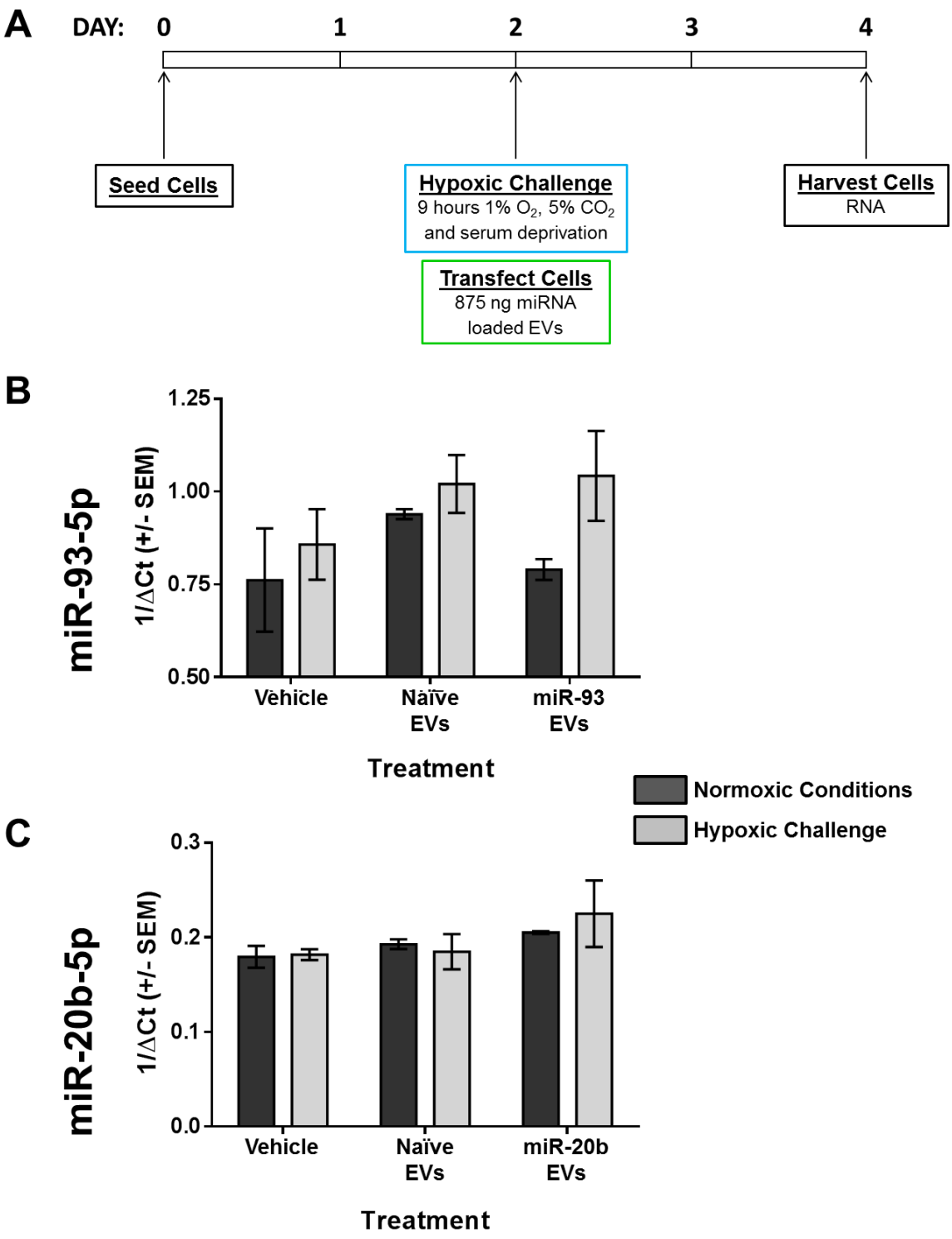

Figure 5.16 - Delivery of miRNA Loaded EVs Post-Hypoxic Challenge
The experimental protocol for post-hypoxic challenge EV delivery is given (A). B50 neuronal cells were seeded in 12 well plates on Day 0. Cells were subjected to a 9 hour hypoxic challenge on Day 2. Immediately following reoxygenation (post hypoxic challenge) 875ng of miR-93 or miR-20b loaded EVs were added to the cell culture medium. Cells were harvested on Day 4. The expression of miR-93 (B) and miR-20b (C) was assessed in B50 neuronal cells which had received 875 ng of naïve EVs, miRNA loaded EVs or an equivalent volume of PBS (n=3). miRNA expression was assessed at Day 4, by qRT-PCR. Expression was normalised to that of U87. Data shown is 1/ΔCt values (± SEM). Probability was calculated using a one-way-ANOVA with Tukey's Multiple Comparisons Test.

Modulation of miR-93 and miR-20b expression was not observed *in vitro* following treatment with miRNA loaded EVs. However, this method had previously been used by Dr. Emily Ord, who showed significant up-regulation of miR-520b following delivery of miR-520b loaded EVs to B50 neuronal cells, *in vitro* (Figure 5.16). In the protocol used for this experiment, B50 cells were seeded on Day 0, given 875 ng of naïve EVs, miRNA mimic, EV/miRNA mimic mixture or miR-520b loaded EVs on Day 1 and RNA harvested on Day 3. There was no significant increase in miR-520b expression following treatment with naïve EVs (RQ 1.69 ± 0.13 vs. 1.00 ± 1.77), miRNA mimic (RQ 2.72 ±0.07 vs. 1.00 ± 1.77) or EV/miRNA mimic mixture (RQ 2.89 ± 0.72 vs. 1.00 ± 1.77). However, following treatment with miR-520b loaded EVs expression of miR-520b was significantly increased, more than 1000-fold (RQ 1364.20 ± 78.10 vs. 1.00 ± 1.77).

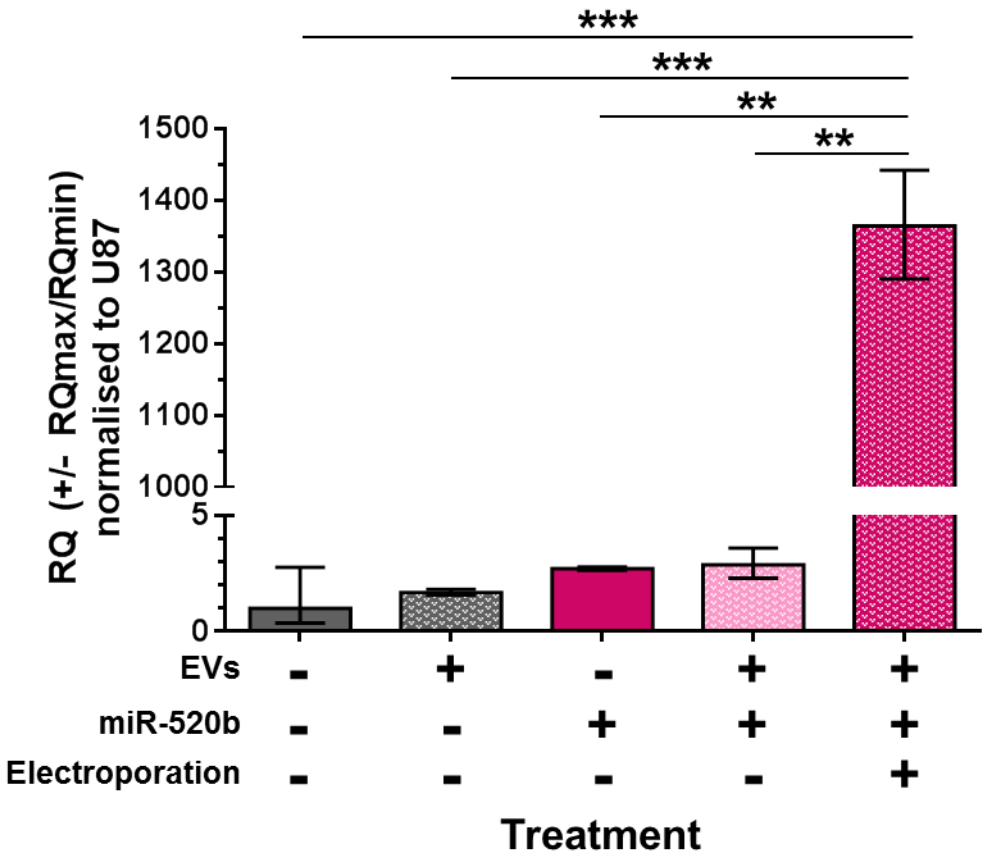

Figure 5.17 – Delivery of miR-520b EVs *In Vitro*
The expression of miR-520b was assessed in B50 neuronal cells which had received 875 ng of naïve EVs, miR-520b mimic, miR-520b/EV mixture, miR-520b loaded EVs or an equivalent volume of PBS (n=5). B50 neuronal cells were seeded on Day 0, EVs were added to cell culture medium on Day 1 and RNA harvested from cells on Day 3. Change in miRNA expression was assessed by qRT-PCR and relative quantification (RQ) calculated from ΔΔCt following normalisation to U87 and compared to miRNA expression in the PBS treated cells. Data shown is RQ ± RQmax/RQmin. Probability was calculated using a one-way-ANOVA with Tukey's Multiple Comparisons Test. Data courtesy of Dr. Emily Ord.

The comparison of the results obtained when modulating miR-93 and miR-20b expression with miRNA loaded EVs in the present study and those obtained by Dr. Emily Ord, using miR-520b loaded EVs in a previous study, led us to the conclusion that there must have been an error in the protocol followed for the synthetic loading (by electroporation) of the miRNA mimic into the EVs (Figure 5.3). As the basal expression of miR-520b in B50 neuronal cells is similar to that of miR-93 and miR-20b, there was no other obvious reason why miR-520b expression should be modulated so radically following treatment with miRNA loaded EVs and miR-93 and miR-20b expression completely unchanged.

5.3.4 Electroporation Protocol Optimisation

As a result of the lack of miRNA modulation in the *in vitro* study we spent a considerable amount of time attempting to troubleshoot the EV electroporation protocol (Figure 5.3) as we hypothesised that it was at this step a mistake must have been made that led to failure of miRNA being loaded into the EVs.

As the protocol had originally been optimised by Dr. Emily Ord she was consulted. After careful re-examination of the protocols used the only difference that could be found was the type of electroporation cuvette used. While the type of electroporation cuvette to be used was not specified in the protocol, Dr. Ord had optimised the protocol using short electrode (1.1 cm) electroporation cuvettes with a 1 mm electrode gap (Cell Projects Ltd). In the present study long electrode (2.2 cm) electroporation cuvettes, also with a 1 mm electrode gap (Cell Projects Ltd) had been used. Both cuvettes hold the same volume but the long electrode cuvettes are designed to be compatible for use with specific electroporators that require longer electrodes.

As a result of this discovery it was hypothesised that the EVs had been successfully electroporated and miRNA mimic loaded into the EVs but at a lower efficiency than previously estimated. The reduced efficiency of miRNA loading into the EVs would result in a lower level of miRNA modulation following delivery with the same low concentration of EVs used by Dr. Ord. To test this hypothesis two different concentrations of miR-93 and miR-20b loaded EVs (from the two batches of miRNA loaded EVs we had created) were delivered to normoxic B50 neuronal cells (Figure 5.18).

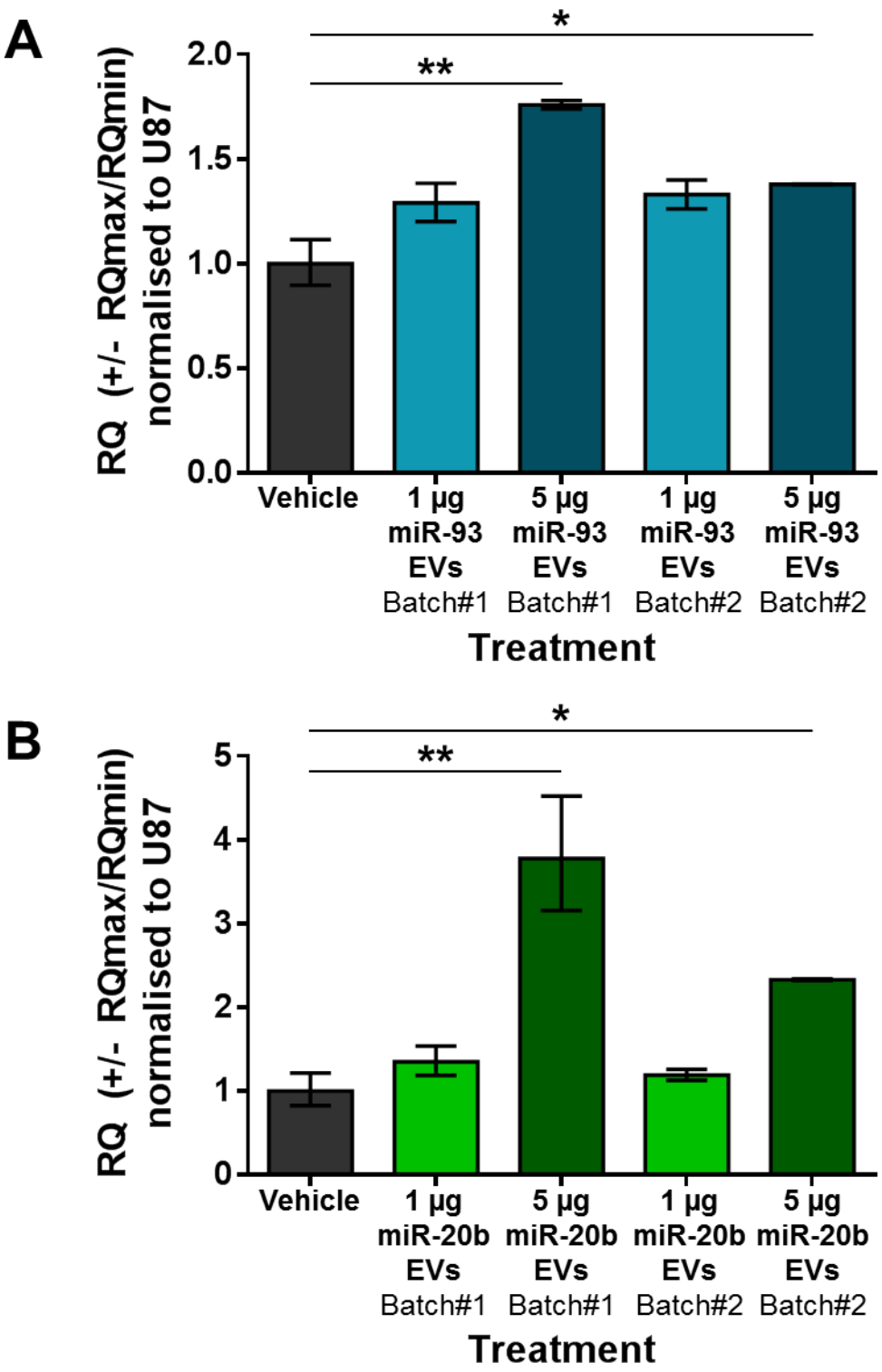

Figure 5.18 – Electroporation Optimisation Results
The expression of miR-93 (A) and miR-20b (B) was assessed in B50 neuronal cells which had received 1 µg or 5 µg of miRNA loaded EVs from the first or second batch of miRNA loaded EVs made or an equivalent volume of PBS (n=1). B50 neuronal cells were seeded on Day 0, EVs were added to cell culture medium on Day 1 and RNA harvested from cells on Day 3. Change in miRNA expression was assessed by qRT-PCR and relative quantification (RQ) calculated from ΔΔCt following normalisation to U87 and compared to miRNA expression in the PBS treated cells. Data shown is RQ ± RQmax/RQmin. Probability was calculated using a one-way-ANOVA with Tukey's Multiple Comparisons Test: *p<0.05; **p<0.01.

miR-93 expression was unchanged following delivery of 1 µg of miR-93 EVs (Batch #1) (RQ 1.29 ± 0.09 vs. 1.00 ± 0.12) as compared to vehicle treated cells but significantly increased following delivery of 5 µg of miR-93 EVs (Batch #1) (RQ 1.76 ± 0.02 vs. 1.00 ± 0.12) (Figure 5.18A). Similarly, miR-93 expression was unchanged following delivery of 1 µg of miR-93 EVs as compared to vehicle treated cells (Batch #2) (RQ 1.33 ± 0.07 vs. 1.00 ± 0.12) but significantly increased following delivery of 5 µg of miR-93 EVs (Batch #2) (RQ 1.38 ± 0.005 vs. 1.00 ± 0.12) (Figure 5.18A).

miR-20b expression was unchanged following delivery of 1 µg of miR-20b EVs (Batch #1) (RQ 1.35 ± 0.19 vs. 1.00 ± 0.22) as compared to vehicle treated cells but significantly increased following delivery of 5 µg of miR-20b EVs (Batch #1) (RQ 3.78 ± 0.75 vs. 1.00 ± 0.22) (Figure 5.18B). Similarly, miR-20b expression was unchanged following delivery of 1 µg of miR-20b EVs (Batch #2) as compared to vehicle treated cells (RQ 1.19 ± 0.07 vs. 1.00 ± 0.22) but significantly increased following delivery of 5 µg of miR-20b EVs (Batch #2) (RQ 2.33 ± 0.007 vs. 1.00 ± 0.22) (Figure 5.18B).

These results suggest that the EVs were electroporated, and miRNAs loaded into them, but not at a level sufficient to modulate expression *in vivo* or *in vitro* at the concentrations at which they had been successfully delivered in the past.

5.4 Discussion

There is an unmet need for novel treatments that not only result in reperfusion but also address specific aspects of stroke pathophysiology, such as cell death, cerebral oedema, oxidative stress and inflammation. As these processes are part of an ischaemic cascade which begins within minutes of stroke onset and rapidly progresses, the success of any ischaemic stroke treatment is dependent on early and effective administration of therapy. Furthermore, therapeutic agents used must be able to cross the BBB to prove effective.

It was hypothesised that intra-nasal delivery of miR-17 family miRNAs, packaged in extracellular vesicles, would be therapeutically beneficial when delivered following experimentally induced stroke in SHRSP rat. The present study was carefully thought out and aimed to assess both the extent of modulation and possible mechanisms of therapeutic efficacy. When modulation of miR-93 and miR-20b was not observed in SHRSP, following delivery of miRNA-loaded EVs post-stroke, further studies investigated modulation of miRNA expression following delivery of miR-20b loaded EVs to naïve rats. Subsequent studies profiled miRNA expression in B50 neuronal cells following delivery of miRNA loaded EVs. As miRNA expression was not modulated following delivery of miR loaded EVs in either the *in vivo* and *in vitro* parts of the study, experimental protocols were re-examined to find the cause of the problem.

One possible cause of the negative results obtained is the fact that long electrode electroporation cuvettes were used instead of short electrode cuvettes, at a critical stage in the experiment, where miRNAs are loaded into EVs. Although the protocol was optimised using short electrode electroporation cuvettes, the long electrode cuvettes are compatible with the shock compartment of the Bio-Rad MicroPulser™ Electroporator (used by our group). The protocol specified that a 400 V electrical pulse was delivered. We initially hypothesised that the longer electrode cuvettes were resulting in reduced electrical field strength, although the voltage applied was the same. Electrical field strength is determined by the following equation:

$$critical\ field\ strength\ (V/cm) = \frac{permeation\ voltage\ of\ the\ membrane}{(0.75\ X\ diameter\ of\ the\ cell/vesicle)}$$

Permeation voltage of the membrane is temperature dependent, which is why cooling of electroporation cuvettes before use is important. To calculate the voltage to be set on the electroporator, the field strength is multiplied by the width of the gap between the electrodes in the cuvette:

$$Voltage = critical\ field\ strength\ (V/cm)\ X\ electrode\ distance$$

It is clear from these equations that electrode length does not determine field strength or voltage delivered. Cell Projects, manufacturers of the electrodes used in the present study, have confirmed that there should be no difference in the electrical field strength delivered between the two types of electrodes, and that both are compatible with the Bio-Rad electroporator used. And yet, if data generated following electroporation with the 2 different cuvettes is compared, it appears that only the short electrodes successfully electroporated EVs, resulting in loading of miRNA mimics.

As our NanoSight data and TEM images show, the naïve EVs isolated from the brain of SHRSP and electroporated EVs did not fall within the size range typically associated with exosomes (30 – 120 nm). EVs used in the present study to deliver miRNAs were larger than this: the mean particle size as assessed by NanoSight was between 172 – 184 nm. A previous study has shown that larger microparticles (500 nm – 1 μM) do not successfully cross the BBB following intra-nasal delivery and instead were delivered to the lungs and intestines (Zhuang et al., 2011). These results suggest that particle size is an important factor for translocation to the brain following intra-nasal delivery. However, the majority of EVs used in the study were significantly smaller than the smallest microparticles delivered in the study mentioned and no modulation of miRNA expression was observed in the lung or kidney. Furthermore, particle size should not affect miRNA modulation *in vitro* and no modulation of miRNA expression was observed *in vivo* or *in vitro*.

However, as electrical field strength is partially determined by the diameter of the vesicles being electroporated, this may have affected electroporation conditions. Larger particles require a smaller applied voltage to deliver the same electrical field strength to the solution. The optimised protocol suggested applying a voltage of 400V. When applying a voltage of 400 V to larger particles

this would result in greater electrical field strength. One would hypothesise that too great a voltage would either increase loading efficiency or result in damage to the EV membrane. However, this theory is contradicted by TEM images of electroporated EVs which demonstrated the presence of intact vesicles.

Other similar studies have demonstrated successful uptake of therapeutic cargo (either miRNA or siRNA) by exosomes at a range of electroporation settings and these are summarised in Table 5.1. It is clear that optimal electroporation settings differ depending on both the cargo being loaded and the cell type from which the exosomes were generated. In general the percentage of cargo loaded is relatively low (~25%), with only one group demonstrating ~55% of cargo loaded into exosomes following electroporation (Bala et al., 2015, Momen-Heravi et al., 2014). The percentage of cargo loaded was not calculated in the present study. However, it is evident that if only relatively small percentages of cargo are loaded into the exosomes following electroporation, if electroporation conditions are sub-optimal then the percentage of cargo loaded may decrease dramatically. This is demonstrated by several studies which show that several parameters including electroporation voltage (Momen-Heravi et al., 2014, Wahlgren et al., 2012), siRNA aggregation (Kooijmans et al., 2013) and exosome aggregation (Hood et al., 2014) can significantly affect the efficiency of cargo loading into exosomes. While the voltage used in the present study was the same as that used in other studies (Alvarez-Erviti et al., 2011, Kooijmans et al., 2013) the electrode distance was smaller (0.1 cm vs. 0.4 cm) meaning that the critical field strength delivered was significantly higher. However, as these same electroporation settings had been used successfully within our group previously this is unlikely to be the cause of the negative results observed in the present study. Furthermore, trehalose was used in our electroporation buffer (as recommended by (Hood et al., 2014)) to prevent exosome aggregation and we did not observe significant exosome aggregation by TEM (data not shown).

Table 5.1 – Summary of studies using electroporation to load cargo into exosomes.
This table gives information about the cell type used to generate the exosomes (and unless otherwise stated exosomes were isolated from cell culture medium), electrode distance in the electroporation cuvettes used, electroporation settings, the cargo loaded and the approximate percentage of cargo loaded into exosomes following electroporation. A '–' indicates there was no information presented in the study on the specific category.

Reference	Cell Type Used to Generate Exosomes	Electroporation Cuvette: Electrode Distance	Electroporation Settings	Cargo	Percentage of Cargo Loaded
(Alvarez-Erviti et al., 2011) *Nature Biotechnology*	Primary dendritic cells harvested from murine bone marrow.	4 mm	400 V, 125 μF	GAPDH siRNA, BACE1 siRNA	~25%
(El-Andaloussi et al., 2012) *Nature Protocols*	Bone marrow dendritic cells and HEK cells	4 mm	400 mV, 125 μF, 10-15 ms pulse	siRNA	~25%
(Wahlgren et al., 2012) *Nucleic Acids Research*	HeLa and lung cancer cells HTB-177. Exosomes from human plasma.	4 mm	150 V, 100 mF	MAPK1 siRNA	~15-35%, depending which exosomes were used.
(Shtam et al., 2013) *Cell Communication & Signalling*	HeLa and HT1080 human fibosarcoma cells.	4 mm	700 V, 350 ms pulse, 20 times	RAD51 and RAD52 siRNA	-
(Kooijmans et al., 2013) *J. of Controlled Release*	Human embryonic kidney HEK293T and mouse neuroblastoma Neuro2A.	4 mm	400 V, 125 μF	Fluorescently labelled siRNA	~25%
(Hood et al., 2014) *Analytical Biochemistry*	Mouse B16-F10 melanoma cells.	4 mm	750 V/cm, single pulse <1 ms	Supramagnetic iron oxide nanoparticles (SPION5)	-
(Tian et al., 2014) *Biomaterials*	Human breast cancer cell lines MDA-MB-231 and MCF-7.	4 mm	350 V, 150 mF	Doxorubicin	up to 20%
(Momen-Heravi et al., 2014) *Nanomedicine*	Murine B cells.	2 mm	150 V, 100 μF	miR-155 mimic or inhibitor	~55%
(Bala et al., 2015) *Nature Scientific Reports*	Murine B cells.	2 mm	150 V, 100 μF	miR-155 mimic	presumed as above
Present Study	SHRSP brain homogenate.	1 mm	400 V, 10-15 ms pulse	miR-93 and miR-20b mimic	-

The protein content of EV suspensions was measured by BCA protein assay and used as an estimate of the concentration of EVs within each sample, as recommended in the Nature Protocols study which was used as the basis for our protocol (El-Andaloussi et al., 2012). An alternative method would be to use a NanoSight to measure the number of EVs within each sample. As the NanoSight measurements could be variable depending on how concentrated or dilute a sample was, it was decided that BCA protein assay was the best way to measure EV concentration. However, if errors were made at this stage in the experiment, it is possible that EV samples (naïve or electroporated) could be over-diluted and so result in a lower than calculated dose of EVs being delivered. However, as BCA assays were used regularly in our group and by Dr. Emily Ord in her experiments, I do not believe that this explains the differences observed in miRNA modulation between the two experiments.

A further possibility is that differences in the biology of the miRNAs themselves could explain differences in miRNA modulation. The miRNA mimics used in the present study were purchased from Life Technologies. Mimics used in experiments performed by Dr. Emily Ord were also purchased from Life Technologies. Furthermore, Life Technology miRNA mimics have been used regularly in our research group and without problem in the past. As the data presented in Chapter 3 shows, it is easier to modulate miRNAs with lower endogenous expression or they can be modulated to a greater extent with identical doses of miRNA modulating agents. However, as the endogenous expression of miR-520b is between that of miR-93 and miR-20b this does not explain differences in miRNA modulation observed.

It is difficult to discover the exact reason for the failure of miRNA modulation following delivery of miRNA loaded EVs and it is possible that it is the combined result of a number of small errors. The protocols were optimised by a member of our research group, using the same animals and equipment as were to be used in the present study. It was therefore believed that no further optimisation was needed before starting the *in vivo* study shown here. With hindsight it is clear that time and money could have been saved if a couple of small optimisation experiments had been carried out *in vitro* prior to starting the *in vivo* study. If time had permitted a further experiment could have been carried out to examine differences in miRNA expression between loaded and naïve exosomes. If

RNA was extracted from both naïve and loaded exosomes then qRT-PCR could be used to examine differences between miR-93 and miR-20b expression in each – this would give an indication of whether or not electroporation had been successful.

Other methods of loading cargo into exosomes include transfection of exosome producing cells, cell activation and simple incubation. The most commonly used method for loading miRNA into exosomes in the literature is that of transfecting the exosome producing cells so that they over-express a certain miRNA which is then packaged into exosomes endogenously by the cell (Chen et al., 2014, Katakowski et al., 2013, Kosaka et al., 2012, Munoz et al., 2013, Ohno et al., 2013, Pan et al., 2012, Zhang et al., 2010, Xin et al., 2013b). While this method has been used to successfully to generate exosomes that modulate miRNA expression both *in vitro* and *in vivo* the cell engineering necessary to optimise conditions so that large amounts of the desired miRNA are loaded into exosomal lumen can be extremely time intensive. This method would also be problematic if patients' own cells were to be used as exosome donors to generate non-immunogenic exosomes. miRNA can be loaded into exosomes following simple incubation of exosomes and cargo (Bryniarski et al., 2013) and also by using chemical transfection reagents. However chemical transfection was found to be a less successful method than electroporation at loading siRNA into exosomes when the two methods were compared (Shtam et al., 2013, Wahlgren et al., 2012). Cells can also be activated to induce modulation of exosome loading (Xin et al., 2012). This method has been used in the setting of ischaemic stroke, when mesenchymal stromal cells (MSCs) were treated with brain extracts from rat MCAO brain, resulting in increased expression of miR-133b in exosomes produced by the MSCs (Xin et al., 2012). This method is problematic in that it is difficult to control the response of the cells to the activating agent. A subsequent study by the same group used lentiviral vectors to transfect the cells, resulting in over-expression of miR-133b and subsequent increased loading of miR-133b into exosomes (Xin et al., 2013b).

The discovery that miRNAs were not efficiently loaded into EVs, a critical step in all the experiments presented in this study, was extremely disappointing. The data presented in this study is therefore uninterpretable in the context of currently published literature. These experiments are important and if the technical issues had been corrected in time would have determined whether intra-nasal delivery of miRNA loaded EVs held promise as a novel therapy in the setting of pre-clinical experimental stroke. Intra-nasal delivery of miRNA loaded EVs post-stroke, is novel, clinically relevant and remains a therapy of interest in the pre-clinical stroke studies carried out by our research group.

Chapter 6 General Discussion

6.1 Summary

Stroke remains a largely unmet clinical need. The primary treatment for stroke is still rt-PA which was first tested in a clinical trial over twenty years ago. Furthermore it is estimated that less than 10% of patients receive this treatment (Adeoye et al., 2011, Menon et al., 2015, Saver et al., 2013). Recent advances in mechanical clot retrieval have demonstrated that endovascular treatment is an additional treatment option offering improved outcome (e.g MR CLEAN clinical trial (Berkhemer et al., 2015)). Furthermore, the creation of specialised stroke units is associated with improved outcome (Stroke Unit Trialists' Collaboration, 2013). Despite this and although stroke incidence has fallen as a result of interventions improving control of cardiovascular risk, stroke remains one of the highest causes of death and serious disability worldwide. Numerous pre-clinical studies have significantly improved our understanding of the ischaemic cascade and the pathophysiology of stroke. They have further demonstrated that neuroprotective and neuro-restorative strategies may hold promise but these have failed to make the transition from “bench to bedside” despite appearing to be highly effective in rodents. This thesis has investigated whether miRNAs (especially those packaged within exosomes) are dysregulated following ischaemic stroke and whether they can be modulated therapeutically to improve outcome following stroke.

Early studies (Chapter 3) investigated whether candidate miRNAs, miR-494 and miR-21, held promise as therapeutic agents for ischaemic stroke. While data supporting the therapeutic use of miR-494 was lacking, data concerning miR-21 modulation held more promise. miR-21 is increased significantly in the brain of SHRSP rats at 72 hours following tMCAO. While modulation of miR-21 expression *in vitro* did not result in modulation of PTEN or PDCD4 (target gene) expression or in increased cell survival in cerebral endothelial cells it was hypothesised that this could be a result of miRNA mimics not being functionally processed by the cells to which they were delivered. Further experiments would address whether or not this was the case and carry out more comprehensive gene expression and functional outcome assays to determine exactly what effect miR-21 modulation has *in vitro*. Wire myography experiments revealed abnormal basal nitric oxide activity in the aortae of miR-21$^{-/-}$ mice, consistent with a detrimental phenotype associated with a loss of miR-21 expression (Breen,

2015). Further experiments would address the effect of gain or loss of miR-21 expression on cerebral blood vessels, such as the MCA, providing information of the importance of miR-21 modulation in the brain and whether or not its modulation was likely to prove therapeutically beneficial in the setting of ischaemic stroke.

This thesis has primarily focussed on the identification of dysregulated exosomal miRNAs in human ischaemic stroke patients and subsequent investigation of these same miRNAs in pre-clinical models of stroke (Chapter 4). Exosomes were isolated from serum of stroke patients that had been collected 48 hours post-stroke onset. Profiling of exosomal miRNA content in ischaemic stroke patients found 9 miRNAs whose expression was increased significantly in the serum of ischaemic stroke patients in comparison to non-stroke controls. Of these, 7 miRNAs were significantly increased in the serum of SVD stroke patients in comparison to non-stroke controls. While exosomal miRNA signalling has been demonstrated in other cardiovascular disease settings (Bang et al., 2014a, Hergenreider et al., 2012) this is the first study, to our knowledge, to profile exosomal miRNA expression in ischaemic stroke patients. Other studies have demonstrated that specific miRNA sequences are preferentially selected for extracellular transport (Montecalvo et al., 2012) or are packaged differently (Palma et al., 2012) demonstrating that miRNAs are not randomly secreted in exosomes from cells. The data presented in this thesis are consistent with our hypothesis that specific miRNAs are actively packaged into exosomes as a result of ischaemic stroke (or contribute to the cause thereof) and that as a result the circulating exosomal miRNA profile is significantly altered. When total miRNA expression was profiled in the serum of the same stroke (and control) population (albeit smaller ‘n’) there were no significantly dysregulated miRNAs detected (Breen, 2015) highlighting the importance of profiling exosomal miRNA. Furthermore, these data in conjunction with the presented study are consistent with the hypothesis that a number of miRNAs are selectively and actively packaged into exosomes.

Importantly, in comparison to a number of studies that have profiled total miRNA expression in ischaemic stroke patients the present study had access to a non-stroke patient population that was aged, hypertensive and had significant risk of stroke. Therefore differences in exosomal miRNA expression can be more

readily attributed to ischaemic stroke (vs. more general cardiovascular disease). Profiling of miR-17 family miRNA expression in our pre-clinical models revealed significantly higher miR-17 expression in naïve SHRSP rats as compared to normotensive WKY rats but no significant differences between total and exosomal circulating miRNA expression in SHRSP following either tMCAO or pMCAO. SHRSP are believed by some to be a model of human cerebral SVD (in part; no animal model can fully mimic human SVD). In human patients exosomal miRNA expression was significantly increased in SVD stroke subtype versus other stroke subtypes - it is therefore possible that the presented data are consistent with the hypothesis that dysregulated miRNAs detected in human SVD stroke patients are packaged into exosomes as a result of underlying cerebral vascular disease which predisposes patients to suffer a stroke. Cerebral ischaemia as a result of ischaemic stroke may result in further increases in expression of these miRNAs, explaining why exosomal miRNA expression was increased in large artery and cardioembolic patients but to a much lesser extent.

It has been suggested that embolic MCAO (Overgaard et al., 1992) is a more clinically relevant model of human stroke (Hossmann, 2012) than tMCAO. Embolic MCAO involves the insertion of an embolus at the origin of the MCA, occluding blood supply to the brain. The embolus is subsequently broken down by the administration of rtPA. Reperfusion is therefore protracted (as opposed to immediate with removal of intraluminal suture in tMCAO model) and so the infarct expands into the penumbral area within 3 hours. When reperfusion is immediate this infarct expansion is delayed, unnaturally, by 6-12 hours (Hossmann, 2012). However, as the majority of patients (77.5%) in the present study did not receive rtPA, these patients are perhaps best reflected by the pMCAO model which we used in this study. Furthermore, as we examined miRNA expression in our pre-clinical tMCAO model at 24 and 72 hours post-stroke when infarct expansion would have completed we would not expect to see significant differences by using an embolic model of stroke. However, future studies should take this issue into consideration.

While the presented study gave no indication that exosomal miRNAs would be useful as biomarkers or predictors of clinical outcome this may well reflect the extremely heterogeneous nature of a stroke patient population and is also consistent with the idea that dysregulated miRNA expression is not only changed

as a result of ischaemic stroke but predisposes to some degree. Further studies would investigate (if possible) exosomal miRNA expression at more acute time points (<48 hours, as used in present study) as well as longer time points and would compare both total and exosomal miRNA expression at all time points.

Finally, the use of exosomal packaged miRNAs as a therapeutic agent was investigated. Electroporation was used to load exosomes harvested from the brains of SHRSP rats with miR-93 or miR-20b mimic. miR-93 and miR-20b exosomes were subsequently delivered *in vivo* via intra-nasal delivery to SHRSP and *in vitro* to a neuronal cell line. While miRNA loaded exosomes did not modulate miRNA expression it is believed that this was the result of technical problems. Future studies would optimise electroporation conditions further and investigate efficacy of alternative methods of loading miRNA into exosomes, such as transfection of exosome producing cells which has been used successfully to load exosomes with miRNAs previously (Johnsen et al., 2014). The *in vivo* experiments that had been planned are important and remain of interest but delivery times and stroke model used could be refined to make the model as clinically relevant as possible, as has been discussed above.

6.2 Future Perspectives

As has already been discussed no neuroprotective or neuro-restorative strategies have yet made the transition from “bench to bedside” despite promising results in rodent stroke models. While this translational roadblock has now been recognised and suggestions have been made as to how to overcome this, this is a huge challenge for pre-clinical stroke research. Every effort therefore should be made to ensure that all pre-clinical studies, including our own, adhere to basic good practice guidelines (ARRIVE and STAIR amongst others (Fisher et al., 2009, Kilkenny et al., 2010, Macleod et al., 2009, STAIR, 1999)). Furthermore, pre-clinical study design should be improved to avoid “preventable attrition” (Dirnagl, 2016). This includes increasing internal validity by randomisation and blinding to improve reproducibility. Larger group sizes should be used in animal studies to increase statistical power and to reduce the reporting of inflated effect sizes. Furthermore the publication of negative results should be encouraged – it is estimated that only 50% of clinical medicine studies are ever published (Chan et al., 2014) and it is thought that this percentage could be

significantly less in pre-clinical medicine (Dirnagl, 2016). Furthermore the use of appropriate animal models (both comorbid and aged) would improve external validity. While some of these suggestions come at a cost, making them unfeasible for some research groups, every effort should be made to ensure studies are carefully planned and rigorously performed to overcome this translational roadblock that is holding back the development of desperately needed novel treatments for ischaemic stroke patients.

A further challenge in the search for novel therapeutic interventions for stroke is that of delivery. As “time is brain” (Saver, 2006) it is important to deliver therapeutic interventions as rapidly as possible following stroke. For this reason delivery methods commonly used in pre-clinical ischaemic stroke studies such as invasive stereotactic injection or ICV infusion delivery of therapeutic agents may not be suitable for use in a clinical setting, aside from other safety and cost considerations. As therapeutic agents must cross the BBB to be effective, systemic delivery is not always an option. Relatively novel, non-invasive delivery methods, such as intra-nasal, where therapeutic agents can rapidly cross the BBB (Lochhead and Thorne, 2012) have already been used to deliver miRNA modulating agents with therapeutic effect in pre-clinical models of Alzheimer’s Disease and ICH (Kim et al., 2014, Lee et al., 2012). However, the PISCES trial (in which neural stem cells were administered between 6-60 months post-stroke) (Kalladka et al., 2016) has demonstrated that if the primary aim of the intervention is to promote repair and regeneration then delivery can be delayed and stereotactic administration may become a viable option.

miRNAs are attractive candidates for therapeutic modulation in the setting of ischaemic stroke, as a result of their ability to alter the expression of multiple genes involved in stroke pathophysiology. Due to their small size and conserved sequence miRNA modulating agents are now readily available for most miRNAs. However, given the potential of one miRNA to target many genes, off-target effects are a significant consideration (van Rooij and Kauppinen, 2014). This highlights the importance of targeted delivery of miRNA modulating agents – a challenge which may be circumvented by the use of targeted exosomes (Johnsen et al., 2014). Despite the many challenges associated with successful and therapeutically effective miRNA modulation, a successful phase II clinical trial in which miR-122 was modulated to treat hepatitis-C virus infection resulted in

long-lasting dose-dependent antiviral activity and was well tolerated (Janssen et al., 2013). This proves that miRNA modulation is feasible therapeutically in human patients and is an inspiration for future studies seeking to modulate miRNA expression following ischaemic stroke.

In the present study microarray technology was used to identify dysregulated exosomal miRNAs. While array technology is a useful tool for profiling large numbers of miRNAs in numerous samples simultaneously, some studies have used RNA Sequencing (RNA-Seq) and Next Generation Sequencing (NGS) technologies to investigate changes in RNA and non-coding RNA expression both in human patients and in pre-clinical models of stroke (Dykstra-Aiello et al., 2015, Meller et al., 2016, Zhang et al., 2016a). RNA-Seq is a deep-sequencing technology that involves the conversion of a RNA population to a library of cDNA fragments, to which adapters are attached on to one or both ends. Sequencing experiments can be performed with or without amplification, with each molecule being sequenced in a high-throughput manner, with the reads (short sequences) subsequently aligned to a reference genome (Wang et al., 2009). RNA-Seq is beneficial in comparison to microarray technology in that it has the ability to identify novel RNAs, including lncRNAs. Microarray technology, on the other hand, is limited by its ability only to detect previously identified transcripts or miRNAs. Furthermore RNA-Seq can profile changes in differing RNA types in parallel, for example profiling mRNAs, lncRNAs, miRNAs, snoRNAs and piwi-interacting RNAs (piRNAs) in the same samples (for example, (Muller et al., 2015)). This can give an in depth understanding of interactions within the transcriptome, such as interactions between RNA-RNA and miRNA-mRNA, and helps to identify functionality of dysregulated RNAs. Finally, RNA-Seq has greater sensitivity for RNAs with low expression. Therefore, if RNA-Seq had been used in the present study, there may not have been problems with the low sample input and a larger number of dysregulated miRNAs may have been identified. However, the cost of RNA-Seq is prohibitive (~10 times that of microarray) and so only a small number of samples would have been profiled. The benefits and limitations of each have to be weighed against each other. If RNA-Seq technology becomes more widely used and the price falls it would be interesting to use this technology in the cohort of patients examined in the present study.

Finally, exosomes remain an exciting prospect in the drive towards personalised medicine. Numerous studies have demonstrated both the importance of exosome based paracrine signalling and the suitability of using exosomes for drug delivery. However this field is still in relative infancy and a number of questions still need to be answered (Johnsen et al., 2014). These include whether or not exosome producing cells would need to be self-derived to be non-immunogenic, which method of exosome loading is most appropriate and whether this changes for the type of cargo being loaded. Perhaps the most interesting question is whether the further development of targeting (via peptides on the surface) of exosomes will allow for specific drug delivery *in vivo* – if exosomes were to be used to deliver miRNA mimics or anti-miRs this would substantially reduce the possibility of off-target effects following intravenous delivery.

6.3 Concluding Remarks

In summary, the findings presented in this thesis confirm (as was hypothesised) that packaging of miRNAs into exosomes is significantly dysregulated in stroke patients and that as a result the circulating exosomal miRNA profile is altered. Further studies are needed to elucidate the functional importance of this dysregulation and whether exosomal miRNAs can be used therapeutically in the setting of ischaemic stroke.

List of References

ABRAMI, L., BRANDI, L., MOAYERI, M., BROWN, M. J., KRANTZ, B. A., LEPPLA, S. H. & VAN DER GOOT, F. G. 2013. Hijacking multivesicular bodies enables long-term and exosome-mediated long-distance action of anthrax toxin. *Cell Rep,* 5**,** 986-96.

ABRAMOV, A. Y., SCORZIELLO, A. & DUCHEN, M. R. 2007. Three distinct mechanisms generate oxygen free radicals in neurons and contribute to cell death during anoxia and reoxygenation. *J Neurosci,* 27**,** 1129-38.

ABRAMOVITZ, M., ADAM, M., BOIE, Y., CARRIERE, M., DENIS, D., GODBOUT, C., LAMONTAGNE, S., ROCHETTE, C., SAWYER, N., TREMBLAY, N. M., BELLEY, M., GALLANT, M., DUFRESNE, C., GAREAU, Y., RUEL, R., JUTEAU, H., LABELLE, M., OUIMET, N. & METTERS, K. M. 2000. The utilization of recombinant prostanoid receptors to determine the affinities and selectivities of prostaglandins and related analogs. *Biochim Biophys Acta,* 1483**,** 285-93.

ADAMS, H. P., BENDIXEN, B. H., KAPPELLE, L. J., BILLER, J., LOVE, B. B., GORDON, D. L. & MARSH, E. E. 1993. Classification of subtype of acute ischemic stroke. Definitions for use in a multicenter clinical trial. TOAST. Trial of Org 10172 in Acute Stroke Treatment. *Stroke,* 24**,** 35-41.

ADAMSON, J., BESWICK, A. & EBRAHIM, S. 2004. Is stroke the most common cause of disability? *J Stroke Cerebrovasc Dis,* 13**,** 171-7.

ADEOYE, O., HORNUNG, R., KHATRI, P. & KLEINDORFER, D. 2011. Recombinant tissue-type plasminogen activator use for ischemic stroke in the United States: a doubling of treatment rates over the course of 5 years. *Stroke,* 42**,** 1952-5.

AHO, K., HARMSEN, P., HATANO, S., MARQUARDSEN, J., SMIRNOV, V. E. & STRASSER, T. 1980. Cerebrovascular disease in the community: results of a WHO collaborative study. *Bull World Health Organ,* 58**,** 113-30.

ALLAN, S. M. & ROTHWELL, N. J. 2001. Cytokines and acute neurodegeneration. *Nat Rev Neurosci,* 2**,** 734-44.

ALVAREZ-ERVITI, L., SEOW, Y., YIN, H., BETTS, C., LAKHAL, S. & WOOD, M. J. 2011. Delivery of siRNA to the mouse brain by systemic injection of targeted exosomes. *Nat Biotechnol,* 29**,** 341-5.

AMARENCO, P. & LABREUCHE, J. 2009. Lipid management in the prevention of stroke: review and updated meta-analysis of statins for stroke prevention. *Lancet Neurol,* 8**,** 453-63.

ANDERSEN, K. K., OLSEN, T. S., DEHLENDORFF, C. & KAMMERSGAARD, L. P. 2009. Hemorrhagic and ischemic strokes compared: stroke severity, mortality, and risk factors. *Stroke,* 40**,** 2068-72.

ANKARCRONA, M., DYPBUKT, J. M., BONFOCO, E., ZHIVOTOVSKY, B., ORRENIUS, S., LIPTON, S. A. & NICOTERA, P. 1995. Glutamate-induced neuronal death: a succession of necrosis or apoptosis depending on mitochondrial function. *Neuron,* 15**,** 961-73.

ARAI, K., JIN, G., NAVARATNA, D. & LO, E. H. 2009. Brain angiogenesis in developmental and pathological processes: neurovascular injury and angiogenic recovery after stroke. *FEBS J,* 276**,** 4644-52.

ARNAIZ, S. L., CORONEL, M. F. & BOVERIS, A. 1999. Nitric oxide, superoxide, and hydrogen peroxide production in brain mitochondria after haloperidol treatment. *Nitric Oxide,* 3**,** 235-43.

ARROYO, J. D., CHEVILLET, J. R., KROH, E. M., RUF, I. K., PRITCHARD, C. C., GIBSON, D. F., MITCHELL, P. S., BENNETT, C. F., POGOSOVA-AGADJANYAN, E. L., STIREWALT, D. L., TAIT, J. F. & TEWARI, M. 2011. Argonaute2 complexes carry a population of circulating microRNAs independent of vesicles in human plasma. *Proc Natl Acad Sci U S A,* 108**,** 5003-8.

ARVIDSSON, A., COLLIN, T., KIRIK, D., KOKAIA, Z. & LINDVALL, O. 2002. Neuronal replacement from endogenous precursors in the adult brain after stroke. *Nat Med,* 8**,** 963-70.

ASCHNER, J. L., LUM, H., FLETCHER, P. W. & MALIK, A. B. 1997. Bradykinin- and thrombin-induced increases in endothelial permeability occur independently of

phospholipase C but require protein kinase C activation. *J Cell Physiol,* 173**,** 387-96.

ASTRUP, J., SYMON, L., BRANSTON, N. M. & LASSEN, N. A. 1977. Cortical evoked potential and extracellular K+ and H+ at critical levels of brain ischemia. *Stroke,* 8**,** 51-7.

AZUMA-MUKAI, A., OGURI, H., MITUYAMA, T., QIAN, Z. R., ASAI, K., SIOMI, H. & SIOMI, M. C. 2008. Characterization of endogenous human Argonautes and their miRNA partners in RNA silencing. *Proc Natl Acad Sci U S A,* 105**,** 7964-9.

BAEK, D., VILLEN, J., SHIN, C., CAMARGO, F. D., GYGI, S. P. & BARTEL, D. P. 2008. The impact of microRNAs on protein output. *Nature,* 455**,** 64-71.

BAILEY, E. L., MCCULLOCH, J., SUDLOW, C. & WARDLAW, J. M. 2009. Potential animal models of lacunar stroke: a systematic review. *Stroke,* 40**,** e451-8.

BALA, S., CSAK, T., MOMEN-HERAVI, F., LIPPAI, D., KODYS, K., CATALANO, D., SATISHCHANDRAN, A., AMBROS, V. & SZABO, G. 2015. Biodistribution and function of extracellular miRNA-155 in mice. *Scientific Reports,* 5**,** 10721.

BAMFORD, J., SANDERCOCK, P., DENNIS, M., BURN, J. & WARLOW, C. 1991. Classification and natural history of clinically identifiable subtypes of cerebral infarction. *Lancet,* 337**,** 1521-6.

BANG, C., BATKAI, S., DANGWAL, S., GUPTA, S. K., FOINQUINOS, A., HOLZMANN, A., JUST, A., REMKE, J., ZIMMER, K., ZEUG, A., PONIMASKIN, E., SCHMIEDL, A., YIN, X., MAYR, M., HALDER, R., FISCHER, A., ENGELHARDT, S., WEI, Y., SCHOBER, A., FIEDLER, J. & THUM, T. 2014a. Cardiac fibroblast-derived microRNA passenger strand-enriched exosomes mediate cardiomyocyte hypertrophy. *J Clin Invest*.

BANG, C., BATKAI, S., DANGWAL, S., GUPTA, S. K., FOINQUINOS, A., HOLZMANN, A., JUST, A., REMKE, J., ZIMMER, K., ZEUG, A., PONIMASKIN, E., SCHMIEDL, A., YIN, X., MAYR, M., HALDER, R., FISCHER, A., ENGELHARDT, S., WEI, Y., SCHOBER, A., FIEDLER, J. & THUM, T. 2014b. Cardiac fibroblast-derived microRNA passenger strand-enriched exosomes mediate cardiomyocyte hypertrophy. *J Clin Invest,* 124**,** 2136-46.

BARON, J. C. 1999. Mapping the ischaemic penumbra with PET: implications for acute stroke treatment. *Cerebrovasc Dis,* 9**,** 193-201.

BARTEL, D. P. 2009. MicroRNAs: target recognition and regulatory functions. *Cell,* 136**,** 215-33.

BEHM-ANSMANT, I., REHWINKEL, J., DOERKS, T., STARK, A., BORK, P. & IZAURRALDE, E. 2006. mRNA degradation by miRNAs and GW182 requires both CCR4:NOT deadenylase and DCP1:DCP2 decapping complexes. *Genes & Development,* 20**,** 1885-1898.

BELAYEV, L., BUSTO, R., ZHAO, W. & GINSBERG, M. D. 1996. Quantitative evaluation of blood-brain barrier permeability following middle cerebral artery occlusion in rats. *Brain Res,* 739**,** 88-96.

BERKHEMER, O. A., FRANSEN, P. S. S., BEUMER, D., VAN DEN BERG, L. A., LINGSMA, H. F., YOO, A. J., SCHONEWILLE, W. J., VOS, J. A., NEDERKOORN, P. J., WERMER, M. J. H., VAN WALDERVEEN, M. A. A., STAALS, J., HOFMEIJER, J., VAN OOSTAYEN, J. A., LYCKLAMA À NIJEHOLT, G. J., BOITEN, J., BROUWER, P. A., EMMER, B. J., DE BRUIJN, S. F., VAN DIJK, L. C., KAPPELLE, L. J., LO, R. H., VAN DIJK, E. J., DE VRIES, J., DE KORT, P. L. M., VAN ROOIJ, W. J. J., VAN DEN BERG, J. S. P., VAN HASSELT, B. A. A. M., AERDEN, L. A. M., DALLINGA, R. J., VISSER, M. C., BOT, J. C. J., VROOMEN, P. C., ESHGHI, O., SCHREUDER, T. H. C. M. L., HEIJBOER, R. J. J., KEIZER, K., TIELBEEK, A. V., DEN HERTOG, H. M., GERRITS, D. G., VAN DEN BERG-VOS, R. M., KARAS, G. B., STEYERBERG, E. W., FLACH, H. Z., MARQUERING, H. A., SPRENGERS, M. E. S., JENNISKENS, S. F. M., BEENEN, L. F. M., VAN DEN BERG, R., KOUDSTAAL, P. J., VAN ZWAM, W. H., ROOS, Y. B. W. E. M., VAN DER LUGT, A., VAN OOSTENBRUGGE, R. J., MAJOIE, C. B. L. M. & DIPPEL, D. W. J. 2015. A Randomized Trial of Intraarterial Treatment for Acute Ischemic Stroke. *New England Journal of Medicine,* 372**,** 11-20.

BERNARD, S. A., GRAY, T. W., BUIST, M. D., JONES, B. M., SILVESTER, W., GUTTERIDGE, G. & SMITH, K. 2002. Treatment of comatose survivors of out-of-hospital cardiac arrest with induced hypothermia. *N Engl J Med,* 346**,** 557-63.

BHATIA, R., HILL, M. D., SHOBHA, N., MENON, B., BAL, S., KOCHAR, P., WATSON, T., GOYAL, M. & DEMCHUK, A. M. 2010. Low rates of acute recanalization with intravenous recombinant tissue plasminogen activator in ischemic stroke: real-world experience and a call for action. *Stroke,* 41**,** 2254-8.

BOHNSACK, M. T., CZAPLINSKI, K. & GORLICH, D. 2004. Exportin 5 is a RanGTP-dependent dsRNA-binding protein that mediates nuclear export of pre-miRNAs. *RNA,* 10**,** 185-91.

BONFOCO, E., KRAINC, D., ANKARCRONA, M., NICOTERA, P. & LIPTON, S. A. 1995. Apoptosis and necrosis: two distinct events induced, respectively, by mild and intense insults with N-methyl-D-aspartate or nitric oxide/superoxide in cortical cell cultures. *Proc Natl Acad Sci U S A,* 92**,** 7162-6.

BOVERIS, A. & CHANCE, B. 1973. The mitochondrial generation of hydrogen peroxide. General properties and effect of hyperbaric oxygen. *Biochem J,* 134**,** 707-16.

BREEN, C. R. 2015. *The Role of miRNAs in Stroke.* Unpublished doctoral thesis, University of Glasgow.

BRENNAN, A. M., SUH, S. W., WON, S. J., NARASIMHAN, P., KAUPPINEN, T. M., LEE, H., EDLING, Y., CHAN, P. H. & SWANSON, R. A. 2009. NADPH oxidase is the primary source of superoxide induced by NMDA receptor activation. *Nat Neurosci,* 12**,** 857-63.

BROWN, R. D., WHISNANT, J. P., SICKS, J. D., O'FALLON, W. M. & WIEBERS, D. O. 1996. Stroke incidence, prevalence, and survival: secular trends in Rochester, Minnesota, through 1989. *Stroke,* 27**,** 373-80.

BRYNIARSKI, K., PTAK, W., JAYAKUMAR, A., PULLMANN, K., CAPLAN, M. J., CHAIROUNGDUA, A., LU, J., ADAMS, B. D., SIKORA, E., NAZIMEK, K., MARQUEZ, S., KLEINSTEIN, S. H., SANGWUNG, P., IWAKIRI, Y., DELGATO, E., REDEGELD, F., BLOKHUIS, B. R., WOJCIKOWSKI, J., DANIEL, A. W., GROOT KORMELINK, T. & ASKENASE, P. W. 2013. Antigen-specific, antibody-coated, exosome-like nanovesicles deliver suppressor T-cell microRNA-150 to effector T cells to inhibit contact sensitivity. *J Allergy Clin Immunol,* 132**,** 170-81.

BUCK, B. H., LIEBESKIND, D. S., SAVER, J. L., BANG, O. Y., YUN, S. W., STARKMAN, S., ALI, L. K., KIM, D., VILLABLANCA, J. P., SALAMON, N., RAZINIA, T. & OVBIAGELE, B. 2008. Early neutrophilia is associated with volume of ischemic tissue in acute stroke. *Stroke,* 39**,** 355-60.

BULLER, B., LIU, X., WANG, X., ZHANG, R. L., ZHANG, L., HOZESKA-SOLGOT, A., CHOPP, M. & ZHANG, Z. G. 2010. MicroRNA-21 protects neurons from ischemic death. *Febs j,* 277**,** 4299-307.

BUSCHOW, S. I., NOLTE-'T HOEN, E. N., VAN NIEL, G., POLS, M. S., TEN BROEKE, T., LAUWEN, M., OSSENDORP, F., MELIEF, C. J., RAPOSO, G., WUBBOLTS, R., WAUBEN, M. H. & STOORVOGEL, W. 2009. MHC II in dendritic cells is targeted to lysosomes or T cell-induced exosomes via distinct multivesicular body pathways. *Traffic,* 10**,** 1528-42.

CAI, X., HAGEDORN, C. H. & CULLEN, B. R. 2004. Human microRNAs are processed from capped, polyadenylated transcripts that can also function as mRNAs. *RNA,* 10**,** 1957-66.

CAMPBELL , B. C. V., MITCHELL , P. J., KLEINIG , T. J., DEWEY , H. M., CHURILOV , L., YASSI , N., YAN , B., DOWLING , R. J., PARSONS , M. W., OXLEY , T. J., WU , T. Y., BROOKS , M., SIMPSON , M. A., MITEFF , F., LEVI , C. R., KRAUSE , M., HARRINGTON , T. J., FAULDER , K. C., STEINFORT , B. S., PRIGLINGER , M., ANG , T., SCROOP , R., BARBER , P. A., MCGUINNESS , B., WIJERATNE , T., PHAN , T. G., CHONG , W., CHANDRA , R. V., BLADIN , C. F., BADVE , M., RICE , H., DE VILLIERS , L., MA , H., DESMOND , P. M., DONNAN , G. A. & DAVIS , S. M. 2015. Endovascular Therapy for Ischemic Stroke with Perfusion-Imaging Selection. *New England Journal of Medicine,* 372**,** 1009-1018.

CARAYON, K., CHAOUI, K., RONZIER, E., LAZAR, I., BERTRAND-MICHEL, J., ROQUES, V., BALOR, S., TERCE, F., LOPEZ, A., SALOME, L. & JOLY, E. 2011.

Proteolipidic composition of exosomes changes during reticulocyte maturation. *J Biol Chem,* 286**,** 34426-39.

CARDEN, D. L. & GRANGER, D. N. 2000. Pathophysiology of ischaemia-reperfusion injury. *J Pathol,* 190**,** 255-66.

CHAN, A. W., SONG, F., VICKERS, A., JEFFERSON, T., DICKERSIN, K., GOTZSCHE, P. C., KRUMHOLZ, H. M., GHERSI, D. & VAN DER WORP, H. B. 2014. Increasing value and reducing waste: addressing inaccessible research. *Lancet,* 383**,** 257-66.

CHE, X., YE, W., PANGA, L., WU, D. C. & YANG, G. Y. 2001. Monocyte chemoattractant protein-1 expressed in neurons and astrocytes during focal ischemia in mice. *Brain Res,* 902**,** 171-7.

CHELOUFI, S., DOS SANTOS, C. O., CHONG, M. M. W. & HANNON, G. J. 2010. A dicer-independent miRNA biogenesis pathway that requires Ago catalysis. *Nature,* 465**,** 584-589.

CHEN, F., DU, Y., ESPOSITO, E., LIU, Y., GUO, S., WANG, X., LO, E. H., XING, C. & JI, X. 2015. Effects of Focal Cerebral Ischemia on Exosomal Versus Serum miR126. *Translational Stroke Research,* 6**,** 478-484.

CHEN, L., CHARRIER, A., ZHOU, Y., CHEN, R., YU, B., AGARWAL, K., TSUKAMOTO, H., LEE, L. J., PAULAITIS, M. E. & BRIGSTOCK, D. R. 2014. Epigenetic regulation of connective tissue growth factor by MicroRNA-214 delivery in exosomes from mouse or human hepatic stellate cells. *Hepatology,* 59**,** 1118-29.

CHEN, X., BA, Y., MA, L., CAI, X., YIN, Y., WANG, K., GUO, J., ZHANG, Y., CHEN, J., GUO, X., LI, Q., LI, X., WANG, W., ZHANG, Y., WANG, J., JIANG, X., XIANG, Y., XU, C., ZHENG, P., ZHANG, J., LI, R., ZHANG, H., SHANG, X., GONG, T., NING, G., WANG, J., ZEN, K., ZHANG, J. & ZHANG, C. Y. 2008. Characterization of microRNAs in serum: a novel class of biomarkers for diagnosis of cancer and other diseases. *Cell Res,* 18**,** 997-1006.

CHEN, Z. L. & STRICKLAND, S. 1997. Neuronal death in the hippocampus is promoted by plasmin-catalyzed degradation of laminin. *Cell,* 91**,** 917-25.

CHENG, Y., JI, R., YUE, J., YANG, J., LIU, X., CHEN, H., DEAN, D. B. & ZHANG, C. 2007. MicroRNAs are aberrantly expressed in hypertrophic heart: do they play a role in cardiac hypertrophy? *Am J Pathol,* 170**,** 1831-40.

CHI, W., MENG, F., LI, Y., WANG, Q., WANG, G., HAN, S., WANG, P. & LI, J. 2014. Downregulation of miRNA-134 protects neural cells against ischemic injury in N2A cells and mouse brain with ischemic stroke by targeting HSPA12B. *Neuroscience,* 277**,** 111-22.

CHIU, Y. L. & RANA, T. M. 2003. siRNA function in RNAi: a chemical modification analysis. *Rna,* 9**,** 1034-48.

CHO, B. B. & TOLEDO-PEREYRA, L. H. 2008. Caspase-independent programmed cell death following ischemic stroke. *J Invest Surg,* 21**,** 141-7.

CHO, Y. S., CHALLA, S., MOQUIN, D., GENGA, R., RAY, T. D., GUILDFORD, M. & CHAN, F. K. 2009. Phosphorylation-driven assembly of the RIP1-RIP3 complex regulates programmed necrosis and virus-induced inflammation. *Cell,* 137**,** 1112-23.

CHRISTIANSON, H. C., SVENSSON, K. J., VAN KUPPEVELT, T. H., LI, J.-P. & BELTING, M. 2013. Cancer cell exosomes depend on cell-surface heparan sulfate proteoglycans for their internalization and functional activity. *Proceedings of the National Academy of Sciences,* 110**,** 17380-17385.

CIFUENTES, D., XUE, H., TAYLOR, D. W., PATNODE, H., MISHIMA, Y., CHELOUFI, S., MA, E., MANE, S., HANNON, G. J., LAWSON, N. D., WOLFE, S. A. & GIRALDEZ, A. J. 2010. A Novel miRNA Processing Pathway Independent of Dicer Requires Argonaute2 Catalytic Activity. *Science,* 328**,** 1694-1698.

CIPOLLONE, F., FELICIONI, L., SARZANI, R., UCCHINO, S., SPIGONARDO, F., MANDOLINI, C., MALATESTA, S., BUCCI, M., MAMMARELLA, C. & SANTOVITO, D. 2011. A unique microRNA signature associated with plaque instability in humans. *Stroke,* 42**,** 2556-2563.

COLOMBO, M., RAPOSO, G. & THERY, C. 2014. Biogenesis, secretion, and intercellular interactions of exosomes and other extracellular vesicles. *Annu Rev Cell Dev Biol,* 30**,** 255-89.

CRICK, F. 1970. Central dogma of molecular biology. *Nature,* 227**,** 561-3.

CRICK, F. H. 1958. On protein synthesis. *Symp Soc Exp Biol,* 12**,** 138-63.

DAVIS, B. N., HILYARD, A. C., LAGNA, G. & HATA, A. 2008. SMAD proteins control DROSHA-mediated microRNA maturation. *Nature,* 454**,** 56-61.

DEL ZOPPO, G. J., SCHMID-SCHONBEIN, G. W., MORI, E., COPELAND, B. R. & CHANG, C. M. 1991. Polymorphonuclear leukocytes occlude capillaries following middle cerebral artery occlusion and reperfusion in baboons. *Stroke,* 22**,** 1276-83.

DENG, X., ZHONG, Y., GU, L., SHEN, W. & GUO, J. 2013. MiR-21 involve in ERK-mediated upregulation of MMP9 in the rat hippocampus following cerebral ischemia. *Brain Res Bull,* 94**,** 56-62.

DENLI, A. M., TOPS, B. B., PLASTERK, R. H., KETTING, R. F. & HANNON, G. J. 2004. Processing of primary microRNAs by the Microprocessor complex. *Nature,* 432**,** 231-5.

DENZER, K., VAN EIJK, M., KLEIJMEER, M. J., JAKOBSON, E., DE GROOT, C. & GEUZE, H. J. 2000. Follicular dendritic cells carry MHC class II-expressing microvesicles at their surface. *J Immunol,* 165**,** 1259-65.

DHARAP, A., BOWEN, K., PLACE, R., LI, L. C. & VEMUGANTI, R. 2009. Transient focal ischemia induces extensive temporal changes in rat cerebral microRNAome. *J Cereb Blood Flow Metab,* 29**,** 675-87.

DIEDERICHS, S. & HABER, D. A. 2007. Dual role for argonautes in microRNA processing and posttranscriptional regulation of microRNA expression. *Cell,* 131**,** 1097-108.

DIMITRIJEVIC, O. B., STAMATOVIC, S. M., KEEP, R. F. & ANDJELKOVIC, A. V. 2006. Effects of the chemokine CCL2 on blood-brain barrier permeability during ischemia-reperfusion injury. *J Cereb Blood Flow Metab,* 26**,** 797-810.

DIMMELER, S. & YLA-HERTTUALA, S. 2014. 14q32 miRNA cluster takes center stage in neovascularization. *Circ Res,* 115**,** 680-2.

DING, G., JIANG, Q., LI, L., ZHANG, L., ZHANG, Z. G., LEDBETTER, K. A., GOLLAPALLI, L., PANDA, S., LI, Q., EWING, J. R. & CHOPP, M. 2008. Angiogenesis detected after embolic stroke in rat brain using magnetic resonance T2*WI. *Stroke,* 39**,** 1563-8.

DIRNAGL, U. 2016. Thomas Willis Lecture: Is Translational Stroke Research Broken, and if So, How Can We Fix It? *Stroke,* 47**,** 2148-53.

DIRNAGL, U., HAKIM, A., MACLEOD, M., FISHER, M., HOWELLS, D., ALAN, S. M., STEINBERG, G., PLANAS, A., BOLTZE, J., SAVITZ, S., IADECOLA, C. & MEAIRS, S. 2013. A concerted appeal for international cooperation in preclinical stroke research. *Stroke,* 44**,** 1754-60.

DIRNAGL, U., IADECOLA, C. & MOSKOWITZ, M. A. 1999. Pathobiology of ischaemic stroke: an integrated view. *Trends Neurosci,* 22**,** 391-7.

DJEBALI, S., DAVIS, C. A., MERKEL, A., DOBIN, A., LASSMANN, T., MORTAZAVI, A., TANZER, A., LAGARDE, J., LIN, W., SCHLESINGER, F., XUE, C., MARINOV, G. K., KHATUN, J., WILLIAMS, B. A., ZALESKI, C., ROZOWSKY, J., RODER, M., KOKOCINSKI, F., ABDELHAMID, R. F., ALIOTO, T., ANTOSHECHKIN, I., BAER, M. T., BAR, N. S., BATUT, P., BELL, K., BELL, I., CHAKRABORTTY, S., CHEN, X., CHRAST, J., CURADO, J., DERRIEN, T., DRENKOW, J., DUMAIS, E., DUMAIS, J., DUTTAGUPTA, R., FALCONNET, E., FASTUCA, M., FEJES-TOTH, K., FERREIRA, P., FOISSAC, S., FULLWOOD, M. J., GAO, H., GONZALEZ, D., GORDON, A., GUNAWARDENA, H., HOWALD, C., JHA, S., JOHNSON, R., KAPRANOV, P., KING, B., KINGSWOOD, C., LUO, O. J., PARK, E., PERSAUD, K., PREALL, J. B., RIBECA, P., RISK, B., ROBYR, D., SAMMETH, M., SCHAFFER, L., SEE, L. H., SHAHAB, A., SKANCKE, J., SUZUKI, A. M., TAKAHASHI, H., TILGNER, H., TROUT, D., WALTERS, N., WANG, H., WROBEL, J., YU, Y., RUAN, X., HAYASHIZAKI, Y., HARROW, J., GERSTEIN, M., HUBBARD, T., REYMOND, A., ANTONARAKIS, S. E., HANNON, G., GIDDINGS, M. C., RUAN, Y., WOLD, B., CARNINCI, P., GUIGO, R. & GINGERAS, T. R. 2012. Landscape of transcription in human cells. *Nature,* 489**,** 101-8.

DOEPPNER, T. R., DOEHRING, M., BRETSCHNEIDER, E., ZECHARIAH, A., KALTWASSER, B., MÜLLER, B., KOCH, J. C., BÄHR, M., HERMANN, D. M. & MICHEL, U. 2013. MicroRNA-124 protects against focal cerebral ischemia via mechanisms involving Usp14-dependent REST degradation. *Acta neuropathologica,* 126**,** 251-265.

DREIER, J. P. 2011. The role of spreading depression, spreading depolarization and spreading ischemia in neurological disease. *Nat Med,* 17**,** 439-47.

DUAN, X., ZHAN, Q., SONG, B., ZENG, S., ZHOU, J., LONG, Y., LU, J., LI, Z., YUAN, M. & CHEN, X. 2014. Detection of platelet microRNA expression in patients with diabetes mellitus with or without ischemic stroke. *Journal of diabetes and its complications,* 28**,** 705-710.

DUECK, A., ZIEGLER, C., EICHNER, A., BEREZIKOV, E. & MEISTER, G. 2012. microRNAs associated with the different human Argonaute proteins. *Nucleic Acids Res,* 40**,** 9850-62.

DUGAN, L. L., SENSI, S. L., CANZONIERO, L. M., HANDRAN, S. D., ROTHMAN, S. M., LIN, T. S., GOLDBERG, M. P. & CHOI, D. W. 1995. Mitochondrial production of reactive oxygen species in cortical neurons following exposure to N-methyl-D-aspartate. *J Neurosci,* 15**,** 6377-88.

DYKSTRA-AIELLO, C., JICKLING, G. C., ANDER, B. P., ZHAN, X., LIU, D., HULL, H., ORANTIA, M., HO, C. & STAMOVA, B. 2015. Intracerebral Hemorrhage and Ischemic Stroke of Different Etiologies Have Distinct Alternatively Spliced mRNA Profiles in the Blood: a Pilot RNA-seq Study. *Transl Stroke Res,* 6**,** 284-9.

EBERT, M. S. & SHARP, P. A. 2010. MicroRNA sponges: Progress and possibilities. *RNA,* 16**,** 2043-2050.

EHRENREICH, H., WEISSENBORN, K., PRANGE, H., SCHNEIDER, D., WEIMAR, C., WARTENBERG, K., SCHELLINGER, P. D., BOHN, M., BECKER, H., WEGRZYN, M., JAHNIG, P., HERRMANN, M., KNAUTH, M., BAHR, M., HEIDE, W., WAGNER, A., SCHWAB, S., REICHMANN, H., SCHWENDEMANN, G., DENGLER, R., KASTRUP, A. & BARTELS, C. 2009. Recombinant human erythropoietin in the treatment of acute ischemic stroke. *Stroke,* 40**,** e647-56.

EL-ANDALOUSSI, S., LEE, Y., LAKHAL-LITTLETON, S., LI, J., SEOW, Y., GARDINER, C., ALVAREZ-ERVITI, L., SARGENT, I. L. & WOOD, M. J. 2012. Exosome-mediated delivery of siRNA in vitro and in vivo. *Nat Protoc,* 7**,** 2112-26.

ELMEN, J., LINDOW, M., SILAHTAROGLU, A., BAK, M., CHRISTENSEN, M., LIND-THOMSEN, A., HEDTJARN, M., HANSEN, J. B., HANSEN, H. F., STRAARUP, E. M., MCCULLAGH, K., KEARNEY, P. & KAUPPINEN, S. 2008. Antagonism of microRNA-122 in mice by systemically administered LNA-antimiR leads to up-regulation of a large set of predicted target mRNAs in the liver. *Nucleic Acids Res,* 36**,** 1153-62.

EMERGING RISK FACTORS COLLABORATION, T. 2010. Diabetes mellitus, fasting blood glucose concentration, and risk of vascular disease: a collaborative meta-analysis of 102 prospective studies. *The Lancet,* 375**,** 2215-2222.

FAN, X., WANG, E., WANG, X., CONG, X. & CHEN, X. 2014. MicroRNA-21 is a unique signature associated with coronary plaque instability in humans by regulating matrix metalloproteinase-9 via reversion-inducing cysteine-rich protein with Kazal motifs. *Exp Mol Pathol,* 96**,** 242-9.

FASSBENDER, K., ROSSOL, S., KAMMER, T., DAFFERTSHOFER, M., WIRTH, S., DOLLMAN, M. & HENNERICI, M. 1994. Proinflammatory cytokines in serum of patients with acute cerebral ischemia: kinetics of secretion and relation to the extent of brain damage and outcome of disease. *J Neurol Sci,* 122**,** 135-9.

FEIGIN, V. L., FOROUZANFAR, M. H., KRISHNAMURTHI, R., MENSAH, G. A., CONNOR, M., BENNETT, D. A., MORAN, A. E., SACCO, R. L., ANDERSON, L., TRUELSEN, T., O'DONNELL, M., VENKETASUBRAMANIAN, N., BARKER-COLLO, S., LAWES, C. M., WANG, W., SHINOHARA, Y., WITT, E., EZZATI, M., NAGHAVI, M., MURRAY, C., GLOBAL BURDEN OF DISEASES, I., RISK FACTORS, S. & THE, G. B. D. S. E. G. 2014. Global and regional burden of stroke during 1990-2010: findings from the Global Burden of Disease Study 2010. *Lancet,* 383**,** 245-54.

FICHTLSCHERER, S., DE ROSA, S., FOX, H., SCHWIETZ, T., FISCHER, A., LIEBETRAU, C., WEBER, M., HAMM, C. W., ROXE, T., MULLER-ARDOGAN, M., BONAUER, A., ZEIHER, A. M. & DIMMELER, S. 2010. Circulating microRNAs in patients with coronary artery disease. *Circ Res,* 107**,** 677-84.

FISHER, M. & BASTAN, B. 2012. Identifying and utilizing the ischemic penumbra. *Neurology,* 79**,** S79-85.

FISHER, M., FEUERSTEIN, G., HOWELLS, D. W., HURN, P. D., KENT, T. A., SAVITZ, S. I. & LO, E. H. 2009. Update of the stroke therapy academic industry roundtable preclinical recommendations. *Stroke,* 40**,** 2244-50.

FONAROW, G. C., SMITH, E. E., SAVER, J. L., REEVES, M. J., BHATT, D. L., GRAU-SEPULVEDA, M. V., OLSON, D. M., HERNANDEZ, A. F., PETERSON, E. D. & SCHWAMM, L. H. 2011. Timeliness of tissue-type plasminogen activator therapy in acute ischemic stroke: patient characteristics, hospital factors, and outcomes associated with door-to-needle times within 60 minutes. *Circulation,* 123**,** 750-8.

FORSTERMANN, U., CLOSS, E. I., POLLOCK, J. S., NAKANE, M., SCHWARZ, P., GATH, I. & KLEINERT, H. 1994. Nitric oxide synthase isozymes. Characterization, purification, molecular cloning, and functions. *Hypertension,* 23**,** 1121-31.

FREDERICKSON, C. J., GIBLIN, L. J., KREZEL, A., MCADOO, D. J., MUELLER, R. N., ZENG, Y., BALAJI, R. V., MASALHA, R., THOMPSON, R. B., FIERKE, C. A., SARVEY, J. M., DE VALDENEBRO, M., PROUGH, D. S. & ZORNOW, M. H. 2006. Concentrations of extracellular free zinc (pZn)e in the central nervous system during simple anesthetization, ischemia and reperfusion. *Exp Neurol,* 198**,** 285-93.

FREY, W. H., LIU, J., CHEN, X., THORNE, R. G., FAWCETT, J. R., ALA, T. A. & RAHMAN, Y.-E. 1997. Delivery of 125I-NGF to the Brain via the Olfactory Route. *Drug Delivery,* 4**,** 87-92.

FREY, W. H. N. 1991. *Neurologic Agents for Nasal Administration to the Brain*. Geneva, Switzerland patent application PCT/US1990/007099.

FRIEDMAN, R. C., FARH, K. K., BURGE, C. B. & BARTEL, D. P. 2009. Most mammalian mRNAs are conserved targets of microRNAs. *Genome Res,* 19**,** 92-105.

FURUKAWA, K., FU, W., LI, Y., WITKE, W., KWIATKOWSKI, D. J. & MATTSON, M. P. 1997. The actin-severing protein gelsolin modulates calcium channel and NMDA receptor activities and vulnerability to excitotoxicity in hippocampal neurons. *J Neurosci,* 17**,** 8178-86.

GALASSO, S. L. & DYCK, R. H. 2007. The Role of Zinc in Cerebral Ischemia. *Molecular Medicine,* 13**,** 380-387.

GALLO, A., TANDON, M., ALEVIZOS, I. & ILLEI, G. G. 2012. The majority of microRNAs detectable in serum and saliva is concentrated in exosomes. *PLoS One,* 7**,** e30679.

GAN, C., WANG, C. & TAN, K. 2012. Circulatory microRNA-145 expression is increased in cerebral ischemia. *Genet Mol Res,* 11**,** 147-152.

GE, X.-T., LEI, P., WANG, H.-C., ZHANG, A.-L., HAN, Z.-L., CHEN, X., LI, S.-H., JIANG, R.-C., KANG, C.-S. & ZHANG, J.-N. 2014. miR-21 improves the neurological outcome after traumatic brain injury in rats. *Scientific Reports,* 4**,** 6718.

GE, X., HAN, Z., CHEN, F., WANG, H., ZHANG, B., JIANG, R., LEI, P. & ZHANG, J. 2015. miR-21 alleviates secondary blood–brain barrier damage after traumatic brain injury in rats. *Brain Research,* 1603**,** 150-157.

GE, X., HUANG, S., GAO, H., HAN, Z., CHEN, F., ZHANG, S., WANG, Z., KANG, C., JIANG, R., YUE, S., LEI, P. & ZHANG, J. 2016. miR-21-5p alleviates leakage of injured brain microvascular endothelial barrier in vitro through suppressing inflammation and apoptosis. *Brain Research*.

GIDDAY, J. M., GASCHE, Y. G., COPIN, J. C., SHAH, A. R., PEREZ, R. S., SHAPIRO, S. D., CHAN, P. H. & PARK, T. S. 2005. Leukocyte-derived matrix metalloproteinase-9 mediates blood-brain barrier breakdown and is proinflammatory after transient focal cerebral ischemia. *Am J Physiol Heart Circ Physiol,* 289**,** H558-68.

GIRALDEZ, A. J., MISHIMA, Y., RIHEL, J., GROCOCK, R. J., VAN DONGEN, S., INOUE, K., ENRIGHT, A. J. & SCHIER, A. F. 2006. Zebrafish MiR-430 promotes deadenylation and clearance of maternal mRNAs. *Science,* 312**,** 75-9.

GIROUARD, H., WANG, G., GALLO, E. F., ANRATHER, J., ZHOU, P., PICKEL, V. M. & IADECOLA, C. 2009. NMDA receptor activation increases free radical production through nitric oxide and NOX2. *J Neurosci,* 29**,** 2545-52.

GOLDIE, B. J., DUN, M. D., LIN, M., SMITH, N. D., VERRILLS, N. M., DAYAS, C. V. & CAIRNS, M. J. 2014. Activity-associated miRNA are packaged in Map1b-enriched exosomes released from depolarized neurons. *Nucleic Acids Res,* 42**,** 9195-208.

GOYAL , M., DEMCHUK , A. M., MENON , B. K., EESA , M., REMPEL , J. L., THORNTON , J., ROY , D., JOVIN , T. G., WILLINSKY , R. A., SAPKOTA , B. L., DOWLATSHAHI , D., FREI , D. F., KAMAL , N. R., MONTANERA , W. J., POPPE , A. Y., RYCKBORST , K. J., SILVER , F. L., SHUAIB , A., TAMPIERI , D., WILLIAMS , D., BANG , O. Y., BAXTER , B. W., BURNS , P. A., CHOE , H., HEO , J.-H., HOLMSTEDT , C. A., JANKOWITZ , B., KELLY , M., LINARES , G., MANDZIA , J. L., SHANKAR , J., SOHN , S.-I., SWARTZ , R. H., BARBER , P. A., COUTTS , S. B., SMITH , E. E., MORRISH , W. F., WEILL , A., SUBRAMANIAM , S., MITHA , A. P., WONG , J. H., LOWERISON , M. W., SAJOBI , T. T. & HILL , M. D. 2015. Randomized Assessment of Rapid Endovascular Treatment of Ischemic Stroke. *New England Journal of Medicine,* 372**,** 1019-1030.

GRAU, A. J., REIS, A., BUGGLE, F., AL-KHALAF, A., WERLE, E., VALOIS, N., BERTRAM, M., BECHER, H. & GROND-GINSBACH, C. 2001. Monocyte function and plasma levels of interleukin-8 in acute ischemic stroke. *J Neurol Sci,* 192**,** 41-7.

GRAY, W. D., FRENCH, K. M., GHOSH-CHOUDHARY, S., MAXWELL, J. T., BROWN, M. E., PLATT, M. O., SEARLES, C. D. & DAVIS, M. E. 2015. Identification of therapeutic covariant microRNA clusters in hypoxia-treated cardiac progenitor cell exosomes using systems biology. *Circ Res,* 116**,** 255-63.

GREEN, D. R. & REED, J. C. 1998. Mitochondria and apoptosis. *Science,* 281**,** 1309-12.

GREENBERG, D. A. & JIN, K. 2006. Growth factors and stroke. *NeuroRx,* 3**,** 458-65.

GREGORY, R. I., YAN, K. P., AMUTHAN, G., CHENDRIMADA, T., DORATOTAJ, B., COOCH, N. & SHIEKHATTAR, R. 2004. The Microprocessor complex mediates the genesis of microRNAs. *Nature,* 432**,** 235-40.

GRIBKOFF, V. K., STARRETT, J. E., JR., DWORETZKY, S. I., HEWAWASAM, P., BOISSARD, C. G., COOK, D. A., FRANTZ, S. W., HEMAN, K., HIBBARD, J. R., HUSTON, K., JOHNSON, G., KRISHNAN, B. S., KINNEY, G. G., LOMBARDO, L. A., MEANWELL, N. A., MOLINOFF, P. B., MYERS, R. A., MOON, S. L., ORTIZ, A., PAJOR, L., PIESCHL, R. L., POST-MUNSON, D. J., SIGNOR, L. J., SRINIVAS, N., TABER, M. T., THALODY, G., TROJNACKI, J. T., WIENER, H., YELESWARAM, K. & YEOLA, S. W. 2001. Targeting acute ischemic stroke with a calcium-sensitive opener of maxi-K potassium channels. *Nat Med,* 7**,** 471-7.

GU, Z., KAUL, M., YAN, B., KRIDEL, S. J., CUI, J., STRONGIN, A., SMITH, J. W., LIDDINGTON, R. C. & LIPTON, S. A. 2002. S-nitrosylation of matrix metalloproteinases: signaling pathway to neuronal cell death. *Science,* 297**,** 1186-90.

GUBERN, C., CAMOS, S., BALLESTEROS, I., RODRIGUEZ, R., ROMERA, V. G., CANADAS, R., LIZASOAIN, I., MORO, M. A., SERENA, J., MALLOLAS, J. & CASTELLANOS, M. 2013. miRNA expression is modulated over time after focal ischaemia: up-regulation of miR-347 promotes neuronal apoptosis. *Febs j,* 280**,** 6233-46.

GUDURIC-FUCHS, J., O'CONNOR, A., CULLEN, A., HARWOOD, L., MEDINA, R. J., O'NEILL, C. L., STITT, A. W., CURTIS, T. M. & SIMPSON, D. A. 2012. Deep sequencing reveals predominant expression of miR-21 amongst the small non-coding RNAs in retinal microvascular endothelial cells. *Journal of Cellular Biochemistry,* 113**,** 2098-2111.

GUO, D., LIU, J., WANG, W., HAO, F., SUN, X., WU, X., BU, P., ZHANG, Y., LIU, Y., LIU, F., ZHANG, Q. & JIANG, F. 2013. Alteration in abundance and compartmentalization of inflammation-related miRNAs in plasma after intracerebral hemorrhage. *Stroke,* 44**,** 1739-42.

GUO, F., HAN, X., ZHANG, J., ZHAO, X., LOU, J., CHEN, H. & HUANG, X. 2014. Repetitive Transcranial Magnetic Stimulation Promotes Neural Stem Cell

Proliferation via the Regulation of MiR-25 in a Rat Model of Focal Cerebral Ischemia. *PLoS ONE,* 9**,** e109267.
GUO, H., INGOLIA, N. T., WEISSMAN, J. S. & BARTEL, D. P. 2010. Mammalian microRNAs predominantly act to decrease target mRNA levels. *Nature,* 466**,** 835-840.
HA, M. & KIM, V. N. 2014. Regulation of microRNA biogenesis. *Nat Rev Mol Cell Biol,* 15**,** 509-24.
HACKE , W., KASTE , M., BLUHMKI , E., BROZMAN , M., DÁVALOS , A., GUIDETTI , D., LARRUE , V., LEES , K. R., MEDEGHRI , Z., MACHNIG , T., SCHNEIDER , D., VON KUMMER , R., WAHLGREN , N. & TONI , D. 2008. Thrombolysis with Alteplase 3 to 4.5 Hours after Acute Ischemic Stroke. *New England Journal of Medicine,* 359**,** 1317-1329.
HAINSWORTH, A. H., BRITTAIN, J. F. & KHATUN, H. 2012. Pre-clinical models of human cerebral small vessel disease: utility for clinical application. *J Neurol Sci,* 322**,** 237-40.
HAINSWORTH, A. H. & MARKUS, H. S. 2008. Do in vivo experimental models reflect human cerebral small vessel disease? A systematic review. *J Cereb Blood Flow Metab,* 28**,** 1877-91.
HALLENBECK, J. M. 2002. The many faces of tumor necrosis factor in stroke. *Nat Med,* 8**,** 1363-8.
HAMMOND, S. M., BERNSTEIN, E., BEACH, D. & HANNON, G. J. 2000. An RNA-directed nuclease mediates post-transcriptional gene silencing in Drosophila cells. *Nature,* 404**,** 293-6.
HAMMOND, S. M., BOETTCHER, S., CAUDY, A. A., KOBAYASHI, R. & HANNON, G. J. 2001. Argonaute2, a link between genetic and biochemical analyses of RNAi. *Science,* 293**,** 1146-50.
HANSON, P. I. & CASHIKAR, A. 2012. Multivesicular body morphogenesis. *Annu Rev Cell Dev Biol,* 28**,** 337-62.
HARING, H. P., BERG, E. L., TSURUSHITA, N., TAGAYA, M. & DEL ZOPPO, G. J. 1996. E-selectin appears in nonischemic tissue during experimental focal cerebral ischemia. *Stroke,* 27**,** 1386-91; discussion 1391-2.
HARRAZ, M. M., EACKER, S. M., WANG, X., DAWSON, T. M. & DAWSON, V. L. 2012. MicroRNA-223 is neuroprotective by targeting glutamate receptors. *Proceedings of the National Academy of Sciences,* 109**,** 18962-18967.
HAZARIKA, S., FARBER, C. R., DOKUN, A. O., PITSILLIDES, A. N., WANG, T., LYE, R. J. & ANNEX, B. H. 2013. MicroRNA-93 Controls Perfusion Recovery After Hindlimb Ischemia by Modulating Expression of Multiple Genes in the Cell Cycle PathwayClinical Perspective. *Circulation,* 127**,** 1818-1828.
HEART PROTECTION STUDY COLLABORATIVE GROUP, T. 2002. MRC/BHF Heart Protection Study of cholesterol lowering with simvastatin in 20,536 high-risk individuals: a randomised placebo-controlled trial. *Lancet,* 360**,** 7-22.
HENDRICKSON, D. G., HOGAN, D. J., MCCULLOUGH, H. L., MYERS, J. W., HERSCHLAG, D., FERRELL, J. E. & BROWN, P. O. 2009. Concordant Regulation of Translation and mRNA Abundance for Hundreds of Targets of a Human microRNA. *PLoS Biology,* 7**,** e1000238.
HERGENREIDER, E., HEYDT, S., TREGUER, K., BOETTGER, T., HORREVOETS, A. J., ZEIHER, A. M., SCHEFFER, M. P., FRANGAKIS, A. S., YIN, X., MAYR, M., BRAUN, T., URBICH, C., BOON, R. A. & DIMMELER, S. 2012. Atheroprotective communication between endothelial cells and smooth muscle cells through miRNAs. *Nat Cell Biol,* 14**,** 249-56.
HERTZ, L. 2008. Bioenergetics of cerebral ischemia: a cellular perspective. *Neuropharmacology,* 55**,** 289-309.
HOLLER, N., ZARU, R., MICHEAU, O., THOME, M., ATTINGER, A., VALITUTTI, S., BODMER, J. L., SCHNEIDER, P., SEED, B. & TSCHOPP, J. 2000. Fas triggers an alternative, caspase-8-independent cell death pathway using the kinase RIP as effector molecule. *Nat Immunol,* 1**,** 489-95.
HOOD, J. L., SCOTT, M. J. & WICKLINE, S. A. 2014. Maximizing exosome colloidal stability following electroporation. *Anal Biochem,* 448**,** 41-9.

HOPPER, I., BILLAH, B., SKIBA, M. & KRUM, H. 2011. Prevention of diabetes and reduction in major cardiovascular events in studies of subjects with prediabetes: meta-analysis of randomised controlled clinical trials. *Eur J Cardiovasc Prev Rehabil,* 18**,** 813-23.

HOSSMANN, K. A. 2012. The two pathophysiologies of focal brain ischemia: implications for translational stroke research. *J Cereb Blood Flow Metab,* 32**,** 1310-6.

HSU, S. D., CHU, C. H., TSOU, A. P., CHEN, S. J., CHEN, H. C., HSU, P. W., WONG, Y. H., CHEN, Y. H., CHEN, G. H. & HUANG, H. D. 2008. miRNAMap 2.0: genomic maps of microRNAs in metazoan genomes. *Nucleic Acids Res,* 36**,** D165-9.

HUANG, J., CHOUDHRI, T. F., WINFREE, C. J., MCTAGGART, R. A., KISS, S., MOCCO, J., KIM, L. J., PROTOPSALTIS, T. S., ZHANG, Y., PINSKY, D. J. & CONNOLLY, E. S., JR. 2000. Postischemic cerebrovascular E-selectin expression mediates tissue injury in murine stroke. *Stroke,* 31**,** 3047-53.

HUANG, L. G., LI, J. P., PANG, X. M., CHEN, C. Y., XIANG, H. Y., FENG, L. B., SU, S. Y., LI, S. H., ZHANG, L. & LIU, J. L. 2015. MicroRNA-29c Correlates with Neuroprotection Induced by FNS by Targeting Both Birc2 and Bak1 in Rat Brain after Stroke. *CNS neuroscience & therapeutics*.

HUANG, S. E., ZHAO, J., HUANG, D., ZHUO, L., LIAO, S. & JIANG, Z. 2016. Serum miR-132 is a risk marker of post-stroke cognitive impairment. *Neuroscience Letters,* 615**,** 102-106.

HUANG, Z. G., XUE, D., PRESTON, E., KARBALAI, H. & BUCHAN, A. M. 1999. Biphasic opening of the blood-brain barrier following transient focal ischemia: effects of hypothermia. *Can J Neurol Sci,* 26**,** 298-304.

HUMPHREYS, D. T., WESTMAN, B. J., MARTIN, D. I. & PREISS, T. 2005. MicroRNAs control translation initiation by inhibiting eukaryotic initiation factor 4E/cap and poly(A) tail function. *Proc Natl Acad Sci U S A,* 102**,** 16961-6.

HUNTER, M. P., ISMAIL, N., ZHANG, X., AGUDA, B. D., LEE, E. J., YU, L., XIAO, T., SCHAFER, J., LEE, M.-L. T., SCHMITTGEN, T. D., NANA-SINKAM, S. P., JARJOURA, D. & MARSH, C. B. 2008. Detection of microRNA Expression in Human Peripheral Blood Microvesicles. *PLoS ONE,* 3**,** e3694.

HURLEY, J. H. & HANSON, P. I. 2010. Membrane budding and scission by the ESCRT machinery: it's all in the neck. *Nat Rev Mol Cell Biol,* 11**,** 556-66.

HYPOTHERMIA AFTER CARDIAC ARREST STUDY GROUP, T. 2002. Mild Therapeutic Hypothermia to Improve the Neurologic Outcome after Cardiac Arrest. *New England Journal of Medicine,* 346**,** 549-556.

IADECOLA, C. & ANRATHER, J. 2011. The immunology of stroke: from mechanisms to translation. *Nat Med,* 17**,** 796-808.

IBRAHIM, A. & MARBÁN, E. 2016. Exosomes: Fundamental Biology and Roles in Cardiovascular Physiology. *Annual Review of Physiology,* 78**,** 67-83.

IMMORDINO, M. L., DOSIO, F. & CATTEL, L. 2006. Stealth liposomes: review of the basic science, rationale, and clinical applications, existing and potential. *International Journal of Nanomedicine,* 1**,** 297-315.

INTERCOLLEGIATE STROKE WORKING PARTY, T. 2012. National clinical guideline for stroke. London: Royal College of Physicians.

INTERCOLLEGIATE STROKE WORKING PARTY, T. 2015. Clinical Audit April - June 2015. *In:* ROYAL COLLEGE OF PHYSICIANS SENTINEL STROKE NATIONAL AUDIT PROGRAME (SSNAP), T. (ed.). London: Royal College of Physicians.

INTERCOLLEGIATE STROKE WORKING PARTY, T. 2016. National clinical guideline for stroke. *In:* RUDD, T. (ed.). London: Royal College of Physicians.

JACKSON, R. J., HELLEN, C. U. T. & PESTOVA, T. V. 2010. The mechanism of eukaryotic translation initiation and principles of its regulation. *Nat Rev Mol Cell Biol,* 11**,** 113-127.

JANSSEN , H. L. A., REESINK , H. W., LAWITZ , E. J., ZEUZEM , S., RODRIGUEZ-TORRES , M., PATEL , K., VAN DER MEER , A. J., PATICK , A. K., CHEN , A., ZHOU , Y., PERSSON , R., KING , B. D., KAUPPINEN , S., LEVIN , A. A. & HODGES , M. R. 2013. Treatment of HCV Infection by Targeting MicroRNA. *New England Journal of Medicine,* 368**,** 1685-1694.

JARRY, J., SCHADENDORF, D., GREENWOOD, C., SPATZ, A. & VAN KEMPEN, L. C. 2014. The validity of circulating microRNAs in oncology: five years of challenges and contradictions. *Mol Oncol,* 8**,** 819-29.

JAZBUTYTE, V. & THUM, T. 2010. MicroRNA-21: from cancer to cardiovascular disease. *Curr Drug Targets,* 11**,** 926-35.

JEYASEELAN, K., LIM, K. Y. & ARMUGAM, A. 2008. MicroRNA expression in the blood and brain of rats subjected to transient focal ischemia by middle cerebral artery occlusion. *Stroke,* 39**,** 959-966.

JI, R., CHENG, Y., YUE, J., YANG, J., LIU, X., CHEN, H., DEAN, D. B. & ZHANG, C. 2007. MicroRNA expression signature and antisense-mediated depletion reveal an essential role of MicroRNA in vascular neointimal lesion formation. *Circ Res,* 100**,** 1579-88.

JIA, L., HAO, F., WANG, W. & QU, Y. 2015. Circulating miR-145 is associated with plasma high-sensitivity C-reactive protein in acute ischemic stroke patients. *Cell Biochemistry and Function,* 33**,** 314-319.

JICKLING, G. C., ANDER, B. P., ZHAN, X., NOBLETT, D., STAMOVA, B. & LIU, D. 2014. microRNA Expression in Peripheral Blood Cells following Acute Ischemic Stroke and Their Predicted Gene Targets. *PloS one,* 9**,** e99283.

JOHNSEN, K. B., GUDBERGSSON, J. M., SKOV, M. N., PILGAARD, L., MOOS, T. & DUROUX, M. 2014. A comprehensive overview of exosomes as drug delivery vehicles - endogenous nanocarriers for targeted cancer therapy. *Biochim Biophys Acta,* 1846**,** 75-87.

JOHNSTONE, R. M., ADAM, M., HAMMOND, J. R., ORR, L. & TURBIDE, C. 1987. Vesicle formation during reticulocyte maturation. Association of plasma membrane activities with released vesicles (exosomes). *J Biol Chem,* 262**,** 9412-20.

JOVIN, T. G., CHAMORRO, A., COBO, E., DE MIQUEL, M. A., MOLINA, C. A., ROVIRA, A., SAN ROMÁN, L., SERENA, J., ABILLEIRA, S., RIBÓ, M., MILLÁN, M., URRA, X., CARDONA, P., LÓPEZ-CANCIO, E., TOMASELLO, A., CASTAÑO, C., BLASCO, J., AJA, L., DORADO, L., QUESADA, H., RUBIERA, M., HERNANDEZ-PÉREZ, M., GOYAL, M., DEMCHUK, A. M., VON KUMMER, R., GALLOFRÉ, M. & DÁVALOS, A. 2015. Thrombectomy within 8 Hours after Symptom Onset in Ischemic Stroke. *New England Journal of Medicine,* 372**,** 2296-2306.

KALLADKA, D., SINDEN, J., POLLOCK, K., HAIG, C., MCLEAN, J., SMITH, W., MCCONNACHIE, A., SANTOSH, C., BATH, P. M., DUNN, L. & MUIR, K. W. 2016. Human neural stem cells in patients with chronic ischaemic stroke (PISCES): a phase 1, first-in-man study. *The Lancet,* 388**,** 787-796.

KAMIYA, T., KATAYAMA, Y., KASHIWAGI, F. & TERASHI, A. 1993. The role of bradykinin in mediating ischemic brain edema in rats. *Stroke,* 24**,** 571-5; discussion 575-6.

KANG, H., DAVIS-DUSENBERY, B. N., NGUYEN, P. H., LAL, A., LIEBERMAN, J., VAN AELST, L., LAGNA, G. & HATA, A. 2012. Bone morphogenetic protein 4 promotes vascular smooth muscle contractility by activating microRNA-21 (miR-21), which down-regulates expression of family of dedicator of cytokinesis (DOCK) proteins. *J Biol Chem,* 287**,** 3976-86.

KATAKOWSKI, M., BULLER, B., ZHENG, X., LU, Y., ROGERS, T., OSOBAMIRO, O., SHU, W., JIANG, F. & CHOPP, M. 2013. Exosomes from marrow stromal cells expressing miR-146b inhibit glioma growth. *Cancer Lett,* 335**,** 201-4.

KATSURA, K., KRISTIAN, T. & SIESJO, B. K. 1994. Energy metabolism, ion homeostasis, and cell damage in the brain. *Biochem Soc Trans,* 22**,** 991-6.

KAWAMATA, T., SEITZ, H. & TOMARI, Y. 2009. Structural determinants of miRNAs for RISC loading and slicer-independent unwinding. *Nat Struct Mol Biol,* 16**,** 953-60.

KAWAMATA, T. & TOMARI, Y. 2010. Making RISC. *Trends Biochem Sci,* 35**,** 368-76.

KERNIE, S. G. & PARENT, J. M. 2010. Forebrain neurogenesis after focal Ischemic and traumatic brain injury. *Neurobiol Dis,* 37**,** 267-74.

KHANNA, S., RINK, C., GHOORKHANIAN, R., GNYAWALI, S., HEIGEL, M., WIJESINGHE, D. S., CHALFANT, C. E., CHAN, Y. C., BANERJEE, J. & HUANG, Y. 2013. Loss of miR-29b following acute ischemic stroke contributes to neural cell

death and infarct size. *Journal of Cerebral Blood Flow & Metabolism,* 33**,** 1197-1206.

KHVOROVA, A., REYNOLDS, A. & JAYASENA, S. D. 2003. Functional siRNAs and miRNAs exhibit strand bias. *Cell,* 115**,** 209-16.

KILKENNY, C., BROWNE, W. J., CUTHILL, I. C., EMERSON, M. & ALTMAN, D. G. 2010. Improving bioscience research reporting: the ARRIVE guidelines for reporting animal research. *PLoS Biol,* 8**,** e1000412.

KIM, J.-M., LEE, S.-T., CHU, K., JUNG, K.-H., KIM, J. H., YU, J.-S., KIM, S., KIM, S. H., PARK, D.-K., MOON, J., BAN, J., KIM, M., LEE, S. K. & ROH, J.-K. 2014. Inhibition of Let7c MicroRNA Is Neuroprotective in a Rat Intracerebral Hemorrhage Model. *PLoS ONE,* 9**,** e97946.

KIM, J. M., JUNG, K. H., CHU, K., LEE, S. T., BAN, J., MOON, J., KIM, M., LEE, S. K. & ROH, J. K. 2015. Atherosclerosis-Related Circulating MicroRNAs as a Predictor of Stroke Recurrence. *Transl Stroke Res,* 6**,** 191-7.

KITAMURA, Y., IIDA, Y., ABE, J., MIFUNE, M., KASUYA, F., OHTA, M., IGARASHI, K., SAITO, Y. & SAJI, H. 2006a. In vivo measurement of presynaptic Zn2+ release during forebrain ischemia in rats. *Biol Pharm Bull,* 29**,** 821-3.

KITAMURA, Y., IIDA, Y., ABE, J., MIFUNE, M., KASUYA, F., OHTA, M., IGARASHI, K., SAITO, Y. & SAJI, H. 2006b. Release of vesicular Zn2+ in a rat transient middle cerebral artery occlusion model. *Brain Res Bull,* 69**,** 622-5.

KOOIJMANS, S. A., STREMERSCH, S., BRAECKMANS, K., DE SMEDT, S. C., HENDRIX, A., WOOD, M. J., SCHIFFELERS, R. M., RAEMDONCK, K. & VADER, P. 2013. Electroporation-induced siRNA precipitation obscures the efficiency of siRNA loading into extracellular vesicles. *J Control Release,* 172**,** 229-38.

KOSAKA, N., IGUCHI, H., YOSHIOKA, Y., HAGIWARA, K., TAKESHITA, F. & OCHIYA, T. 2012. Competitive interactions of cancer cells and normal cells via secretory microRNAs. *J Biol Chem,* 287**,** 1397-405.

KOZOMARA, A. & GRIFFITHS-JONES, S. 2014. miRBase: annotating high confidence microRNAs using deep sequencing data. *Nucleic Acids Res,* 42**,** D68-73.

KRICHEVSKY, A. M. & GABRIELY, G. 2009. miR-21: a small multi-faceted RNA. *J Cell Mol Med,* 13**,** 39-53.

KRUPINSKI, J., KUMAR, P., KUMAR, S. & KALUZA, J. 1996. Increased Expression of TGF-β1 in Brain Tissue After Ischemic Stroke in Humans. *Stroke,* 27**,** 852-857.

KRUTZFELDT, J., RAJEWSKY, N., BRAICH, R., RAJEEV, K. G., TUSCHL, T., MANOHARAN, M. & STOFFEL, M. 2005. Silencing of microRNAs in vivo with 'antagomirs'. *Nature,* 438**,** 685-9.

KUEHBACHER, A., URBICH, C., ZEIHER, A. M. & DIMMELER, S. 2007. Role of Dicer and Drosha for endothelial microRNA expression and angiogenesis. *Circ Res,* 101**,** 59-68.

KUROIWA, T., TING, P., MARTINEZ, H. & KLATZO, I. 1985. The biphasic opening of the blood-brain barrier to proteins following temporary middle cerebral artery occlusion. *Acta Neuropathol,* 68**,** 122-9.

LACKLAND, D. T., ROCCELLA, E. J., DEUTSCH, A. F., FORNAGE, M., GEORGE, M. G., HOWARD, G., KISSELA, B. M., KITTNER, S. J., LICHTMAN, J. H., LISABETH, L. D., SCHWAMM, L. H., SMITH, E. E. & TOWFIGHI, A. 2014. Factors influencing the decline in stroke mortality: a statement from the American Heart Association/American Stroke Association. *Stroke,* 45**,** 315-53.

LAKHAL, S. & WOOD, M. J. A. 2011. Exosome nanotechnology: An emerging paradigm shift in drug delivery. *BioEssays,* 33**,** 737-741.

LAN, Y. F., CHEN, H. H., LAI, P. F., CHENG, C. F., HUANG, Y. T., LEE, Y. C., CHEN, T. W. & LIN, H. 2012. MicroRNA-494 reduces ATF3 expression and promotes AKI. *J Am Soc Nephrol,* 23**,** 2012-23.

LANDER, E. S., LINTON, L. M., BIRREN, B., NUSBAUM, C., ZODY, M. C., BALDWIN, J., DEVON, K., DEWAR, K., DOYLE, M., FITZHUGH, W., FUNKE, R., GAGE, D., HARRIS, K., HEAFORD, A., HOWLAND, J., KANN, L., LEHOCZKY, J., LEVINE, R., MCEWAN, P., MCKERNAN, K., MELDRIM, J., MESIROV, J. P., MIRANDA, C., MORRIS, W., NAYLOR, J., RAYMOND, C., ROSETTI, M., SANTOS, R., SHERIDAN, A., SOUGNEZ, C., STANGE-THOMANN, Y., STOJANOVIC, N.,

SUBRAMANIAN, A., WYMAN, D., ROGERS, J., SULSTON, J., AINSCOUGH, R., BECK, S., BENTLEY, D., BURTON, J., CLEE, C., CARTER, N., COULSON, A., DEADMAN, R., DELOUKAS, P., DUNHAM, A., DUNHAM, I., DURBIN, R., FRENCH, L., GRAFHAM, D., GREGORY, S., HUBBARD, T., HUMPHRAY, S., HUNT, A., JONES, M., LLOYD, C., MCMURRAY, A., MATTHEWS, L., MERCER, S., MILNE, S., MULLIKIN, J. C., MUNGALL, A., PLUMB, R., ROSS, M., SHOWNKEEN, R., SIMS, S., WATERSTON, R. H., WILSON, R. K., HILLIER, L. W., MCPHERSON, J. D., MARRA, M. A., MARDIS, E. R., FULTON, L. A., CHINWALLA, A. T., PEPIN, K. H., GISH, W. R., CHISSOE, S. L., WENDL, M. C., DELEHAUNTY, K. D., MINER, T. L., DELEHAUNTY, A., KRAMER, J. B., COOK, L. L., FULTON, R. S., JOHNSON, D. L., MINX, P. J., CLIFTON, S. W., HAWKINS, T., BRANSCOMB, E., PREDKI, P., RICHARDSON, P., WENNING, S., SLEZAK, T., DOGGETT, N., CHENG, J. F., OLSEN, A., LUCAS, S., ELKIN, C., UBERBACHER, E., FRAZIER, M., et al. 2001. Initial sequencing and analysis of the human genome. *Nature,* 409**,** 860-921.

LANDTHALER, M., YALCIN, A. & TUSCHL, T. 2004. The human DiGeorge syndrome critical region gene 8 and Its D. melanogaster homolog are required for miRNA biogenesis. *Curr Biol,* 14**,** 2162-7.

LEE, R. C., FEINBAUM, R. L. & AMBROS, V. 1993. The C. elegans heterochronic gene lin-4 encodes small RNAs with antisense complementarity to lin-14. *Cell,* 75**,** 843-54.

LEE, S. T., CHU, K., JUNG, K. H., KIM, J. H., HUH, J. Y., YOON, H., PARK, D. K., LIM, J. Y., KIM, J. M., JEON, D., RYU, H., LEE, S. K., KIM, M. & ROH, J. K. 2012. miR-206 regulates brain-derived neurotrophic factor in Alzheimer disease model. *Ann Neurol,* 72**,** 269-77.

LEE, Y., AHN, C., HAN, J., CHOI, H., KIM, J., YIM, J., LEE, J., PROVOST, P., RADMARK, O., KIM, S. & KIM, V. N. 2003. The nuclear RNase III Drosha initiates microRNA processing. *Nature,* 425**,** 415-9.

LEE, Y., JEON, K., LEE, J. T., KIM, S. & KIM, V. N. 2002. MicroRNA maturation: stepwise processing and subcellular localization. *EMBO J,* 21**,** 4663-70.

LEE, Y., KIM, M., HAN, J., YEOM, K. H., LEE, S., BAEK, S. H. & KIM, V. N. 2004. MicroRNA genes are transcribed by RNA polymerase II. *EMBO J,* 23**,** 4051-60.

LEIST, M., VOLBRACHT, C., KUHNLE, S., FAVA, E., FERRANDO-MAY, E. & NICOTERA, P. 1997. Caspase-mediated apoptosis in neuronal excitotoxicity triggered by nitric oxide. *Mol Med,* 3**,** 750-64.

LENNOX, K. A. & BEHLKE, M. A. 2010. A direct comparison of anti-microRNA oligonucleotide potency. *Pharm Res,* 27**,** 1788-99.

LEUNG, L. Y., CHAN, C. P., LEUNG, Y. K., JIANG, H. L., ABRIGO, J. M., WANG DE, F., CHUNG, J. S., RAINER, T. H. & GRAHAM, C. A. 2014. Comparison of miR-124-3p and miR-16 for early diagnosis of hemorrhagic and ischemic stroke. *Clin Chim Acta,* 433**,** 139-44.

LEVIN, A. A. 1999. A review of the issues in the pharmacokinetics and toxicology of phosphorothioate antisense oligonucleotides. *Biochim Biophys Acta,* 1489**,** 69-84.

LEWERENZ, J., DARGUSCH, R. & MAHER, P. 2010. Lactacidosis modulates glutathione metabolism and oxidative glutamate toxicity. *J Neurochem,* 113**,** 502-14.

LEWIS, B. P., SHIH, I. H., JONES-RHOADES, M. W., BARTEL, D. P. & BURGE, C. B. 2003. Prediction of mammalian microRNA targets. *Cell,* 115**,** 787-98.

LEWSEY, J. D., GILLIES, M., JHUND, P. S., CHALMERS, J. W., REDPATH, A., BRIGGS, A., WALTERS, M., LANGHORNE, P., CAPEWELL, S., MCMURRAY, J. J. & MACINTYRE, K. 2009. Sex differences in incidence, mortality, and survival in individuals with stroke in Scotland, 1986 to 2005. *Stroke,* 40**,** 1038-43.

LI, P., TENG, F., GAO, F., ZHANG, M., WU, J. & ZHANG, C. 2015a. Identification of Circulating MicroRNAs as Potential Biomarkers for Detecting Acute Ischemic Stroke. *Cell Mol Neurobiol,* 35**,** 433-47.

LI, S. H., SU, S. Y. & LIU, J. L. 2015b. Differential Regulation of microRNAs in Patients with Ischemic Stroke. *Curr Neurovasc Res,* 12**,** 214-21.

LIAO, Y. C., WANG, Y. S., GUO, Y. C., LIN, W. L., CHANG, M. H. & JUO, S. H. 2014. Let-7g improves multiple endothelial functions through targeting transforming growth factor-beta and SIRT-1 signaling. *J Am Coll Cardiol,* 63**,** 1685-94.

LIFE TECHNOLOGIES, T. 2011. *Optimized protocol with low sample input for profiling human microRNA using the OpenArray® platform.* [Online]. Life Technologies Corporation. Available: https://tools.thermofisher.com/content/sfs/brochures/cms_097637.pdf [Accessed April 27 2016].

LIU, C. G., CALIN, G. A., MELOON, B., GAMLIEL, N., SEVIGNANI, C., FERRACIN, M., DUMITRU, C. D., SHIMIZU, M., ZUPO, S., DONO, M., ALDER, H., BULLRICH, F., NEGRINI, M. & CROCE, C. M. 2004a. An oligonucleotide microchip for genome-wide microRNA profiling in human and mouse tissues. *Proc Natl Acad Sci U S A,* 101**,** 9740-4.

LIU, D. Z., JICKLING, G. C., ANDER, B. P., HULL, H., ZHAN, X., COX, C., SHROFF, N., DYKSTRA-AIELLO, C., STAMOVA, B. & SHARP, F. R. 2015a. Elevating microRNA-122 in blood improves outcomes after temporary middle cerebral artery occlusion in rats. *Journal of Cerebral Blood Flow & Metabolism*.

LIU, J., CARMELL, M. A., RIVAS, F. V., MARSDEN, C. G., THOMSON, J. M., SONG, J. J., HAMMOND, S. M., JOSHUA-TOR, L. & HANNON, G. J. 2004b. Argonaute2 is the catalytic engine of mammalian RNAi. *Science,* 305**,** 1437-41.

LIU, P., ZHAO, H., WANG, R., WANG, P., TAO, Z., GAO, L., YAN, F., LIU, X., YU, S., JI, X. & LUO, Y. 2015b. MicroRNA-424 protects against focal cerebral ischemia and reperfusion injury in mice by suppressing oxidative stress. *Stroke,* 46**,** 513-9.

LIU, X., LI, F., ZHAO, S., LUO, Y., KANG, J., ZHAO, H., YAN, F., LI, S. & JI, X. 2013a. MicroRNA-124–Mediated Regulation of Inhibitory Member of Apoptosis-Stimulating Protein of p53 Family in Experimental Stroke. *Stroke,* 44**,** 1973-1980.

LIU, X. S., CHOPP, M., WANG, X. L., ZHANG, L., HOZESKA-SOLGOT, A., TANG, T., KASSIS, H., ZHANG, R. L., CHEN, C. & XU, J. 2013b. MicroRNA-17-92 cluster mediates the proliferation and survival of neural progenitor cells after stroke. *Journal of Biological Chemistry,* 288**,** 12478-12488.

LIU, X. S., CHOPP, M., WANG, X. L., ZHANG, L., HOZESKA-SOLGOT, A., TANG, T., KASSIS, H., ZHANG, R. L., CHEN, C., XU, J. & ZHANG, Z. G. 2013c. MicroRNA-17-92 cluster mediates the proliferation and survival of neural progenitor cells after stroke. *J Biol Chem,* 288**,** 12478-88.

LIU, Y., ZHANG, J., HAN, R., LIU, H., SUN, D. & LIU, X. 2015c. Downregulation of serum brain specific microRNA is associated with inflammation and infarct volume in acute ischemic stroke. *Journal of Clinical Neuroscience,* 22**,** 291-295.

LIU, Y. P. & BERKHOUT, B. 2011. miRNA cassettes in viral vectors: Problems and solutions. *Biochimica et Biophysica Acta (BBA) - Gene Regulatory Mechanisms,* 1809**,** 732-745.

LIVAK, K. J. & SCHMITTGEN, T. D. 2001. Analysis of Relative Gene Expression Data Using Real-Time Quantitative PCR and the $2^{-\Delta\Delta CT}$ Method. *Methods,* 25**,** 402-408.

LLAVE, C., XIE, Z., KASSCHAU, K. D. & CARRINGTON, J. C. 2002. Cleavage of Scarecrow-like mRNA targets directed by a class of Arabidopsis miRNA. *Science,* 297**,** 2053-6.

LOCHHEAD, J. J. & THORNE, R. G. 2012. Intranasal delivery of biologics to the central nervous system. *Advanced Drug Delivery Reviews,* 64**,** 614-628.

LONG, G., WANG, F., LI, H., YIN, Z., SANDIP, C., LOU, Y., WANG, Y., CHEN, C. & WANG, D. W. 2013. Circulating miR-30a, miR-126 and let-7b as biomarker for ischemic stroke in humans. *BMC neurology,* 13**,** 178.

LONGA, E. Z., WEINSTEIN, P. R., CARLSON, S. & CUMMINS, R. 1989. Reversible middle cerebral artery occlusion without craniectomy in rats. *Stroke,* 20**,** 84-91.

LÖTVALL, J., HILL, A. F., HOCHBERG, F., BUZÁS, E. I., DI VIZIO, D., GARDINER, C., GHO, Y. S., KUROCHKIN, I. V., MATHIVANAN, S., QUESENBERRY, P., SAHOO, S., TAHARA, H., WAUBEN, M. H., WITWER, K. W. & THÉRY, C. 2014. Minimal experimental requirements for definition of extracellular vesicles and their

functions: a position statement from the International Society for Extracellular Vesicles. *2014*.

LU, J., GETZ, G., MISKA, E. A., ALVAREZ-SAAVEDRA, E., LAMB, J., PECK, D., SWEET-CORDERO, A., EBERT, B. L., MAK, R. H., FERRANDO, A. A., DOWNING, J. R., JACKS, T., HORVITZ, H. R. & GOLUB, T. R. 2005. MicroRNA expression profiles classify human cancers. *Nature,* 435**,** 834-8.

LUENGO-FERNANDEZ, R., GRAY, A. M., BULL, L., WELCH, S., CUTHBERTSON, F., ROTHWELL, P. M. & OXFORD VASCULAR, S. 2013. Quality of life after TIA and stroke: ten-year results of the Oxford Vascular Study. *Neurology,* 81**,** 1588-95.

LUENGO-FERNANDEZ, R., LEAL, J. & GRAY, A. 2014. Research Spend in the UK. *In:* STROKE ASSOCIATION, T. (ed.). London: The Stroke Association.

LUND, E., GUTTINGER, S., CALADO, A., DAHLBERG, J. E. & KUTAY, U. 2004. Nuclear export of microRNA precursors. *Science,* 303**,** 95-8.

MACLEOD, M. R., FISHER, M., O'COLLINS, V., SENA, E. S., DIRNAGL, U., BATH, P. M., BUCHAN, A., VAN DER WORP, H. B., TRAYSTMAN, R., MINEMATSU, K., DONNAN, G. A. & HOWELLS, D. W. 2009. Good laboratory practice: preventing introduction of bias at the bench. *Stroke,* 40**,** e50-2.

MACRAE, I. M. 2011. Preclinical stroke research--advantages and disadvantages of the most common rodent models of focal ischaemia. *Br J Pharmacol,* 164**,** 1062-78.

MARKUS, R., REUTENS, D. C., KAZUI, S., READ, S., WRIGHT, P., PEARCE, D. C., TOCHON-DANGUY, H. J., SACHINIDIS, J. I. & DONNAN, G. A. 2004. Hypoxic tissue in ischaemic stroke: persistence and clinical consequences of spontaneous survival. *Brain,* 127**,** 1427-36.

MARTIN, R. L., LLOYD, H. G. & COWAN, A. I. 1994. The early events of oxygen and glucose deprivation: setting the scene for neuronal death? *Trends Neurosci,* 17**,** 251-7.

MATRANGA, C., TOMARI, Y., SHIN, C., BARTEL, D. P. & ZAMORE, P. D. 2005. Passenger-strand cleavage facilitates assembly of siRNA into Ago2-containing RNAi enzyme complexes. *Cell,* 123**,** 607-20.

MEISTER, G., LANDTHALER, M., PATKANIOWSKA, A., DORSETT, Y., TENG, G. & TUSCHL, T. 2004. Human Argonaute2 mediates RNA cleavage targeted by miRNAs and siRNAs. *Mol Cell,* 15**,** 185-97.

MELLER, R., PEARSON, A. N., HARDY, J. J., HALL, C. L., MCGUIRE, D., FRANKEL, M. R. & SIMON, R. P. 2016. Blood transcriptome changes after stroke in an African American population. *Ann Clin Transl Neurol,* 3**,** 70-81.

MELO, SONIA A., SUGIMOTO, H., O'CONNELL, JOYCE T., KATO, N., VILLANUEVA, A., VIDAL, A., QIU, L., VITKIN, E., PERELMAN, LEV T., MELO, CARLOS A., LUCCI, A., IVAN, C., CALIN, GEORGE A. & KALLURI, R. 2014. Cancer Exosomes Perform Cell-Independent MicroRNA Biogenesis and Promote Tumorigenesis. *Cancer Cell,* 26**,** 707-721.

MENON, B. K., SAVER, J. L., GOYAL, M., NOGUEIRA, R., PRABHAKARAN, S., LIANG, L., XIAN, Y., HERNANDEZ, A. F., FONAROW, G. C., SCHWAMM, L. & SMITH, E. E. 2015. Trends in endovascular therapy and clinical outcomes within the nationwide Get With The Guidelines-Stroke registry. *Stroke,* 46**,** 989-95.

MILLER, A. A., DRUMMOND, G. R., SCHMIDT, H. H. & SOBEY, C. G. 2005. NADPH oxidase activity and function are profoundly greater in cerebral versus systemic arteries. *Circ Res,* 97**,** 1055-62.

MIRNA THERAPEUTICS, I. 2016. *A Multicenter Phase I Study of MRX34, MicroRNA miR-RX34 Liposomal Injection* [Online]. Bethesda (MD): National Library of Medicine (US). 2000-2016. Available: https://clinicaltrials.gov/ct2/show/NCT01829971?term=mirna+therapeutics&rank=115 [Accessed 19 September 2016.

MOBIUS, W., VAN DONSELAAR, E., OHNO-IWASHITA, Y., SHIMADA, Y., HEIJNEN, H. F., SLOT, J. W. & GEUZE, H. J. 2003. Recycling compartments and the internal vesicles of multivesicular bodies harbor most of the cholesterol found in the endocytic pathway. *Traffic,* 4**,** 222-31.

MOMEN-HERAVI, F., BALA, S., BUKONG, T. & SZABO, G. 2014. Exosome-mediated delivery of functionally active miRNA-155 inhibitor to macrophages. *Nanomedicine: Nanotechnology, Biology and Medicine,* 10**,** 1517-1527.

MONTECALVO, A., LARREGINA, A. T., SHUFESKY, W. J., STOLZ, D. B., SULLIVAN, M. L., KARLSSON, J. M., BATY, C. J., GIBSON, G. A., ERDOS, G., WANG, Z., MILOSEVIC, J., TKACHEVA, O. A., DIVITO, S. J., JORDAN, R., LYONS-WEILER, J., WATKINS, S. C. & MORELLI, A. E. 2012. Mechanism of transfer of functional microRNAs between mouse dendritic cells via exosomes. *Blood,* 119**,** 756-66.

MOON, J.-M., XU, L. & GIFFARD, R. G. 2013. Inhibition of microRNA-181 reduces forebrain ischemia-induced neuronal loss. *Journal of Cerebral Blood Flow & Metabolism,* 33**,** 1976-1982.

MOREL, L., REGAN, M., HIGASHIMORI, H., NG, S. K., ESAU, C., VIDENSKY, S., ROTHSTEIN, J. & YANG, Y. 2013. Neuronal exosomal miRNA-dependent translational regulation of astroglial glutamate transporter GLT1. *J Biol Chem,* 288**,** 7105-16.

MOURELATOS, Z., DOSTIE, J., PAUSHKIN, S., SHARMA, A., CHARROUX, B., ABEL, L., RAPPSILBER, J., MANN, M. & DREYFUSS, G. 2002. miRNPs: a novel class of ribonucleoproteins containing numerous microRNAs. *Genes Dev,* 16**,** 720-8.

MOZAFFARIAN, D., BENJAMIN, E. J., GO, A. S., ARNETT, D. K., BLAHA, M. J., CUSHMAN, M., DAS, S. R., DE FERRANTI, S., DESPRES, J. P., FULLERTON, H. J., HOWARD, V. J., HUFFMAN, M. D., ISASI, C. R., JIMENEZ, M. C., JUDD, S. E., KISSELA, B. M., LICHTMAN, J. H., LISABETH, L. D., LIU, S., MACKEY, R. H., MAGID, D. J., MCGUIRE, D. K., MOHLER, E. R., 3RD, MOY, C. S., MUNTNER, P., MUSSOLINO, M. E., NASIR, K., NEUMAR, R. W., NICHOL, G., PALANIAPPAN, L., PANDEY, D. K., REEVES, M. J., RODRIGUEZ, C. J., ROSAMOND, W., SORLIE, P. D., STEIN, J., TOWFIGHI, A., TURAN, T. N., VIRANI, S. S., WOO, D., YEH, R. W. & TURNER, M. B. 2015. Heart Disease and Stroke Statistics-2016 Update: A Report From the American Heart Association. *Circulation*.

MUKHOPADHYAY, P., DAS, S., AHSAN, M. K., OTANI, H. & DAS, D. K. 2012. Modulation of microRNA 20b with resveratrol and longevinex is linked with their potent anti-angiogenic action in the ischaemic myocardium and synergestic effects of resveratrol and gamma-tocotrienol. *J Cell Mol Med,* 16**,** 2504-17.

MULLER, S., RAULEFS, S., BRUNS, P., AFONSO-GRUNZ, F., PLOTNER, A., THERMANN, R., JAGER, C., SCHLITTER, A. M., KONG, B., REGEL, I., ROTH, W. K., ROTTER, B., HOFFMEIER, K., KAHL, G., KOCH, I., THEIS, F. J., KLEEFF, J., WINTER, P. & MICHALSKI, C. W. 2015. Next-generation sequencing reveals novel differentially regulated mRNAs, lncRNAs, miRNAs, sdRNAs and a piRNA in pancreatic cancer. *Mol Cancer,* 14**,** 94.

MUNOZ, J. L., BLISS, S. A., GRECO, S. J., RAMKISSOON, S. H., LIGON, K. L. & RAMESHWAR, P. 2013. Delivery of Functional Anti-miR-9 by Mesenchymal Stem Cell-derived Exosomes to Glioblastoma Multiforme Cells Conferred Chemosensitivity. *Mol Ther Nucleic Acids,* 2**,** e126.

NAGAOKA, A., IWATSUKA, H., SUZUOKI, Z. & OKAMOTO, K. 1976. Genetic predisposition to stroke in spontaneously hypertensive rats. *Am J Physiol,* 230**,** 1354-9.

NAGESH, V., WELCH, K. M., WINDHAM, J. P., PATEL, S., LEVINE, S. R., HEARSHEN, D., PECK, D., ROBBINS, K., D'OLHABERRIAGUE, L., SOLTANIAN-ZADEH, H. & BOSKA, M. D. 1998. Time course of ADCw changes in ischemic stroke: beyond the human eye! *Stroke,* 29**,** 1778-82.

NAMURA, S., ZHU, J., FINK, K., ENDRES, M., SRINIVASAN, A., TOMASELLI, K. J., YUAN, J. & MOSKOWITZ, M. A. 1998. Activation and cleavage of caspase-3 in apoptosis induced by experimental cerebral ischemia. *J Neurosci,* 18**,** 3659-68.

NATIONAL INSTITUTE FOR HEALTH AND CARE EXCELLENCE, T. 2008. Stroke and transient ischaemic attack in over 16s: diagnosis and initial management. *In:* NICE (ed.) *NICE Guideline.* NICE.

NATIONAL INSTITUTE FOR HEALTH AND CARE EXCELLENCE, T. 2011. Hypertension in adults: diagnosis and management. *In:* NICE (ed.) *NICE Guidelines.* NICE.

NATIONAL INSTITUTE FOR HEALTH AND CARE EXCELLENCE, T. 2014. Cardiovascular disease: risk assessment and reduction, including lipid modification. *In:* NICE (ed.) *NICE Guideline.* NICE.

NATIONAL INSTITUTE FOR HEALTH AND CARE EXCELLENCE, T. 2015. Atrial fibrillation. *In:* NICE (ed.) *NICE Guideline.* NICE.

NATIONAL INSTITUTE OF NEUROLOGICAL DISORDERS, T. & STROKE RT-PA STROKE STUDY GROUP, T. 1995. Tissue Plasminogen Activator for Acute Ischemic Stroke. *New England Journal of Medicine,* 333**,** 1581-1588.

NI, J., WANG, X., CHEN, S., LIU, H., WANG, Y., XU, X., CHENG, J., JIA, J. & ZHEN, X. 2015. MicroRNA let-7c-5p protects against cerebral ischemia injury via mechanisms involving the inhibition of microglia activation. *Brain, Behavior, and Immunity,* 49**,** 75-85.

NICHOLLS, D. & ATTWELL, D. 1990. The release and uptake of excitatory amino acids. *Trends Pharmacol Sci,* 11**,** 462-8.

NOR, A. M., DAVIS, J., SEN, B., SHIPSEY, D., LOUW, S. J., DYKER, A. G., DAVIS, M. & FORD, G. A. 2005. The Recognition of Stroke in the Emergency Room (ROSIER) scale: development and validation of a stroke recognition instrument. *The Lancet Neurology,* 4**,** 727-734.

NOTTROTT, S., SIMARD, M. J. & RICHTER, J. D. 2006. Human let-7a miRNA blocks protein production on actively translating polyribosomes. *Nat Struct Mol Biol,* 13**,** 1108-14.

O'COLLINS, V. E., MACLEOD, M. R., DONNAN, G. A., HORKY, L. L., VAN DER WORP, B. H. & HOWELLS, D. W. 2006. 1,026 experimental treatments in acute stroke. *Ann Neurol,* 59**,** 467-77.

O'DONNELL, M. J., XAVIER, D., LIU, L., ZHANG, H., CHIN, S. L., RAO-MELACINI, P., RANGARAJAN, S., ISLAM, S., PAIS, P., MCQUEEN, M. J., MONDO, C., DAMASCENO, A., LOPEZ-JARAMILLO, P., HANKEY, G. J., DANS, A. L., YUSOFF, K., TRUELSEN, T., DIENER, H.-C., SACCO, R. L., RYGLEWICZ, D., CZLONKOWSKA, A., WEIMAR, C., WANG, X. & YUSUF, S. 2010. Risk factors for ischaemic and intracerebral haemorrhagic stroke in 22 countries (the INTERSTROKE study): a case-control study. *The Lancet,* 376**,** 112-123.

OBAD, S., DOS SANTOS, C. O., PETRI, A., HEIDENBLAD, M., BROOM, O., RUSE, C., FU, C., LINDOW, M., STENVANG, J., STRAARUP, E. M., HANSEN, H. F., KOCH, T., PAPPIN, D., HANNON, G. J. & KAUPPINEN, S. 2011. Silencing of microRNA families by seed-targeting tiny LNAs. *Nat Genet,* 43**,** 371-8.

OHAB, J. J., FLEMING, S., BLESCH, A. & CARMICHAEL, S. T. 2006. A neurovascular niche for neurogenesis after stroke. *J Neurosci,* 26**,** 13007-16.

OHNO, S., TAKANASHI, M., SUDO, K., UEDA, S., ISHIKAWA, A., MATSUYAMA, N., FUJITA, K., MIZUTANI, T., OHGI, T., OCHIYA, T., GOTOH, N. & KURODA, M. 2013. Systemically injected exosomes targeted to EGFR deliver antitumor microRNA to breast cancer cells. *Mol Ther,* 21**,** 185-91.

OKADA, Y., COPELAND, B. R., FITRIDGE, R., KOZIOL, J. A. & DEL ZOPPO, G. J. 1994a. Fibrin contributes to microvascular obstructions and parenchymal changes during early focal cerebral ischemia and reperfusion. *Stroke,* 25**,** 1847-53; discussion 1853-4.

OKADA, Y., COPELAND, B. R., MORI, E., TUNG, M. M., THOMAS, W. S. & DEL ZOPPO, G. J. 1994b. P-selectin and intercellular adhesion molecule-1 expression after focal brain ischemia and reperfusion. *Stroke,* 25**,** 202-11.

OLIVIERI, F., ANTONICELLI, R., SPAZZAFUMO, L., SANTINI, G., RIPPO, M. R., GALEAZZI, R., GIOVAGNETTI, S., D'ALESSANDRA, Y., MARCHESELLI, F., CAPOGROSSI, M. C. & PROCOPIO, A. D. 2014. Admission levels of circulating miR-499-5p and risk of death in elderly patients after acute non-ST elevation myocardial infarction. *International Journal of Cardiology,* 172**,** e276-e278.

OLSEN, P. H. & AMBROS, V. 1999. The lin-4 regulatory RNA controls developmental timing in Caenorhabditis elegans by blocking LIN-14 protein synthesis after the initiation of translation. *Dev Biol,* 216**,** 671-80.

ORD, E. N. J., SHIRLEY, R., VAN KRALINGEN, J. C., GRAVES, A., MCCLURE, J. D., WILKINSON, M., MCCABE, C., MACRAE, I. M. & WORK, L. M. 2012. Positive

impact of pre-stroke surgery on survival following transient focal ischemia in hypertensive rats. *Journal of Neuroscience Methods,* 211**,** 305-308.

OUYANG, Y. B., LU, Y., YUE, S., XU, L. J., XIONG, X. X., WHITE, R. E., SUN, X. & GIFFARD, R. G. 2012. miR-181 regulates GRP78 and influences outcome from cerebral ischemia in vitro and in vivo. *Neurobiol Dis,* 45**,** 555-63.

OVERGAARD, K., SEREGHY, T., BOYSEN, G., PEDERSEN, H., HOYER, S. & DIEMER, N. H. 1992. A rat model of reproducible cerebral infarction using thrombotic blood clot emboli. *J Cereb Blood Flow Metab,* 12**,** 484-90.

PACHER, P., BECKMAN, J. S. & LIAUDET, L. 2007. Nitric oxide and peroxynitrite in health and disease. *Physiol Rev,* 87**,** 315-424.

PALMA, J., YADDANAPUDI, S. C., PIGATI, L., HAVENS, M. A., JEONG, S., WEINER, G. A., WEIMER, K. M., STERN, B., HASTINGS, M. L. & DUELLI, D. M. 2012. MicroRNAs are exported from malignant cells in customized particles. *Nucleic Acids Res,* 40**,** 9125-38.

PAN, Q., RAMAKRISHNAIAH, V., HENRY, S., FOURASCHEN, S., DE RUITER, P. E., KWEKKEBOOM, J., TILANUS, H. W., JANSSEN, H. L. & VAN DER LAAN, L. J. 2012. Hepatic cell-to-cell transmission of small silencing RNA can extend the therapeutic reach of RNA interference (RNAi). *Gut,* 61**,** 1330-9.

PANDI, G., NAKKA, V. P., DHARAP, A., ROOPRA, A. & VEMUGANTI, R. 2013. MicroRNA miR-29c down-regulation leading to de-repression of its target DNA methyltransferase 3a promotes ischemic brain damage. *PloS one,* 8**,** e58039.

PARENT, J. M., VEXLER, Z. S., GONG, C., DERUGIN, N. & FERRIERO, D. M. 2002. Rat forebrain neurogenesis and striatal neuron replacement after focal stroke. *Ann Neurol,* 52**,** 802-13.

PARK, K. P., ROSELL, A., FOERCH, C., XING, C., KIM, W. J., LEE, S., OPDENAKKER, G., FURIE, K. L. & LO, E. H. 2009. Plasma and brain matrix metalloproteinase-9 after acute focal cerebral ischemia in rats. *Stroke,* 40**,** 2836-42.

PAROLINI, I., FEDERICI, C., RAGGI, C., LUGINI, L., PALLESCHI, S., DE MILITO, A., COSCIA, C., IESSI, E., LOGOZZI, M., MOLINARI, A., COLONE, M., TATTI, M., SARGIACOMO, M. & FAIS, S. 2009. Microenvironmental pH is a key factor for exosome traffic in tumor cells. *J Biol Chem,* 284**,** 34211-22.

PEERSCHKE, E. I., YIN, W. & GHEBREHIWET, B. 2010. Complement activation on platelets: implications for vascular inflammation and thrombosis. *Mol Immunol,* 47**,** 2170-5.

PENG, G., YUAN, Y., WU, S., HE, F., HU, Y. & LUO, B. 2015. MicroRNA let-7e Is a Potential Circulating Biomarker of Acute Stage Ischemic Stroke. *Transl Stroke Res,* 6**,** 437-45.

PEREZ-GONZALEZ, R., GAUTHIER, S. A., KUMAR, A. & LEVY, E. 2012. The exosome secretory pathway transports amyloid precursor protein carboxyl-terminal fragments from the cell into the brain extracellular space. *J Biol Chem,* 287**,** 43108-15.

PETERSEN, C. P., BORDELEAU, M. E., PELLETIER, J. & SHARP, P. A. 2006. Short RNAs repress translation after initiation in mammalian cells. *Mol Cell,* 21**,** 533-42.

PILLAI, R. S., BHATTACHARYYA, S. N., ARTUS, C. G., ZOLLER, T., COUGOT, N., BASYUK, E., BERTRAND, E. & FILIPOWICZ, W. 2005. Inhibition of translational initiation by Let-7 MicroRNA in human cells. *Science,* 309**,** 1573-6.

PUBLIC HEALTH ENGLAND, T. 2013. *National Cardiovascular Disease (CVD) profiles* [Online]. Public Health England. Available: http://www.sepho.org.uk/NationalCVD/NationalCVDProfiles.aspx [Accessed 26 January 2016.

PUSIC, A. D. & KRAIG, R. P. 2014. Youth and environmental enrichment generate serum exosomes containing miR-219 that promote CNS myelination. *Glia,* 62**,** 284-99.

QIU, J., ZHOU, X.-Y., ZHOU, X.-G., CHENG, R., LIU, H.-Y. & LI, Y. 2013. Neuroprotective effects of microRNA-210 on hypoxic-ischemic encephalopathy. *BioMed research international,* 2013.

QU, Y., WU, J., CHEN, D., ZHAO, F., LIU, J., YANG, C., WEI, D., FERRIERO, D. M. & MU, D. 2014. MiR-139-5p inhibits HGTD-P and regulates neuronal apoptosis induced by hypoxia-ischemia in neonatal rats. *Neurobiol Dis,* 63**,** 184-93.

RAITOHARJU, E., LYYTIKAINEN, L. P., LEVULA, M., OKSALA, N., MENNANDER, A., TARKKA, M., KLOPP, N., ILLIG, T., KAHONEN, M., KARHUNEN, P. J., LAAKSONEN, R. & LEHTIMAKI, T. 2011. miR-21, miR-210, miR-34a, and miR-146a/b are up-regulated in human atherosclerotic plaques in the Tampere Vascular Study. *Atherosclerosis,* 219**,** 211-7.

RAPOSO, G., NIJMAN, H. W., STOORVOGEL, W., LIEJENDEKKER, R., HARDING, C. V., MELIEF, C. J. & GEUZE, H. J. 1996. B lymphocytes secrete antigen-presenting vesicles. *J Exp Med,* 183**,** 1161-72.

READ, S. J., HIRANO, T., ABBOTT, D. F., SACHINIDIS, J. I., TOCHON-DANGUY, H. J., CHAN, J. G., EGAN, G. F., SCOTT, A. M., BLADIN, C. F., MCKAY, W. J. & DONNAN, G. A. 1998. Identifying hypoxic tissue after acute ischemic stroke using PET and 18F-fluoromisonidazole. *Neurology,* 51**,** 1617-21.

REEVES, M. J., BUSHNELL, C. D., HOWARD, G., GARGANO, J. W., DUNCAN, P. W., LYNCH, G., KHATIWODA, A. & LISABETH, L. 2008. Sex differences in stroke: epidemiology, clinical presentation, medical care, and outcomes. *Lancet Neurol,* 7**,** 915-26.

REHWINKEL, J. A. N., BEHM-ANSMANT, I., GATFIELD, D. & IZAURRALDE, E. 2005. A crucial role for GW182 and the DCP1:DCP2 decapping complex in miRNA-mediated gene silencing. *RNA,* 11**,** 1640-1647.

REN, J., ZHANG, J., XU, N., HAN, G., GENG, Q., SONG, J., LI, S., ZHAO, J. & CHEN, H. 2013. Signature of Circulating MicroRNAs as Potential Biomarkers in Vulnerable Coronary Artery Disease. *PLoS ONE,* 8**,** e80738.

REN, X. P., WU, J., WANG, X., SARTOR, M. A., QIAN, J., JONES, K., NICOLAOU, P., PRITCHARD, T. J. & FAN, G. C. 2009. MicroRNA-320 is involved in the regulation of cardiac ischemia/reperfusion injury by targeting heat-shock protein 20. *Circulation,* 119**,** 2357-66.

RICE, M. E. 2011. H2O2: a dynamic neuromodulator. *Neuroscientist,* 17**,** 389-406.

RIPPE, C., BLIMLINE, M., MAGERKO, K. A., LAWSON, B. R., LAROCCA, T. J., DONATO, A. J. & SEALS, D. R. 2012. MicroRNA changes in human arterial endothelial cells with senescence: relation to apoptosis, eNOS and inflammation. *Exp Gerontol,* 47**,** 45-51.

ROSELL, A., ALVAREZ-SABÍN, J., ARENILLAS, J. F., ROVIRA, A., DELGADO, P., FERNÁNDEZ-CADENAS, I., PENALBA, A., MOLINA, C. A. & MONTANER, J. 2005. A Matrix Metalloproteinase Protein Array Reveals a Strong Relation Between MMP-9 and MMP-13 With Diffusion-Weighted Image Lesion Increase in Human Stroke. *Stroke,* 36**,** 1415-1420.

ROSELL, A., CUADRADO, E., ORTEGA-AZNAR, A., HERNANDEZ-GUILLAMON, M., LO, E. H. & MONTANER, J. 2008. MMP-9-positive neutrophil infiltration is associated to blood-brain barrier breakdown and basal lamina type IV collagen degradation during hemorrhagic transformation after human ischemic stroke. *Stroke,* 39**,** 1121-6.

ROSOMOFF, H. L. 1957. Hypothermia and cerebral vascular lesions: Ii. experimental middle cerebral artery interruption followed by induction of hypothermia. *A.M.A. Archives of Neurology & Psychiatry,* 78**,** 454-464.

ROSS, T. M., MARTINEZ, P. M., RENNER, J. C., THORNE, R. G., HANSON, L. R. & FREY, W. H., 2ND 2004. Intranasal administration of interferon beta bypasses the blood-brain barrier to target the central nervous system and cervical lymph nodes: a non-invasive treatment strategy for multiple sclerosis. *J Neuroimmunol,* 151**,** 66-77.

ROTHWELL, P. M., COULL, A. J., SILVER, L. E., FAIRHEAD, J. F., GILES, M. F., LOVELOCK, C. E., REDGRAVE, J. N., BULL, L. M., WELCH, S. J., CUTHBERTSON, F. C., BINNEY, L. E., GUTNIKOV, S. A., ANSLOW, P., BANNING, A. P., MANT, D., MEHTA, Z. & OXFORD VASCULAR, S. 2005. Population-based study of event-rate, incidence, case fatality, and mortality for all acute vascular events in all arterial territories (Oxford Vascular Study). *Lancet,* 366**,** 1773-83.

SABATEL, C., MALVAUX, L., BOVY, N., DEROANNE, C., LAMBERT, V., GONZALEZ, M.-L. A., COLIGE, A., RAKIC, J.-M., NOËL, A., MARTIAL, J. A. & STRUMAN, I.

2011. MicroRNA-21 Exhibits Antiangiogenic Function by Targeting RhoB Expression in Endothelial Cells. *PLoS ONE,* 6**,** e16979.

SAKA, O., MCGUIRE, A. & WOLFE, C. 2009. Cost of stroke in the United Kingdom. *Age Ageing,* 38**,** 27-32.

SARKAR, J., GOU, D., TURAKA, P., VIKTOROVA, E., RAMCHANDRAN, R. & RAJ, J. U. 2010. MicroRNA-21 plays a role in hypoxia-mediated pulmonary artery smooth muscle cell proliferation and migration. *Am J Physiol Lung Cell Mol Physiol,* 299**,** L861-71.

SAUNDERSON, S. C., DUNN, A. C., CROCKER, P. R. & MCLELLAN, A. D. 2014. CD169 mediates the capture of exosomes in spleen and lymph node. *Blood,* 123**,** 208-16.

SAVER, J. L. 2006. Time is brain--quantified. *Stroke,* 37**,** 263-6.

SAVER, J. L., FONAROW, G. C., SMITH, E. E. & ET AL. 2013. TIme to treatment with intravenous tissue plasminogen activator and outcome from acute ischemic stroke. *JAMA,* 309**,** 2480-2488.

SAVER, J. L., GOYAL, M., BONAFE, A., DIENER, H.-C., LEVY, E. I., PEREIRA, V. M., ALBERS, G. W., COGNARD, C., COHEN, D. J., HACKE, W., JANSEN, O., JOVIN, T. G., MATTLE, H. P., NOGUEIRA, R. G., SIDDIQUI, A. H., YAVAGAL, D. R., BAXTER, B. W., DEVLIN, T. G., LOPES, D. K., REDDY, V. K., DU MESNIL DE ROCHEMONT, R., SINGER, O. C. & JAHAN, R. 2015. Stent-Retriever Thrombectomy after Intravenous t-PA vs. t-PA Alone in Stroke. *New England Journal of Medicine,* 372**,** 2285-2295.

SAYED, D., HONG, C., CHEN, I. Y., LYPOWY, J. & ABDELLATIF, M. 2007. MicroRNAs play an essential role in the development of cardiac hypertrophy. *Circ Res,* 100**,** 416-24.

SCHINZEL, A. C., TAKEUCHI, O., HUANG, Z., FISHER, J. K., ZHOU, Z., RUBENS, J., HETZ, C., DANIAL, N. N., MOSKOWITZ, M. A. & KORSMEYER, S. J. 2005. Cyclophilin D is a component of mitochondrial permeability transition and mediates neuronal cell death after focal cerebral ischemia. *Proc Natl Acad Sci U S A,* 102**,** 12005-10.

SEGGERSON, K., TANG, L. & MOSS, E. G. 2002. Two genetic circuits repress the Caenorhabditis elegans heterochronic gene lin-28 after translation initiation. *Dev Biol,* 243**,** 215-25.

SEGURA, E., GUERIN, C., HOGG, N., AMIGORENA, S. & THERY, C. 2007. CD8+ dendritic cells use LFA-1 to capture MHC-peptide complexes from exosomes in vivo. *J Immunol,* 179**,** 1489-96.

SEGURA, E., NICCO, C., LOMBARD, B., VERON, P., RAPOSO, G., BATTEUX, F., AMIGORENA, S. & THERY, C. 2005. ICAM-1 on exosomes from mature dendritic cells is critical for efficient naive T-cell priming. *Blood,* 106**,** 216-23.

SELBACH, M., SCHWANHAUSSER, B., THIERFELDER, N., FANG, Z., KHANIN, R. & RAJEWSKY, N. 2008. Widespread changes in protein synthesis induced by microRNAs. *Nature,* 455**,** 58-63.

SELVAMANI, A., SATHYAN, P., MIRANDA, R. C. & SOHRABJI, F. 2012. An antagomir to microRNA Let7f promotes neuroprotection in an ischemic stroke model. *PloS one,* 7**,** e32662.

SELVAMANI, A., WILLIAMS, M. H., MIRANDA, R. C. & SOHRABJI, F. 2014. Circulating miRNA profiles provide a biomarker for severity of stroke outcomes associated with age and sex in a rat model. *Clinical Science,* 127**,** 77-89.

SEPRAMANIAM, S., ARMUGAM, A., LIM, K. Y., KAROLINA, D. S., SWAMINATHAN, P., TAN, J. R. & JEYASEELAN, K. 2010. MicroRNA 320a functions as a novel endogenous modulator of aquaporins 1 and 4 as well as a potential therapeutic target in cerebral ischemia. *Journal of Biological Chemistry,* 285**,** 29223-29230.

SEPRAMANIAM, S., TAN, J. R., TAN, K. S., DESILVA, D. A., TAVINTHARAN, S., WOON, F. P., WANG, C. W., YONG, F. L., KAROLINA, D. S., KAUR, P., LIU, F. J., LIM, K. Y., ARMUGAM, A. & JEYASEELAN, K. 2014. Circulating microRNAs as biomarkers of acute stroke. *Int J Mol Sci,* 15**,** 1418-32.

SHAN, S. W., FANG, L., SHATSEVA, T., RUTNAM, Z. J., YANG, X., DU, W., LU, W. Y., XUAN, J. W., DENG, Z. & YANG, B. B. 2013. Mature miR-17-5p and passenger

miR-17-3p induce hepatocellular carcinoma by targeting PTEN, GalNT7 and vimentin in different signal pathways. *J Cell Sci,* 126**,** 1517-30.
SHIRLEY, R., ORD, E. N. & WORK, L. M. 2014. Oxidative Stress and the Use of Antioxidants in Stroke. *Antioxidants (Basel),* 3**,** 472-501.
SHOAMANESH, A., PREIS, S. R., BEISER, A. S., KASE, C. S., WOLF, P. A., VASAN, R. S., BENJAMIN, E. J., SESHADRI, S. & ROMERO, J. R. 2016. Circulating biomarkers and incident ischemic stroke in the Framingham Offspring Study. *Neurology,* 87**,** 1206-1211.
SHTAM, T. A., KOVALEV, R. A., VARFOLOMEEVA, E. Y., MAKAROV, E. M., KIL, Y. V. & FILATOV, M. V. 2013. Exosomes are natural carriers of exogenous siRNA to human cells in vitro. *Cell Commun Signal,* 11**,** 88.
SIMATS, A., GARCÍA-BERROCOSO, T. & MONTANER, J. 2016. Neuroinflammatory biomarkers: From stroke diagnosis and prognosis to therapy. *Biochimica et Biophysica Acta (BBA) - Molecular Basis of Disease,* 1862**,** 411-424.
SKOG, J., WURDINGER, T., VAN RIJN, S., MEIJER, D. H., GAINCHE, L., SENA-ESTEVES, M., CURRY, W. T., JR., CARTER, B. S., KRICHEVSKY, A. M. & BREAKEFIELD, X. O. 2008. Glioblastoma microvesicles transport RNA and proteins that promote tumour growth and provide diagnostic biomarkers. *Nat Cell Biol,* 10**,** 1470-6.
SNAPYAN, M., LEMASSON, M., BRILL, M. S., BLAIS, M., MASSOUH, M., NINKOVIC, J., GRAVEL, C., BERTHOD, F., GOTZ, M., BARKER, P. A., PARENT, A. & SAGHATELYAN, A. 2009. Vasculature guides migrating neuronal precursors in the adult mammalian forebrain via brain-derived neurotrophic factor signaling. *J Neurosci,* 29**,** 4172-88.
SORENSEN, J. C., MATTSSON, B., ANDREASEN, A. & JOHANSSON, B. B. 1998. Rapid disappearance of zinc positive terminals in focal brain ischemia. *Brain Res,* 812**,** 265-9.
SØRENSEN, S. S., NYGAARD, A.-B., NIELSEN, M.-Y., JENSEN, K. & CHRISTENSEN, T. 2014. miRNA expression profiles in cerebrospinal fluid and blood of patients with acute ischemic stroke. *Translational stroke research,* 5**,** 711-718.
SOTGIU, S., ZANDA, B., MARCHETTI, B., FOIS, M. L., ARRU, G., PES, G. M., SALARIS, F. S., ARRU, A., PIRISI, A. & ROSATI, G. 2006. Inflammatory biomarkers in blood of patients with acute brain ischemia. *European Journal of Neurology,* 13**,** 505-513.
SPITE, M. & SERHAN, C. N. 2010. Novel lipid mediators promote resolution of acute inflammation: impact of aspirin and statins. *Circ Res,* 107**,** 1170-84.
STAIR 1999. Recommendations for standards regarding preclinical neuroprotective and restorative drug treatment. *Stroke,* 30**,** 2752-2758.
STAMATOVIC, S. M., KEEP, R. F., KUNKEL, S. L. & ANDJELKOVIC, A. V. 2003. Potential role of MCP-1 in endothelial cell tight junction 'opening': signaling via Rho and Rho kinase. *J Cell Sci,* 116**,** 4615-28.
STARY, C. M., XU, L., SUN, X., OUYANG, Y. B., WHITE, R. E., LEONG, J., LI, J., XIONG, X. & GIFFARD, R. G. 2015. MicroRNA-200c contributes to injury from transient focal cerebral ischemia by targeting Reelin. *Stroke,* 46**,** 551-6.
STATHER, P. W., SYLVIUS, N., WILD, J. B., CHOKE, E., SAYERS, R. D. & BOWN, M. J. 2013. Differential MicroRNA Expression Profiles in Peripheral Arterial Disease. *Circ Cardiovasc Genet*.
STOORVOGEL, W., STROUS, G. J., GEUZE, H. J., OORSCHOT, V. & SCHWARTZ, A. L. 1991. Late endosomes derive from early endosomes by maturation. *Cell,* 65**,** 417-27.
STROKE ASSOCIATION, T. 2016. State of the Nation - Stroke Statistics.
STROKE UNIT TRIALISTS' COLLABORATION, T. 2013. Organised inpatient (stroke unit) care for stroke. *Cochrane Database Syst Rev***,** Cd000197.
SU, H., TROMBLY, M. I., CHEN, J. & WANG, X. 2009. Essential and overlapping functions for mammalian Argonautes in microRNA silencing. *Genes Dev,* 23**,** 304-17.

SUN, Y., GUI, H., LI, Q., LUO, Z. M., ZHENG, M. J., DUAN, J. L. & LIU, X. 2013. MicroRNA-124 Protects Neurons Against Apoptosis in Cerebral Ischemic Stroke. *CNS neuroscience & therapeutics,* 19**,** 813-819.

TABARA, H., SARKISSIAN, M., KELLY, W. G., FLEENOR, J., GRISHOK, A., TIMMONS, L., FIRE, A. & MELLO, C. C. 1999. The rde-1 gene, RNA interference, and transposon silencing in C. elegans. *Cell,* 99**,** 123-32.

TAGAMI, M., NARA, Y., KUBOTA, A., SUNAGA, T., MAEZAWA, H., FUJINO, H. & YAMORI, Y. 1987. Ultrastructural characteristics of occluded perforating arteries in stroke-prone spontaneously hypertensive rats. *Stroke,* 18**,** 733-40.

TAGUCHI, A., SOMA, T., TANAKA, H., KANDA, T., NISHIMURA, H., YOSHIKAWA, H., TSUKAMOTO, Y., ISO, H., FUJIMORI, Y., STERN, D. M., NARITOMI, H. & MATSUYAMA, T. 2004. Administration of CD34+ cells after stroke enhances neurogenesis via angiogenesis in a mouse model. *J Clin Invest,* 114**,** 330-8.

TAKAHASHI, Y., NISHIKAWA, M., SHINOTSUKA, H., MATSUI, Y., OHARA, S., IMAI, T. & TAKAKURA, Y. 2013. Visualization and in vivo tracking of the exosomes of murine melanoma B16-BL6 cells in mice after intravenous injection. *J Biotechnol,* 165**,** 77-84.

TAN, J. R., TAN, K. S., KOO, Y. X., YONG, F. L., WANG, C. W., ARMUGAM, A. & JEYASEELAN, K. 2013. Blood microRNAs in low or no risk ischemic stroke patients. *International journal of molecular sciences,* 14**,** 2072-2084.

TAN, K. S., ARMUGAM, A., SEPRAMANIAM, S., LIM, K. Y., SETYOWATI, K. D., WANG, C. W. & JEYASEELAN, K. 2009. Expression profile of MicroRNAs in young stroke patients. *PloS one,* 4**,** e7689.

TARKOWSKI, E., ROSENGREN, L., BLOMSTRAND, C., WIKKELSO, C., JENSEN, C., EKHOLM, S. & TARKOWSKI, A. 1995. Early intrathecal production of interleukin-6 predicts the size of brain lesion in stroke. *Stroke,* 26**,** 1393-8.

TAY, J., TIAO, J., HUGHES, Q., GILMORE, G. & BAKER, R. 2016. Therapeutic Potential of miR-494 in Thrombosis and Other Diseases: A Review. *Australian Journal of Chemistry***,** -.

THÉRY, C., AMIGORENA, S., RAPOSO, G. & CLAYTON, A. 2006. Isolation and Characterization of Exosomes from Cell Culture Supernatants and Biological Fluids. *Current Protocols in Cell Biology.* John Wiley & Sons, Inc.

THOMSON, D. W., BRACKEN, C. P., SZUBERT, J. M. & GOODALL, G. J. 2013. On measuring miRNAs after transient transfection of mimics or antisense inhibitors. *PLoS One,* 8**,** e55214.

THORNBERRY, N. A. & LAZEBNIK, Y. 1998. Caspases: enemies within. *Science,* 281**,** 1312-6.

THORNE, R. G., EMORY, C. R., ALA, T. A. & FREY, W. H., 2ND 1995. Quantitative analysis of the olfactory pathway for drug delivery to the brain. *Brain Res,* 692**,** 278-82.

THORNE, R. G., PRONK, G. J., PADMANABHAN, V. & FREY, W. H., 2ND 2004. Delivery of insulin-like growth factor-I to the rat brain and spinal cord along olfactory and trigeminal pathways following intranasal administration. *Neuroscience,* 127**,** 481-96.

THUM, T., GALUPPO, P., WOLF, C., FIEDLER, J., KNEITZ, S., VAN LAAKE, L. W., DOEVENDANS, P. A., MUMMERY, C. L., BORLAK, J., HAVERICH, A., GROSS, C., ENGELHARDT, S., ERTL, G. & BAUERSACHS, J. 2007. MicroRNAs in the human heart: a clue to fetal gene reprogramming in heart failure. *Circulation,* 116**,** 258-67.

TIAN, Y., LI, S., SONG, J., JI, T., ZHU, M., ANDERSON, G. J., WEI, J. & NIE, G. 2014. A doxorubicin delivery platform using engineered natural membrane vesicle exosomes for targeted tumor therapy. *Biomaterials,* 35**,** 2383-90.

TOWNSEND, N., BHATNAGAR, P., WILKINS, E., WICKRAMASINGHE, K. & RAYNER, M. 2015. Cardiovascular disease statistics, 2015. London.

TRAMS, E. G., LAUTER, C. J., SALEM, N., JR. & HEINE, U. 1981. Exfoliation of membrane ecto-enzymes in the form of micro-vesicles. *Biochim Biophys Acta,* 645**,** 63-70.

TSAI, P.-C., LIAO, Y.-C., WANG, Y.-S., LIN, H.-F., LIN, R.-T. & JUO, S. 2012. Serum microRNA-21 and microRNA-221 as potential biomarkers for cerebrovascular disease. *Journal of vascular research,* 50**,** 346-354.

TSUJI, K., AOKI, T., TEJIMA, E., ARAI, K., LEE, S. R., ATOCHIN, D. N., HUANG, P. L., WANG, X., MONTANER, J. & LO, E. H. 2005. Tissue plasminogen activator promotes matrix metalloproteinase-9 upregulation after focal cerebral ischemia. *Stroke,* 36**,** 1954-9.

VALADI, H., EKSTROM, K., BOSSIOS, A., SJOSTRAND, M., LEE, J. J. & LOTVALL, J. O. 2007. Exosome-mediated transfer of mRNAs and microRNAs is a novel mechanism of genetic exchange between cells. *Nat Cell Biol,* 9**,** 654-659.

VAN GIJN, J. & RINKEL, G. J. 2001. Subarachnoid haemorrhage: diagnosis, causes and management. *Brain,* 124**,** 249-78.

VAN ROOIJ, E. & KAUPPINEN, S. 2014. Development of microRNA therapeutics is coming of age. *EMBO Mol Med,* 6**,** 851-64.

VAN ROOIJ, E., SUTHERLAND, L. B., LIU, N., WILLIAMS, A. H., MCANALLY, J., GERARD, R. D., RICHARDSON, J. A. & OLSON, E. N. 2006. A signature pattern of stress-responsive microRNAs that can evoke cardiac hypertrophy and heart failure. *Proceedings of the National Academy of Sciences of the United States of America,* 103**,** 18255-18260.

VICKERS, K. C., PALMISANO, B. T., SHOUCRI, B. M., SHAMBUREK, R. D. & REMALEY, A. T. 2011. MicroRNAs are transported in plasma and delivered to recipient cells by high-density lipoproteins. *Nat Cell Biol,* 13**,** 423-33.

VILA, N., CASTILLO, J., DAVALOS, A. & CHAMORRO, A. 2000. Proinflammatory cytokines and early neurological worsening in ischemic stroke. *Stroke,* 31**,** 2325-9.

VILA, N., CASTILLO, J., DAVALOS, A., ESTEVE, A., PLANAS, A. M. & CHAMORRO, A. 2003. Levels of anti-inflammatory cytokines and neurological worsening in acute ischemic stroke. *Stroke,* 34**,** 671-5.

VINCIGUERRA, A., FORMISANO, L., CERULLO, P., GUIDA, N., CUOMO, O., ESPOSITO, A., DI RENZO, G., ANNUNZIATO, L. & PIGNATARO, G. 2014. MicroRNA-103-1 selectively downregulates brain NCX1 and its inhibition by anti-miRNA ameliorates stroke damage and neurological deficits. *Molecular Therapy,* 22**,** 1829-1838.

WAHLGREN, J., DE, L. K. T., BRISSLERT, M., VAZIRI SANI, F., TELEMO, E., SUNNERHAGEN, P. & VALADI, H. 2012. Plasma exosomes can deliver exogenous short interfering RNA to monocytes and lymphocytes. *Nucleic Acids Res,* 40**,** e130.

WANG, F., ZHAO, X. Q., LIU, J. N., WANG, Z. H., WANG, X. L., HOU, X. Y., LIU, R., GAO, F., ZHANG, M. X., ZHANG, Y. & BU, P. L. 2012. Antagonist of microRNA-21 improves balloon injury-induced rat iliac artery remodeling by regulating proliferation and apoptosis of adventitial fibroblasts and myofibroblasts. *J Cell Biochem,* 113**,** 2989-3001.

WANG, M., LI, W., CHANG, G. Q., YE, C. S., OU, J. S., LI, X. X., LIU, Y., CHEANG, T. Y., HUANG, X. L. & WANG, S. M. 2011. MicroRNA-21 regulates vascular smooth muscle cell function via targeting tropomyosin 1 in arteriosclerosis obliterans of lower extremities. *Arterioscler Thromb Vasc Biol,* 31**,** 2044-53.

WANG, P., LIANG, J., LI, Y., LI, J., YANG, X., ZHANG, X., HAN, S., LI, S. & LI, J. 2014a. Down-regulation of miRNA-30a alleviates cerebral ischemic injury through enhancing beclin 1-mediated autophagy. *Neurochem Res,* 39**,** 1279-91.

WANG, W., SUN, G., ZHANG, L., SHI, L. & ZENG, Y. 2014b. Circulating MicroRNAs as Novel Potential Biomarkers for Early Diagnosis of Acute Stroke in Humans. *Journal of Stroke and Cerebrovascular Diseases,* 23**,** 2607-2613.

WANG, X., ZHANG, X., REN, X.-P., CHEN, J., LIU, H., YANG, J., MEDVEDOVIC, M., HU, Z. & FAN, G.-C. 2010. MicroRNA-494 Targeting Both Proapoptotic and Antiapoptotic Proteins Protects Against Ischemia/Reperfusion-Induced Cardiac InjuryClinical Perspective. *Circulation,* 122**,** 1308-1318.

WANG, Y., HUANG, J., MA, Y., TANG, G., LIU, Y., CHEN, X., ZHANG, Z., ZENG, L., WANG, Y., OUYANG, Y. B. & YANG, G. Y. 2015. MicroRNA-29b is a therapeutic

target in cerebral ischemia associated with aquaporin 4. *J Cereb Blood Flow Metab,* 35**,** 1977-84.

WANG, Y., RUDD, A. G. & WOLFE, C. D. 2013. Age and ethnic disparities in incidence of stroke over time: the South London Stroke Register. *Stroke,* 44**,** 3298-304.

WANG, Y., ZHANG, Y., HUANG, J., CHEN, X., GU, X., WANG, Y., ZENG, L. & YANG, G.-Y. 2014c. Increase of circulating miR-223 and insulin-like growth factor-1 is associated with the pathogenesis of acute ischemic stroke in patients. *BMC neurology,* 14**,** 77.

WANG, Z., GERSTEIN, M. & SNYDER, M. 2009. RNA-Seq: a revolutionary tool for transcriptomics. *Nat Rev Genet,* 10**,** 57-63.

WARDLAW, J. M., SMITH, C. & DICHGANS, M. 2013. Mechanisms of sporadic cerebral small vessel disease: insights from neuroimaging. *Lancet Neurol,* 12**,** 483-97.

WEBER, M., BAKER, M. B., MOORE, J. P. & SEARLES, C. D. 2010. MiR-21 is induced in endothelial cells by shear stress and modulates apoptosis and eNOS activity. *Biochemical and Biophysical Research Communications,* 393**,** 643-648.

WEI, N., XIAO, L., XUE, R., ZHANG, D., ZHOU, J., REN, H., GUO, S. & XU, J. 2015. MicroRNA-9 Mediates the Cell Apoptosis by Targeting Bcl2l11 in Ischemic Stroke. *Mol Neurobiol*.

WELTEN, S. M., BASTIAANSEN, A. J., DE JONG, R. C., DE VRIES, M. R., PETERS, E. A., BOONSTRA, M. C., SHEIKH, S. P., LA MONICA, N., KANDIMALLA, E. R., QUAX, P. H. & NOSSENT, A. Y. 2014. Inhibition of 14q32 MicroRNAs miR-329, miR-487b, miR-494, and miR-495 increases neovascularization and blood flow recovery after ischemia. *Circ Res,* 115**,** 696-708.

WEN, Y., ZHANG, X., DONG, L., ZHAO, J., ZHANG, C. & ZHU, C. 2015. Acetylbritannilactone Modulates microRNA-155-Mediated Inflammatory Response in Ischemic Cerebral Tissues. *Mol Med*.

WEZEL, A., WELTEN, S. M. J., RAZAWY, W., LAGRAAUW, H. M., DE VRIES, M. R., GOOSSENS, E. A. C., BOONSTRA, M. C., HAMMING, J. F., KANDIMALLA, E. R., KUIPER, J., QUAX, P. H. A., NOSSENT, A. Y. & BOT, I. 2015. Inhibition of MicroRNA-494 Reduces Carotid Artery Atherosclerotic Lesion Development and Increases Plaque Stability. *Annals of Surgery,* 262**,** 841-848.

WHITE, I. J., BAILEY, L. M., AGHAKHANI, M. R., MOSS, S. E. & FUTTER, C. E. 2006. EGF stimulates annexin 1-dependent inward vesiculation in a multivesicular endosome subpopulation. *Embo j,* 25**,** 1-12.

WHITELEY, W., JACKSON, C., LEWIS, S., LOWE, G., RUMLEY, A., SANDERCOCK, P., WARDLAW, J., DENNIS, M. & SUDLOW, C. 2009. Inflammatory Markers and Poor Outcome after Stroke: A Prospective Cohort Study and Systematic Review of Interleukin-6. *PLOS Medicine,* 6**,** e1000145.

WIGHTMAN, B., HA, I. & RUVKUN, G. 1993. Posttranscriptional regulation of the heterochronic gene lin-14 by lin-4 mediates temporal pattern formation in C. elegans. *Cell,* 75**,** 855-62.

WIKLANDER, O. P., NORDIN, J. Z., O'LOUGHLIN, A., GUSTAFSSON, Y., CORSO, G., MAGER, I., VADER, P., LEE, Y., SORK, H., SEOW, Y., HELDRING, N., ALVAREZ-ERVITI, L., SMITH, C. I., LE BLANC, K., MACCHIARINI, P., JUNGEBLUTH, P., WOOD, M. J. & ANDALOUSSI, S. E. 2015. Extracellular vesicle in vivo biodistribution is determined by cell source, route of administration and targeting. *J Extracell Vesicles,* 4**,** 26316.

WOLF, P. A., ABBOTT, R. D. & KANNEL, W. B. 1991. Atrial fibrillation as an independent risk factor for stroke: the Framingham Study. *Stroke,* 22**,** 983-8.

WONG, L. L., ARMUGAM, A., SEPRAMANIAM, S., KAROLINA, D. S., LIM, K. Y., LIM, J. Y., CHONG, J. P. C., NG, J. Y. X., CHEN, Y.-T., CHAN, M. M. Y., CHEN, Z., YEO, P. S. D., NG, T. P., LING, L. H., SIM, D., LEONG, K. T. G., ONG, H. Y., JAUFEERALLY, F., WONG, R., CHAI, P., LOW, A. F., LAM, C. S. P., JEYASEELAN, K. & RICHARDS, A. M. 2015. Circulating microRNAs in heart failure with reduced and preserved left ventricular ejection fraction. *European Journal of Heart Failure,* 17**,** 393-404.

WORLD HEALTH ORGANISATION, T. 2014. *The top 10 causes of death* [Online]. World Health Organisation. Available: http://www.who.int/mediacentre/factsheets/fs310/en/ [Accessed 26 January 2016.

WU, L., FAN, J. & BELASCO, J. G. 2006. MicroRNAs direct rapid deadenylation of mRNA. *Proc Natl Acad Sci U S A,* 103**,** 4034-9.

XIN, H., LI, Y., BULLER, B., KATAKOWSKI, M., ZHANG, Y., WANG, X., SHANG, X., ZHANG, Z. G. & CHOPP, M. 2012. Exosome-mediated transfer of miR-133b from multipotent mesenchymal stromal cells to neural cells contributes to neurite outgrowth. *Stem Cells,* 30**,** 1556-64.

XIN, H., LI, Y., CUI, Y., YANG, J. J., ZHANG, Z. G. & CHOPP, M. 2013a. Systemic administration of exosomes released from mesenchymal stromal cells promote functional recovery and neurovascular plasticity after stroke in rats. *J Cereb Blood Flow Metab,* 33**,** 1711-5.

XIN, H., LI, Y., LIU, Z., WANG, X., SHANG, X., CUI, Y., ZHANG, Z. G. & CHOPP, M. 2013b. MiR-133b Promotes Neural Plasticity and Functional Recovery After Treatment of Stroke with Multipotent Mesenchymal Stromal Cells in Rats Via Transfer of Exosome-Enriched Extracellular Particles. *Stem Cells,* 31**,** 2737-2746.

XIONG, R., WANG, Z., ZHAO, Z., LI, H., CHEN, W., ZHANG, B., WANG, L., WU, L., LI, W., DING, J. & CHEN, S. 2014. MicroRNA-494 reduces DJ-1 expression and exacerbates neurodegeneration. *Neurobiology of Aging,* 35**,** 705-714.

XU, L.-J., OUYANG, Y.-B., XIONG, X., STARY, C. M. & GIFFARD, R. G. 2015. Post-stroke treatment with miR-181 antagomir reduces injury and improves long-term behavioral recovery in mice after focal cerebral ischemia. *Experimental Neurology,* 264**,** 1-7.

YAMORI, Y. & HORIE, R. 1977. Developmental course of hypertension and regional cerebral blood flow in stroke-prone spontaneously hypertensive rats. *Stroke,* 8**,** 456-61.

YAMORI, Y., HORIE, R., HANDA, H., SATO, M. & FUKASE, M. 1976. Pathogenetic similarity of strokes in stroke-prone spontaneously hypertensive rats and humans. *Stroke,* 7**,** 46-53.

YANG, G., PEI, Y., CAO, Q. & WANG, R. 2012. MicroRNA-21 represses human cystathionine gamma-lyase expression by targeting at specificity protein-1 in smooth muscle cells. *J Cell Physiol,* 227**,** 3192-200.

YANG, J.-S., MAURIN, T., ROBINE, N., RASMUSSEN, K. D., JEFFREY, K. L., CHANDWANI, R., PAPAPETROU, E. P., SADELAIN, M., O'CARROLL, D. & LAI, E. C. 2010. Conserved vertebrate mir-451 provides a platform for Dicer-independent, Ago2-mediated microRNA biogenesis. *Proceedings of the National Academy of Sciences,* 107**,** 15163-15168.

YANG, X., DU, W. W., LI, H., LIU, F., KHORSHIDI, A., RUTNAM, Z. J. & YANG, B. B. 2013. Both mature miR-17-5p and passenger strand miR-17-3p target TIMP3 and induce prostate tumor growth and invasion. *Nucleic Acids Res,* 41**,** 9688-704.

YANG, Y. & ROSENBERG, G. A. 2011. Blood-brain barrier breakdown in acute and chronic cerebrovascular disease. *Stroke,* 42**,** 3323-8.

YANG, Z. B., ZHANG, Z., LI, T. B., LOU, Z., LI, S. Y., YANG, H., YANG, J., LUO, X. J. & PENG, J. 2014. Up-regulation of brain-enriched miR-107 promotes excitatory neurotoxicity through down-regulation of glutamate transporter-1 expression following ischaemic stroke. *Clin Sci (Lond),* 127**,** 679-89.

YAO, R., MA, Y., DU, Y., LIAO, M., LI, H., LIANG, W., YUAN, J., MA, Z., YU, X., XIAO, H. & LIAO, Y. 2011. The altered expression of inflammation-related microRNAs with microRNA-155 expression correlates with Th17 differentiation in patients with acute coronary syndrome. *Cell Mol Immunol,* 8**,** 486-95.

YEKTA, S., SHIH, I. H. & BARTEL, D. P. 2004. MicroRNA-directed cleavage of HOXB8 mRNA. *Science,* 304**,** 594-6.

YI, R., QIN, Y., MACARA, I. G. & CULLEN, B. R. 2003. Exportin-5 mediates the nuclear export of pre-microRNAs and short hairpin RNAs. *Genes Dev,* 17**,** 3011-6.

YILMAZ, G. & GRANGER, D. N. 2010. Leukocyte recruitment and ischemic brain injury. *Neuromolecular Med,* 12**,** 193-204.

YIN, K. J., DENG, Z., HUANG, H., HAMBLIN, M., XIE, C., ZHANG, J. & CHEN, Y. E. 2010. miR-497 regulates neuronal death in mouse brain after transient focal cerebral ischemia. *Neurobiol Dis,* 38**,** 17-26.

YING, W., HAN, S. K., MILLER, J. W. & SWANSON, R. A. 1999. Acidosis potentiates oxidative neuronal death by multiple mechanisms. *J Neurochem,* 73**,** 1549-56.

YODA, M., KAWAMATA, T., PAROO, Z., YE, X., IWASAKI, S., LIU, Q. & TOMARI, Y. 2010. ATP-dependent human RISC assembly pathways. *Nat Struct Mol Biol,* 17**,** 17-23.

YU, H., WU, M., ZHAO, P., HUANG, Y., WANG, W. & YIN, W. 2015. Neuroprotective effects of viral overexpression of microRNA-22 in rat and cell models of cerebral ischemia-reperfusion injury. *J Cell Biochem,* 116**,** 233-41.

YU, S. P., YEH, C. H., SENSI, S. L., GWAG, B. J., CANZONIERO, L. M., FARHANGRAZI, Z. S., YING, H. S., TIAN, M., DUGAN, L. L. & CHOI, D. W. 1997. Mediation of neuronal apoptosis by enhancement of outward potassium current. *Science,* 278**,** 114-7.

YU, S. W., ANDRABI, S. A., WANG, H., KIM, N. S., POIRIER, G. G., DAWSON, T. M. & DAWSON, V. L. 2006. Apoptosis-inducing factor mediates poly(ADP-ribose) (PAR) polymer-induced cell death. *Proc Natl Acad Sci U S A,* 103**,** 18314-9.

ZECHARIAH, A., ELALI, A. & HERMANN, D. M. 2010. Combination of tissue-plasminogen activator with erythropoietin induces blood-brain barrier permeability, extracellular matrix disaggregation, and DNA fragmentation after focal cerebral ischemia in mice. *Stroke,* 41**,** 1008-12.

ZENG, L., LIU, J., WANG, Y., WANG, L., WENG, S., CHEN, S. & YANG, G.-Y. 2012. Cocktail blood biomarkers: prediction of clinical outcomes in patients with acute ischemic stroke. *European neurology,* 69**,** 68-75.

ZENG, L., LIU, J., WANG, Y., WANG, L., WENG, S., TANG, Y., ZHENG, C., CHENG, Q., CHEN, S. & YANG, G.-Y. 2011. MicroRNA-210 as a novel blood biomarker in acute cerebral ischemia. *Front Biosci (Elite Ed),* 3**,** 1265-1272.

ZHAI, F., ZHANG, X., GUAN, Y., YANG, X., LI, Y., SONG, G. & GUAN, L. 2012. *Expression profiles of microRNAs after focal cerebral ischemia/reperfusion injury in rats*.

ZHANG, D. W., SHAO, J., LIN, J., ZHANG, N., LU, B. J., LIN, S. C., DONG, M. Q. & HAN, J. 2009. RIP3, an energy metabolism regulator that switches TNF-induced cell death from apoptosis to necrosis. *Science,* 325**,** 332-6.

ZHANG, H., KOLB, F. A., JASKIEWICZ, L., WESTHOF, E. & FILIPOWICZ, W. 2004. Single processing center models for human Dicer and bacterial RNase III. *Cell,* 118**,** 57-68.

ZHANG, J., YUAN, L., ZHANG, X., HAMBLIN, M. H., ZHU, T., MENG, F., LI, Y., CHEN, Y. E. & YIN, K. J. 2016a. Altered long non-coding RNA transcriptomic profiles in brain microvascular endothelium after cerebral ischemia. *Experimental Neurology,* 277**,** 162-170.

ZHANG, L., DONG, L. Y., LI, Y. J., HONG, Z. & WEI, W. S. 2012. miR-21 represses FasL in microglia and protects against microglia-mediated neuronal cell death following hypoxia/ischemia. *Glia,* 60**,** 1888-95.

ZHANG, R., CHOPP, M., ZHANG, Z., JIANG, N. & POWERS, C. 1998. The expression of P- and E-selectins in three models of middle cerebral artery occlusion. *Brain Res,* 785**,** 207-14.

ZHANG, X. Y., SHEN, B. R., ZHANG, Y. C., WAN, X. J., YAO, Q. P., WU, G. L., WANG, J. Y., CHEN, S. G., YAN, Z. Q. & JIANG, Z. L. 2013. Induction of thoracic aortic remodeling by endothelial-specific deletion of microRNA-21 in mice. *PLoS One,* 8**,** e59002.

ZHANG, Y., CHENG, L., CHEN, Y., YANG, G.-Y., LIU, J. & ZENG, L. 2016b. Clinical predictor and circulating microRNA profile expression in patients with early onset post-stroke depression. *Journal of Affective Disorders,* 193**,** 51-58.

ZHANG, Y., LIU, D., CHEN, X., LI, J., LI, L., BIAN, Z., SUN, F., LU, J., YIN, Y., CAI, X., SUN, Q., WANG, K., BA, Y., WANG, Q., WANG, D., YANG, J., LIU, P., XU, T., YAN, Q., ZHANG, J., ZEN, K. & ZHANG, C. Y. 2010. Secreted monocytic miR-150 enhances targeted endothelial cell migration. *Mol Cell,* 39**,** 133-44.

ZHAO, H., TAO, Z., WANG, R., LIU, P., YAN, F., LI, J., ZHANG, C., JI, X. & LUO, Y. 2014. MicroRNA-23a-3p attenuates oxidative stress injury in a mouse model of focal cerebral ischemia-reperfusion. *Brain Res,* 1592**,** 65-72.

ZHAO, H., WANG, J., GAO, L., WANG, R., LIU, X., GAO, Z., TAO, Z., XU, C., SONG, J., JI, X. & LUO, Y. 2013. MiRNA-424 protects against permanent focal cerebral ischemia injury in mice involving suppressing microglia activation. *Stroke,* 44**,** 1706-13.

ZHOU, J., WANG, K. C., WU, W., SUBRAMANIAM, S., SHYY, J. Y., CHIU, J. J., LI, J. Y. & CHIEN, S. 2011. MicroRNA-21 targets peroxisome proliferators-activated receptor-alpha in an autoregulatory loop to modulate flow-induced endothelial inflammation. *Proc Natl Acad Sci U S A,* 108**,** 10355-60.

ZHOU, J. & ZHANG, J. 2014. Identification of miRNA-21 and miRNA-24 in plasma as potential early stage markers of acute cerebral infarction. *Mol Med Rep,* 10**,** 971-6.

ZHU, F., LIU, J. L., LI, J. P., XIAO, F., ZHANG, Z. X. & ZHANG, L. 2014. MicroRNA-124 (miR-124) regulates Ku70 expression and is correlated with neuronal death induced by ischemia/reperfusion. *J Mol Neurosci,* 52**,** 148-55.

ZHUANG, X., TENG, Y., SAMYKUTTY, A., MU, J., DENG, Z., ZHANG, L., CAO, P., RONG, Y., YAN, J., MILLER, D. & ZHANG, H. G. 2016. Grapefruit-derived Nanovectors Delivering Therapeutic miR17 Through an Intranasal Route Inhibit Brain Tumor Progression. *Mol Ther,* 24**,** 96-105.

ZHUANG, X., XIANG, X., GRIZZLE, W., SUN, D., ZHANG, S., AXTELL, R. C., JU, S., MU, J., ZHANG, L., STEINMAN, L., MILLER, D. & ZHANG, H. G. 2011. Treatment of brain inflammatory diseases by delivering exosome encapsulated anti-inflammatory drugs from the nasal region to the brain. *Mol Ther,* 19**,** 1769-79.

ZILE, M. R., MEHURG, S. M., ARROYO, J. E., STROUD, R. E., DESANTIS, S. M. & SPINALE, F. G. 2011. Relationship between the temporal profile of plasma microRNA and left ventricular remodeling in patients after myocardial infarction. *Circ Cardiovasc Genet,* 4**,** 614-9.

ZIVIN, J. A., FISHER, M., DEGIROLAMI, U., HEMENWAY, C. C. & STASHAK, J. A. 1985. Tissue plasminogen activator reduces neurological damage after cerebral embolism. *Science,* 230**,** 1289-92.